Manual of diagnostic ultrasound

volume 1

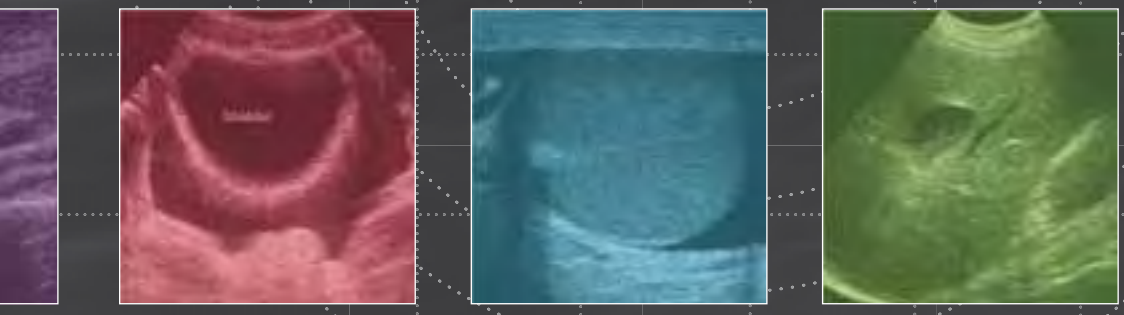

Second edition

World Health Organization

Manual of diagnostic ultrasound

volume 1

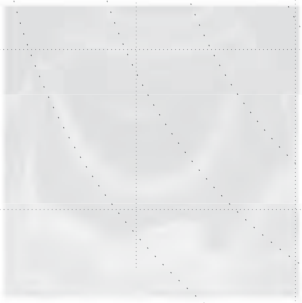

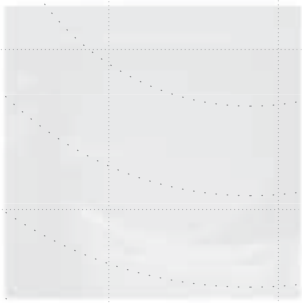

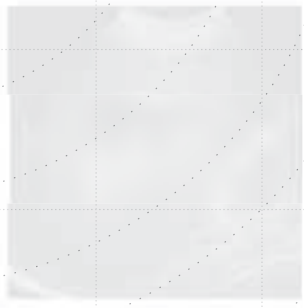

Second edition

World Health Organization

WHO Library Cataloguing-in-Publication Data

WHO manual of diagnostic ultrasound. Vol. 1. -- 2nd ed / edited by Harald Lutz, Elisabetta Buscarini.

1.Diagnostic imaging. 2.Ultrasonography. 3.Pediatrics - instrumentation. I.Lutz, Harald. II.Buscarini, Elisabetta. III. World Health Organization. IV.World Federation for Ultrasound in Medicine and Biology.

ISBN 978 92 4 154745 1 (NLM classification: WN 208)

Production editor: Melanie Lauckner
Design & layout: Sophie Guetaneh Aguettant and Cristina Ortiz

Printed in Malta by Gutenberg Press Ltd.

Contents

Foreword

No medical treatment can or should be considered or given until a proper diagnosis has been established.

For a considerable number of years after Roentgen first described the use of ionizing radiation – at that time called 'X-rays' – for diagnostic imaging in 1895, this remained the only method for visualizing the interior of the body. However, during the second half of the twentieth century new imaging methods, including some based on principles totally different from those of X-rays, were discovered. Ultrasonography was one such method that showed particular potential and greater benefit than X-ray-based imaging.

During the last decade of the twentieth century, use of ultrasonography became increasingly common in medical practice and hospitals around the world, and several scientific publications reported the benefit and even the superiority of ultrasonography over commonly used X-ray techniques, resulting in significant changes in diagnostic imaging procedures.

With increasing use of ultrasonography in medical settings, the need for education and training became clear. Unlike the situation for X-ray-based modalities, no international and few national requirements or recommendations exist for the use of ultrasonography in medical practice. Consequently, fears of 'malpractice' due to insufficient education and training soon arose.

WHO took up this challenge and in 1995 published its first training manual in ultrasonography. The expectations of and the need for such a manual were found to be overwhelming. Thousands of copies have been distributed worldwide, and the manual has been translated into several languages. Soon, however, rapid developments and improvements in equipment and indications for the extension of medical ultrasonography into therapy indicated the need for a totally new ultrasonography manual.

The present manual is the first of two volumes. Volume 2 includes paediatric examinations and gynaecology and musculoskeletal examination and treatment. As editors, both volumes have two of the world's most distinguished experts in ultrasonography: Professor Harald Lutz and Professor Elisabetta Buscarini. Both have worked intensively with clinical ultrasonography for years, in addition to conducting practical training courses all over the world. They are also distinguished representatives of the World Federation for Ultrasound in Medicine and Biology and the Mediterranean and African Society of Ultrasound.

We are convinced that the new publications, which cover modern diagnostic and therapeutic ultrasonography extensively, will benefit and inspire medical professionals in improving 'health for all' in both developed and developing countries.

Harald Østensen,
Cluny, France

Acknowledgements

The editors **Harald T Lutz** and **Elisabetta Buscarini** wish to thank all the members of the Board of the World Federation for Ultrasound in Medicine and Biology (WFUMB) for their support and encouragement during preparation of this manual. **Professor Lotfi Hendaoui** is gratefully thanked for having carefully read over the completed manuscript.
The editors also express their gratitude to and appreciation of those listed below, who supported preparation of the manuscript by contributing as co-authors and by providing illustrations and competent advice.

Marcello Caremani: Department of Infectious Diseases, Public Hospital, Arezzo, Italy
Jin Young Choi: Department of Radiology, Yonsei University College of Medicine, Seoul, Republic of Korea
Josef Deuerling: Department of Internal Medicine, Klinikum Bayreuth, Bayreuth, Germany
Klaus Dirks: Department of Internal Medicine, Klinikum Bayreuth, Bayreuth, Germany
Hassen A Gharbi: Department of Radiology, Ibn Zohr, Coté El Khandra, Tunis, Tunisia
Joon Koo Han: Department of Radiology 28, Seoul National University Hospital Seoul, Republic of Korea
Michael Kawooya: Department of Radiology, Mulago Hospital, Kampala, Uganda
Ah Young Kim: Department of Radiology, Asan Medical Center, Ulsan University, Seoul, Republic of Korea
Se Hyung Kim: Department of Radiology, Seoul National University Hospital, Seoul, Republic of Korea
Jae Young Lee: Department of Radiology, Seoul National University Hospital, Seoul, Republic of Korea
Jeung Min Lee: Department of Radiology, Seoul National University Hospital, Seoul, Republic of Korea
Guido Manfredi: Department of Gastroenterology, Maggiore Hospital, Crema, Italy
Mark Robinson: Department of Radiology, The Royal Gwent Hospital, Newport, Wales
Richard Soldner: Engineer, Herzogenaurach, Germany

Chapter 1

Basic physics

1

Basic physics

Definition

Ultrasound is the term used to describe sound of frequencies above 20 000 Hertz (Hz), beyond the range of human hearing. Frequencies of 1–30 megahertz (MHz) are typical for diagnostic ultrasound.

Diagnostic ultrasound imaging depends on the computerized analysis of reflected ultrasound waves, which non-invasively build up fine images of internal body structures. The resolution attainable is higher with shorter wavelengths, with the wavelength being inversely proportional to the frequency. However, the use of high frequencies is limited by their greater attenuation (loss of signal strength) in tissue and thus shorter depth of penetration. For this reason, different ranges of frequency are used for examination of different parts of the body:

- 3–5 MHz for abdominal areas
- 5–10 MHz for small and superficial parts and
- 10–30 MHz for the skin or the eyes.

Generation of ultrasound

Piezoelectric crystals or materials are able to convert mechanical pressure (which causes alterations in their thickness) into electrical voltage on their surface (the piezoelectric effect). Conversely, voltage applied to the opposite sides of a piezoelectric material causes an alteration in its thickness (the indirect or reciprocal piezoelectric effect). If the applied electric voltage is alternating, it induces oscillations which are transmitted as ultrasound waves into the surrounding medium. The piezoelectric crystal, therefore, serves as a transducer, which converts electrical energy into mechanical energy and vice versa.

Ultrasound transducers are usually made of thin discs of an artificial ceramic material such as lead zirconate titanate. The thickness (usually 0.1–1 mm) determines the ultrasound frequency. The basic design of a plain transducer is shown in Fig. 1.1.

In most diagnostic applications, ultrasound is emitted in extremely short pulses as a narrow beam comparable to that of a flashlight. When not emitting a pulse (as much as 99% of the time), the same piezoelectric crystal can act as a receiver.

Fig. 1.1. Basic design of a single-element transducer

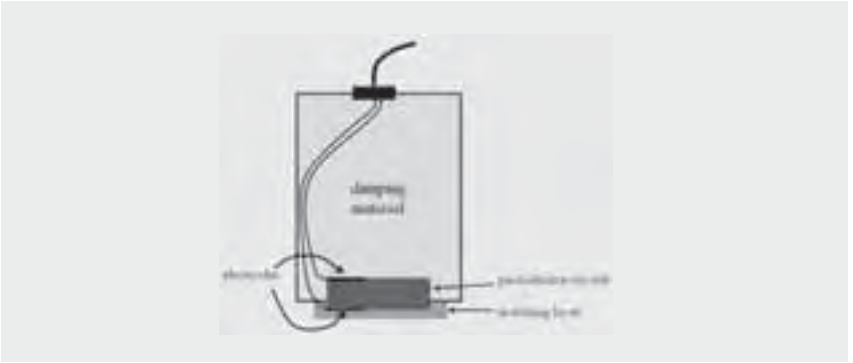

Properties of ultrasound

Sound is a vibration transmitted through a solid, liquid or gas as mechanical pressure waves that carry kinetic energy. A medium must therefore be present for the propagation of these waves. The type of waves depends on the medium. Ultrasound propagates in a fluid or gas as longitudinal waves, in which the particles of the medium vibrate to and fro along the direction of propagation, alternately compressing and rarefying the material. In solids such as bone, ultrasound can be transmitted as both longitudinal and transverse waves; in the latter case, the particles move perpendicularly to the direction of propagation. The **velocity of sound** depends on the density and compressibility of the medium. In pure water, it is 1492 m/s (20 °C), for example. The relationship between frequency (f), velocity (c) and wavelength (λ) is given by the relationship:

$$\lambda = \frac{c}{f} \qquad (1.1)$$

As it does in water, ultrasound propagates in soft tissue as longitudinal waves, with an average velocity of around 1540 m/s (fatty tissue, 1470 m/s; muscle, 1570 m/s). The construction of images with ultrasound is based on the measurement of distances, which relies on this almost constant propagation velocity. The velocity in bone (ca. 3600 m/s) and cartilage is, however, much higher and can create misleading effects in images, referred to as artefacts (see below).

The wavelength of ultrasound influences the **resolution** of the images that can be obtained; the higher the frequency, the shorter the wavelength and the better the resolution. However, attenuation is also greater at higher frequencies.

The kinetic energy of sound waves is transformed into heat (thermal energy) in the medium when sound waves are absorbed. The use of ultrasound for thermotherapy was the first use of ultrasound in medicine.

Energy is lost as the wave overcomes the natural resistance of the particles in the medium to displacement, i.e. the viscosity of the medium. Thus, absorption increases with the viscosity of the medium and contributes to the attenuation of the ultrasound beam. Absorption increases with the frequency of the ultrasound.

Bone absorbs ultrasound much more than soft tissue, so that, in general, ultrasound is suitable for examining only the surfaces of bones. Ultrasound energy cannot reach

the areas behind bones. Therefore, ultrasound images show a black zone behind bones, called an **acoustic shadow**, if the frequencies used are not very low (see Fig. 5.2).

Reflection, scattering, diffraction and refraction (all well-known optical phenomena) are also forms of interaction between ultrasound and the medium. Together with absorption, they cause attenuation of an ultrasound beam on its way through the medium. The total attenuation in a medium is expressed in terms of the distance within the medium at which the intensity of ultrasound is reduced to 50% of its initial level, called the 'half-value thickness'.

In soft tissue, attenuation by absorption is approximately 0.5 decibels (dB) per centimetre of tissue and per megahertz. Attenuation limits the depth at which examination with ultrasound of a certain frequency is possible; this distance is called the 'penetration depth'. In this connection, it should be noted that the reflected ultrasound echoes also have to pass back out through the same tissue to be detected. Energy loss suffered by distant reflected echoes must be compensated for in the processing of the signal by the ultrasound unit using echo gain techniques ((depth gain compensation (DGC) or time gain compensation (TGC)) to construct an image with homogeneous density over the varying depth of penetration (see section on Adjustment of the equipment in Chapter 2 and Fig. 2.4).

Reflection and refraction occur at acoustic boundaries (interfaces), in much the same way as they do in optics. Refraction is the change of direction that a beam undergoes when it passes from one medium to another. Acoustic interfaces exist between media with different acoustic properties. The acoustic properties of a medium are quantified in terms of its **acoustic impedance**, which is a measure of the degree to which the medium impedes the motion that constitutes the sound wave. The acoustic impedance (z) depends on the density (d) of the medium and the sound velocity (c) in the medium, as shown in the expression:

$$z = dc \qquad (1.2)$$

The difference between the acoustic impedance of different biological tissues and organs is very small. Therefore, only a very small fraction of the ultrasound pulse is reflected, and most of the energy is transmitted (Fig. 1.2). This is a precondition for the construction of ultrasound images by analysing echoes from successive reflectors at different depths.

The greater the difference in acoustic impedance between two media, the higher the fraction of the ultrasound energy that is reflected at their interface and the higher the attenuation of the transmitted part. Reflection at a smooth boundary that has a diameter greater than that of the ultrasound beam is called 'specular reflection' (see Fig. 1.3).

Air and gas reflect almost the entire energy of an ultrasound pulse arriving through a tissue. Therefore, an **acoustic shadow** is seen behind gas bubbles. For this reason, ultrasound is not suitable for examining tissues containing air, such as the healthy lungs. For the same reason, a coupling agent is necessary to eliminate air between the transducer and the skin.

The boundaries of tissues, including organ surfaces and vessel walls, are not smooth, but are seen as 'rough' by the ultrasound beam, i.e. there are irregularities at a scale similar to the wavelength of the ultrasound. These interfaces cause non-specular reflections, known as back-scattering, over a large angle. Some of these reflections will reach the transducer and contribute to the construction of the image (Fig. 1.3).

Fig. 1.2. Specular reflection. (a) Transducer emitting an ultrasound pulse. (b) Normally, most of the energy is transmitted at biological interfaces. (c) Gas causes total reflection

Fig. 1.3. Specular reflection. Smooth interface (left), rough interface (right). Back-scattering is characteristic of biological tissues. The back-scattered echo e1 will reach the transducer

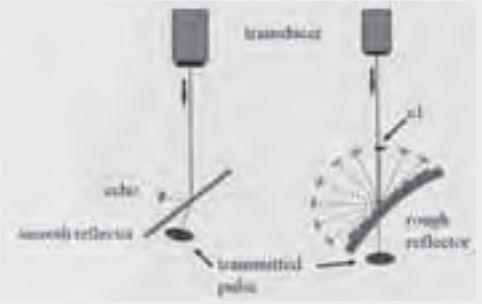

A similar effect is seen with very small reflectors, those whose diameters are similar to that of the wavelength of the ultrasound beam. These reflectors are called 'scatterers'. They reflect (scatter) ultrasound over a wide range of angles, too (Fig. 1.4).

Shape of the ultrasound beam

The three-dimensional **ultrasound field** from a focused transducer can be described as a beam shape. Fig. 1.5 is a two-dimensional depiction of the three-dimensional beam shape. An important distinction is made between the near field (called the Fresnel zone) between the transducer and the focus and the divergent far field (called the Fraunhofer zone) beyond the focus. The border of the beam is not smooth, as the energy decreases away from its axis.

Fig. 1.4. Scatterer. Part of the back-scattered echoes (e7) will reach the transducer

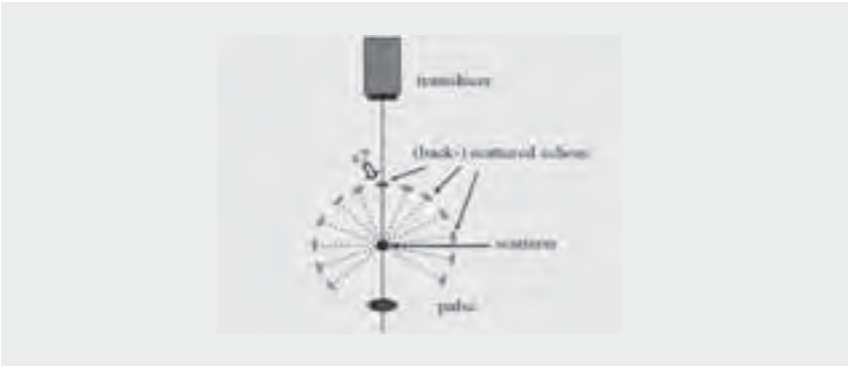

Fig. 1.5. Ultrasound field

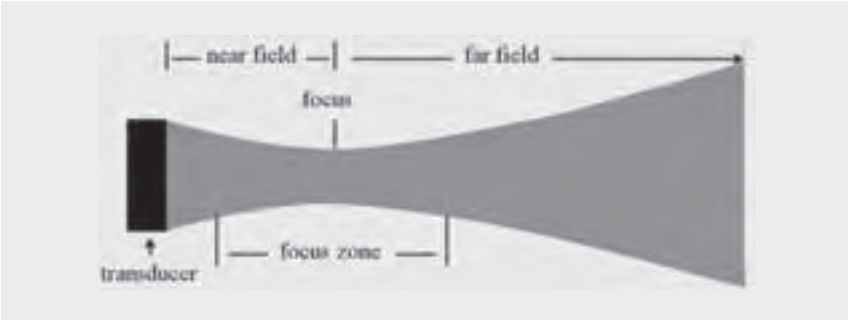

The focus zone is the narrowest section of the beam, defined as the section with a diameter no more than twice the transverse diameter of the beam at the actual focus. If attenuation is ignored, the focus is also the area of highest intensity. The length of the near field, the position of the focus and the divergence of the far field depend on the frequency and the diameter (or aperture) of the active surface of the transducer. In the case of a plane circular transducer of radius R, the near field length (L_0) is given by the expression:

$$L_0 \sim \frac{0.8R^2}{\lambda} \qquad (1.3)$$

The divergence angle (x) of the ultrasound beam in the far field is given by the expression:

$$\frac{\sin x}{2} \sim \frac{0.6\lambda}{R} \qquad (1.4)$$

The diameter of the beam in the near field corresponds roughly to the radius of the transducer. A small aperture and a large wavelength (low frequency) lead to a

Fig. 1.6. Focusing of transducers. Ultrasound field of a plane and a concave transducer (left) and of multiarray transducers, electronically focused for short and far distances and depths; (see also Fig. 1.7)

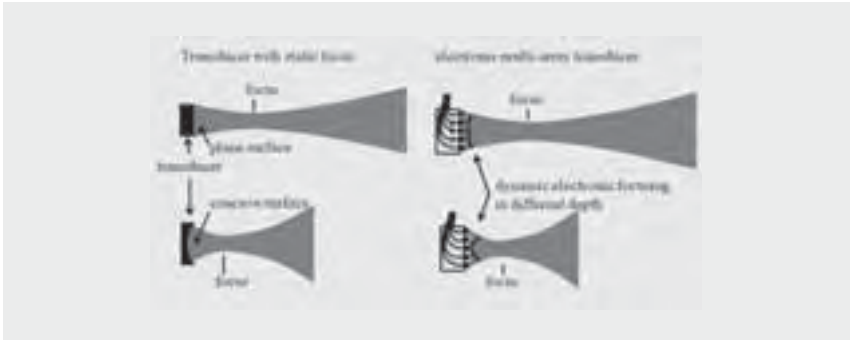

Fig. 1.7. Dynamic electronic focusing during receive to improve lateral resolution over a larger depth range

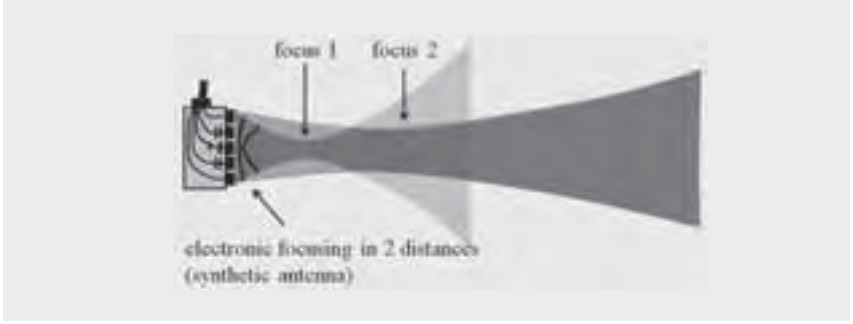

short near field and greater divergence of the far field, while a larger aperture or higher frequency gives a longer near field but less divergence. The focal distance, $L_{0,}$ as well as the diameter of the beam at the focal point can be modified by additional focusing, such as by use of a concave transducer (Fig. 1.6) or an acoustic lens (static focus). The use of electronic means for delaying parts of the signal for the different crystals in an array system enables variable focusing of the composite ultrasound beam, adapted to different depths during receive (dynamic focusing; Fig. 1.6 and Fig. 1.7).

The form and especially the diameter of the beam strongly influence the **lateral resolution** and thus the quality of the ultrasound image. The focus zone is the zone of best resolution and should always be positioned to coincide with the region of interest. This is another reason for using different transducers to examine different regions of the body; for example, transducers with higher frequencies and mechanical focusing should be used for short distances (small-part scanner). Most modern transducers have electronic focusing to allow adaption of the aperture to specific requirements (dynamic focusing, Fig. 1.7).

Spatial resolution

Spatial resolution is defined as the minimum distance between two objects that are still distinguishable. The lateral and the axial resolution must be differentiated in ultrasound images.

Lateral resolution (Fig. 1.8) depends on the diameter of the ultrasound beam. It varies in the axial direction, being best in the focus zone. As many array transducers can be focused in only one plane, because the crystals are arranged in a single line, lateral resolution is particularly poor perpendicular to that plane.

The axial resolution (Fig. 1.9) depends on the pulse length and improves as the length of the pulse shortens. Wide-band transducers (transducers with a high transmission bandwidth, e.g. 3–7 MHz) are suitable for emitting short pulses down to nearly one wavelength.

Fig. 1.8. Lateral resolution. The objects at position 'a' can be depicted separately because their separation is greater than the diameter of the ultrasound beam in the focus zone. The distance between the objects at 'b' is too small to allow them to be distinguished. The objects at 'c' are the same distance apart as those at 'a' but cannot be separated because the diameter of the beam is greater outside the focus zone

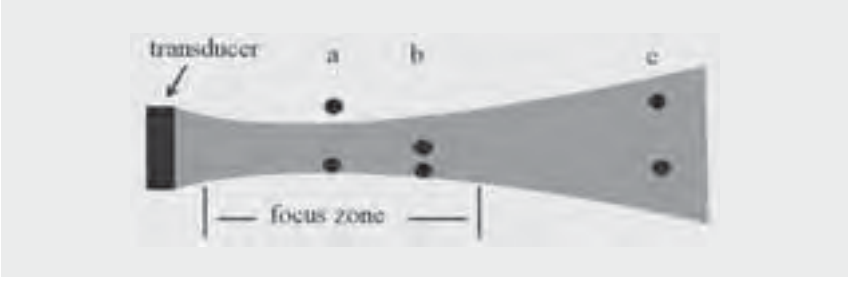

Fig. 1.9. Axial resolution. The objects at positions '1' and '2' can be depicted separately because their distance is greater than the pulse length *a*, whereas the distance between the objects at '3' and '4' is too small for them to be depicted separately

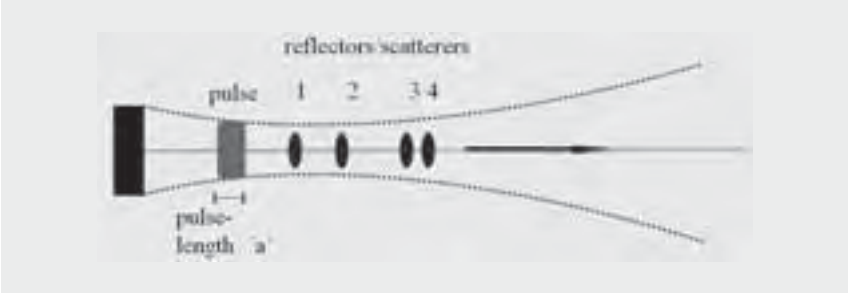

Echo

Echo is the usual term for the reflected or back-scattered parts of the emitted ultrasound pulses that reach the transducer. For each echo, the intensity and time delay are measured

at the transducer and electronically processed to allow calculation of the distance travelled. The displayed results form the basis of diagnostic ultrasound images.

The origin of echoes reflected from broad boundaries, such as the surface of organs or the walls of large vessels, is easily identified. However, scatterers that are very small in relation to the ultrasound beam exist at high density in the soft tissues and organs. Because of their large number, single scatterers cannot be registered separately by the ultrasound beam, and the superimposed signals cannot be related to specific anatomical structures. These image components are called 'speckle'.

Although the idea that each echo generated in the tissue is displayed on the screen is an oversimplification, it is reasonable to describe all echoes from an area, an organ or a tumour as an **echo pattern** or **echo structure** (see Fig. 2.12 and Fig. 2.13).

Doppler effect

The **Doppler effect** was originally postulated by the Austrian scientist Christian Doppler in relation to the colours of double stars. The effect is responsible for changes in the frequency of waves emitted by moving objects as detected by a stationary observer: the perceived frequency is higher if the object is moving towards the observer and lower if it is moving away. The difference in frequency (Δf) is called the **Doppler frequency shift**, **Doppler shift** or **Doppler frequency**. The Doppler frequency increases with the speed of the moving object.

The Doppler shift depends on the emitted frequency (f), the velocity of the object (V) and the angle (α) between the observer and the direction of the movement of the emitter (Fig. 1.10), as described by the formula (where c is the velocity of sound in the medium being transversed):

$$\Delta f = \frac{f}{c} V \cos\alpha \qquad (1.5)$$

When the angle α is 90° (observation perpendicular to the direction of movement), no Doppler shift occurs (cos 90° = 0)

Fig. 1.10. Doppler effect. The observer hears the correct frequency from the car in position *'b'* (α = 90°), whereas the signal from position 'a' (α = 45°) sounds lower and that from position 'c' (α = 135°) higher than the emitted sound

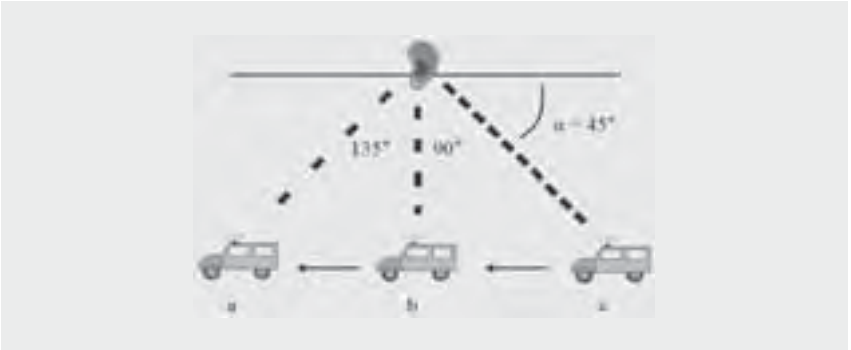

In medicine, Doppler techniques are used mainly to analyse blood flow (Fig. 1.11). The observed Doppler frequency can be used to calculate blood velocity because the velocity of the ultrasound is known and the angle of the vessels to the beam direction can be measured, allowing angle correction. It must be noted that a Doppler shift occurs twice in this situation: first, when the ultrasound beam hits the moving blood cells and, second, when the echoes are reflected back by the moving blood cells. The blood velocity, *V*, is calculated from the Doppler shift by the formula:

$$V = c \cdot \frac{\Delta f}{2f} \cdot \cos\alpha \qquad (1.6)$$

Fig. 1.11. Doppler analysis of blood flow (arrow). The Doppler shift occurs twice. The shift observed depends on the orientation of the blood vessel relative to the transducer

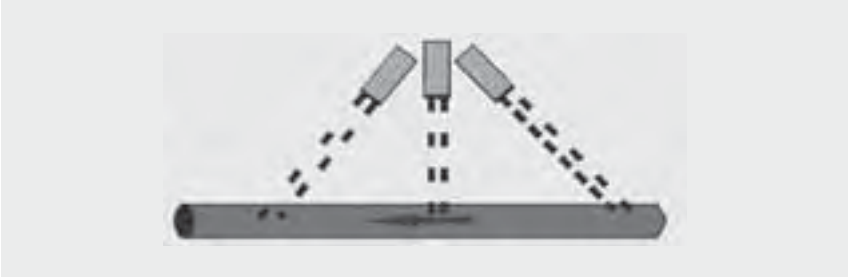

Physiological blood flow causes a Doppler shift of 50–16 000 Hz (frequencies in the audible range), if ultrasound frequencies of 2–10 MHz are used. The equipment can be set up to emit sounds at the Doppler frequency to help the operator monitor the outcome of the examination.

Ultrasound techniques

The echo principle forms the basis of all common ultrasound techniques. The distance between the transducer and the reflector or scatterer in the tissue is measured by the time between the emission of a pulse and reception of its echo. Additionally, the intensity of the echo can be measured. With Doppler techniques, comparison of the Doppler shift of the echo with the emitted frequency gives information about any movement of the reflector. The various ultrasound techniques used are described below.

A-mode

A-mode (A-scan, amplitude modulation) is a one-dimensional examination technique in which a transducer with a single crystal is used (Fig. 1.12). The echoes are displayed on the screen along a time (distance) axis as peaks proportional to the intensity (amplitude) of each signal. The method is rarely used today, as it conveys limited information, e.g. measurement of distances.

B-mode

B-mode (brightness modulation) is a similar technique, but the echoes are displayed as points of different grey-scale brightness corresponding to the intensity (amplitude) of each signal (Fig. 1.12).

Fig. 1.12. A-mode and one-dimensional B-mode. The peak heights in A-mode and the intensity of the spots in B-mode are proportional to the strength of the echo at the relevant distance

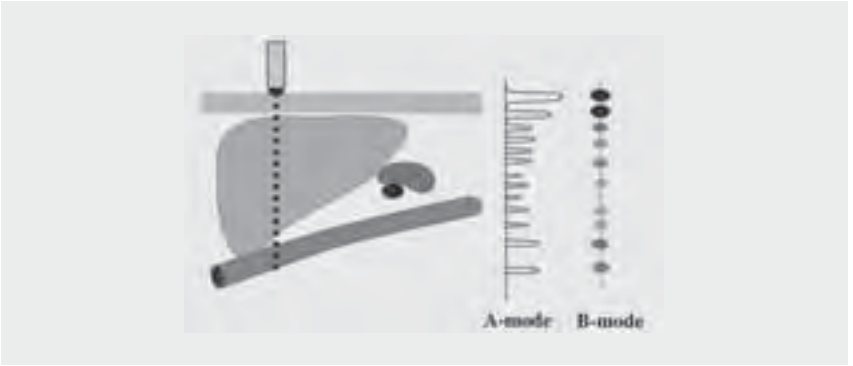

M-mode or TM-mode

M-mode or TM-mode (time motion) is used to analyse moving structures, such as heart valves. The echoes generated by a stationary transducer (one-dimensional B-mode) are recorded continuously over time (Fig. 1.13).

Fig. 1.13. TM-mode. (a) The echoes generated by a stationary transducer when plotted over time form lines from stationary structures or curves from moving parts. (b) Original TM-mode image (lower image) corresponding to the marked region in the B-scan in the upper image (liver and parts of the heart)

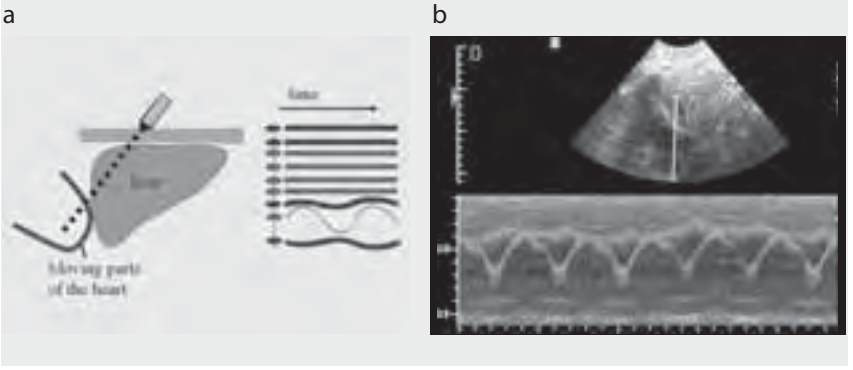

B-scan, two-dimensional

The arrangement of many (e.g. 256) one-dimensional lines in one plane makes it possible to build up a two-dimensional (2D) ultrasound image (2D B-scan). The single lines are generated one after the other by moving (rotating or swinging) transducers or by electronic multielement transducers.

Rotating transducers with two to four crystals mounted on a wheel and swinging transducers ('wobblers') produce a sector image with diverging lines (mechanical sector scanner; Fig. 1.14).

Fig. 1.14. Two-dimensional B-scan. (a) A rotating transducer generates echoes line by line. (b) In this early image (from 1980), the single lines composing the ultrasound image are still visible

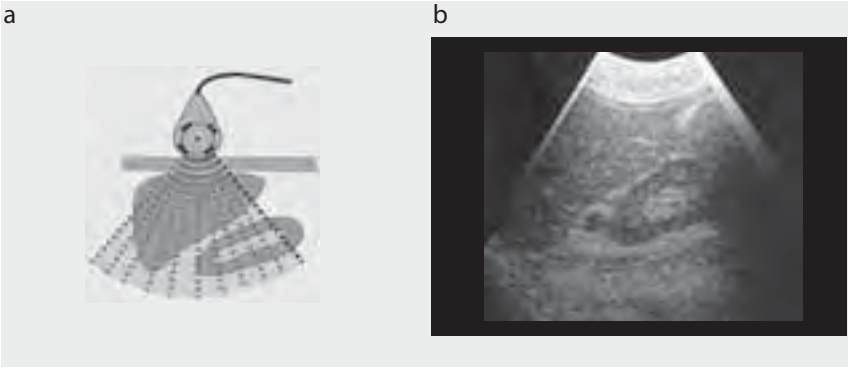

Electronic transducers are made from a large number of separate elements arranged on a plane (**linear array**) or a curved surface (**curved array**). A group of elements is triggered simultaneously to form a single composite ultrasound beam that will generate one line of the image. The whole two-dimensional image is constructed step-by-step, by stimulating one group after the other over the whole array (Fig. 1.15). The lines can run parallel to form a rectangular (linear array) or a divergent image (curved array). The **phased array technique** requires use of another type of electronic multielement transducer, mainly for echocardiography. In this case, exactly delayed electronic excitation of the elements is used to generate successive ultrasound beams in different directions so that a sector image results (electronic sector scanner).

Construction of the image in fractions of a second allows direct observation of movements in real time. A sequence of at least 15 images per second is needed for real-time observation, which limits the number of lines for each image (up to 256) and, consequently, the width of the images, because of the relatively slow velocity of sound. The **panoramic-scan technique** was developed to overcome this limitation. With the use of high-speed image processors, several real-time images are constructed to make one large (panoramic) image of an entire body region without loss of information, but no longer in real time.

A more recent technique is **tissue harmonic imaging**, in which the second harmonic frequencies generated in tissue by ultrasound along the propagation path are used to construct an image of higher quality because of the increased lateral resolution arising from the narrower harmonic beam. The echoes of gas-filled microbubbles

Fig. 1.15. Linear and curved array transducer, showing ultrasound beams generated by groups of elements

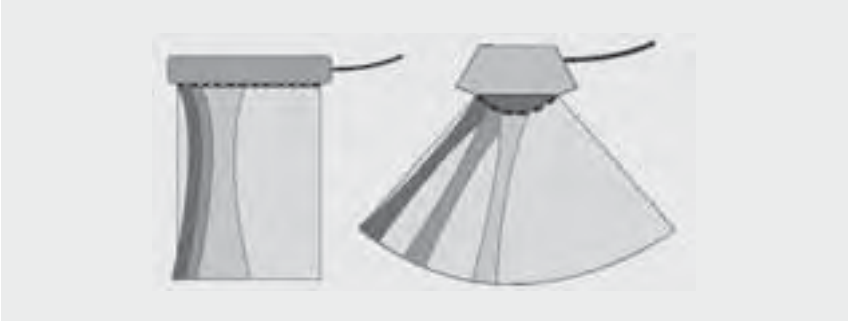

(contrast agents) are rich in harmonics as well. Thus microbubbles can be detected by Doppler schemes even in very small vessels with very low flow at the microvascular level (**contrast harmonic imaging**).

Many technical advances have been made in the electronic focusing of array transducers (**beam forming**) to improve spatial resolution, by elongating the zone of best lateral resolution and suppressing side lobes (points of higher sound energy falling outside the main beam). Furthermore, use of complex pulses from wide-band transducers can improve axial resolution and penetration depth. The elements of the array transducers are stimulated individually by precisely timed electronic signals to form a synthetic antenna for transmitting composite ultrasound pulses and receiving echoes adapted to a specific depth. Parallel processing allows complex image construction without delay.

Three- and four-dimensional techniques

The main prerequisite for construction of **three-dimensional (3D)** ultrasound images is very fast data acquisition. The transducer is moved by hand or mechanically perpendicular to the scanning plane over the region of interest.

The collected data are processed at high speed, so that real-time presentation on the screen is possible. This is called the **four-dimensional (4D) technique** (4D = 3D + real time). The 3D image can be displayed in various ways, such as transparent views of the entire volume of interest or images of surfaces, as used in obstetrics and not only for medical purposes. It is also possible to select two-dimensional images in any plane, especially those that cannot be obtained by a 2D B-scan (Fig. 1.16).

B-flow

B-flow is a special B-scan technique that can be used to show movement without relying upon the Doppler effect. The echoes from moving scatterers (particularly blood cells in blood vessels) are separated from stationary scatterers by electronic comparison of echoes from successive pulses (autocorrelation). These very weak echoes are amplified and depicted as moving dots on the screen. This technique is effective in showing the inner surface of blood vessels, but, unlike Doppler methods (see below), it provides no information about flow velocity (Fig. 1.17).

Fig. 1.16. 3D ultrasound image of the liver. The 3D data collected (left, image 3) can provide 2D sections in different planes (right, images 1, 2 and 4)

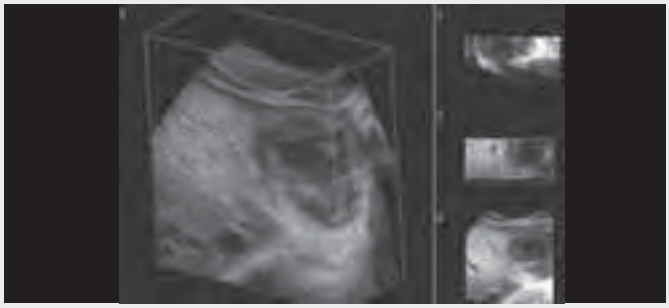

Fig. 1.17. B-flow image of an aorta with arteriosclerosis. This technique gives a clear delineation of the inner surface of the vessel (+…+ measures the outer diameter of the aorta)

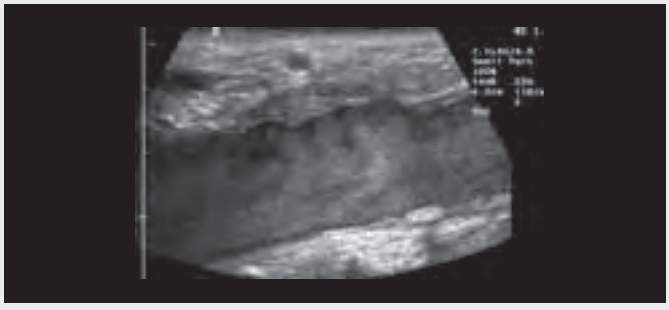

Doppler techniques

In these techniques, the **Doppler effect** (see above) is used to provide further information in various ways, as discussed below. They are especially important for examining blood flow.

Continuous wave Doppler

The transducer consists of two crystals, one permanently emitting ultrasound and the other receiving all the echoes. No information is provided about the distance of the reflector(s), but high flow velocities can be measured (Fig. 1.18).

Pulsed wave Doppler

In this technique, ultrasound is emitted in very short pulses. All echoes arriving at the transducer between the pulses in a certain time interval (termed the gate) are registered and analysed (Fig. 1.19). A general problem with all pulsed Doppler techniques is the analysis of high velocities: the range for the measurement of Doppler frequencies is

limited by the pulse repetition frequency (PRF). When the Doppler frequency is higher than the pulse repetition frequency, high velocities are displayed as low velocities in the opposite direction (spectral Doppler) or in the wrong colour (colour Doppler). This phenomenon is known as 'aliasing' and is directly comparable to the effect seen in movies where car wheels rotating above a certain speed appear to be turning backward. A correct display is possible only for Doppler frequencies within the range ± one half the pulse repetition frequency, known as the **Nyquist limit**. As a consequence, Doppler examination of higher velocities requires lower ultrasound frequencies and a high pulse repetition frequency, whereas low velocities can be analysed with higher frequencies, which allow better resolution.

Fig. 1.18. Schematic representation of the principle of continuous wave Doppler

Fig. 1.19. Schematic representation of pulsed wave Doppler. The gate is adjusted to the distance of the vessel and the echoes within the gate are analysed (the Doppler angle α is 55° in this example)

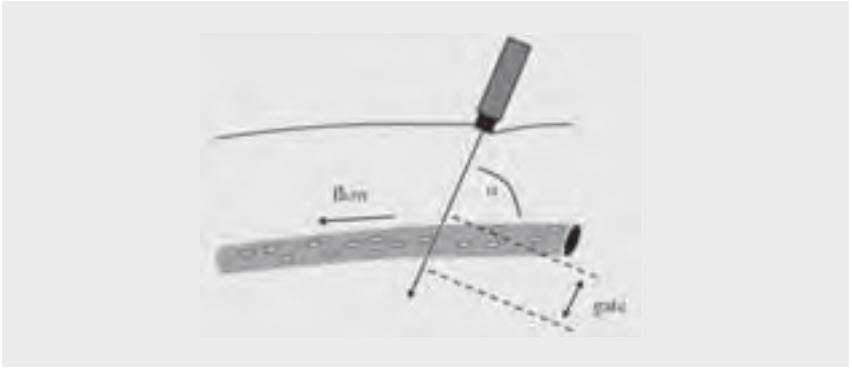

Spectral Doppler

The flow of blood cells in vessels is uneven, being faster in the centre. Doppler analysis, therefore, shows a spectrum of different velocities towards or away from the transducer, observed as a range of frequencies. All this information can be displayed together on the screen. The velocity is displayed on the vertical axis. Flow towards the transducer is positive (above the baseline), while flow away is negative (below the baseline). The number of signals for each velocity determines the brightness of the corresponding point on the screen. The abscissa corresponds to the time base. The **spectral Doppler**

approach combined with the B-scan technique is called the **duplex technique**. The B-scan shows the location of the vessel being examined and the angle between it and the ultrasound beam, referred to as the Doppler angle. This angle should always be less than 60°, and if possible around 30°, to obtain acceptable results. The integrated display demonstrates the detailed characteristics of the flow. The combination of B-scan with colour Doppler and spectral Doppler is called the **triplex technique** (Fig. 1.20).

Fig. 1.20. Spectral Doppler, triplex technique. The upper B-scan shows the vessel, the Doppler angle (axis arrow) and the gate. The lower part of the image shows the spectrum of the velocities over time (two cycles). Note the different velocities: peak velocity in systole (V_{peak}), maximal velocity over time (V_{max}, white plot), most frequent velocity (V_{mode}, black plot) and average velocity (V_{mean})

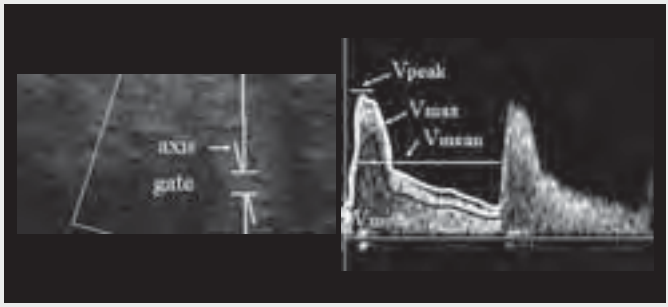

Additionally, the cross-section of the vessel can be determined from the image. The volume blood flow (*Vol*) can then be calculated by multiplying the cross-section (*A*) by the average (over time and across the vessel) flow velocity (TAV_{mean}):

$$Vol = A \cdot TAV_{mean} \tag{1.7}$$

However, measurement of the cross-section and the Doppler angle, which affects the calculated flow velocity, is difficult and often imprecise.

The velocity curves in a Doppler display yield indirect information about the blood flow and about the resistance of the vessel to flow. Highly resistant arteries show very low flow or even no flow in late diastole, whereas less resistant arteries show higher rates of end-diastolic flow. Indices that are independent of the Doppler angle can be calculated to characterize the flow in the vessels, showing the relation between the systolic peak velocity (V_{max}) and the minimal end-diastolic flow (V_{min}). The commonest index used is the **resistance index** (*RI*):

$$RI = \frac{(V_{max} - V_{min})}{V_{max}} \tag{1.8}$$

The **pulsatility index** (*PI*) is another common index used to characterize oscillations in blood flow, including the time-averaged maximal velocity (TAV_{max}):

$$PI = \frac{(V_{max} - V_{min})}{TAV_{max}} \qquad (1.9)$$

Narrowing of a vessel (stenosis) causes acceleration of the flow within the stenotic section (in a closed system), and post-stenotic turbulence is seen as 'spectral broadening' on a spectral Doppler display. The grade of the stenosis (*St*) (as a percentage) can be estimated from the calculated average flow velocity before (V_1) and within (V_2) the stenotic section of the vessel using the formula:

$$St = 100(1 - \frac{V_1}{V_2}) \qquad (1.10)$$

Colour Doppler and **power Doppler** displays are used as duplex systems integrated into the B-scan image.

Colour Doppler (CD) imaging displays the average blood velocity in a vessel, based on the mean Doppler frequency shift of the scatterers (the blood cells). The echoes arising from stationary reflectors and scatterers are displayed as grey-scale pixels to form the B-scan image. The echoes from moving scatterers are analysed by the Doppler technique separately in a selected window and are displayed in the same image as colour-coded pixels (Fig. 1.21). The direction of the flow is shown by different colours, usually red and blue. The disadvantages of colour Doppler are the angle dependence and aliasing artefacts.

Fig. 1.21. Colour Doppler. The echoes from moving targets (blood cells) within the window are colour-coded and depicted here in black (see also Fig. 4.11)

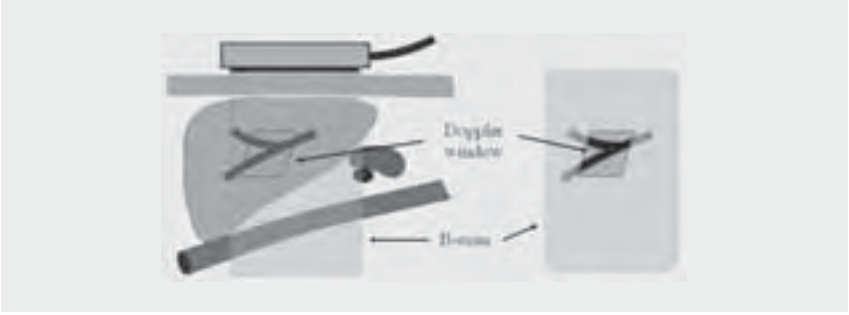

Power Doppler (PD, also known as **colour Doppler energy** or **ultrasound angiography**) is based on the total integrated power of the Doppler signal. In general, it is up to five times more sensitive in detecting blood flow than colour Doppler, being in particular more sensitive to slow blood flow in small vessels; however, it gives no information about the direction of flow.

Contrast agents

The echoes from blood cells in the vessels are much weaker than those arising in tissue. Therefore, contrast agents administered intravenously into the systemic circulation were initially used to obtain stronger signals from blood flow. These agents are microbubbles, which are more or less stabilized or encapsulated gas bubbles, and are somewhat smaller than red blood cells. Use of these contrast agents considerably improves the visibility of small vessels and slow flow with colour and power Doppler. However, the most important advantage of contrast agents is that they allow a more detailed image of the static and dynamic vascularity of organs or tumours. Analysis of the appearance of the contrast agents in the early phase after application (fill-in) and later (wash-out) shows characteristic patterns of various tumours (dynamic enhancement pattern), and enables their differentiation. Another benefit is that the contrast between lesions and the surrounding normal tissue may increase because of their different vascularity. Thus, small lesions, which are not seen in conventional ultrasound images because of their low contrast, become visible.

Special software programmes and equipment are needed when contrast agents are used. Contrast harmonic imaging is a technique similar to tissue harmonic imaging (see above) for improving the signals from microbubbles.

Artefacts

Artefacts are features of an ultrasound image that do not correspond to real structures, i.e. they do not represent a real acoustic interface with regard to shape, intensity or location (Table 1.1, Table 1.2, Fig. 1.22, Fig. 1.23, Fig. 1.24, Fig. 1.25, Fig. 1.26, Fig. 1.27, Fig. 1.28, Fig. 1.29, Fig. 1.30, Fig. 1.31, Fig. 1.32). Features that result from incorrect adjustment of the instrument settings are, by this definition, not true artefacts.

Artefacts may adversely affect image quality, but they are not difficult to recognize in the majority of cases. In certain situations, they hamper correct diagnosis (e.g. cysts) or lead to false diagnosis of a pathological condition where none exists. In other cases, they may actually facilitate diagnosis (e.g. stones).

Table 1.1. Common B-scan artefacts

Term/origin	Appearance	Diagnostic significance
Acoustic shadow (see Fig. 1.22, Fig. 1.23): total reflection on a strong reflector (gas, foreign body) or extensive absorption (bones)	Echo-free zone behind the interface, a **complete shadow**. Less than total weakening of the ultrasound causes an **incomplete shadow**. Echoes from behind the interface are still seen but appear very weak. Shadows behind gas often show a second superimposed artefact ('dirty shadow').	Limits the examination of body regions behind gas or bones but is useful for diagnosing stones, calcifications or foreign bodies.
Tangential artefact (**lateral shadow**): total lateral deflection of the sound beam onto the sides of smooth structures (cysts, vessels)	Small, echo-free, dark zone behind both flanks of such a structure, like a shadow	Regarded as a sign of a cyst or a benign tumour with a capsule
Echo enhancement (**acoustic enhancement**) (Fig. 1.24): structures that attenuate ultrasound less than the surrounding tissue lead to over-amplification of the echoes behind.	Echoes behind such structures appear too bright.	Regarded as a sonographic symptom of a cystic lesion but sometimes also seen behind benign and malignant tumours
Reverberation (Fig. 1.25): echoes are reflected partially by interfaces on their way back (internal reflections) or at the surface of the transducer itself. The echo is then reflected for a second time at the interface of its origin but twice the time is needed before it is recorded by the transducer. This may occur several times, the echoes becoming weaker after each reflection.	The structures that cause internal reflections are displayed two or more times at double or multiple distances from the transducer, always in the same order as the original structures, but weaker.	These echoes become especially conspicuous in echo-free areas close to the transducer (bladder, gallbladder, cysts). As they occur mainly in the abdominal wall, they can be identified, because they do not move with the abdominal structures during breathing.
Mirror artefact (Fig. 1.26): a strong smooth reflector reflects the beam to the side, where it causes further reflections or back-scatter. These echoes follow the same path back to the transducer and are wrongly displayed in straight extension of the original beam direction (a special type of internal reflection or reverberation).	These artefacts are seen only in echo-free areas. Structures of the liver seen above the diaphragm (the surface of the air-filled lung acting as the mirror) are a typical example.	An image or lesion of the liver or the kidney may, for example, be seen above the diaphragm and be misinterpreted as a lesion of the lung.
Comet tail artefact (or ring-down artefact) (Fig. 1.27): if two interfaces lie close together, they can cause many internal reflections at very short intervals and send a large number of echoes back to the transducer.	In the ultrasound image, a small bright 'tail' is seen behind these interfaces, sometimes for only a very short time.	This artefact is typical of a group of small air bubbles ('dirty shadow') and of the wall of the gallbladder in cholesterolosis. It also occurs behind puncture needles if their angle to the ultrasound beam is around 90°.
Partial volume effect (Fig. 1.28): if an ultrasound beam hits a cyst smaller than the beam cross-section, the echoes from the wall appear to come from inside the cyst (artificial sedimentation).	Small cystic lesions show echoes inside.	Small cysts may be misinterpreted as solid lesions.
Overpenetration: the bladder and other large fluid-filled structures do not attenuate the ultrasound pulses. They can generate reflections beyond the selected depth that return late or only after the next pulse. These echoes are displayed in the image as if generated by the second pulse.	Echoes appear within a normally echo-free area, such as the bladder.	Such wrong echoes, called 'ghost echoes', must be distinguished from real echoes by changing the scan direction.
Velocity artefact (Fig. 1.29): if an ultrasound beam passes through a structure with a considerably higher sound velocity (e.g. cartilage), echoes from structures beyond are displayed closer to the transducer.	Structures behind tissues with higher sound velocity are distorted in the ultrasound image.	The border of the lung appears to undulate behind the ribs due to such distortion.

Table 1.2. Common disturbances and artefacts in Doppler techniques

Term/origin	Appearance	Diagnostic significance
Tissue vibration (bruit): restriction of blood flow by a stenosis or by an arteriovenous fistula causes vibrations of the surrounding tissue, which are transmitted by the pulsating blood pressure.	Disseminated colour pixels in the tissue around a stenosis.	Indication of a severe stenosis
Flash: corresponds to the vibration artefact. The pulsation of the heart is transmitted to the adjacent structures, e.g. the cranial parts of the liver.	A short but intense colour coding of all pixels within the Doppler window during systole	Disturbs examination of the vessels in the region close to the heart
Blooming (Fig. 1.30): amplification of the signals causes 'broadening' of the vessels.	The area of colour-coded pixels is broader than the diameter of the vessel.	Blurred border of the vessel and inaccurate demarcation of the inner surface of the wall
Twinkling (Fig. 1.31): caused by certain stones, calcifications and foreign bodies with a rough surface.	Colour-coded stones or calcifications with a mosaic-like pattern	Sometimes helpful for detecting small kidney stones
Change of angle of incidence: the ultrasound beam impinges on a vessel running across the scanning plane at different angles.	Despite a constant flow velocity in one direction, the signals from the vessel are displayed in different colours depending on the angle between the vessel and the ultrasound beam. If it is 'hidden' at an angle of 90°, no coloured pixel is seen.	The inhomogeneous depiction of the vessel is not an artefact but a correct depiction, depending on the actual angle of each part of the image.

Fig. 1.22. (a) Several gallstones (arrow) cause a complete acoustic shadow (S), whereas a small 4-mm gallstone (b) causes only an incomplete shadow (S). The small shadow in (b) at the edge of the gallbladder (arrow) corresponds to a tangential artefact (see Fig. 1.24)

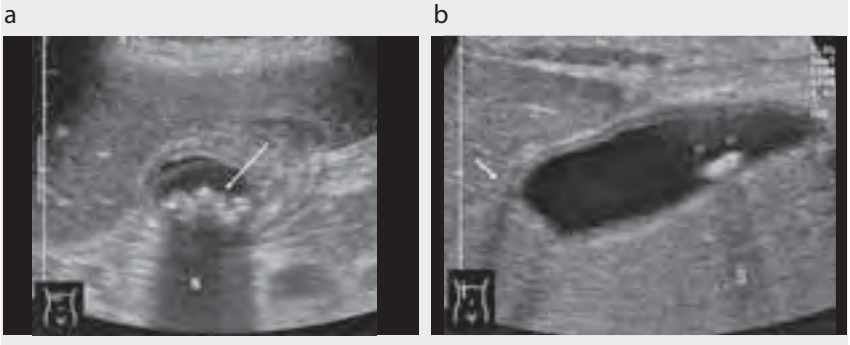

Fig. 1.23. Air bubbles cause 'dirty' shadows. (a) Gas in an abscess (arrow) causes a strong echo, a shadow and reverberation artefacts, which superimpose the shadow (A, abscess; I, terminal ileum). (b) Air in the jejunum causes a 'curtain' of shadows and reverberation artefacts, which cover the whole region behind the intestine

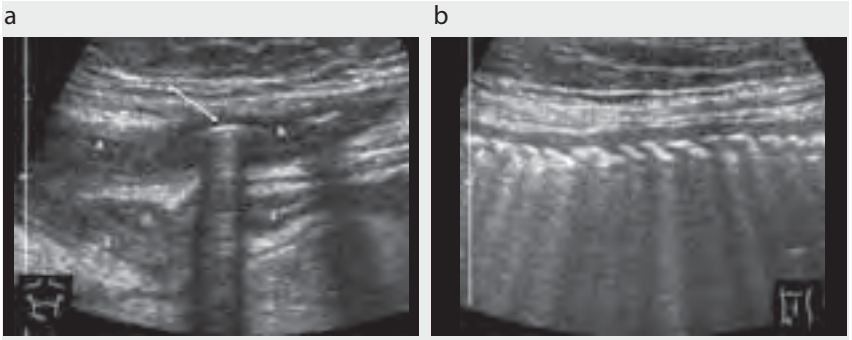

Fig. 1.24. A small cyst in the liver causes two artefacts. A brighter zone behind the cyst is caused by echo enhancement, whereas slight shadows on both sides of this zone are tangential artefacts due to the smooth border of the cyst

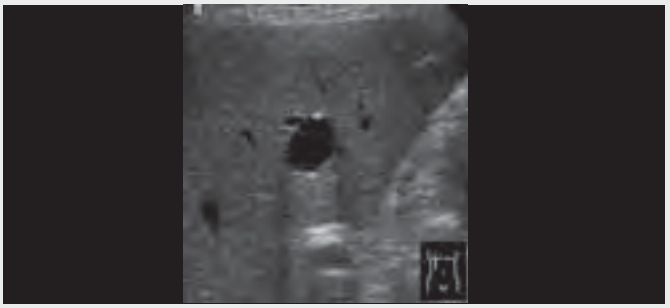

Fig. 1.25. Reverberation artefacts. (a) A 'cloud' of small artefacts (arrow) is seen in the gallbladder. (b) The structures between the wall and the border of the air (1) are repeated several times behind this border (2)

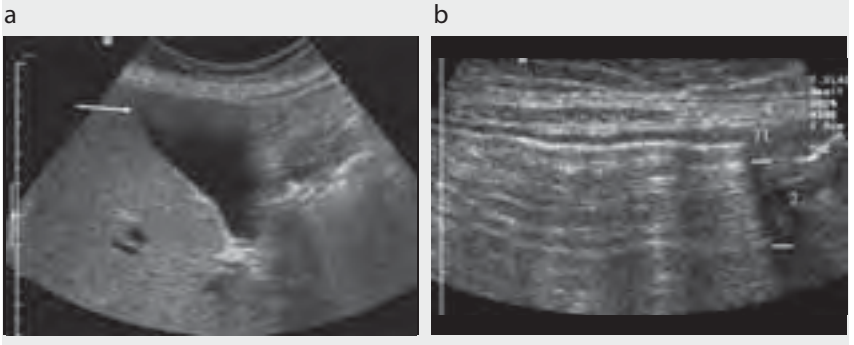

Fig. 1.26. Mirror artefact. The air-containing lung behind the diaphragm reflects all the ultrasound pulses. (a) Structures of the liver are seen behind this border (arrow) as artefacts. (b) The cross-section of a vessel indicates the direction of the original pulse reflected by this mirror (arrow). The echoes from the path between the mirror and the vessel and back are depicted falsely along a straight line (dotted line) behind the diaphragm

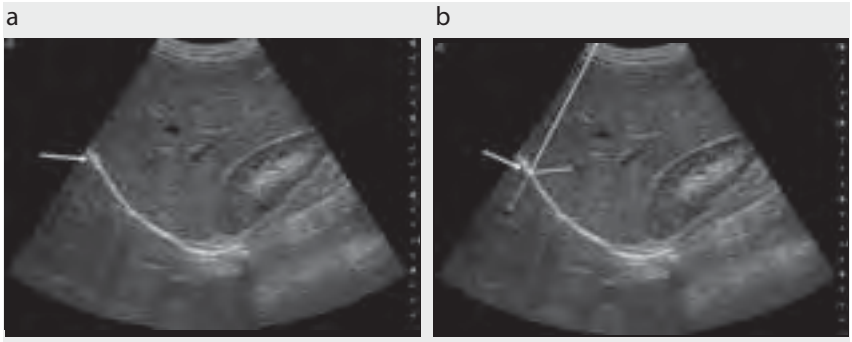

Fig. 1.27. Comet tail (or ring-down) artefact. The small artefacts (broad open arrow) are typical of cholesterolosis of the gallbladder (see Fig. 8.17). A shadow (S) is caused by a gallstone (thin arrow)

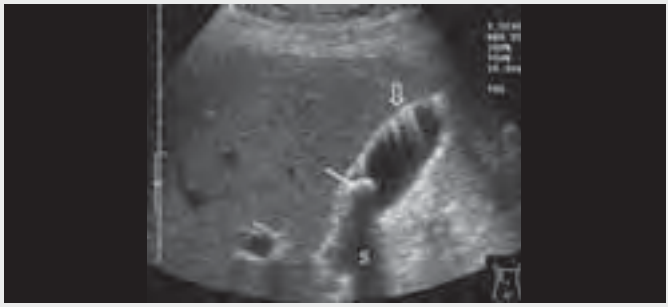

Fig. 1.28. Partial volume effect. (a) The cyst (c) is smaller than the diameter of the ultrasound beam. The beam generates weak echoes from the wall, which are depicted within the cyst. (b) These artefacts are seen in two small cysts (arrows) of the right kidney (RN).The other larger cysts (z) are echo free. The lesion (T) at the lower pole is a true echo-poor small carcinoma. This image illustrates very well the diagnosis problems that are sometimes caused by artefacts

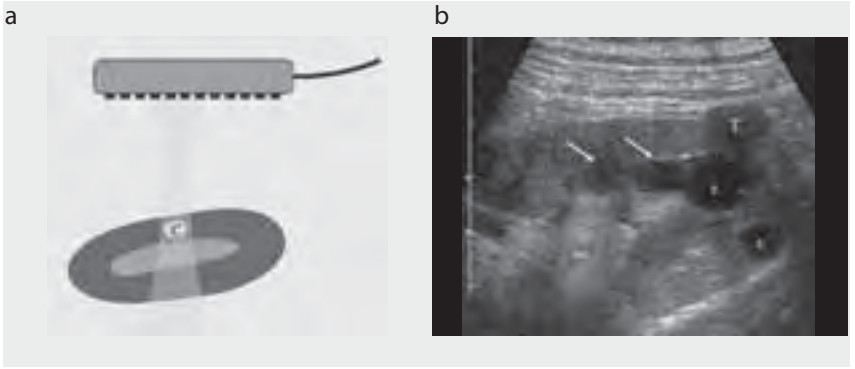

Fig. 1.29. Velocity artefact. The higher sound velocity in the cartilage (car) of the ribs causes distortion of the echoes at the border of the lung (arrows), so that the contour appears to be undulating (see also Fig. 5.2; int, intercostal muscles)

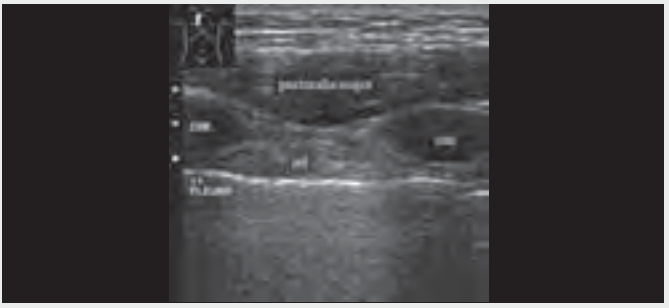

Fig. 1.30. Blooming: (a) the colour-coded signals (white and black) show a wider diameter of the splenic vessel than that correctly measured by B-scan (b)

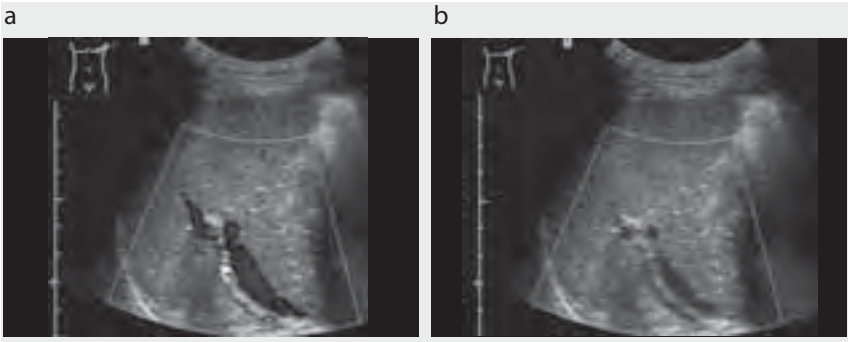

Fig. 1.31. 'Twinkling'. (a) B-scan shows a strong echo of a renal stone and an incomplete shadow (arrow). (b) With colour Doppler, the stone (arrow) is colour-coded with a mosaic-like multicoloured pattern (here black and white spots)

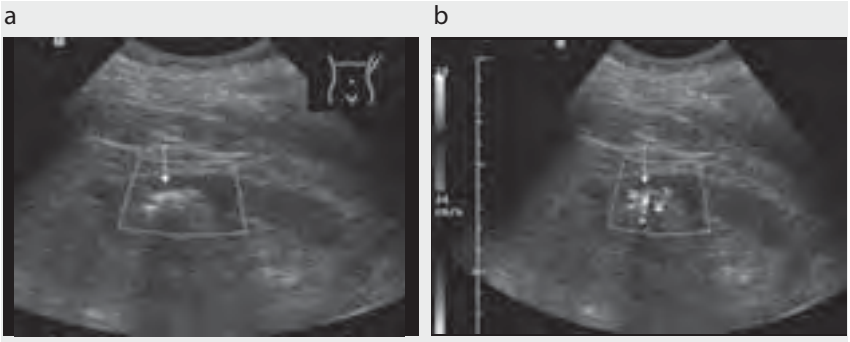

Fig. 1.32. Change of angle of incidence. The curved vessel (iliac artery) is oriented at different angles with respect to the ultrasound beam (thick arrows). The constant flow in one direction (thin arrows) is Doppler-coded red in some sections (seen here as white) and blue in others (black arrows)

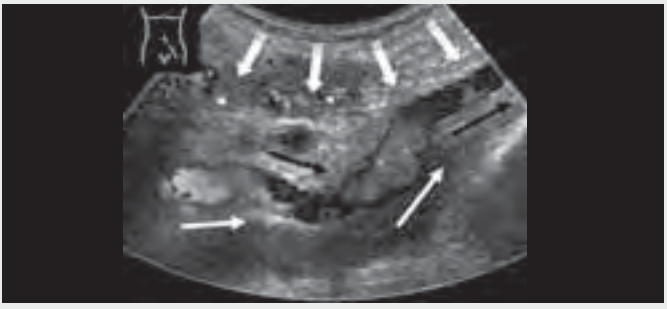

Adverse effects

The kinetic energy of ultrasound waves can cause adverse effects in tissue. Non-thermal effects include cavitation, direct mechanical damage to cells by acceleration, movement of particles in fluid (acoustic streaming) and aggregation of particles or cells. Cavitation is the formation of voids, or bubbles, in a biological structure during the rarefaction phase of a sound wave. These bubbles may grow with changes in pressure or collapse during the positive pressure phase. The risk of cavitation is low at the ultrasound intensities used in medical diagnosis. Furthermore, diagnostic ultrasound is applied in very short pulses. Nevertheless, as very small gas bubbles may serve as cavitation centres, the recent introduction of microbubble contrast agents has stimulated and renewed discussion about this phenomenon.

Direct mechanical damage to cell membranes, the occurrence of high temperatures or formation of free radicals may also occur. However, the Committee on Ultrasound Safety of the World Federation for Ultrasound in Medicine and Biology has stated that no adverse biological effects have been seen in the large number of studies that have been carried out to date. A **mechanical index** has been introduced to indicate the relative risk for adverse biological effects resulting from mechanical effects during an ultrasound examination. This index is calculated in real time by the ultrasound equipment and displayed so that the operator is aware of any risk.

The generation of heat in tissues is an important limiting factor in the diagnostic use of ultrasound. The temperature rise in tissue depends on the absorbed ultrasound energy and the volume within which the absorption occurs. The energy absorbed is therefore higher with stationary ultrasound emitters (transducer fixed, e.g. Doppler, TM-mode) than with scanning methods (transducer moved during examination, e.g. B-scan). Furthermore, the thermal effect is reduced by convection, especially in the bloodstream. The embryo is particularly sensitive to long exposure to ultrasound, especially during prolonged Doppler examinations.

The **thermal index** (TI) is displayed in real time as an indication of the maximum temperature rise that may occur in a tissue during a prolonged ultrasound examination. Depending on the method used, the appropriate index to use is specified as:

- TIS for superficial tissue (e.g. the thyroid or the eyes); this indicator can also be used for endoscopic ultrasound;
- TIC for superficial bones (e.g. examination of the brain through the skull);
- TIB for bone tissue in the ultrasound beam (e.g. examination of a fetus).

Ultrasound that produces a rise in temperature of less than 1 °C above the normal physiological level of 37 °C is deemed without risk by the Committee on Ultrasound Safety of the World Federation for Ultrasound in Medicine and Biology.

For more details see chapter on Safety in Volume 2 of this manual.

Chapter 2

Examination technique: general rules and recommendations

2

Examination technique: general rules and recommendations

Range of application

All body regions that are not situated behind expanses of bone or air-containing tissue, such as the lungs, are accessible to transcutaneous ultrasound. Bone surfaces (fractures, osteolytic lesions) and the surfaces of the lungs or air-void parts can also be demonstrated. Examinations through thin, flat bones are possible at lower frequencies. It is also possible to bypass obstacles with endoprobes (endoscopic sonography). Thus, transcutaneous ultrasound is used mainly for evaluating:

- neck: thyroid gland, lymph nodes, abscesses, vessels (angiology);
- chest: wall, pleura, peripherally situated disorders of the lung, mediastinal tumours and the heart (echocardiography);
- abdomen, retroperitoneum and small pelvis: parenchymatous organs, fluid-containing structures, gastrointestinal tract, great vessels and lymph nodes, tumours and abnormal fluid collections; and
- extremities (joints, muscles and connective tissue, vessels).

General indications (B-scan and duplex techniques)

The general indications are:

- presence, position, size and shape of organs;
- stasis, concretions and dysfunction of hollow organs and structures;
- tumour diagnosis and differentiation of focal lesions;
- inflammatory diseases;
- metabolic diseases causing macroscopic alterations of organs;
- abnormal fluid collection in body cavities or organs, including ultrasound-guided diagnostic and therapeutic interventions;
- evaluating transplants;
- diagnosis of congenital defects and malformations.

Additionally, ultrasound is particularly suitable for checks in the management of chronic diseases and for screening, because it is risk-free, comfortable for patients and cheaper than other imaging modalities.

Preparation

In general, no preparation is needed for an ultrasound examination; however, for certain examinations of the abdomen, a period of fasting is useful or necessary. To avoid problems due to meteorism, dietary restrictions (no gas-producing foods), physical exercise (walking before the examination) and even premedication (antifoaming agents) are recommended. Special preparation is only necessary for certain examinations and these are discussed in the relevant chapters of this manual.

Positioning

The ultrasound examination is usually carried out with the patient in the supine position. As further described in the specific chapters, it is often useful to turn the patient in an oblique position or to scan from the back in a prone position, e.g. when scanning the kidneys. Ultrasound also allows examination of the patient in a sitting or standing position, which may help in certain situations to diagnose stones or fluid collection (e.g. pleural effusion).

Coupling agents

A coupling agent is necessary to ensure good contact between the transducer and the skin and to avoid artefacts caused by the presence of air between them. The best coupling agents are water-soluble gels, which are commercially available. Water is suitable for very short examinations. Disinfectant fluids can also be used for short coupling of the transducer during guided punctures. Oil has the disadvantage of dissolving rubber or plastic parts of the transducer.

The composition of a common coupling gel is as follows:

- 10.0 g carbomer
- 0.25 g ethylenediaminetetraacetic acid (EDTA)
- 75.0 g propylene glycol
- 12.5 g trolamine and up to 500 ml demineralized water.

Dissolve the EDTA in 400 ml of water. When the EDTA has dissolved, add the propylene glycol. Then add the carbomer to the solution and stir, if possible with a high-speed stirrer, until the mixture forms a gel without bubbles. Add up to 500 ml of demineralized water to the gel.

Precaution: Be careful not to transmit infectious material from one patient to the next via the transducer or the coupling gel. The transducer and any other parts that come into direct contact with the patient must be cleaned after each examination. The minimum requirements are to wipe the transducer after each examination and to clean it with a suitable disinfectant every day and after the examination of any patient who may be infectious.

A suitable method for infectious patients, e.g. those infected with human immunodeficiency virus (HIV) and with open wounds or other skin lesions, is to slip a disposable glove over the transducer and to smear some jelly onto the active surface of the transducer.

Equipment

Generally, modern ultrasound equipment consists of 'all-round scanners'. Two transducers, usually a curved array for the range 3–5 MHz and a linear array for the range greater than 5 MHz to 10 MHz, as a 'small-part scanner' can be used as 'general-purpose scanners' for examination of all body regions with the B-scan technique (Fig. 2.1).

Fig. 2.1. Choice of transducer and frequency. Generally, superficial structures are examined at 7.5 MHz; however, this frequency is not in general suitable for abdominal work and is limited to examination of superficial structures. (a) At 7.5 MHz, only the ventral surface of the liver can be displayed. (b) The liver and the adjacent structures can be examined completely at 3.5 MHz

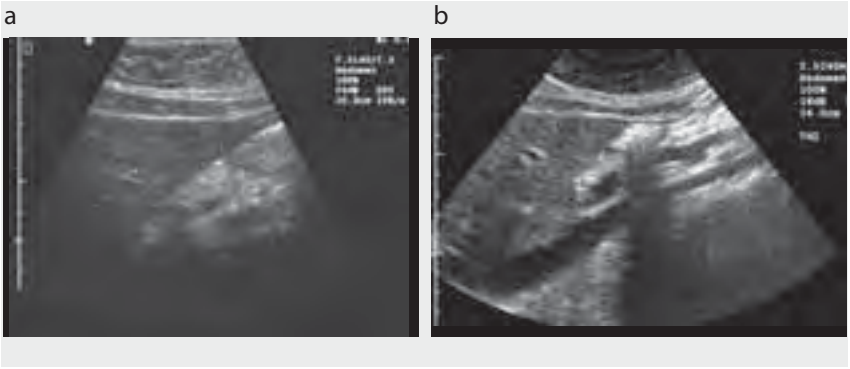

Examinations of the skin and eyes and the use of endoprobes require special transducers and more expensive equipment to enable the use of higher frequencies. For echocardiography, different transducers, i.e. electronic sector scanners (phased array technique) are required.

An integrated Doppler technique is necessary for echocardiography and angiology, and is also useful for most other applications. Special software is needed for the use of contrast agents.

Adjustment of the equipment

Correct adjustment of an ultrasound scanner is not difficult, as the instruments offer a wide range of possible settings. Most instruments have a standard setting for each transducer and each body region. This standard can be adapted to the needs of each operator.

When starting with these standards, only slight adaptation to the individual patient is necessary.

- The choice of frequency (and transducer) depends on the penetration depth needed. For examination of the abdomen, it may be useful to start with a lower frequency (curved array, 3.5 MHz) and to use a higher frequency if the region of interest is close to the transducer, e.g. the bowel (Fig. 2.1, Fig. 11.26).
- Adaptation to the penetration depth needed: the whole screen should be used for the region of interest (Fig. 2.2).
- The mechanical index should be as low as possible (< 0.7 in adults).

- The time gain compensation (TGC) setting must compensate for attenuation, e.g. depending on the abdominal wall, to obtain a homogeneous image. It is useful to find a good TGC setting when scanning a homogeneous section of the tissue, e.g. the right liver lobe in the abdomen, before moving the transducer to the region of interest (Fig. 2.3, Fig. 2.4, Fig. 2.5).
- The focus, or zone of best resolution, should always be adjusted to the point of interest.

Fig. 2.2. Use of the screen. (a) Incorrect adaptation of the screen: the region of interest fills only a small part of the screen. (b) Correct adaptation of the screen

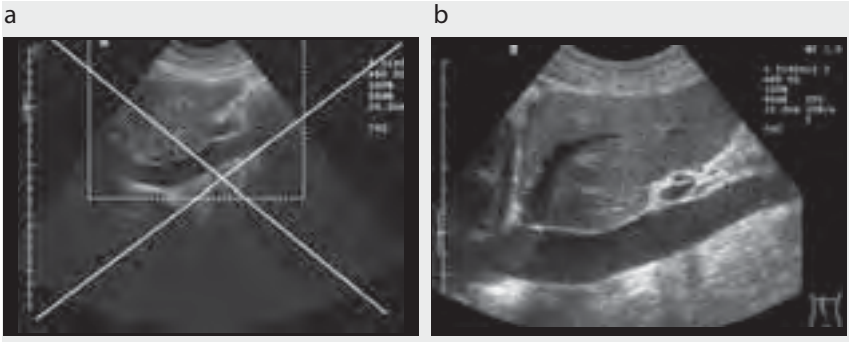

Fig. 2.3. (a) Operating console of an ultrasound machine. Control knobs must be adjusted for each patient. R (range), penetration depth; F (focus), region of best resolution; TGC, time (depth) gain compensation (see Fig. 2.4); Z (zoom), enlarges regions of interest; G, Doppler gain; V, Doppler velocity (pulse repetition frequency). (b) B-image (not the same equipment as in (a)), shows correct (homogeneous pattern of normal liver tissue), TGC curve (arrow) and focus zone, which should be slightly deeper and level with the focal nodular hyperplasia lesion. The thermal index (TIS) and the mechanical index (MI) are indicated. Note that these indices are considerably higher in the colour Doppler image (B-scan 0.6 and 0.5, respectively, versus Doppler 2.3 and 0.8). (c) The Doppler velocity and the Doppler window are correctly adjusted to the size of the lesion and the expected velocity range in the vessels

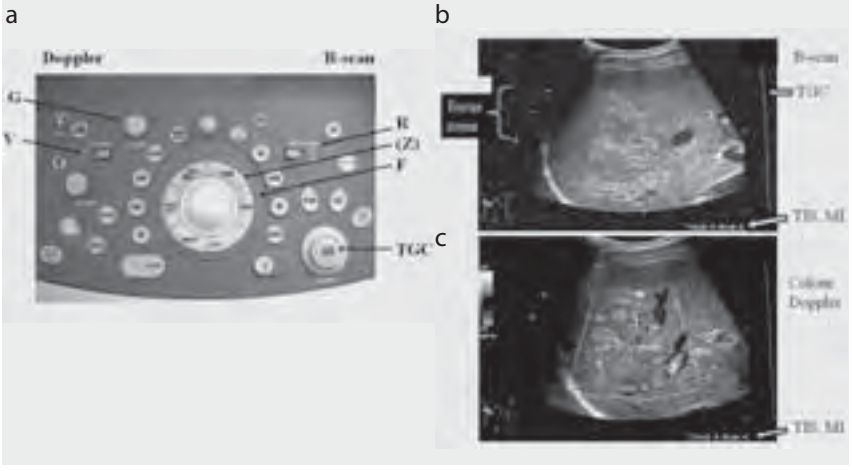

Fig. 2.4. Time gain compensation (TGC). The TGC is always adjusted according to each patient's circumstances. (a) An overall gain in compensation (B-mode: gain) and gradual regulation are possible. (b) The loss of intensity, or decline in the echoes at a greater distance, is compensated for by the TGC, as shown in the diagram and (c) the ultrasound image with the displayed TGC line (arrow) for 3.5 MHz. This compensation is not sufficient for 7 MHz (see Fig. 2.1)

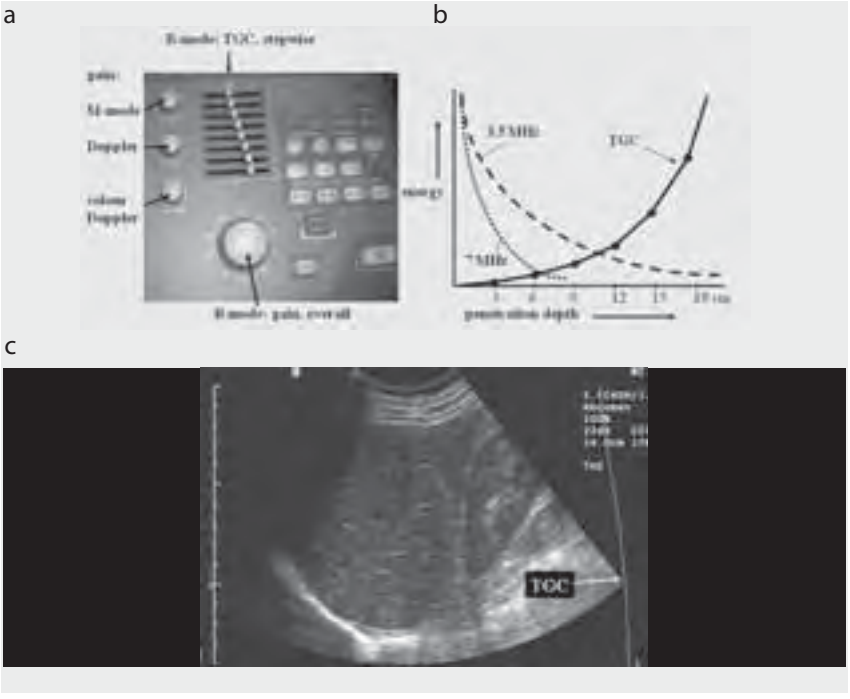

Fig. 2.5. TGC adjustment. Two examples of incorrect adjustment: (a) The lower part of the ultrasound image is too dark because the TGC adjustment is too weak, whereas in (b) the adjustment for the middle part is too high, causing an inhomogeneous image of the liver with a zone that is too bright in the middle part

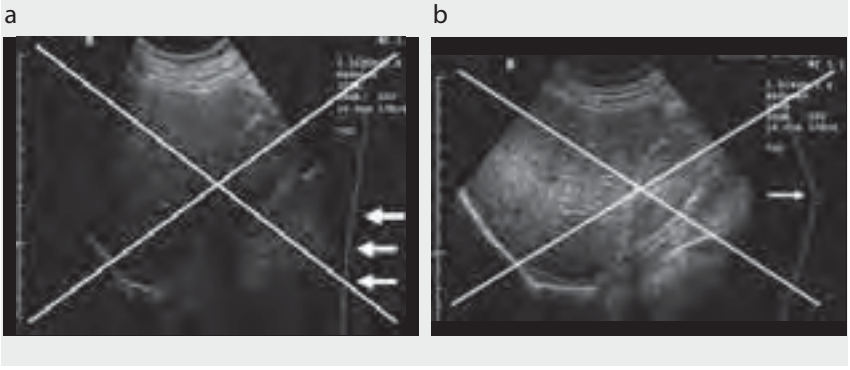

- The zoom should be used mainly for the final investigation of detail and for preparing the documentation.
- If there are problems, use of the image optimizer knob and returning to the standard settings may help.

Guidelines for the examination

- Know the patient's problem and medical history. An advantage of ultrasound is that the patient's doctor can carry out the examination, and this provides a good opportunity to talk to the patient about his or her problem.
- Make sure that the settings of the equipment and the orientation of the transducer are correct in relation to the image. This will avoid misinterpretations due to inhomogeneous images with areas that are too dark or too bright and with artefacts.
- Conduct a systematic and complete examination of the whole body region, even if there is an obvious palpable mass or a localized point of pain.
- Start with an anatomically constant area and move to the more variable area (e.g. from the liver to the region of the pancreas or the intestine).
- Move the transducer in a slow constant pattern, while maintaining the defined scanning plane. Hold the transducer motionless when the patient moves, e.g. during respiration. It is possible to move a transducer in many directions by tilting it in the scanning plane and moving it perpendicularly, but with a combination of all these movements the less experienced operator will lose the orientation of the image (Fig. 2.6, Fig. 2.7).
- Use anatomically constant, easily visualized structures for orientation (e.g. liver, aorta or fluid-filled bladder) and normal structures for comparison (e.g. right and left kidney or kidney and liver).
- Examine each organ, structure or tumour in at least two planes. **In this way, one can avoid missing small lesions or misinterpreting artefacts as real alterations.**
- Use palpation to displace fluid or gas from the bowel, to test the consistency of tumours and organs and to localize points of pain.
- Continue the entire examination even if pathological conditions are found. Only a complete examination will avoid that only a less important alteration (e.g. gallstones) is found but the main diagnosis (e.g. pancreatic cancer) is missed.
- In clinically difficult situations or when the findings are doubtful, repeat the examination a short time later. Such repeat examinations can be carried out even at the bedside. This is particularly useful with trauma patients and patients in intensive care.

Fig. 2.6. Movements of a transducer. The transducer can be moved in its scanning plane in a longitudinal direction (a), turned about itself (b), or tilted in the scanning plane (c) or in a perpendicular direction (d)

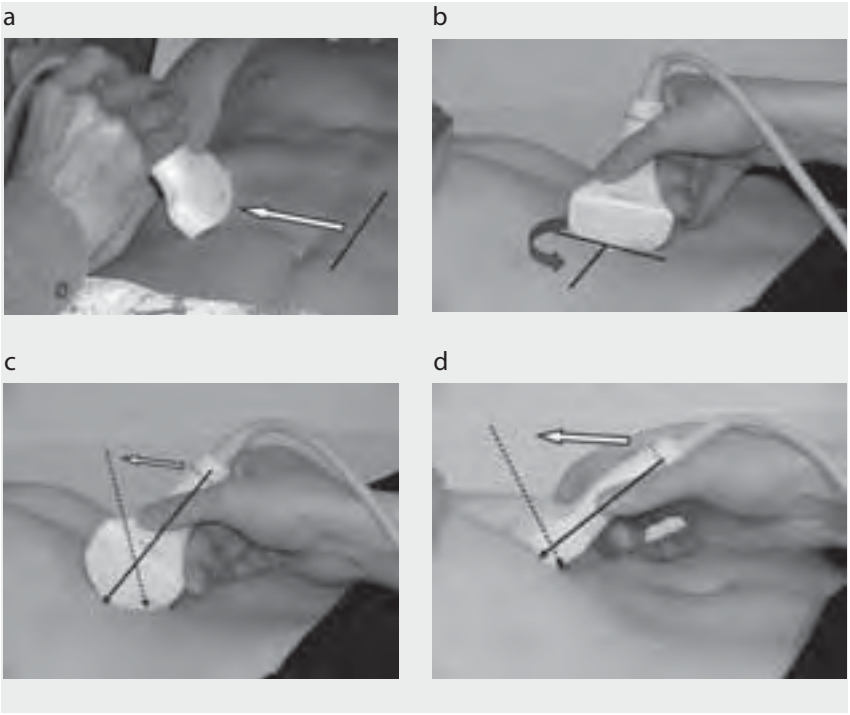

Fig. 2.7. Imaging of the right liver lobe and the right kidney obtained by tilting the transducer in different directions (I and II)

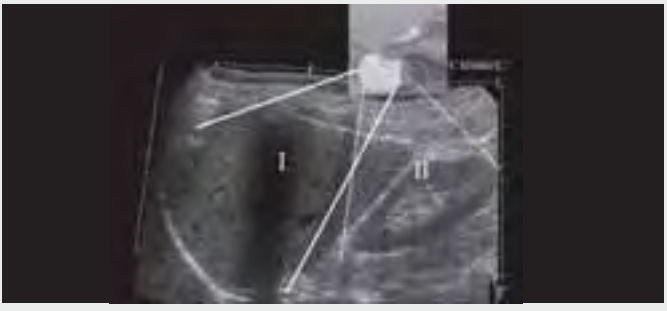

Documentation

As a rule, both a written report and pictorial documentation should be prepared for each ultrasound examination.

The written report should include:

- a description of the problem that led to the examination;
- a list of the organs (region) examined (generally, it is not necessary to describe normal findings but to note measurements only);
- a description of pathological findings (the descriptions should be concise and clear, but without over-interpretation.); and
- the diagnosis or decision.

Pictorial documentation of pathological findings in two planes is necessary, but documentation of a normal finding (one representative scan of the organ or body region examined) is also useful, e.g. for later check-up examinations.

Interpretation of the ultrasound image

Organs, structures within organs, vessels, tumours and fluid collections are evaluated by B-scan in terms of their:

- presence (aplasia?);
- position (displaced?);
- outer contour or border (which gives information about the surface of an organ or tumour as well as about its relation to the adjacent structures*)*;
- mobility (fixed?);
- consistency (palpation under ultrasonic observation);
- echo pattern; and
- attenuation.

Evaluation of the **presence**, **position** and **size** of an organ is based on the known normal anatomy. A simple determination of organ diameter is sufficient for most routine evaluations, provided the shape is normal. The volume (V) of round- or oval-shaped organs is calculated on the basis of their three perpendicular diameters a, b and c, following the formula for an ellipsoid:

$$V = 0.5 \cdot a \cdot b \cdot c \qquad (2.1)$$

Formulas for special problems, e.g. pleural effusion, are discussed in specific chapters of this book. The volume of organs and structures with complicated shapes can be calculated by the 3D technique.

Evaluation of the **contour** of an organ, and particularly of a neoplastic lesion, should give information about both the smooth or irregular surface and any sharp or blurred (ill-defined) demarcation lines (Fig. 2.8, Fig. 2.9, Fig. 2.10). The latter should include the relation to the surrounding tissue, e.g. any overlap with a natural border, such as a capsule, or infiltration into adjacent structures. The possibilities of contour evaluation are limited by the imaging geometry of ultrasound. The fine surface irregularities of a cirrhotic liver, for example, can be shown, especially since the surface

Fig. 2.8. Evaluation of the margin or contour of a lesion (e.g. in the liver). The margin of both lesions is sharp. The cyst (a) is echo free, the haemangioma (b) shows a homogeneous echo-rich pattern

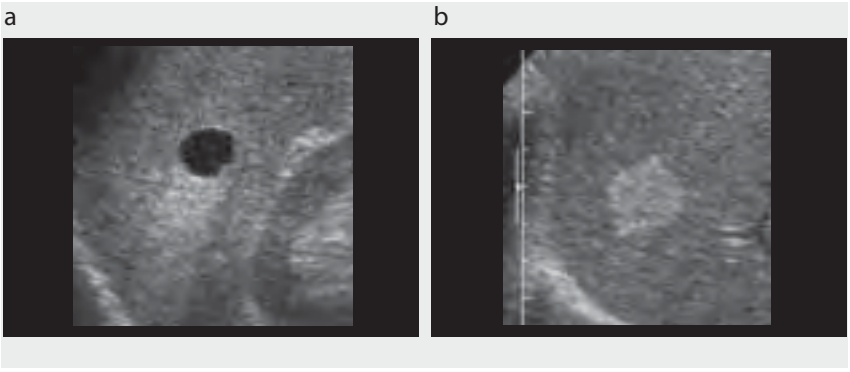

Fig. 2.9. Evaluation of the contour (margin) of two echo-poor liver lesions. (a) The echo-poor metastasis has a blurred outline, particularly at the cranial side (arrow), whereas the malignant lymphoma (b) shows a partial (dorsal side), rather sharp but altogether irregular outline. Slight echo enhancement is seen behind the lymphoma

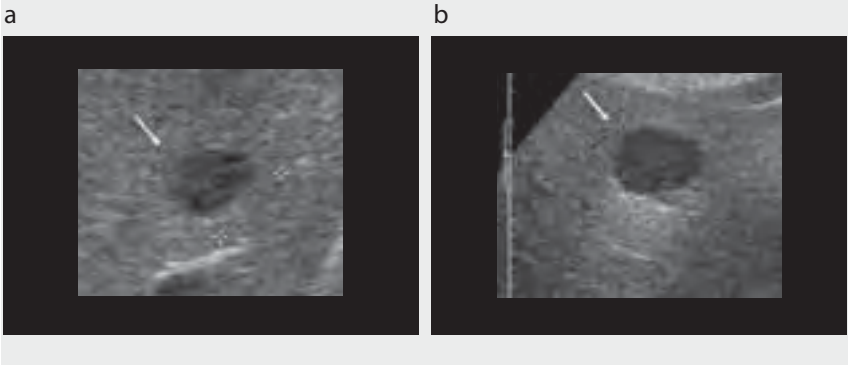

is approximately perpendicular to the ultrasound beam (Fig. 2.11). The contour of an organ such as the pancreas, however, may appear to be irregular, particularly on the sides, as a result of the coarse boundary echoes.

Evaluation of the **echo pattern** (also known as echo structure, echo texture, echogenicity) of an organ, tissue or tumour is based on an analysis of the intensity and distribution of the internal echoes that are not due to discernible anatomical structures, such as vessels, septa or ducts. Single echoes are either weak, average or strong (Fig. 2.12).

The **echo pattern** is analysed on the basis of the number and strength of the echoes and their distribution (Fig. 2.13):

- echo free – echo poor (hypoechogenic) – average – echo rich (hyperechogenic); and
- homogeneous or inhomogeneous.

Fig. 2.10. Contour sign. (a) The lesion in the liver has a smooth outline and a tangential artefact (see Fig. 1.24), but is nevertheless a hepatocellular carcinoma (HCC), probably with a capsule. The pattern is average, similar to that of the surrounding liver tissue. (b) The metastasis in the abdominal wall shows an irregular shape and an echo-poor pattern

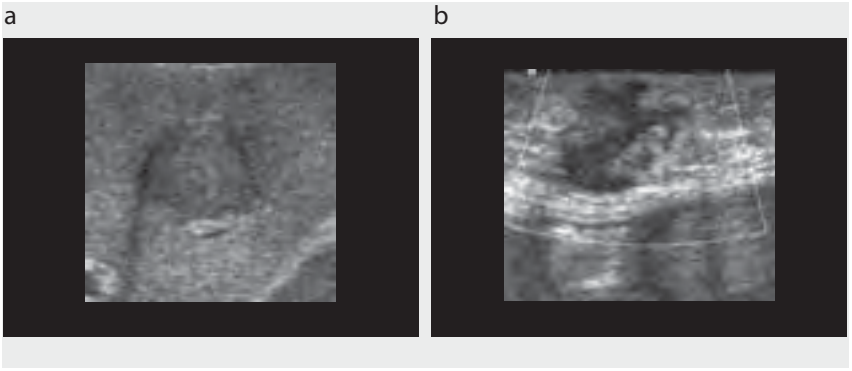

Fig. 2.11. Surface of the liver. (a) The normal healthy liver has a smooth surface. The echo structure of the normal liver is homogeneous and of normal brightness. (b) The cirrhotic liver has an irregular surface. (The echo pattern of the cirrhotic liver is slightly inhomogeneous (coarsened)

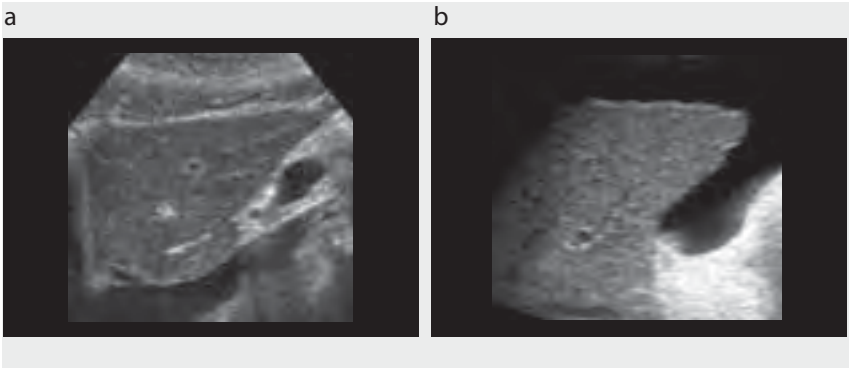

Echo free: no (real) echoes within a lesion, e.g. a cyst (Fig. 2.8, Fig. 2.13). This diagnosis requires the correct gain and the identification of artefacts (see section on Artifacts in Chapter 1). Furthermore, only fluid in the strict physical sense is really echo free. Other types of fluid (e.g. blood, abscesses or exudates) contain small particles (e.g. blood cells, fibrin) and cause weak echoes (Fig. 2.12).

Echo poor: an echo pattern consisting of only a few weak echoes (see Fig. 2.9).

An echo pattern appears to be **echo rich** if the tissue causes many weak echoes or a few strong echoes. In both situations, this region appears 'bright' on the screen. For the first type of echo-rich pattern, the term 'echo dense' is occasionally used. Generally, none of these types of echo-rich pattern is differentiated (Fig. 2.8, Fig. 2.9, Fig. 2.10, Fig. 2.11, Fig. 2.12, Fig. 2.13, Fig. 2.14).

Fig. 2.12. Quality of echoes. The echoes in the upper part of the left lesion are weak, while those of the liver are average. In the right lesion, strong echoes caused by gas are seen. Both lesions (abscesses) show an inhomogeneous pattern; the one on the left is echo poor and the other partially echo rich. Behind the right-hand lesion, a tangential artefact is seen

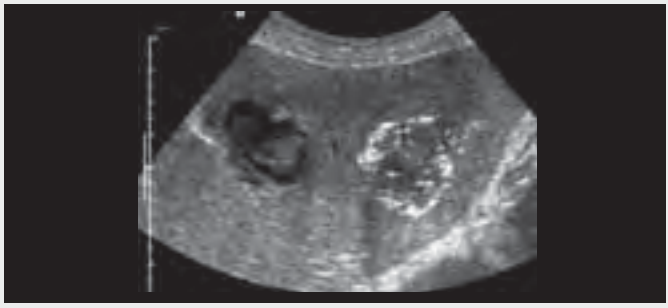

Fig. 2.13. Echo structure (echo pattern). (a) The ultrasonic structure of the liver and the parenchyma of the kidney are echo poor and homogeneous; the pattern in the centre of the kidney is echo rich. A small cyst (arrow) is echo free. (b) The liver shows an inhomogeneous echo-rich structure caused by echo-rich metastases

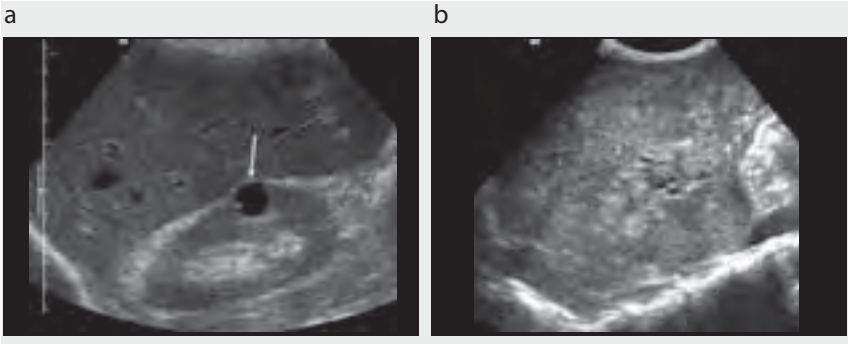

Increased **attenuation** of ultrasound in an organ may indicate pathological alterations, such as fibrosis; however, experience is needed to recognize this sonographic symptom, as no objective parameters exist (Fig. 2.14).

Fig. 2.14. Attenuation. (a) The fatty liver shows a typical homogeneous echo-rich pattern. (b) The echo structure of the left liver is echo rich near the ventral surface, but the dorsal parts appear more echo poor. Provided the adjustment of the TGC is correct, this indicates higher than average attenuation of the ultrasound, as seen in fibrosis

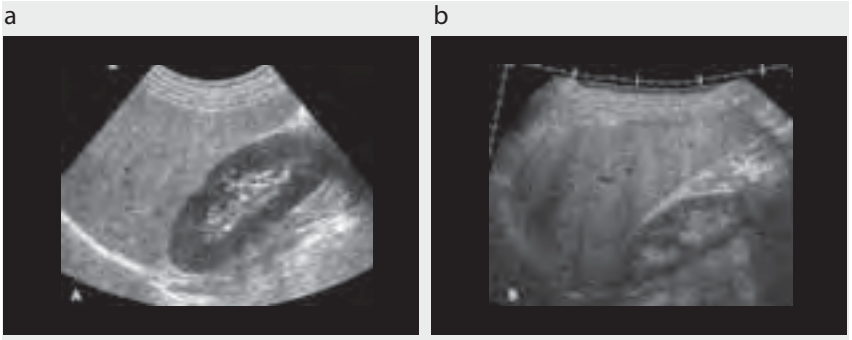

Duplex technique

In interpreting Doppler information in an ultrasound image, account should be taken of the principal problems and limitations of the Doppler technique: angle dependency and aliasing.

A suitable angle (< 60°) must be found for the ultrasound beam to reach the vessel of interest, especially if measurements (spectral Doppler) are to be made. The angle is less problematic for colour Doppler imaging, but colour pixels may be missed if the angle is close to 90° (see Fig. 1.32). Power Doppler images are not affected by this problem but give no information about the flow direction.

The window for the Doppler examination should be as small as possible, as its width and length determine the time needed for the construction of one image and, therefore, the image frequency (Fig. 1.19, Fig. 1.20, Fig. 1.21). The distal border of the window, or the penetration depth for the Doppler ultrasound, limits the pulse repetition frequency because a second pulse can be emitted only if the echoes of the adjusted depth have reached the transducer. The pulse repetition frequency limits the flow velocity, which can be depicted without aliasing (see section on Doppler techniques in Chapter 1). Initially, it is useful to adjust the settings to a relatively low velocity (17–24 cm/s) to depict the slow flow velocities in the veins. For the same reason, the filter should be low to avoid suppressing slow flow signals with those caused by the movement of the wall. For the examination of veins and arteries, the wall filter should be adjusted to 50–100 Hz and 200 Hz, respectively. If aliasing (see section on Doppler techniques in Chapter 1) occurs in the arteries, the pulse repetition frequency can gradually be adapted to higher velocities. The baseline can also be shifted to avoid aliasing in the arteries (Fig. 2.15) because the velocity in the veins in the opposite direction is slow.

The gain of the Doppler signals should be high so that single colour pixels are seen in the tissue, especially if thrombosis is suspected. If no colour-coded signals are seen in a vessel, the angle and adjustment, particularly of the pulse repetition frequency, should be checked. If they are correct, spectral Doppler should also be used to obtain a definite diagnosis.

Fig. 2.15. Aliasing. (a) The spectral Doppler depiction (duplex technique) of the flow in the aorta shows aliasing. The peak velocity signals, 80–120 cm/s, are shown below the baseline (arrow). (b) Correct depiction as a result of shifting the baseline (arrow)

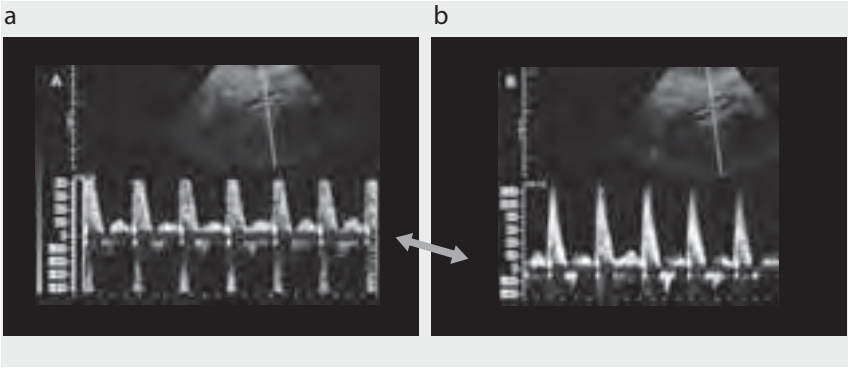

In an artery, the colour Doppler technique will yield high systolic flow and give a good signal. In diastole, however, the flow may become very slow or even reverse (high-resistance flow), resulting in a weak signal and an unsatisfactory image of the vessel. With persistence, it is possible to extend the peak flow to get a better colour Doppler image (Fig. 2.16).

B-scan provides information about the anatomy of vessels, including diagnoses of dilatation, aneurysms and alterations of the wall and stenosis. Thrombosis in a vessel can also be demonstrated.

The colour Doppler technique permits detection of small vessels and gives information about flow and direction. Power Doppler is more sensitive for examining small vessels and slow flow but does not provide information about the direction of flow. In particular, it is used to estimate the vascularity of a structure or a mass.

Estimation of flow velocity from the brightness of colour pixels is rather approximate. Even turbulent flow, caused by stenosis, is not reliable.

Use of spectral Doppler (triplex technique) is needed for a more accurate analysis of the flow, e.g. direction, velocity and dynamic course. A condition required for an exact analysis is a Doppler angle of < 60° (best, ~30°), which may be difficult to achieve in the abdomen. Each measurement should be made a least three times, and the average finding should be used. Attention should be paid to specific conditions, such as a change in flow, which depend on the activity of the region or tissues it supplies.

Fig. 2.16. Colour Doppler and spectral Doppler of the abdominal aorta. (a) The colour Doppler image shows red (here bright) signals, because it is made in systole, whereas the image in (b) shows blue signals (here dark), indicating reverse flow in early diastole. Both phases are indicated in the spectral Doppler (c)

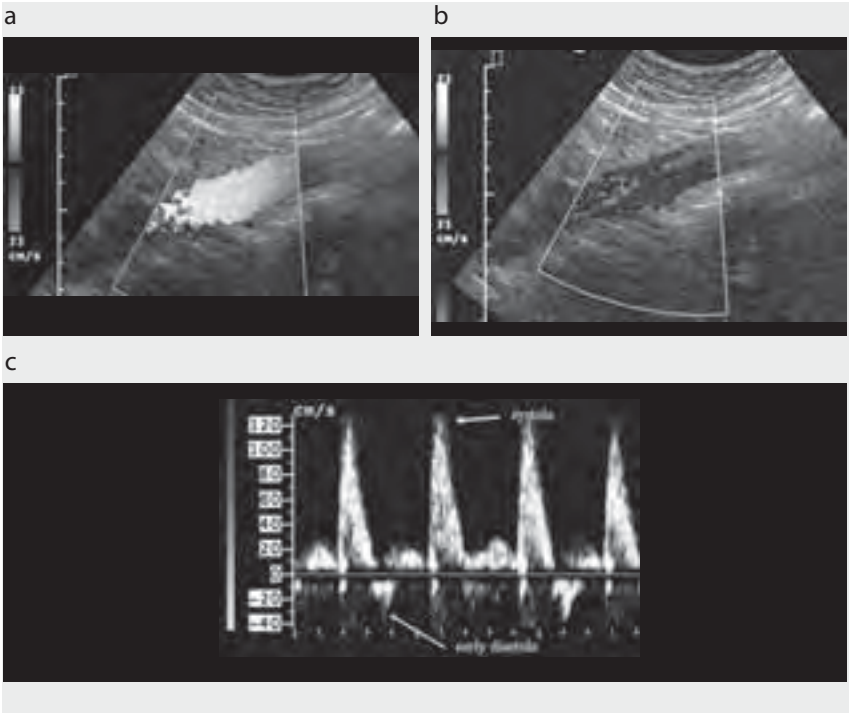

Chapter 3

Interventional ultrasound

3

Interventional ultrasound

Definitions

Interventional ultrasound is defined as any diagnostic or therapeutic procedure performed under ultrasound guidance for any tissue or organ that is visualized by ultrasound.

Diagnostic procedures: ultrasound-guided aspiration of fluid or cystic fluid for biochemical or cytological and culture examinations as well as for cytological or tissue sampling with fine (outer calibre < 1 mm) or coarse needles for microscopic examination. The needle calibre is generally expressed in terms of gauges (Table 3.1).

Table 3.1. Needle calibre: conversion from millimetres to gauge

Millimetres (mm)	Gauge
Fine needle: calibre ≤ 1 mm	
0.5	23
0.6	22
0.7	21
0.8	20
0.9	19
Coarse needle: calibre ≥ 1 mm	
1.0	18
1.1	17
1.3	16
1.4	15
1.6	14
1.8	13
2.0	12

Therapeutic procedures: drainage of fluid collections (e.g. abscesses, parasitic cysts) by needle or catheter; injection into a tumour or echinococcal cyst of necrotizing substances (e.g. ethanol) and positioning of radiofrequency needle electrodes to obtain a thermal lesion.

Over the past 10 years, due to improvements in imaging techniques, indications for diagnostic procedures have progressively decreased and they have been replaced by imaging and/or laboratory data when they are considered sufficient for diagnosis.

Indications for therapeutic procedures have been increasing, so that there is now, for example, consensus that percutaneous abscess drainage is the treatment of choice for abdominal abscesses.

Ultrasound-guided procedures: general clinical rules

Ultrasound-guided diagnostic procedures should be performed only if a diagnosis cannot be made with other less or non-invasive methods (i.e. diagnostic imaging).

Pathological diagnostic confirmation should imply a definite benefit for the patient.

Therapeutic procedures should be as effective, or more effective, than more conventional invasive methods (e.g. surgery).

Before any ultrasound-guided procedure is carried out, a coagulation parameter check is mandatory: prothrombin activity should be 50% or greater, the international normalized ratio less than 1.5 and the platelet count 50 000 per ml or more.

Before any ultrasound-guided procedure is performed, the patient's informed consent should be obtained.

Contraindications: Uncooperative patients; severe blood-clotting impairment (patients must be asked about their intake of anticoagulant or antiaggregant drugs.)

Diagnostic procedures

Ultrasound-guided diagnostic procedures include cytological or tissue sampling and fluid collection by needle aspiration.

Technical notes

Needles

Fine needles are subdivided into aspirative needles for cytological sampling and cutting needles for tissue sampling (Fig. 3.1, Fig. 3.2).

Aspirative needles have an inner removable stylet. The prototype of aspirative needles was the spinal needle (Fig. 3.1). Cellular material is collected by aspiration, which is obtained by connecting the needle to a 10-ml syringe (which can also be connected to an aspiration handle).

Fig. 3.1. Types of aspirative needle and inner stylet

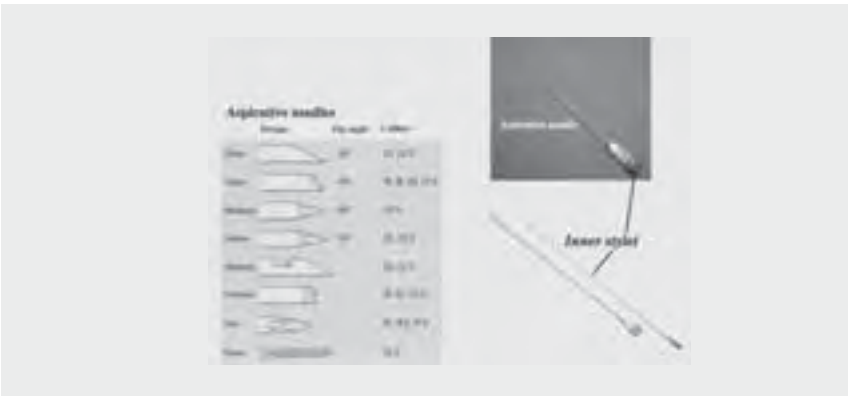

The main types of cutting needles are the Menghini (end-cutting needle) (Fig. 3.2) and the Tru-Cut (side-cutting needle). The Menghini needle has an inner retractable stylet attached to the syringe piston to avoid aspiration of the tissue core when suction is applied. The Tru-Cut needle has an outer cutting cannula and an inner one with a 20-mm notch, in which the biopsy specimen is trapped. The notch is located immediately before the tip (Table 3.2).

Fluid aspiration can be performed with either fine or coarse aspirative needles, depending on the fluid characteristics (e.g. viscosity, presence of debris).

Fig. 3.2. End-cutting needle showing needle tip

Table 3.2. Types of needles with relevant calibre and cost in US$ (averaged worldwide, for 2009)

Type	Calibre (gauge)	Cost (US$)
Aspirative		
Chiba	18–22	12
Spinal	18–25	6
Cutting		
Menghini	15–23	35
Tru-Cut	14–20	20

Approach

The approach depends on the target organ and the site of the focal lesion and can be either subcostal or intercostal. The depth of the target is calculated.

Biopsy with aspirative needle

The skin of the patient is disinfected with iodine, which also serves as a sterile contact medium. The fine needle is guided towards the target either with the **free-hand technique** or with the help of a **guidance apparatus** attached to the probe or directly introduced through the biopsy channel of the transducer (Fig. 3.3).

Fine needles can be inserted directly into the skin and subcutaneous tissue and then directed to the target. The tip of the needle should be seen on the ultrasound screen during the biopsy. Lesion areas, which are usually necrotic (echo poor, central), should

be avoided during sampling to improve the quality and quantity of the material collected (see Fig. 3.4). When the needle tip is in the correct position, the inner stylet is removed and the needle is attached to the syringe. Suction is applied, and the needle is moved backward and forward five to ten times. The syringe's piston is released before the needle is withdrawn to avoid contamination with material from different tissue layers.

Fig. 3.3. (a) In the free-hand technique, the needle is inserted close to the probe and the needle track is monitored by slight adjustments to the probe's inclination. (b) The needle is inserted into the channel of the guidance apparatus connected to the probe

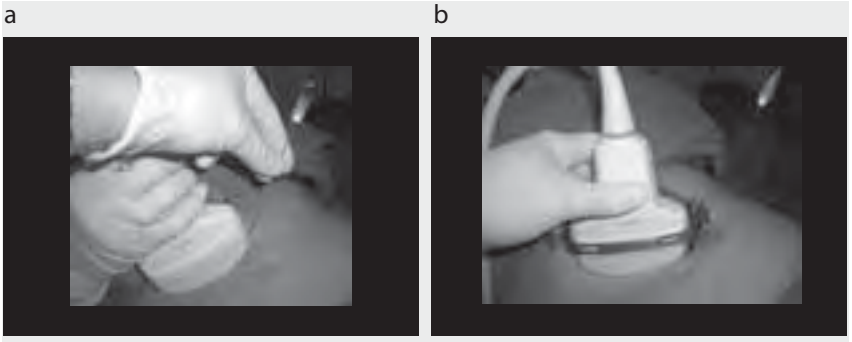

The biopsy needle is disconnected, and the syringe is filled with air and reconnected to the biopsy needle. The material inside the needle is sprayed onto slides and smeared. It is preferable to check the adequacy of the material collected by immediate staining; if this is not possible, the biopsy should be repeated two or three times to ensure that an adequate sample has been obtained.

Biopsy with cutting needle

Cutting needles, even those of calibre < 1 mm, have a blunter tip than aspirative needles. Therefore, a local anaesthetic (e.g. 2–3 ml lidocaine) is infiltrated subcutaneously into the muscle layer after the skin has been disinfected. This is particularly necessary when larger calibre needles (< 18 gauge) are used. The skin is then pricked with a small lancet to facilitate the entrance of the needle. The biopsy is performed according to the type of needle. The Menghini needle is introduced into the superior margin of the target, suction is applied to the syringe and the needle is advanced rapidly for 2–3 cm and retracted. The Tru-Cut needle is also positioned at the proximal border of the target. The internal cannula is advanced, the tissue is trapped in the notch and finally cut by the outer sheath.

Post-biopsy control

The patient's vital parameters should be observed for 2 h after the intervention, especially if the biopsy was performed with a coarse needle or if the patient's coagulative status is abnormal although within the suggested limits. Thereafter, in the absence of any troubling signs or symptoms, the patient can be discharged with the recommendation to seek advice for any medical complaint within the following 7 days.

A negative biopsy result does not rule out a malignancy or, conversely, the need to confirm the benign nature of the biopsied lesion formally.

Indications

Liver

Malignant tumours

Ultrasound-guided biopsy is very accurate for diagnosing malignant liver tumours (Fig. 3.4, Fig. 3.5, Fig. 3.6, Fig. 3.7). Metastases can be typed by examining a cytological sample obtained with an aspirative needle (fine-needle biopsy (FNB)); sensitivity is very high at 92.7% and specificity is 100%. Cytological typing of hepatocellular carcinoma (HCC) can present some difficulties because, in well-differentiated forms, tumour hepatocytes are very similar to normal hepatocytes, whereas in poorly differentiated forms the hepatic histotype can be misinterpreted and an erroneous diagnosis of metastasis made. In such cases, it is advisable to perform a double biopsy: one for cytological examination (fine-needle biopsy with an aspirative needle) and one for histology (fine-needle biopsy with a cutting needle). In this way, sensitivity is increased to 97.5% and the specificity is 100%. According to current diagnostic policy, a biopsy should not be performed on nodular lesions with an α-fetoprotein value higher than 400 ng/ml or if two imaging techniques confirm a diagnosis of HCC.

Fig. 3.4. Fine-needle biopsy of a large hepatic lesion: hepatocellular carcinoma. Note that on the needle track a portion of normal parenchyma is interposed between the lesion and liver capsule; the needle is directed to the more echo-rich area of the tumour to improve the sampling adequacy

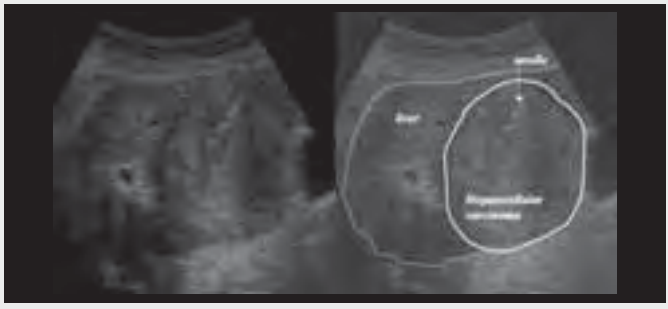

Fig. 3.5. Fine-needle biopsy of a small hepatic lesion: liver metastasis

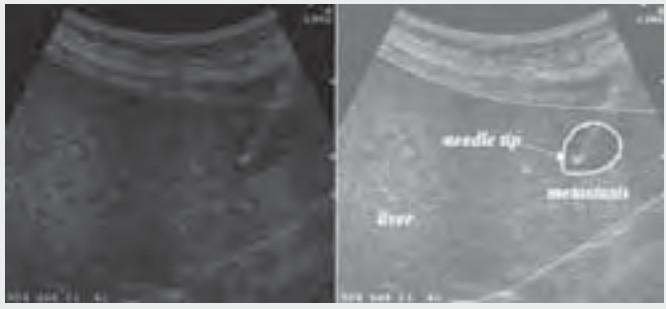

Fig. 3.6. Fine-needle biopsy of a small, ill-defined hepatic lesion: cholangiocarcinoma

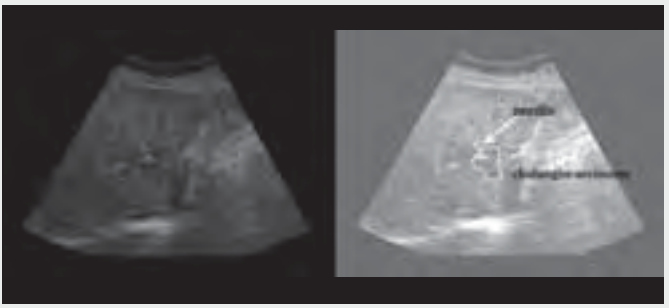

Fig. 3.7. Fine-needle biopsy of a large hepatic lesion with irregular borders: cholangiocarcinoma

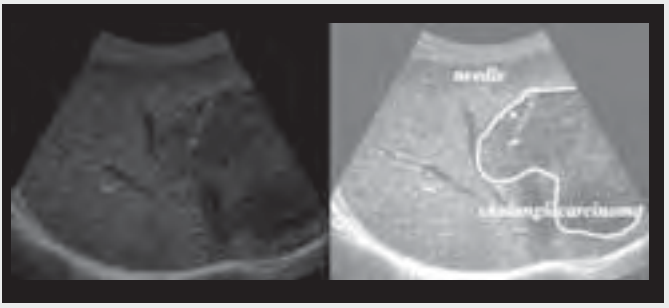

Benign tumours

Haemangioma is the commonest benign liver tumour, and generally ultrasound is diagnostic. In some instances, however, its presentation can be very atypical and puncture is advised. Unfortunately, the diagnostic accuracy of fine-needle biopsy is not satisfactory because the material obtained is filled with blood, and few endothelial cells are present. Furthermore, major complications (haemorrhage) or even death has been reported after biopsy of liver haemangioma.

Two other benign liver tumours – much rarer than angioma – are adenoma and focal nodular hyperplasia, which is really a pseudotumour. Imaging with a combination of at least two coincident techniques generally suffices to characterize focal nodular hyperplasia, while diagnosis of an adenoma is more difficult. A combination biopsy (cytology and histology) should be performed with caution because both focal nodular hyperplasia and adenoma have rich vascularization. Histological sampling is better performed with coarse cutting needles (1.2–1.4 mm).

Simple cysts and hydatid cyst

Generally, ultrasonic diagnosis of simple cysts is to be recommended. In an oncological context, however, a pathological diagnosis may be necessary. Cystic fluid can easily be aspirated and a cytological examination performed.

Hydatid cysts are usually diagnosed by a combination of serology and imaging. In some cases, an examination of the aspirated fluid may be useful. Experience has shown that puncturing a hydatid cyst is only rarely complicated by anaphylactic shock.

Pyogenic abscess and amoebic abscess

Material obtained by ultrasound-guided aspiration of pyogenic abscess is creamy-yellow and foul-smelling. Multiple sets of culture increase the diagnostic yield of blood cultures. Ultrasound-guided aspiration of an amoebic abscess should be performed when the diagnosis is uncertain. The aspirated fluid is viscous, yellow or dark-brown ('anchovy sauce'). In both these forms, the aspiration should be performed with 19- to 20-gauge needles because of the viscosity of the material.

Chronic liver disease (cirrhosis, chronic hepatitis)

When clinical, laboratory and imaging data require histological confirmation, a biopsy can be performed with a subcostal or intercostal approach. A cutting needle (14–18 gauge) can be used.

Gallbladder

The gallbladder can be punctured under ultrasound guidance, using a transhepatic approach, to diagnose gallbladder masses.

Pancreas

Pancreatic masses

The pathological diagnosis of a pancreatic mass ensures correct management of patients (Fig. 3.8, Fig. 3.9). If the tumour is resectable, surgery can be carried out to avoid the time and difficulties involved in intraoperative biopsy. In patients with non-resectable tumours, appropriate palliative treatment can be planned. Moreover, fine-needle biopsy allows diagnosis of malignancies other than adenocarcinoma, such as neuroendocrine tumours, lymphoma or metastases, which require different management. In one series of 510 patients with pancreatic masses, either benign or malignant, the diagnostic effectiveness of fine-needle biopsy was found to be very high (Table 3.3), except for neuroendocrine tumours.

Fig. 3.8. Fine-needle biopsy of a large pancreatic lesion: pancreatic carcinoma

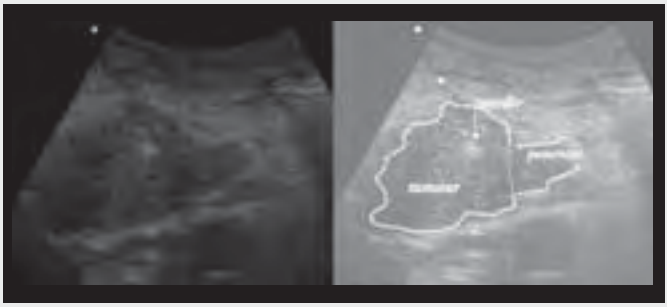

Fig. 3.9. Fine-needle biopsy of a large cystic pancreatic lesion: pancreatic cystadenoma. Bioptic access was transhepatic

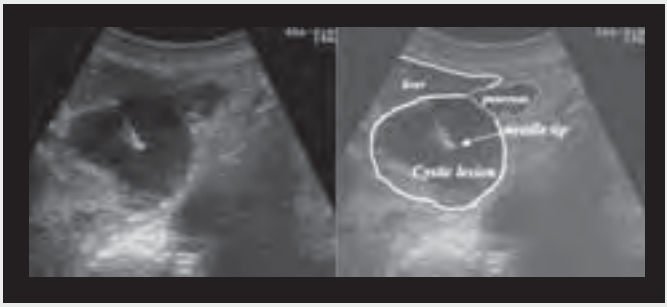

Table 3.3. Results of different fine-needle biopsy procedures for the diagnosis of pancreatic lesions; the differences in the results are not statistically significant

	Cytology (287 patients)	Histology (95 patients)	Cytology + histology (128 patients)
Sensitivity (%)	87	94	97
Specificity (%)	100	100	100

Spleen

Spleen biopsies are performed infrequently because of the risk of post-procedural bleeding. Moreover, the indications for spleen biopsy, which include staging or restaging of lymphoma, are decreasing. Spleen biopsy can, however, be a highly effective diagnostic tool in selected cases of focal lesions, organomegaly or fever of unknown origin. In addition, it has an acceptable complication rate (Fig. 3.10).

Fig. 3.10. Fine-needle biopsy of a large cystic lesion of the spleen: metastasis

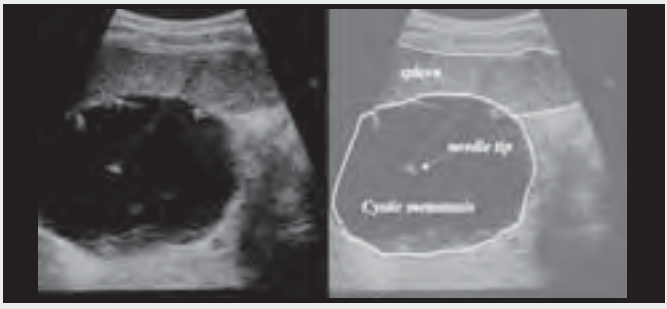

Kidney

Imaging techniques cannot always differentiate between a benign and a malignant kidney mass. In such instances, fine-needle biopsy is easy to perform, with satisfactory diagnostic accuracy. Cutting needles (18 gauge) guided by ultrasound can readily be used to obtain kidney tissue to characterize diffuse nephropathy.

Gastrointestinal masses

The origin of gastrointestinal masses varies, occurring either in the gastrointestinal tract or independently of it. Intestinal gas, which degrades the ultrasound image, can be displaced by compressing the intestine with the probe. Sampling is preferably performed with a fine aspirative needle (cytology examination). A liquid mass can easily be aspirated with a fine needle. Many potential pathological conditions are possible: haematoma, very large kidney cysts or ovarian cysts, mesenteric cysts, lymphangioma, atypical location of a pancreatic pseudocyst, necrotic tumours and hydatid cysts. The aspirated material should be used for culture, cytological examinations and laboratory tests, such as amylase and tumour markers. Other retroperitoneal or abdominal (lymphadenopathy) masses can also be aspirated under ultrasound guidance (Fig. 3.11, Fig. 3.12).

Fig. 3.11. Fine-needle biopsy of a huge retroperitoneal mass: sarcoma

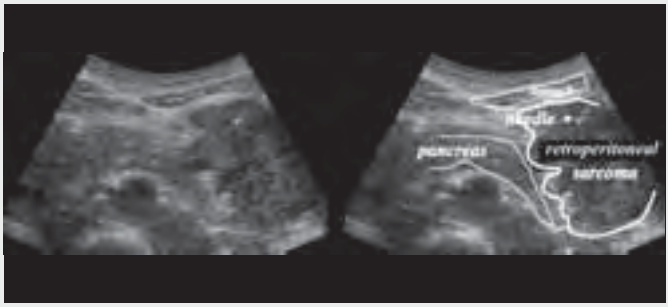

Lung

Ultrasonography is a useful alternative to other imaging techniques (e.g. fluoroscopy and computed tomography (CT)) to guide biopsy of subpleural lung lesions. The technique is simple and rapid and can be carried out at the bedside.

Bone

Although sonography cannot be used to study bone lesions, ultrasound images are clear enough to perform an ultrasound-guided biopsy on some patients with lytic lesions characterized by disruption of the cortical structure. Within these limits, the diagnostic accuracy is very good.

Fig. 3.12. Fine-needle biopsy of abdominal lymphadenopathy; the biopsy access was transhepatic

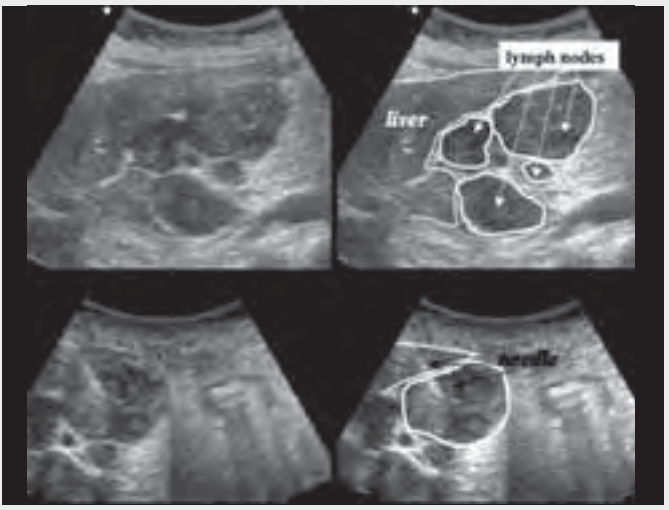

Diagnostic or therapeutic procedures

Pericardiocentesis, **pleurocentesis** and **paracentesis** are procedures with either a diagnostic or therapeutic purpose.

Pericardiocentesis

Ultrasound guidance reduces the risks for lung or heart injury, and the procedure is much safer and easier than the previously used blind puncture technique. Cytological and culture examinations can establish the diagnosis in many instances. Generally, the procedure has a simultaneous therapeutic value, when the amount of pericardial fluid could interfere with cardiac contractions. Sometimes, a permanent catheter may be necessary, which can be positioned by the Seldinger technique (see section on Catheter insertion techniques in this chapter).

Pleurocentesis

The procedure is still performed with a blind technique, in which the fluid collected is substantial. Ultrasound guidance facilitates correct needle insertion and positioning, particularly when small amounts of fluid or septated collections are involved.

Paracentesis

Ultrasound guidance ensures the correct positioning of the needle when the sample to be collected is small or loculated (Fig. 3.13).

Fig. 3.13. Paracentesis: correct positioning of the needle

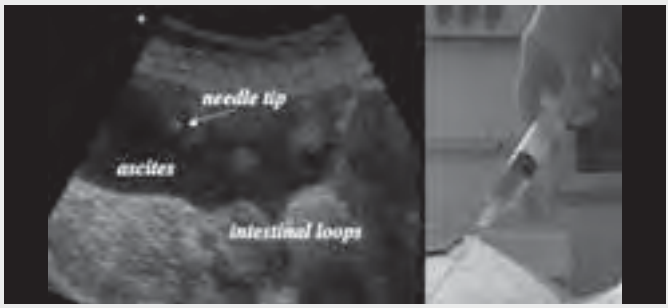

Therapeutic procedures

Abdominal abscess drainage is the first line of treatment for infected or symptomatic fluid collection. Almost all abscesses are amenable to percutaneous drainage. When a coexisting problem, such as a bowel leak, requires surgery, drainage provides useful temporization for the surgeon. Catheter insertion procedures include the trocar and Seldinger techniques. Ultrasound, CT and fluoroscopy are the imaging guidance systems most commonly used. Preferably, the procedure is performed by positioning a large catheter under ultrasound guidance. The catheter is left in situ until draining has stopped.

Technical notes

Catheters of different lengths and calibres are available (Table 3.4). Most are characterized by a terminal part configured as a 'pigtail' (or J-shaped), which can prevent inadvertent catheter withdrawal (Fig. 3.14).

Table 3.4. Conversion from French units to inches and millimetres

French catheter scale (outside diameter)	Inches	mm
4	0.053	1.35
6	0.079	2
8	0.105	2.7
10	0.131	3.3
12	0.158	4
14	0.184	4.7
16	0.210	5.3
18	0.236	6
20	0.263	6.7
22	0.288	7.3
24	0.315	8

Fig. 3.14. Catheter structure. Withdrawal of the inner stylet and sheath allows the tip to assume a J-shaped curvature

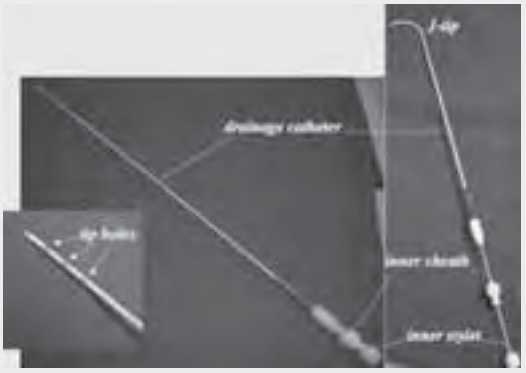

Catheter insertion techniques

Basically, there are two methods for inserting a catheter into an abscess: the trocar technique and the Seldinger technique.

Trocar technique

A catheter mounted on a trocar is directly inserted into the collection site. The depth of the target should be accurately measured and the track of the trocar carefully followed on the ultrasound screen. When the calibre of the catheter is large (> 8 French), accurate placement can be made by using a guiding needle previously inserted into the abscess. Thereafter, a small skin incision is made alongside the needle, and the trocar is advanced parallel to the guiding needle. When the catheter is in position, the inner stylet of the trocar is retracted, some millilitres of pus aspirated, and the trocar then removed.

Seldinger technique

An 18 to 20-gauge needle is inserted into the collection site and a guide wire passed through the needle. After needle insertion and aspiration of a few millilitres of fluid, a guide wire is inserted and the needle is withdrawn. The catheter is directed over the guide and into place at the collection site. The first step of the procedure is realized under ultrasound guidance. It may be necessary to use dilators of increasing calibre to obtain an adequate track for introduction of the catheter.

An advantage of the trocar technique is its relative simplicity, whereas the Seldinger technique allows more accurate location of the catheter.

Management of the catheter

A primary mechanism for internal catheter retention is the catheter configuration. The so-called pigtail-shaped catheter or J-shaped tip (Fig. 3.14), which is widely used, prevents inadvertent catheter withdrawal. The catheter should be fixed externally by suturing it to the patient's skin. Most catheters have external fixation devices.

Once abscess decompression has been achieved, the catheter should be flushed every 8–12 h with 10–15 ml of saline to clear it and to eliminate plugs, which may cause obstruction. The procedure should be performed cautiously to avoid catheter dislodgement. Catheter output, the characteristics of the drained material and any changes in these characteristics should be carefully recorded. Output reduction while the abscess is incompletely drained may indicate the presence of a clog in the tube, in which case the catheter should be changed. Suspicion of a fistula with adjacent organs or other structures should be confirmed by injecting contrast fluid into the abscess through the catheter. The presence of sepsis should delay this radiological check.

Indications

Liver

Pyogenic abscess

The pus is characteristically creamy and unpleasant smelling. Needle aspiration (even with a fine needle) is recommended as the first diagnostic procedure, as it allows assessment of the thickness of the purulent material and, thus, facilitates the choice of catheter. A first culture should be performed. If the abscess is large, use of a catheter is generally mandatory (Fig. 3.15, Fig. 3.16). It is left in situ for a few days after drainage has stopped (with the catheter open).

Fig. 3.15. Catheter drainage of a large pyogenic abscess of the liver

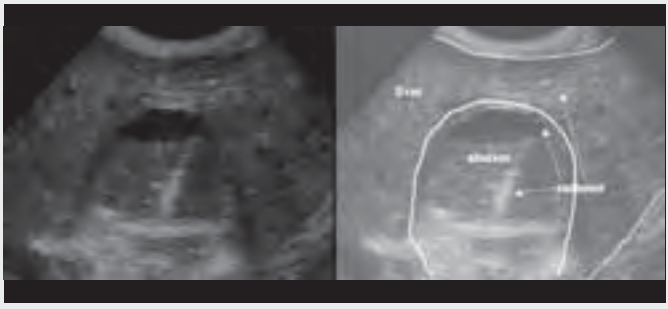

Amoebic abscess

The pus is yellow or dark-brown ('anchovy sauce') and, typically, odourless. The treatment is similar to that described for pyogenic abscess. The results of percutaneous drainage are very satisfactory for both kinds of abscess.

Echinococcal cyst

Hydatid cyst can be treated by ultrasound-guided puncture with the PAIR technique (puncture, aspiration of contents, injection of scolicide solution and reaspiration of the injected liquid), which represents an alternative to surgery and medical treatment. Preliminary aspiration of cystic fluid (10–20 ml) for parasitological and biological examination is performed. The fluid is typically as limpid as pure water. The therapeutic procedure (Fig. 3.17) is generally performed with a 14–18 gauge needle, preferably with a transhepatic approach. Catheter insertion is only sometimes useful but is mandatory for large cysts and thick material. After fluid aspiration, 95% ethanol or 30% hypertonic

saline solution is introduced in a quantity equivalent to about one third of the aspirated fluid to ensure an effective concentration of the scolicide in the cyst. After 10 min, the ethanol or saline solution is reaspirated. A variation involves repeating the ethanol injection (about 100 ml) every 3 days without reaspiration. Treatment with a specific drug is advisable. The procedure is effective and safe: prolonged follow-up has not shown leakage of hydatid fluid or passage of ethanol or saline solution into the bile system. The operator must, however, bear in mind the risk of chemical cholangitis; therefore, a rapid test for bilirubin should be performed on the fluid from the cyst, before scolicide injection.

Fig. 3.16. Pus from a pyogenic abscess is yellow (a), whereas that from amoebic abscess is typically brown (b)

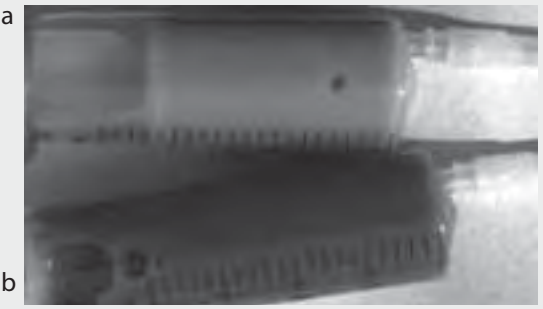

Fig. 3.17. PAIR technique study of a hepatic hydatid cyst. The catheter is clearly visible inside the cyst. Reaspiration of scolicide progressively empties the cyst

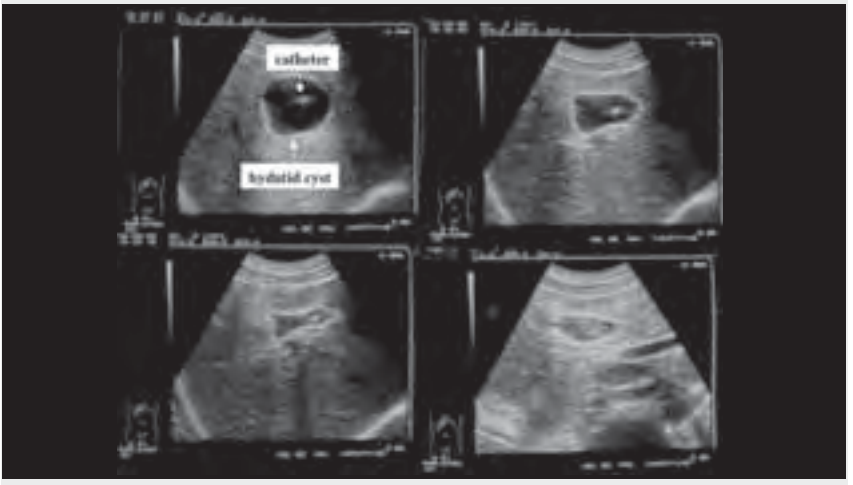

Pancreas

Pancreatic **pseudocyst**

These are collections of pancreatic juice encapsulated by a connective wall of varying thickness, without an epithelial lining. They originate from the pancreas and, in many instances, communicate with pancreatic ducts. They are usually found within or adjacent to the pancreas in the lesser peritoneal sac. Occasionally, pseudocysts dissect the mesentery and can be found anywhere in the abdomen. Two pathogenic mechanisms are responsible for pseudocyst development. In the first, there is an episode of acute pancreatitis with gland inflammation, exudates and eventual disruption of the ductular system. The second mechanism is related to the course of chronic pancreatitis. Most pseudocysts resolve with conservative management. When the presumed duration of collection of pancreatic juice is less than 6 weeks, treatment should be avoided to allow maturation of the pseudocyst wall. Percutaneous drainage of pseudocysts requires the use of large-bore catheters, as the collection fluid is rich in fibrin plugs and gross necrotic debris. The time needed to cure pseudocysts by percutaneous drainage is generally very long and sometimes takes months. **Pancreatic abscesses** (Fig. 3.18) and other **abdominal collections** (Fig. 3.19) can also be drained under ultrasound guidance.

Fig. 3.18. (a–d) Catheter drainage of a large pancreatic collection. The catheter is visible within the collection (black and white arrows), which is progressively emptied

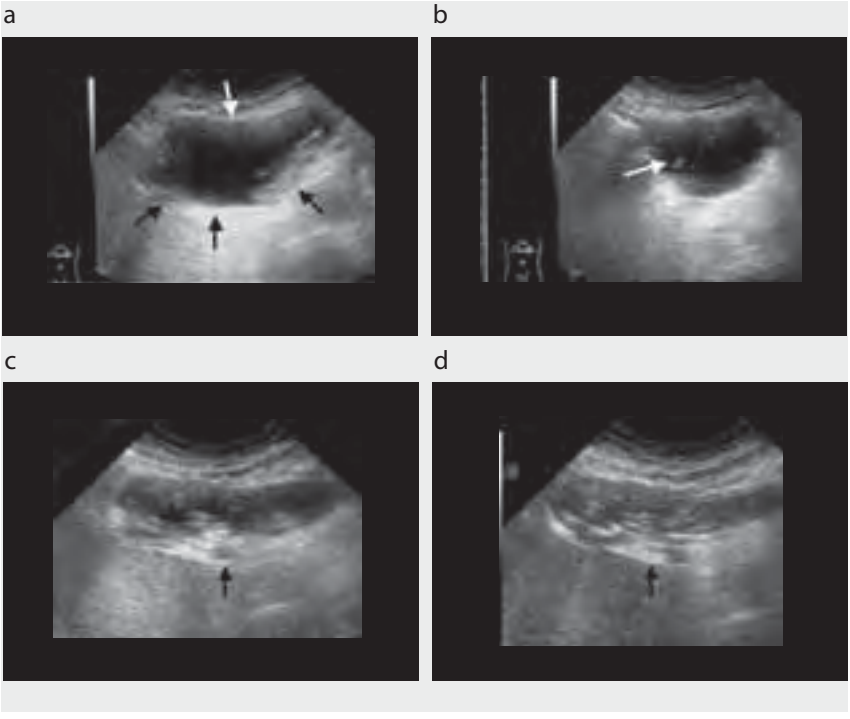

Fig. 3.19. (a, b) Needle drainage of a renal abscess (abs) due to *Escherichia coli*. The needle (n) track is marked with arrows; k, kidney

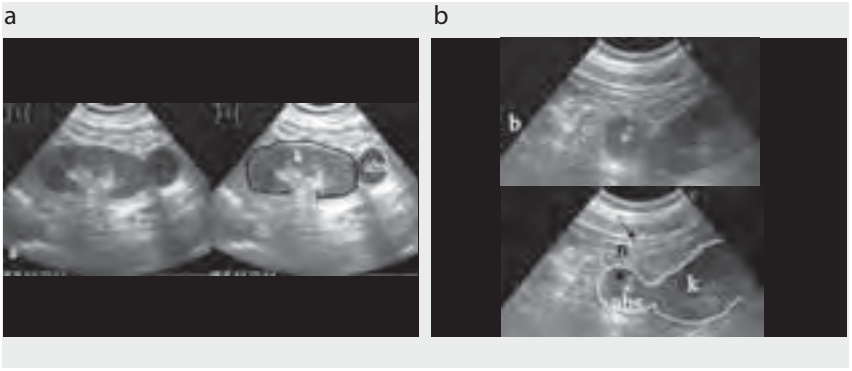

Percutaneous treatment of malignant liver tumours

Metastases of HCC and colorectal cancer are the most frequent liver malignancies, for which the only prospect for cure is surgical resection. Liver transplantation is the therapy of choice only in selected cases of HCC. The number of patients suitable for liver resection is sharply limited by many factors: multicentre tumours, non-resectable location, advanced liver cirrhosis and comorbidity. Methods for local tumour ablation have thus been proposed, and some ultrasound-guided procedures have gained ground.

HCC can be treated by ultrasound-guided procedures, such as percutaneous ethanol injection, or by creating a thermal lesion with a radiofrequency electrode (radiofrequency ablation). It is generally accepted that single tumours of less than 5 cm in diameter or multiple tumours (diameter < 3 cm) can be treated. The results obtained appear similar to those for surgical resection. Percutaneous ethanol injection (Fig. 3.20) is a more straightforward procedure, but it requires many sessions. It is performed, without anaesthesia, by inserting, under ultrasound guidance, a fine needle (22 gauge) into different tumour sites. Access is intercostal or subcostal, and 2–5 ml of 95% ethanol is injected at each session. The injection is generally painful, although is rarely judged unbearable. The total amount of injected ethanol can be calculated from Shiina's formula, in which a correction factor is introduced into the sphere volume calculation: $4/3\ \pi\ (r + 0.5)^3$, where r is the tumour radius and 0.5 the correction factor.

In radiofrequency ablation (Fig. 3.21), the patient is connected to the radiofrequency generator by an active electrode and a dispersive electrode. A mild sedative is administered, before the skin is pricked with a small lancet under local anaesthesia. Access is intercostal or subcostal. The radiofrequency generator is activated, and a temperature of about 100 °C is reached around the electrode tip and maintained for 10–20 min. Recent approaches to wider thermal necrosis have centred on modifying the needle electrodes: expandable electrodes enlarge the surface of the active electrode by means of extensible hooks (expandable system); and internal cooling of the needle electrode prevents adjacent tissue desiccation and hence allows higher power input (cooled system).

The results obtained by either percutaneous ethanol injection or radiofrequency ablation are examined by techniques such as CT and magnetic resonance imaging (MRI). In a substantial proportion of cases, the tumour is found to be completely necrotized at the end of treatment. Studies of the long-term therapeutic efficacy of

Fig. 3.20. Percutaneous ethanol injection of a small HCC located in segment 8 of the liver: ethanol is injected after the needle tip is demonstrated in the tumour

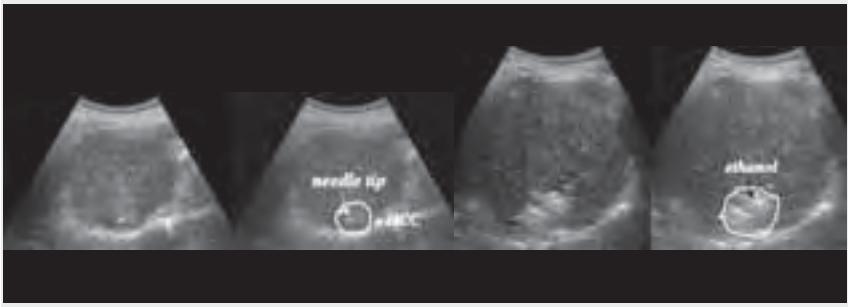

Fig. 3.21. Radiofrequency thermal ablation of a small HCC located in segment 8 of the liver. After the needle-electrode hooks are deployed within the tumour, exposure to radiofrequency (RF) is activated until completion of thermal ablation

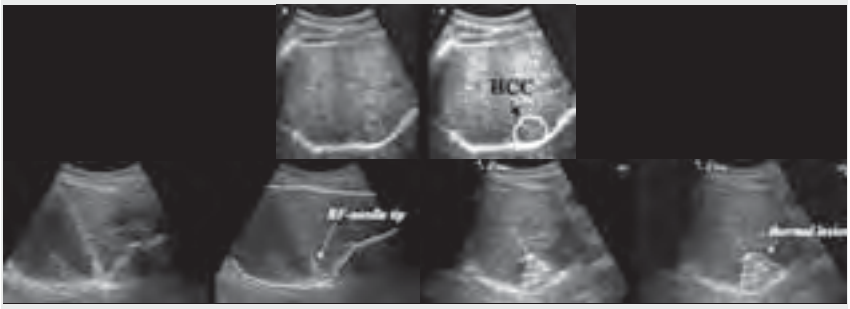

percutaneous ethanol injection and radiofrequency ablation for small HCCs show similar survival rates (about 40–50% at 5 years), which are comparable to those after surgical resection. Recurrences after these procedures are high (65–90% at 5 years), with a disease-free survival rate of about 25% at 3 years. A lower incidence of local recurrence is seen with radiofrequency ablation. Another advantage of this procedure is that tumour ablation can be achieved in only one or two sessions, while a large number of sessions are required for percutaneous ethanol injection over many weeks.

Percutaneous ethanol injection is ineffective for treating liver metastases, and this indication for the procedure has been abandoned. The percutaneous therapeutic option is offered by radiofrequency ablation, which has been used to treat metastases from colorectal cancer and is associated with almost the same number and kind of limitations as those for HCC.

Complications of interventional ultrasonography

Complications of diagnostic and therapeutic procedures have been examined in many multicentre studies. Studies carried out in a single institution are rare because few centres carry out enough procedures to be able to make such analyses. However, multicentre studies tend to underreport data, and data on therapeutic procedures are, in some settings, difficult to analyse. As some of these procedures (particularly drainage of abdominal abscesses and pancreatic collections) are carried out on severely ill patients, it is difficult or impossible to distinguish between procedure-related complications and the disease outcome. For local treatment of liver tumours (by percutaneous ethanol injection or radiofrequency ablation), the patient's condition is relatively good and patients are closely followed after treatment. Complications due to these two procedures are, thus, clearly reported.

Diagnostic procedures

The risks associated with these diagnostic procedures are low: the mortality rate in the multicentre surveys lies in the range 0.001–0.031%. In a recent survey of 16 648 ultrasound-guided liver procedures in one centre, no deaths were observed. The rate of major complications has been estimated as 0.05%, one third of which is due to haemorrhage. One problem that is still the subject of discussion is tumour seeding along the needle track; however, the risk seems to be low (three cases in 100 000 biopsies).

The major caveats to performing ultrasound-guided diagnostic procedures are as follows:

- The risk increases with the use of large needles.
- Puncture of vascular lesions (haemangioma, angiosarcoma) presents a high risk for bleeding.
- It is hazardous to biopsy a normal pancreas because of a false impression of the presence of a 'mass'.
- Pancreatitis may occur after biopsy; the risk for puncturing a phaeochromocytoma is high and should be avoided (diagnosis on the basis of imaging and clinical syndrome).
- Puncture of carcinoid metastases to the liver can cause a carcinoid crisis (somatostatin analogues should be available during puncture).
- Puncture of a hydatid cyst may cause anaphylaxis (check serology whenever such a lesion is suspected; resuscitation drugs and instruments should be available during puncture).
- An aneurysm may be misinterpreted as a lesion (check the lesion with colour Doppler ultrasound before biopsy).

Therapeutic procedures

Percutaneous ethanol injection

In a multicentre survey of 1066 patients with small HCC (greatest diameter, < 5 cm) treated for a mean of 6.7 sessions with a fine needle, one death occurred (0.09%) and 34 major complications (3.2%) were found, 9 of which were haemorrhagic.

Radiofrequency ablation

In two large multicentre studies involving two different techniques (the cooled system and the expandable system), the mortality rate ranged from 0.09% to 0.3%. The major complication rate was 2.2–3.2%. Tumour seeding was observed in 0.04–0.3% of cases.

Treatment of hydatid cyst

No major complications were found in 163 patients with echinococcal cysts treated by PAIR. However, in a large series treated by alcohol injection, without reaspiration, one death was observed due to anaphylactic shock.

Chapter 4

Neck

4

Neck

Indications

The indications for ultrasonography of the neck are:

- diseases of the thyroid gland
- suspected parathyroidal adenoma
- malignant lymphoma, staging and follow-up
- palpable masses (lymph nodes, tumours, cervical cysts)
- abscesses.

Examination technique

Equipment, transducer

A linear or curved array is used, at least 5 MHz or, better, 7.5–10 MHz.

If an abdominal transducer of only 3 MHz is available, a water bag placed between the transducer and the skin permits a rough examination of the neck.

The Doppler technique is useful, especially for examining the thyroid (differentiation of toxic adenomas, diagnosis of autoimmune disorders and some thyroid carcinomas) and for differentiation of enlarged lymph nodes.

Preparation

No specific preparation is necessary.

Position of the patient

The preferred position for examining a patient is supine, with the neck hyper-extended (neck roll). Examination in a sitting position is also possible.

Scanning technique

The initial scans (B-scan) should be transverse, with the strong echoes of the air in the trachea (marking the midline) and the large vessels on both sides used as 'landmarks'. These scans should be followed by longitudinal scans (see Fig. 4.1, Fig. 4.2).

Afterwards, if indicated, examination, with colour Doppler of the whole thyroid gland (Grave-Basedow disease) or nodules and enlarged lymph nodes and tumours, may be necessary, always after the B-scan technique is used.

Fig. 4.1. (a) Topography of the thyroid (Th). (b) Typical transverse scan. Smm, sternocleidomastoid muscle; Stm, sternothyroidal muscle; Om, omohyoid muscle; Ca, common carotid artery; Jv, jugular vein; Tr, trachea; P, parathyroid gland; Rn, recurrent nerve; Vn, vagus nerve; O, oesophagus

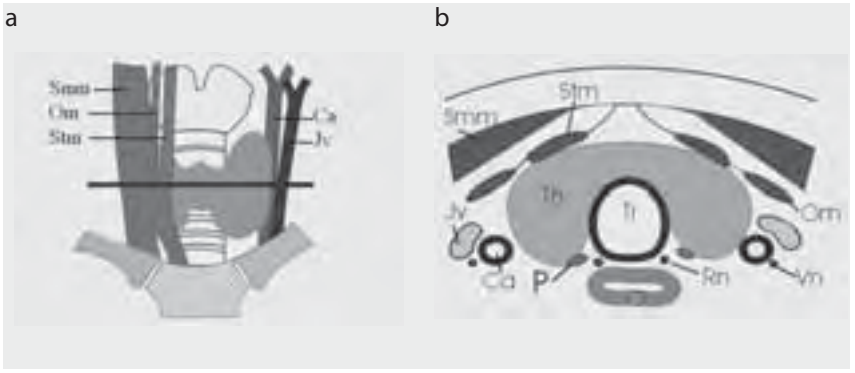

Fig. 4.2. Transducer placement corresponding to Fig. 4.1, Fig 4.2, Fig. 4.3

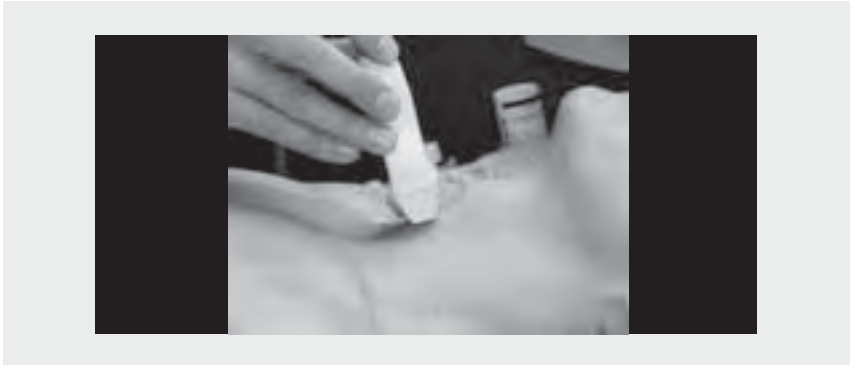

Normal findings

Thyroid gland

The thyroid is shaped like the letter 'H', with an oval lobe on each side of the trachea connected by the isthmus (Fig. 4.3, Fig. 4.4). The pyramidal process, originating from the isthmus and developing in the midline upwards, is a rare inborn variant. Abnormalities, such as the sublingual thyroid or a unilateral gland, are also very rare.

The two lower arteries (inferior thyroid artery) enter the capsule of the thyroid on the dorsal side of the lower poles. The two upper arteries (superior thyroid artery) originating from the external carotid artery enter the upper poles.

The thyroid gland consists of small lobules, each containing around 25 follicles. The content of the follicles depends on their function. It also determines the echo pattern (Fig. 4.3).

The echo pattern of the thyroid gland is homogeneous and echo rich (normofollicular stage), giving a strong contrast to the echo-poor pattern of the surrounding muscles,

Fig. 4.3. (a) Transverse scan of the normal thyroid (Th), panoramic view. The echo-rich pattern of the thyroid contrasts well with the muscles (Fig. 4.1). The air in the trachea (Tr) causes an acoustic shadow and reverberation artefacts. Note the large vessels on both sides. Jv, jugular vein; Ca, common carotid artery; Om, omohyoid muscle; Smm, sternocleidomastoid muscle; Stm, sternothyroidal muscle. (b) Schematic representation of the relation between thyroid function and sonographic pattern. Macrofollicular echo-rich nodules are typical of endemic goitre, normofollicular pattern is the normal finding. A microfollicular echo-poor pattern is typical in Grave-Basedow disease, and an echo-poor pattern caused by cellular infiltration is seen in Hashimoto thyroiditis and in carcinomas

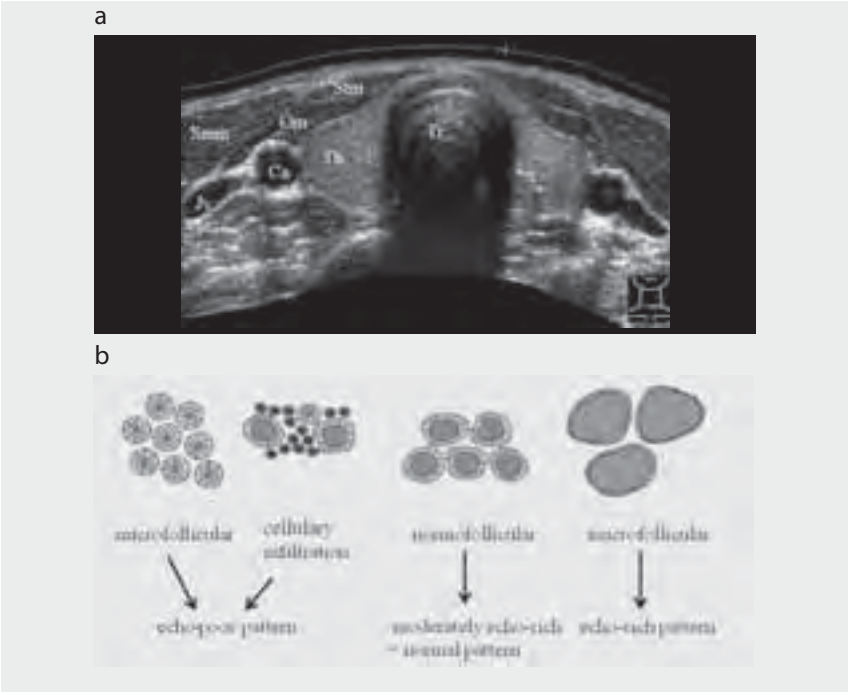

Fig. 4.4. Normal left lobe (31 × 9 mm) and oesophagus, longitudinal scan

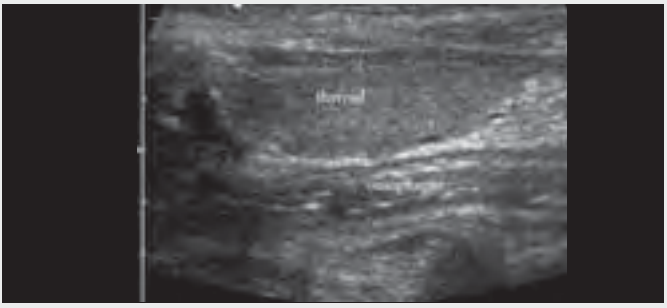

which can serve as a reference. The outline is regular and smooth. The bright echoes behind the isthmus are caused by air within the trachea. The section of the lobes is round or triangular in transverse scans and oval in longitudinal scans (Fig. 4.3, Fig. 4.4).

The size of each lobe is 5–6 cm (length (*a*)) × 2–4 cm (width (*b*)) × 1–2.5 cm (thickness (*c*)). The volume of the whole gland is up to 20 ml in females and 25 ml in males and is determined by adding the volumes (*V*) of both lobes, each calculated from the formula:

$$V = 0.5 \cdot a \cdot b \cdot c \qquad (4.1)$$

The intensive blood circulation can be demonstrated with colour and power Doppler techniques. The peak flow velocity in the thyroid arteries is less than 25 cm/s.

Parathyroid glands

Usually, normal parathyroid glands cannot be found by ultrasound. However, it may be possible to visualize them if a good quality machine with a high frequency (> 7 MHz) is used and if the location of the glands is normal – close to the superior or inferior thyroid artery.

Oesophagus

The cervical oesophagus can be seen in longitudinal scans behind the thyroid as a tubular or target-like structure if this area is scanned with the transducer moved to the left-hand side to avoid the shadow of air within the trachea (Fig. 4.3, Fig. 4.4).

Vessels

The large vessels (the carotid artery and the jugular vein) are behind the sternocleidomastoid muscles and lateral to the thyroid gland. The jugular vein shows as an oval shape and may collapse in certain phases of respiration or from the pressure of the transducer. The carotid artery is round and shows stronger wall echoes than the vein (Fig. 4.3).

Lymph nodes

The number of the lymph nodes is especially high in the neck. High-frequency ultrasound frequently demonstrates normal lymph nodes, which are usually oval, with a maximum diameter of 8 mm. The pattern is echo poor with an echo-rich hilus. In older people, the pattern becomes increasingly echo rich due to fatty degeneration, mostly starting from the hilus (see Fig. 4.5). The lymph nodes of older people are more difficult to detect because of their low contrast with the surrounding soft tissue. The normal vessels, which branch out symmetrically from the hilus ('hilar vascularity'), can be evaluated with high-resolution power Doppler.

Muscles

The muscles are echo poor with a striated structure. They are important as anatomical landmarks and serve as a reference point for evaluating the echo pattern of the thyroid.

Fig. 4.5. Normal lymph node (arrow) between vessels (Jv (jugular vein), Ca (common carotid artery)) and muscle (Smm (sternocleidomastoid muscle)). The oval shape and the echo-rich hilus are characteristic

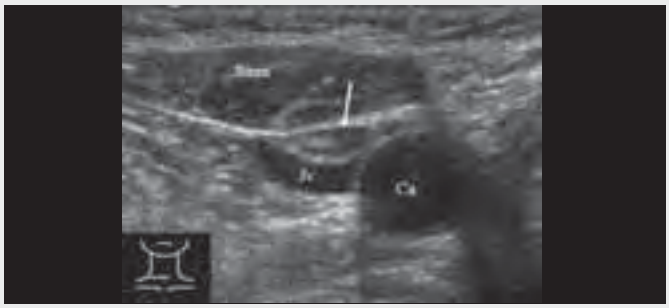

Pathological findings

Thyroid

Congenital abnormalities

Failure of the thyroid to descend during embryogenesis leads to an ectopic thyroid or to an abnormal lobe in the midline (pyramidal lobe). The size of the isthmus is variable. The absence of one lobe is very rare. Abnormalities of the vessels are more common, e.g. a fifth artery (thyroid ima artery).

Endemic goitre (iodine-deficiency goitre)

Endemic goitre is very common in areas of iodine deficiency. Enlargement of the thyroid is a lifelong disorder in which the thyroid is enlarged with a homogeneous, echo-rich pattern in the early stage of the disorder (Fig. 4.6, see also Fig. 4.5).

The pattern becomes inhomogeneous (nodular goitre, Fig. 4.7), mainly in middle-aged patients, because of inhomogeneous growth of the cells and the development of macrofollicular echo-rich nodules. Degenerative alterations, such as cystic degeneration of the nodules and calcification, may also occur. Liquid parts of the nodules are echo free and may imitate cysts. Calcifications cause strong echoes, sometimes with acoustic shadows.

Autoimmune disorders of the thyroid

A common sonographic finding in autoimmune disorders of the thyroid is an echo-poor pattern.

Grave-Basedow disease

In this disease, autoantibodies against the thyroid-stimulating hormone receptor stimulate the thyroid in the same way as the hormone. The disease occurs more often in young (female) adults, but can be seen at any age. The younger the patient, the more characteristic are the symptoms of hyperthyroidism.

Fig. 4.6. Simple goitre (iodine deficiency) with a volume of 54 ml

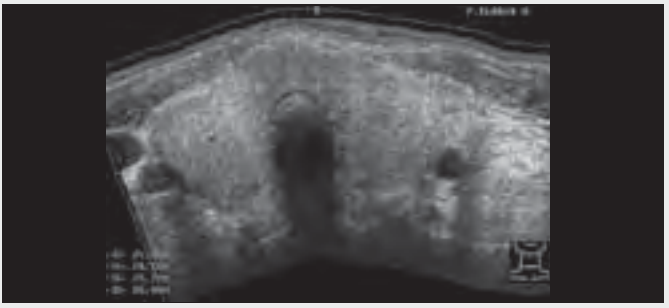

Fig. 4.7. Nodular goitre (iodine deficiency) with a volume of 96 ml. Typical inhomogeneous and echo-rich pattern

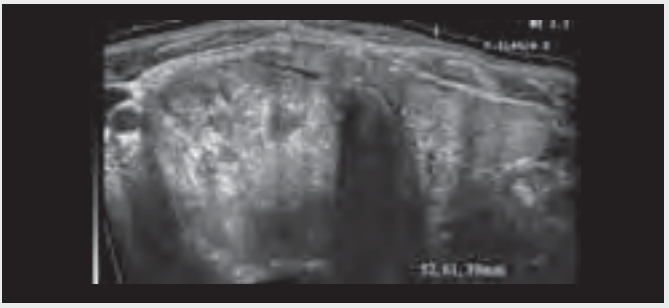

Ultrasound can be used to visualize a moderately enlarged thyroid with a characteristic echo-poor, homogeneous or slightly inhomogeneous pattern corresponding histologically to hyperplastic but empty follicles (Fig. 4.8).

Colour and power Doppler examinations demonstrate striking hypervascularity (Fig. 4.9). The flow in the feeding arteries is rapid, at more than 100 cm/s; a decrease to less than 40 cm/s on treatment is interpreted as a sign of a good prognosis.

Focal lesions (nodules) within the echo-poor thyroid in Grave-Basedow disease are independent of the basic disease and should be considered separately.

Autoimmune thyroiditis (Hashimoto thyroiditis)

In this disease, lymphoplasmacellular infiltration slowly destroys the gland. This infiltration causes an echo-poor pattern of the thyroid, which develops over a long time. In the initial stage, the gland may be slightly enlarged; in the later (atrophic) stage, however, the thyroid becomes small with a volume of less than 10 ml (Fig. 4.10).

Colour Doppler ultrasound demonstrates hypervascularity, which is not as marked as in Grave-Basedow disease. The flow in the feeding arteries is less rapid.

Fig. 4.8. Grave-Basedow disease. The moderately enlarged thyroid shows a characteristically echo-poor pattern without contrast with the muscles (m, M). The outline of the right lobe is marked. The image is composed of transverse scans of the right and left lobes. Ca, common carotid artery

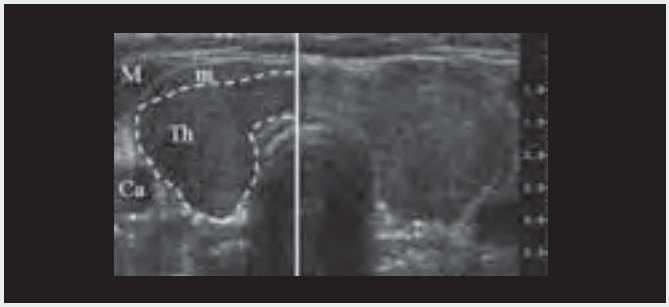

Fig. 4.9. Grave-Basedow disease. (a) Colour Doppler (white) demonstrates hypervascularity. (b) Spectral Doppler shows the acceleration of the flow in the feeding artery (ca. 50 cm/s)

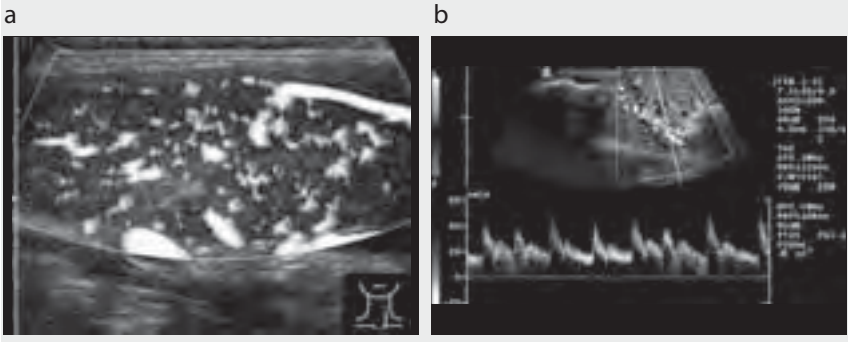

In the early stage, hyperfunction may occur, and differentiation from Grave-Basedow disease becomes difficult. The typical clinical feature of the later stage is hypothyroidism.

Toxic adenoma, toxic goitre

The proliferation of autonomic cells, stimulated by iodine deficiency, leads to autonomic, toxic nodules or a diffuse functional autonomy causing hormone production independent of stimulation by thyroid-stimulating hormone. When the volume of the autonomic tissue is greater than 5–10 ml (depending on the iodine supply), hyperthyroidism results. The incidence of this type of hyperthyroidism is, therefore, higher than that of Grave-Basedow disease in areas of iodine deficiency. The disorder develops in a long-standing simple goitre and is seen mainly in the elderly (Fig. 4.11).

Fig. 4.10. Hashimoto thyroiditis. Note: (a) the echo-poor pattern (B-scan) of the small gland; (b) hypervascularity (power Doppler). Smm, sternocleidomastoid muscle; Ca, common carotid artery; Jv, jugular vein

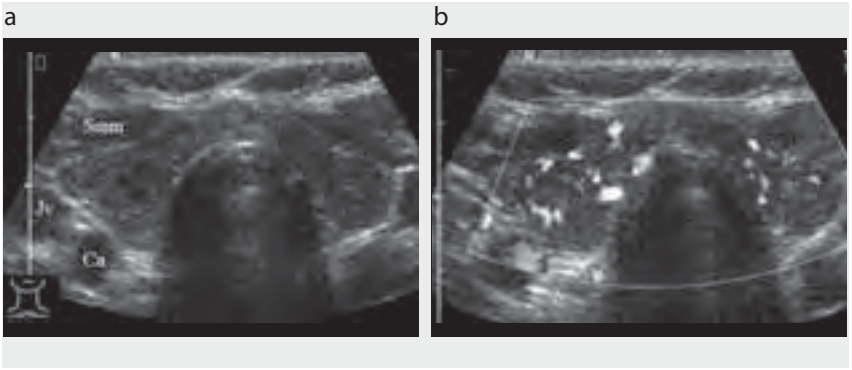

Fig. 4.11. Toxic adenoma. (a) Oval nodule (9 mm) with echo-poor halo. (b) Doppler technique shows a hypervascular pattern and the vascular halo

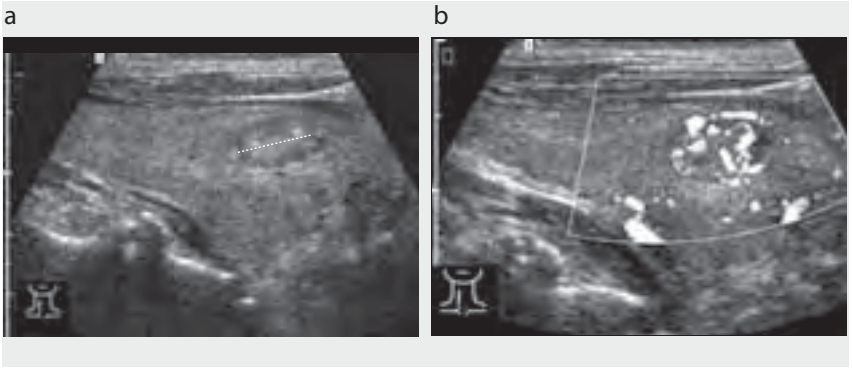

A typical autonomic adenoma is echo poor. The Doppler technique demonstrates hypervascularity (compared with the surrounding tissue) within the nodule and a halo consisting of vessels. Warm or toxic nodules may show a more echo-rich pattern in up to 30% of people, and hypervascularity may be missing in regressive nodules. Currently, there are no reliable sonographic signs to indicate the warm or toxic nature of a nodule. There is therefore no specific echo pattern for diffuse autonomy. A diagnosis of toxic nodule can be assumed only if others (e.g. Grave-Basedow disease, toxic adenoma) are excluded (Table 4.1).

Caution! Highly differentiated carcinomas of the thyroid are also hypervascular but without a halo.

Hypothyroidism

In adults, hypothyroidism is a consequence of the loss of thyroid tissue caused by thyroiditis, radiation therapy to the neck, radioiodine ablation or surgical resection of the thyroid. In most cases, ultrasound demonstrates a small thyroid (< 10 ml). A

Table 4.1. Clinical and sonographic differential diagnosis of hyperthyroidism

Ultrasound B-scan	Doppler	Additional aspects	Disorder
Symmetric goitre, echo-poor pattern	Hypervascularity, high velocity	Anti-TSH ophthalmopathy	Grave-Basedow disease
Moderate enlargement, echo-poor pattern	Hypervascularity	Anti-thyroid peroxidase	Hashimoto thyroiditis (initial stage)
Nodule, echo-poor, halo	Hypervascular halo	TSH	Toxic adenoma
Normal thyroid	Normal finding	TSH	Diffuse autonomy or thyreotoxicosis caused by drugs

TSH, thyroid-stimulating hormone.

characteristic echo-poor pattern is found in the late, atrophic stage of Hashimoto thyroiditis. The echo pattern in other cases is relatively normal or less homogeneous.

Thyroiditis

Pyogenic thyroiditis is very rare. Symptoms such as tenderness, swelling and redness are more often caused by pyogenic inflammation of the soft tissue around the thyroid. Ultrasound demonstrates dislocation of the thyroid and inflammation of the soft tissue (see below).

Subacute thyroiditis (giant cell thyroiditis, de Quervain thyroiditis) is thought to be viral in origin, because this disease often follows respiratory tract infections. Pain radiating to the mandible and the ear is a typical symptom.

An ultrasound B-scan shows an echo-poor area with a blurred margin. The gland may be slightly enlarged (Fig. 4.12). The lesions are more or less hypovascular than the surrounding thyroid tissue.

Chronic fibrosing thyroiditis (Riedel thyroiditis) is extremely rare. An irregular echo pattern caused by blurred echo-poor, nodular lesions is reported in a few cases.

Fig. 4.12. De Quervain thyroiditis. (a) Transverse (30 × 20 mm) and (b) longitudinal (46 × 24 mm) scan of the left lobe. Note the inflamed lymph node (Ln, 9 mm × 6 mm). The border of the slightly echo-poor inflamed area is better seen in the longitudinal scan. Ca, common carotid artery, Jv, jugular vein, M, muscles, TR, trachea

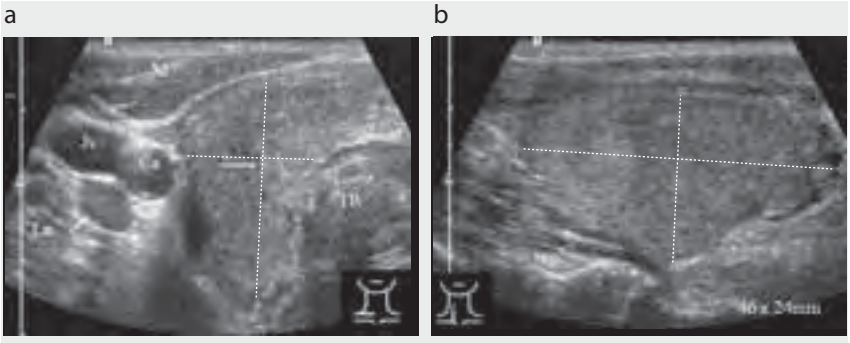

Focal lesions

Cysts and cystic lesions

True cysts of the thyroid are very rare, and most cystic echo-free lesions are cystic-degenerated nodules. The echo pattern of the solid parts determines its clinical classification. A typical event is the sudden onset of pain coupled with a palpable swelling caused by bleeding into the cyst (e.g. when practising sports). In these cases, ultrasound demonstrates a cloud of echoes floating in the fluid. The puncture shows brownish fluid ('chocolate cyst') (Fig. 4.13).

Fig. 4.13. Cystic lesions of the thyroid with haemorrhage ('chocolate cysts'). (a) Floating echoes (21 mm). (b) Sedimented blood cells. Note the echoes of the puncture needle (arrows). Ca, common carotid artery; Jv, jugular vein; Smm, sternocleidomastoid muscle

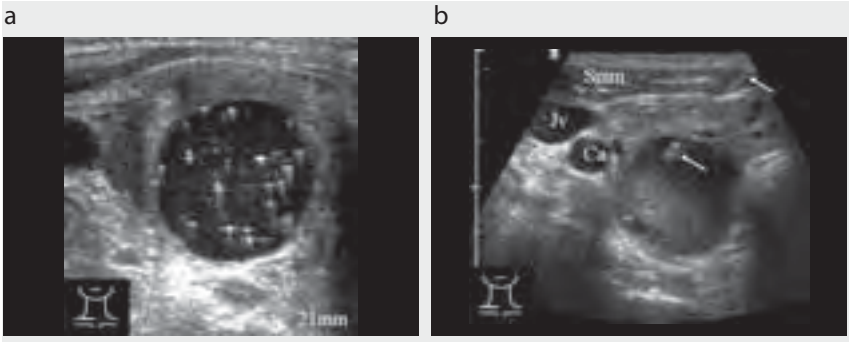

Solid nodules

Nodules in the thyroid are found in up to 50% of asymptomatic persons. Malignant tumours of the thyroid are rare. Nevertheless, differentiation of benign and malignant nodules is a challenge in the ultrasonic diagnosis of the thyroid.

Benign lesions

True adenomas are encapsulated, grow slowly and are mainly microfollicular. Adenomas vary in their function. Warm or toxic adenomas are highly differentiated and can accumulate iodine independently of thyroid-stimulating hormone regulation (see above).

Depending on the follicular structure, adenomas are mostly echo poor (microfollicular, Fig. 4.14) or more echo rich and rather homogeneous. Their contour is smooth. An echo-poor halo (B-scan) with vessels around the nodule is characteristic of a benign adenoma and is, therefore, best demonstrated with colour Doppler. Warm adenomas often show hypervascularity (Fig. 4.15).

Hyperplastic nodules develop over several years in cases of endemic goitre, caused by the differential growth ability of the thyroid cells. These lesions are not true neoplasms. Owing to their normofollicular or macrofollicular structure, they are often echo rich with an echo-poor halo. Degenerative alterations, such as cystic parts or calcifications, are common, causing a complex sonographic pattern with echo-free areas and strong echoes (Fig. 4.16, Fig. 4.17).

Fig. 4.14. Adenoma (21 mm) with a complex echo pattern caused by calcification, regressive cystic components and an echo-poor halo

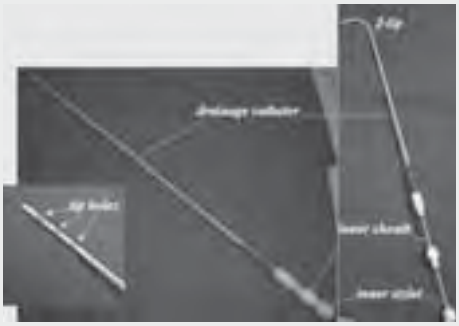

Fig. 4.15. (a) B-scan of an adenoma of the thyroid. shows an echo-poor pattern and a halo. (b) Power Doppler shows signals in the nodule and the vascular halo

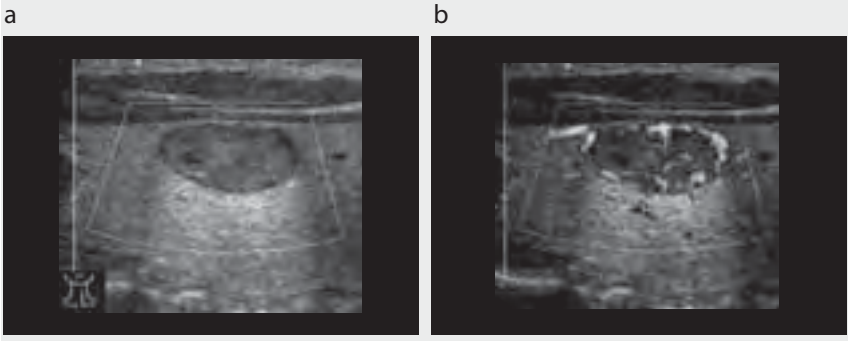

Fig. 4.16. Nodule with a moderately echo-poor pattern surrounding tissue

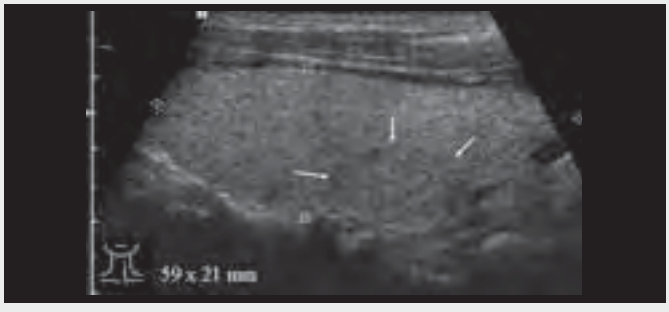

Fig. 4.17. Echo-rich nodule (8 mm) and echo-poor nodule with halo (19 mm)

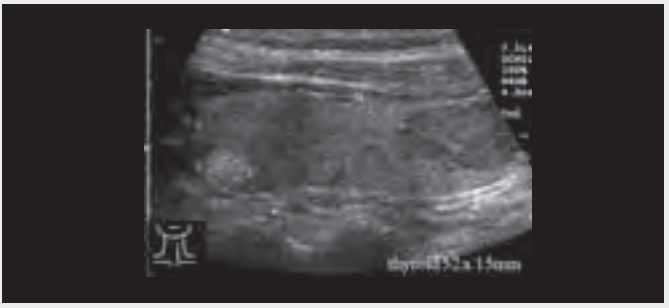

Malignant tumours

Papillary and **follicular carcinomas** are the commonest thyroid carcinomas (ca. 70% and 15%, respectively). They are highly differentiated and grow slowly. **Anaplastic carcinoma** is less common, especially in areas with no iodine deficiency (ca. 5–10%), and is a carcinoma of older patients (> 65 years). **Medullary carcinoma** arises from the C cells. It occurs sporadically or as part of multiple endocrine neoplasia (IIa or IIb) (Fig. 4.18, Fig. 4.19, Fig. 4.20, Fig. 4.21, Fig. 4.22, Fig. 4.23). **Metastases**, mainly from lung cancer and malignant lymphomas, may involve the thyroid gland.

Fig. 4.18. Small papillary carcinoma (9 mm). (a) B-scan shows an echo-poor lesion with a slightly irregular contour, partially blurred halo-free outline and without a halo. (b) Power Doppler shows a feeding vessel but no vascular halo

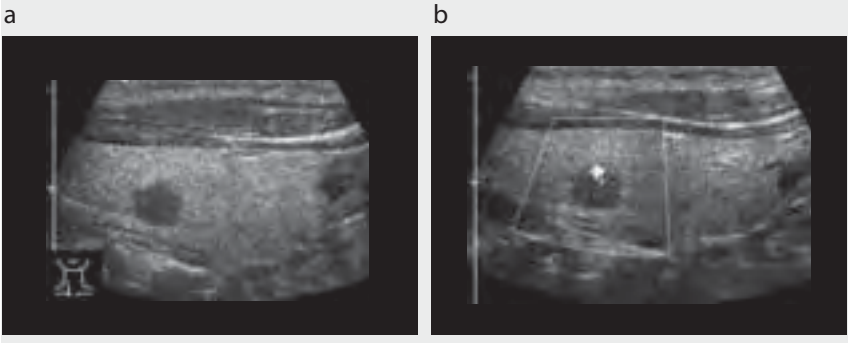

The malignant tumours are echo poor and slightly inhomogeneous, although an inhomogeneous pattern is difficult to recognize in smaller lesions. An extremely echo-poor pattern is found in malignant lymphomas and anaplastic carcinomas. Lack of a halo is typical. The contour is irregular and may show pseudopods or spicula. Interruption of the thyroid capsule and infiltration of the surrounding tissue can be visualized. When the sagittal diameter is greater than the transverse diameter, the finding is usually suspect.

Fig. 4.19. Papillary carcinoma (between arrow, 19 mm) of the thyroid with dispersed stronger echoes indicating microcalcification causing an incomplete shadow

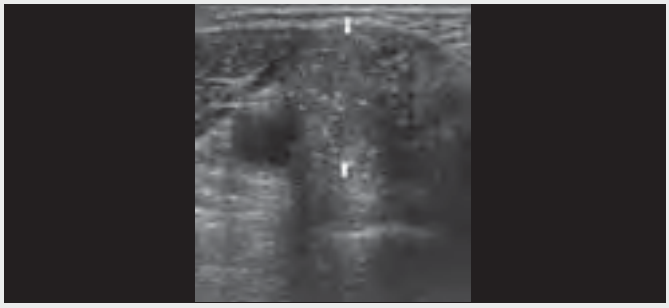

Fig. 4.20. Follicular carcinoma (19 mm). Note the irregular contour, the penetration through the capsule (arrow) and the complex echo pattern with spotted calcifications (shadows)

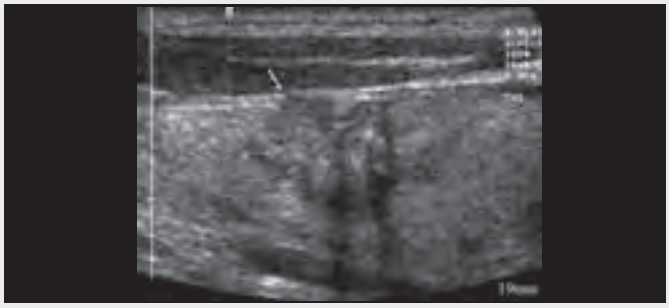

Fig. 4.21. Large anaplastic carcinoma (diameter, 67 mm) arising in a nodular endemic goitre. The carcinoma in the left lobe is echo poor; the pattern in the right lobe and the isthmus is echo rich. TR, trachea (see Fig. 4.7)

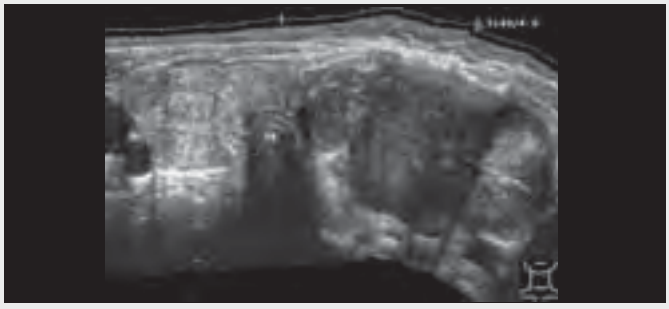

Fig. 4.22. Metastasis (57 mm × 34 mm) from lung cancer in the right thyroid lobe: inhomogeneous, moderately echo-poor pattern, irregular outline

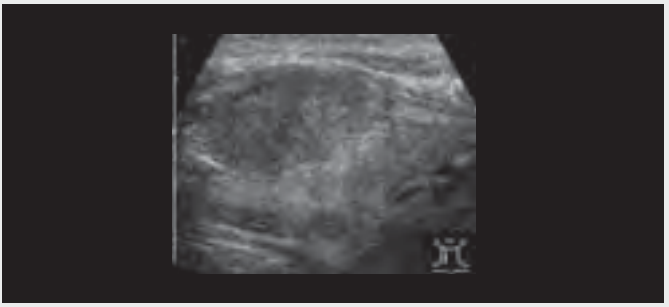

Fig. 4.23. Malignant lymphoma (secondary) in the left thyroid lobe (18 mm × 22 mm)

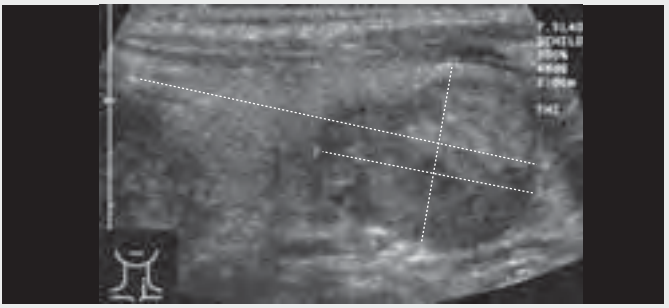

Dispersed strong echoes arising from microcalcifications are characteristic in papillary carcinoma. Spotted calcifications also occur in medullary and anaplastic carcinomas. Occasionally, small echo or cystic parts are seen in papillary carcinomas.

The Doppler technique shows hypervascularity in highly differentiated carcinomas, but without a vascular halo. Anaplastic carcinomas, most of the metastases and the lymphomas are hypovascular when compared to the thyroid.

Post-treatment thyroid

Providing the patient with information about the treatment (disease and method) is a prerequisite for post-treatment check-ups This is especially important after surgery.

After resection of an endemic goitre, relatively large nodular relapses (Fig. 4.24) with inhomogeneous echo patterns on both sides of the trachea may be seen. Lack of the isthmus is typical of the post-operative situation. After subtotal resection, it is sometimes difficult to identify small thyroid remnants, especially if they are not echo rich.

Examination of the lymph nodes is the main objective of follow-up checks after surgical treatment of carcinomas. Enlarged, rounded lymph nodes are suspect (see

Fig. 4.24. Relapse of a nodular endemic goitre (no isthmus) with large nodules with inhomogeneous echotexture

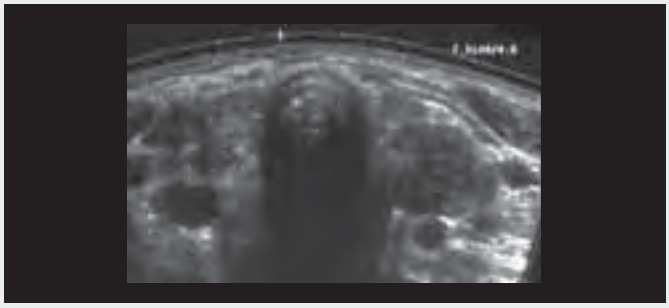

below). It is interesting that lymph node metastases of highly differentiated carcinomas show a hypervascularity similar to that of the primary tumours.

In Grave-Basedow disease, the typical echo-poor pattern disappears with functional remission after treatment. A reduction in the elevated flow velocity in the feeding arteries appears to be an early sign of successful treatment. In contrast, the echo-poor pattern of Hashimoto thyroiditis is seen in all phases, independent of function.

Radioiodine ablation of the thyroid or radiation of the neck (lymphomas) causes a reduction of thyroid tissue and ultimately leads to a small thyroid.

Warm or toxic adenomas treated successfully with alcohol instillation (see below) not only become smaller and more echo rich, but their hypervascularity disappears.

Parathyroid glands

Ultrasound is the first-line method for preoperative localization of orthotopic adenomas of the parathyroid glands in primary hyperthyroidism and for diagnosis of hyperplasia of the parathyroid glands in patients with renal failure.

Orthotopic adenomas are more or less echo poor, smooth nodules at the dorsal border of the thyroid. Their shape is variable, mostly oval, but sometimes moderately long, triangular or lobed. The pattern is more echo poor than that of the normal thyroid but may become complex, with more echo-rich and echo-free areas due to regressive alterations.

Colour Doppler enables identification of the feeding vessels (Fig. 4.25, Fig. 4.26).

Branchial cervical cysts

Medial thyroglossal cysts are located in the midline below the hyoid, above the thyroid. They are usually diagnosed in childhood.

Lateral cervical cysts are located at the anterior margin of the sternocleidomastoid muscle. They grow slowly and sometimes become visible or symptomatic in young adults. Ultrasound demonstrates a lesion with the typical signs of a cyst (round or oval, smooth outline, echo free). In some symptomatic cases, a cervical cyst shows a more or less echo-rich, homogeneous pattern, caused by a secondary infection (Fig. 4.27). A cystic cutaneous fistula may develop.

Fig. 4.25. Adenoma of the parathyroid (p, 12 mm × 4 mm), echo-poor pattern, lobulated shape

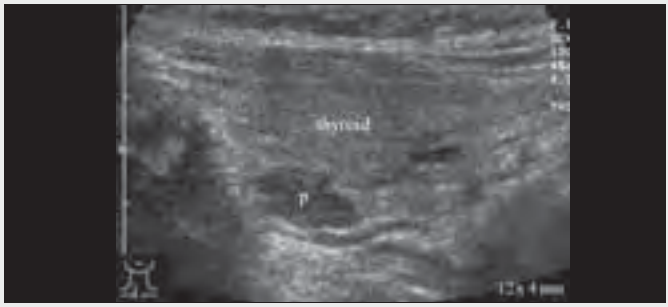

Fig. 4.26. Adenoma of the parathyroid. Echo-poor pattern showing irregular outline. Power Doppler shows the vessels inside the adenoma. Oe, oesophagus

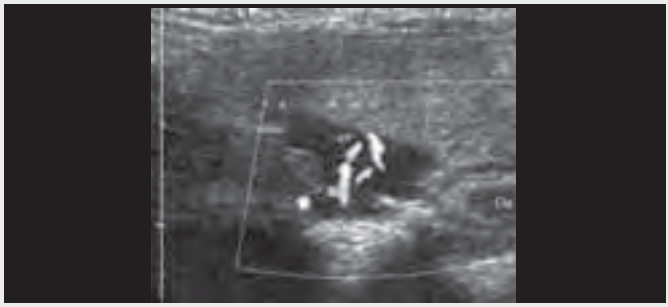

Fig. 4.27. Lateral cervical cyst (diameter, 33 mm). The homogeneous echoes within the cyst are caused by a secondary inflammation. Cranially, note an enlarged, echo-poor inflammatory lymph node

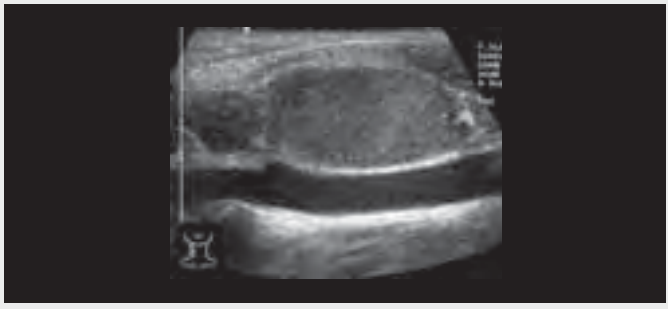

Primary tumours in the neck

Primary tumours in the neck are rare in adults.

Lipomas and lipofibromas originating from the skin are situated in the nucha. Their pattern is echo rich, and the margins are smooth (Fig. 4.28).

Glomangioma arising from the carotid glomus is demonstrated in the carotid bifurcation as a homogeneous, echo-poor, hypervascular tumour.

Malignant tumours of the deeper layers arise in the oesophagus, the larynx or the hypopharynx. They are visualized as echo-poor, inhomogeneous masses with irregular outlines, often infiltrating the surrounding structures (e.g. the thyroid).

Fig. 4.28. Fibrolipoma (diameter, 54 mm) in the neck. The location, the oval shape and the echo pattern are characteristic

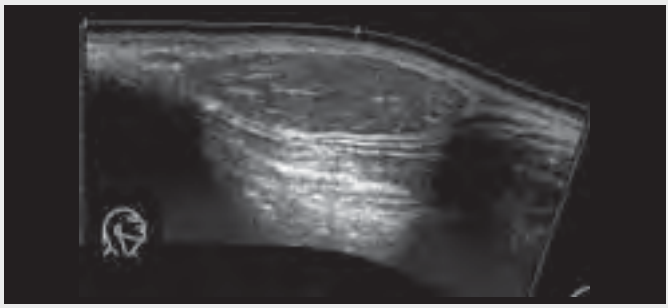

Inflammation of the soft tissue

Inflammation of the cervical soft tissue usually originates from a neighbouring structure, such as the tonsils, or lymphogenously or iatrogenically. The echo pattern may be very poor (abscess) or complex and echo rich with strong echoes (gas) (Fig. 4.29). The distension depends on the fascias and anatomical structures. Structures such as muscles or the thyroid are swollen. In the jugular vein, thrombosis may occur as a complication or, in some cases, as the initial focus (Fig. 4.30). In these cases, the vein is no longer compressible and the wall is thickened. The thrombus itself is echo poor.

Colour Doppler demonstrates hyperaemia of inflamed tissue or avascular abscesses.

Typical peritonsillar abscesses can be demonstrated as echo-poor lesions medial to the large vessels by using the air echoes inside the larynx and the moving echoes of the tongue as anatomical landmarks.

Lymph node diseases

Enlarged lymph nodes are often found in the neck. Reactive hyperplasia may be the commonest cause of lymphadenopathy, but malignant lymphomas and metastases of tumours of the head, the neck or the lung and even distant metastases (e.g. stomach cancer) are also common. Diagnosis is usually made by palpation, often by patients themselves. Several studies have shown, however, that ultrasound is useful in detecting nonpalpable 'occult' metastases and for the staging and follow-up of lymphomas.

Fig. 4.29. Abscess behind the (displaced) left thyroid lobe. B-scan shows an inhomogeneous, echo-poor area with some gas echoes (arrow). A line of strong air echoes indicates the trachea. Ca, common carotids artery; Jv, jugular vein

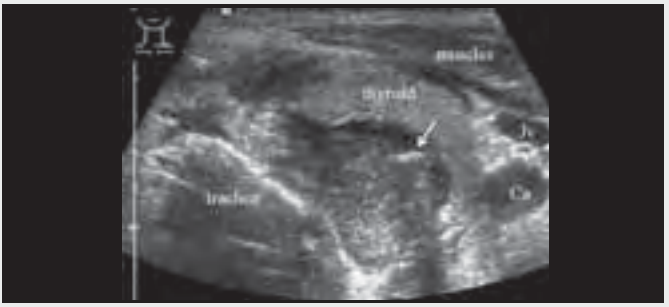

Fig. 4.30. Inflammatory thrombosis of the left jugular vein. The vein is dilated (compared with the carotid artery) and filled with echo-rich thrombotic material. The wall is echo poor (arrow). Ca, common carotid artery

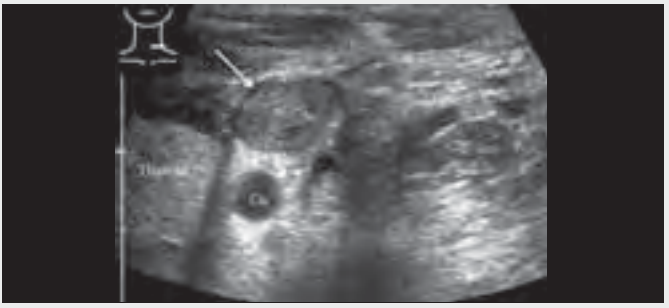

Lymph nodes involved in **inflammatory diseases** are usually enlarged, but their architecture is not destroyed (Fig. 4.31, Fig. 4.32). Ultrasound therefore visualizes enlarged, oval lymph nodes with smooth contours. The long (longitudinal) diameter is greater than 5–10 mm. The ratio of the long to the short axis remains greater than 1.5. The pattern is more or less echo poor, and the echo-rich hilus is discernible. Colour Doppler shows hyperaemia but normal vascular architecture, with vessels branching out from the hilus ('hilar vascularity') (Fig. 4.32 (a)). The resistance index in inflammatory lymph nodes is less than 0.65.

Abscess formation may cause echo-free areas, and they may break through the capsule into the surrounding tissue.

Granulomatous inflammation (*Boeck disease*), tuberculosis or *Mycobacterium avium-intracellulare* complex infection often result in atypical sonographic findings of the lymph nodes involved, similar to the findings for malignant lymph nodes. The enlarged lymph nodes are rounder, and the patterns become inhomogeneous

Fig. 4.31. Enlarged inflammatory lymph nodes (LK). B-scan shows an echo-poor pattern but an echo-rich hilus (transverse scan through the short axis of the lymph node). Ca, common carotid artery

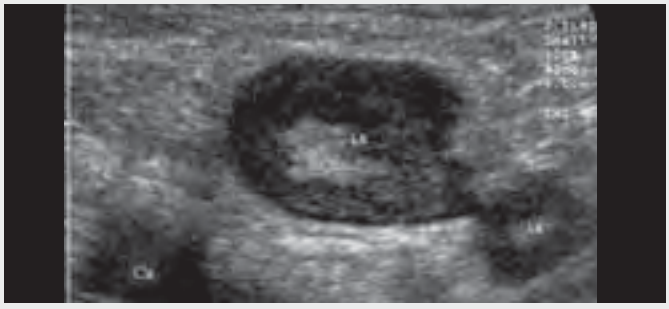

Fig. 4.32. Power Doppler view of cervical lymph nodes. (a) Inflammatory lymph node shows hilar vascularity. (b) Lymph node metastasis (diameter, 28 mm) with peripheral vascularity

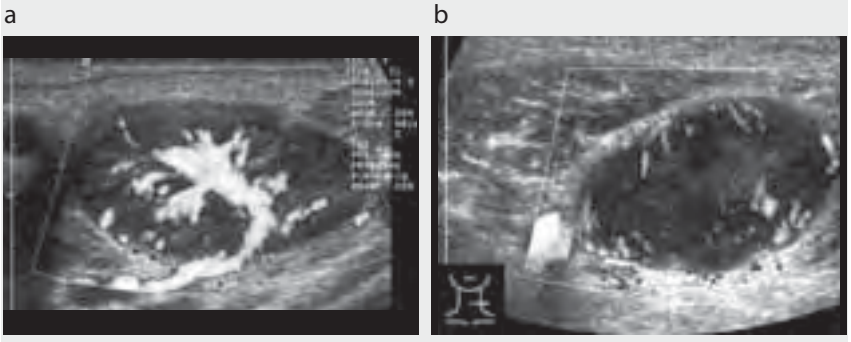

with echo-poor granulomas or echo-free caseation. Atypical vessel architecture, displacement of vessels due to caseation and a higher resistance index (up to 0.72) are described in cases of **tuberculosis**.

Metastatic lymph nodes are moderately or considerably enlarged, with a more rounded shape. The pattern is less echo poor and inhomogeneous, and the hilus sign is often missing. The contour is irregular, with short pseudopods, indicating infiltration through the capsule (Fig. 4.33). The vascular pattern is irregular, with vessels penetrating the capsule ('peripheral vascularity') (Fig. 4.32b) and the resistance index is high (> 0.8–0.9).

The lymph nodes involved in **malignant lymphomas** are extremely echo poor. They are oval, round or polygonal if arranged in a conglomerate. The margin is smooth (Fig. 4.34). The vascular pattern is variable and often regular, as in inflammatory hyperplasia, and the resistance index is less elevated (around 0.65–0.75).

Fig. 4.33. Lymph node metastasis (24 mm × 18 mm) from lung cancer: inhomogeneous, echo-poor pattern compared with the pattern of the thyroid. The jugular vein (Jv) is displaced. Ca, common carotid artery

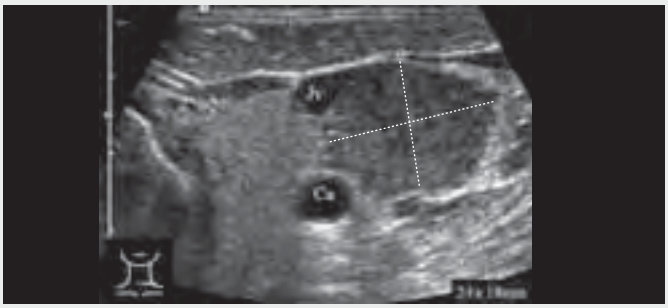

Fig. 4.34. Conglomerate of enlarged cervical lymph nodes, non-Hodgkin lymphoma: echo-poor pattern, oval or polygonal shape, no hilus sign. Smm, sternocleidomastoid muscle

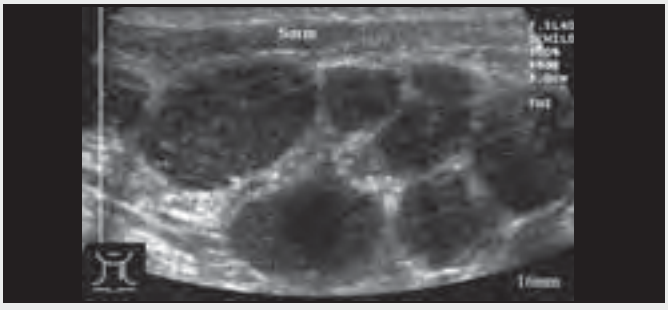

Differential diagnosis

Goitre

Generally, differentiation of an enlarged thyroid is not difficult.

An endemic goitre shows an echo-rich, homogeneous or mostly inhomogeneous echo pattern, with echo-rich macrofollicular nodules and regressive alterations. Echo-poor sections in endemic goitre, especially if connected with fast growth, are suspect and may indicate malignancy.

Large malignant tumours cause asymmetric enlargement of the thyroid and show an echo-poor, heterogeneous pattern. Dispersed stronger echoes in the mass are caused by calcifications (microcalcification). They should not be misinterpreted as an echo-rich pattern.

In Grave-Basedow disease, the thyroid is symmetrically enlarged and echo poor, with a smooth margin and a regular shape. Hypervascularity is striking and nearly pathognomonic. The similar Hashimoto thyroiditis, with a slight echo-poor enlargement, can be differentiated by less rapid flow in the feeding arteries or more easily by clinical aspects (no ophthalmopathy) and the analysis of antibodies (Table 4.2).

Table 4.2. Differentiation of the enlarged thyroid (goitre)

Ultrasound B-scan	Doppler	Other aspects/function	Diagnosis
Symmetric or asymmetric goitre, echo-rich, mostly inhomogeneous, regressive alterations	–	Normal function, late-stage hypothyroidism and hyperthyroidism (toxic adenoma(s) possible)	Endemic goitre
Asymmetric, echo-poor, irregular outline	Sometimes hypervascular	Fast-growing goitre	Malignant tumour
Symmetric, echo-poor, smooth margin	Hypervascular, high flow	Hyperthyroidism (ophthalmopathy), TSH antibodies	Grave-Basedow disease
Symmetric, echo-poor moderate enlargement	Hypervascular	Hyperthyroidism or normal function, TPO antibodies	Hashimoto thyroiditis, initial stage

TSH, thyroid-stimulating hormone; TPO, thyroid peroxidase.

Small thyroid

Small thyroids (< 10 ml) in adults are consequences of inflammatory disease or therapy. Any previous surgical reduction or radioiodine treatment should be established from the case history. A small thyroid with a regular echo pattern, associated with hypothyroidism, can also be due to previous radiation therapy (e.g. for malignant lymphoma). An echo-poor pattern is typical in the atrophic stage of Hashimoto thyroiditis.

Echo-poor nodule

Differentiation of focal lesions in the thyroid gland is the most challenging aspect of sonographic diagnosis of the thyroid. Nodules are very common and mostly asymptomatic. Malignant tumours are rare and, in the early stage, are also asymptomatic.

Echo-rich lesions are hyperplastic nodules or benign adenomas. Echo-poor nodules are a problem, as many adenomas and malignant tumours show this ultrasonic feature. Additionally, warm and toxic adenomas as well as highly differentiated carcinomas are hypervascular. In many cases, a fine-needle biopsy is required to establish a final diagnosis, although there are several sonographic signs that should raise suspicions of malignancy (Table 4.3). The presence of only one of these symptoms should be investigated by puncture; if three or more of these signs are present, malignancy is likely. The sonographic criteria for malignant focal lesions of the thyroid are:

- echo-poor, inhomogeneous pattern
- microcalcifications
- no halo (B-scan)
- greater sagittal diameter
- size > 3 cm

- blurred margin
- irregular contour
- infiltration of surrounding structures
- high attenuation
- hypervascularity within the nodule but with no vascular halo (Doppler) and
- enlarged lymph nodes.

It is also useful to look at other symptoms and findings. A history of radiation therapy of the neck, a family history of thyroid nodules, fast growth of the nodule or enlarged lymph nodes are suspect. Proof of a warm, toxic nodule by scintigraphy or a low level of thyroid-stimulating hormone (but not hyperthyroidism itself) exclude a carcinoma. The differential diagnoses of echo-poor lesions is illustrated in Table 4.3.

Table 4.3. Differential diagnoses of echo-poor focal lesions of the thyroid

Disorder	Echo pattern	Contour	Doppler
Follicular adenoma	Halo	Smooth	Hypervascular
Carcinoma, highly differentiated	Heterogeneous, no halo, microcalcifications	Irregular, blurred	Hypervascular, no vascular halo
Carcinoma, poorly differentiated	Heterogeneous	Irregular, blurred	Hypovascular
De Quervain thyroiditis	Homogeneous	Blurred	Hypovascular
Abscess (acute thyroiditis)	Echo free	Blurred	Avascular
Parathyroid adenoma	Heterogeneous	Smooth, variable shape	Feeding vessels

Other lesions and masses in the neck

It is generally not difficult to differentiate between thyroid tumours and tumours of other structures. Tumours of the lymph nodes are situated lateral to the great vessels. Carcinomas of the hypopharynx, larynx or cervical oesophagus are situated behind the thyroid, but may infiltrate the gland from the dorsal surface. Rare tumours and masses, such as glomangiomas or cervical cysts, are also characterized by a typical location.

Ultrasound-guided fine-needle biopsy

Fine-needle biopsy is a good complement to ultrasonography of the thyroid and the neck. If the general recommendations and rules discussed in Chapter 3 are followed, biopsy of lesions in the neck is particularly easy, almost without risk and can be carried out on outpatients.

Fine-needle biopsy of thyroid nodules is done mainly by aspiration, as described above. A second biopsy is recommended for less experienced operators to avoid false or insufficient results. A complementary biopsy with a cutting needle may be useful for the diagnosis of lymphomas and anaplastic carcinomas.

All suspect lesions should be investigated by fine-needle biopsy of the thyroid, if a diagnosis cannot be made with non-invasive tests. De Quervain thyroiditis can be diagnosed with cytological proof of the characteristic giant cells.

In the same way, lesions and masses outside the thyroid, especially unclear tumours, abscesses and suspicious lymph nodes, can be punctured. To avoid fistulas, if an atypical, possibly tuberculous, lymph node is punctured, it is useful to shift the skin over the lesion before inserting the needle.

Finally, an ultrasound-guided puncture can be used to treat hot adenomas of the thyroid or of the parathyroid gland by percutaneous injection of 96% ethanol. The position of the needle has to be controlled precisely to avoid injury to the recurrent nerve. Colour Doppler demonstrates a decrease in hypervascularity after successful treatment, while a B-scan shows regression in the size of the nodule and a less echo-poor pattern.

Chapter 5

Chest

5

Chest

Indications

The fact that ultrasound is reflected completely by the bony thorax and by the air-filled lungs led to the mistaken notion that sonography is not a helpful diagnostic tool for the chest. In recent years, however, technical advances and new scientific evidence have led to a steadily broadening spectrum of applications of sonography to diseases of the chest: chest-wall lesions can be depicted, and pleural effusion and peripheral lung consolidation have become useful sonic windows. Although the sonographic image does not provide a complete overview of the chest, it is useful for certain indications:

Symptoms:

- chest pain
- dyspnoea
- fever
- inflow congestion.

Physical examination:

- palpable mass
- percussion dullness or damping
- rale.

In addition to X-ray, CT and magnetic resonance imaging (MRI):

- differentiation of solids and liquids
- infiltration of the pleura or chest wall
- vascularization
- breathing dynamics.

Examination technique

Equipment, transducer

Any equipment used for sonographic examination of the abdomen and small parts may also be used to examine the thorax. Ultrasound examination of the chest wall and the axilla and supraclavicular regions generally requires a linear probe with frequencies of 5–8 MHz. Recently introduced probes of 10–13 MHz are excellent for evaluating lymph nodes. For investigating the lung, a convex or sector probe of 3–5 MHz provides adequate depth of penetration.

Preparation

No specific preparation is necessary.

Position of the patient

Usually, the dorsal and lateral images are obtained with the patient sitting, whereas the supine position is used for visualizing the ventral side. When the arms are raised and crossed behind the head, the intercostal spaces are extended.

Scanning technique

The transducer is moved along the intercostal spaces in the dorsal-to-ventral direction and in longitudinal and transverse positions. Bedridden and intensive-care patients are examined by turning them to the oblique position on the bed. During every stage of the examination, the user should determine the breath-related movement of the pleura, the so-called 'gliding sign', in combination with respiratory manoeuvres, such as coughing or sniffing. The diaphragm is examined from the abdomen, in the subcostal section by the transhepatic route on the right side and, to a lesser extent, through the spleen on the left side.

Normal findings

Fig. 5.1, Fig. 5.2 and Fig. 5.3 show the normal aspect of the chest.

Fig. 5.1. Chest wall in the third intercostal space. Ultrasound imaging is limited by total reflection from the aerated lung, so-called visceral pleura (arrows): an echogenic, breathing-dependent, sliding line. M, pectoralis muscle

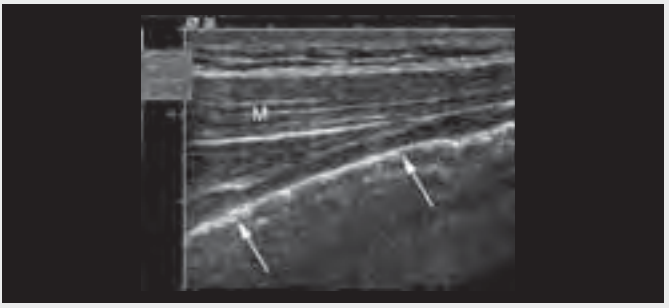

Fig. 5.2. (a) The visceral pleura (arrow) dorsal to the rib cartilage (C) is shifted ventrally towards the transducer as a result of various ultrasound beam rates in cartilage and soft tissue of the chest wall: velocity artefact. (b) The rib (R) absorbs the ultrasound beam and leads to an acoustic shadow

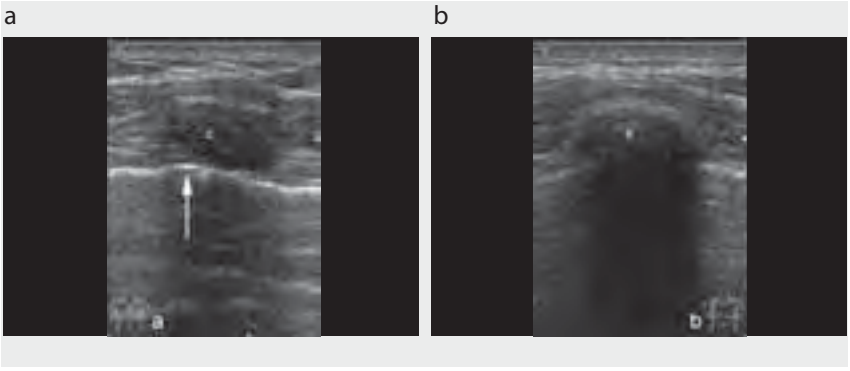

Fig. 5.3. Pleura. The sliding, wide visceral pleura (1) is an artefact caused by total reflection at the air-filled lung. Between the pleural sheets (2), echo-free fluid in the pleural space can be seen. (3) The echogenic parietal pleura)

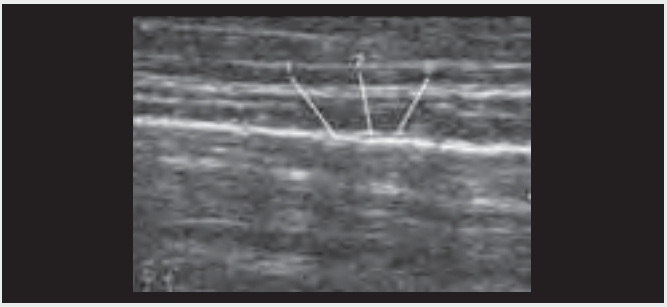

Pathological findings

Chest wall

Soft-tissue lesions

Suspect or unclear findings found during palpation of the chest wall should initially be examined by ultrasound. In most cases, the examiner will find lymph nodes, which are the most clinically relevant finding.

Reactive and inflammatory lymph nodes are seldom larger than 20 mm. Their form is oval or elongated, and the margin is smooth, sharply demarcated and arranged in a string-of-pearls fashion. Depending on the anatomical structure, there is often an echogenic central zone, a so-called 'hilar fat sign' (Fig. 5.4). This echogenic centre becomes larger during the healing phase of inflammatory lymph nodes. Vascularization is regular.

Fig. 5.4. Inflammatory lymph node: oval, smooth, and clearly demarcated. Echo-rich central zone is called the 'hilar fat sign', corresponding to the fatty connective tissue in the central region of the lymph node

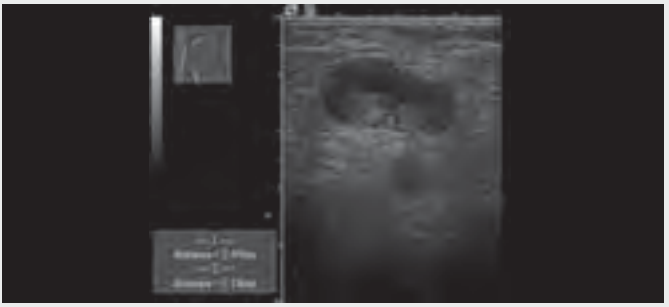

Lymph node metastases appear as round-to-oval inhomogeneous structures, usually with well defined borders. They typically show extracapsular growth with irregular borders and diffused infiltrating growth into vessels and the surrounding tissue (Fig. 5.5). Vascularization is irregular, mostly at the margin and corkscrew-like.

Fig. 5.5. Lymph node metastasis of an epidermoid lung cancer. Rounded, invasive growth into the surrounding tissue, sometimes echo inhomogeneous, with reduced mobility

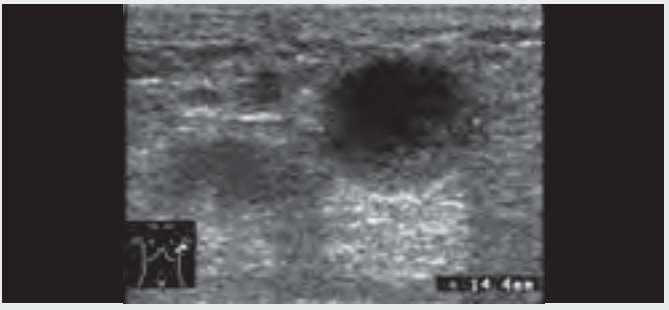

Axillary, supraclavicular and cervical nonpalpable lymph nodes are more easily detected by ultrasound than by CT. This is important for the staging of lung and breast cancers.

A homogeneous, echo-poor, sharply demarcated shape is typical of **malignant lymphomas**. Lymph nodes in centrocytic malignant lymphomas or Hodgkin lymphomas can present as almost echo free and cyst-like. Lymphomatous lymph nodes are round and oval but seldom triangular. Vascularization is enhanced or irregular (Fig. 5.6).

Note: Acute inflammatory lymph nodes are similar to lymphomatous lymph nodes.

Fig. 5.6. Malignant B-cell lymphoma. Smooth margin, sharply demarcated, hypoechoic with enhanced irregular vascularization

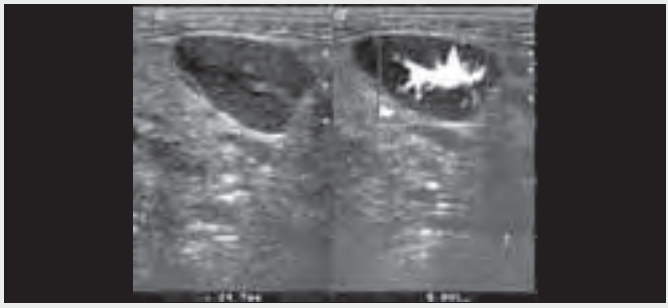

Haematomas can present with varying echo patterns as a result of the number of erythrocytes and the grade of organization. They can first be echo rich, then echo poor and later inhomogeneous.

The echogenicity of **lipomas** depends on their cellular fat content and differences in impedance in the interstitial tissue. The sonographic texture can vary from echo poor to relatively echo rich. The borderline of the surrounding tissue can be incomplete.

Bone

Rib and sternum fractures: it is surprising that rib fractures are diagnosed twice as frequently by sonography than by chest radiography. Conventional X-rays provide an overall view of the chest but have the disadvantage of occasional superimposition. On ultrasonic examination, the patient indicates the site of the pain and the examiner obtains an image by closely following the course of the ribs, looking for typical signs of fracture at the corticalis reflection (see below and Fig. 5.7). Minute dislocations and fissures are visible as a reverberation artefact at the traumatized point, referred to as a 'chimney phenomenon'.

Fig. 5.7. Rib fracture. Step-and-gap formation of 1 mm (arrow), not seen on X-ray. M, intercostal muscle; F, subcutaneous fat

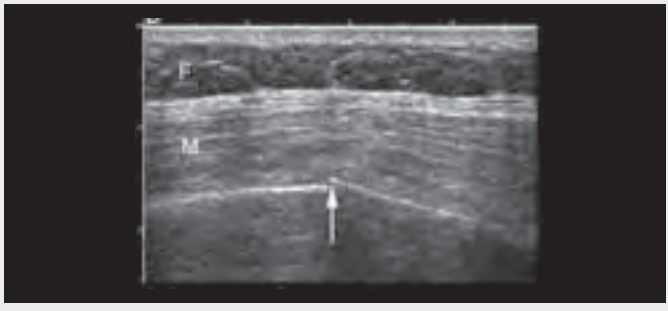

The sonographic signs of rib and sternum fractures, at the site of pain, are:

Direct signs:
- gap
- step
- dislocation.

Indirect signs:
- haematoma
- chimney phenomenon
- pleural effusion
- lung contusion
- skin emphysema.

Note: At the sternum, the synchondrosis of the manubrium should not be misinterpreted as a fracture (Fig. 5.8).

Fig. 5.8. Sternum fracture (F) with dislocation of 5 mm. The hump and cortical interruption of the manubrium (M) should not be misinterpreted as a fracture

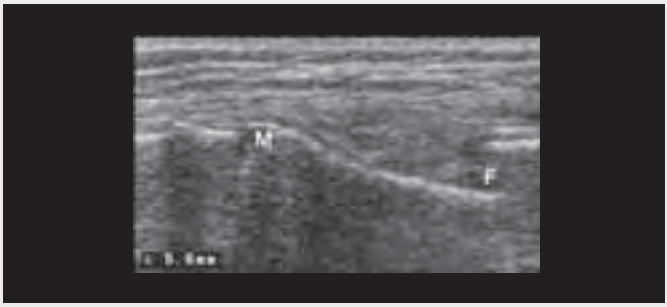

Osteolytic metastases in the bony thorax cause disruption of the corticalis reflex with pathological ultrasound transmission. The echo texture is sometimes poor and hazy (Fig. 5.9). With colour Doppler, corkscrew-like vessel neoformations can be found. During therapy, the size, shape and structure of metastatic osteolysis can be used as follow-up parameters.

Fig. 5.9. Osteolytic rib metastasis (M). The cortical reflection of the rib is disrupted. The ultrasound beam passes through the inhomogeneous metastatic formation to the visceral pleura

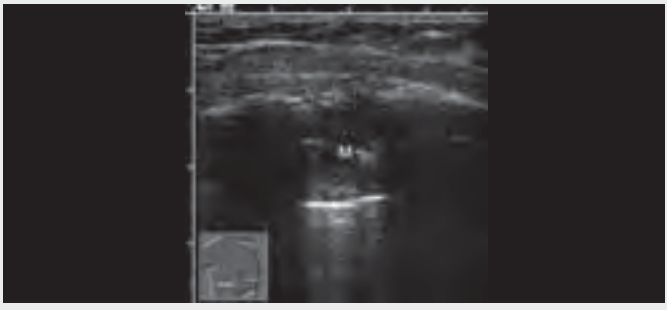

Pleura

The normal pleura is only 0.2–0.4 mm thick and, hence, at the limit of resolution of current ultrasound systems. It is not always possible to visualize sonographically both the pleural blades and the hypoechoic space between them. The finer visceral pleura is submerged in the thick line of total reflection of the ultrasound at the air-filled lung (Fig. 5.3). As soon as the peripheral lung is free of air because of a pathological process, the actual visceral pleura can be marked off as a fine echogenic line.

Pleural effusion

In contrast to X-ray, ultrasound can detect pleural effusions of as little as 5 ml laterodorsally to the angle between the chest wall and the diaphragm, with patients in either a standing or sitting position. By turning the supine patient slightly sidewards, small dorsal effusions can also be identified.

Pleural effusions are echo free as they are liquid formations (Fig. 5.10). Similarly, pleural scars and thickening are also visualized as hypoechoic structures. However, pleural effusion changes its shape with respiration and shows the fluid colour sign, which originates from the lung pulse and respiration shifting of the fluid.

Fig. 5.10. Large, almost echo-free pleural effusion caused by congestive heart failure. The echoes at the margin and in the depth are artefacts

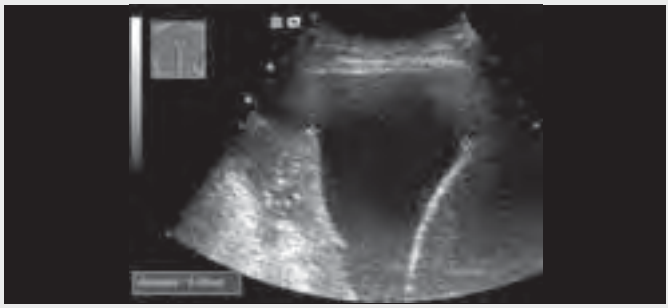

Transudates are almost always echo free, whereas about half of **exudates** are echogenic. The echogenicity of exudates often increases during illness, while transudates become slightly echogenic after puncture. Diffusely distributed, swirling or floating, slight echoes indicate reflecting particles in the fluid, e.g. cells, protein, fibrin or blood. Echoes that swirl with the respiratory or cardiac rhythm clearly indicate fluid collection. Movable strands, fibrinous strings and septations are typical of inflammatory effusions (Fig. 5.11). **Malignant effusions** can also appear to be echo free or septated. Only nodules indicate malignancy (Fig. 5.12).

Volumetry of pleural effusion

Anatomical differences and the various shapes of the chest make pleural effusions highly variable. Thus, the exact volume of an effusion cannot be measured.

Fig. 5.11. Pleural empyema with several cavities, septations and fibrinous bands

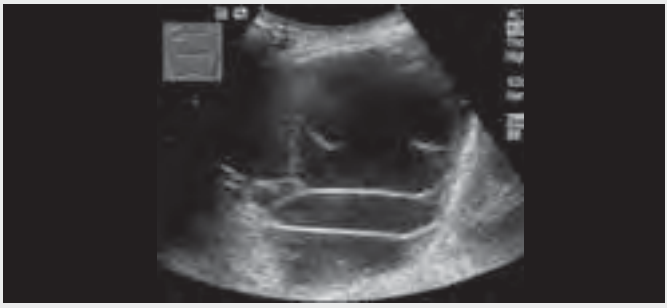

Fig. 5.12. Metastatic (M) nodules of an adenocarcinoma on the thickened and destroyed diaphragm

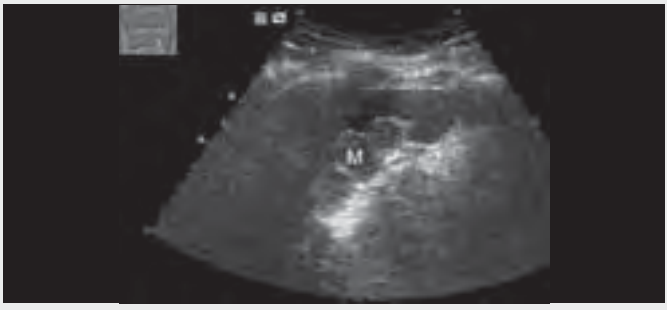

Fig. 5.13. Estimate of the volume of a pleural effusion: lateral plus median subpulmonary height of effusion × 70: corresponds to about 800 ml

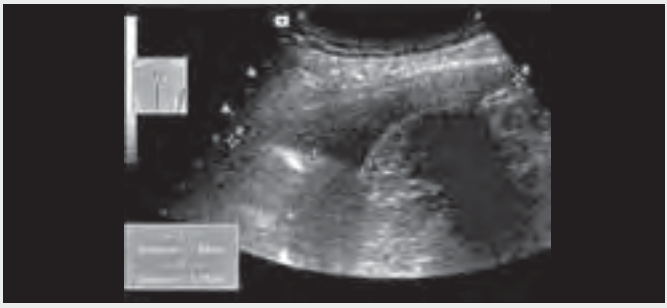

With the patient in the sitting position, the sum of the basal lung–diaphragm distance (in cm) and the lateral height of the effusion (in cm) multiplied by 70 will result in an acceptable estimate of the volume of pleural effusion (Fig. 5.13). In routine clinical follow-up, it is sufficient to measure the subpulmonary and lateral 'water level'.

For bedridden patients, the planimetric square dimension of an effusion in a transverse section multiplied by the maximum craniocaudal length times an empirical factor of 2/3 is a good correlation of real effusion volume. Similar results have been reported by multiplying the maximum thickness of the pleural fluid layer (in cm) by 50 and then taking 800 from the result.

Pneumothorax

The major criterion of pneumothorax is absence of breath-related movement of the visceral pleura, referred to as the 'sliding sign'. Further signs, in comparison with the healthy side, are:

- absence of sliding sign
- broadening of visceral pleura band
- absence of comet-tail artefacts
- horizontal reverberation artefacts and
- lung point.

The extent of the lung collapse and the breadth of major pneumothorax cannot be seen by sonography. The fleeting appearance of lung sliding replacing a pneumothorax pattern is termed the 'lung point' (Fig. 5.14).

Fig. 5.14. Pneumothorax. (a) Healthy side; sliding visceral pleura band; some vertical comet-tail artefacts. (b) Side of pneumothorax; loss of sliding sign; enhanced horizontal reverberation artefacts in the lung

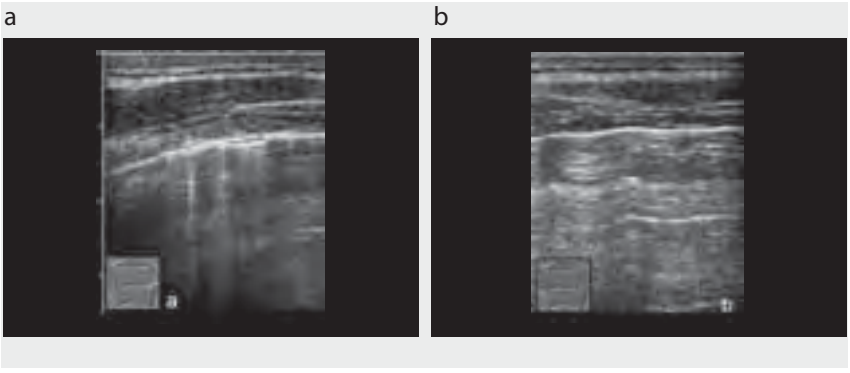

Pleuritis

Pleuritis is most frequently caused by viral infections or tuberculosis. Clinically, pleuritis is difficult to diagnose and often the diagnosis can be made only by excluding other diseases that cause chest pain. A chest X-ray sometimes shows a blurred or even absent contour of the diaphragm; it can also demonstrate an effusion. Pleural alterations, which can be missed by X-ray, are detectable by ultrasonography in up to 90% of cases (Fig. 5.15, Fig. 5.16).

Fig. 5.15. Pleuritis. Rough appearance and interruption of the normally smooth pleura visceralis. Small subpleural echo-poor consolidations

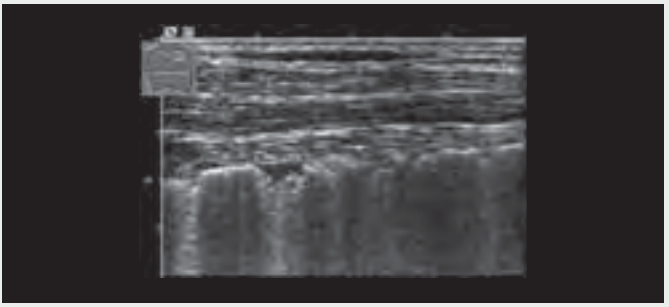

Fig. 5.16. Tuberculous pleuritis. (a) Echo-poor thickening of the pleura visceralis up to 3 mm. (b) Nodular subpleural consolidations. Diagnosis is confirmed by ultrasound-guided biopsy

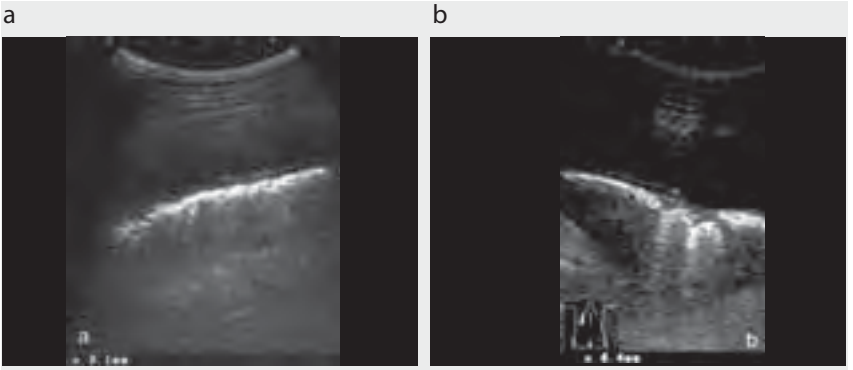

The sonographic findings in pleuritis are:

- rough appearance of pleura visceralis
- interruptions of pleura visceralis
- small subpleural consolidations and
- small effusion.

Pleural mesothelioma

Mesotheliomas are usually visualized as diffuse, irregular thickenings of the pleura. They have very irregular, partly angular, unclear borders. In addition to tumour-like formations, mesotheliomas can also present as extensive, tapestry-like growths with nodules. Large pleural effusions frequently occur with mesotheliomas (Fig. 5.17).

Fig. 5.17. Pleural mesothelioma. Nodular and plate-formed broadening of the pleura. Echo-poor and irregular vascularization

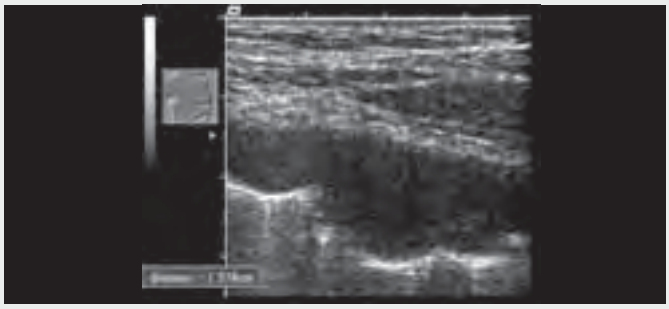

Fig. 5.18. Rupture of the diaphragm (arrows) after a serious blunt-abdominal trauma

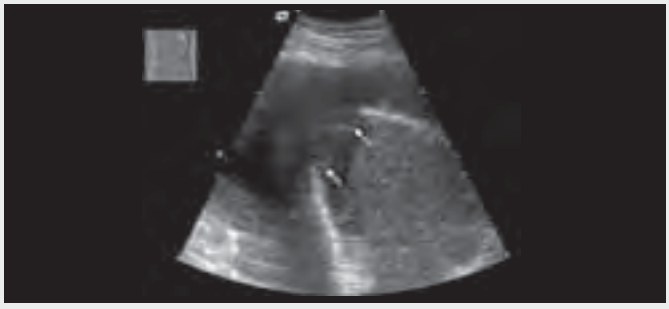

Diaphragm

Real-time sonographic examination is the most suitable method for functional examination of the diaphragm. Normal equilateral up-and-down movement of the diaphragm in harmony with respiration can be observed. Paralysis of the diaphragm attracts the examiner's attention because of absent or paradoxical movement. Ruptures of the diaphragm can also be recognized (Fig. 5.18). One should not be misled by an apparent diaphragm hiatus originating at an artefact corresponding to the outline shadow.

Peripheral pulmonary consolidation

Ultrasound imaging of the lung is not possible in healthy people, because the ultrasound beam is reflected totally at the surface. The prerequisite for lung sonography is that the consolidation extends to the pleura.

Pneumonia

In the early congestive stage of pneumonia, the echo texture of the lung is similar to that of the liver. A marked tree-shaped bronchoaerogram and a large number of

lenticular echo reflections measuring a few millimetres are frequently observed up to the pleura (Fig. 5.19, Fig. 5.20). In a densely subpleural location, one finds a broad, highly hypoechoic strip, which is a superficial fluid alveologram. In viral or fungal pneumonia, less marked air bronchograms are obtained.

Ultrasound images of pneumonia are characterized by an irregular, serrated, somewhat blurred margin. The fluid bronchogram is characterized by anechoic tubular structures in the bronchial tree. A persistent fluid bronchogram arouses suspicion of post-stenotic pneumonitis and should be followed by suitable bronchoscopic clarification. On colour-coded duplex sonography, pneumonia has a typical appearance: circulation is uniformly increased and branched, while the vessels have a normal course. The sonographic findings in pneumonia are:

- hepatoid in the early stage
- air bronchogram
- lenticular air trappings

Fig. 5.19. Lobar pneumonia. Liver-like consolidation of the left upper-lobe with lenticular air trappings and an air bronchogram

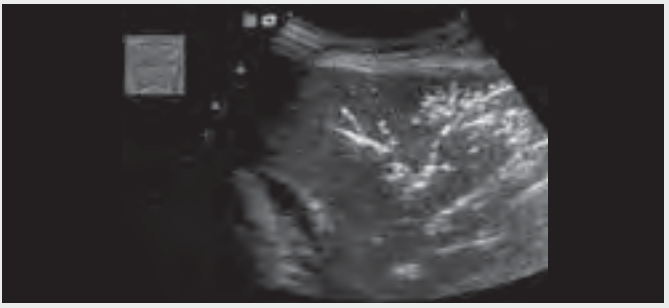

Fig. 5.20. Tree-like air bronchogram in pneumonia

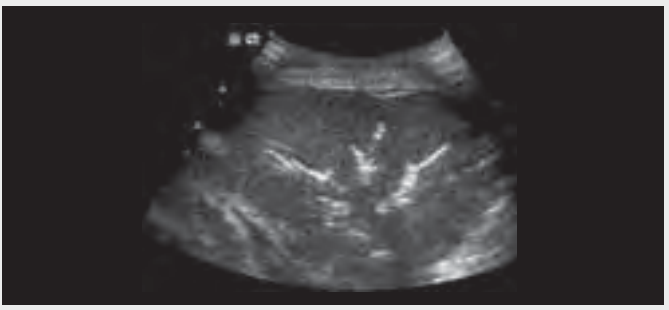

- fluid bronchogram (post-stenotic)
- blurred and serrated margins
- reverberation echoes in the margin and
- hypoechoic abscess formation.

Bacterial pneumonias tend to fuse and form abscesses seen as round or oval, largely anechoic foci (Fig. 5.21). Depending on the formation of a capsule, the margin is smooth and echo dense. In cases of complicated pneumonia, it is useful to obtain a specimen for the detection of pathogens by means of ultrasound-guided aspiration.

When pneumonia is in the healing phase, the infiltrated lung tissue is increasingly ventilated, and the air gives rise to reflection and reverberation artefacts in ultrasonograms. The pneumonia recedes on the ultrasound image and appears smaller than on a chest radiograph, which is consistent with the clinical course (Fig. 5.22).

Fig. 5.21. Small abscess formation (+ — +) in lobar pneumonia. Nearly echo free and rounded. An air inlet indicates the connection to the bronchial system

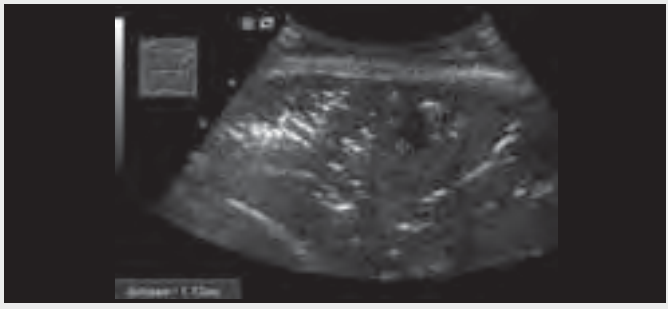

Fig. 5.22. Healing phase of pneumonia. The consolidation is receding and resolving, the air bronchogram is disappearing, air trappings and reverberation artefacts are increasing, all of which are consistent with clinical management

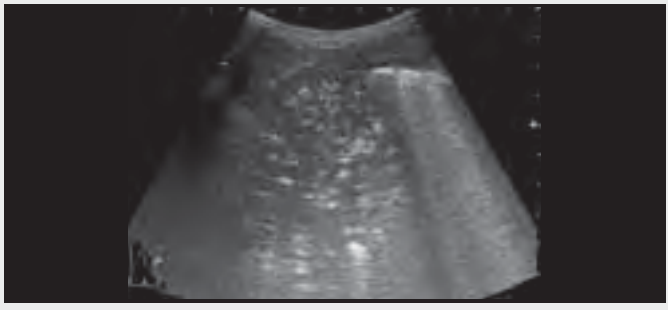

Tuberculosis

Pulmonary tuberculosis is polymorphic on X-ray as well as on chest sonography. The sonogram reveals isolated or numerous subpleural nodular hypoechoic lesions (Fig. 5.16, Fig. 5.17, Fig. 5.18, Fig. 5.19, Fig. 5.20, Fig. 5.21, Fig. 5.22, Fig. 5.23). Imaging of these lesions may be facilitated by the presence of a pleural effusion. Miliary tuberculosis is characterized by nodular dissemination occurring as multiple subpleural nodules measuring a few millimetres. Liquefaction is well demonstrated in the sonogram, although the presence of air in the tuberculous cavern may limit visualization. The patient's response to tuberculostatic treatment can be monitored well by sonography, especially in cases of pleural and subpleural tuberculosis.

The sonographic findings in tuberculosis are:

- pleural effusion
- fragmentation of visceral pleura
- subpleural infiltrations of various forms
- air bronchogram in cases of larger infiltrations and
- broad reflection artefact in cavities

Fig. 5.23. Miliary tuberculosis. Multiple rounded subpleural consolidations up to 5 mm

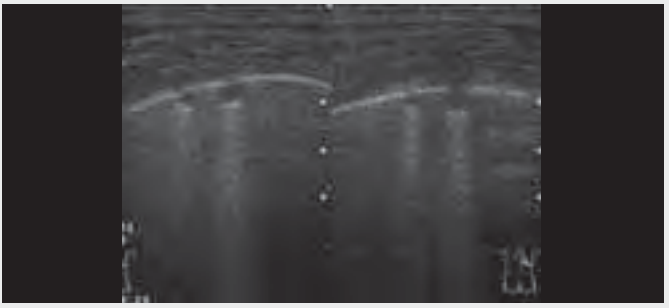

Interstitial lung disease

Diseases of the framework lung cannot be imaged by sonography, and the technique is of little use for their primary diagnosis. Here, the value of sonography lies in the detection of minimal pleural effusions and subpleural infiltrations during follow-up.

Pulmonary embolism

A few minutes after a secondary pulmonary artery has become occluded, the surfactant collapses, and interstitial fluid and erythrocytes flow into the alveolar space. Haemorrhagic congestion offers ideal conditions for ultrasound imaging. These consolidations are open at the periphery along with their base, which creates good conditions for transthoracic sonography. According to the results of new imaging procedures, the frequency of haemorrhagic reperfusionable pulmonary infarction is much higher than previously reported (Fig. 5.24, Fig. 5.25).

Fig. 5.24. Pulmonary embolism: two pleural-based infiltrations

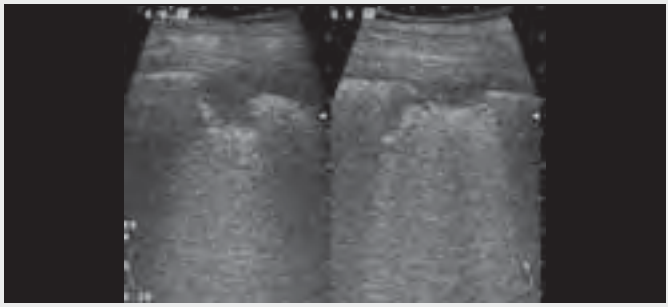

Fig. 5.25. Pulmonary embolism. (a) Triangular pleural-based, homogeneous airless inlets. (b) Concomitant small pleural effusion

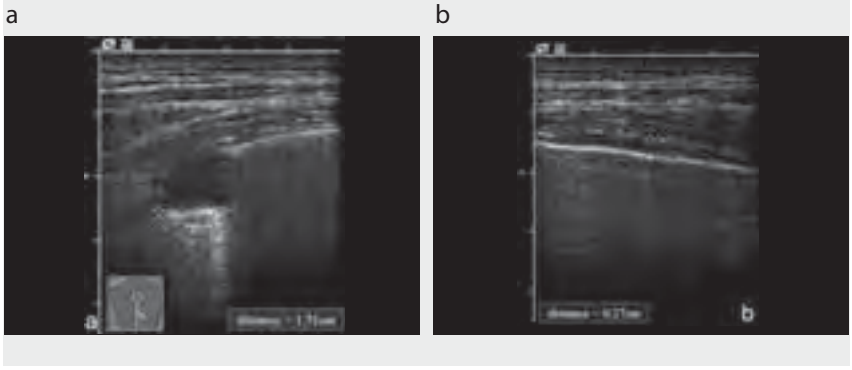

The sonomorphological criteria for a peripheral pulmonary embolism are:

- echo poor
- size, average 16 mm × 12 mm (range, 5–70 mm)
- pleural-based
- triangular > rounded
- central bronchial reflexion
- vascularization stop
- 2.5 lesions per patient
- in two thirds of cases, the location is dorsobasal and
- small pleural effusion.

The overall sensitivity of chest sonography in pulmonary embolism is 80% and the specificity 93% (accuracy 95%). In thromboembolism, chest sonography should be performed in the context of echocardiography and leg vein sonography. Ultrasound can provide three kinds of information: the source in deep veins, the haemodynamic relevance on the way through the heart and the outcome as pulmonary embolism: 'killing three birds with one stone' results in a sensitivity of 92%.

Pulmonary carcinomas and metastases

In sonograms, lung carcinomas and metastases are, for the most part, rounded or polycyclic. Pulmonary malignancies can have a variable echo texture; they are usually hypoechoic, moderately echo dense or very inhomogeneously structured. They frequently have sharp margins and fringed or finger-shaped ramifications into the ventilated lung (Fig. 5.26). The tumour vessels are irregular and shaped like a corkscrew. Dynamic ultrasound examination is better than CT or MRI for depicting malignant invasion of the chest wall or subclavian vessels. The advantages of ultrasound-guided biopsy are manifold: fast availability, low complication rate, absence of electromagnetic radiation and low cost.

The sonographic features of pulmonary carcinomas are:

- hypoechoic, inhomogeneous
- rounded, polycyclic
- sharp, serrated margins
- ramifications and fringes
- infiltration of chest wall and
- irregular vascularization.

Fig. 5.26. (a) Epidermoid lung cancer infiltrating the chest wall, destroying the ribs and intercostal space. Fringes and ramifications. (b) Irregular neovascularization of cancer

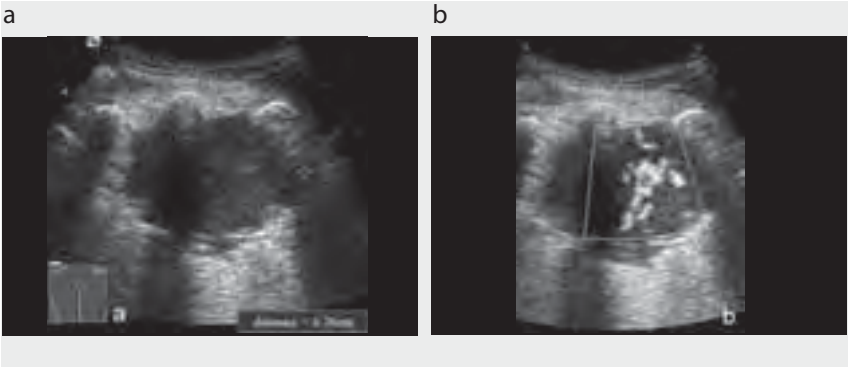

Atelectasis

Lung atelectases are characterized by partial or complete absence of ventilation. **Compression atelectasis** is caused by voluminous pleural effusion. The patient may develop triangular, homogeneous, hypoechoic consolidations shaped like a wedge or a pointed cap and have blurred margins to ventilated lung parenchyma (Fig. 5.27). These are partially reventilated during inspiration and after puncture of the effusion.

A sonographic image of **obstructive atelectasis** is marked by a largely homogeneous, hypoechoic presentation of lung tissue in terms of hepatization. Effusion is absent or very small. Depending on the duration of atelectasis, intraparenchymatous structures may also be seen, including hypoechoic vascular lines and echogenic bronchial reflexes. Secretory congestion of the bronchi presents a fluid bronchogram. On colour Doppler sonography, regular vessels along the bronchi are seen.

In cases of chest trauma, especially serial rib fractures, **pulmonary contusions** are seen better in sonography than in radiographs. Alveolar oedema and alveolar haemorrhage caused by trauma are visualized as hypoechoic, plate-like, blurred lesions with indistinct margins (Fig. 5.28). These are more pronounced in the presence of concomitant pleural effusion.

Fig. 5.27. Compression atelectasis. Triangular, hypoechoic, pointed cap-like transformation of lung parenchyma, surrounded by fluid. Partial reventilation during inspiration

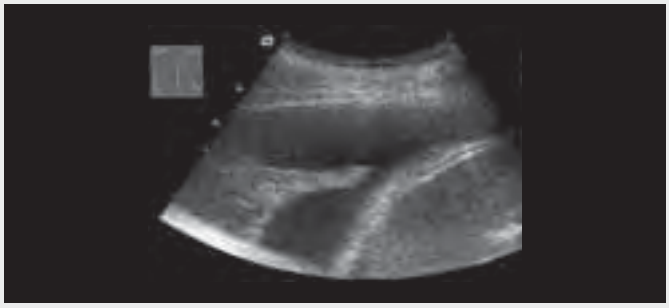

Fig. 5.28. Lung contusion. Plate-formed subpleural haemorrhage (arrows), irregular and blurred demarcation

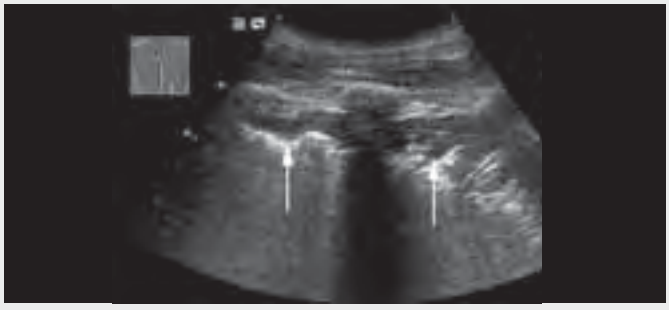

Mediastinum

Most of the clinically relevant space-occupying masses in the adult mediastinum are located in the anterior and mid-mediastinum and are, therefore, readily accessible for sonographic assessment. Sonographic access to the mediastinum is obtained supra- or parasternally; occasionally, the infrasternal path is chosen. A good understanding of anatomy is absolutely essential. Lesions of the anterior superior mediastinum can be identified clearly as solid or cystic. Tumours that appear at the margin of the sternum are easily localized and biopsied. Ultrasound examination may demonstrate regression

Fig. 5.29. Mediastinal lymph node metastases from a small-cell lung cancer (LC) by the suprasternal approach. AO, aorta; BT, branchiocephalic trunk

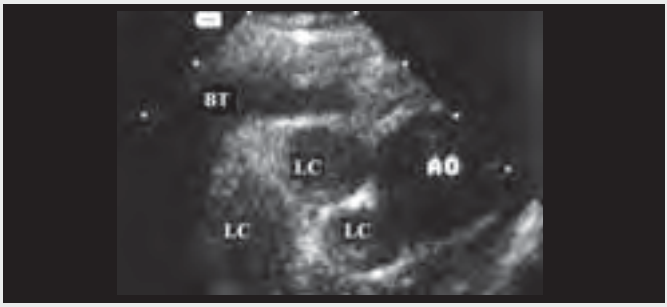

Fig. 5.30. Pericardial effusion (PE) in the parasternal longitudinal approach, caused by viral pericarditis. LV, left ventricle

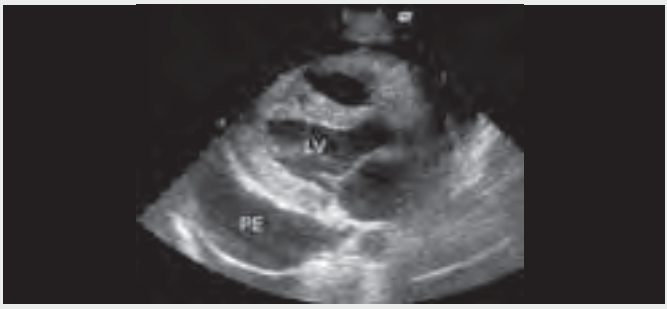

after the treatment of mediastinal lymphoma or metastases (Fig. 5.29). Inflow congestion and superior vena cava syndrome can be cleared by sonography. Colour Doppler may detect collateral vessels. The development of endoscopic ultrasound has opened up new diagnostic possibilities for the detection and analysis of mediastinal lymph nodes.

Pericardium

Pericardial effusion is easily diagnosed, as a left sternal or subcostal approach shows the fluid surrounding the myocardium. Echogenic layers on the myocardium and fibrinous bands may indicate chronic inflammation caused by infection or rheumatic disease (Fig. 5.30). Malignant pericardial effusions sometimes show swirling echoes. Pericardial tamponade is marked sonographically by the collapse of the right atrial and/or ventricular walls during diastole. When the clinical situation is critical, ultrasound allows an immediate, safe pericardial tap. Sometimes, it is difficult to distinguish between epicardial fat pads and true pericardial effusions.

Chapter 6

Abdominal cavity and retroperitoneum

6

Abdominal cavity and retroperitoneum

Indications

The indications of ultrasonography of the abdominal cavity and retroperitoneum are:

- alpable mass
- pain
- fistulas
- ascites
- suspected perforation (free air demonstrable?)
- hernia
- malignant lymphomas (staging, follow-up)
- aortic aneurysm
- venous congestion
- blunt trauma
- suspected postoperative complications

Examination technique

Equipment, transducer

Abdominal scanners, curved array or sector transducer, 3–5 MHz are used for general examinations. Linear array transducers, 5–10 MHz, are best suited for abdominal wall and superficial structures.

Preparation

No specific preparation is required.

Position of the patient

Supine is generally the best, in the left or right oblique or lateral position, with head held high or low, if needed.

Scanning technique

The abdominal wall is examined systematically in longitudinal and transverse scans, starting in the cranial part below the ribs from the midline. The corresponding left and right sides are used for comparison.

The abdominal cavity is usually visualized in examinations of the abdominal organs. For the detection of ascites, the splenic bed, Morison's pouch and the retrovesical space in the small pelvis have to be scanned. For determination of the presence of free air, the region between the surface of the right liver lobe and the abdominal wall must be scanned, with the patient in a slightly left oblique position (the area before the right liver lobe should be the highest point of the cavity).

In the retroperitoneal space, the large vessels and the kidneys (see Chapter 13, Kidneys and ureters) are the anatomical landmarks for orientation. The large vessels should always be visualized in longitudinal and transverse scans from the diaphragm to the bifurcation. To overcome the problem of meteorism, an examination from the flanks (coronal scans) or with the patient in an upright position is recommended. Another method is to displace the gas in the intestinal loops by graded compression of the transducer in the area to be scanned.

Normal findings

Abdominal wall, abdominal cavity and retroperitoneal space

Skin, subcutaneous tissue, muscles and the parietal peritoneum form the anterolateral abdominal wall. On both sides of the linea alba, the rectus abdominis muscles are visualized as echo-poor structures with transverse lines of stronger echoes corresponding to the characteristic inscriptions. The fascial sheath cannot be seen. The three thin muscles (external and internal oblique and transversus abdominis) forming the lateral wall are easily differentiated in younger and muscular individuals. In obese persons, the image consists of a heterogeneous, not clearly structured echo-poor wall (Fig. 6.1, Fig. 6.2). The extraperitoneal fascia forms a thicker structure behind the linea

Fig. 6.1. (a) Abdominal wall Rectus abdominis with inscriptions (arrows). Athlete. Thin layer of extra-abdominal fatty tissue in front of the liver (broad arrow). (b) Abdominal wall. Extra-abdominal fatty tissue behind the wall (m, rectus abdominis) and in front of the liver (f, fatty tissue)

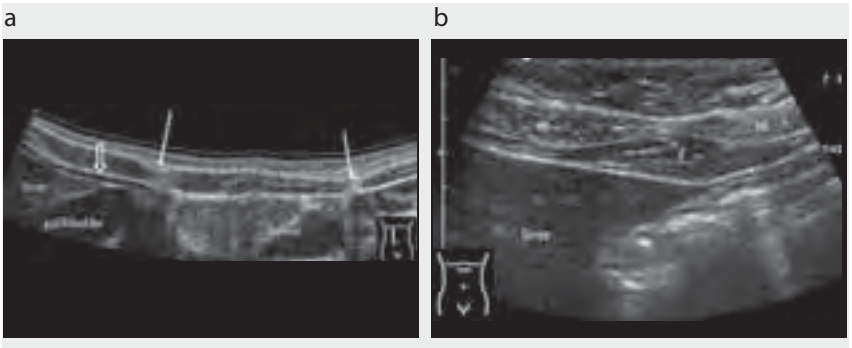

alba cranial to the umbilicus. It appears triangular in a longitudinal scan and rhomboid in transverse scans. It should not be misinterpreted as a mass (Fig. 6.1).

The posterior wall is marked by the strong echoes of the ventral surface of the vertebrae, which absorb all the energy and cause an acoustic shadow. The intervertebral discs also cause strong borderline echoes but do not absorb all the energy, so that echoes behind them are seen. On both sides, echo-poor muscles (psoas muscle and quadratus lumborum) are observable. Depending on age and condition, their diameter and shape differ from person to person (see Fig. 6.3, Fig. 6.4, Fig. 6.5, Fig. 13.9).

The diaphragm forms the 'roof' of the abdomen and appears as a thin, echo-poor layer or structure, but only in those parts that do not border the air-containing lung, e.g. dorsal to the liver or the pillar in front of the aorta (see Fig. 6.5). In the other sections, a line of bright borderline echoes marks the interface between the diaphragm and the lung and hides the thin echo-poor diaphragm (see Fig. 1.26, Fig. 7.5b).

Fig. 6.2. Abdominal wall. Transverse scan shows subcutaneous fat and thin rectus abdominis. The linea alba is marked by an arrow

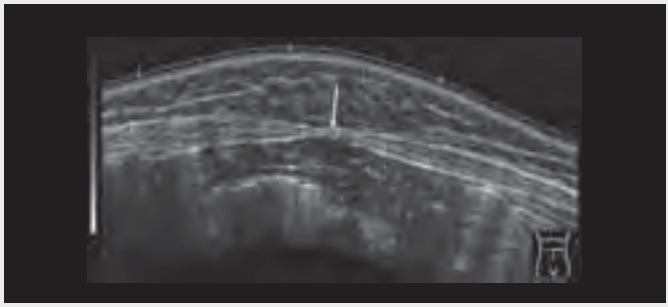

Fig. 6.3. Topography of the abdomen, transverse (a) and longitudinal (b) scan. Abdominal cavity (grey) and retroperitoneal space (white). In (a) k, kidney. (b) The tumour (T) is localized in the retroperitoneal space (axis of the kidney, dotted line) despite its short distance from the ventral abdominal wall.

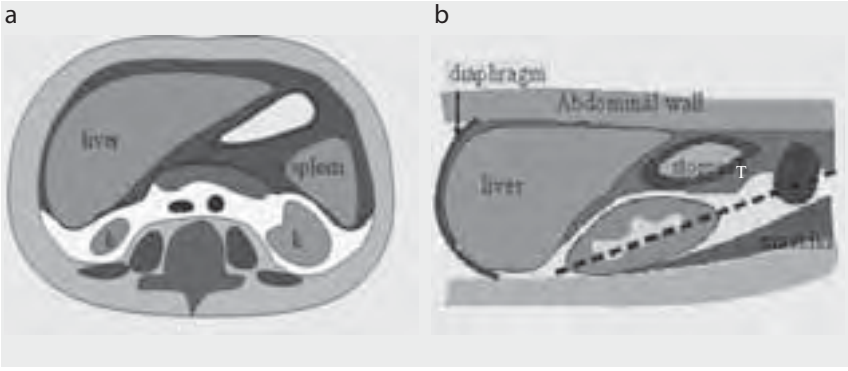

Fig. 6.4. Abdominal and retroperitoneal space. The borderline echoes between the liver and the kidney (arrow) mark the border between the abdomen and the retroperitoneal space, but are not caused by the parietal peritoneum. (p, psoas muscle; s, shadow behind the vertebral column; vc, vena cava; ao, aorta.)

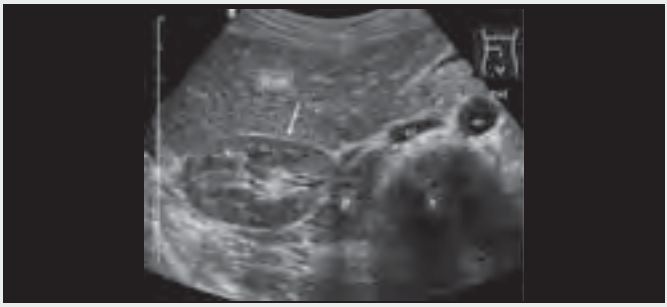

Fig. 6.5. (a, b) Abdominal aorta, coeliac trunk (T) and superior mesenteric artery (sma). The arrows mark the strong echoes of the vertebral bodies. Real echoes arising from the vertebral canal are seen behind a disc (in the bottom right-hand circle)

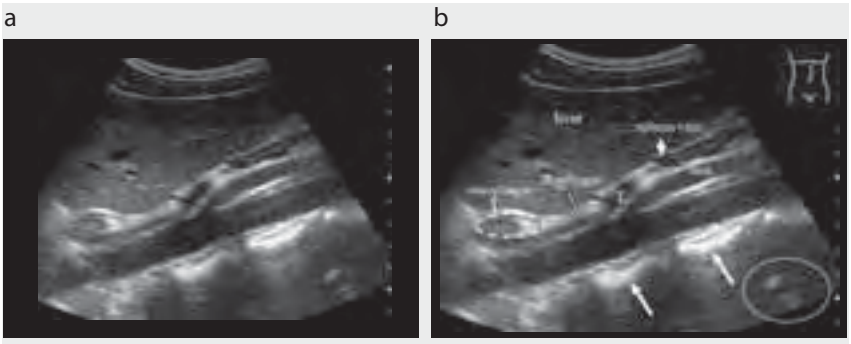

The retroperitoneal space is separated from the abdominal space by the parietal peritoneum, but ultrasound does not generally allow visualization of this thin serous lining. Thin echo lines between intra-abdominal organs and retroperitoneal organs and structures are mostly borderline echoes. The retroperitoneal or intra-abdominal localization of a mass or fluid can be estimated from the proximity of their relation to the retroperitoneal organs, especially the kidneys and the aorta (Fig. 6.3).

The abdominal cavity is separated by ligaments into different but communicating spaces and recesses, which are important for diagnosis and therapy. The mesentery and the retroperitoneal connective tissue appear echo rich and coarse, particularly in obese patients. The medium-size vessels in the ligaments can be seen, if the image is not impaired by meteorism.

Aorta and vena cava

The abdominal **aorta** is easily visualized as a nearly echo-free structure, with strong wall echoes running in front of the vertebral column (distance < 6 mm) from the aortic hiatus to the bifurcation. The internal diameter varies with the patient's age, from 11 mm to 19 mm in the upper part and from 10 mm to 15 mm in the lower part. The coeliac trunk and its branches, the superior and inferior mesenteric artery and the renal arteries can be visualized with ultrasound as well, if meteorism does not impede the examination (Fig. 6.5).

Spectral Doppler shows a relatively high diastolic flow above the renal arteries (low resistance profile) and a low diastolic flow (high resistance) in the lower part. The peak velocity (V_{max}) lies in the range 70–180 cm/s and the mean velocity (V_{mean}) in the range 40–70 cm/s (Fig. 6.6).

Fig. 6.6. Abdominal aorta. Spectral Doppler shows a low-resistance flow (high diastolic flow) in the upper part (a) and a high-resistance flow in the lower part (b)

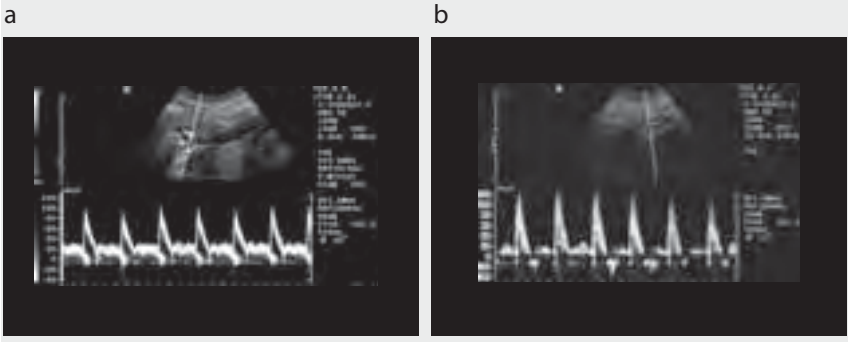

Fig. 6.7. Vena cava. The body of the pancreas is partially covered by shadow(S) arising from air in the distal stomach (smv, superior mesenteric vein)

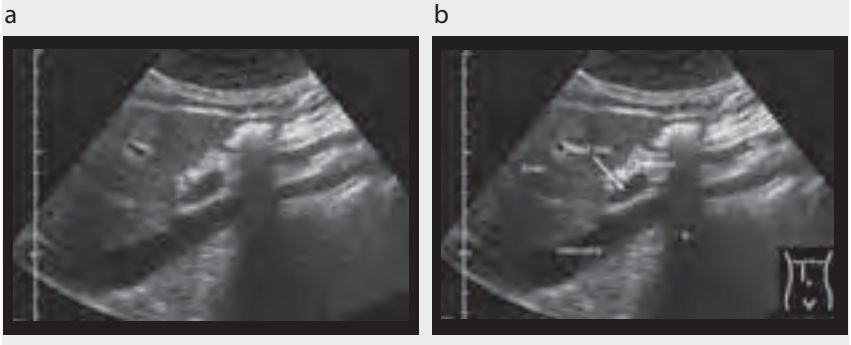

The inferior vena cava runs up the right side, slightly curved in the sagittal plane, with a greater distance from the aorta in the upper part. Its cross-section is oval with a distinctly smaller sagittal diameter, especially in the lower part (Fig. 6.4). The calibre varies with the actual thoracic pressure. The echoes of the wall are weaker (Fig. 6.7). In

front, behind and on both sides of the vessels, large groups of lymph nodes are arranged with long axes of up to 20 mm.

Pathological findings

Abdominal wall

Tumours

Primary tumours of the abdomen wall are rare. Benign **lipomas** and **fibrolipomas** are more or less echo rich, with sharp margins. They do not contrast well with the surrounding fat tissue (see Fig. 4.28). **Desmoid tumours** are associated with a recent pregnancy. Ultrasound demonstrates echo-poor lesions, most with sharp margins. A blurred border indicates infiltration into surrounding tissues. **Metastases** are usually echo poor or heterogeneous with irregular, ill-defined margins (Fig. 6.8).

Fig. 6.8. Metastasis (diameter, 24 mm). The irregular, blurred boundary and the heterogeneous echo-poor structure are characteristic

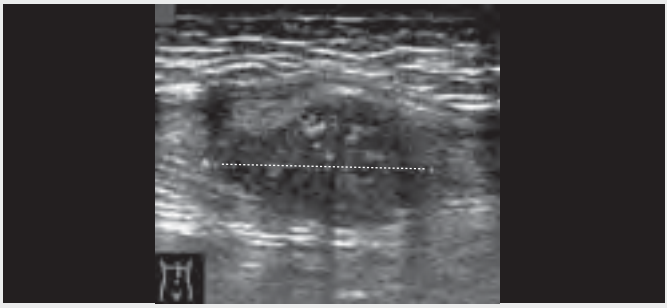

Foreign-body granulomas are characterized by a strong echo in the centre and, often, an annular echo-poor or average structure. Colour Doppler shows a hypervascular zone around the small lesion (small-parts scanner).

Inflammation, fluid collections

An **inflammation** of the wall may occur as a complication of an operation or a trauma. The inflamed area appears more echo dense, with a blurred structure, than the normal wall.

Abscesses are associated with a trauma, a laparotomy or, rarely, an enterocutaneous fistula. Abscesses are oval or irregular, depending on the structures of the wall. The pattern is echo poor or even echo free (Fig. 6.9). Strong echoes indicate gas in the abscess. The margin is often ill defined. Colour Doppler shows no signals in the lesion but a hyperaemic zone around it.

Seromas are also associated with laparotomy. They are echo free or very echo poor, with a sharp margin (Fig. 6.10). It is difficult to distinguish a post-operative seroma from a post-operative abscess if the latter does not show typical symptoms. If the clinical examination is also ambiguous, a guided puncture may identify the nature of the lesion.

Fig. 6.9. Abscess (post-operative). Note the thin, echo-poor fistula (arrow). The sonographic feature is similar to that of a metastasis (see Fig. 6.8), but the history and clinical symptoms are different

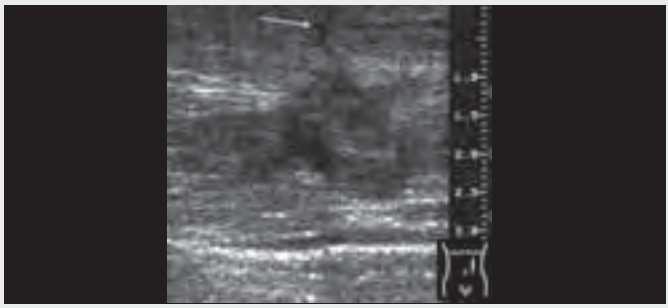

Fig. 6.10. Seroma. Note the sharp margins. The fluid is echo free, apart from some artefacts

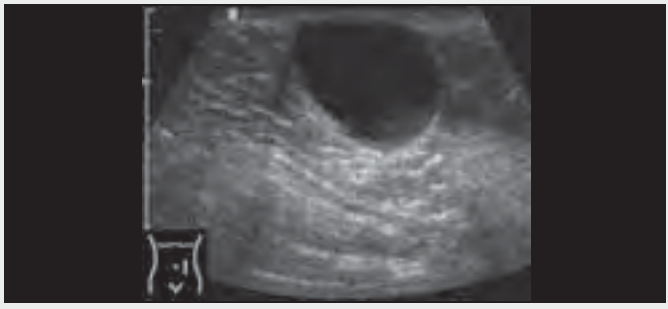

Fig. 6.11. Haematoma (diameter, 131 mm). The echo pattern of the older haematoma is relatively heterogeneous; the margin is irregular but sharp

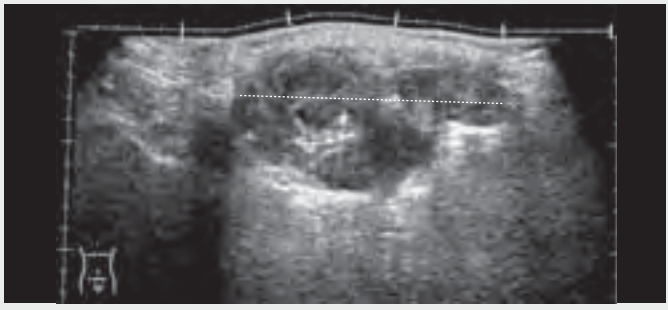

The echo pattern of **haematomas** depends on their stage: bleeding into the tissue initially causes an echo-rich, 'cloud-like' pattern, with irregular, blurred margins. Later, the blood forms a circumscribed echo-poor lesion (Fig. 6.11). Finally, this lesion becomes increasingly echo rich, indicating the organization of the haematoma.

Subcutaneous emphysema

A subcutaneous emphysema of the abdominal wall can be due to a perforating trauma. Ultrasound demonstrates a line of strong echoes within the wall (but not behind the wall, which indicates meteorism). The acoustic shadow covers the deeper layers of the wall and the abdomen.

Hernias

Hernias arise at typically weak parts of the linea alba, mainly above the umbilicus (epigastric hernia), the umbilicus itself (umbilical hernia), the linea semilunaris (Spigelian hernia), the inguinal canal (inguinal hernias) and the femoral ring (femoral hernia). Incisional hernias are late complications of operative wounds. The point of pain or palpation guides the ultrasound examination.

The ultrasound features of a hernia are variable, depending on the content of the hernial sac. The echo pattern of the visceral peritoneum (fat tissue) is echo rich, and intestinal loops can be identified. Lack of movement, a swollen, echo-poor wall of the bowel and fluid (but not ascites) in the sac indicate an incarcerated hernia. The sonographic signs of bowel obstruction (see Chapter 11, Gastrointestinal tract) indicate strangulation. The hernial orifice can be visualized by ultrasound as a gap in the linea alba (epigastric hernia) or at the border of the abdomen, which sometimes allows repositioning (Fig. 6.12, Fig. 6.13, Fig. 6.14, Fig. 6.15).

Fig. 6.12. Incisional hernia (40 mm, larger measure), through the gap in the fascia (indicated by the arrow, 9 mm). The hernia contains fatty tissue only

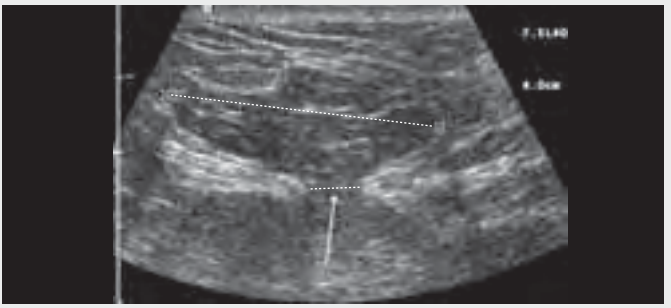

Fig. 6.13. Incisional hernia. The fluid and the swollen wall of the small bowel in the sac indicate an alteration in torsion and obstruction of the blood supply

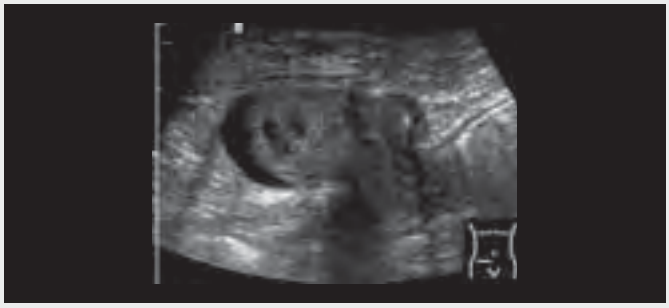

Fig. 6.14. Incarcerated Spigelian hernia (arrows). The hernia causes mechanical obstruction of the small bowel (dilated fluid-filled loops with a swollen wall)

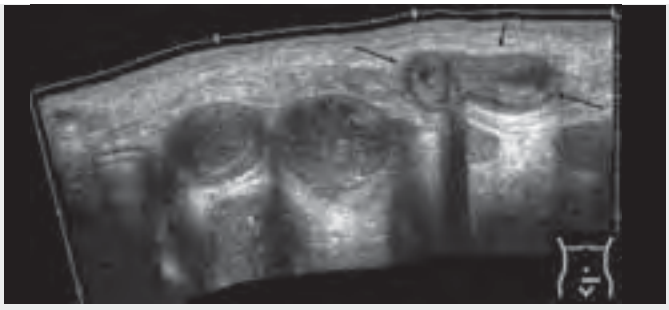

Fig. 6.15. Inguinal hernia (diameter, 18 mm). Fluid in the sac (arrow) and the echo-poor, thickened wall indicate alteration of the bowel (see also Fig. 15.49)

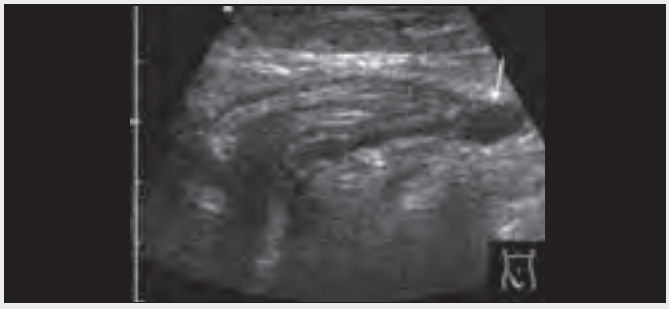

Abdominal cavity

Ascites

The presence of ascites is a common symptom in many types of disorder (Table 6.1).

Small amounts of ascites should be sought in typical recesses, Morison's pouch or Douglas's pouch. Amounts of fluid greater than 10 ml can be demonstrated with ultrasound. The fluid is echo free or very echo poor, which does not exclude an exudate. Fine, dispersed echoes in the fluid suggest haemorrhagic (malignant) ascites or exudates. At a later stage, they are often characterized by filiform echoes. Purulent ascites is less echo poor. Diagnosis of the type and cause of ascites are often more reliable if additional signs are found (Table 6.1, Fig. 6.16, Fig. 6.17, Fig. 6.18, Fig. 6.19, Fig. 6.20, Fig. 6.21, Fig. 6.22, Fig. 6.23, Fig. 6.24, Fig. 6.25).

Table 6.1. Types of ascites

Disorder	Type	Ultrasound findings	Additional findings
Portal hypertension	Transudate	Echo free	Liver, spleen, gallbladder
Venous congestion (heart failure)	Transudate	Echo free	Dilated vena cava, pleural effusion
Nephritic syndrome	Transudate	Echo free	Kidneys
Inflammatory disorder (peritonitis)	Serofibrinous exudates	Echo free or echo poor, filiform echoes (fibrin)	Thickened bowel wall, abscess, gas echoes (perforation)
Tuberculosis	Exudates	Echo poor	Echo-poor lymph nodes, thickened mesentery, complex inflammatory masses (HIV infection)
Pancreatogenic ascites	Exudates	Echo free or echo poor	Pancreatitis
Malignant tumours	Variable, haemorrhagic, chylous	Echo free, fine dispersed echoes	Retracted bowel loops, thickened mesentery, metastases (liver)
Trauma, anticoagulation	Blood	Echo poor or even echo free	Trauma, anticoagulation

Fig. 6.16. Small amount of ascites in Morison's pouch (arrow) and in front of the right liver lobe position 'a'. The small line of ascites in front of the liver 'a' is 'masked' by reverberation echoes

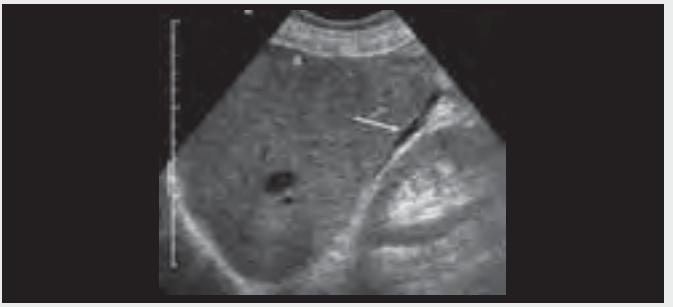

Fig. 6.17. A trace of fluid in Douglas's pouch (arrow). Nearly echo-free blood after a fall

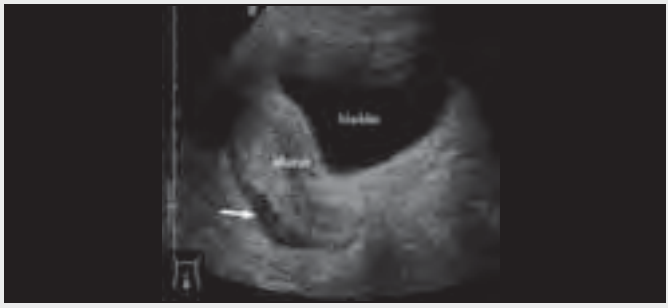

Fig. 6.18. Fluid (bleeding) in the rectouterine space. The uterus and the adnexa (follicles in the right ovary, arrow) are surrounded by the fluid. Note the different appearance of the echo-poor blood and the echo-free fluid in the bladder

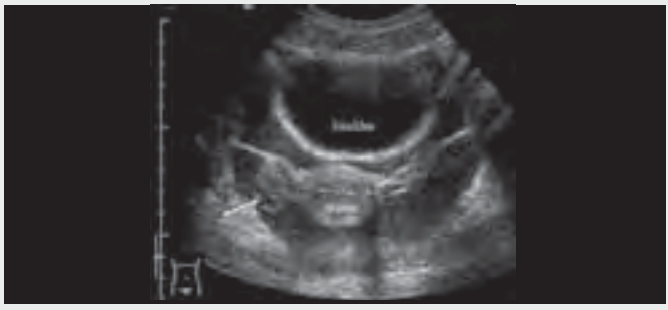

Fig. 6.19. Inflammatory ascites (exudates) with filiform echo lines in the stage of organization (adhesions)

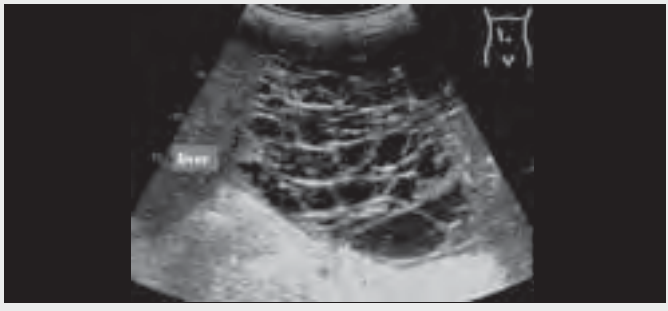

Fig. 6.20. Haemorrhagic, malignant ascites (ovarian cancer), showing faint echoes

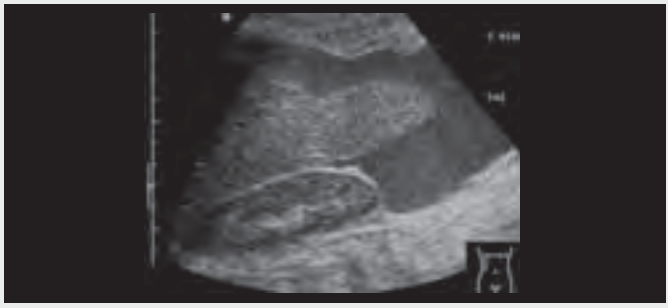

Fig. 6.21. Ascites (transudate) with floating small bowel loops

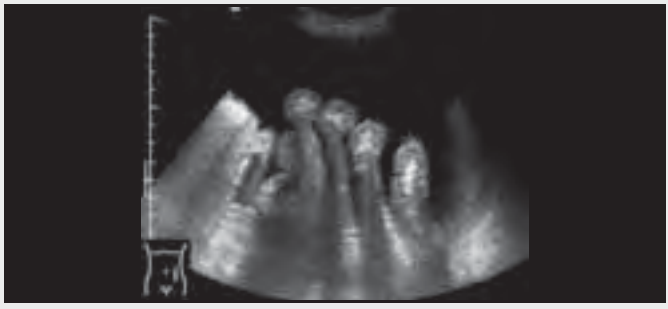

Fig. 6.22. Mesothelioma. The visceral serous lining of the loops and the parietal serosa are thickened (arrow). Close to the abdominal wall, note typical reverberation artefacts. A, ascites

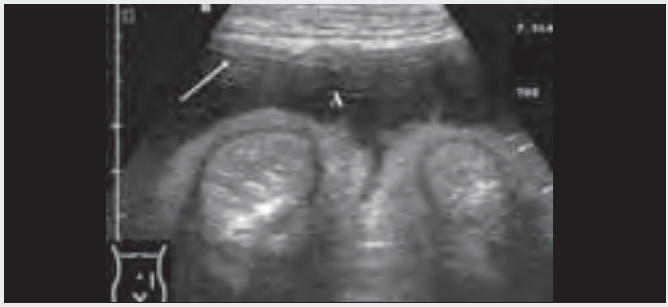

Fig. 6.23. Small amount of ascites between small bowel loops. The ascites does not flow up because of post-operative adhesions. Note the oedema of the small bowel

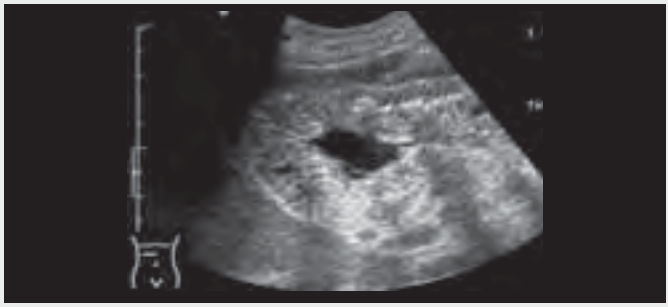

Fig. 6.24. Abscess (localized peritonitis; diameters, 26 mm and 11 mm)). Note the inflamed, thickened wall of the small bowel (D)

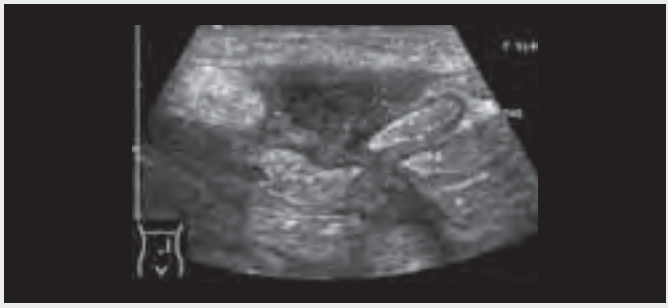

Fig. 6.25. Postoperative haematoma, showing similar sonographic features as abscesses (see also Fig. 6.24, Fig. 6.26)

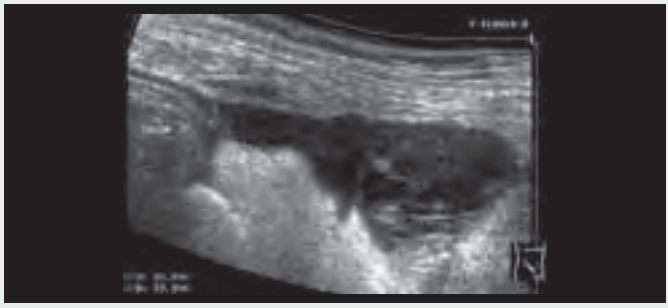

Fig. 6.26. Intra-abdominal abscess. Note that it is difficult to decide whether all the strong gas echoes are within the lumen of the bowel

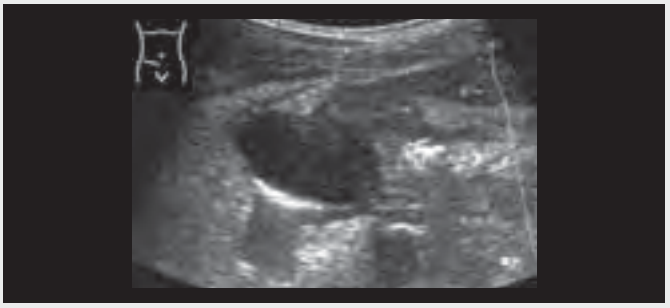

The thickness of the gallbladder wall is a reliable symptom for distinguishing benign ascites caused by portal hypertension or hypalbuminaemia (thickened wall) from malignant ascites (normal wall). Floating small-bowel loops are characteristic of extensive ascites (transudates and some exudates). The loops are often retracted in inflammatory disease or in malignant infiltration of the mesentery. In cases of localized peritonitis or (postoperative) adhesions, the fluid may be more localized and not flow up when the position of the patient changes.

Whenever ascites is seen, all parts and all organs of the abdomen must be examined carefully to find the underlying disorder (see Table 6.1)

Pseudomyxoma peritonei

This term describes a special type of gelatinous ascites, often caused by an ovarian cancer. Ultrasound demonstrates extended ascites with septa.

Quincke oedema

This disorder is caused by a lack of the C1-esterase inhibitor. It may affect the abdomen, causing ascites and oedema of the gastric and intestinal walls. The echo-free ascites and the very echo-poor swelling of the walls disappear within hours or 2–3 days.

Peritonitis

Peritonitis may arise from an infectious disease of an abdominal organ (e.g. appendicitis, diverticulitis) or be caused by a (bowel) perforation. Initially, the peritonitis remains localized. Ultrasound can visualize echo-poor fluid collection surrounded by adhered intestinal loops, often with a thickened, echo-poor wall. Strong gas echoes within the fluid are highly symptomatic of bowel perforation. The sonographic indications of bowel obstruction (see Chapter 11, Gastrointestinal tract) may also be seen. If the peritonitis remains localized, an abscess or a complex inflammatory tumour is visualized by ultrasound. If diffuse peritonitis develops, ascites and unmoving bowel loops (paralytic ileus) are seen.

A special type of ascites is secondary infection of an initially sterile ascites caused by portal hypertension.

Peritoneal tuberculosis

Peritoneal tuberculosis is a common extrapulmonary manifestation that is seen in advanced stages of HIV infection. Usually, ascites occurs secondary to an affection of the small bowel. The course is usually chronic, and two types, 'wet' and 'dry', are differentiated.

The ultrasound findings are not specific but indicative of the clinical background. Ascites, echo free or with filiform echoes, is the leading symptom of the 'wet' type. In the 'dry' form, irregular thickening of the mesentery with a complex echo pattern is seen, but ultrasound usually cannot visualize the small tubercles in the peritoneum. The affected lymph nodes are rounded and echo poor, with small echo-free lesions (caseous degeneration). Only small, localized portions of less echo-poor fluid are found. The affected intestinal loops are matted, and the thickened wall is echo poor. The adhesions of the intestine, the mesentery, small abscesses and enlarged lymph nodes may form large pseudotumours with a complex echo pattern.

Adhesions

Post-operative adhesions between the bowel and the abdominal wall are a common problem. Ultrasound is usually not useful for visualizing these thin bridles directly, but real-time examination of the movement of the intestine gives an indirect indication. The upper and lower parts of the abdomen are scanned with the transducer positioned in the midline and midclavicular line. An easily discernible structure is examined during deep inspiration and expiration. Normally, it shifts more than 6 cm in the upper and less than 4 cm in the lower abdomen. A shift of more than 3 cm is suspect, and no shift confirms the diagnosis.

Retroperitoneal space

Retroperitoneal fluid collections are either haemorrhagic (trauma, anticoagulation therapy, neoplasms, aneurysm) or inflammatory. Additionally, urinomas may occur around the kidney (see Chapter 13, Kidneys and ureters). The fluid is mostly limited to the original site by the various ligaments, which makes it easier to find the causative disorder. Fluid in the anterior pararenal space may be caused by acute necrotizing pancreatitis. Fluid in the medial part is caused by disorders of the large vessels (see section on Aorta and vena cava in this chapter). Fluid in the perirenal space is caused mainly by diseases of the kidneys (see Chapter 13, Kidneys and ureters). Fluid is found behind the kidneys in infections of the psoas muscle, which is due to abscesses or haemorrhage (see Fig. 6.27, Fig. 6.28, see also Fig. 13.63, Fig. 13.64). The latter may occur spontaneously if the patient is on anticoagulant therapy. Abscesses are secondary to inflammatory disorders of the vertebral column (e.g. spondylodiscitis, tuberculous spondylitis) or of the abdomen (appendicitis, fistulas, postoperative complications). The psoas itself may be thickened, with a partially echo-free, irregular pattern, which is best visualized by comparison with the psoas muscle on the other side.

Retroperitoneal fluid collections are mostly echo poor, corresponding to their characteristics (blood, inflammatory exudates).

Cystic lesions

Echo-free and smoothly delineated **mesenteric cysts** are very rare. In endemic areas, parasitic disorders (*Echinococcus granulosus* infections, hydatid disease) have to be taken into consideration if cystic or complex partially cystic lesions are found in the

Fig. 6.27. Psoas haematoma (fresh, anticoagulation therapy). The haematoma localized in front of the muscle appears rather inhomogeneous, with ill-defined borders (arrows)

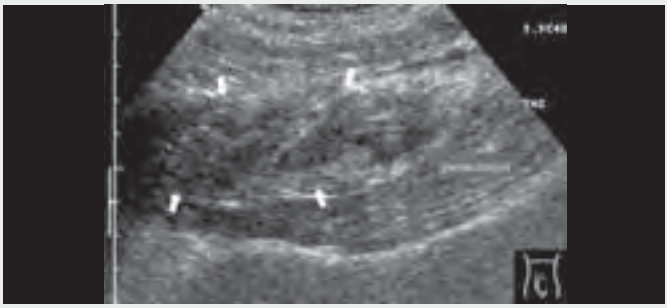

Fig. 6.28. Old haematoma (19 mm × 33 mm) in front of the psoas muscle, 6 weeks after an accident. The rounded haematoma is homogeneous and echo poor with sharp margins. It has the appearance of a tumour

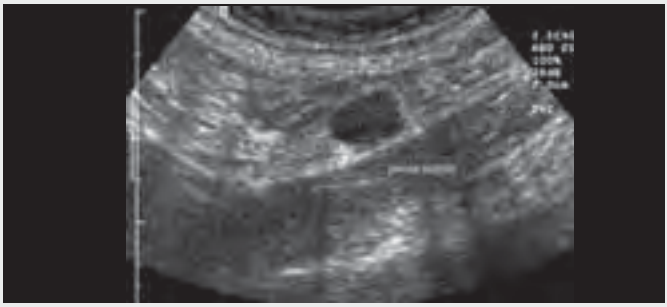

abdominal cavity. **Seromas, biliomas** or **lymphoceles** are echo free and smooth, like serous cysts. They are diagnosed from the clinical background.

Tumours

Primary tumours of the peritoneum and the retroperitoneum are rare. Benign **lymphangiomas** show a complex pattern, with echo-free areas.

Malignant mesotheliomas cause thickening of the parietal and visceral peritoneum, which is visualized as a relatively echo-rich lining of the bowel, organs and the inner surface of the wall, connected by ascites (see Fig. 6.22).

L**iposarcomas** are echo rich and show poor contrast with fat tissue. Other malignant tumours, such as **leiomyosarcoma,** show a more complex, inhomogeneous pattern. Malignant tumours frequently become large, as they may cause no symptoms for a long time. Their size, an inhomogeneous pattern, an irregular shape and a blurred outline indicate malignancy (Fig. 6.29, Fig. 13.65), whereas small, more homogeneous tumours with sharp, smooth borders may be benign. Generally, reliable differentiation is not possible.

Fig. 6.29. Retroperitoneal sarcoma (diameter, 104 mm). Note the inhomogeneous, relatively echo-rich pattern. The aorta (ao) is discernible but not the vena cava

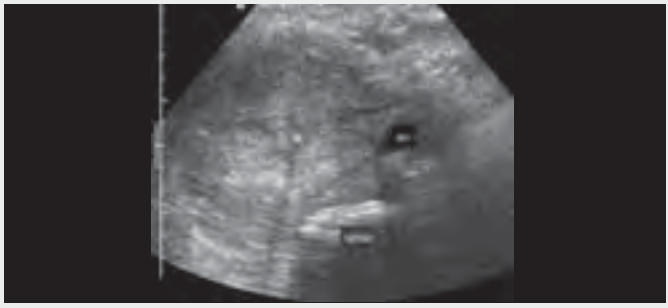

Fig. 6.30. Metastasis (13 mm) in the visceral mesentery of a small bowel loop (arrow), (sb, small bowel; ao, aorta)

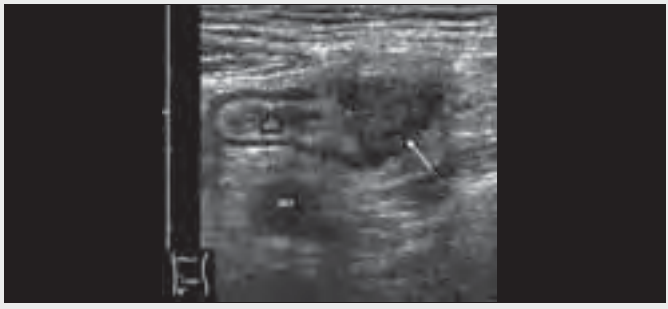

Metastases are commoner in the mesentery and the retroperitoneal lymph nodes (Fig. 6.30, see also Fig. 6.32). Usually, they are echo poor and associated with ascites (Fig. 6.20). Diffuse infiltration of the mesentery causes shrinking and retraction of the intestine. Carcinomatous lymph nodes are enlarged, moderately echo poor and often show an irregular, ill-defined outline. Colour Doppler permits visualization of irregular 'peripheral' vascularity.

Malignant lymphomas

Advanced malignant lymphomas usually involve the retroperitoneal, para-aortic lymph nodes. Not infrequently, they also involve the mesenteric lymph nodes.

The lymph nodes are enlarged, more rounded and echo poor, the hilus sign is missing, the nodes are conglomerated or, less frequently, isolated, and they surround the large vessels. Compression of these vessels, especially of the vena cava, should be diagnosed only if the vessel is dilated distally (Fig. 6.30, Fig. 6.31, Fig. 6.32, Fig. 6.33, Fig. 6.34, Fig. 6.35).

Fig. 6.31. (a) Non-Hodgkin lymphoma with multiple enlarged, echo-poor lymph nodes around the coeliac trunk. (b) Lymphadenitis mesenterica. The slightly enlarged mesenteric lymph nodes are relatively echo rich (hilus sign) and oval

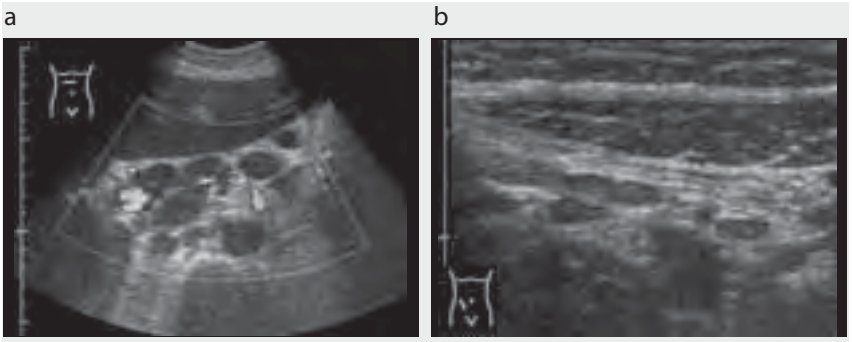

Fig. 6.32. Lymph node metastasis (gastric cancer; diameter, 45 mm) behind the (compressed) vena cava (vc); pv, portal vein

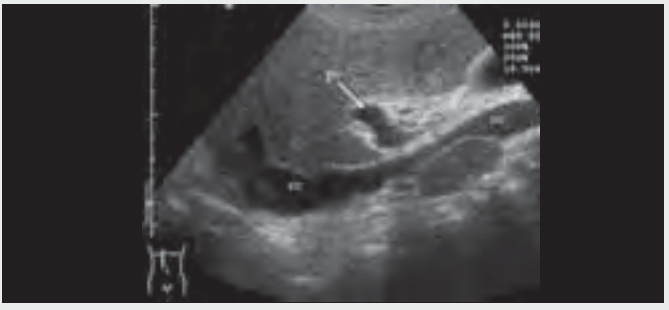

Fig. 6.33. Malignant lymphoma (arrows, 37 mm). The distance between the aorta and the spine is increased. A diagnosis of compression of the vena cava (vc) should not be based on the oval cross-section shown, but only if the section distal to the tumour is dilated (ao, aorta; pv, portal vein)

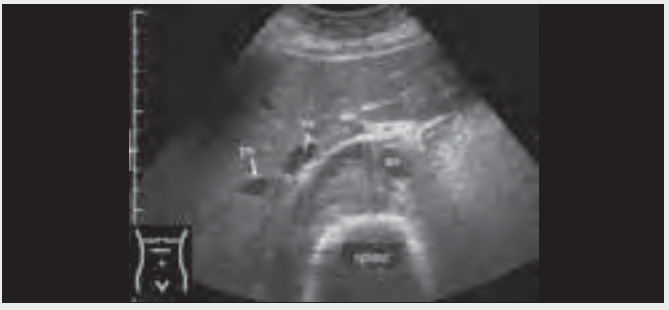

Fig. 6.34. Immunocytoma. Enlarged lymph nodes (arrows) in front of the aorta in the angle of the superior mesenteric artery (sma); t, coeliac trunk)

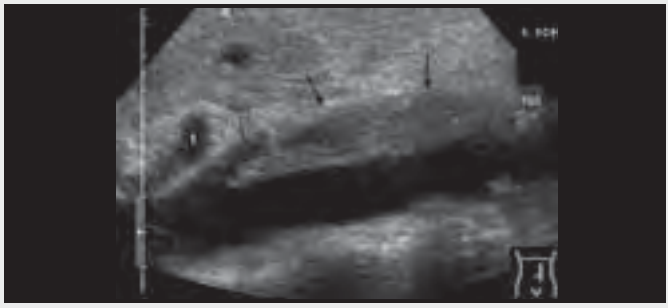

Fig. 6.35. Low-grade non-Hodgkin lymphoma (ln). The enlarged retroperitoneal lymph nodes coat the aorta (ao); sma, superior mesenteric artery; see also Fig. 6.46)

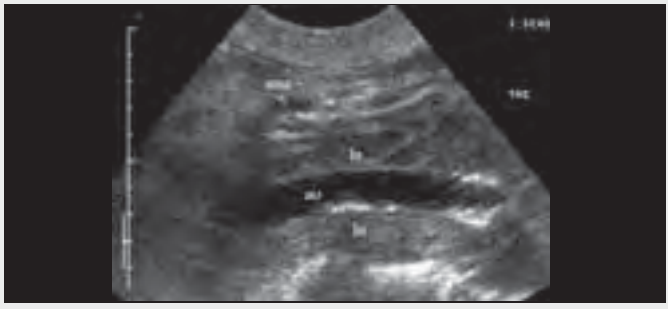

The lymph nodes are hypervascular, as shown by the colour or power Doppler technique. The vascularity varies and may be regular ('hilar' vascularity) or pathological (peripheral vascularity).

Retroperitoneal fibrosis

This disorder is characterized by augmented connective tissue between the renal pelvis and the promontory of the sacrum. The etiology is unknown but, in some cases, the disease occurs as a reaction to aortic aneurysms, retroperitoneal surgery or drugs.

Ultrasound shows an echo-poor mass around the large vessels, sometimes with ill-defined borders. A compression of one or both ureters simultaneously is characteristic (Fig. 6.46 and Fig. 13.61 in Chapter 13, Kidneys and ureters).

Aorta and vena cava

Situs inversus of the great vessels is rare; however, **variations** of the coeliac trunk and of the superior mesenteric artery are common, e.g. a common trunk for the two vessels or origination of the hepatic artery from the superior mesenteric artery.

Arteriosclerosis is characterized by irregular thickening of the wall and elongation of the aorta, evident from the fact that the aorta is curved like an S and cannot be depicted in one scanning plane. The inner surface of the irregular wall can be depicted especially well with B-flow technique (see Fig. 6.36, Fig. 1.17). **Stenosis** can also be visualized with B-scan; however, an exact estimate is possible only with the spectral Doppler technique.

Aneurysms are typical, significant complications and consist of spindle-shaped, focal dilatations with a transverse diameter greater than 3.5 cm. B-scan shows the size and shape of an aneurysm and partial thrombosis. The latter is echo poor and can be clearly distinguished from the residual lumen. A large transverse diameter and an asymmetric thrombosis are regarded as risk factors for perforation. An echo-poor mass around the aneurysm is strongly indicative of perforation into the retroperitoneal space (Fig. 6.37, Fig. 6.38, Fig. 6.39, Fig. 6.40).

Colour Doppler shows the sometimes turbulent or rotating flow and is useful for identifying the vessels branching off. The distance between the aneurysm and the renal arteries is particularly important. In suprarenal aneurysms, the left renal vein should also be identified.

Fig. 6.36. Aortosclerosis (diameter, 16 mm). Localized calcifications cause strong echoes and acoustic shadows (see Fig. 1.17); sma, superior mesenteric artery

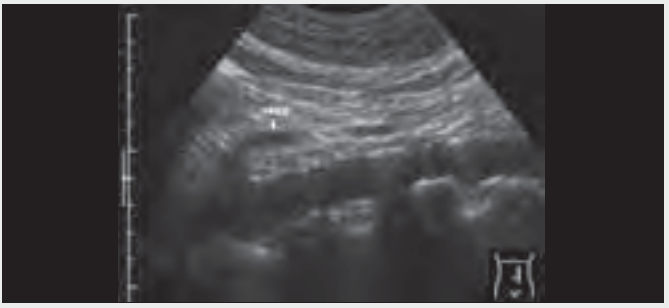

Fig. 6.37. Small aortic aneurysm (diameter, 24 mm; aorta, 15 mm) without thrombosis

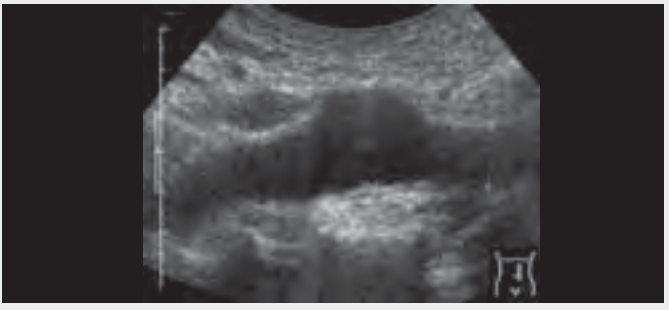

Fig. 6.38. Infrarenal aortic aneurysm (diameter, 47 mm) without thrombosis. Note the natural 'contrast' of the blood (turbulent flow)

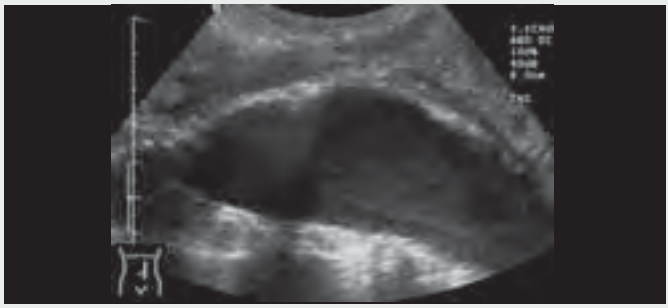

Fig. 6.39. Aortic aneurysm (75 mm × 63 mm). Asymmetric thrombosis

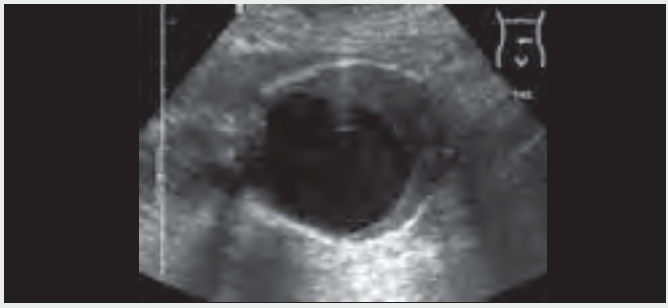

Fig. 6.40. Aortic aneurysm (53 × 49 mm). Circular thrombosis. Colour Doppler shows rotating flow (bright pixels correspond to red and dark pixels to blue)

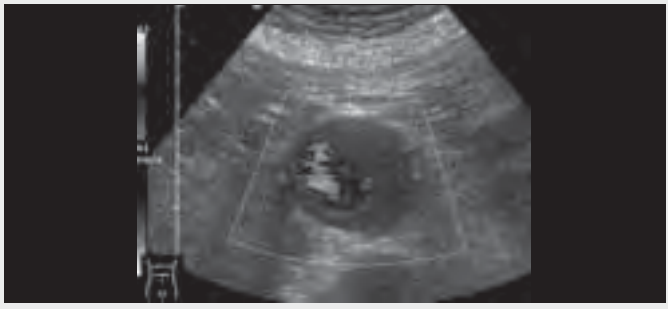

Ultrasound is useful for postoperative check-ups of prostheses, to measure their diameter and detect complications, such as stenosis, obstruction or inflammatory reactions.

Special types of aneurysm are sack-shaped, inflammatory and dissecting aneurysms. Sack-shaped (false) aneurysms of the aorta are rarely seen and are characteristic of medium-size arteries in systemic vasculitis. The term '**inflammatory aneurysm**' refers to a strong inflammatory reaction of surrounding tissue, especially in front of the aorta. The lymph nodes in the region are enlarged. It is related to retroperitoneal fibrosis.

Dissecting aneurysms cause only slight dilatation of the aorta. Careful B-scan examination may show flapping intimal lamellae. Colour Doppler differentiates true and false lumina more clearly, the flow direction in systole and diastole and the connection between the two lumina (Fig. 6.41).

Fig. 6.41. Dissecting aneurysm. (a) B-scan shows slight dilatation and a membrane in the middle of the lumen. (b) Colour Doppler shows different flows in the true (red = bright) and the false lumina (blue = dark)

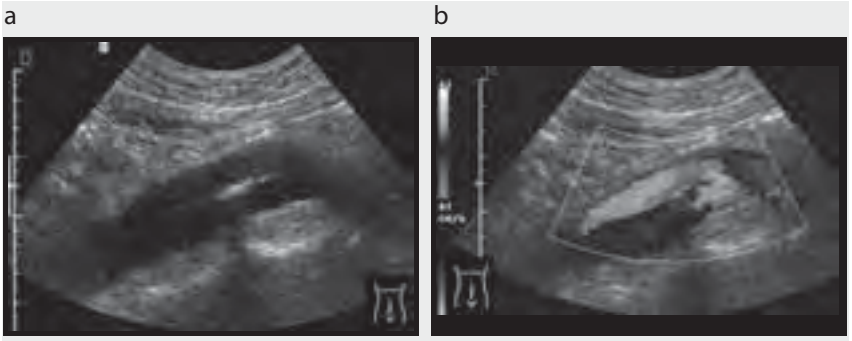

Fig. 6.42. Venous congestion (heart failure). The vena cava is dilated (30 mm), the cross-section round (see Fig. 6.4)

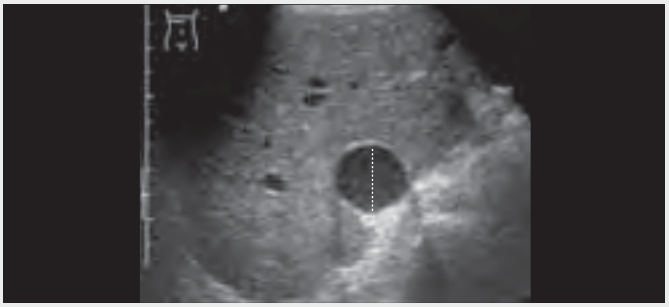

Venous congestion is easily visualized with B-scan: the cross-section of the vein becomes round, the vessel is dilated, and respiratory movements are missing. The feeding vessels, particularly the hepatic veins, are dilated (Fig. 6.42, Fig. 2.2).

A **thrombus** in the vena cava usually originates from a thrombosis of a feeding vein. A thrombus protruding into the lumen of the vena cava is echo poor and easy to detect. The vena cava is not dilated. A fresh thrombosis originating in the vena cava itself may sometimes appear nearly echo free and is, therefore, difficult to detect (Fig. 6.43, Fig. 6.44).

Differentiation between a simple thrombosis and a **tumour thrombosis** is difficult or even impossible with B-scan and colour Doppler. The thin tumour vessels can often be visualized only with contrast agents. Examination of the organ, drained by the vein, permits detection of the nature of the thrombus (see Chapter 13, Kidneys and ureters).

Colour Doppler permits detection of the flow in a thrombotic vein. It is particularly useful for follow-up control of cava filters.

Fig. 6.43. Thrombosis of the vena cava. The vessel is dilated (between calipers, 28 mm) and shows few echoes inside (fresh thrombosis); ao, aorta

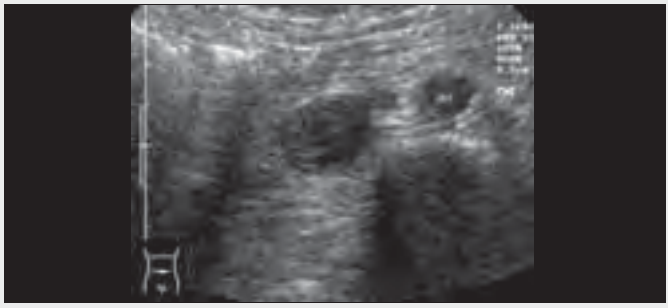

Fig. 6.44. Thrombosis of the left renal vein, protruding into the vena cava (vc)

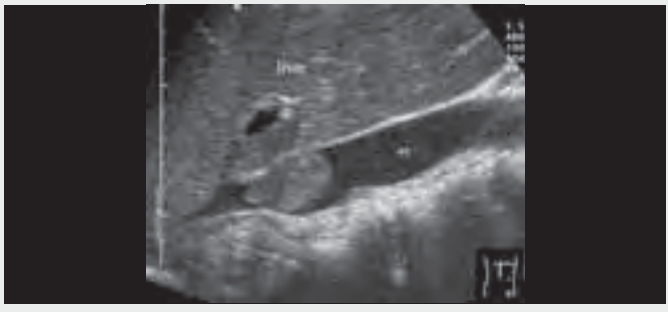

Differential diagnosis

The differential diagnosis of focal lesions in the abdominal wall does not pose problems if the clinical background is taken into account. Differentiation between a more harmless seroma and an abscess after laparotomy is sometimes difficult if there are no clear clinical or sonographic signs of an abscess. Ultrasonic-guided puncture is the

method of choice for clarifying the difference. Benign tumours, such as lipofibromas, and malignant lesions, mainly metastases, can usually be differentiated on the basis of the different echo patterns and the definition of the outline, as described in section on Abdominal wall in this chapter.

Ascites is a common ambiguous symptom of many diseases. Misdiagnosis of a large (ovarian) cyst as an ascites can be avoided, as a giant cyst will displace the intestine, whereas floating small bowel loops are always seen in ascites.

The main clinical problem in differentiation is between benign and malignant ascites. This can be resolved by examining the gallbladder wall: a thickened wall is a reliable sign of benign ascites, especially that caused by portal hypertension. The nature of the fluid itself does not help, as exudates or malignant ascites may appear to be echo-free transudates. In contrast, echoes within the fluid are not seen in transudates but indicate inhomogeneous fluid, exudates, purulent, haemorrhagic or chylous ascites. Generally, examination of the abdominal organs enables diagnosis of the causal disorder, as shown in Table 6.1.

In certain situations it is difficult to decide whether typical gas echoes are caused by gas bubbles in the bowel or from outside it due to perforation or abscess. Therefore, a diagnosis of free air or gas in the abdomen should be made only if gas echoes are detected in front of the right liver. The possibility of interposition of gas-containing colon sections (Chilaiditi syndrome) should be considered (Fig. 6.45).

Tumours in the abdomen pose some difficulties for differential diagnosis. It is not easy to identify the origin of the tumour, which may be an abdominal organ or, more

Fig. 6.45. Gas echoes in front of the right liver lobe. (a) Free gas (arrows) caused by perforation of a duodenal ulcer. (b) Gas inside the colon in Chilaiditi syndrome (colon interposition); gb, gallbladder. The thin wall (arrow) is difficult to see (3.5 MHz)

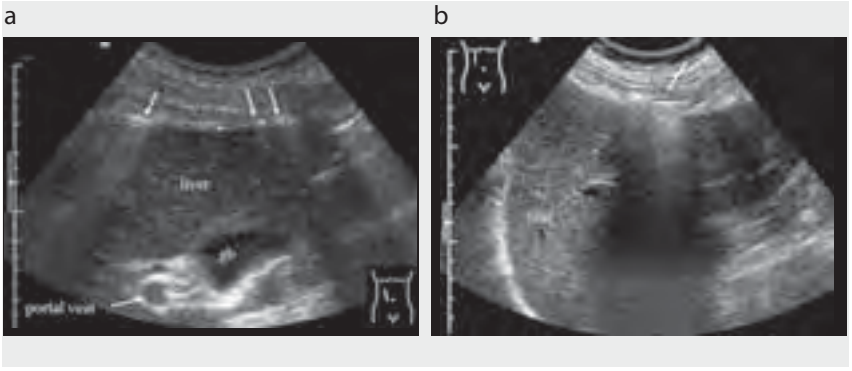

rarely, the connective tissue of the abdominal cavity or retroperitoneal space. Careful examination in different scanning planes, including guided palpation, may establish a connection with a certain organ or structure. Association with clear anatomical structures, such as the kidney or the aorta, can help in identifying the location. It should be noted that a tumour's close connection to the abdominal wall does not exclude a retroperitoneal origin (see Fig. 6.3a).

Differentiation between neoplastic lesions and pseudotumours is also difficult. Pancreatic pseudocysts are typical examples. They may be seen months or years after a

trauma or as an asymptomatic relict of a previous pancreatitis and are not infrequently localized some distance from the pancreas. Aneurysms of medium-size vessels pose a similar problem. They may be thrombosed and have the appearance of a tumour but not associated with an organ if the connection to an artery is not seen initially. Inflammatory pseudotumours consisting of small abscesses, fistulas, intestinal loops, lymph nodes and inflamed connective tissue show a complex pattern. Sometimes, a malignant tumour may cause an inflammatory reaction and have similar sonographic features. Large malignant tumours show a complex pattern, with echo-rich, echo-poor or even cystic sections. Consequently, a mass with cystic parts should not be misinterpreted as a (harmless) cyst.

The retroperitoneal lymph nodes, which are affected by malignant lymphomas or metastasizing carcinomas, represent a special problem for differential diagnosis, as the sonographic features of a partially thrombotic aortic aneurysm and of retroperitoneal fibrosis are similar. A horseshoe kidney also imitates a mass in front of the aorta. The relation of the 'mass' to the vena cava and its outline should resolve the situation, as shown in Table 6.2 and Fig. 6.46.

Table 6.2. Differential diagnoses of echo-poor masses around the aorta

Disorder	Ultrasound findings	Additional findings
Malignant lymphoma	Echo-poor, enlarged lymph nodes on both sides of both vessels. Aorta marked by strong wall echoes. Increased distance between aorta and vertebral column	Mesenteric lymph nodes, enlarged spleen
Retroperitoneal fibrosis	Echo-poor tissue around both vessels, ill-defined border	Hydronephrosis
Aneurysm	Echo-poor thrombosis, strong wall echoes at the surface of the mass	Vena cava not included
Horseshoe kidney	Echo-poor mass in front of the vessels. Smooth, sharp contour, connection to the kidneys	–
Abdominal tumour (colon)	Echo-poor or target-like lesion ('pseudokidney sign') distant to the aorta	–

Fig. 6.46. Differential diagnosis of echo-poor masses and structures around the aorta (see also Table 6.2)

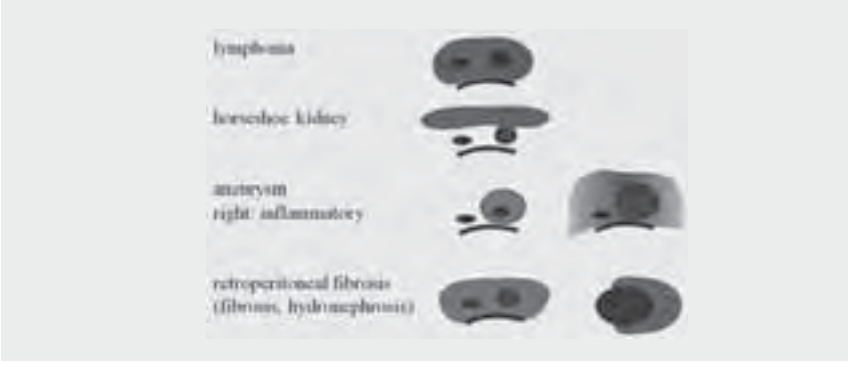

Supplementary methods

Ultrasound-guided puncture is the simplest, most reliable method for establishing a final diagnosis in various situations, such as solid tumours of unclear origin and nature, ascites and other fluid collections (see Chapter 3, Interventional ultrasound).

Chapter 7

Liver

7

Liver

Indications

The indications for ultrasonography of the liver are:

- enlarged liver (hepatomegaly)
- suspected liver abscess
- jaundice
- abdominal trauma
- ascites
- suspected metastases in the liver
- suspected liver mass
- right upper abdominal pain
- screening for endemic echinococcosis.

Examination technique

Equipment transducer

The examination should be carried out with the highest frequency transducer possible, usually 3.5 MHz or 5.0 MHz. Doppler techniques are needed for precise analysis of the vessels.

Preparation

The patient should take nothing by mouth for 8 h before the examination. If fluid is essential to prevent dehydration, only water should be given. If the symptoms are acute, the examination should be undertaken immediately. In the case of infants, if the clinical condition of the patient permits, they should be given nothing by mouth for 3 h before the examination.

Position of the patient

Real-time imaging of the liver is performed with the patient in the supine, left-oblique and left-lateral decubitus positions.

Scanning technique

Scanning should be in the sagittal, transverse and oblique planes, including scans through the intercostal and subcostal spaces (Fig. 7.1).

Fig. 7.1. Scanning area for evaluation of the liver in (a) supine position and (b) left posterior oblique position

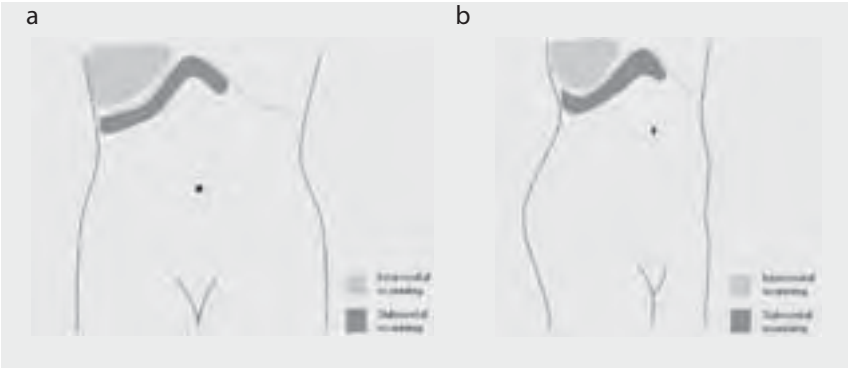

Normal findings

Echo texture

The normal liver parenchyma is homogeneous. Within the homogeneous parenchyma lie the thin-walled hepatic veins, the brightly reflective portal veins, the hepatic arteries and the hepatic duct. The liver texture is comparable to that of the renal parenchyma. The normal liver parenchyma should have a softer, more homogeneous texture than the dense medulla and hypoechoic renal cortex.

Echogenicity

The liver can be as or more echogenic than the kidney (Fig. 7.2); however, it can be less echogenic than the kidney, as the echogenicity of the renal cortex can be increased in some renal diseases (Fig. 7.3). The spleen has about the same echogenicity and the pancreas about the same or slightly greater echogenicity than the liver.

Size

Size is measured as shown in Fig. 7.4. Generally, the liver measures less than 15 cm, with 20 cm representing the upper limit of normal. Hepatomegaly is present when the liver exceeds 20 cm. There is, however, considerable variation.

Normal anatomy

Liver anatomy is based on its vasculature. The right, middle and left hepatic veins course between lobes and segments, and eight segments are distinguished in the Couinaud classification (Fig. 7.5). The middle hepatic vein separates the anterior segment of the right lobe from the medial segment of the left lobe. The right hepatic vein divides the right lobe into anterior and posterior segments, and the left hepatic vein divides the left lobe into medial and lateral segments. The ascending segment of the left portal vein and the fissure for the ligamentum teres also separate the medial segment of the left lobe from the lateral segment.

Fig. 7.2. Normal echo texture and echogenicity of the liver. The liver is isoechoic to the cortex of the right kidney (RK)

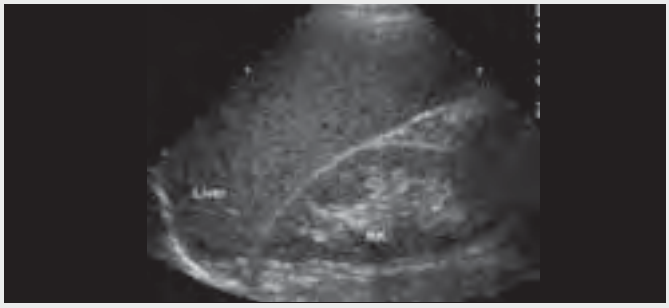

Fig. 7.3. Echogenicity of normal liver and in chronic renal parenchymal disease. Owing to increased renal cortical echo, that of the liver appears to be lower

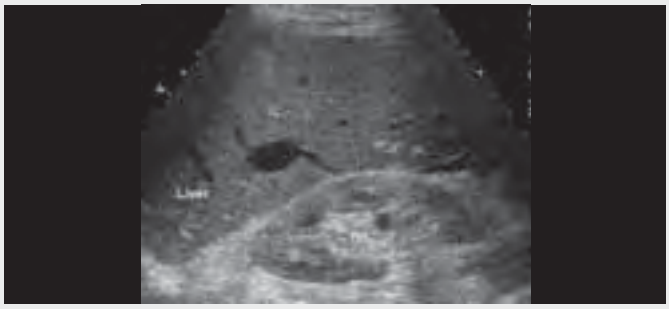

Fig. 7.4. Measurement of the liver, from the inferior tip to the dome on real ultrasonography (a) and diagramatically (b)

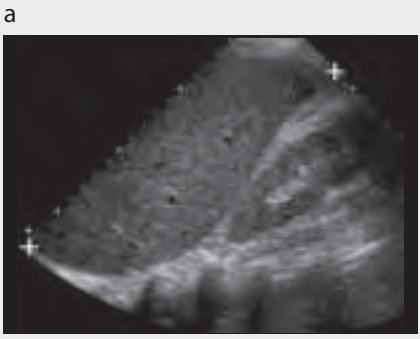

Fig. 7.5. Normal anatomy of the liver. (a) The right hepatic vein (RHV) divides the right anterior segment (RAS) and the right posterior segment (RPS) of the liver. The middle hepatic vein (MHV) (arrow) divides the right lobe and the left lobe, and the left hepatic vein (LHV) divides the left medial segment (LMS) and the left lateral segment (LLS); (IVC, inferior vena cava). (b) The open arrow shows the left hepatic vein, and the long solid arrow indicates the middle hepatic vein (RL, right lobe). (c) The main interlobar fissure (open arrow) divides the right and left lobes of the liver. The umbilical segment (solid arrows) of the left portal vein divides the LMS and the LLS. (d) Open arrow indicates the main interlobar fissure. The fissure for the ligamentum teres (solid arrow) divides the LMS and the LLS. (e–h) The segments are numbered 1–8 according to the Couinaud classification: (e) longitudinal scan at the epigastrium; (f) subcostal oblique ascending scan; (g) subcostal right transverse scan (GB, gallbladder; PV, portal vein); (h) right hypochondrium, longitudinal scan

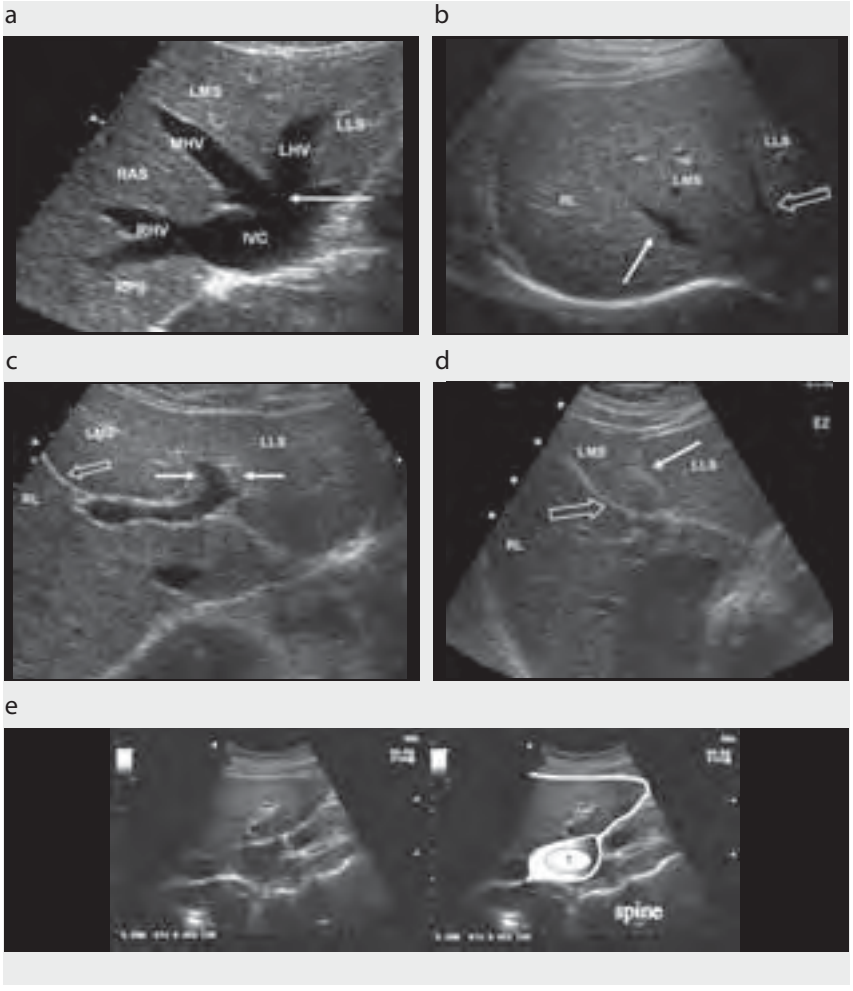

Fig. 7.5. *continued*

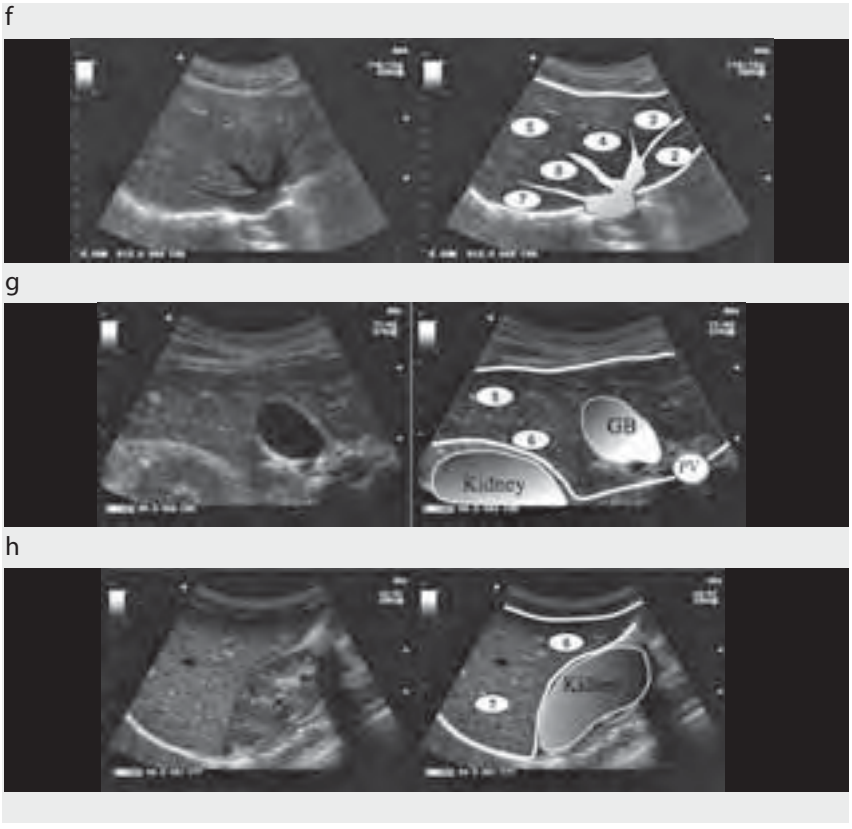

Pathological findings

Infectious diseases

Hepatitis

'Hepatitis' is the general term for inflammatory and infectious disease of the liver, of which there are many causes. Patients with acute and chronic hepatitis may initially present with flu-like and gastrointestinal symptoms, including loss of appetite, nausea, vomiting and fatigue.

In **acute hepatitis**, the liver parenchyma may have diffusely decreased echogenicity, with accentuated brightness of the portal triads, known as 'periportal cuffing' (Fig. 7.6). Hepatomegaly and thickening of the gallbladder wall are associated findings. In most cases, the liver appears normal.

In most cases of **chronic hepatitis**, the liver appears normal. The liver parenchyma may be coarse, with decreased brightness of the portal triads, but the degree of attenuation is not as great as in fatty infiltration (Fig. 7.7). The liver does not increase in size.

Fig. 7.6. Acute hepatitis. (a) The right hepatic lobe shows normal echo texture and normal echogenicity (arrow indicates right pleural effusion). (b) Diffuse thickening (arrows) of the gallbladder is revealed, suggesting gallbladder oedema

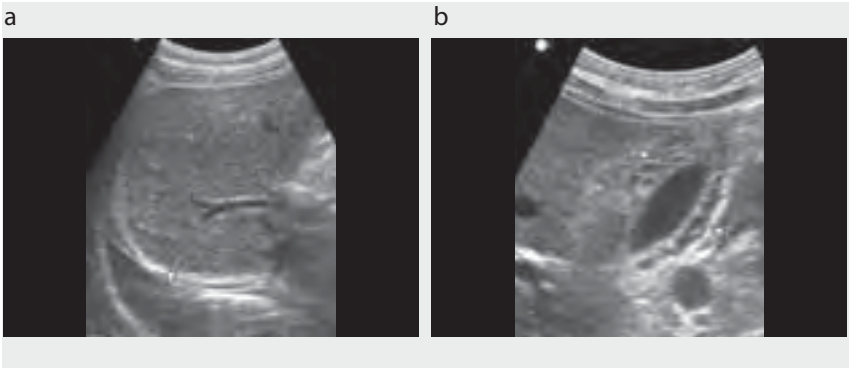

Fig. 7.7. Chronic hepatitis. Note the coarse echo texture of the liver, with increased echogenicity

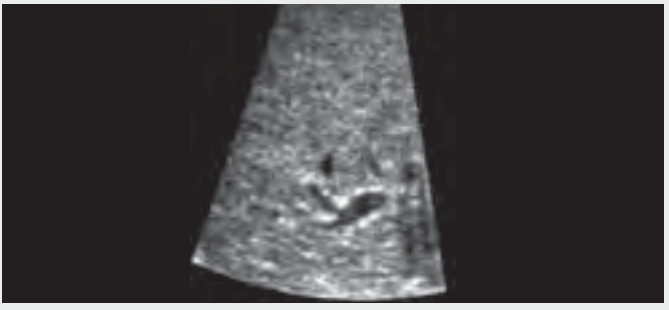

Cirrhosis

Sonographic diagnosis of cirrhosis may be difficult. The specific findings include a coarse liver pattern secondary to fibrosis and nodularity (Fig. 7.8); increased attenuation may be present, with decreased vascular markings. Diffuse steatosis can also manifest as increased attenuation with decreased vascular markings. Hepatosplenomegaly may be present, with ascites surrounding the liver in the early stages of cirrhosis, whereas in advanced stages the liver is often small, with enlargement of the caudate, left lobe or both relative to the right lobe. Isoechoic or hypoechoic regenerative nodules may be seen throughout the liver parenchyma, most of which are less than 1 cm in diameter. Dysplastic nodules are larger than regenerative nodules and can have variable echogenicity. As cirrhosis is considered premalignant, further examination and follow-up are needed.

Fig. 7.8. Liver cirrhosis. (a) Very coarse liver echo texture and surface nodularity (arrows), either gross or micronodular, are demonstrated by ultrasound (a, ascites). (b) The portal vein is dilated by > 1.3 cm in diameter. (c) Recanalization of the umbilical vein (uv) can create a spontaneous portosystemic shunt (g, gallbladder). (d, e) Volumetric changes in cirrhosis, either segmental, caudate (segment 1) hypertrophy (arrows in (d)) or regional right lobe atrophy (arrow in (e)) (a, ascites). (f) Splenomegaly of different degrees can be associated with cirrhosis (s, spleen; k, kidney). (g) Cirrhosis decompensation: ascites and gallbladder wall oedema (arrows) are noted

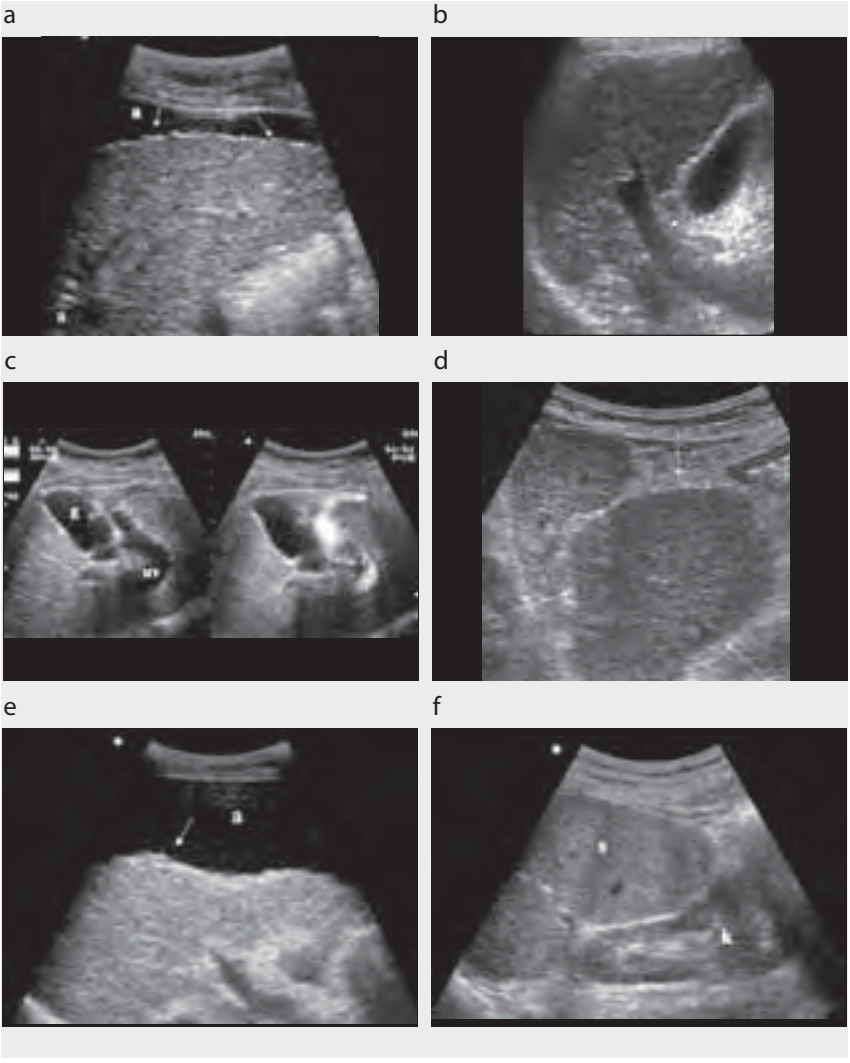

Fig. 7.8. *continued*

g

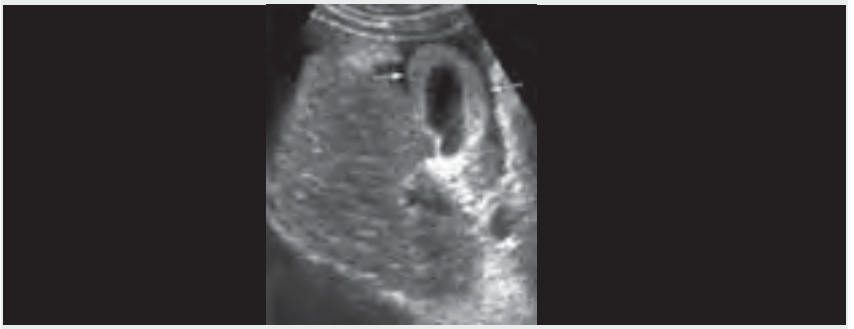

Fig. 7.9. (a, b, c) Mature liver abscesses (arrows): these are complex lesions with irregular, thick walls and septa and inhomogeneous echoes on the inside (arrowhead, diaphragm; asterisk, necrotic debris)

a

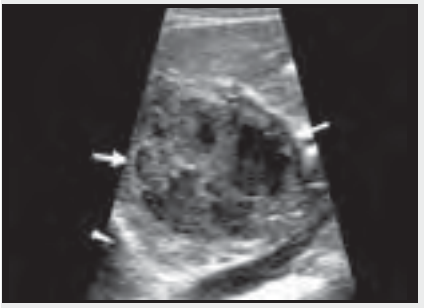

b

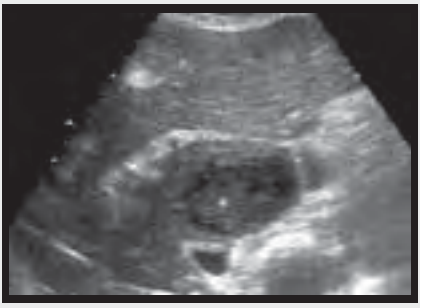

c

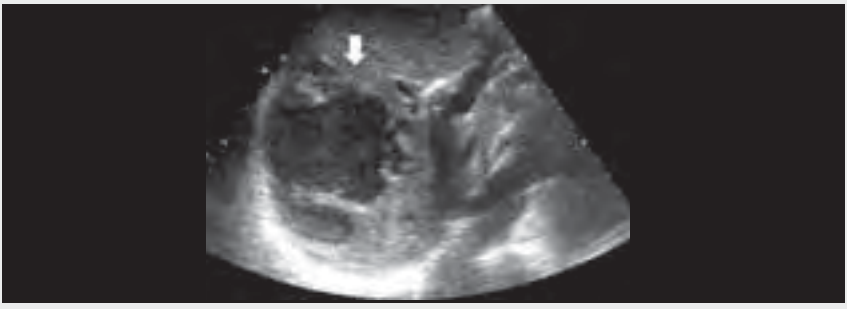

Pyogenic liver abscess

Sonographic identification of a pyogenic abscess depends on the maturity and internal consistency of the lesion. Mature purulent abscesses appear cystic, the fluid ranging from anechoic to highly echogenic (Fig. 7.9). Immature abscesses may appear solid, with altered echogenicity, and are usually hypoechoic (Fig. 7.10). The abscess may have echogenic foci, with a posterior reverberation artefact if gas is present. Fluid-filled interfaces, internal

septations and some debris are found along the posterior margin. The abscess wall can vary from well defined to irregular and thick (Fig. 7.11).

Fig. 7.10. Immature liver abscesses (arrows). Both hypoechoic (a) and isoechoic (b) abscesses appear solid

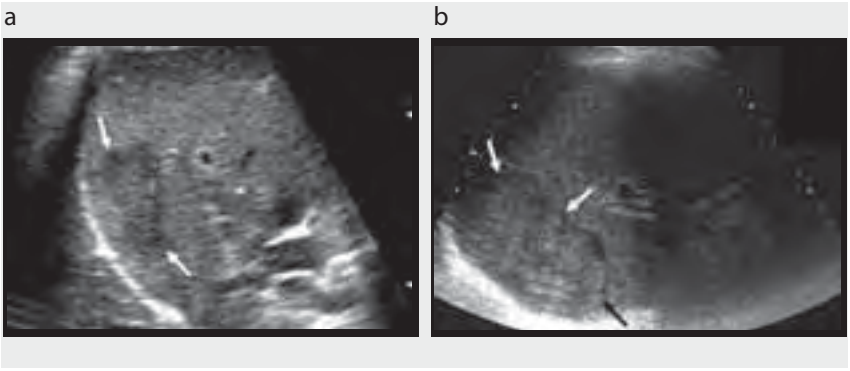

Fig. 7.11. Air-containing liver abscess (arrows). Multiple ring-down artefacts (arrowheads) arise from the abscess

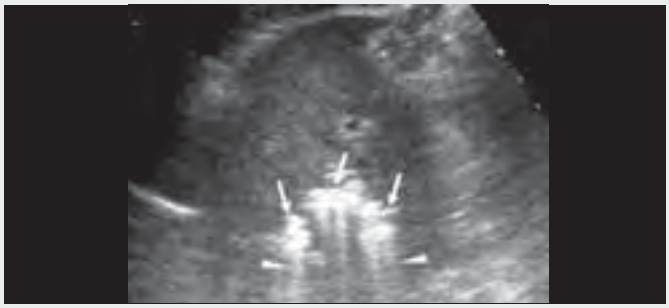

Fungal diseases

Hepatic candidiasis usually occurs in immunocompromised hosts and is transmitted via the bloodstream. The commonest finding is multiple hypoechoic nodules with discrete margins. Other sonographic patterns are 'wheel-within-a-wheel' patterns, multiple small hypoechoic lesions with echogenic central foci, referred to as 'bull's eye' or 'target' lesions (Fig. 7.12), or multiple hyperechoic nodules with posterior shadowing. Of these, the 'wheel-within-a-wheel' and 'bull's eye' patterns suggest that the infection is active, whereas the other two patterns occur later in the course of the disease and suggest that the infection is subsiding.

Fig. 7.12. Hepatic candidiasis. (a) A hypoechoic lesion with an echogenic central focus ('bull's-eye' nodule, arrow) is seen. (b) The typical 'wheel-within-a-wheel' pattern (arrows) seen during the course of the disease consists of a peripheral hypoechoic zone, a second echogenic wheel and a central hypoechoic nidus (arrow)

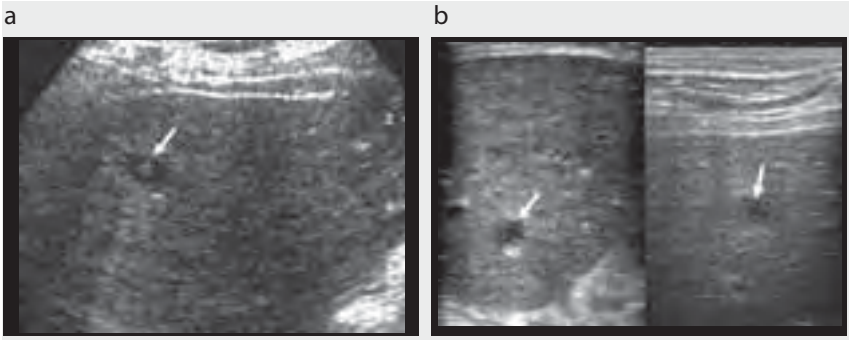

Amoebic abscess

An amoebic abscess is a collection of pus caused by hepatic infection with the parasite *Entamoeba histolytica*. The sonographic appearance of amoebic abscess is nonspecific and similar to that of pyogenic abscesses.

Echinococcal cysts

These cysts are most prevalent in sheep- and cattle-raising countries, especially Australia, the Mediterranean region and the Middle East. The sonographic features of echinococcal cyst are:

- simple cyst containing no internal architecture, except sand
- 'water lily sign', which are cysts with detached endocyst secondary to rupture
- 'cyst-within-a-cyst', with daughter cysts matrix and
- a densely calcified mass (Fig. 7.13).

Septations are frequent and include a honeycomb appearance with fluid collection. If a 'water lily sign' or 'cyst-within-a-cyst' is found, it is specific for echinococcal cyst.

There are two current classifications of hydatid cysts, one by WHO, consisting of cystic echinococcosis (CE) 1–5, and one by Gharbi, which is annotated simply as 1–5.

Hepatic tuberculosis

Involvement of the liver and spleen is common in patients with miliary tuberculosis. Sonography usually demonstrates only nonspecific hepatomegaly; however, the lesions are too small to be seen sonographically. Sometimes, either small, echo-poor nodules or a large mass called a pseudotumour or tuberculoma can appear over the liver (Fig. 7.14). Tuberculomas are frequently echo poor and must be distinguished from metastasis, abscess and primary liver tumour. As the disease progresses, hepatic tuberculosis may involve calcifications. In an analysis of patients with HIV infection and abnormal abdominal CT findings, 20% had liver cirrhosis.

Fig. 7.13. Hydatid cyst of the liver. (a) Type 1. Note the thick membrane (vc, vena cava). (b) Type 2. The membranes are detached (dotted line). (c) Type 3 (arrows). Multivesicular, with typical honeycomb appearance. (d) Type 4. Note the thick, tangled membrane and daughter vesicles (arrows). (e) Type 5. Ultrasound cannot explore the content of a calcified cyst (arrow)

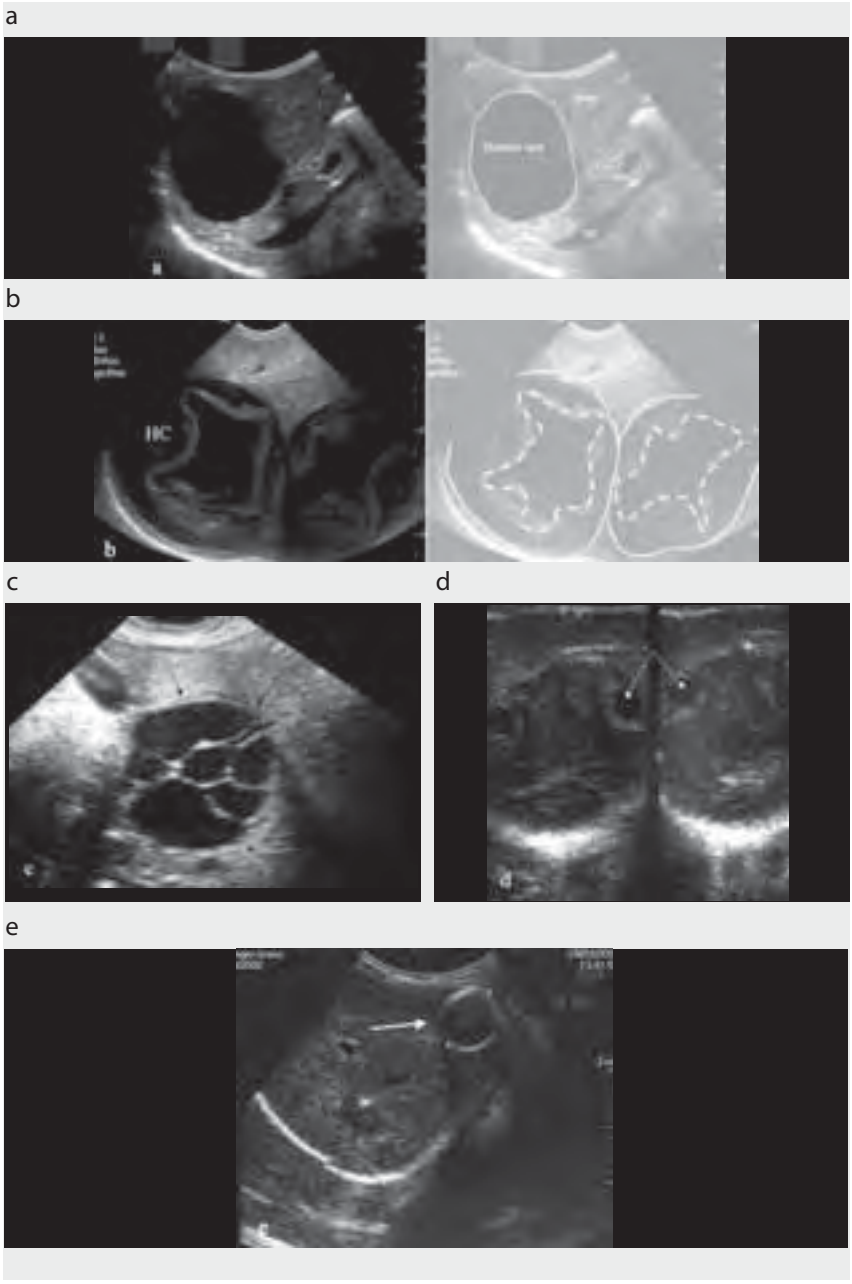

Fig. 7.14. Hepatic tuberculoma. An ill-defined, echo-poor, large mass (arrows) is seen in the right lobe of the liver

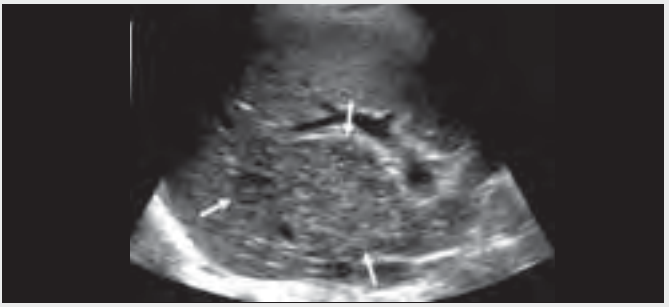

Metabolic disorders

Fatty liver

Sonographically, the liver has increased echogenicity and may be enlarged. Diffuse fatty liver has homogeneously increased echogenicity. The sonographic features of diffuse fatty liver are:

- bright liver, with greater echogenicity than the kidney
- decreased portal vein wall visualization
- poor penetration of the posterior liver and
- hepatomegaly (Fig. 7.15).

Fig. 7.15. Diffuse fatty liver. (a) The liver shows greater echogenicity than the kidney, with poor penetration of the posterior liver. (b) Decreased visualization of the portal vein wall (arrows) is seen

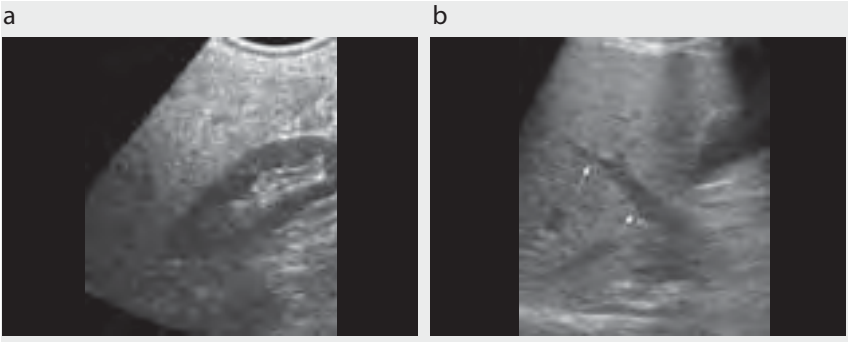

Focal fatty deposits show regions of increased echogenicity on a background of normal liver parenchyma (Fig. 7.16 (a)), whereas focal fatty sparing appears as hypoechoic masses within a dense, fatty-infiltrated liver (Fig. 7.16 (b)). Frequent locations include the region of the porta hepatis, near the falciform ligament, the dorsal

left lobe and the caudate lobe. These deposits tend to be geographically configured, i.e. have a map-like appearance but not nodular or round. The hepatic vessels are usually normal and not displaced in these areas on colour or power Doppler images.

Fig. 7.16. (a) Focal fat deposition (arrow) in the left lobe of the liver (MHV, middle hepatic vein). (b) Focal fatty "sparing" (between calipers) as a hypoechoic mass within a bright liver

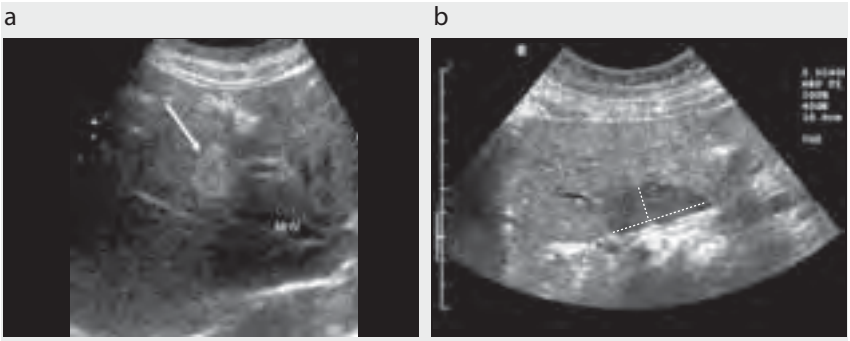

Fig. 7.17. Normal portal vein flow. Note the undulating hepatopetal flow signal

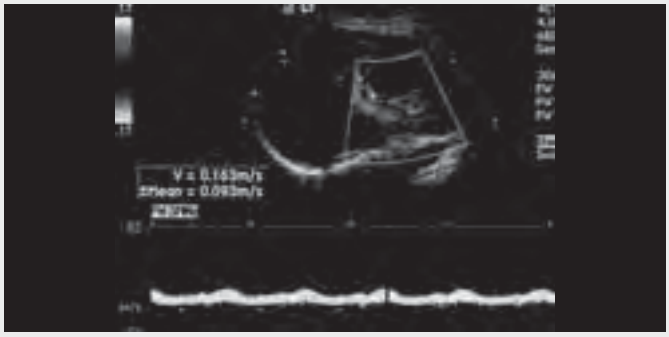

Vascular diseases

Portal hypertension

Sonography can be useful for defining the presence of ascites, hepatosplenomegaly and collateral circulation; the cause of jaundice; and the patency of hepatic vascular channels. The normal portal vein has an undulating hepatopetal flow (Fig. 7.17), whereas the calibre of the portal and splenic veins may be increased by more than 1.3–1.6 cm in portal hypertension. With the development of a porto-systemic shunt, however, the calibre of the veins may decrease. The superior mesenteric and splenic veins are more strongly influenced by respiration and the patient's position. Thus, any increase in size may not be due to portal hypertension. The main sites of porto-systemic shunt are the gastro-oesophageal junction, for the gastric and para-oesophageal varix;

the fissure of the ligamentum teres, for the recanalized umbilical vein; the splenic and left renal hilum, for spleno-renal and gastro-renal shunts; and the mesentery for mesenteric varix. The mean portal venous flow velocity is approximately 15–18 cm/s but varies with respiration and cardiac pulsation. As portal hypertension develops, the flow becomes monophasic. In advanced portal hypertension, the flow becomes biphasic and finally hepatofugal (Fig. 7.18).

Fig. 7.18. Reversed portal venous flow in portal hypertension. Note the biphasic hepatofugal flow signal

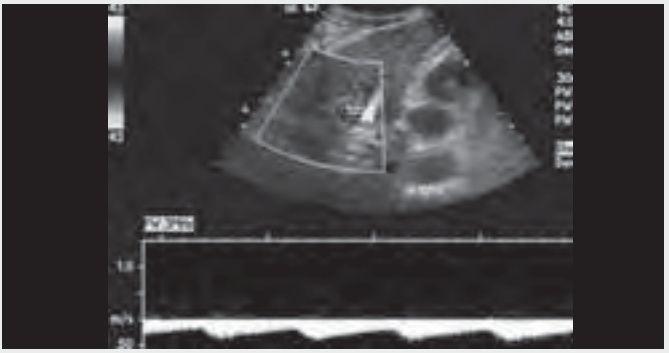

Portal vein thrombosis

Portal vein thrombosis develops secondary to slow flow, hypercoagulable states, inflammation or invasion by a malignancy such as hepatocellular carcinoma, metastatic liver disease, pancreatic carcinoma or primary hepatic vascular leiomyosarcoma of the portal vein. Slow flow is usually secondary to portal hypertension, with shunting of mesenteric and splenic flow away from the liver. Sonography is an accurate means of confirming portal vein thrombosis. In sonography, portal flow is absent, and the vessel may be filled with a hypoechoic thrombus. As an acute thrombus can be hypoechoic or anechoic and may be overlooked, colour Doppler examination is necessary. Doppler sonography is also useful for distinguishing benign from malignant portal vein thrombi in patients with cirrhosis. The following sonographic findings suggest malignant thrombi:

- expansion of involved portal vein
- a periportal tumour connected to the thrombi and
- a pulsatile flow signal within the thrombi (Fig. 7.19).

'Cavernous transformation' of the portal vein manifests as numerous wormlike vessels at the porta hepatis, which represent periportal collateral circulation. This is observed in longstanding thrombus or occlusion, i.e. longer than 12 months.

Hepatic venous obstruction and Budd-Chiari syndrome

As the hepatic veins have thin walls and no adventitia, the walls are less echogenic than those of the portal vein. The flow patterns in the hepatic vein are influenced by heart

Fig. 7.19. Malignant portal vein thrombosis. (a) On the grey-scale image, echogenic material (arrows) is seen within the main portal vein, with dilatation of the portal vein. (b) On a power Doppler image, irregular vascular channels with a pulsatile flow signal are seen within the thrombus (arrows)

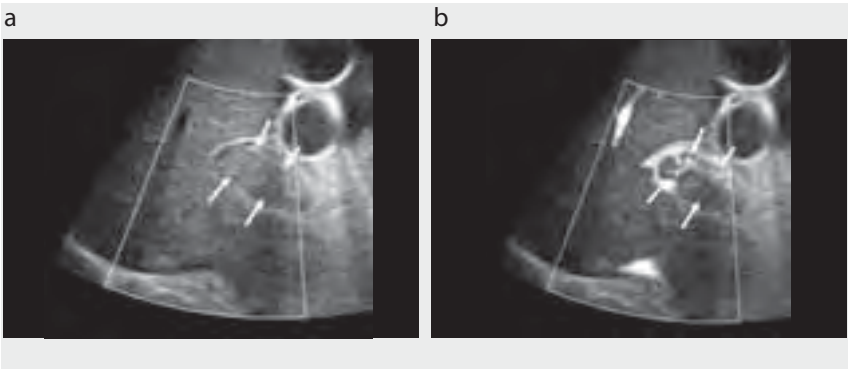

motion. Normal individuals show two prominent antegrade (hepatofugal) waves and one prominent retrograde (hepatopetal) wave; thus, the hepatic veins have a triphasic wave. The larger of the two antegrade waves occurs during systole and is due to atrial relaxation, whereas the other occurs during diastole after opening of the tricuspid valve. The retrograde wave occurs when the right atrium contracts at the end of diastole.

Obliteration of hepatic vein pulsatility should be considered abnormal. In some cases, it may indicate anatomical obstruction between the right atrium and hepatic veins, such as a tumour or Budd-Chiari syndrome.

Hepatic venous obstruction can be due to obstruction of the suprahepatic portion of the inferior vena cava, thrombosis of the main hepatic veins themselves or obstruction at the level of small hepatic venules. Budd-Chiari syndrome generally involves the first two conditions, while hepatic veno-occlusive disease involves the last.

The sonographic findings in Budd-Chiari syndrome include evidence of hepatic vein occlusion and abnormal intrahepatic collaterals. The findings in hepatic vein occlusion include partial or complete disappearance of the hepatic veins, stenosis, dilatation, thick wall echoes, abnormal course, extrahepatic anastomoses and thrombosis.

In Budd-Chiari syndrome, Doppler sonography may show abnormal blood-flow patterns in the hepatic veins and inferior vena cava. The flow in the inferior vena cava, the hepatic veins or both changes from phasic to absent, reversed, turbulent or continuous. The portal blood flow may also be affected, characteristically being either slowed or reversed. Colour Doppler imaging can reveal hepatic venous occlusion, hepatic-systemic collaterals, hepatic vein–portal vein collaterals and anomalous or accessory hepatic veins of increased calibre.

Hepatic veno-occlusive disease

Hepatic veno-occlusive disease is defined as progressive occlusion of the small hepatic venules. Patients with this disease are clinically indistinguishable from those with Budd-Chiari syndrome. Doppler sonography shows normal calibre, patency and phasic flow in the main hepatic veins and inferior vena cava. The flow in the portal vein may be abnormal, being either reversed or 'to-and-fro'.

Focal hepatic lesions

Benign cysts

Simple cysts are usually incidental, because most patients who have them are asymptomatic. Simple cysts are anechoic, with a well demarcated, thin wall and posterior acoustic enhancement (Fig. 7.20). Infrequently, these cysts contain fine linear internal septa. Complications such as haemorrhage or infection may occur and cause pain. Calcification may be seen within the cyst wall and may cause shadowing. In adult polycystic liver disease, the cysts are small (< 2–3 cm) and occur throughout the hepatic parenchyma. Histologically, they are similar to simple hepatic cysts.

Peribiliary cysts are small (0.2–2.5 cm) and are usually located centrally within the porta hepatis or at the junction of the main right and left hepatic ducts. Sonographically, peribiliary cysts can be seen as discrete, clustered cysts or as tubular structures with thin septa, paralleling the bile ducts and portal veins (Fig. 7.21).

Fig. 7.20. A simple cyst in the right lobe of the liver, showing a well demarcated, thin-walled, anechoic lesion (long arrow) with posterior acoustic enhancement (short arrows)

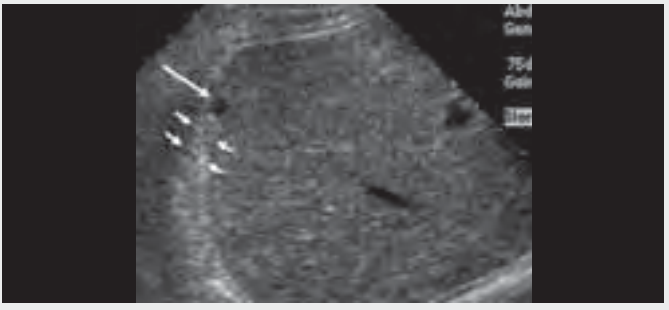

Fig. 7.21. Peribiliary cysts. Colour Doppler sonography shows multiple cysts (arrows) clustered around the portal veins (RPV, right portal vein; LPV, left portal vein; IVC, inferior vena cava)

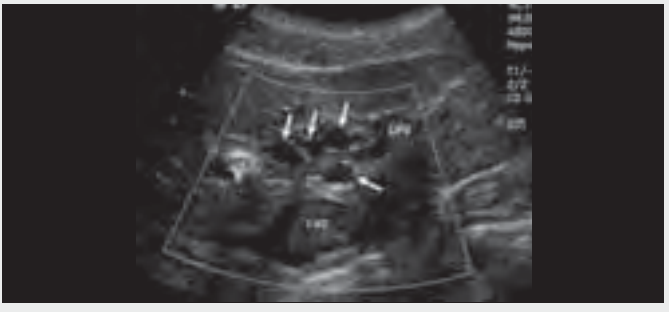

Biliary hamartoma

Bile duct hamartomas are benign liver malformations, which usually show innumerable, well defined, solid nodules less than 1 cm in diameter. The lesions are usually hypoechoic and less commonly hyperechoic. Bright echogenic foci in the liver with distal ring-down artefacts are characteristic (Fig. 7.22).

Fig. 7.22. Biliary hamartoma. Multiple echogenic foci with posterior ring-down artefacts (arrows) are seen in the right lobe of the liver

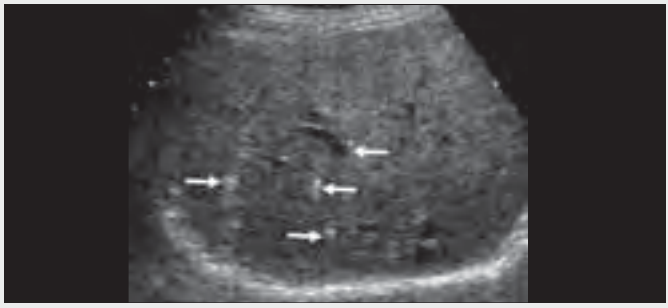

Haemangioma

Haemangiomas are benign congenital tumours consisting of large, blood-filled cystic spaces. They are the commonest benign tumours of the liver. Their sonographic appearance is characteristic: most are less than 3 cm, homogeneous and hyperechoic with acoustic enhancement (Fig. 7.23 (a)). Another typical feature is a heterogeneous central area containing hypoechoic portions with a thin or thick echogenic border (Fig. 7.23 (b)). Haemangiomas are round, oval or lobulated, with well defined borders. Larger haemangiomas may have a mixed pattern, resulting from necrosis. Calcification is rare.

Fig. 7.23. Typical hepatic haemangiomas. (a) A homogeneous hyperechoic nodule with posterior acoustic enhancement (arrows). (b) A hyperechoic nodule (arrows) with a central heterogeneous hypoechoic area

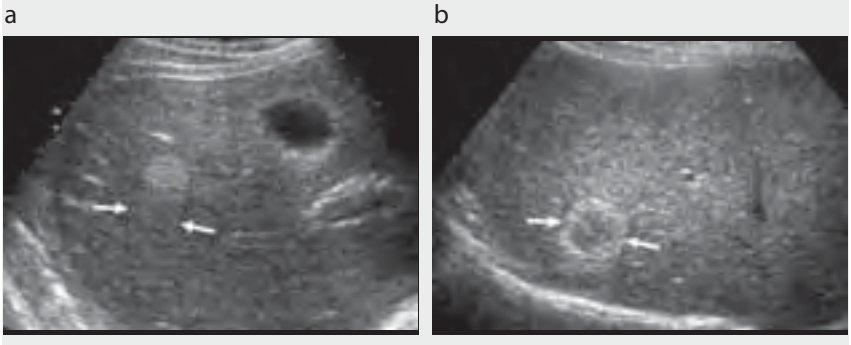

Focal nodular hyperplasia

Focal nodular hyperplasia is the second most common benign liver mass after haemangioma. It is commoner in women than men, particularly among women of childbearing age, and is typically a well circumscribed, usually solitary mass with a central scar. Its excellent blood supply makes haemorrhage, necrosis and calcification rare. On sonography, focal nodular hyperplasia is well defined and hyperechogenic or isoechogenic relative to the liver (Fig. 7.24 (a)). It often manifests as a subtle liver mass that is difficult to differentiate from the adjacent normal liver. Doppler features of focal nodular hyperplasia are highly indicative, in that well developed peripheral and central blood vessels are seen (Fig. 7.24 (b)). The characteristic finding on colour Doppler is intra-tumoral blood vessels within the central scar, with either a linear or a stellate configuration.

Fig. 7.24. Focal nodular hyperplasia. (a) A nearly isoechoic mass (arrows) can be seen in the left lobe of the liver. (b) On colour Doppler sonography, stellate or spoke-wheel-like vascularity (arrowheads) due to centrifugal arterial flow is noted

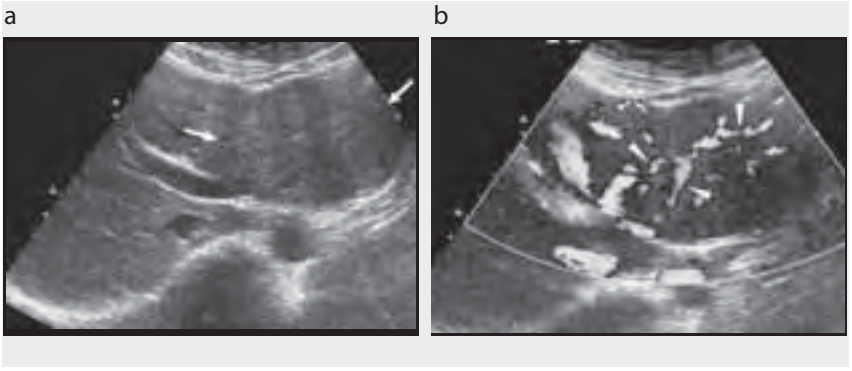

Hepatic adenoma

Hepatic adenoma occurs more commonly in women than men and has been associated with use of oral contraceptives. Patients may present with right upper-quadrant pain secondary to rupture, with bleeding into the tumour. Hepatic adenomas have also been reported in association with glycogen storage or **von Gierke disease**. Because hepatic adenoma has a propensity to haemorrhage and there is a risk for malignant degeneration, surgical resection is recommended. The sonographic appearance of hepatic adenoma is non-specific, and the echogenicity is variable (Fig. 7.25). In haemorrhage, a fluid component may be evident within or around the mass, and free intraperitoneal blood may be seen. The mass may be solitary or multiple. If the liver ruptures, fluid may be found in the peritoneal cavity.

Biliary cystadenoma and biliary cystadenocarcinoma

Biliary cystadenoma is a rare cystic neoplasm occurring primarily in middle-aged women. Although it is usually benign, it tends to recur after subtotal excision and can develop into a malignant cystadenocarcinoma. The most striking feature of the gross pathology of a biliary cystadenoma or cystadenocarcinoma is its multiloculated

Fig. 7.25. Large adenoma of the right liver lobe. (a) Echo-poor oval lesion with (b) multiple vascular signals within the lesion detected by power Doppler

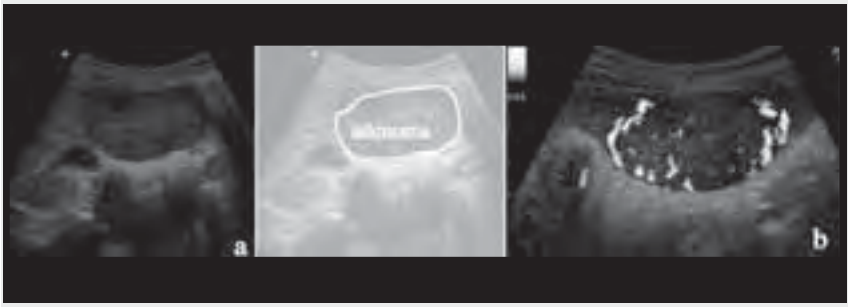

appearance. In patients with biliary cystadenoma, the most common sonographic finding is a septated multilocular cyst with no gross nodules or soft-tissue mass (Fig. 7.26). Although cystadenoma usually cannot be differentiated from cystadenocarcinoma by imaging criteria, the presence of solid nodular masses or coarse calcifications along the wall or septa in a multilocular cystic mass indicates a likely diagnosis of biliary cystadenocarcinoma (Fig. 7.27).

Fig. 7.26. Biliary cystadenoma. A multilocular cystic mass (arrows) with irregular septa is seen

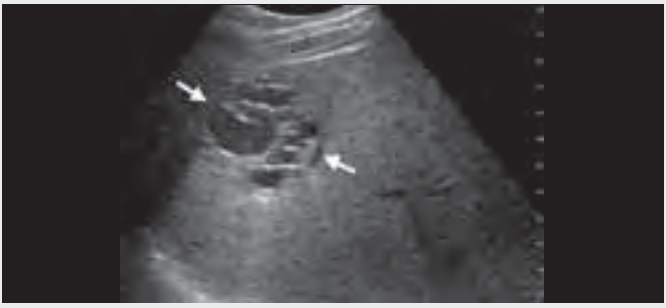

Hepatocellular carcinoma

Hepatocellular carcinoma (HCC) is one of the commonest malignant tumours worldwide and its incidence is increasing, particularly in Africa and Asia. It is strongly associated with cirrhosis (80% of patients with HCC have cirrhosis) and chronic viral hepatitis. Alcoholic cirrhosis is a potential predisposing factor for HCC, and both viral hepatitis B and viral hepatitis C are now widespread. Pathologically, HCC occurs in three forms: solitary, multiple nodules and diffuse infiltrative. The sonographic appearance is variable, but there is a relation to size. Small HCCs (< 3 cm) tend to be hypoechoic (Fig. 7.28). Increasing echogenicity is related to the presence of haemorrhage, fibrosis and necrosis, echogenic lesions being found in about one

Fig. 7.27. Biliary cystadenocarcinoma. A large multilocular cystic mass (long arrows) with thick mural nodules (asterisks) and septa (short arrows) are noted

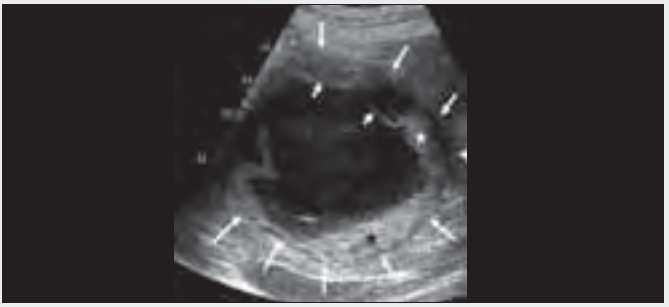

half of large HCCs. Small HCCs may also appear hyperechoic due to fatty change or sinusoidal dilatation. A mosaic pattern, a hypoechoic halo and lateral shadowing are relatively specific findings in HCCs (Fig. 7.28). The mosaic pattern is due to the presence of multiple compartments of different histological origin in a tumour. A hypoechoic halo and lateral shadowing are caused by a fibrous capsule. Portal or hepatic venous invasion of a tumour is considered to be characteristic of HCC and is associated with a poorer prognosis. Colour and spectral Doppler show high-velocity systolic and diastolic signals in HCC due to arteriovenous shunts and low impedance vasculature. The basket pattern and intratumoral vascular pattern are characteristic of HCCs on colour Doppler sonography (Fig. 7.28). Colour and power Doppler techniques are excellent for detecting neovascularity in tumour thrombi within the portal veins, which is diagnostic of HCC even without the demonstration of the parenchymal lesion.

Fibrolamellar hepatocellular carcinoma

Fibrolamellar HCC is a rare form (2%), occurring in young patients without coexisting liver disease. It has a better prognosis than HCC itself. It is typically large, solitary and slow growing, often with calcification and a central fibrosis scar resembling focal nodular hyperplasia.

Metastases

Metastatic disease is the commonest form of neoplastic involvement of the liver. It is most common in association with colon cancer, with decreasing frequency in gastric, pancreatic, breast and lung cancers. The sonographic appearance of metastatic liver disease varies. Knowledge of a prior or concomitant malignancy and features of disseminated malignancy at the time of sonography are helpful for correct interpretation of sonographically detected liver masses. They may present as a single liver lesion, but do so more commonly as multiple focal masses. Although there are no absolutely confirmatory features of metastatic disease on sonography, the presence of multiple solid nodules of different sizes and the presence of a hypoechoic halo surrounding a liver mass are indicative of metastasis (Fig. 7.29).

Hyperechoic metastases are generally from a gastrointestinal tumour, a renal cell carcinoma, a carcinoid, a choriocarcinoma or an islet cell tumour, and the echogenicity

Fig. 7.28. Small hepatocellular carcinoma (HCC). (a) A small, low echoic tumour measuring 1.7 cm in diameter (arrow) with slight heterogeneous internal echogenicity and a subtle hypoechoic halo; the coarse echo texture indicates chronic liver disease. (b) Echogenic HCC nodule with a subtle hypoechoic halo. (c) This tumour has two echoic areas, with a sharp distinction within the tumour (node-intra-node pattern). Note, in (b) and (c), the hypoechoic halo (long arrows), lateral shadowing (short arrows) and posterior enhancement. (d) Echo-rich, inhomogeneous HCC with hypoechoic halo. (e) Echo-poor HCC with extracapsular growth. (f)–(h) In larger tumours, the echo texture is complex (mosaic pattern and multiple tumour vascular signals are found). Colour Doppler sonography of HCC: (g) basket pattern in which peritumoral and intratumoral vessels are seen (arrows indicate the tumour margin); (h) in the intratumoral vascular pattern, the feeding vessel goes directly into the tumour and branches within it (arrows indicate the tumour margin)

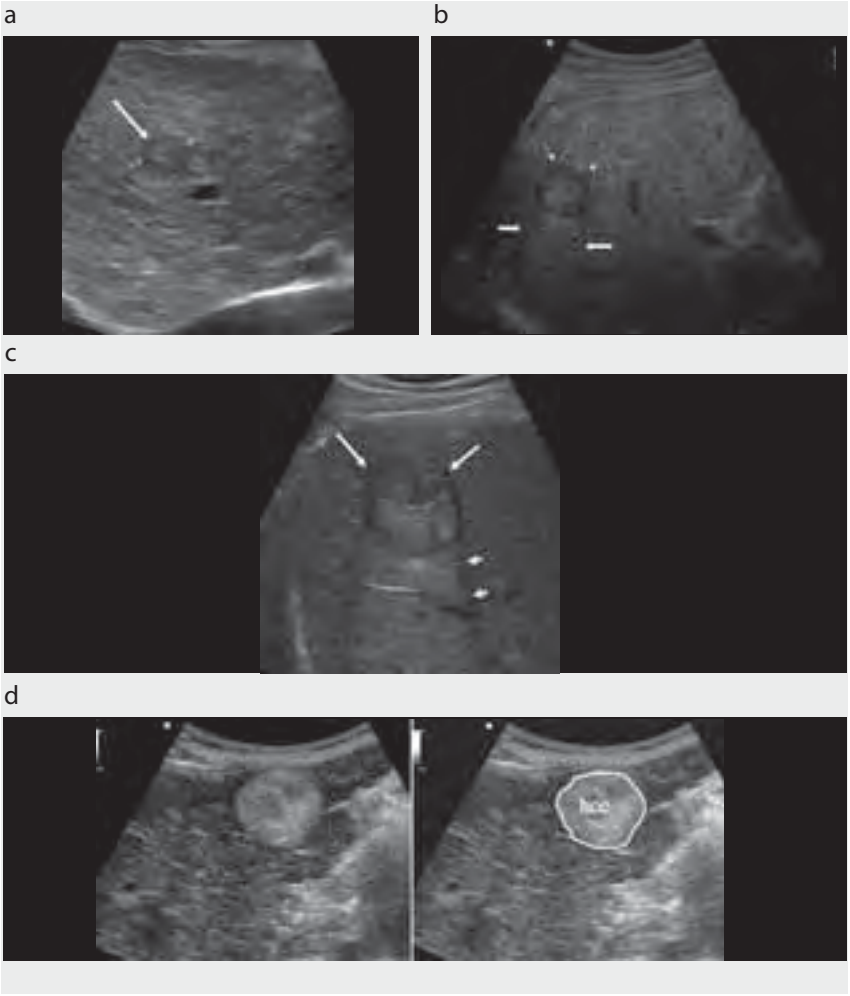

Fig. 7.28. *continued*

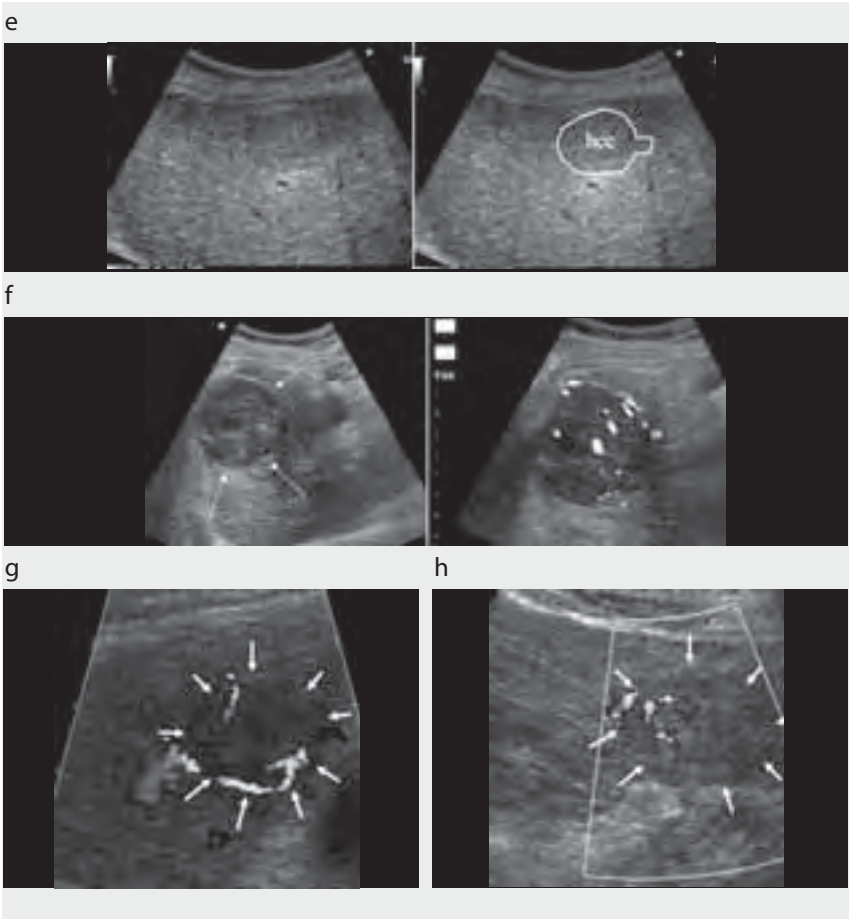

of the lesion increases with the vascularity of the tumour (Fig. 7.29). Hypoechoic metastases are typical after breast or lung cancer, but metastases from gastric, pancreatic or oesophageal cancer may also be hypoechoic. Calcific metastases have marked echogenicity and posterior shadowing (Fig. 7.30). They are most frequently associated with mucinous adenocarcinoma. Cystic metastases can generally be differentiated from benign hepatic cysts by their irregular thick walls, mural nodules, fluid–fluid levels and internal septation. Cystadenocarcinoma of the ovary and pancreas and mucinous carcinoma of the colon may be associated with cystic metastases in the liver. More often, cystic neoplasms occur secondary to extensive necrosis, most commonly in metastatic sarcoma (Fig. 7.31). Metastatic neuroendocrine tumours and large necrotic colorectal metastases can be predominantly cystic.

Diffuse infiltrative metastases, which may be confused with chronic liver disease, can occur after breast cancer, lung cancer and malignant melanoma. The 'bull's-eye' pattern or 'target' sign indicates a hyperechoic or isoechoic lesion with a peripheral hypoechoic halo and is the result of compression, fibrosis or hypervascularity of adjacent liver parenchyma (see Fig. 7.29). Clinically, the presence of this hypoechoic halo is an important sign of malignancy, such as metastases and HCCs (see Fig. 7.28 and Fig. 7.29).

Fig. 7.29. Multiple metastatic tumours from a carcinoid. Multiple hyperechoic nodules (arrows) have a peripheral hyperechoic halo with a 'target' or 'bull's-eye' pattern

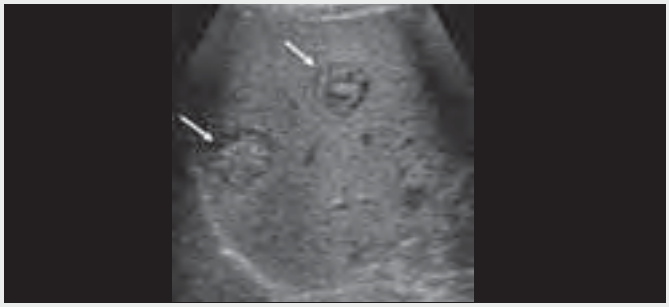

Fig. 7.30. Calcified metastatic tumours from colon cancer. Multiple, very bright echogenic nodules with posterior shadowing are noted

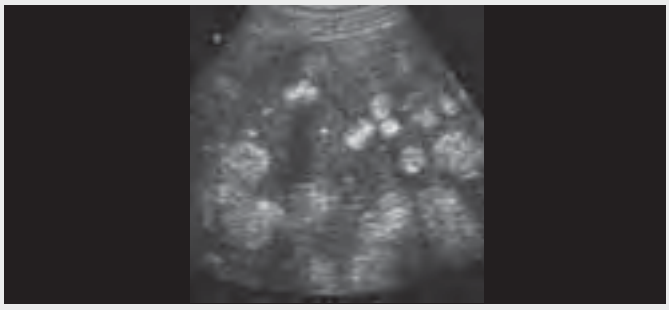

Fig. 7.31. Multiple solid and cystic metastases from gastrointestinal stromal tumours. (a) Multiple hypoechoic nodules (arrows) with a central cystic area are seen. (b) Some nodules show complete or partial cystic change due to extensive tumour necrosis

a

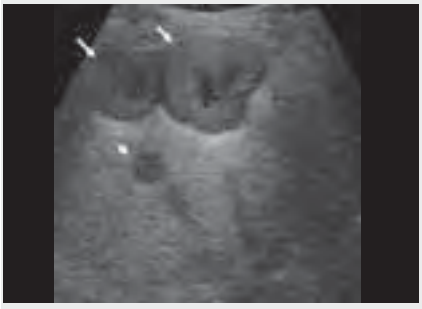

b

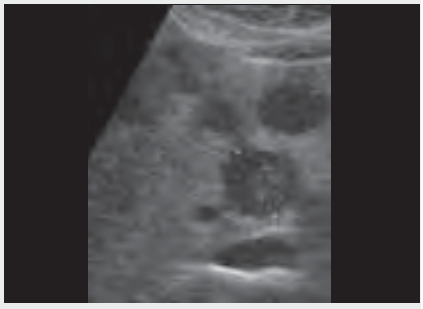

Intrahepatic cholangiocarcinoma

Intrahepatic cholangiocarcinoma is the second commonest primary hepatic malignant tumour after HCC, accounting for 5–30% of all primary malignant hepatic tumours. They can be classified as peripheral tumours. On sonography, most occur as a single, homogeneous, hypoechoic mass (Fig. 7.32). When detected, they are usually ill defined and poorly reflective. Commonly, dilated intrahepatic bile ducts are seen, which terminate at the level of the tumour. Occasionally, a tumour is intraluminal or causes focal thickening of the bile duct wall, resulting in stenosis in the absence of a mass. The tumour may be multifocal. As a rule, portal vein tumour thrombus is rare.

Fig. 7.32. Intrahepatic cholangiocarcinoma. In the right lobe of the liver, a large, ill-defined, heterogeneous, echo-poor mass (arrows) with multiple intratumoral echogenic spots can be seen

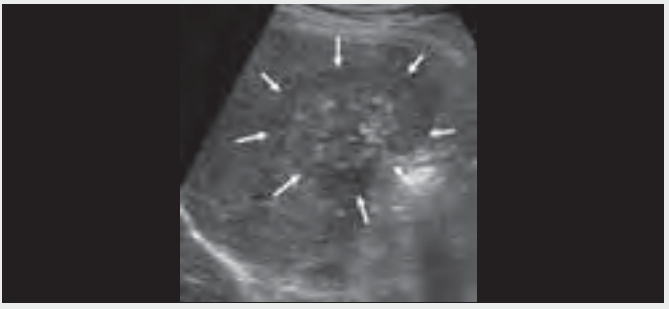

Lymphoma

Primary liver lymphoma is rare, and secondary liver lymphoma is also uncommon. Lymphomatous involvement of the liver appears either as a normal or a diffuse alteration of parenchymal echoes with hepatomegaly or as homogeneous hypoechoic masses (Fig. 7.33), which tend to have posterior acoustic enhancement. The pattern of multiple hypoechoic hepatic masses is more typical of primary non-Hodgkin lymphoma of the liver or lymphoma associated with HIV/AIDS.

Fig. 7.33. Lymphoma of the liver. (a) Multiple echo-poor tumours are seen throughout the liver. (b) Some tumours show a typical 'bull's-eye' pattern

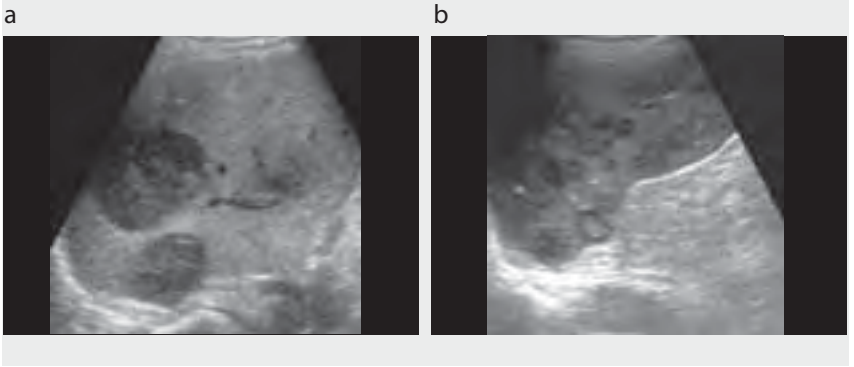

Epithelioid haemangioendothelioma

Hepatic epithelioid haemangioendothelioma is a rare tumour of vascular origin that occurs almost exclusively in adults. It is difficult to diagnose on clinical grounds because of its non-specific signs and symptoms and misinterpretation of pathological specimens. On sonography, these tumours usually consist of discrete, mostly peripheral, individual tumour nodules measuring 2–4 cm. As the nodules grow and coalesce with time, they may show peripheral, confluent tumour masses. The echogenicity of the tumours varies, although they are usually hypoechogenic.

Angiosarcoma

Angiosarcoma is a malignant tumour arising from vascular endothelial cells. It is associated with exposure to various toxic materials, such as polyvinyl chloride, arsenic and Thorotrast (previously used as an intravascular contrast agent). The condition occurs almost exclusively in adults, predominantly in men. The tumours are usually large, unencapsulated and nodular or multinodular. Their sonographic appearance is commonly that of a large mass of mixed echogenicity, associated with necrosis and haemorrhage. If these tumours show a diffuse infiltrative pattern, they cannot be differentiated from diffuse hepatocellular disease.

Trauma

Abdominal trauma most frequently affects the spleen, kidney and liver. CT is used more often than sonography to evaluate the presence and extent of liver laceration, while sonography is usually used to monitor serially the pattern of healing. In the sonographic findings of acute trauma to the liver, fresh haemorrhage is echogenic. Within the first week, a hepatic laceration becomes more hypoechoic and distinct as blood becomes resolved (Fig. 7.34). Septations and internal echoes develop 2–4 weeks after trauma. A subcapsular haematoma may appear as anechoic, hypoechoic, septated lenticular or curvilinear. Fluid in the right upper quadrant or in the right upper quadrant and pelvic recess may suggest hepatic injury, as opposed to splenic, renal or enteric injury.

Fig. 7.34. Liver laceration. (a) The irregularly lacerated lesion (arrows) has a track-like zone, which in (b) is shown as an echo-poor zone with a central anechoic area. It suggests resolution of a haematoma in the lacerated zone

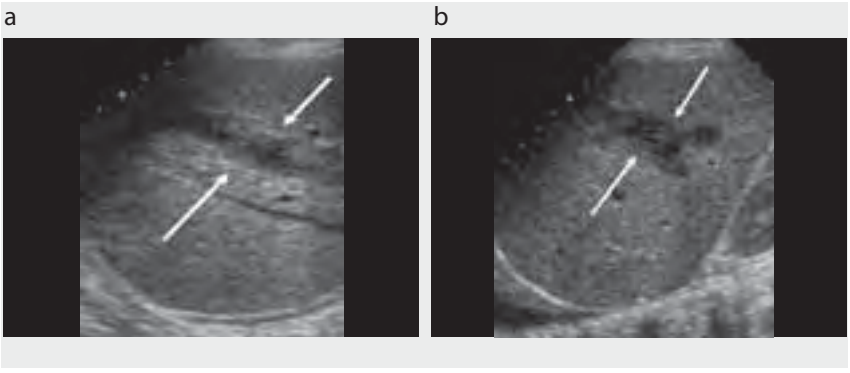

Chapter 8

Gallbladder and bile ducts

8

Gallbladder and bile ducts

Indications

The indications for ultrasonography of the gallbladder and bile ducts are:

- pain in the right upper abdomen (raises suspicion of gallstones or cholecystitis)
- jaundice
- palpable right upper abdominal mass
- recurrent symptoms of peptic ulcer
- fever of unknown origin.

Examination technique

Equipment, transducer

For adults, use a 3.5-MHz transducer. For children and thin adults, use a 5-MHz transducer.

Preparation

The patient should take nothing by mouth for 8 h before the examination. If fluid is required, only water should be given. If the symptoms are acute, proceed with the examination. Clinical conditions permitting, infants should be given nothing by mouth for 3 h before the examination.

Position of the patient

Start with the patient lying in the supine position. It may be necessary to turn patients onto the left side or to examine them in the erect position or on their hands and knees. Apply coupling agent liberally to the right upper abdomen and then to the left upper abdomen, because, whatever the symptoms, both sides should be scanned. For the scans, ask patients to hold their breath with the abdomen 'pushed out' in full expiration.

Scanning technique

Start by placing the transducer centrally at the top of the abdomen (the xiphoid angle). Angle the beam to the right side of the patient to image the liver and adjust the gain to obtain the best image.

Start with longitudinal scans, followed by transverse; add intercostal scans if needed. Then turn the patient on the left side and make oblique scans at different angles. The best method for visualizing the proximal common duct and the gallbladder is a right anterior oblique view with the patient in a left posterior oblique or left lateral decubitus position during deep inspiration (Fig. 8.1).

Fig. 8.1. Right anterior oblique view for visualization of the proximal common bile duct and the gallbladder

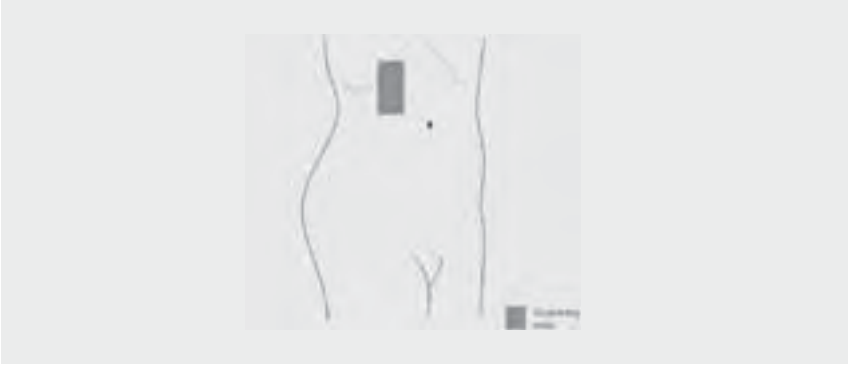

Sonographic evaluation of the bile ducts should include the following five images (Fig. 8.2):

- a subcostal oblique view to assess the ductal confluence anterior to the portal vein bifurcation at the porta hepatis;
- a transverse left lobe view for evaluation of left intrahepatic ducts (recumbent H view);
- a right coronal intercostal view for evaluation of the right intrahepatic ducts;
- a hepatoduodenal ligament view for assessment of the extrahepatic duct from the common hepatic duct to the pancreas head; and
- views of the pancreas head to assess the distal common bile duct.

If there is excessive gas in the bowel, the patient should be examined standing (sitting will not usually displace bowel gas).

In most patients, the gallbladder is best imaged using the liver as an acoustic window. It is recommended that the gallbladder be imaged with the patient in the supine, left posterior oblique, left lateral decubitus and semiprone positions. In each position, it is important to visualize the gallbladder neck, because stones may be hidden in this region. The interlobar fissure can be a valuable anatomical landmark for localizing the gallbladder when the latter is contracted or when it is small and filled with stones (Fig. 8.3). Visualization with the patient on the hands and knees can demonstrate gallstones more clearly, as they can move anteriorly.

Fig. 8.2. Five basic images for evaluating the bile ducts and each scanning location: (a) a subcostal oblique view (IHD, intrahepatic duct; RPV, right portal vein; LPV, left portal vein); (b) a transverse left lobe view; (c) a view of the right coronal intercostals (S5, segment 5; S7, segment 7; S8, segment 8); (d) a view of the hepatoduodenal ligament (PC, pancreas; PV, portal vein; IVC, inferior vena cava; and (e) view of the pancreas head (GDA, gastroduodenal artery; SV, splenic vein; CD, common hepatic and common bile ducts; Ao, aorta). (f) Diagram showing the scanning areas used to obtain each of the five basic images (a, subcostal oblique view; b, transverse left lobe view; c, right coronal intercostal view; d, hepatoduodenal ligament view; e, pancreatic head view)

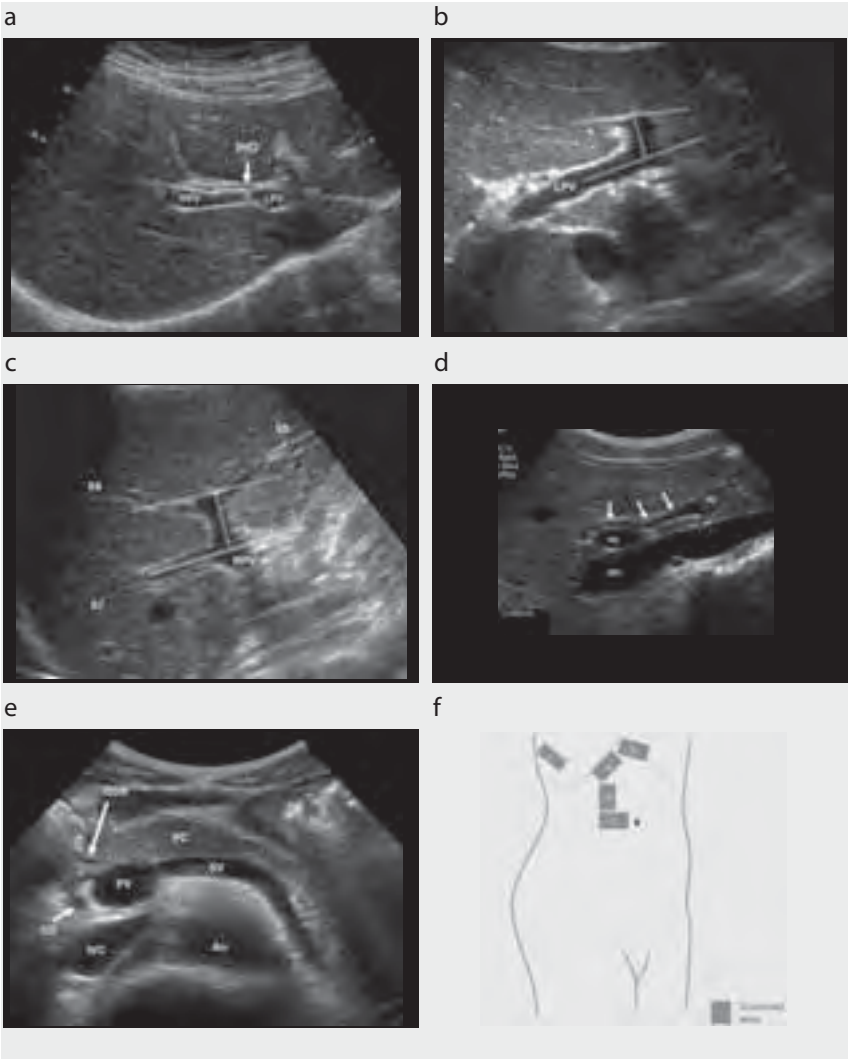

Fig. 8.3. (a) The interlobar fissure (arrow) appears as a hyperechoic line and connects the right portal vein to the gallbladder. (b) Diagram showing the scanning area used to visualize the interlobar fissure

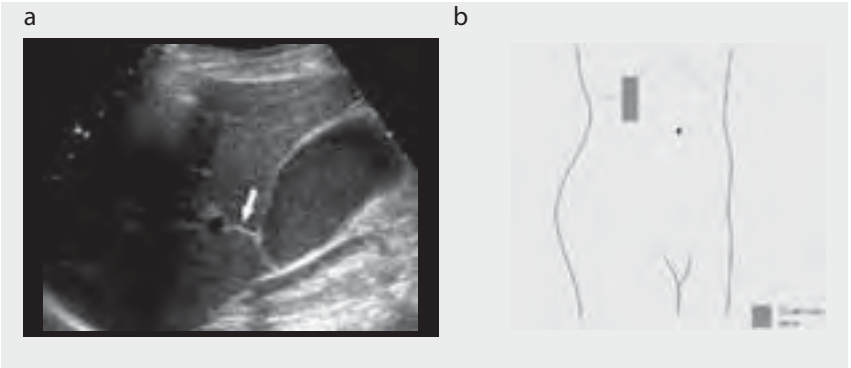

Normal findings

The biliary system consists of the right and left hepatic ducts, the common hepatic duct, the common bile duct, the gallbladder and the cystic duct. The intrahepatic bile ducts travel in the portal triads adjacent to the portal veins and hepatic arteries. The orientation of the bile ducts with respect to the portal veins is variable. At the porta hepatis, the main right and left hepatic ducts join to form the common hepatic duct. The common bile duct descends into the posterior and lateral aspect of the pancreas head before entering the ampulla. The term 'common duct' is used for the common hepatic duct and common bile duct together. In a longitudinal view of the porta hepatis, the common duct is seen anterior to the portal vein. The right hepatic artery is seen between the common duct and the portal vein.

The intrahepatic ducts are considered normal if their diameter is 2 mm or less and not more than 40% of the diameter of the adjacent portal vein (Fig. 8.4). The common hepatic duct, high in the porta hepatis as it crosses over the right hepatic artery, has an internal diameter of less than 4 mm (Fig. 8.5). A duct with a diameter of 5 mm is acceptable, while one with a diameter of 6 mm requires further investigation.

The gallbladder is an elongated, pear-shaped sac lying below the liver. It is divided into a fundus, a body and a neck, which continues into the cystic duct. The wall of the gallbladder consists of a mucosal layer (hyperechoic), a smooth muscle layer (hypoechoic), a perimuscular connective tissue layer (hyperechoic) and a serosal layer (hypoechoic). The intrahepatic gallbladder is usually in the plane of the interlobar fissure that divides into the right and left lobe (see Fig. 8.3). The transverse diameter of the normal gallbladder is less than 4 cm, while its longitudinal diameter is less than 10 cm; its wall thickness is less than 3 mm. The most accurate measurements of the gallbladder wall are made from the anterior subhepatic wall in a long-axis image (Fig. 8.6).

Fig. 8.4. (a) Dilated intrahepatic duct (arrow). Intrahepatic ducts are considered dilated if they measure ≥ 2 mm in diameter or more than 40% of the diameter of the adjacent portal vein (PV). (b) Diagram showing the scanning area used to obtain image shown in (a)

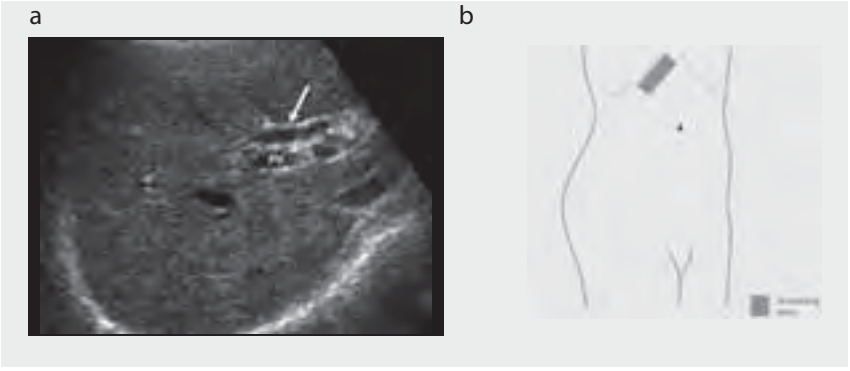

Fig. 8.5. (a) Hepatoduodenal ligament view shows the inferior vena cava (1), right portal vein (2), common duct (3), gallbladder (4), right hepatic artery (RHA) and right renal artery (RRA). The diameter of the common duct is measured at its proximal portion (open arrow) in this view. (b) Diagram showing the scanning area used to obtain the image shown in (a)

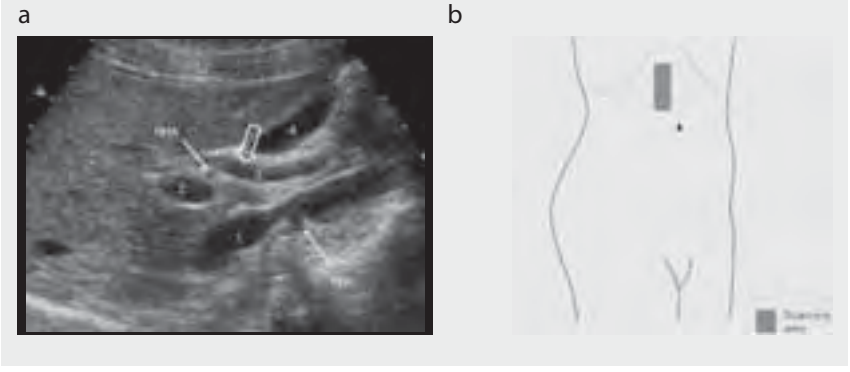

Fig. 8.6. Measurement of the gallbladder wall. The most accurate measurements are obtained from the anterior subhepatic gallbladder wall (arrows) in a long-axis or transverse image

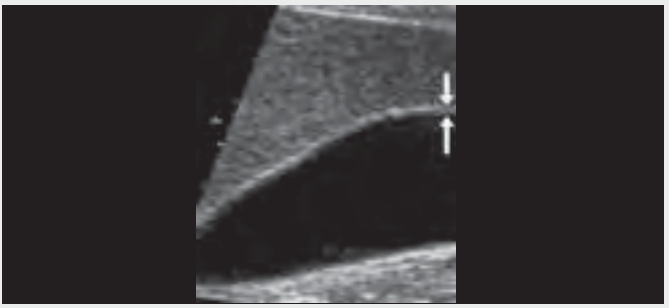

Pathological findings

Gallbladder

Stones

Sonography plays the primary role in imaging the gallbladder. The typical sonographic appearance of gallstones is a mobile intraluminal echogenic focus with an associated acoustic shadow (Fig. 8.7). Small stones attenuate the beam less than larger stones and therefore produce less well defined shadows.

Fig. 8.7. (a) A large gallbladder stone with posterior shadowing. (b) Multiple small stones (wide arrow) with posterior shadowing (thin arrow)

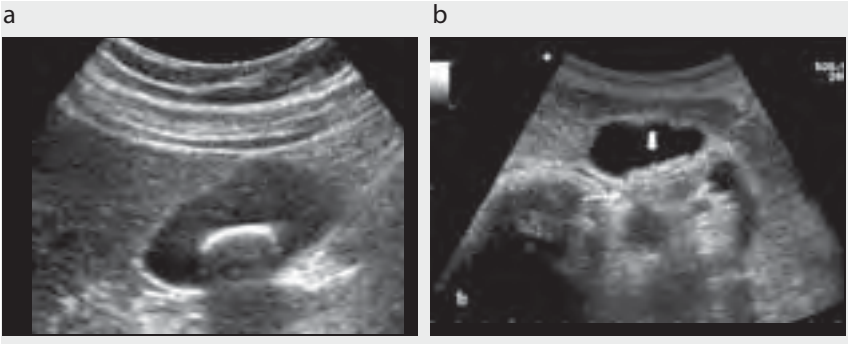

It is important to optimize the focal zone of the transducer and to use higher frequency transducers to differentiate shadowing from small stones. The patient's position should be shifted during the procedure to demonstrate the presence of the stones as well as to differentiate them from polyps and other entities. Detection of mobility is important in ruling out a polyp.

When the gallbladder is filled with small stones or with a single large stone, the gallbladder fossa appears as two echogenic lines. The echogenic line seen in the near field is the gallbladder wall, and the echogenic line with posterior shadowing is a stone (Fig. 8.8). Such shadowing is termed a 'wall–echo–shadow complex'. Some stones appear to float.

Fig. 8.8. Two large stones filling the gallbladder, with a wall–echo–shadow complex. The longest arrow indicates the perimuscular layer of the gallbladder wall, the intermediate arrow the lumen of the gallbladder or thickened muscular layer and the shortest arrow the anterior surface of stones

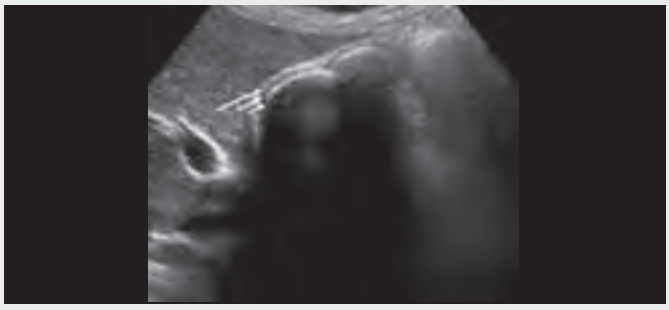

Sludge

Gallbladder sludge consists of a combination of cholesterol crystals and granules of calcium bilirubinate in thick, viscous bile. The sonographic appearance of sludge is that of amorphous, low-level echoes, with the gallbladder in a dependent position with no acoustic shadowing. Tumefactive biliary sludge can mimic polypoid tumours (Fig. 8.9). Lack of internal vascularity, mobility and a normal wall are signs of the presence of sludge. The artefactual echo caused by the section thickness and side-lobe artefact can also mimic sludge. These artefacts can be reduced by appropriate focusing, by centring the gallbladder in the field of view and by optimizing the gain settings.

Fig. 8.9. (a, b) Mass-like sludge in the gallbladder. The sludge (arrows) is mobile, as seen by changing the patient's position

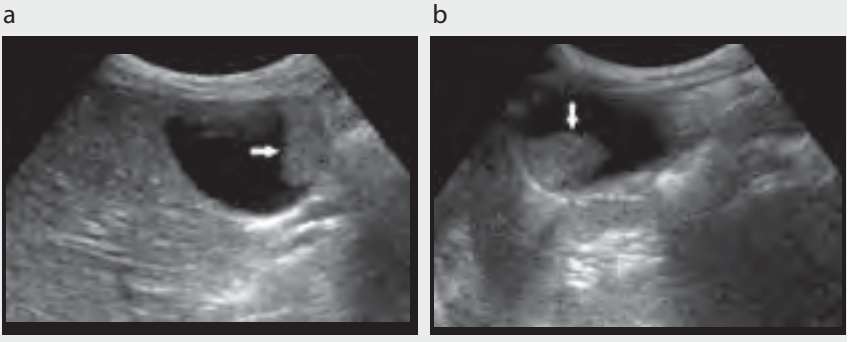

Acute calculous cholecystitis

This type of cholecystitis is caused by impaction of gallstones in the cystic duct or the gallbladder neck, resulting in obstruction, with luminal distension, ischaemia, superinfection and, eventually, necrosis of the gallbladder. The sonographic features of acute calculous cholecystitis include:

- calculi in the gallbladder;
- thickening of the anterior gallbladder wall;
- positive Murphy's sign;
- distension of the gallbladder (volume > 70 ml);
- impacted stone in the cystic duct or gallbladder neck;
- pericystic fluid collection (sign of actual or impending perforation);
- intraluminal wall desquamation; and
- hypervascularization of the gallbladder wall on colour and power Doppler sonography (Fig. 8.10).

Fig. 8.10. Acute calculous cholecystitis: (a) a stone impacted in the gallbladder neck (short arrow) and thickening of the anterior gallbladder wall (long arrow); (b) hypervascularization of the gallbladder wall (arrows) is seen on power Doppler sonography

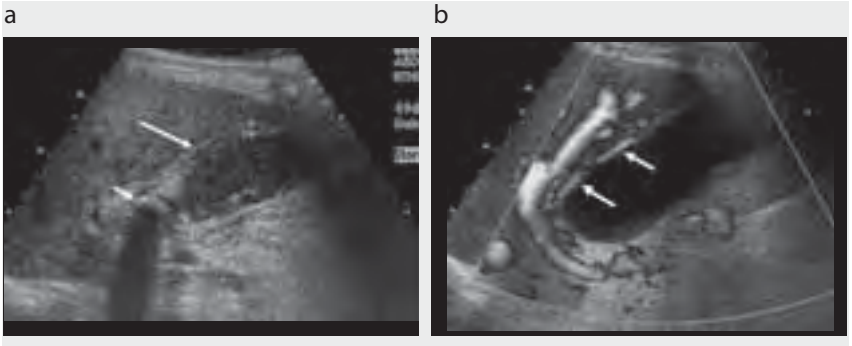

Gallstones are the single most important finding in cases of acute calculous cholecystitis. In the absence of stones, other sonographic findings suggesting acute cholecystitis may indicate the need for cholescintigraphy. The sonographic Murphy's sign refers to focal tenderness directly over the gallbladder when pressure is applied by the transducer; it has 94% sensitivity and 85% specificity. To avoid a false positive for Murphy's sign, it is best to apply pressure with the transducer over areas other than the gallbladder first and then to compress the gallbladder. Murphy's sign is positive in only 33% of patients with acute gangrenous cholecystitis.

Diffuse gallbladder wall thickening should be differentiated from wall thickening due to other causes, such as hepatitis, AIDS, congestive heart failure, hypoalbuminaemia, ascites, adenomyomatosis and chronic cholecystitis. Occasionally, normal individuals have a thickened gallbladder wall due to poor postprandial distension of the gallbladder. On colour or power Doppler sonography, increased blood flow in the distal half of the gallbladder suggests acute cholecystitis. Although none of the signs described above is pathognomonic of acute cholecystitis, the combination of several findings should lead to the correct diagnosis.

Acute acalculous cholecystitis

The sonographic abnormalities in acalculous cholecystitis are similar to those in calculous cholecystitis, other than gallbladder stones. As the sonographic findings in early acalculous cholecystitis may be subtle or nonspecific, a follow-up examination 24–48 h later may be valuable. In the appropriate clinical setting, progressive wall thickening is highly suggestive of acalculous cholecystitis. In children, acute cholecystitis may be acalculous, with increased gallbladder-wall thickening, signs of hydrops, a positive sonographic Murphy's sign and increased diameter of the common bile duct, with sludge.

Gangrenous cholecystitis

In 20–30% of patients with acute cholecystitis, gangrenous changes develop, which are characterized pathologically by intramural haemorrhage, necrosis and microabscess formation. Sonographic findings in gangrenous cholecystitis include bands of non-layering, echogenic tissue within the lumen, representing sloughed membranes and blood (Fig. 8.11). The gallbladder wall is irregular, with small intramural fluid collections, which represent abscesses or haemorrhage.

Fig. 8.11. Gangrenous cholecystitis. The gallbladder wall is diffusely thickened, with an irregular, striated appearance (short arrows). Sloughed membrane is seen (long, thin arrow). In the gallbladder lumen, sludge is noted

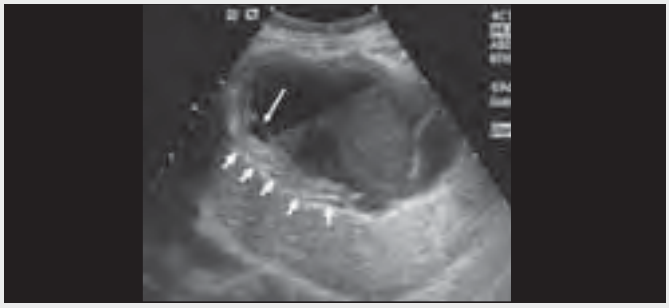

Perforation

Gallbladder perforation occurs in 5–10% of cases and requires immediate cholecystectomy or percutaneous cholecystostomy because of the high mortality rate (greater than 20%). Diabetes, malignancy and use of immunosuppressive drugs predispose to perforation. The commonest site of perforation is the gallbladder fundus, because of its relatively poor blood supply. Sealed-off perforation, in which fluid leaking from the gallbladder is localized around it, is commoner than acute free perforation. The sonographic features of gallbladder perforation vary from a well circumscribed collection of fluid to a solid hypoechoic mass around a deformed gallbladder (Fig. 8.12). Perforation of the gallbladder may extend into the adjacent liver parenchyma, forming an intrahepatic abscess collection (Fig. 8.12). The 'sonographic hole sign', caused by focal interruption of the gallbladder wall, is a direct sign of perforation.

Fig. 8.12. Perforation of the gallbladder. A hypoechoic abscess (black arrows) is seen between the gallbladder (GB) and the liver. Disruption of the gallbladder wall indicates a perforation site (white arrow)

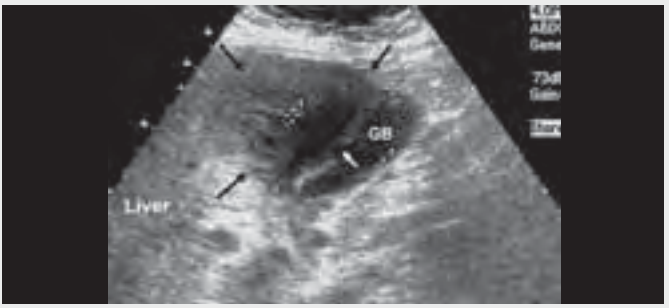

Emphysematous cholecystitis

Emphysematous cholecystitis is a rare infection caused by gas-forming bacteria, such as *Escherichia coli* or *clostridia*, within either the wall or lumen of the gallbladder. The condition predominates in male, elderly and diabetic patients. Surgical or percutaneous intervention is required because of the poor prognosis and high mortality rate due to this condition. The sonographic findings in emphysematous cholecystitis include echogenic lines with posterior 'dirty' shadowing in the gallbladder wall, with or without echogenic spots, and posterior 'dirty' shadowing in the gallbladder or a bright echogenic band with diffuse acoustic shadowing within the gallbladder fossa (Fig. 8.13). It may be difficult to differentiate from a 'porcelain' gallbladder, except that the latter shows posterior clear shadowing. Cholecystoenteric fistula, which can have gas bubbles, does not result in intramural gas in the gallbladder.

Fig. 8.13. Emphysematous cholecystitis (arrow). Note the difference from the wall–echo–shadow complex and gallbladder stones shown in Fig. 8.8

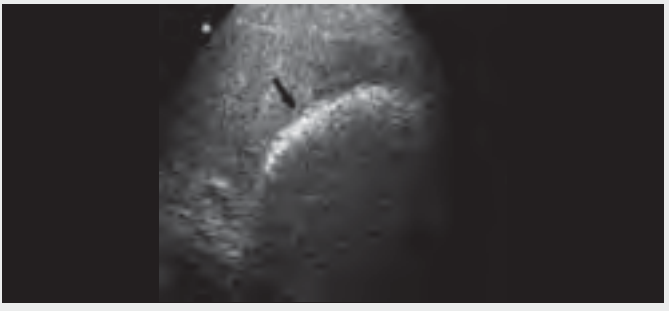

Porcelain gallbladder

Calcification of the gallbladder wall develops as a result of chronic inflammation. The resulting 'porcelain' is associated with a high incidence of gallbladder cancer; thus, prophylactic cholecystectomy is recommended. On sonography, a hyperechoic, curved line or band with posterior acoustic shadowing (Fig. 8.14) is seen in the gallbladder fossa. Intraluminal stones are not usually seen because of the posterior shadowing.

Fig. 8.14. Porcelain gallbladder (arrows). A hyperechoic, curved line with posterior acoustic shadowing is seen in the gallbladder fossa

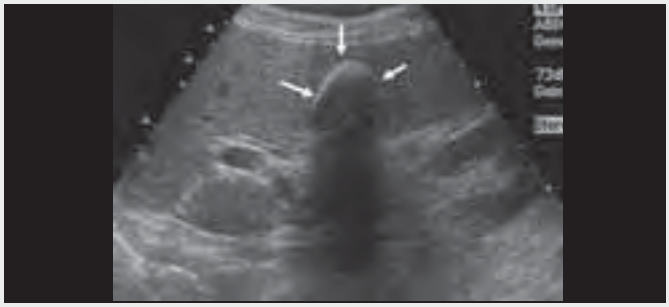

Xanthogranulomatous cholecystitis

Xanthogranulomatous cholecystitis is a rare variation of chronic cholecystitis. It occurs most commonly between the sixth and seventh decades of life and has a slight female predominance. The disease results in formation of ill-defined yellow xanthogranulomas. The most characteristic sonographic finding is the presence of hypoechoic nodules or bands in the gallbladder wall (Fig. 8.15). Cholelithiasis and a thickened gallbladder wall are frequent findings. Xanthogranulomatous cholecystitis can mimic gallbladder cancer, with extensive mural thickening and extensive adhesions involving the transverse colon, liver and duodenum.

Fig. 8.15. Xanthogranulomatous cholecystitis. Multiple hypoechoic nodules (arrowhead) are seen in the thickened gallbladder wall, with a stone in the gallbladder neck (arrow)

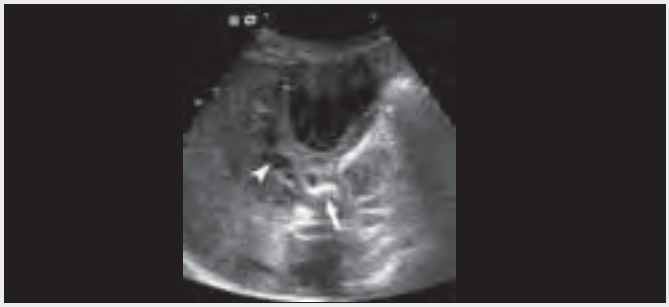

Adenomyomatosis

Adenomyomatosis is a hyperplastic change in the gallbladder wall characterized by proliferation of multiple mucosal invaginations, known as Rokitansky-Aschoff sinuses, with smooth muscle proliferation. These sinuses commonly contain concentrated bile or cholesterol crystals. Adenomyomatosis may be focal, segmental or diffuse (Fig. 8.16). The focal form of adenomyomatosis, called adenomyoma, most commonly occurs in the fundus. Sonographic findings for adenomyomatosis include tiny echogenic foci with comet-tail artefacts, intramural cystic spaces and focal, segmental or diffuse gallbladder-wall thickening. The comet-tail artefacts may result from intramural calculi or cholesterol crystal deposition.

Fig. 8.16. Adenomyomatosis of the gallbladder: (a) diffuse type with echogenic foci (arrows), (b) segmental type and (c) focal type (arrow), as shown, respectively in (d)

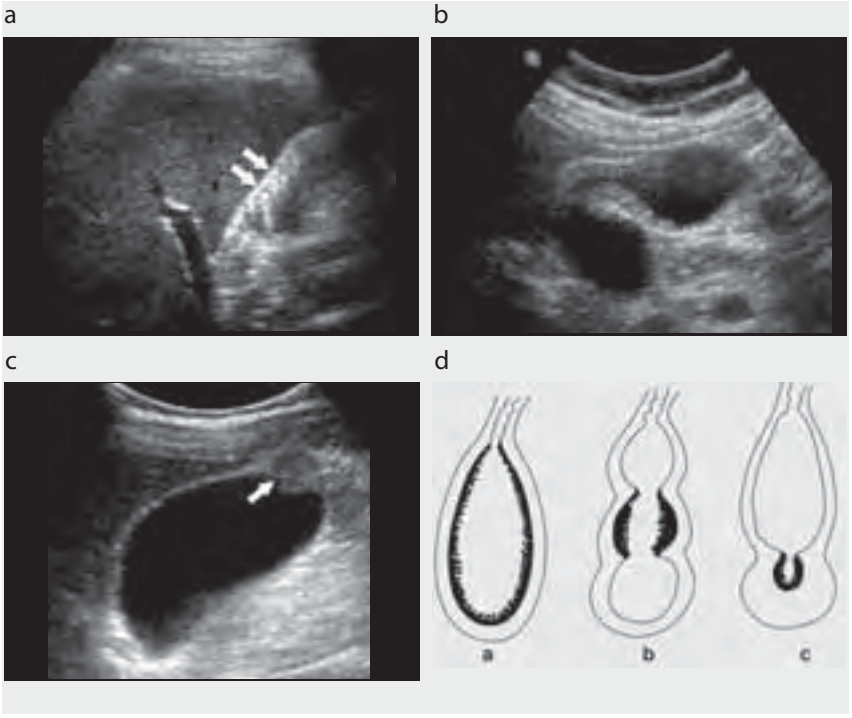

Polyps

Polyps of the gallbladder can be divided into non-neoplastic and neoplastic. Non-neoplastic polyps include cholesterol and inflammatory types; neoplastic polyps are adenomas, adenocarcinomas, leiomyomas and lipomas. Metastatic tumours, such as melanoma, can manifest as polypoid masses. Differentiation of benign and malignant polyps is critical clinically. Multiple polyps less than 10 mm in diameter are usually benign, whereas malignancy is highly suspected in polyps with more than 10 mm in diameter. A rapid change in size on follow-up sonography also suggests malignancy. On sonography, a polyp appears as a protruding echogenic tumour attached to the gallbladder wall. Unlike stones, polyps are not mobile and do not have posterior acoustic shadowing.

Cholesterol polyps account for 50–60% of all polypoid gallbladder lesions. These polyps are less than 1 cm in diameter in more than 90% of cases and multiple in 20–60%. Although it is not easy to distinguish cholesterol polyps from adenomas on sonography, they tend to have high echogenicity and weak posterior comet-tail artefacts (Fig. 8.17). Cholesterol polyps are usually multiple and generally less than 5 mm, which is diagnostic. In contrast, gallbladder adenomas are almost always solitary. Cholesterol polyps, especially those greater than 1 cm, may have internal hypoechoic areas or tiny hyperechoic material depositions.

Inflammatory polyps develop by focal protrusion of inflammatory tissue during cholecystitis. These polyps are usually less than 5 mm.

Adenomas are divided into those with a pedunculated or a sessile appearance. They are larger than non-neoplastic polyps, commonly measuring more than 1 cm. Because adenomas can contain foci of malignant transformation, special care should be taken when a polyp is larger than 1 cm. For adenomas more than 1 cm in diameter, resection should be considered. Adenomas tend to be homogeneously hyperechoic (Fig. 8.18) but become more heterogeneous as they grow.

Fig. 8.17. Cholesterolosis. Note multiple comet-tail artefacts (arrow)

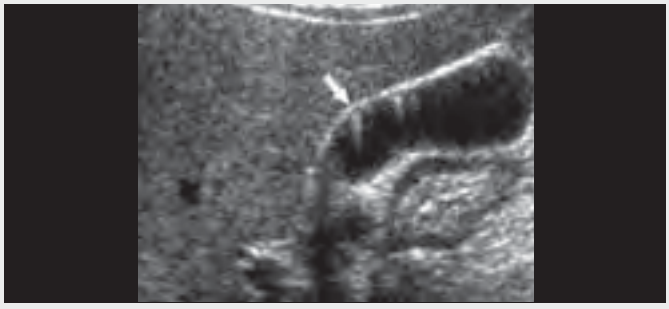

Fig. 8.18. Adenoma of the gallbladder, showing a non-mobile hyperechoic mass without posterior shadowing

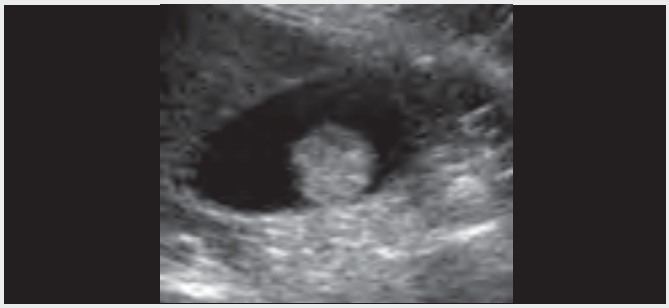

Gallbladder carcinoma

Gallbladder carcinoma occurs mainly in the elderly and is three times commoner in women than in men. It is associated with gallstones (64–98% of cases) and porcelain gallbladder (4–25% of cases) and rarely with colonic polyposis or inflammatory bowel disease. Gallbladder carcinoma occurs in three gross morphological patterns: a mass replacing the gallbladder, a thickened wall mass or an intraluminal polypoid mass (Fig. 8.19). Sonographically, a mass replacing the gallbladder appears as a large, irregular fungating mass with low echogenicity. This is the commonest type, accounting for 40–65% of gallbladder carcinomas. Often, this type accompanies gallstones and involves direct extension into the liver, invasion of the adjacent biliary tree and lymphatic metastasis. An intraluminal polypoid mass tends to have a better prognosis, because it is commonly limited to the mucosa or the muscular layer. This type is seen as a well defined intraluminal, round or oval mass with a broad base. The thickened wall mass ranges from minimal malignant change of the mucosa to focal or diffuse, irregular wall thickening. It is important to differentiate a wall-thickening gallbladder cancer from chronic cholecystitis, although this may sometimes be impossible. Gallbladder carcinoma usually shows focal or diffuse disruption of the hyperechoic perimuscular connective tissue layer and irregular wall thickening, whereas chronic cholecystitis shows smooth wall thickening with preservation of the perimuscular connective tissue layer.

Fig. 8.19. The three potential presentations of gallbladder carcinomas: (a) a soft tissue mass that completely replaces the gallbladder and resides in the gallbladder fossa is seen; (b) focal eccentric wall thickening of the fundus and body of the gallbladder is noted; and (c) a large polypoid mass is seen in the gallbladder

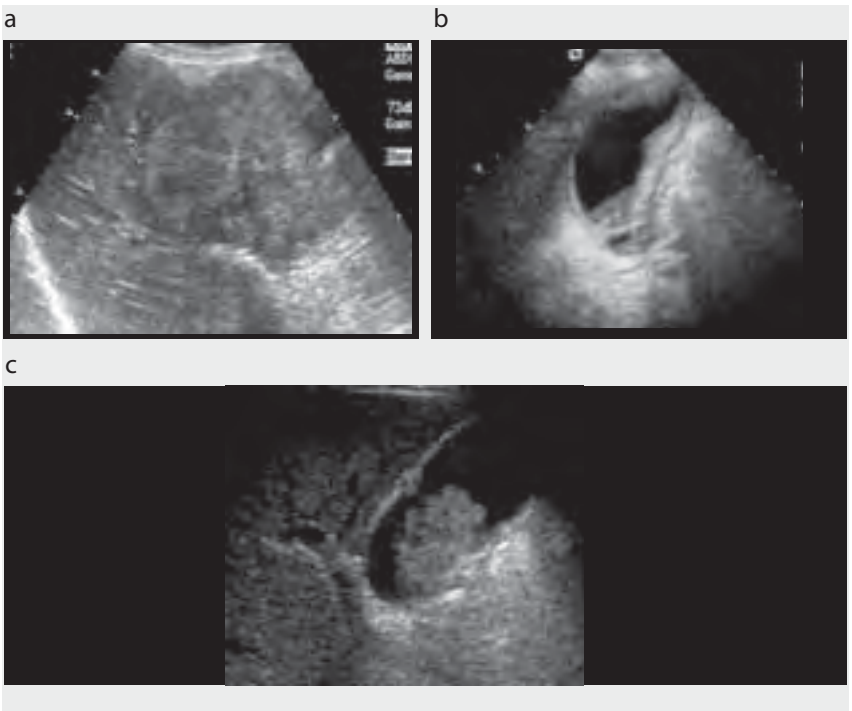

Bile ducts

Dilatation

Intrahepatic duct dilatation is always a significant ultrasound finding, particularly when the 'shotgun' ('parallel channel') sign is seen. When the bile ducts are enlarged by more than 2 mm or represent more than 40% of the diameter of the adjacent portal vein, a diagnosis of ductal dilatation can be made (see Fig. 8.4). The subcostal oblique view of the porta hepatis is the most sensitive for detecting dilatation of the intrahepatic bile duct. Occasionally, the appearance of prominent blood vessels in the liver is misinterpreted as dilated bile ducts on grey-scale ultrasound. Colour Doppler imaging is often useful in these circumstances.

The extrahepatic duct is considered to be dilated when the common hepatic duct is more than 6 mm in diameter (see Fig. 8.5).

The bile duct diameters in elderly patients and patients who have undergone cholecystectomy may be greater than the threshold level of 6 mm without obstruction.

Cholangitis

Bacterial cholangitis

Bacterial cholangitis is almost always associated with biliary obstruction. The clinical triad for bacterial cholangitis is fever, right upper quadrant pain and jaundice. Sonography is an excellent first imaging tool for evaluating patients with suspected cholangitis. The sonographic features of bacterial cholangitis are biliary dilatation, biliary stones or sludge, bile duct wall thickening and liver abscess (Fig. 8.20). In the majority of patients, sonography can reveal the cause and level of bile duct obstruction.

Fig. 8.20. Bacterial cholangitis. Thickening of the wall of the dilated intrahepatic ducts (arrows), with increased periductal echogenicity noted (LPV, left portal vein)

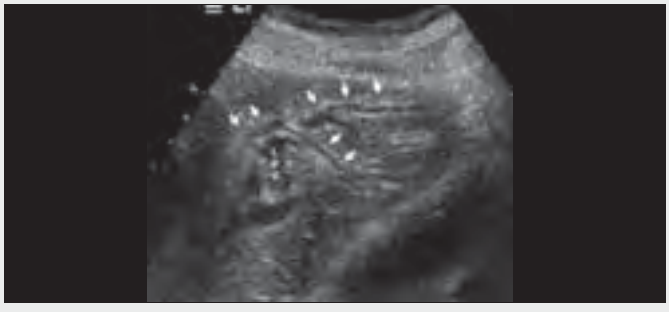

Primary sclerosing cholangitis

The sonographic hallmark of sclerosing cholangitis in the common duct is smooth or irregular wall thickening. Multifocal strictures and beaded narrowing develop in the intrahepatic ducts (Fig. 8.21).

Fig. 8.21. Marked thickening of the common bile duct (CBD) in a patient with sclerosing cholangitis (HA, hepatic artery; PV, portal vein)

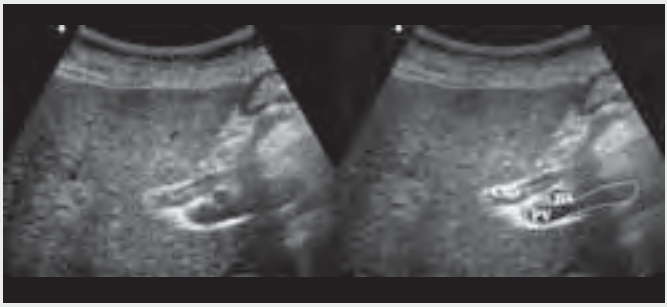

AIDS-related cholangitis

Sonographic findings for AIDS-related cholangitis include intrahepatic and extrahepatic bile duct wall thickening, intrahepatic focal stricture and dilatation and an echogenic nodule at the end of distal common bile duct, which indicates an inflamed, stenosed papilla of Vater.

Recurrent pyogenic cholangitis

Recurrent pyogenic cholangitis, also known as 'oriental cholangitis' or 'intrahepatic pigmented stone disease', is characterized by the development of intrahepatic pigmented stones, recurrent abdominal pain, fever and jaundice. The sonographic features of this condition are intrahepatic and extrahepatic duct stones, biliary dilatation, segmental or focal intrahepatic duct dilatation with atrophy of the affected segment or lobe of the liver, biliary duct wall thickening and increased periportal echo (Fig. 8.22).

Fig. 8.22. Recurrent pyogenic cholangitis. (a) The hepatoduodenal ligament view shows the dilated common bile duct and a common bile duct (CBD) stone (arrow), and (b) the transverse left lobe view shows irregularly dilated intrahepatic ducts and multiple intrahepatic duct stones (arrows) without posterior acoustic shadowing. Atrophy of the left lobe is also seen

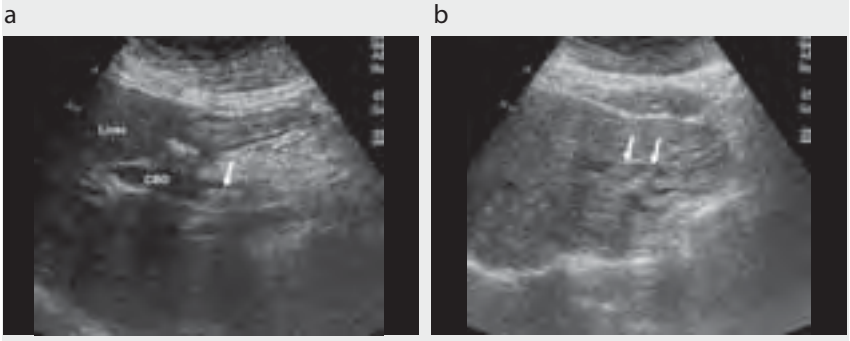

Stones

Intrahepatic duct stones

Intrahepatic duct stones (Fig. 8.23) are easily detected when they appear as highly echogenic foci with posterior shadowing and associated ductal dilatation. When the affected ducts are filled with stones or there is abundant sludge or pus between the stones, however, they may be misinterpreted as calcified masses or parenchymal calcification.

Fig. 8.23. Intrahepatic duct stones. The transverse left lobe view shows multiple echogenic stones (long arrows) with strong posterior acoustic shadowing. Slightly echogenic materials (short arrow) indicate sludge

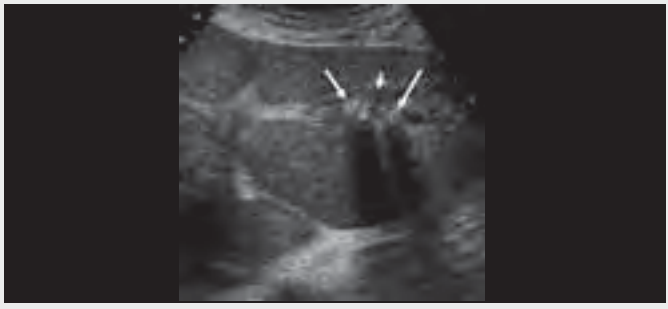

Extrahepatic duct stones

Most stones are seen in the distal common bile duct near the pancreas. A transverse scan of the intrapancreatic portion of the common bile duct (possibly with the patient sitting up after ingestion of water) can be helpful for detecting stones (Fig. 8.24). On sonography, the stones appear as rounded echogenic lesions with posterior acoustic shadowing (Fig. 8.24). Small stones or stones in a non-dilated duct might not show good acoustic shadowing.

Choledochal cysts

Choledochal cysts appear as true cysts in the liver, with or without an apparent communication with the bile ducts. They can appear as a fusiform dilatation of the common bile duct (Todani I type), a diverticulum from the common bile duct (Todani II type), an invagination of the common bile duct into the duodenum (choledochocoele, Todani III type) or multiple biliary dilatation of an intrahepatic or an extrahepatic biliary tree (Todani IV type). The cystic structures may contain sludge, stones or even a solid neoplasm (Fig. 8.25).

Mirizzi syndrome

Mirizzi syndrome is an uncommon cause of extrahepatic bile duct obstruction. It is due to an impacted stone in the cystic duct, which creates extrinsic compression of the common hepatic duct. Sonographically, Mirizzi syndrome appears as an impacted stone causing extrinsic biliary obstruction at the level of cystic duct insertion, in conjunction with acute or chronic cholecystitis (Fig. 8.26).

Fig. 8.24. Extrahepatic duct stones. (a) The hepatoduodenal ligament view obtained without ingestion of water shows a dilated common bile duct (short arrows); the distal common bile duct is hidden by gastric gas (long arrow). (b) The hepatoduodenal ligament view obtained after ingestion of 500 ml water shows a distal common bile duct stone with weak posterior shadowing (long arrow) through the water-filled stomach (short arrow)

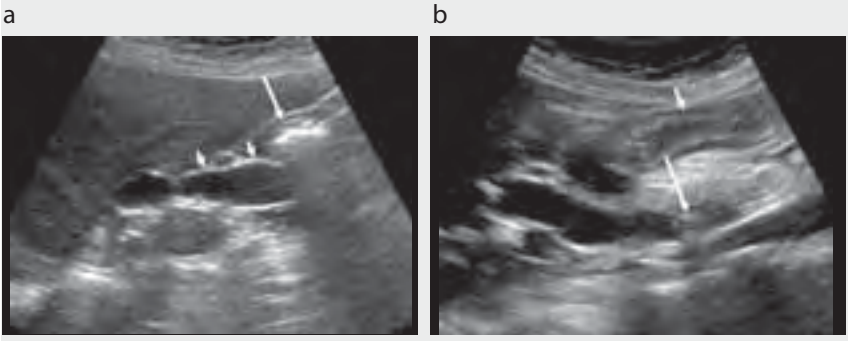

Fig. 8.25. Choledochal cyst, Todani IV type. The subcostal oblique view shows a cystic dilatation of the right hepatic duct, which contains large echogenic stones (long arrow) with weak posterior shadowing. The left intrahepatic ducts also show cystic dilatations and echogenic materials (short arrows) within the ducts

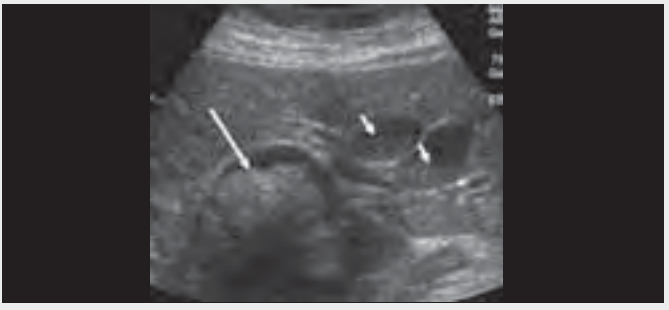

Biliary parasites

Biliary ascariasis appears as a tube or as parallel echogenic bands within the bile ducts on the longitudinal view of sonography (Fig. 8.27). On the transverse view, a 'target' appearance is seen, made up of the rounded worm surrounded by the duct wall. Movement of the worm during the scan is confirmatory.

Klatskin tumour (hilar cholangiocarcinoma)

Dilatation of the intrahepatic bile ducts is the most frequently seen abnormality in patients with cholangiocarcinoma. Klatskin tumours classically manifest as segmental dilatation and non-union of the right and left ducts at the porta hepatis. These findings may be the first and only clues to the presence of this pathological condition, because

Fig. 8.26. Mirizzi syndrome. (a) A dilated common hepatic duct (CHD) and a cystic duct stone (asterisk); and (b) a thickened, collapsed gallbladder (GB) and a cystic duct stone (asterisk) are seen

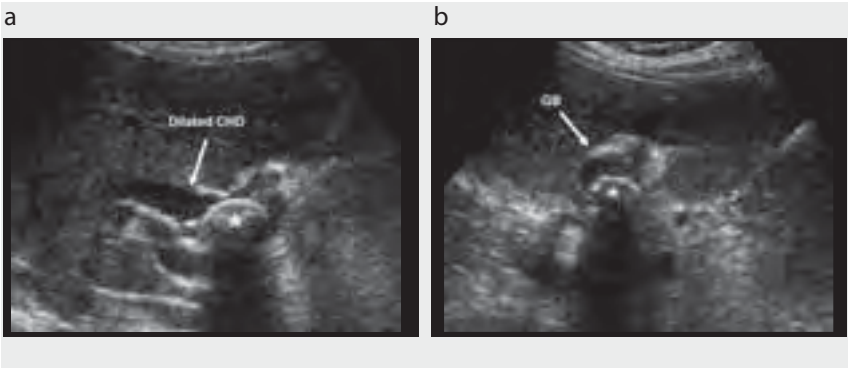

Fig. 8.27. Biliary ascariasis. A parallel echogenic band (arrow) within the dilated common bile duct is seen on the hepatoduodenal ligament view

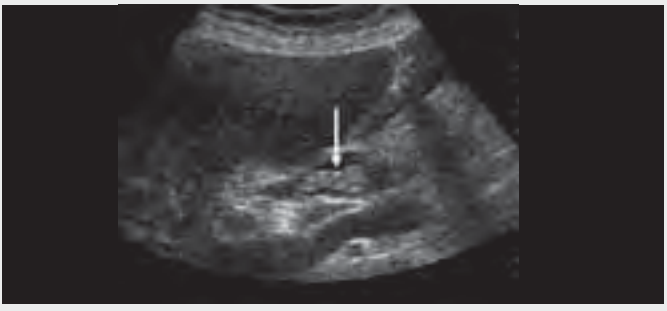

Klatskin tumour most commonly appears as an isoechoic infiltrative mass that may be inferred from the distance that separates the dilated segmental ducts (Fig. 8.28). Subtle alterations in liver echogenicity and pressure effects on adjacent vascular structures, especially the portal vein, may also be helpful. Vascular involvement, lymphadenopathy and the extent of ductal involvement influence the resectability of hilar cholangiocarcinoma. Klatskin tumour may be mimicked by inflammatory cholangitis (AIDS, sclerosing cholangitis), oriental cholangitis, benign biliary tumour, invasive hepatoma or gallbladder cancer. Metastatic adenopathy to the porta hepatis from primary tumours such as those of the gastrointestinal tract, pancreas or breast and lymphoma may occasionally mimic hilar cholangiocarcinoma. Occasionally, a discrete metastasis from the breast or colon or a melanoma may be seen as a polypoid intraluminal ductal mass.

Fig. 8.28. Klatskin tumour. The subcostal oblique view shows an isoechoic infiltrative mass (arrows) in the hepatic hilar area, with isolation of each intrahepatic duct in the right anterior segment (S8), the right posterior segment (S7) and the left lobe (LL)

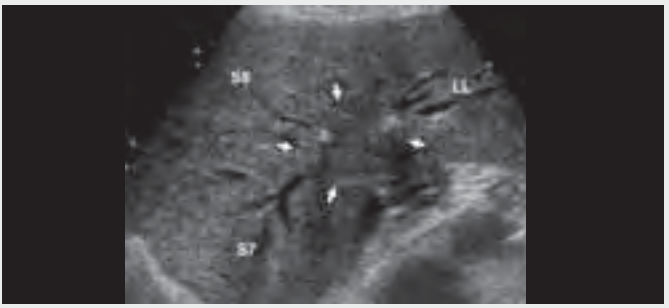

Extrahepatic bile duct tumours

Cholangiocarcinomas of the distal common bile duct are usually small and have a better prognosis than the more central Klatskin tumours. A short stricture or, less often, a polypoid mass is identified (Fig. 8.29). The tumours may be mimicked by ampullary papillomas, adenomas, blood clots or benign strictures.

Aspects of the differential diagnosis of pathological lesions in the gallbladder and bile ducts and typical pitfalls and errors are summarized in Table 8.1.

Fig. 8.29. Polypoid cholangiocarcinoma of the common bile duct. The hepatoduodenal ligament view shows an intraluminal, echo-poor mass (arrow) filling the distal common bile duct, with dilatation of the proximal duct. No associated wall thickening or posterior shadowing is seen

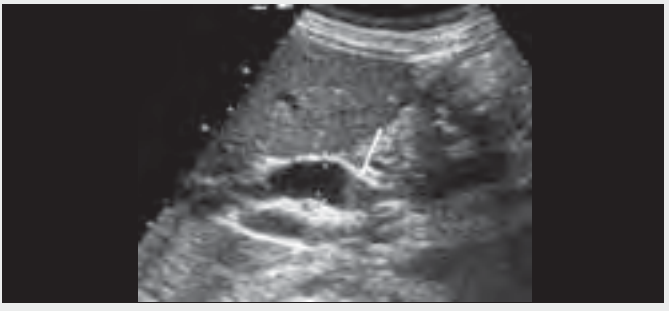

Table 8.1. Gallbladder and bile ducts: differential diagnosis of pathological conditions

Finding and differential point	Differential diagnosis	Pitfalls
Echogenic lesions in the gallbladder		
Mobile or posterior shadowing	Stones Sludge	Bowel gas Pseudosludge
Fixed	Polyp Adhesive stone Slow-moving tumefactive sludge	
Thickening of the gallbladder wall		
Focal	Adenomyomatosis Gallbladder cancer	Folded gallbladder Phrygian cap
Diffuse	Acute cholecystitis Chronic cholecystitis Xanthogranulomatous cholecystitis Adenomyomatosis Gallbladder wall oedema Gallbladder cancer	Collapsed gallbladder due to poor preparation
No visualization of the gallbladder		
Wall–echo–shadow complex	Stones	
Echogenic line or band	Emphysematous cholecystitis Porcelain gallbladder	Bowel gas
Soft tissue tumour	Gallbladder cancer	
Echogenic lesions in the bile duct		
Posterior shadowing	Stones Pneumobilia	Adjacent bowel gas Surgical clips Pancreatic calcifications
No posterior shadowing	Sludge Polypoid diseases Ascariasis	
Thickening of the bile duct wall		
	Bacterial cholangitis Sclerosing cholangitis AIDS cholangitis Recurrent pyogenic cholangitis Cholangiocarcinoma Metastasis Intramural varix Ascariasis	
Focal stricture	Bacterial cholangitis Cholangiocarcinoma Choledochal cyst Metastasis Benign stricture	
No demonstrable stricture	Stones Polypoid cancer Periampullary cancer Senile change Postcholecystectomy dilatation Choledochal cyst Ascariasis	Dilated hepatic artery Gallbladder neck

Chapter 9

Pancreas

9

Pancreas

Indications

The indications for ultrasonography of the pancreas are:

- midline upper abdominal pain, acute or chronic
- jaundice
- upper abdominal mass
- persistent fever, especially with upper abdominal tenderness
- suspected malignant disease
- recurrent chronic pancreatitis
- suspected complications of acute pancreatitis, especially pseudocyst or abscess
- polycystic kidney disease with cysts in the liver or spleen
- direct abdominal trauma, particularly in children.

Examination technique

Equipment, transducer

As for any other ultrasound study, the highest frequency transducer possible should be used to visualize adequately the structure being examined. For adults, the transducer frequency may vary from 3 MHz to 5 MHz; for children, a 5-MHz or 7.5-MHz transducer can be used routinely. The focal zone of the transducer should be matched to the depth of the pancreas. The transducer gain control must be adjusted to optimize visualization of the entire pancreas.

Preparation

It is best to perform an ultrasound examination of the pancreas on patients who have fasted overnight. If this is not possible, the patient should have been fasting for at least 6–8 h. The purpose of fasting is threefold. First, because the biliary system and pancreas are intimately related, they are usually examined together. If gallstones, dilated ducts or choledocholithiasis are seen, an examination of the pancreas should be performed; and, conversely, if the pancreas is abnormal, the gallbladder and ducts are always evaluated. Fasting promotes greater dilatation of the gallbladder, which facilitates its evaluation. Second, fasting ensures that the stomach is empty. Because the stomach is directly anterior to the pancreas, its contents affect transmission of the sonic beam to the pancreas. Third, fasting tends to result in less bowel gas, which also improves visualization of the pancreas.

Position of the patient

The examination is generally begun with the patient in the supine position (see Fig. 9.1).

Scanning technique

The goal of every pancreatic ultrasound examination is to visualize the gland in its entirety. To do this, the examiner should find or produce a suitable acoustic window through which the pancreas can be visualized. For transverse scans, the left lobe of the liver is used as often as possible as a window into the pancreatic bed (Fig. 9.1 (a)). Visualization of the abdominal aorta and inferior vena cava ensures that adequate depth penetration has been attained to image the pancreas. Sagittal scanning begins in the midline (Fig. 9.1 (b)), with identification of the great vessels, and proceeds to the right until the right kidney is seen and then left to the splenic hilum (or until the pancreas is obscured by gastric or colonic gas). To improve evaluation of the pancreas, especially if it is poorly seen with the patient supine, the water technique can be used: have the patient drink 250–500 ml of water, which may replace stomach gas and provide a sonic window into the pancreas. A semi-erect position with water ingestion may also prove useful (Fig. 9.1 (c, d). The water should be drunk through a straw to keep air intake to a minimum. If the water is allowed to stand overnight, it will contain fewer microbubbles. As the pancreatic tail is adjacent to the splenic hilum, the former can be imaged in the oblique coronal plane with the patient in the supine (30–45°) right posterior oblique position (Fig. 9.1 (e, f). The examination can sometimes be more successful if the patient is in the decubitus position. By moving the patient progressively from the left to the right lateral decubitus position, portions of the pancreas may be visualized as the water distends the gut lumen. In the right lateral decubitus position, fluid in the gastric antrum and duodenum can be seen, nicely outlining the pancreas (Fig. 9.1 (g)).

Normal findings

Certain anatomical landmarks should be identified in scans of the pancreas, in the following order: (1) aorta, (2) inferior vena cava, (3) superior mesenteric artery, (4) superior mesenteric vein, (5) splenic vein, (6) gastric wall and (7) common bile duct.

The pancreas can be localized with ultrasound by identifying its parenchymal architecture and the surrounding anatomical landmarks. The level of the pancreas is known to change slightly with the phase of respiration: at maximal inspiration and expiration, the organ can shift 2–8 cm in the craniocaudal axis. These respiratory migrations should be taken into account when imaging the pancreas and especially during ultrasound-guided biopsy. The pancreas is a nonencapsulated, retroperitoneal structure that lies in the anterior pararenal space between the duodenal loop and the splenic hilum over a length of 12.5–15 cm.

Fig. 9.1. Pancreas. (a) Transverse scan in the supine position. (b) Sagittal scan in the supine position. (c) Transverse scan in the semi-erect position. (d) Result of a transverse scan in the semi-erect position with water ingestion. The fluid-filled stomach (ST) is seen anterior to the pancreatic head (H) and body (B) (SMV, superior mesenteric vein; SMA, superior mesenteric artery; IVC, inferior vena cava; Ao, aorta; V, vertebra). (e) Oblique coronal scan in 45° right posterior oblique position. (f) Result of a coronal scan of spleen clearly demonstrates the pancreatic tail (T) anterior to the splenic vein (SV) through a sonic window of the spleen (S). (g) Result of a transverse scan in the right lateral decubitus position with the water technique. In this position, the fluid-filled gastric antrum (An) and duodenum (D) facilitate visualization of the head (H) and body (B) of the pancreas and the distal common bile duct (CBD) (MPV, main portal vein)

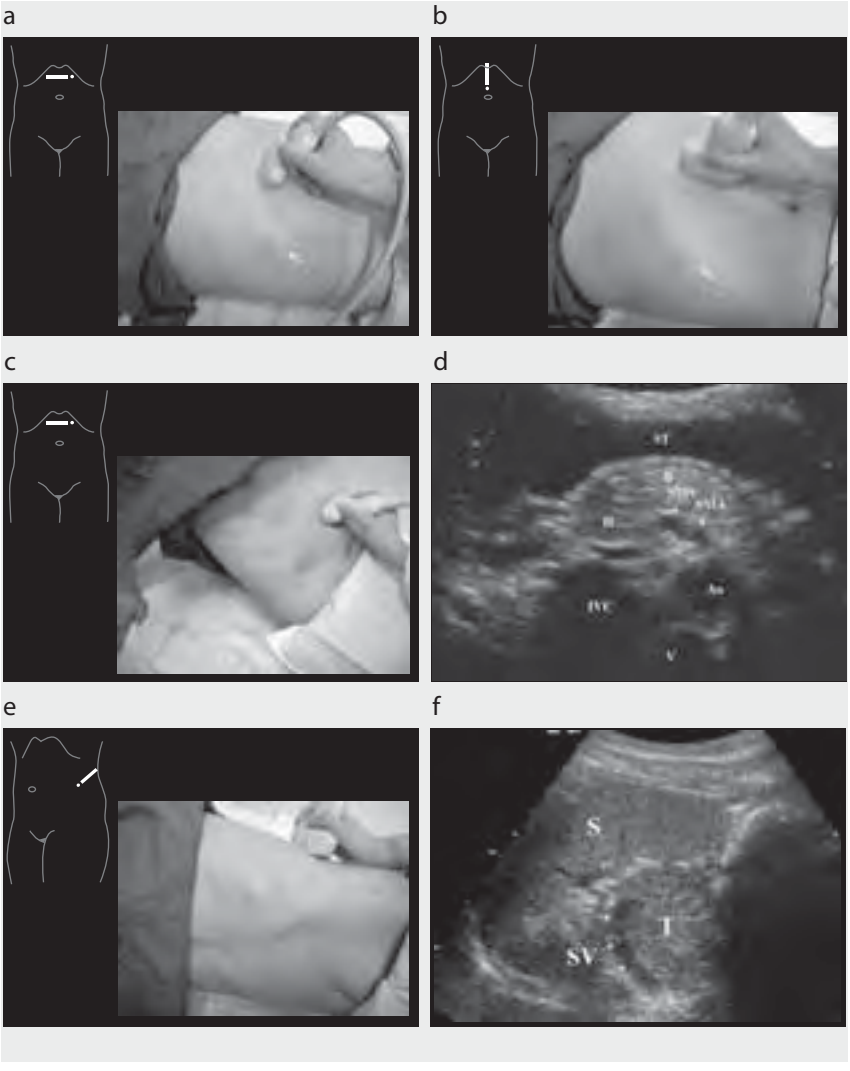

Fig. 9.1. *continued*

g

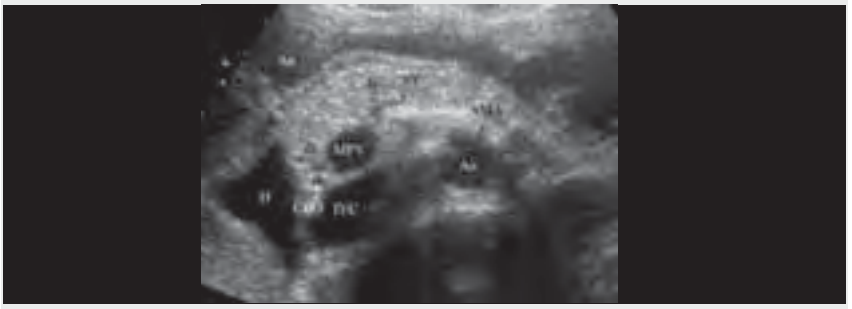

Transverse scan

The head, uncinate process, neck, body and tail constitute the different parts of the pancreas (Fig. 9.2 (a)). The superior mesenteric artery is surrounded by brightly echogenic fat at the root of the mesentery. Anterior to the superior mesenteric artery and in its transverse course is the splenic vein, forming the dorsal border of the pancreas from the splenic hilum to its confluence with the superior mesenteric vein at the neck of the pancreas. At this point, the head and the uncinate process actually wrap around the venous confluence, which forms the portal vein, and pancreatic tissue is seen both anterior and posterior to the vein. The uncinate process represents the medial extension of the head and lies behind the superior mesenteric vessels. The superior mesenteric vessels run posterior to the neck of the pancreas, separating the head from the body. No anatomical landmark separates the body from the tail, but the left lateral border of the vertebral column is considered to be the arbitrary plane demarcating these two segments. Two other important landmarks are the common bile duct and the gastroduodenal artery. In the transverse scan, the gastroduodenal artery is visible anterior to the neck of the pancreas and the common bile duct at the posterior aspect of the head of the pancreas (Fig. 9.2 (a)). The right margin of the pancreas is formed by the second portion of the duodenum (see Fig. 9.1 (g)). Anterior to the pancreas lies the lesser sac, which under normal circumstances is only a potential space and is thus not visible, and the stomach, identified by the alternating hyper- and hypoechoic layers of its submucosa and muscularis propria, respectively.

Sagittal scan

On the right, and lateral to the head, a sagittal right paramedian scan shows the inferior vena cava, on which the head of the pancreas lies (Fig. 9.2 (b)). At the level of the neck, the superior mesenteric vein is seen posterior to the pancreas (Fig. 9.2 (c)). The uncinate process of the head is seen posterior to the superior mesenteric vein. The third portion of the duodenum projects inferiorly (Fig. 9.2 (c)). A longitudinal view of the aorta shows the body of the pancreas situated between the coeliac axis and the superior mesenteric artery (Fig. 9.2 (d)). At the levels of the body and the tail, the stomach lies anteriorly (Fig. 9.2 (e)). A cross-section of the splenic vein is seen posteriorly, whereas a cross-section of the splenic artery appears cephalad (Fig. 9.2 (e)).

Fig. 9.2. (a) Transverse scan demonstrates the pancreas, with a homogeneous texture, consisting of five parts: the uncinate process (U), head (H), neck (N), body (B) and tail (T). The superior mesenteric vein (SMV) and the left lateral border of the vertebral column are considered to be the anatomical plane demarcating these segments. The splenic vein (SV) forms the dorsal border of the gland. Note that the pancreas actually wraps around the confluence of the splenic and the superior mesenteric veins, with the uncinate process lying posterior to the vein. The gastroduodenal artery (GDA) and the common bile duct (CBD) are visualized anterior to the neck and the posterior aspect of the head, respectively. (b) Longitudinal right paramedian sagittal scan at the level of the pancreas head shows the inferior vena cava (IVC), on which the head (H) of the pancreas lies (RA, right renal artery). (c) Sagittal scans at the level of the neck, (d) slightly to the left of the neck and (e) the body show the relations between the pancreas and the surrounding great vessels. (Ao, aorta; CA, coeliac axis; D, duodenum; L, liver; PC, portal confluence; SA, splenic artery; SMA, superior mesenteric artery; ST, stomach)

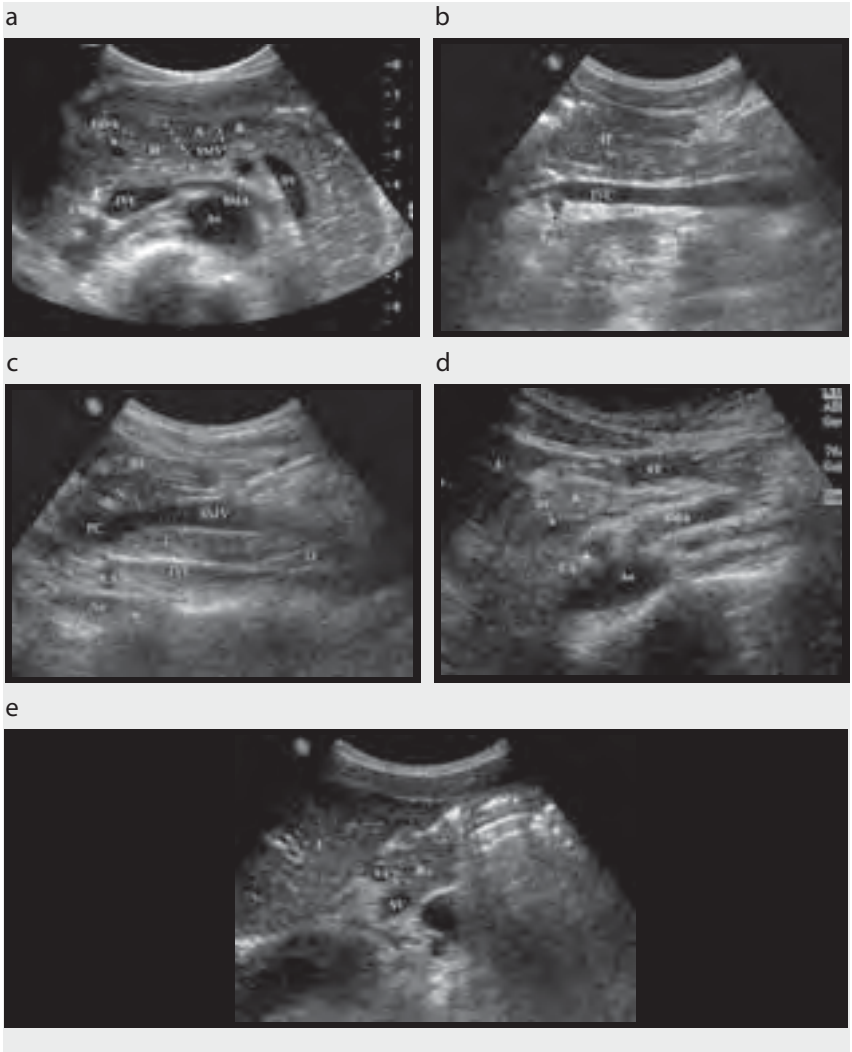

Pancreatic duct

The pancreatic duct may be seen as a single echogenic line within the gland (Fig. 9.3 (a)). Occasionally, the duct contains sufficient fluid to appear tubular, with both echogenic walls imaged (Fig. 9.3 (b)). This is still considered normal, as long as the internal diameter of the duct does not exceed 2–2.5 mm. Visualization of the duct has been reported in up to 86% of normal people.

Fig. 9.3. Normal pancreatic duct on transverse scan: (a) single-line pancreatic duct (arrows) and (b) double-line pancreatic duct (arrows). Even though the pancreatic duct is seen as a tubular structure rather than a single echogenic line, it is still considered normal because the internal diameter does not exceed 2–2.5 mm and the walls are parallel. (Ao, aorta; IVC, inferior vena cava; PC, portal confluence; SMA, superior mesenteric artery; SV, splenic vein)

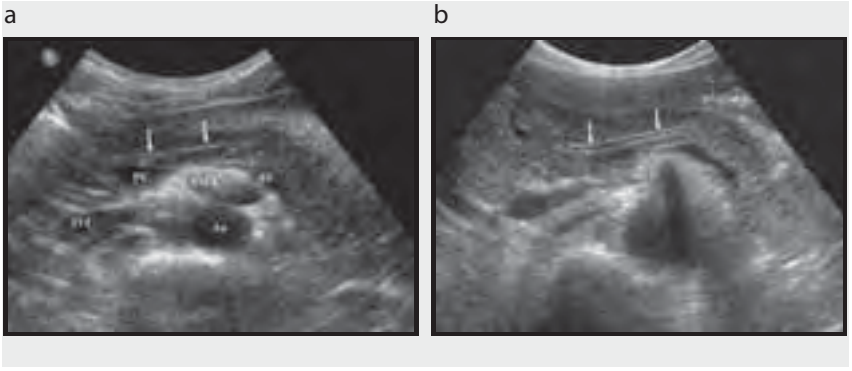

Echotexture of the pancreas

The normal pancreas is usually homogeneous, but a mottled appearance may sometimes be seen. The texture of the pancreas varies with age (Fig. 9.4 (a–c)). In infants and young children, the gland may be more hypoechoic than the normal liver. This is attributed to the preponderance of glandular tissue and the relative paucity of both fat and fibrous elements. With ageing and obesity, the pancreas becomes more echogenic as a result of the presence of fatty infiltration; in up to 35% of cases, it may be as echogenic as the adjacent retroperitoneal fat. These changes are considered to be due to normal ageing and are not associated with pancreatic insufficiency. The increased echogenicity resulting from excessive body fat is reversible. Other causes of fatty infiltration of the pancreas include chronic pancreatitis, dietary deficiency, viral infection, corticosteroid therapy, cystic fibrosis, diabetes mellitus, hereditary pancreatitis and obstruction caused by a stone or a pancreatic carcinoma.

Size of the pancreas

The normal size of the pancreas is a matter of some debate. Most authors consider that normal anteroposterior measurements are approximately 3.5 cm for the head, 2.0 cm for the neck, 2.5 cm for the body and 2.5 cm for the tail. The pancreas may appear larger in obese patients because it blends with the excessive retroperitoneal fat. The size of the pancreas diminishes with age. In practice, focal enlargement or localized change in texture are more significant than an aberrant measurement.

Fig. 9.4. The pancreas is generally more echogenic than the spleen and liver, the degree of echogenicity being variable. Different degrees of hyperechogenicity of the pancreas are shown in (a)–(c)

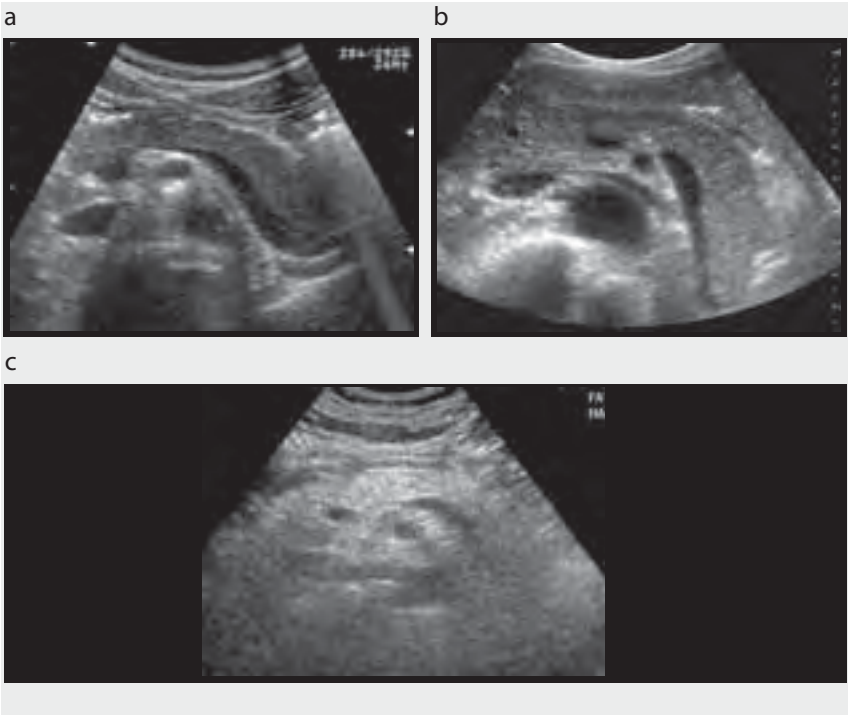

Pathological findings

Acute pancreatitis

Acute inflammation of the pancreas has numerous causes; however, acquired conditions such as alcohol abuse and biliary calculi account for the majority of cases. The classic sonographic findings in acute pancreatitis should include diffuse enlargement of the gland with a generalized decrease in its echogenicity (Fig. 9.5 (a)). Hypoechoic focal enlargement of the pancreas can occur in acute inflammation, generally confined to the head; focal enlargement confined to the tail would be unusual in pancreatitis and more suggestive of a neoplasm. The role of ultrasound in diagnosing acute pancreatitis lies in the detection of gallstones or common bile duct calculi, survey of possible complications, such as peripancreatic fluid (Fig. 9.5 (b–e)), follow-up of complications arising from acute pancreatitis and guidance for interventional procedures. The usefulness of ultrasound is limited to early investigation of acute pancreatitis or traumatic pancreatic injury, whereas CT has been shown to be useful in predicting the outcome of acute pancreatic inflammation and for detecting necrosis and fracture of pancreatitis.

Other complications, such as haemorrhage, pseudocyst formation (Fig. 9.5 (f, g)) and pseudoaneurysm (Fig. 9.5 (h)) of adjacent vessels, may be found on ultrasound examination. A **pancreatic pseudocyst** is a fluid collection that has developed a well defined, non-epithelialized wall in response to extravasated enzymes. It is generally

spherical and distinct from other structures. Fluid must collect over 4–6 weeks in order for the fluid collection to enclose itself by forming a wall consisting of collagen and vascular granulation tissue. Pseudocysts account for 10–20% of cases of acute pancreatitis. Classically, a pseudocyst is seen on sonographic examination as a well defined, smooth-walled anechoic structure with acoustic enhancement (Fig. 9.5 (f–g)). **Pseudoaneurysm** may be related to pancreatitis or may occur secondary to pseudocyst formation. Strong suspicion is crucial for the diagnosis of a pseudoaneurysm because it can mistaken for as a pseudocyst, a much commoner complication of this condition.

Fig. 9.5. Acute pancreatitis. (a) Transverse scan shows a diffusely enlarged pancreas (arrows) with homogeneous hypoechogenicity (IVC, inferior vena cava; PC, portal confluence; SMA, superior mesenteric artery; SV, splenic vein). (b) Transverse scan slightly to the left of (a) demonstrates a diffusely enlarged pancreas (arrows) with heterogeneous echogenic fluid (arrowheads) anterior to the tail of the pancreas; the margin (asterisk) of the pancreatic tail becomes indistinct. (c) Enhanced CT scan shows inflammatory changes of the pancreas and extensive fluid collection (arrows) around the pancreatic tail (T). (d) Transverse scan of another patient with proven pancreatitis shows relatively homogeneous, echo-poor fluid (white and black arrows) anterior and posterior to the pancreatic body (B) and tail (T). (e) Enhanced CT scan shows walled-off, irregular-shaped fluid collection (arrows) around the pancreatic body (B) and tail (T). (f) Pseudocyst (PS) of the pancreatic body (P); transverse scan demonstrates elongated pseudocyst containing echogenic debris (arrow) anterior to the pancreas body. (g) Coronal scan of spleen (S) shows a pseudocyst (PS) in the splenic hilum. (h) Pseudoaneurysm of the splenic artery and haematoma formation; transverse scan shows a large, well demarcated, heterogeneous, echogenic, mass-like lesion (arrows) in the tail (T) of the pancreas (SMV, superior mesenteric vein). (i) Enhanced CT scan demonstrates a 1-cm pseudoaneurysm (arrow) of the splenic artery and a huge surrounding haematoma (arrowheads)

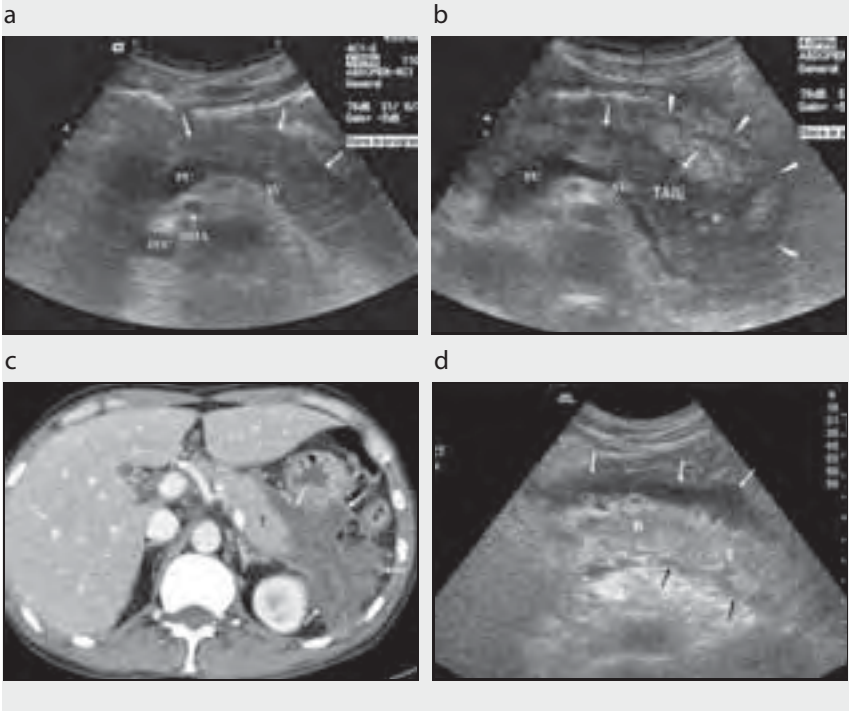

Fig. 9.5. *continued*

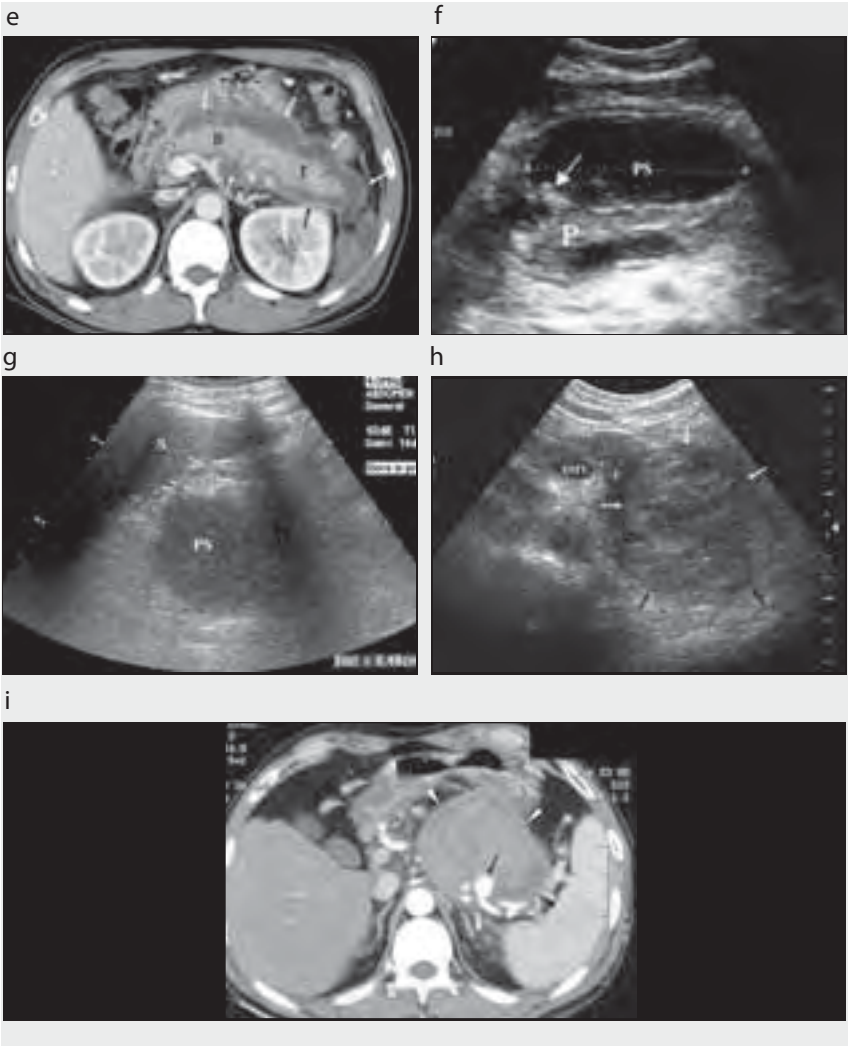

Chronic pancreatitis

Chronic pancreatitis is caused by progressive, irreversible destruction of the pancreas by repeated bouts of mild or subclinical pancreatitis resulting from high alcohol intake or biliary tract disease. Sonographically, chronic pancreatitis shows irregular areas of increased echogenicity representing fibrosis or calcification. The increase in echogenicity in chronic pancreatitis is more patchy and more heterogeneous than the normal increase in the echotexture of the pancreas that results from fatty replacement of glandular tissue. In chronic pancreatitis, the volume of the pancreas is usually diminished and often difficult to outline. Sonographic findings in chronic pancreatitis consist of changes in the size and echotexture of the pancreas, focal mass lesions, calcifications, pancreatic duct dilatation and pseudocyst formation (Fig. 9.6). Pseudocyst formation has been reported in 25–60% of patients with chronic pancreatitis.

Fig. 9.6. Chronic pancreatitis. (a) Transverse image of the pancreas shows a dilated and irregular duct (arrows). Note multiple pancreatic calcifications (arrowheads) scattered throughout the pancreas. (b) Transverse scan shows a markedly dilated duct (asterisks). The bright focus with shadowing within the dilated duct is consistent with a calculus (arrow). (c) Another example of pancreatic duct calculus. Transverse image shows a dilated duct (asterisk). The bright echogenic focus (arrow) with posterior shadowing is consistent with a calculus. (d) Transverse scan of patient with chronic pancreatitis reveals a large pseudocyst (PS) with inner fluid debris (arrows). Note multiple calcifications (arrowheads) with posterior shadowing in the pancreatic body. (e) A contrast-enhanced CT scan confirms the sonographic findings

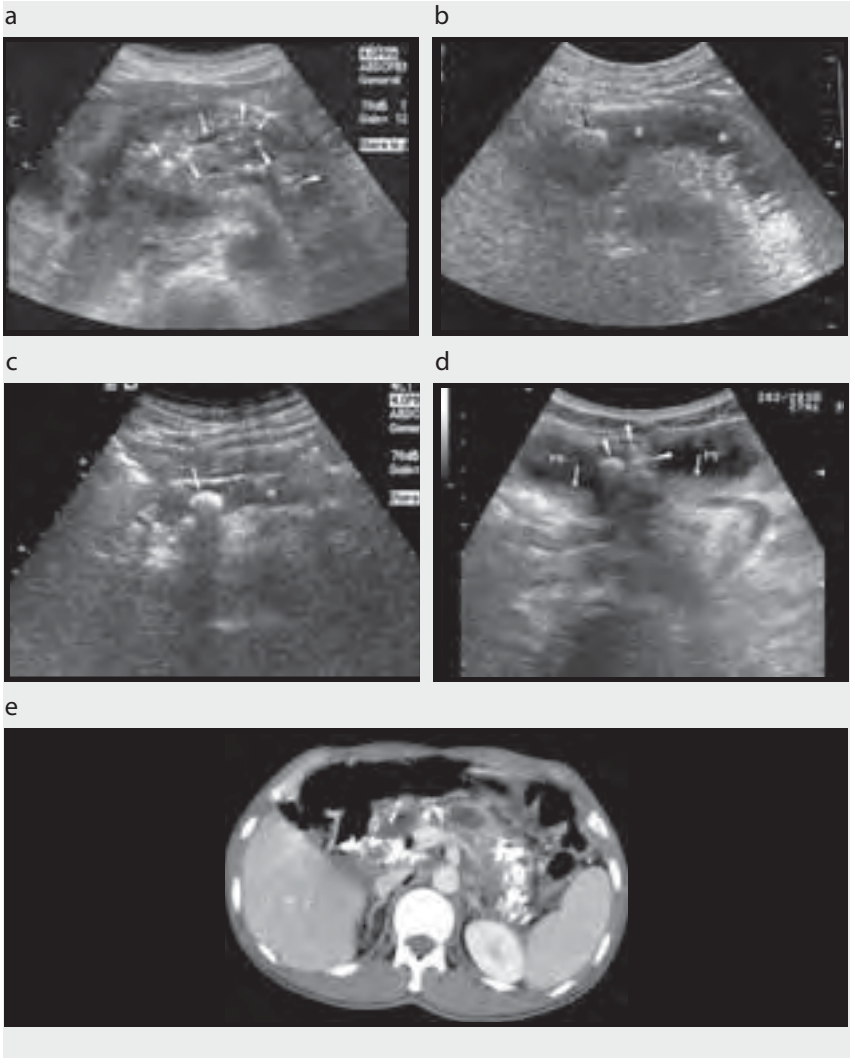

Neoplasms

Adenocarcinoma

Pancreatic carcinoma is the fifth leading cause of death from cancer among both males and females in western countries. The incidence appears to correlate with increasing age worldwide. This neoplasm is extremely rare in people under 40 years of age, and two-thirds of patients are over 60 years of age. Tumours arising in the pancreatic head present earlier because of the associated bile duct obstruction. Tumours in the body and tail of the pancreas present later with less specific symptoms, most commonly weight loss, pain, jaundice and vomiting when the gastrointestinal tract is invaded by the tumour.

The commonest sonographic finding in pancreatic carcinoma is a poorly defined, homogeneous or inhomogeneous hypoechoic mass in the pancreas (Fig. 9.7). Dilatation of the pancreatic duct proximal to a pancreatic mass is also a common finding (Fig. 9.7 (a)). Other sonographic findings include bile duct dilatation (Fig. 9.7 (b)), atrophic change of the gland proximal to an obstructing mass and encasement of adjacent major vessels (Fig. 9.7 (c, d)). Dilatation of the common bile duct associated with the pancreatic duct is known as the 'double-duct sign'. Necrosis, seen as a cystic area within the mass, is a rare manifestation of pancreatic carcinoma (Fig. 9.7 (e)).

Cystic neoplasms

Cystic neoplasms represent approximately 10–15% of pancreatic cysts and only about 1% of pancreatic malignancies. Two distinct forms of cystic neoplasm of the pancreas are recognized; both are generally easily distinguished from the much commoner carcinoma.

Microcystic cystadenoma (serous cystadenoma) is always histologically benign and frequently found in elderly women. It is composed of cysts that are so small (1–2 mm) that the net effect is that of a hyperechoic mass, frequently with lobular outlines (Fig. 9.8 (a)). A central echogenic stellate scar is an inconstant feature of this tumour. Oligocystic serous cystadenoma, which has fewer but much larger cysts, is known to be a variant of serous cystadenoma and accounts for 10–25% of serous cystadenomas of the pancreas. Sonographic findings in oligocystic serous cystadenoma are similar to those of mucinous cystadenoma; however, lobulating outer margins and more frequent pancreatic duct dilatation proximal to the lesion can allow differentiation of oligocystic serous cystadenoma (Fig. 9.8 (b)).

Mucinous cystic neoplasms (macrocystic adenoma, mucinous cystadenoma, cystadenocarcinoma) are composed of one or more macroscopic (> 2 cm) cysts, which may have thin or thick walls and single or multiple locules (Fig. 9.8 (c)). Unlike microcystic adenomas, the macrocystic form has malignant potential. It is difficult to differentiate between benign and malignant forms solely on the basis of sonographic criteria, but thicker walls and solid excrescences raise suspicion of malignancy.

Intraductal papillary mucin-producing tumours are mucinous cystic neoplasms that have been reported under different names: mucinous ductal ectasia, papillary adenocarcinoma, ductectatic tumour, intraductal mucin-hypersecreting neoplasm and mucin villous adenomatosis. In 1997, the unified term 'intraductal papillary mucin-producing tumour' was adopted. These tumours originate from the main pancreatic duct or its branches. Their histology ranges from benign to frankly malignant. The main pancreatic duct type presents as segmental, diffuse dilatation of the main duct with or without side-branch dilatation (Fig. 9.8 (d)). The branch duct type manifests as a single or multicystic mass with a microcystic or macrocystic appearance (Fig. 9.8 (e)). This tumour is differentiated from other cystic neoplasms by evidence of communication with the pancreatic duct.

Fig. 9.7. Carcinomas. (a) Transverse sonogram shows an ill-defined hypoechoic mass (arrows) involving the pancreatic head. An irregularly dilated pancreatic duct (PD) is seen in the proximal portion of the mass (SMA, superior mesenteric artery; SV, splenic vein). (b) Sagittal scan through the porta hepatis shows a markedly dilated bile duct. The common bile duct (CBD) terminates in a solid hypoechoic mass (M) in the pancreatic head (MPV, main portal vein). (c) Transverse scan demonstrates the coeliac axis (CA) arising from the aorta (Ao). A hypoechoic soft-tissue cuff (arrows) is seen along both walls of the coeliac axis (CHA, common hepatic artery; M, mass). (d) Oblique sagittal colour Doppler view shows a mass (arrows) in the pancreatic head encasing the portal confluence (PC) with turbulent flow. Note the echogenic lines (arrowheads) caused by a tube inserted for biliary decompression. (e) Coronal scan of the spleen (S) depicts a large hypoechoic mass (arrows) involving the pancreatic tail with infrequent cystic areas (C), suggesting intratumoral necrosis

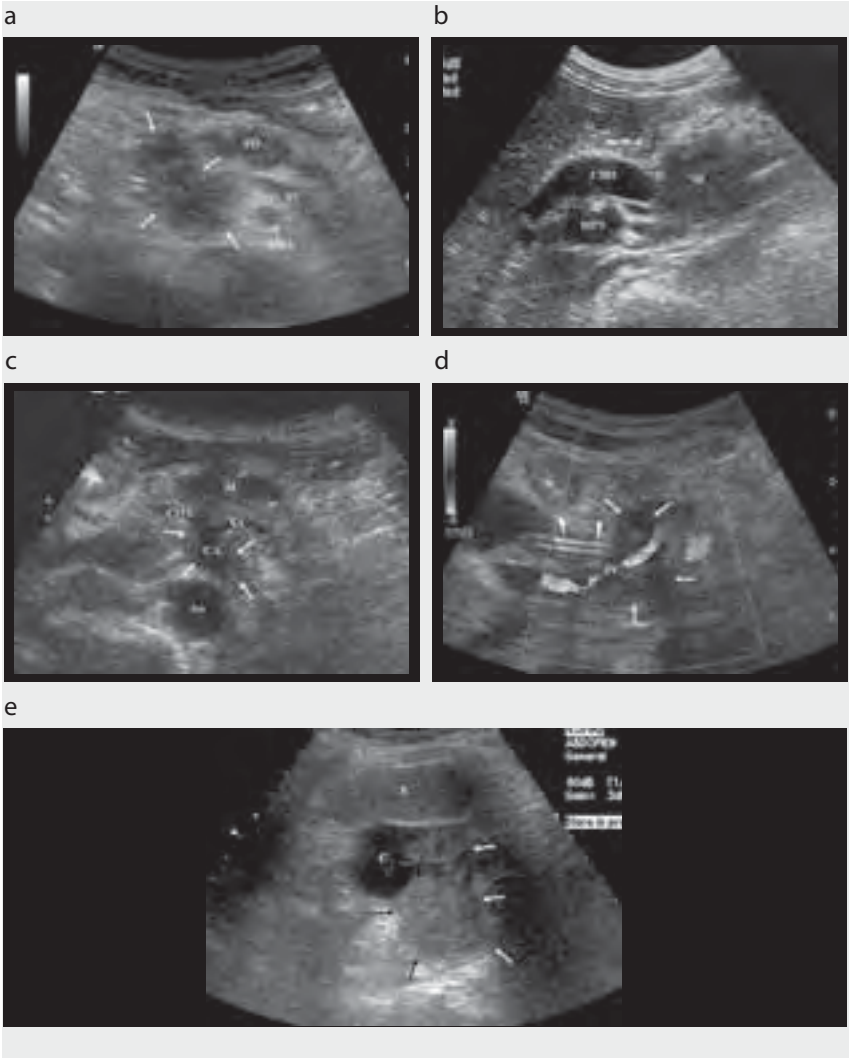

Fig. 9.8. Cystic neoplasms of the pancreas. (a) Microcystic serous cystadenoma. Transverse sonogram demonstrates a heterogeneously echogenic, solid-appearing mass (arrows) with small cystic components in the head of the pancreas. Note posterior acoustic enhancement (arrowheads) behind the mass (PC, portal confluence; SMA, superior mesenteric artery; SV, splenic vein). (b) Oligocystic serous cystadenoma. Coronal scan of the left upper quadrant shows a cystic lesion (C) of approximately 2 cm in the pancreatic tail. Note lobulating outer margin of the lesion (S, spleen; LK, left kidney). (c) Macrocystic mucinous cystadenoma. Transverse scan shows a unilocular cystic lesion (C) of approximately 2 cm at the junction of the pancreatic body and tail. The pancreatic duct is not dilated (Ao, aorta). (d) Transverse scan reveals marked dilatation of the main pancreatic duct (MPD), which is filled with amorphous echoic material. (e) Transverse sonogram shows a lobulating cystic lesion (C) in the pancreatic body with mild main pancreatic duct dilatation (arrows)

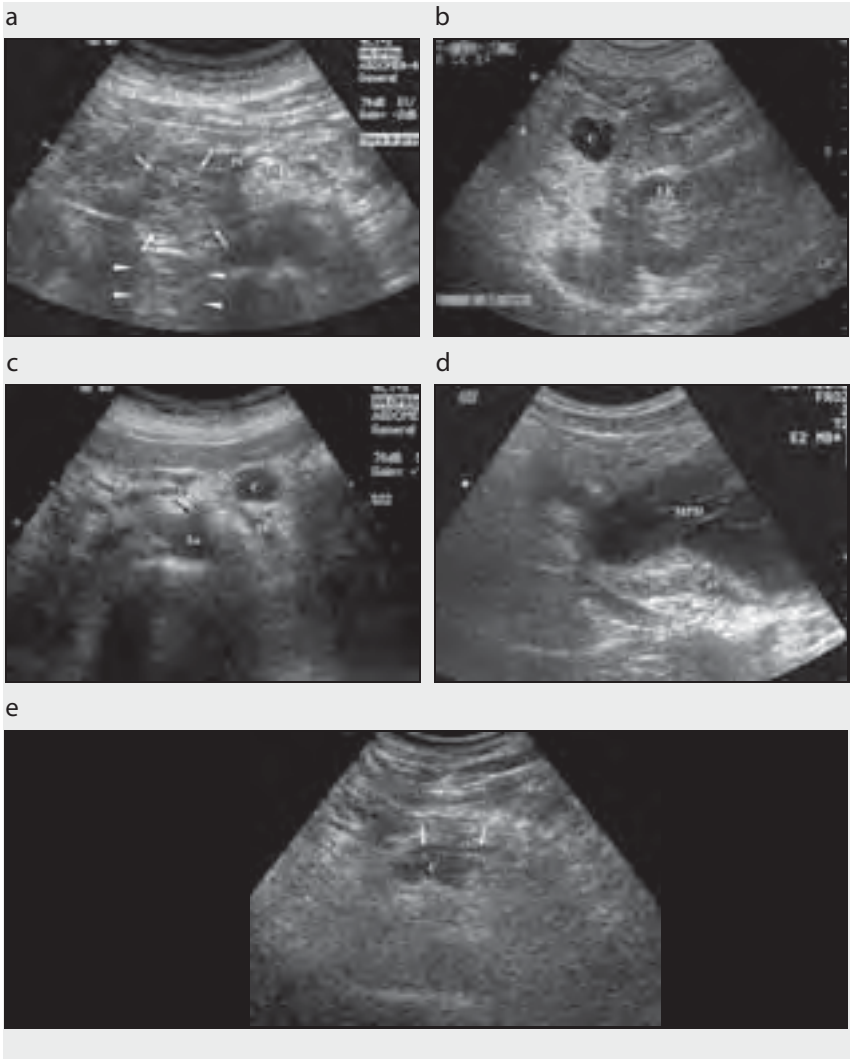

Neuroendocrine tumours

Neuroendocrine tumours of the pancreas appear to arise from multipotent stem cells in the ductal epithelium and are evenly distributed throughout the gland. Necrosis, haemorrhage and calcification are more prominent in larger, malignant types, but malignancy cannot be differentiated microscopically; only dissemination provides indisputable evidence of malignancy. Even malignant tumours are slow growing, and spread beyond the regional lymph nodes and liver is rare. Neuroendocrine tumours are classified as functioning or nonfunctioning, and functioning tumours are subcategorized into insulinoma, gastrinoma, glucagonoma, VIPoma, somatostatinoma and carcinoid, according to their secreting hormones.

The usual neuroendocrine tumours are hypoechoic and well defined, without calcification or necrosis (Fig. 9.9 (a)); however, these lesions can be isoechoic and detectable only by contour changes. Larger tumours can be hypoechoic or echogenic and irregular and may contain calcifications or areas of necrosis (Fig. 9.9 (b)).

Fig. 9.9. Neuroendocrine tumours. (a) Insulinoma. Transverse view demonstrates a well defined hypoechoic mass (M) in the pancreatic body (Ao, aorta; SV, splenic vein). (b) Malignant tumour. On transverse scan, a large heterogeneous hypoechoic mass (M) is seen in the head of the pancreas. STO, stomach

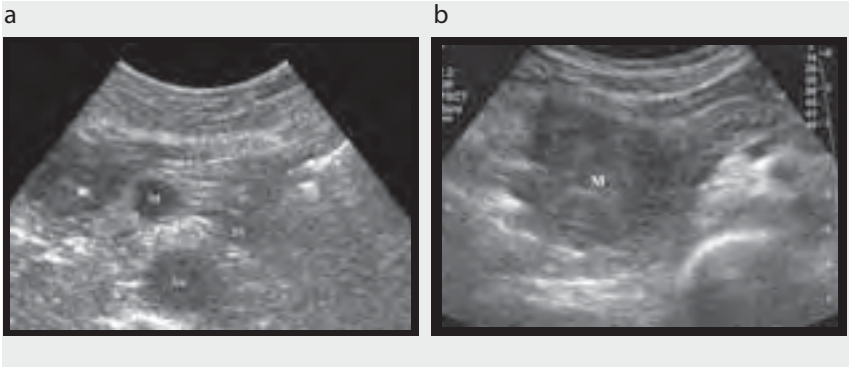

Chapter 10

Spleen

10

Spleen

Indications

The indications for ultrasonography of the spleen are:

- splenomegaly (enlarged spleen);
- left abdominal mass;
- blunt abdominal trauma;
- left upper-abdominal pain (an erect abdominal X-ray, including both sides of the diaphragm, is also needed if perforation of the bowel is suspected);
- suspected subphrenic abscess (pyrexia of unknown origin);
- jaundice combined with anaemia;
- echinococcosis (hydatid disease);
- ascites or localized intra-abdominal fluid;
- suspected malignancy, especially lymphoma or leukaemia.

Examination technique

Equipment, transducer

The average adult is scanned with a curved 2- to 5-MHz transducer. Children and very slender adults may be scanned with a curved 5- to 7-MHz probe. If necessary, linear array transducers can be used for more detail.

Preparation

Patients should fast for 8 h before the examination. If fluid is essential to prevent dehydration, only water should be given. If the symptoms are acute, proceed with the examination. Clinical conditions permitting, infants should fast for 3 h before the examination.

For acutely ill patients (e.g. trauma, sudden abdominal pain, post-surgical pyrexia), no preparation is needed.

Position of the patient

The patient should be supine initially and later lying on the right side with the left arm stretched up over the head. Apply coupling agent over the lower chest, the upper abdomen and left flank. The patient should take a deep breath and hold it when a specific area is being scanned.

Scanning technique

Start by placing the transducer centrally at the top of the abdomen (the xiphoid angle). Angle the beam to the right side of the patient to image the liver; adjust the gain to obtain the best image.

Scan the patient in the supine and right lateral decubitus positions. The patient can be examined in various degrees of inspiration to maximize the window to the spleen. A modest inspiration depresses the central portion of the left hemidiaphragm and spleen inferiorly so that they can be visualized.

Scan from below the costal margin, angling the beam towards the diaphragm, then in the ninth intercostal space downwards. Repeat through all the lower intercostal spaces, first with the patient supine and then with the patient lying on the right side (Fig. 10.1). The plane of section should then be swept posteriorly and anteriorly to view the entire spleen. An oblique plane of the section along the intercostal space can avoid rib shadowing.

Longitudinal scans from the anterior to the posterior axillary lines and transverse upper-abdominal scans should also be performed. A transverse scan from the intercostal approach may help to localize a lesion within the spleen anteriorly and posteriorly (Fig. 10.2). Scan the liver also, particularly when the spleen is enlarged.

Fig. 10.1. Technique for scanning the spleen. The supine and the right lateral decubitus position are required for scanning the spleen

Fig. 10.2. Longitudinal and transverse scans of the spleen. Longitudinal scans should be performed from the anterior to the posterior axillary lines

Normal findings

It is important to identify the:

- left hemidiaphragm
- splenic hilum
- splenic vein and its relation to the pancreas
- left kidney
- left edge of the liver and
- pancreas.

The spleen has impressions for the kidney (posteromedially), stomach (anteromedially) and colon (inferiorly). The splenic hilus is the reference point to ensure correct identification of the spleen and should be used as the entry point for the splenic vessels. The hilar vessels are located between the stomach and kidney (Fig. 10.3). The spleen is somewhat variable in shape: it may be elongated or plump and occasionally show clefts and lobulations, which are normal developmental variants. The significance of splenic clefts lies in the fact that they may be mistaken for fractures. Accessory spleens are encountered in approximately 10% of the population and are most frequently found near the hilum. It is important to identify the left diaphragm and the upper edge of the spleen.

Fig. 10.3. Oblique scan: normal spleen and left kidney

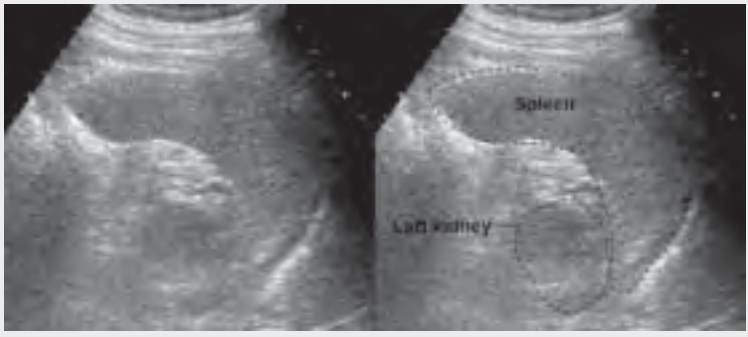

Echo pattern

The normal spleen has a uniform homogeneous texture and is slightly less echogenic than the liver.

Common errors in scanning the spleen

The following may be mistaken for splenic lesions:

- a kidney lesion
- the tail of the pancreas
- adrenal tumours or
- the stomach.

Identify these organs before looking at the spleen.
Non-visualization of spleen may occur in the presence of:

- asplenic syndrome
- polysplenia syndrome
- traumatic fragmentation of the spleen or
- wandering spleen.

Pathological findings

Enlarged spleen or splenomegaly

There are no absolute criteria for the size of the spleen on ultrasound; however, its normal dimensions in the adult are approximately 11–12 cm × 7 cm × 4 cm. When the spleen is longer than 12 cm from pole to pole, splenomegaly is considered to be present. The splenic length measured through the splenic hilum correlates relatively well with CT volumes and is considered to be a good indicator of splenic size in routine clinical practice.

Splenomegaly may be due to:

- tropical diseases, which includes idiopathic splenomegaly, malaria and trypanosomiasis;
- leishmaniasis or schistosomiasis;
- sickle-cell disease (unless infracted);
- congestive splenomegaly (heart failure, portal hypertension, portal or splenic vein thrombosis) (Fig. 10.4);
- neoplasm (leukaemia, lymphoma, metastasis or primary neoplasm);
- metabolic disease (Gaucher disease, amyloidosis, haemochromatosis);
- infection (bacterial, tuberculosis, typhoid fever, rubella or infectious mononucleosis); or
- extramedullary haematopoiesis (myelofibrosis).

Fig. 10.4. (a) Splenomegaly due to portal hypertension. (b) Note liver cirrhosis and portal vein dilatation

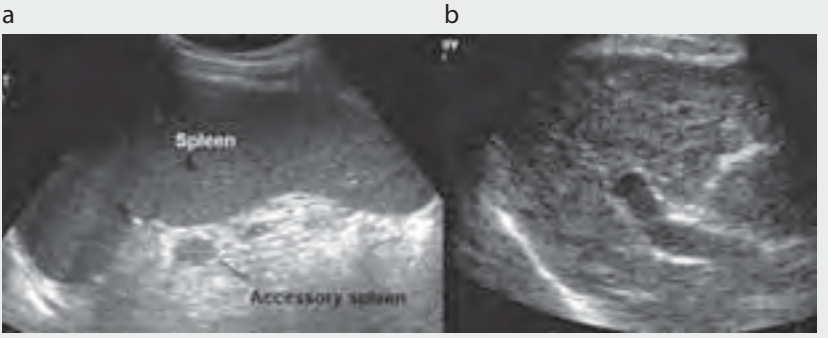

Whenever there is splenomegaly, examine the liver for size and echogenicity. Also examine the splenic and portal veins, the inferior vena cava, the hepatic veins and the mesentery. The region near the hilum of the spleen should be scanned for tubular structures due to varicosities.

Focal splenic lesions

Cystic lesion

If there is a clearly demarcated, echo-free mass with posterior acoustic enhancement, congenital cysts (epidermoid cyst, true cyst) can be differentiated by the presence of an inner endothelial lining. Splenic cysts are usually located within the spleen (Fig. 10.5).

Fig. 10.5. Longitudinal scans: a congenital cyst in the spleen, found incidentally

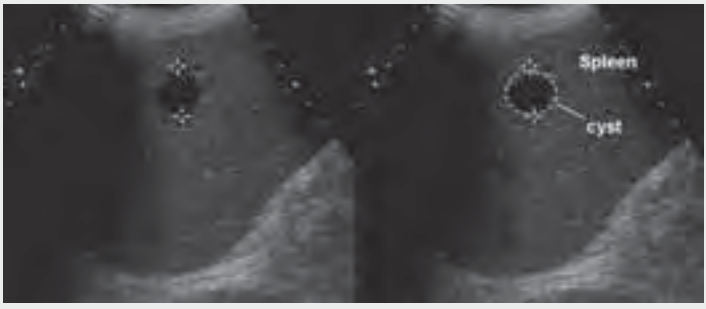

Pseudocysts

Pseudocysts are usually solitary and may contain echoes as a result of haemorrhage or infection (Fig. 10.6). Infection or haemorrhage may also result in debris and echogenic contents within thick-walled pseudocysts. Echogenic foci with acoustic shadowing may be found and is due to calcification within the wall.

Fig. 10.6. Transverse scans: a pseudocyst in the spleen. Note internal echogenic debris and wall

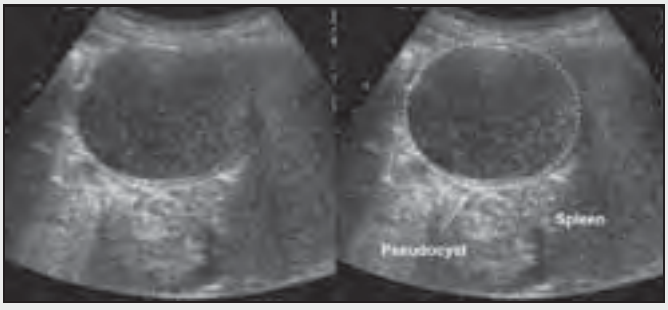

Echinococcal (hydatid) cysts

These are usually clearly defined, with a double wall (the pericyst and the cyst wall), and are often septate. There are markedly enhanced back-wall echoes and, often, marked variation in the thickness of the wall of the cyst.

Abscess

Scan in different projections. A hypoechoic cystic area containing debris with an irregular outline and associated with fever, leukocytosis and local tenderness suggests a splenic abscess (Fig. 10.7). Other findings in a splenic abscess include gas, progressive enlargement of the lesion, subcapsular extension and collections of extracapsular fluid.

Examine the liver for other abscesses. Mortality is likely if diagnosis and treatment are delayed. The sonographic findings can be variable. In questionable cases, fine-needle aspiration can be useful for diagnosis. Percutaneous catheter drainage, guided by sonography, can be safely and successfully performed.

Fig. 10.7. Abscess in the spleen

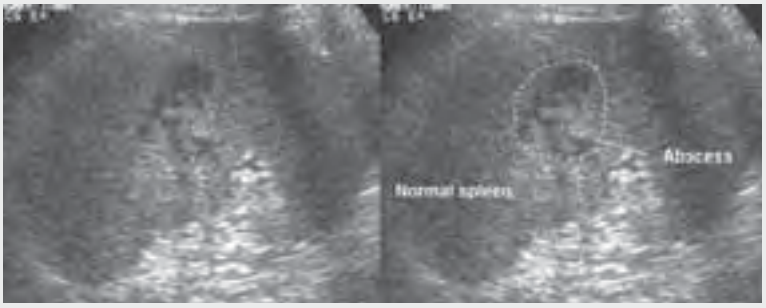

Amoebic abscesses are very rare in the spleen; bacterial abscesses are commoner.

Multiple nodules may also be found in patients with splenic infections, particularly in those who are immunocompromised (Fig. 10.8). The so-called 'wheels-within-wheels' appearance of target lesions suggests micro-abscesses caused by fungus or miliary tuberculosis.

Intrasplenic masses

Splenic masses may be single or multiple and well defined or irregular in outline.

Malignant tumours

The commonest malignant neoplasms involving the spleen are **lymphomas**, which may produce either focal hypoechoic masses or diffuse enlargement of the spleen (Fig. 10.9). Splenomegaly is a frequent finding in lymphoma, but a normal-sized spleen does not exclude the diagnosis.

Fig. 10.8. (a) Micro-abscess (arrows) in an immunocompromised patient. (b) Small hypoechoic nodules are more clearly seen on contrast-enhanced ultrasound

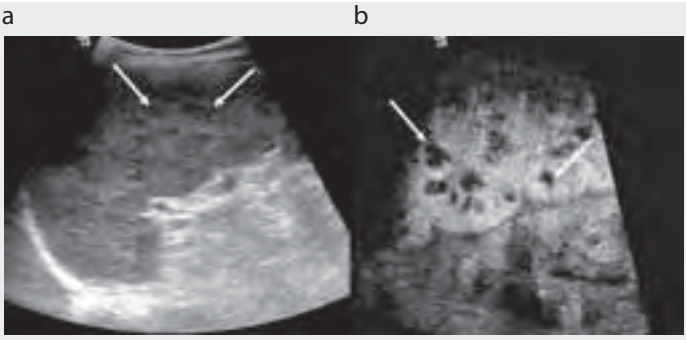

Fig. 10.9. Longitudinal scan: lymphoma of the spleen

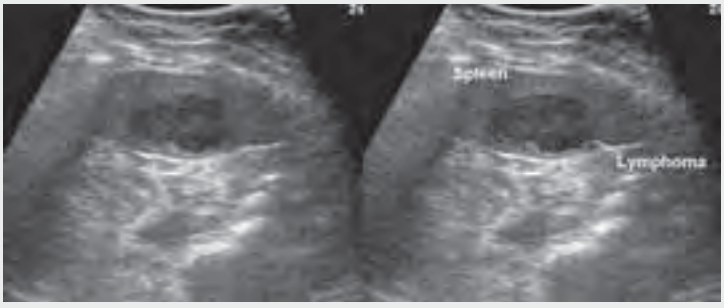

Malignant tumours of the spleen, either primary or metastatic, are very rare. Metastatic deposits from primary tumours of the lungs, breast, ovary and stomach can produce multiple foci of varying echotexture. Multifocal or diffuse lesions, mixed or hyperechoic patterns and target lesions (usually larger than 1 cm) tend to indicate malignancy (Fig. 10.10).

Splenic infarction

Splenic infarcts are typically seen in patients prone to embolic phenomena. Ultrasound often shows a peripheral, wedge-shaped region of hypoechogenicity (Fig. 10.11). Splenic infarcts may initially be large and then become small and echogenic as fibrosis occurs.

Haemangiomas

Haemangiomas are most often well defined focal, echogenic lesions (Fig. 10.12). Although splenic haemangiomas may have an echogenic appearance similar to that of the liver, the sonographic appearance is variable. Lymphangiomas may also occur in the spleen and appear as a multiloculated cystic mass with internal septations (Fig. 10.13).

Fig. 10.10. Metastasis in the spleen from hepatocellular carcinoma. Metastatic tumours of the spleen may manifest as multiple hypoechoic nodules scattered through the splenic parenchyma

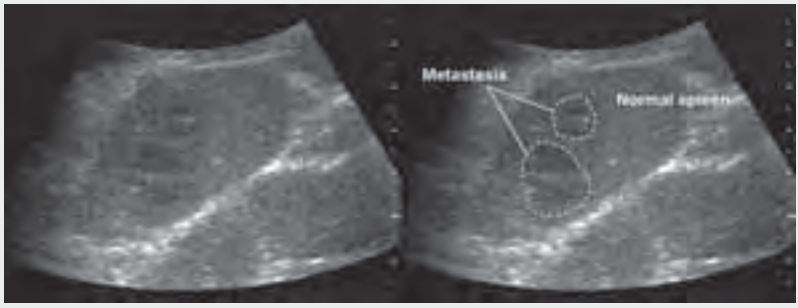

Fig. 10.11. Longitudinal scan of a splenic infarct. Ultrasound shows a mixed echoic area in the periphery of the spleen

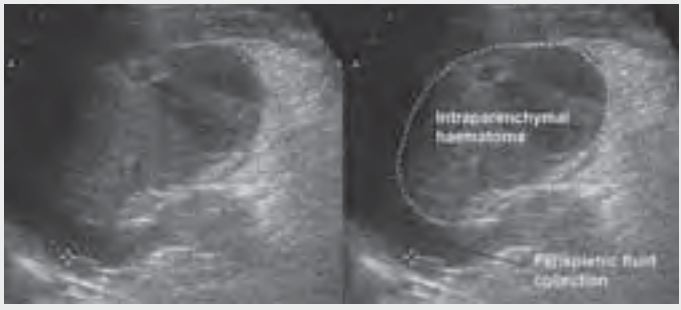

Fig. 10.12. Transverse scan: haemangioma in the spleen. Transverse scan shows a well defined hyperechoic mass with internal hypoechoic area in the spleen

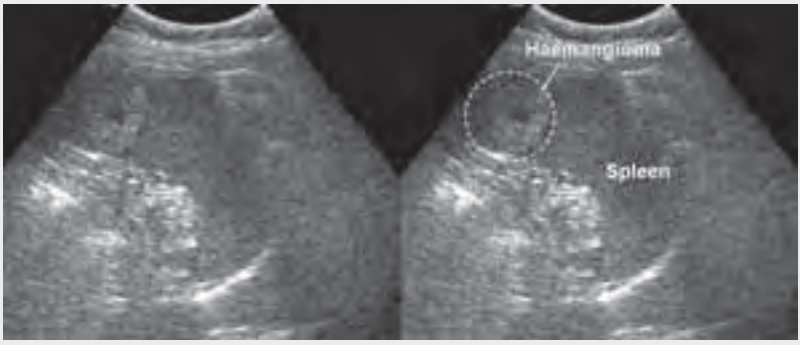

Fig. 10.13. Lymphangioma in the spleen

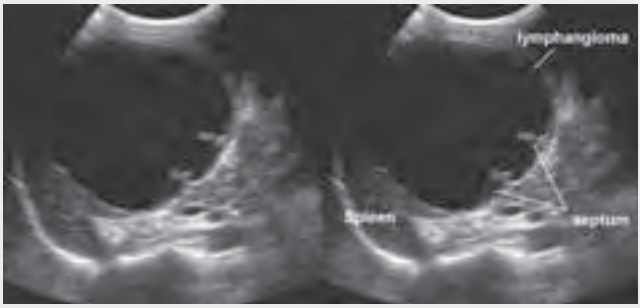

Enlarged splenic vein

A normal splenic vein does not exclude portal hypertension; however, the presence of portosystemic collateral vessels, ascites and cirrhosis of the liver indicates portal hypertension. If the splenic vein appears large and remains larger than 10 mm in diameter on normal respiration, portal hypertension should be suspected. A portal vein that is larger than 13 mm in diameter and does not vary with respiration is strongly correlated with portal hypertension (Fig. 10.14).

Fig. 10.14. Two patients with dilatation of the splenic vein and multiple varicosities, the results of portal hypertension

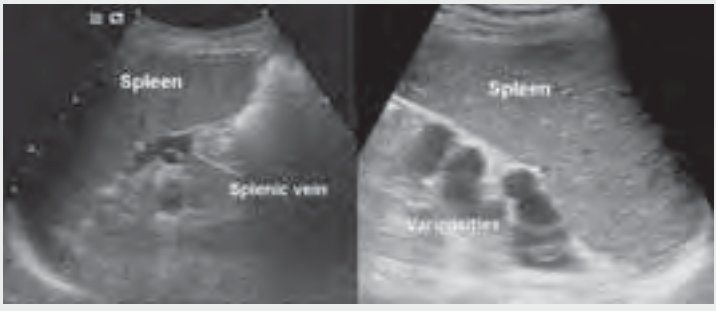

Trauma

Ultrasound can be very useful and highly accurate in the diagnosis of subcapsular and pericapsular haematomas of the spleen. The advantages of ultrasound in assessing splenic trauma include speed, portability with no delay of therapeutic measures and absence of ionizing radiation.

The examination should include a survey of the outline of the spleen to identify any area of local enlargement, followed by a survey of the abdomen to determine whether free intraperitoneal fluid is present. Repeat the scan after a few days if the clinical condition of the patient does not improve.

If there is free intraperitoneal or subphrenic fluid and an irregular splenic outline, a splenic tear or injury is likely. If the fluid collection is half-moon-shaped and follows the contour of the spleen, it suggests subcapsular haematoma (Fig. 10.15). More irregularly shaped fluid collections are seen in perisplenic haematomas.

Fig. 10.15. An intercostal scan after blunt abdominal trauma. Subcapsular and intraparenchymal haematomas are seen

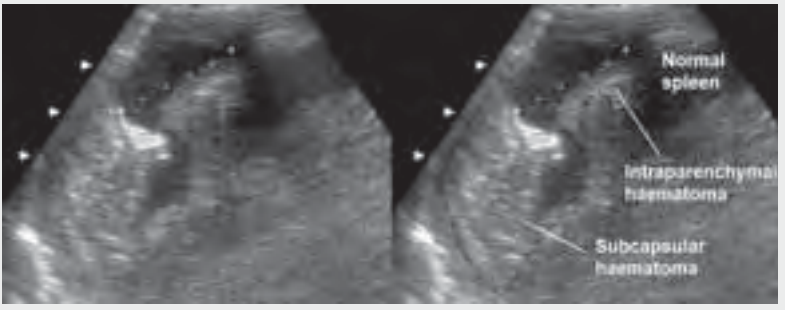

Immediately after a traumatic accident, the haematoma is liquid and can easily be differentiated from splenic parenchyma; however, within hours or days, the echogenicity of the perisplenic clot may closely resemble that of normal splenic parenchyma. An accessory spleen (Fig. 10.16) and a haemangioma (Fig. 10.17) may have a similar appearance.

Old, temporally remote splenic injuries often present sonographically as almost purely cystic collections or calcified masses consisting of irregular clumps of calcification or curvilinear, dense echogenicity.

Haematoma

If the capsule of the injured spleen remains intact, an intraparenchymal or subcapsular haematoma may result (Fig. 10.18). The echogenicity of a haematoma depends on the stage at which the scan is performed.

Fig. 10.16. An accessory spleen. This could be mistaken for a haematoma or the result of a torn spleen

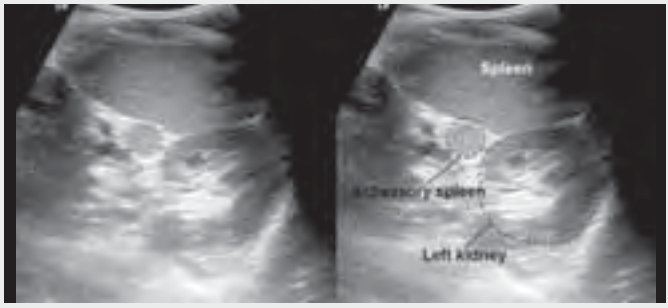

Fig. 10.17. An enlarged spleen due to portal hypertension, in which a solitary haemangioma was an incidental finding. It could be mistaken for an old haematoma

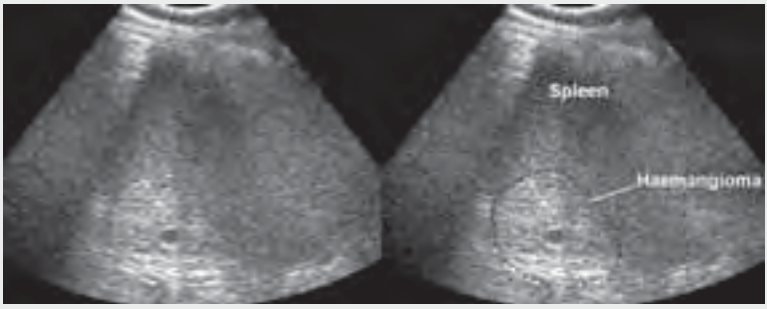

Fig. 10.18. Intraparenchymal haematoma of the spleen and perisplenic fluid collection

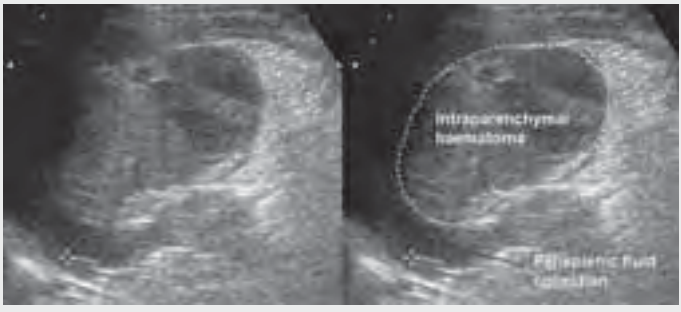

Chapter 11

Gastrointestinal tract

11

Gastrointestinal tract

Preliminary note

Both the cervical and distal abdominal part of the oesophagus can be visualized by transcutaneous ultrasound. As the thoracic part is hidden behind the gas-containing lung and the spine, the wall of this major part of the oesophagus can be visualized only by endoscopic ultrasound. Generally, the stomach and the small and large bowel are accessible to transcutaneous ultrasound, whereas the rectum, especially the distal part, can be examined by endoscopic ultrasound much better than externally through the fluid-filled bladder.

High-frequency transducers (5–7.5 MHz, linear or curved array) of good quality are needed for a detailed ultrasound examination of the gastrointestinal tract. Use of the transcutaneous technique permits differentiation of the layers of the wall. In this way, a thickening not only of the whole wall but also of a single layer or the destruction of layers by an infiltrating process can be visualized. With a transducer of lower frequency or of lower quality, especially a sector scanner, only marked alterations, e.g. bowel obstruction, can be visualized.

Five layers of the wall of the gastrointestinal tract can be differentiated by high-frequency transcutaneous ultrasound and by endoscopic ultrasound (Fig. 11.1, lines 1–5, numbered from the lumen). The echo-rich lines 1 and 5 are due to interface echoes that arise at the border between the (fluid-filled) lumen and the wall (layer 1) and the wall and the surrounding tissue (layer 5), respectively. The other ultrasonic layers correspond to the anatomical layers shown in Fig. 11.1. The echo-poor layer 2 corresponds to the mucosa; the echo-rich layer 3 corresponds to the submucosa, which includes the echoes from the muscularis mucosae. This anatomical layer can be visualized in the stomach by using transducers with very high frequencies (> 10 MHz, endoscopic ultrasound probes) only as a thin echo-rich line, separated by a small echo-poor line from the submucosa. The fourth echo-poor layer corresponds to the muscularis propria. In the deeper parts of the colon and in the rectum, a thin echo-rich line can be visualized, which marks the border between the inner circular muscle layer and the outer longitudinal muscles.

Distinguishing the anatomical layers of the wall of the gastrointestinal tract depends on the frequency and the quality of the transducer on the one hand and, on the other, on the thickness of the layers. The layers of the gastric wall or the rectum can be readily visualized, but not those of the wall of the small bowel, because the thickness of the different layers of the bowel wall lies in the range of the axial resolution of the ultrasound transducers used.

The physical properties of ultrasound itself are responsible for a further phenomenon. Echo-rich layers often appear too thick, as the strong interface echoes between the border of echo-poor (mucosa and muscularis propria) and echo-rich layers (submucosa) add to the echo-rich layer in the ultrasound image.

Fig. 11.1. Scan through the body of the water-filled stomach (water-contrast method). The anatomical layers of the anterior and posterior wall can be seen even at 3.5 MHz. The borderline echoes of the posterior wall are neither very striking (layer 1) nor discernible from the surrounding tissue (layer 5)

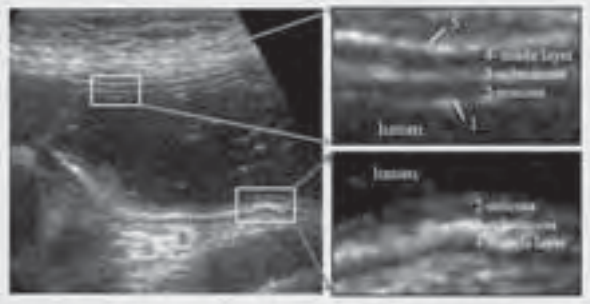

Oesophagus

Indications

There are no clear indications for ultrasonography of the oesophagus for pathological conditions, because the major part is not accessible to transcutaneous ultrasound. In some situations, difficulties in swallowing may be an indication to examine the cervical and abdominal parts of the oesophagus (and the stomach), if an endoscopic examination is not immediately possible.

Examination technique

For the abdominal part of the oesophagus, see below.

Equipment, transducer

Small-parts transducer, linear or curved array, minimum frequency 5 MHz.

Preparation

No specific preparation is necessary.

Position of the patient

The patient should lie in a supine position.

Scanning technique

The cervical part of the oesophagus can be visualized with transverse scans from the (left) side, to avoid the acoustic shadow from the air in the trachea. Additional longitudinal scans can be performed lateral to the trachea.

Normal findings

The cervical part of the oesophagus can be seen as a tubular structure behind the thyroid gland (see Fig. 4.4) The cross-section shows a ring-like structure with an outer echo-poor ring corresponding to the wall (diameter, < 3 mm). The strong echoes in the centre mark the lumen. The movements of the wall during swallowing can be visualized.

Pathological findings

A tumour of the cervical part of the oesophagus can be seen as an echo-poor mass with an irregular outline behind the thyroid (Fig. 11.2). Infiltration of the thyroid or into the surrounding tissue can be seen directly or may be assumed if no movement is seen during swallowing. Enlarged echo-poor lymph nodes raise suspicion of metastases.

Fig. 11.2. Oesophageal carcinoma: echo-poor thickened wall and stenotic lumen (bright echoes) of the lower cervical part of the oesophagus behind the thyroid. Shadow behind air echoes cranial to the tumour

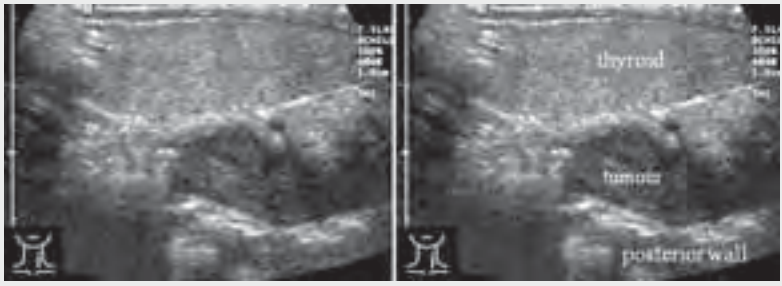

Stomach, including distal oesophagus and proximal duodenum

Indications

The indications for ultrasonography of the stomach are:

- pain in the upper abdomen
- dysphagia and vomiting
- palpable mass in the upper abdomen
- suspected dysfunction (e.g. suspected neuropathy in diabetes)
- suspected submucosal tumour (gastroscopy)
- giant folds (gastroscopy).

In principle, examination of the stomach is included in an ultrasonic examination of the upper abdomen. A more selective examination of the stomach is useful if endoscopy is not available.

In certain differential diagnoses arising during gastroscopy, transabdominal ultrasonography of the stomach is as useful as endoscopic ultrasound.

Examination technique

Equipment, transducer

The usual 3.5-MHz abdominal scanner, curved array or sector, is used for the first orientation. A 5- to 7.5-MHz linear array or curved array transducer can be used for a detailed examination of the wall.

Preparation

The stomach should be empty (fasting period, 4–6 h), as the gastric contents mask pathological conditions.

For a selective examination, the water-contrast method (hydrosonography) is advisable. After a fasting period, the patient drinks around 500 ml of water or juice (without carbon dioxide). It is useful to administer 20–40 mg scopolamine *N*-butyl bromide (Buscopan®) intravenously to stop peristalsis and to achieve good distension of the stomach.

Position of the patient

Supine position, as for the other organs of the upper abdomen.

The water-contrast method is used for examinations in different positions, to bring the fluid into and the air outside the region examined: the head-low position should be assumed for the proximal part, the head-high or sitting position for the distal parts, and the left-lateral and right-lateral positions for the middle part.

Scanning technique

The antrum is most easily visualized in cross-section with a longitudinal scan (relative to the body's axis) over the aorta for the first orientation (Fig. 11.3). The middle parts are visualized by transverse and oblique scans (relative to the stomach). The distal part of the oesophagus and the entrance to the stomach are visualized by longitudinal and transverse scans with a tilted transducer, with the left liver lobe as an acoustic window. The fundus may be missed if the stomach contains only air and if the left liver lobe is very small. Under these circumstances, the water-contrast technique should be used if a disorder in this region is suspected.

Normal findings

The distal parts of the oesophagus and the cardia are visualized as tubular (longitudinal scan) or ring-like structures, with bright echoes in the centre (Fig. 11.4 and also Fig. 11.14). If the stomach is empty, only the anterior wall can normally be seen. The strong echoes behind the anterior wall and the acoustic shadow behind it are caused by air within the lumen. The posterior wall is usually covered by these artefacts. The antrum is always visible as a ring-like structure behind or below the lower edge of the left liver lobe.

Fig. 11.3. Topography of the stomach and its connection to adjacent organs. The lines demonstrate typical scan planes. (a) 1, Longitudinal scan of the upper part; 2, Axis of the antrum; 3, Cross-section of the antrum. (b) Transverse scan of the upper abdomen (om, omentum; vc, vena cava; ao, aorta; b, bursa). The scan line demonstrates the scan plan for Fig. 11.4

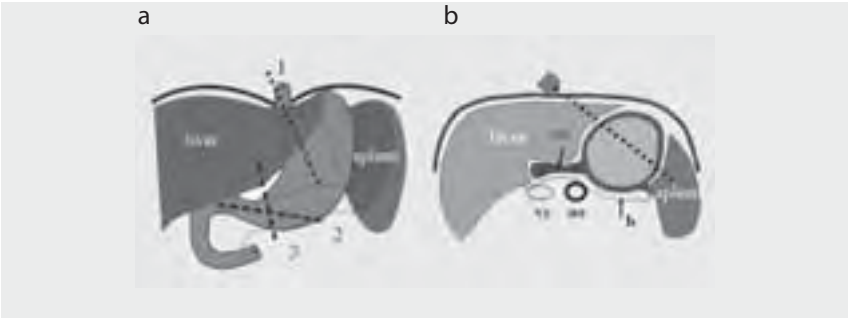

Fig. 11.4. (a, b) Cardia (thin arrow) and body of the stomach between the liver and the spleen. Note the bright line behind the spleen corresponding to the diaphragm (thick arrow). (Ao, aorta)

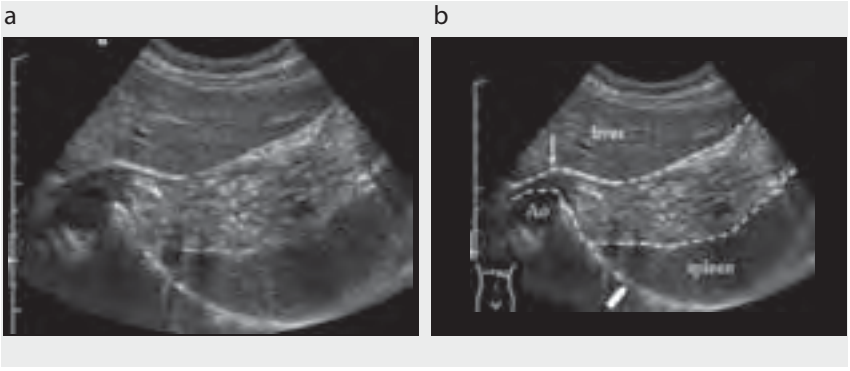

The different layers of the wall can be visualized well with a high-resolution transducer (Fig. 11.1 and Fig. 11.5). The thickness of the wall is 3–6 mm and up to 8 mm in the pylorus region. An exact measurement of the thickness is possible only with the stomach extended, because of the mucosal folds (Fig. 11.5 and Fig. 11.6). All parts of the stomach can be shown more clearly with the water-contrast method.

The duodenum turns backward and runs along the head of the pancreas. The wall is much thinner (< 2 mm). The lumen of the duodenal bulb is marked by strong air echoes (Fig. 11.6 (b)).

Fig. 11.5. Body of the stomach. (a) The layers of the wall of the water-filled body are well delineated (3.5-MHz probe). (b) With a 7.5-MHz probe, the details of the wall are clearly discernible. Bright echoes caused by air bubbles

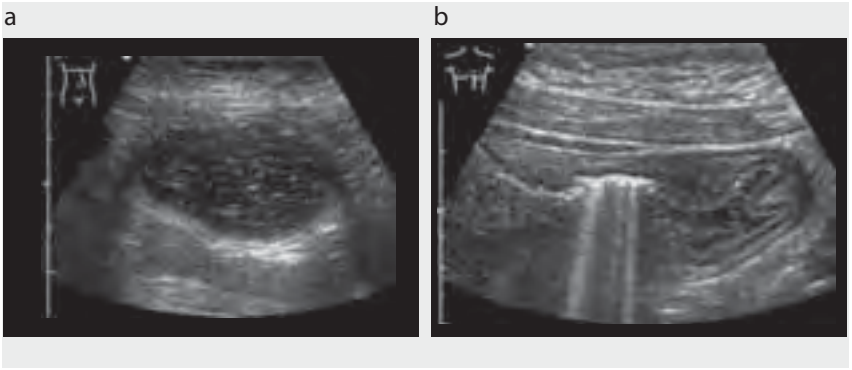

Fig. 11.6. Antrum. (a) Transverse scan. The muscle layer is thick close to the pylorus. The mucosal layer is gyriform, and the lumen is marked only by a single bright echo line (layer 1), because the stomach is empty (pa, pancreas; ao, aorta). (b) Antrum and pylorus, longitudinal scan. Water-filled lumen, air (arrow) in the duodenal bulb

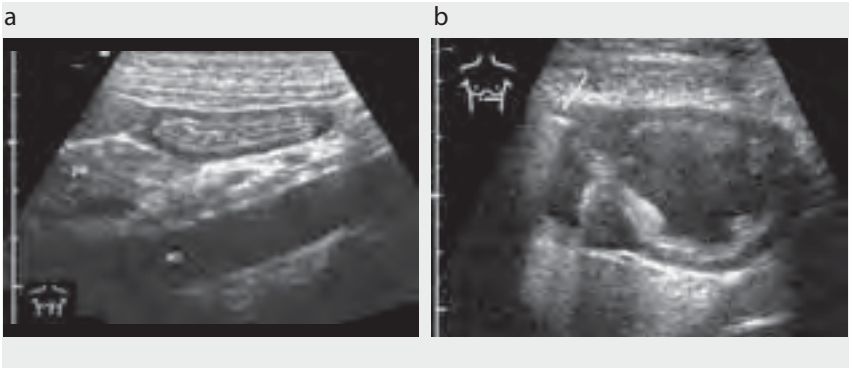

Pathological findings

Functional disorders

Dysfunction

Symptoms of dysfunction of the upper digestive tract can be seen in various organic disorders, such as hiatus hernias and achalasia, or may occur as complications of gastric or duodenal ulcers or tumours.

In a remarkable number of patients who suffer from symptoms such as feeling full, nausea, bloating and pain, no organic alterations can be found. The symptoms are therefore thought to be due to disturbances of motility. The complex is referred to as 'functional dyspepsia' or 'non-ulcer dyspepsia' (NUD).

A disturbance of motility is also seen in patients with diabetes mellitus or other disorders connected with a disorder of the vagus nerve.

Hiatus hernia

Absence of the oesophageal-gastric junction and a digestive tract of diameter greater than 16 mm at the level of the diaphragm are regarded as sonographic symptoms of a hiatus hernia. If the increased diameter is due to a thickened wall, however, a tumour should be suspected.

Achalasia

In achalasia, the distal section of the oesophagus shows a triangular shape, with the apex at the diaphragm (Fig. 11.7). Again, thickening of the wall suggests a tumour ('pseudoachalasia', see also Fig. 11.15).

Fig. 11.7. (a, b) Achalasia. The fluid-filled distal oesophagus is considerably dilated. A tangential artefact causes an acoustic shadow (S) which covers the gastroesophageal junction

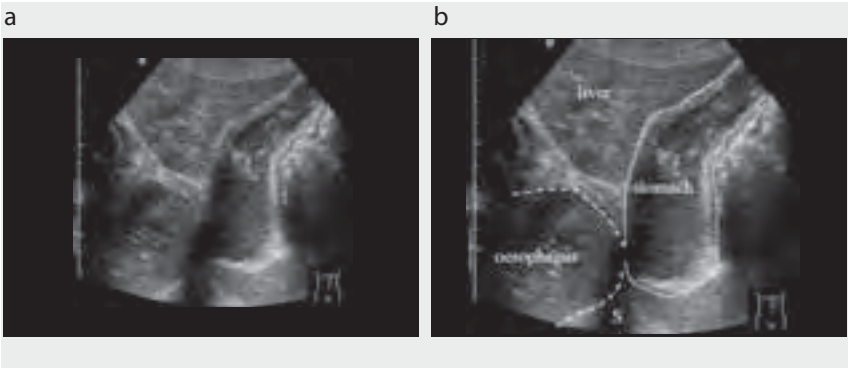

Functional dyspepsia (non-ulcer dyspepsia)

An abnormal distribution of the food in the stomach is characteristic for this disorder. With ultrasound, the distension of the antrum is easier to visualize than the abnormal small proximal part of the stomach. The cross-section of the antrum is measured at the level of the aorta 10 min after a meal. A cross-sectional area less than 3.5 cm^2 is seen as normal, while a cross-sectional area greater than 4.5 cm^2 is typical for patients with non-ulcer dyspepsia.

Diabetes

The width of the antrum, measured over time after a test meal, can be used to calculate gastric emptying. The emptying time is extended in patients with diabetes, especially in those with vegetative neuropathy. In an advanced stage of diabetes, the stomach may be considerably distended (Fig. 11.8).

Fig. 11.8. Diabetic neuropathy. Dilated stomach filled with fluid and chyme (transverse diameter between calipers, 148 mm)

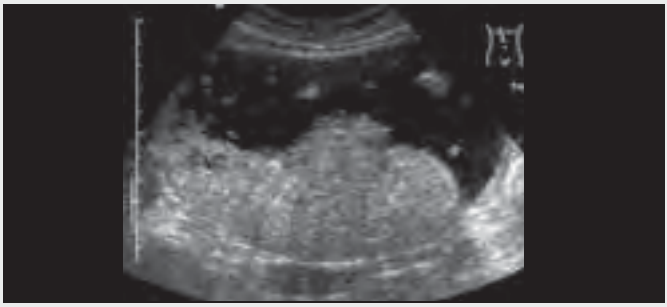

Gastritis

Gastritis may cause swelling of the mucosa and submucosa and thus thickening of the gastric wall. The layers remain distinguishable, and the fourth layer (muscularis propria) is not involved. Such thickening of the gastric wall is discrete in most cases of gastritis associated with chronic *Helicobacter pylori* infection and cannot be visualized by ultrasound. In the acute stage, however, moderate swelling can be seen in marked cases. Remarkable swelling of the mucosa with a more echo-rich pattern is seen in patients with *H. pylori*-associated giant-fold gastritis (Fig. 11.9).

Similar findings are made in various other types of gastritis, such as granulomatous, lymphatic and especially eosinophilic gastritis. The last-mentioned may be associated with swelling of the bowel wall and with ascites. The same pattern can be found in a parasitic gastritis disease caused by *Anisakis marina* infection.

Fig. 11.9. Giant-fold gastritis (*Helicobacter pylori*). Transverse scan through the distal body. The wall is 14 mm thick; the echo-poor fourth layer is still discernible. The narrowed lumen is marked by air echoes

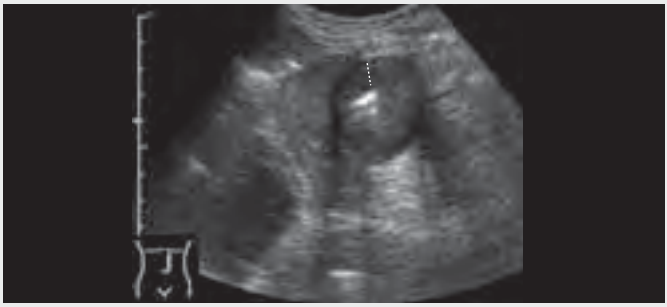

Other benign diseases

Benign diseases that cause similar swelling of the gastric wall are listed in Table 11.1.

Table 11.1. Benign diseases that cause thickening of the gastric wall

Disease	Gastric wall	Further ultrasonic findings
Giant-fold gastritis	Layers 2 and 3: up to 30 mm	
Lymphatic gastritis	Moderate swelling	
Eosinophilic gastritis	Moderate swelling	Bowel, ascites
Anisakis marina infection	Moderate swelling	Small bowel involved, ascites
Ménétrier disease	Marked thickening, echo-rich mucosa	
Angioneurotic oedema (Quincke disease)	Swelling of the whole wall	Bowel involved, ascites
Portal hypertension	Wall thickened in consequence of augmented submucosal venous vessels (Doppler)	Signs of portal hypertension
Cardial congestion	Mild thickening due to congestion	Vena cava dilated
Acute graft rejection	Moderate thickening	
Inflammatory diseases of neighbouring organs (e.g. pancreatitis)	Inflammatory oedematous thickening of all layers	Disorder of an adjacent organ

Ulcers

Gastric ulcers are usually situated on the small curvature of the distal part of the stomach. They cause local swelling of the wall without a clear demarcation. The different layers are still visible. The tissue around an acute ulcer is echo rich as the result of an inflammatory reaction. The transition to the normal wall is graduated. In later stages, echo-poor granulation tissue may be seen. The ulcer itself can be demonstrated with the water-contrast method as a small crater (Fig. 11.10).

Fig. 11.10. (a, b) Gastric ulcer penetrating through all layers into the pancreas

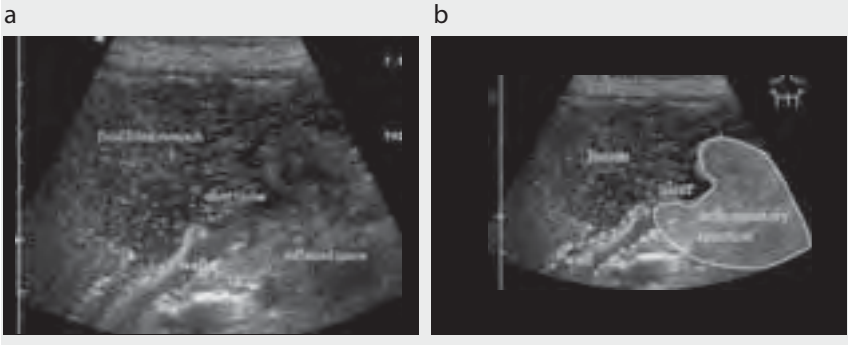

Duodenal ulcers cause considerable swelling of the whole wall of the duodenal bulb. The ulcer is often marked by a strong air echo at the level of the wall (Fig. 11.11 and Fig. 11.12). Demonstration of larger vessels in the base of an ulcer by the Doppler technique indicates a high risk for bleeding (Fig. 11.13).

Free perforation of an ulcer can be diagnosed by the demonstration of free air in the abdomen. Penetration of air bubbles through the wall can sometimes be seen (see Fig. 6.45). Penetration of an ulcer into adjacent organs may cause visible swelling of the structures involved. Stenosis of the pyloric channels leads to distension of the stomach, which, filled with fluid and food, may reach the pelvis.

Ultrasound is suitable for visualizing ulcers in the distal stomach (water contrast) and the duodenal bulb in many cases but cannot be used to exclude ulcers, especially atypical gastric ulcers situated elsewhere.

Fig. 11.11. Duodenal ulcer marked by a strong echo (arrow). The wall of the bulb is swollen and more echo rich than the normal wall of the distal stomach

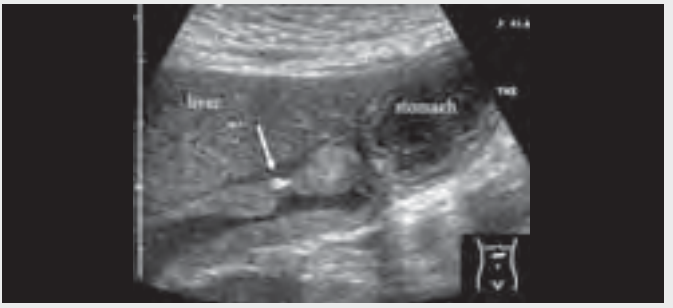

Fig. 11.12. Penetrating duodenal ulcer. Air bubbles mark the ulcer (arrow), which seem to be outside the wall. Additionally, a little fluid is visible, but no free air is seen in the abdomen, indicating that there is no free perforation

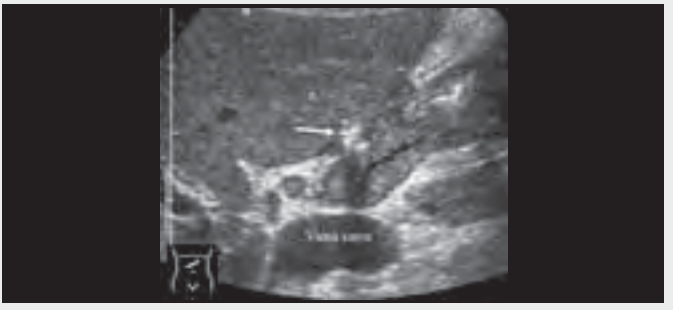

Fig. 11.13. (a, b) Duodenal ulcer marked by an air echo (A) in the swollen wall. Close to the ulcer, a vessel is visualized by power Doppler (arrow). The line marks the duodenum; the interrupted line marks the narrowed lumen

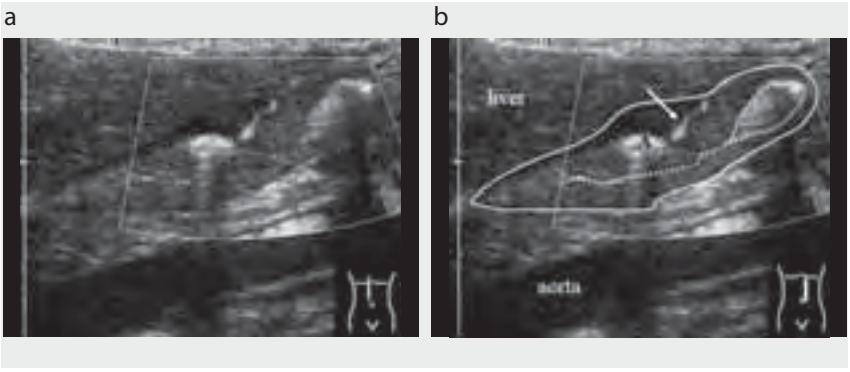

Neoplasms

Gastric carcinoma

Gastric cancers are echo poor, the echo pattern being similar to that of the normal mucosa. Their boundary is sharply defined. They infiltrate throughout the wall and destroy the typical layers. Small carcinomas limited to the mucosal and submucosal layer (early gastric carcinomas, stage 1 tumours) can be visualized only if a high-resolution transducer and the water-contrast method are used or by endoscopic ultrasound (see also Fig. 11.17). Advanced carcinomas cause localized thickening of the wall. In cross-section, a ring-like figure consisting of the echo-poor thickened wall and the stenotic lumen, marked by strong echoes, is seen and is termed a 'cockade', 'pseudokidney sign' or 'target-like lesion' (Fig. 11.14, Fig. 11.15, Fig. 11.16, Fig. 11.17, Fig. 11.18, Fig. 11.19).

Diffuse growing carcinomas cause thickening of the entire gastric wall by up to 10–15 mm. The wall is rigid on palpation. The various thickened layers may remain distinguishable.

Enlarged, round, echo-poor lymph nodes are highly indicative of metastases but can also be caused by an inflammatory reaction.

Fig. 11.14. Normal cardia, transverse scan distal to the hiatus (arrow) (vc, vena cava; ao, aorta)

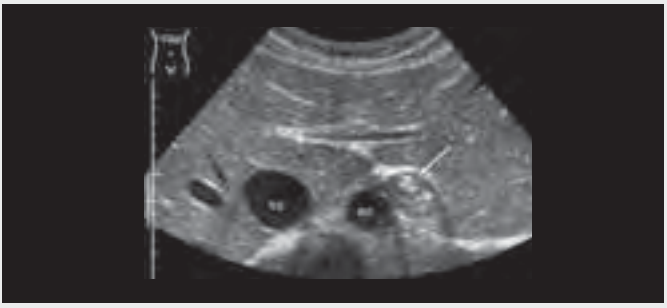

Fig. 11.15. Carcinoma of the cardia (arrows). Transverse scan as in Fig. 11.14 (cl, caudate lobe)

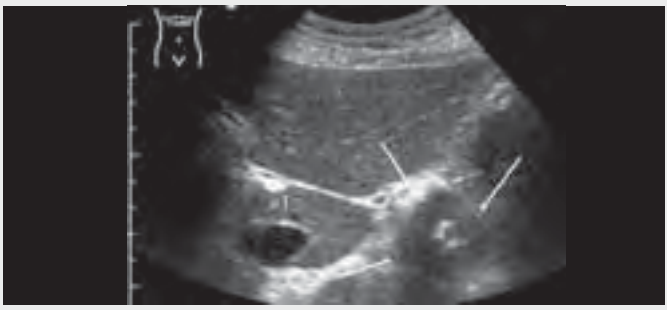

Fig. 11.16. Small, advanced carcinomas of the stomach (different cases). (a) Cross-section shows an irregular thickened wall at the lesser curvature. (b) Longitudinal scan shows localized but considerable neoplastic echo-poor thickening of the wall (16 mm) with an abrupt border at the normal wall (arrow). The inner surface is marked by air echoes

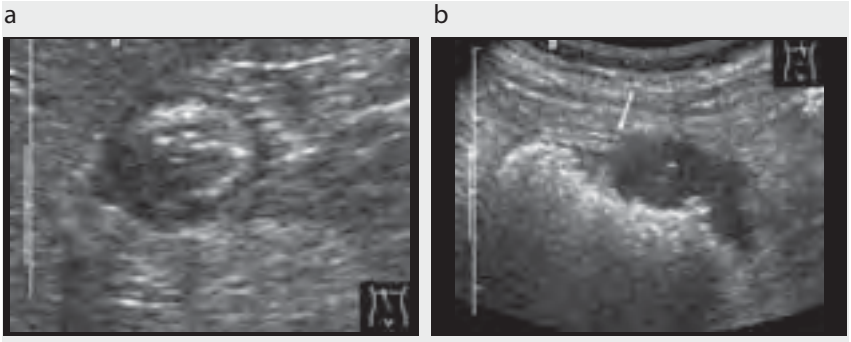

Fig. 11.17. Small gastric cancer. The tumour does not infiltrate the muscle layer, as clearly demonstrated with a 7.5-MHz probe and the water-contrast technique (diameter of wall, 14 mm)

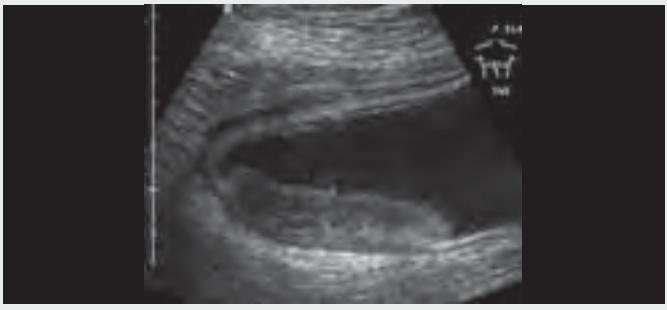

Fig. 11.18. Advanced carcinoma of the antrum (19 mm) causing distal stenosis of the stomach

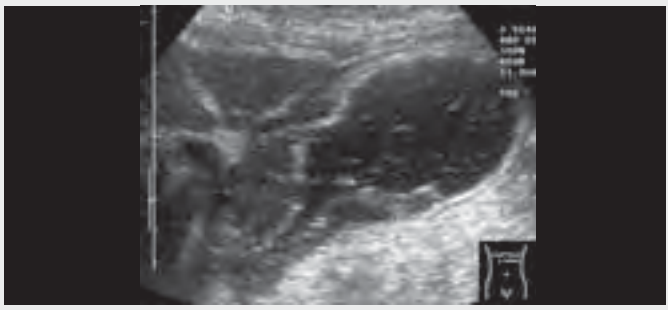

Fig. 11.19. Diffuse gastric cancers, linitis plastica (different cases). Cross-section (a) and longitudinal scan (b) show that the entire stomach wall is homogeneously thickened (12 mm). The different layers are still seen, and the lumen is narrowed (7.5 MHz)

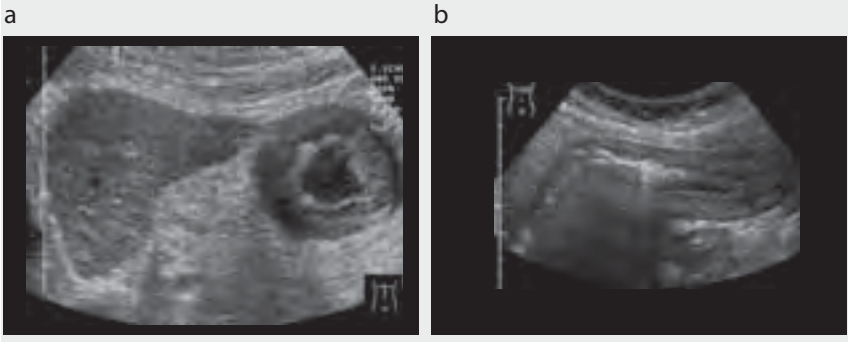

Malignant lymphoma

Malignant lymphomas are extremely echo poor and often appear to be almost echo free. Involved lymph nodes show the same echo-poor pattern.

Early low-grade lymphomas (lymphomas of the mucosa-associated lymphoid tissue, MALT) may grow only on the inner surface, causing thickening of the mucosal layer and an irregular inner surface. Advanced lymphomas destroy the layers and cause echo-poor thickening of the whole gastric wall. Other types are more localized, like carcinomas.

Ultrasound is useful for following up lymphomas. The success of treatment is demonstrated as soon as the thickness decreases and the different layers become visible again (Fig. 11.20, Fig. 11.21, Fig. 11.22).

Fig. 11.20. (a, b) Low-grade MALT lymphoma of the stomach. Transverse and longitudinal scans show thickened dorsal wall (10 mm) with an irregular pattern

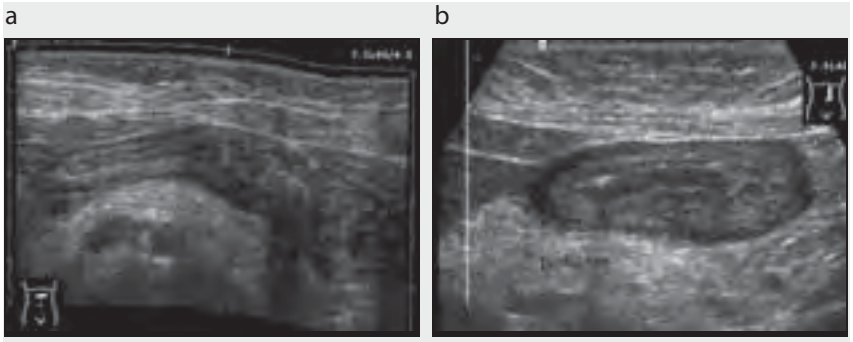

Fig. 11.21. Localized but advanced MALT lymphoma (longitudinal scan through the distal stomach, water contrast)

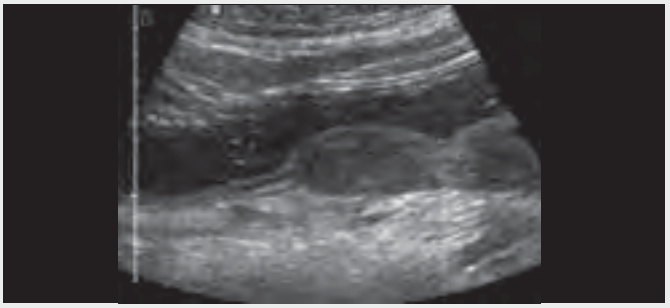

Fig. 11.22. MALT lymphoma spreading throughout the mucosa of the stomach (thickened mucosal layer of the anterior wall) and forming a malignant ulcer in the dorsal wall. (The lymphoma and the layers of the wall are clearly demonstrated using water contrast)

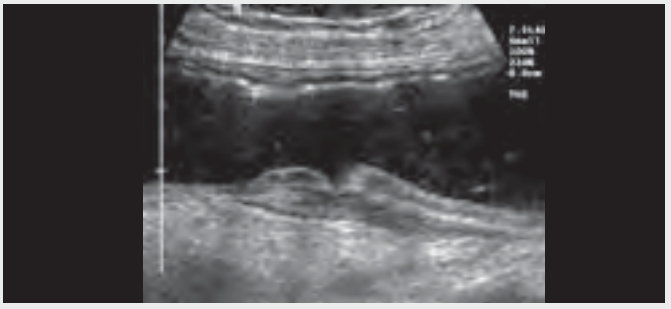

Submucosal tumours

Rare submucosal tumours appear on ultrasound as round tumours with a less echo-poor, slightly irregular echo pattern. From the lumen, such tumours are covered with two or three layers (interface plus mucosal and, mostly, submucosal layer), the so-called 'bridging sign' (Fig. 11.23 and Fig. 11.24). Usually, they are found accidentally but sometimes as a source of bleeding if ulceration of the mucosa has developed. The origin of a submucosal tumour found during ultrasonic examination of the abdomen may first remain unclear but can be revealed by use of the water-contrast technique. During gastroscopy, only a protrusion of the normal mucosa is seen. To differentiate between a submucosal tumour and an impression by a process outside the stomach, ultrasound is the best method. As the nature of these tumours, mainly gastrointestinal stroma tumours (GIST), is uncertain, ultrasonically guided puncture for a complementary histochemical examination might be useful.

Fig. 11.23. Submucosal tumour (gastrointestinal stroma tumour). An echo-poor, inhomogeneous mass at the greater curvature fills the lumen. For a clear diagnosis, the water-contrast method is required

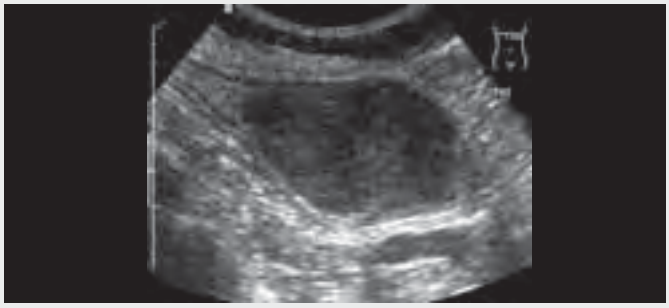

Fig. 11.24. Leiomyoma of the stomach. Three layers (arrow) are seen between the water-filled lumen and the tumour (T), which clearly indicates its origin in the fourth layer ('bridging sign')

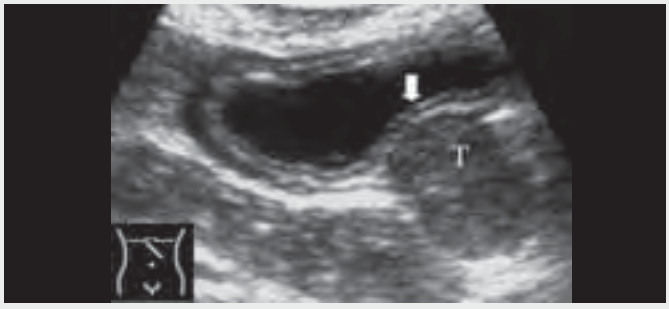

Differential diagnosis

A thickened gastric wall without discernible layers is strongly indicative of malignancy, advanced cancer or malignant lymphoma. A thickened wall with the typical layers still visible is a more ambiguous finding. Malignancy cannot be excluded, as the layers are often discernible in carcinomas of the diffuse type (linitis plastica); however, all diffuse inflammatory and other disorders are possible, as listed with some differential aspects in Table 11.1. A normal (not thickened) muscle layer is considered to be a sign of a benign disorder, but a low-grade malignant lymphoma may involve the mucosa exclusively in the earlier stages.

A localized thickened wall is indicative of a carcinoma or a circumscribed lymphoma. An ulcer might also be diagnosed differentially, especially if the lesion is small and located in the distal part of the stomach. The transition of a tumour to the normal wall is abrupt, whereas the reactive thickened wall in benign ulcers shows a graduated transition to the normal wall. Although ultrasound can be used for some differential diagnoses, mentioned above, it is not usually suitable for distinguishing between benign and malignant ulcers.

Submucosal tumours are round and do not involve the lumen. They therefore differ clearly from the 'pseudokidney sign' of typical gastric carcinomas. The ultrasonic finding of bright echoes in the centre of gastric carcinomas (marking the narrowed lumen) also distinguish gastric tumours from solid tumours of the neighbouring organs. Differentiation of larger submucosal tumours from solid tumours of the surrounding structures is, however, often possible only with the water-contrast method.

Other epithelial tumours of the stomach, such as carcinoid tumours, are seen as small polyps by gastroscopy. They are of no interest for transcutaneous ultrasonography.

Distension of the stomach without signs of a distal tumour may be due to an ulcer in the pylorus channel but may also be seen in an advanced stage of vegetative (diabetic) neuropathy.

Small and large bowel

Indications

The indications for ultrasonography of the small and large bowel are:

- bowel obstruction
- abdominal pain
- suspected appendicitis
- diarrhoea lasting longer than a few days (complications?)
- diverticulitis
- pseudomembranous colitis (in the emergency unit)
- chronic inflammatory bowel disease (diagnosis and management)
- extrapulmonary tuberculosis
- malignant lymphoma.

Generally, ultrasound is not suitable for diagnosing carcinomas of the large bowel, as only advanced tumours can be visualized. It may, however, be useful for finding (advanced) tumours, especially lymphomas, in the small bowel, which is not easily accessible by endoscopy.

Imaging modalities such as ultrasound are not needed to diagnose or manage acute infective enterocolitis but are useful in looking for complications or other disorders in cases with an uncommon (long) course.

Examination technique

Equipment, transducer

A 3- to 5-MHz curved or linear array transducer is used first. Subsequently, small-parts transducers with higher frequencies (5–7.5 MHz) are used to see details. Transducers of 5–7.5 MHz are necessary for examining the appendix.

Preparation

Generally, no preparation is required.

As discussed for examination of the stomach, the water-contrast technique gives a good contrast between the lumen and the wall. Hydrocolonosonography is, therefore, recommended by some authors for delineation of the inner surface of the wall and to visualize small lesions. For this technique, the colon must be cleaned by laxative intestinal lavage, as for colonoscopy. Immediately before the examination 1–1.5 litres of water must be instilled into the colon rectally. Intravenous application of 20 mg scopolamine *N*-butyl bromide (Buscopan) is useful to stop peristalsis and for better distension of the colon.

If examination of the small bowel is indicated, it may be useful for the patient to drink up to 500 ml of water or another suitable fluid.

Position of the patient

The patient should be in the supine position. When the water-contrast method is used, the patient may also be turned in an oblique position.

Scanning technique

It is useful to start with a longitudinal scan of the right liver lobe to check that the instrument has the correct setting. Then, longitudinal scans of the whole abdomen are carried out, with the liver, kidneys and aorta as landmarks. Additionally, transverse and oblique scans are made of the whole abdomen. Gas in the bowel can be displaced by applying slight pressure with the transducer.

For examination of the appendix, the landmarks are the caecum, the terminal ileum and the iliac vessels. The examination is carried out by application of slight pressure in longitudinal and oblique scans. Examination of a patient with acute appendicitis should always include the neighbouring organs, especially the terminal ileum, the lymph nodes and the organs of the small pelvis.

Normal findings

The duodenum is relatively fixed and can be visualized around the head of the pancreas and in its further course to the ligament of Treitz. It is identifiable mainly on the basis of its content, disturbing gas or echo-poor fluid.

The 14–16 loops of the bowel are situated in the middle part of the abdomen, surrounded by the colon. The wall is less than 3 mm thick and consists of an outer, echo-poor layer, corresponding to the muscle layer, and an inner, echo-rich layer due to the submucosa and the interface echoes between the folds of the mucosa and the lumen (Fig. 11.25). When there is water inside the lumen, ultrasound can reveal the complex inner surface of the mucosa, with the longer villi of the jejunum and the shorter villi

of the ileum (Fig. 11.26, see also Fig. 11.50). The last loop of the ileum is not difficult to identify; it is located in the left lower quadrant, with a course from caudal, medial and dorsal to the caecum, which is situated more laterally, cranially and ventrally. The complex structure of the ileocaecal valve can be seen with high-quality ultrasound (Fig. 11.27). The peristaltic movement of the bowel can be visualized, especially if the loops are filled with fluid.

Fig. 11.25. Small bowel. (a) Empty loops with a diameter of 8 mm. (b) Fluid-filled terminal ileum and the normal appendix behind (arrow; diameter, 3.5 mm; ia, iliac artery)

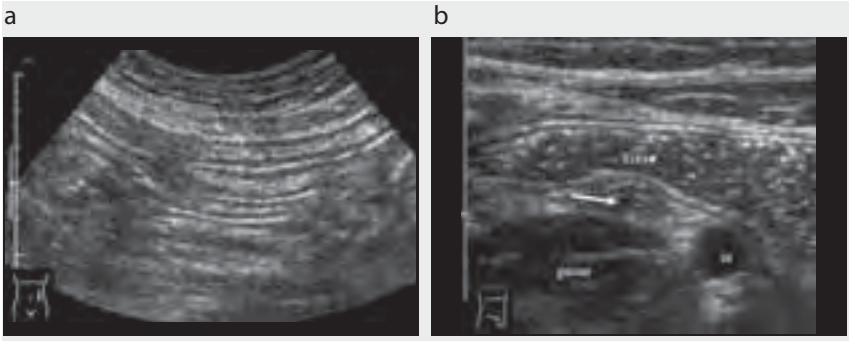

Fig. 11.26. Small bowel loops, demonstrated with high-resolution ultrasound (7.5 MHz). Note the fine pattern of the Kerckring folds (jejunum)

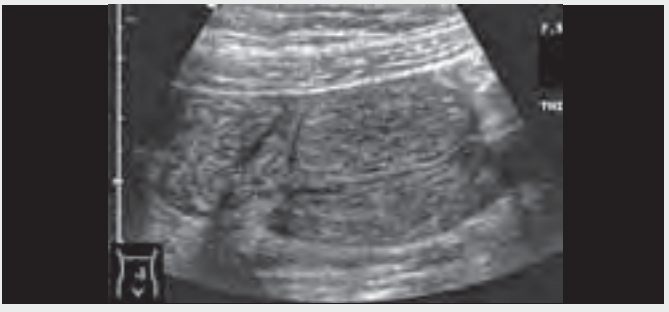

The colon is identified by its larger diameter, the haustra coli and its typical course. In the proximal segments, strong echoes due to gas are common. In the left-sided colon, echo-poor content is not uncommon. The anatomically fixed ascending colon is seen on the right side, with the right flexure close to the gall-bladder. The transverse part has a more variable course, whereas the course of the descending colon is fixed on the left side in front of the iliopsoas muscle. The sigmoid shows no haustra and turns to the midline and backward to the dorsal wall of the bladder. The distal and upper parts of the sigmoid can be demonstrated by using the full bladder as an acoustic window (Fig. 11.27, Fig. 11.28, Fig. 11.29).

Fig. 11.27. Ileocaecal valve (arrow; C, caecum; I, ileum)

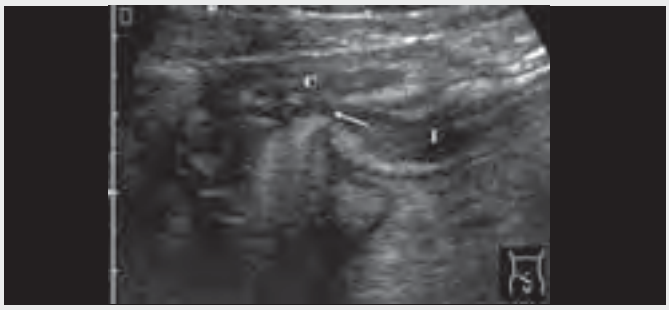

Fig. 11.28. Descending colon, transverse scan. The echo-poor part of the wall corresponds to the muscle (m) layers

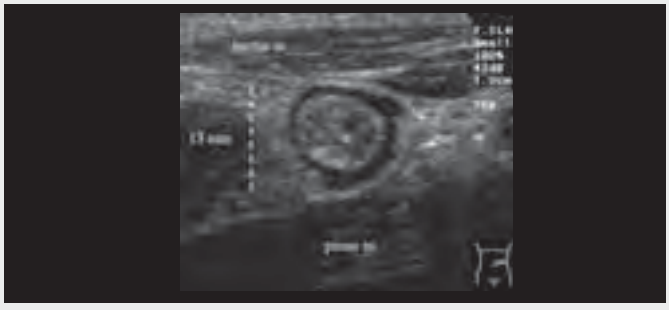

Fig. 11.29. Colon. (a) Fluid-filled descending colon. (b) Gas-containing caecum. The shadow originating at the front of intestinal gas covers the dorsal wall and the structures behind the colon

a

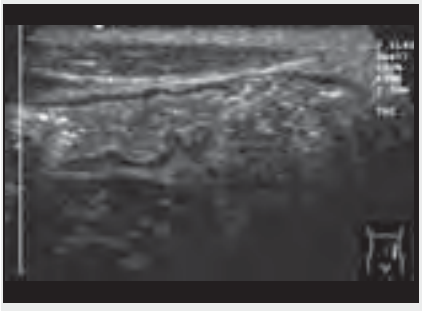

b

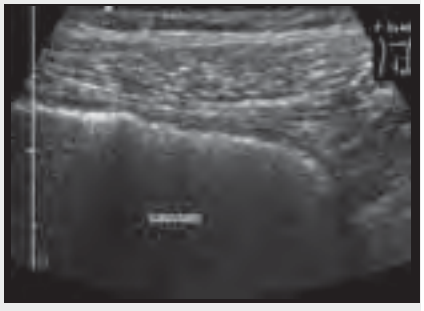

The appendix (Fig. 11.25 (b)) originates 3 cm distal to the ileocaecal valve on the medial side; in 66% of cases, it is located behind the caecum ('retrocaecal'). With ultrasound, it is sometimes possible to demonstrate the normal appendix, but this cannot be done routinely, as it is a tubular structure about 8 cm long with a diameter of 3–6 mm. It differs from the ileum in that it has a blind end and does not show peristaltic movement.

Pathological findings

Inflammatory bowel disease

Enterocolitis

When the bowel is infected with certain microorganisms, the mucosa and submucosa swell and there is augmented secretion of fluid and hyperperistalsis. Ultrasound shows a thickened, echo-poor wall, while the contents of the segments are more or less echo free. The hyperperistalsis can be visualized in real time. A small amount of ascites may be seen between the intestinal loops. The mesenteric lymph nodes may be moderately enlarged. Their pattern is less echo poor, and the echo-rich 'hilus sign' is still seen (Fig. 11.30 and Fig. 11.31; see also Fig. 6.31(b)).

Fig. 11.30. Bacterial enteritis (two cases). The echo-poor mucosa of the terminal ileum is thickened, but the deeper layers are not affected. Several echo-poor lymph nodes are seen. (a) longitudinal scan (wall, 4 mm; C, caecum; ia, iliac artery). (b) Cross-section (wall, 6.5 mm)

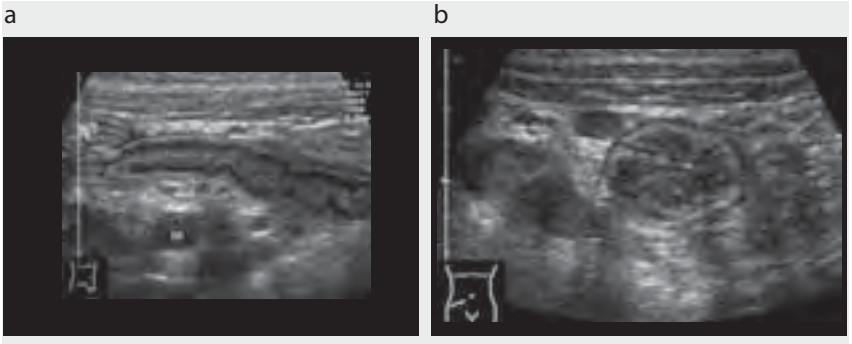

Pseudomembranous colitis

This antibiotic-associated infection, caused by *Clostridium difficile*, is a typical complication of seriously ill patients in intensive care units, although it may be seen in other patients treated with antibiotics and with less severe disease.

Ultrasound shows echo-poor thickening of the colon segments involved. This ultrasonic indication is not specific but, with clinical background information, is typical enough for diagnosis of this disease (Fig. 11.32).

Fig. 11.31. Infectious colitis. The wall is thickened (7 mm), mainly due to swelling of the mucosal and submucosal layers. Enlarged, echo-poor lymph nodes (ln) in the neighbourhood. (a) Longitudinal scan, (b) transverse scan of the descending colon

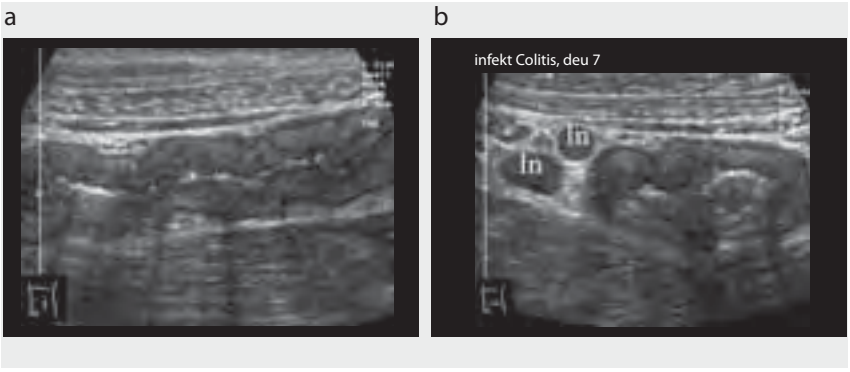

Fig. 11.32. Pseudomembranous colitis (serious case). The whole wall of the descending colon is heavily swollen (thickness, 14 mm) and altogether echo poor

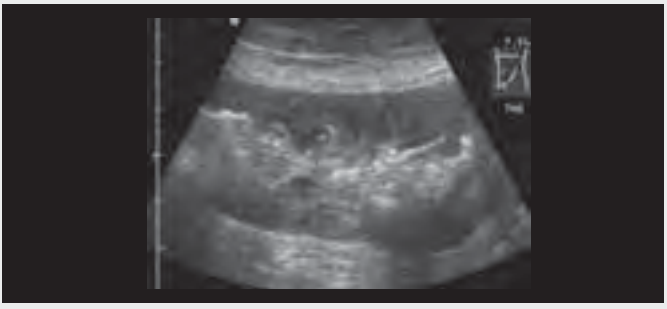

Whipple disease

The ultrasonic features of this rare bacterial disorder are similar to those of other acute inflammatory diseases of the small bowel, with fluid-filled intestinal loops and hyperperistalsis. However, a remarkably echo-rich wall and enlarged lymph nodes with an echo-rich pattern are characteristic.

Diverticulitis

Diverticula, or, more precisely, pseudodiverticula, are common in developed countries. In most cases, they are located in the sigmoid and descending colon. True diverticula are seen in all parts of the colon. Ultrasound can be used to visualize them as small areas within the wall, marked by a strong air echo (Fig. 11.33).

Diverticulitis develops with erosion of the inner surface, followed by microperforation of the diverticula and an inflammatory reaction of the surrounding tissue. It is visualized by ultrasound as a small, echo-poor lesion on the outside of the thickened wall, covered

by an echo-rich cap of fatty tissue (Fig. 11.34 (a)). The condition causes acute abdominal pain and is easy to locate if the transducer follows the pain point.

Ultrasound is also useful for following up the course of this disease, whether it heals or whether there are complications, such as abscesses within the surrounding tissue, which are seen as echo-poor areas (Fig. 11.34 (b)). A further complication, free perforation, is established by the demonstration of gas bubbles as moving strong echoes with artefacts in the abdomen, especially in front of the liver. A colovesicular fistula is another typical complication. Involvement of the bladder can be shown as an echo-poor structure between the sigmoid and the bladder, a swollen wall and echoes and gas artefacts within the bladder.

Fig. 11.33. Diverticulosis. Two diverticula are marked by strong gas echoes at the level of the muscle layer of the wall (arrows)

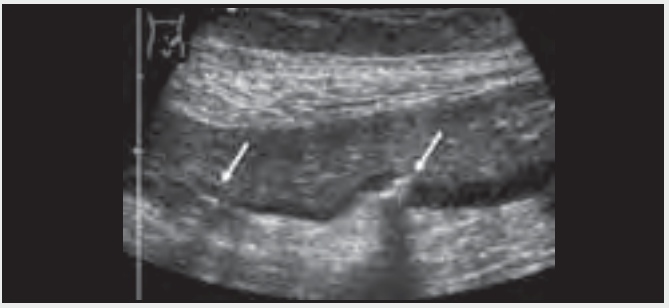

Fig. 11.34. Diverticulitis. (a) The peridiverticulitis (left) is limited by an echo-rich cap of fatty tissue. (b) The peridiverticular inflammation (D) is not limited but forms an echo-poor abscess with an irregular margin. The sigmoid itself shows an echo-poor, thickened wall (10 mm)

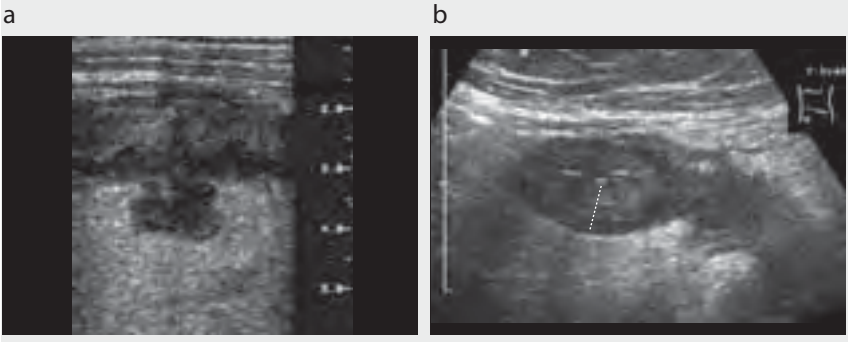

Tuberculosis

Intestinal tuberculosis most commonly involves the small bowel and the ileocaecal region. Ultrasound shows a localized, often circumferential, echo-poor thickening of the wall (Fig. 11.35). If the lumen is fluid-filled, typical ulceration of the mucosa

Fig. 11.35. Tuberculosis of the colon (HIV-infected patient), with echo-poor thickening of the whole wall (compare with Fig. 11.32 and also Fig. 11.46)

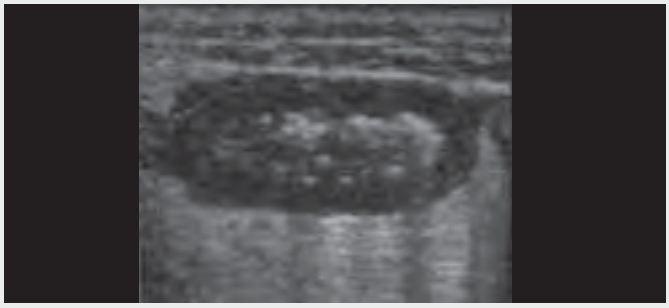

may be seen. The adjacent mesenteric lymph nodes are enlarged. An almost echo-free area corresponds to the characteristic caseation. In later stages, calcifications are also characteristic. The involvement of the peritoneum causes ascites and adhesions. Intestinal loops, conglomerated lymph nodes and fibrotic mesentery may form an inhomogeneous conglomerated mass, often with ascites.

Chronic inflammatory bowel diseases

Crohn disease is characterized by a granulomatous inflammation that affects all parts of the gastrointestinal tract, but usually the distal ileum and parts of the colon. Several segments of the bowel may be affected discontinuously. The inflammation itself involves the whole wall in a discontinuous pattern. Fistulas, abscesses and bowel obstruction are typical complications of this disease.

Ulcerative colitis is limited to the colon, starting in the rectum and spreading upwards. Ultrasound reveals a thickened, echo-poor wall. The different layers remain discernible. Ultrasound images of the acute stages of Crohn disease and of ulcerative colitis are similar to those of the thickened bowel wall seen in acute inflammatory enterocolitis. Differences in the segments of the bowel affected may help differentiate between Crohn disease and ulcerative colitis (Table 11.2, Fig. 11.36, Fig. 11.37, Fig. 11.38).

Table 11.2. Differential diagnostic aspects of chronic inflammatory bowel disease

Disease	Pattern	Wall	Complications
Crohn disease	All parts of the gastrointestinal tract, discontinuously	Discontinuous transmural thickening	Fistulas, abscesses, inflammatory conglomerates, stenosis and obstruction
Ulcerative colitis	Colon, starting in the rectum, spreads continuously	Thickening of the mucosal and submucosal layers Late stage: loss of haustra, thin wall	Free perforation, toxic megacolon, carcinoma

Fig. 11.36. Crohn disease, acute stage. Ultrasound demonstrates thickening of the mucosal and submucosal layer, with blurred borders. Note the oblique and transverse muscles. The arrow marks the ileocaecal valve

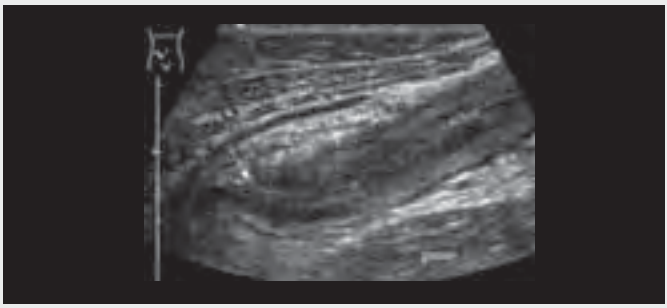

Fig. 11.37. Crohn disease of the colon, subacute stage. The thickening of the wall is caused by swelling of the echo-poor mucosal and particularly the echo-rich submucosal layer. (a) Longitudinal scan; wall, 7 mm. (b) Transverse scan; wall, 8.5 mm

a b

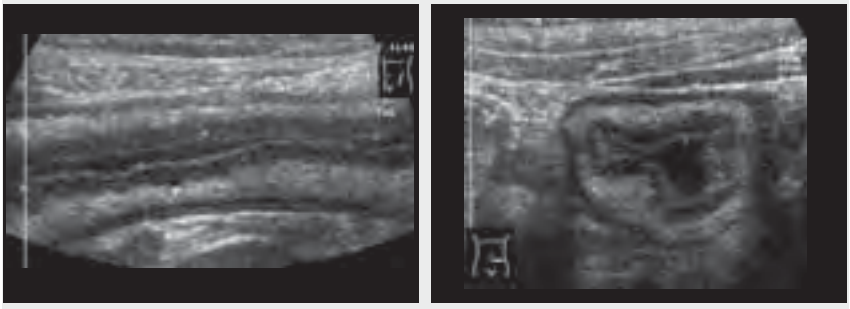

Fig. 11.38. Ulcerative colitis. Thickening of the wall is due to swelling of the mucosa in the acute stage. (a) Wall, 6.5 mm. (b) At a later stage (wall, 5.5 mm), the sonographic features are similar to those seen in Crohn disease

a b

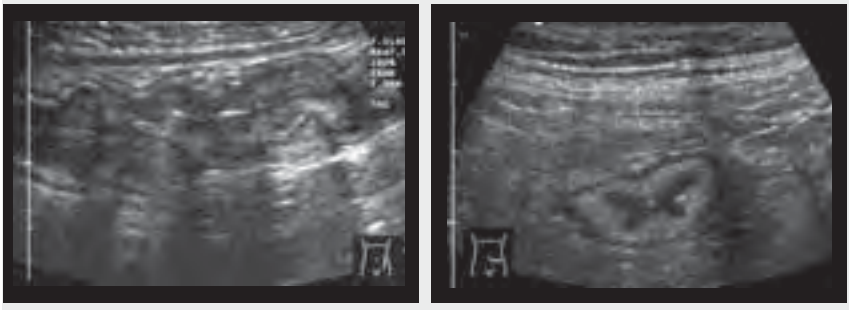

When the Doppler technique is used, augmentation of colour pixels is a sign of hyperaemia, which is indicative of an active inflammatory process. The flow in the feeding artery, mainly the superior mesenteric artery, is increased and changes to that of a low-resistance artery with a high diastolic flow (Fig. 11.39).

Fig. 11.39. Doppler technique in chronic inflammatory bowel disease. (a) Ulcerative colitis. Power Doppler shows augmented signals in the colon wall (4.5 mm), indicating an acute inflammatory stage. (b) Crohn disease. Spectral Doppler shows a low-resistance profile in the superior mesenteric artery in the fasting stage as a symptom of hyperaemia of the affected intestine

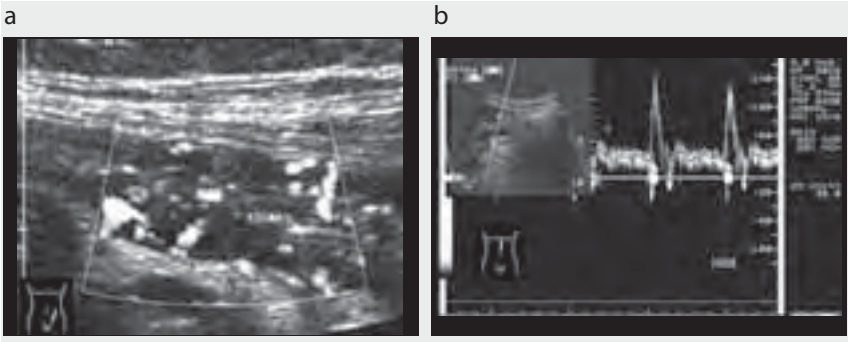

Fistulas (enterocutaneous) are visualized as irregular, echo-poor tubular structures. The echo-poor pattern corresponds to inflammation around the fistula. The fistula itself is marked by some stronger echoes in the centre of the lesion. Fistulas between two loops may form a conglomerate of intestinal loops, echo-free fluid and echo-poor inflammatory tissue (Fig. 11.40).

Narrowing of the lumen can be visualized clearly by ultrasound (Fig. 11.41). In this stage, the passage of gas bubbles can still be observed. If stenosis is complete, the typical mechanical obstruction, with dilated fluid-filled loops, before stenosis can be seen (Fig. 11.41). The Doppler technique is helpful for distinguishing between stenosis caused by an inflamed, thickened wall (more colour pixels) and cicatricial stenosis (fewer colour pixels).

Free perforation may occur as a complication of ulcerative colitis. Another typical problem is toxic megacolon. Ultrasound demonstrates a segment with a thin wall and a diameter of > 6–7 cm filled by strong gas echoes. In the late, inactive stage of the disease, a small echo-poor colon without haustra may be seen.

Ischaemic diseases of the bowel

Various vascular diseases can cause acute (mesenteric infarction) or chronic underperfusion of bowel segments, the upper part of the descending colon being the most commonly involved. Ultrasound shows an echo-poor wall without discernible layers or movement. The border between the affected segment and the normal wall is abrupt, in contrast to inflammatory segments, which show a graduated transition to the normal wall (Fig. 11.42).

Fig. 11.40. Crohn disease. Abscess (echo-poor, inhomogeneous lesion with a strong gas echo; diameter, 57 mm) and enterocutaneous fistulas (pseudopodias)

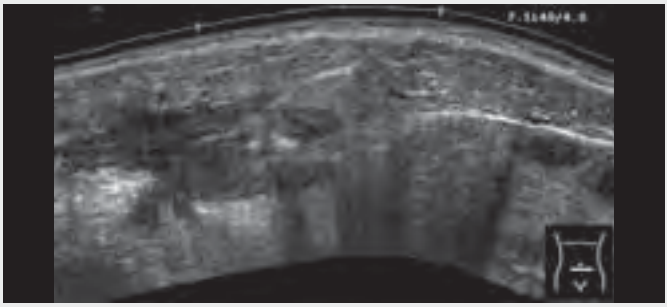

Fig. 11.41. Crohn disease. Stenosis in a lower ileum loop (dotted line) causes bowel obstruction (dilated fluid-filled loops, O). Gas echo (arrow) at the beginning of the stenotic segment

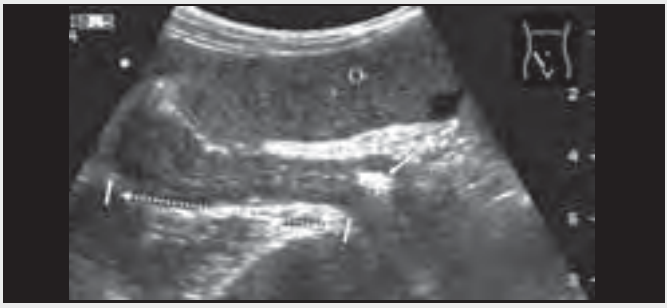

Fig. 11.42. (a, b). Ischaemic colitis. Note the echo-poor thickened wall (7 mm) and the narrowed lumen, without discernible layers, and the abrupt border to the normal colon

a

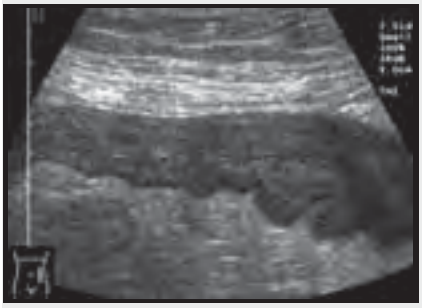

b

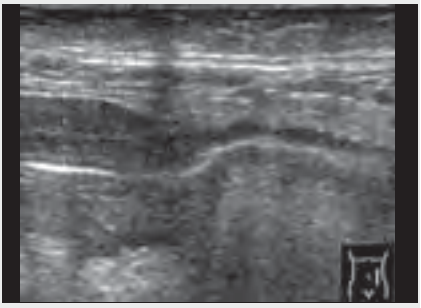

The Doppler technique shows lack of flow signals only if the whole wall is affected. If underperfusion is limited to the mucosa, flow signals are seen on the outside of the wall. Arteriosclerotic stenosis or vasculitis can be visualized with B-scan and colour Doppler technique if the lesion is located in the trunk of the superior or inferior mesenteric artery. Colour Doppler also shows the turbulent flow, but the grade of stenosis must be determined using the spectral Doppler technique.

The ischaemia results in a paralytic ileus. Ultrasound shows dilated intestinal loops with a more or less echo-free content, but without peristalsis. Therefore, sedimentation of the echoes in the fluid is seen. Ascites is visible between the loops during the course of the disease. The demonstration of strong echoes moving in the portal vein indicates a poor prognosis, as these echoes are due to gas bubbles from a gangrenous bowel wall. In contrast, the appearance of colour pixels in the wall indicates a good prognosis (Fig. 11.43).

Fig. 11.43. Ischaemic colitis, prognostic signs. Case (a): single power Doppler signals indicate residual blood supply (good prognosis); case (b): gas bubbles (strong echoes) moving in the intrahepatic branches of the portal vein indicate gangrene of the bowel (poor prognosis)

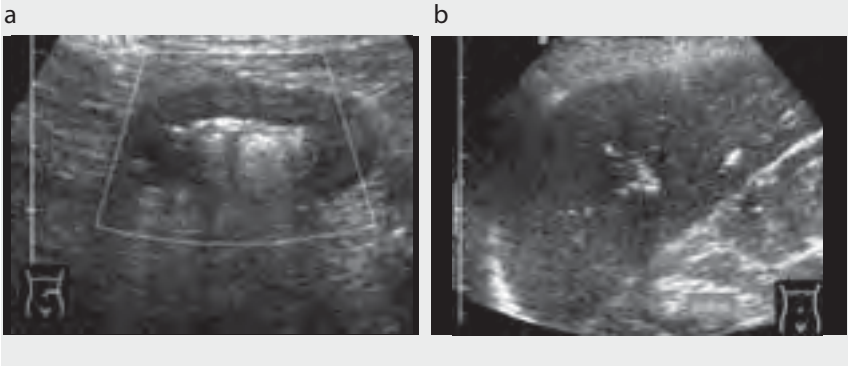

Coeliac disease (gluten-sensitive enteropathy, sprue in adults)

Ultrasound can be used to visualize an abnormally dilated duodenum and dilated, fluid-filled small bowel loops with hyperperistalsis. The inner surface of the wall is flat due to the characteristic atrophy of the villi (Fig. 11.44).

Radiation colitis

Chronic damage of the colon is seen after (pelvic) irradiation. Ultrasound shows an echo-poor wall, sometimes with an inhomogeneous pattern due to scars. The lumen may be narrowed. Colour Doppler examination shows reduced flow.

Tumours

Carcinoma of the colon is one of the commonest malignant tumours in developed countries. The typical sonographic signs of advanced tumours are a localized, one-sided or circumferential thickened wall and an echo-poor pattern, without discernible layers. The typical aspect is known as 'cockade' or 'pseudokidney sign'. The transition

Fig. 11.44. Coeliac disease (adult). Slightly dilated, fluid-filled small bowel with a flat inner surface and hyperperistalsis

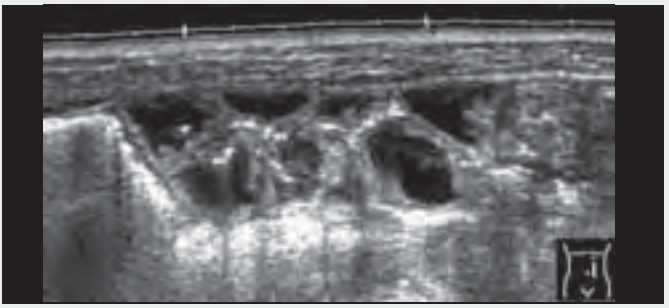

Fig. 11.45. Carcinoma of the small bowel. Characteristic sonographic feature with an echo-poor wall and a narrowed lumen marked by bright echoes

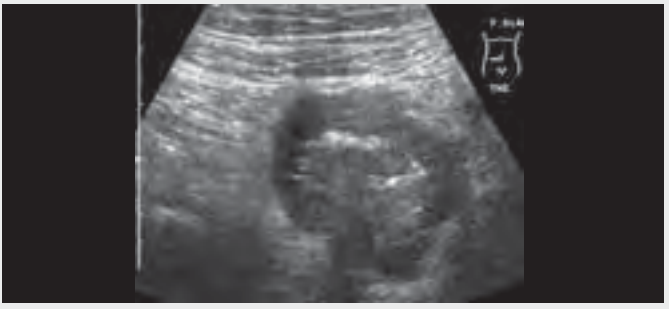

Fig. 11.46. Colon carcinomas (several cases). (a) Cross-section shows the characteristic sonographic pattern of an advanced carcinoma (pseudokidney sign; wall, 11 mm). (b) Longitudinal scan demonstrates an obstruction due to an advanced carcinoma (stenotic lumen, marked by a thin line of bright gas echoes, dilated section (marked by arrows) with heterogeneous fluid proximal to the stenosis)

a

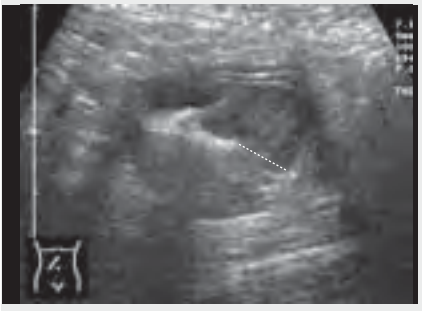

b

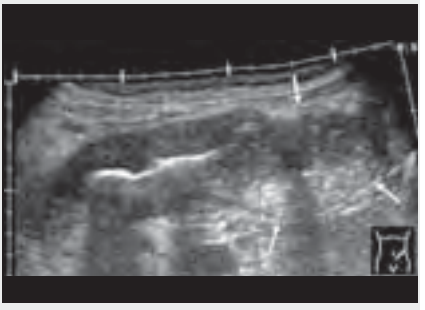

between a neoplasm and the normal wall is usually abrupt (Fig. 11.45 and Fig. 11.46).

The tumour may cause mechanical obstruction (Fig. 11.46). Enlarged, echo-poor lymph nodes and ascites are signs of advanced stage.

Despite the typical aspect of advanced bowel cancer, ultrasound is not generally suitable for detecting carcinomas of the bowel. A negative result on an ultrasound examination does not exclude colon cancer.

Other benign and malignant tumours of the small and large bowel, such as carcinoid tumours, are rarer. Ultrasound can show localized thickening of the wall or a round mass with a smooth surface inside the lumen if the tumour measures 2–3 cm or more. The tumours are echo poor, with the exception of echo-rich lipomas.

Visualization of smaller tumours with the water (contrast) technique is possible but is not diagnostic, as their type and their nature cannot be determined by ultrasound.

Malignant lymphomas of the bowel result in an extremely echo-poor pattern of the mostly circular, thickened wall. The outline can be more irregular than that of carcinomas. The lymph nodes are usually involved.

Secondary lymphomas may extend longitudinally over a longer segment of the bowel. They spread over the surface and do not always destroy the layers. The sonographic aspect of secondary lymphomas resembles that of (chronic) inflammatory diseases (Fig. 11.47).

Fig. 11.47. Malignant lymphoma of the terminal ileum (patient with immunodeficiency). Note the considerably thickened (11 mm), echo-poor wall and the stenotic lumen

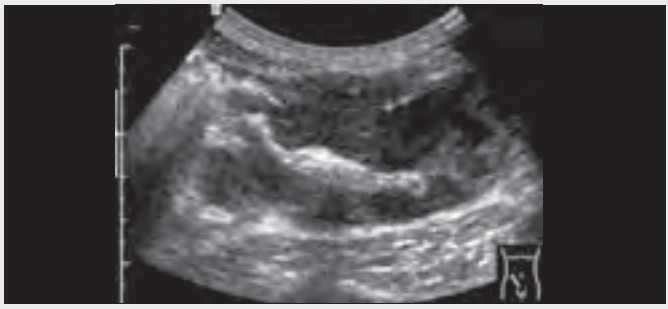

Bowel (ileus) obstruction

Bowel obstruction is a typical complication of various diseases of the bowel. Independent of the causal disease, the ultrasound findings are relatively uniform, with dilated, fluid-filled small bowel loops (Fig. 11.48, Fig. 11.49). In paralytic ileus, no peristalsis is seen, and the only movement of the content is due to respiration and pulsation of vessels.

Violent but frustrated peristalsis is the typical sign of mechanical occlusion. The nature of the occlusion is not always detectable by ultrasound. Neoplastic or inflammatory tumours as well as stones or benign stenosis in Crohn disease can be demonstrated, as described above. The commonest type of obstruction, the adhesion ileus, can be suspected only after exclusion of other causes but cannot be demonstrated directly by ultrasound. The height of the occlusion of the small bowel can be estimated from analysis of the Kerckring folds (Fig. 11.50).

Fig. 11.48. Ileus obstruction. Dilated loops are characteristic. The sedimented contents and the ascites between the loops are signs of paralytic ileus or the late stage of mechanical obstruction

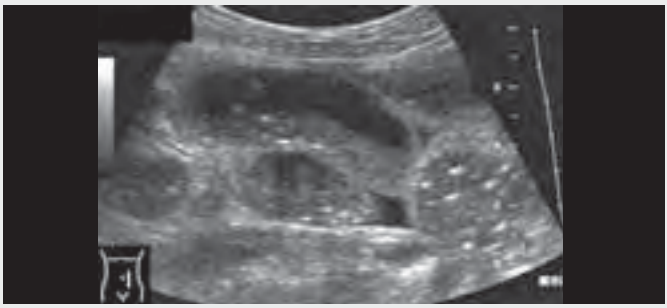

Fig. 11.49. Mechanical obstruction. Real-time scan shows futile movement in both directions (arrow)

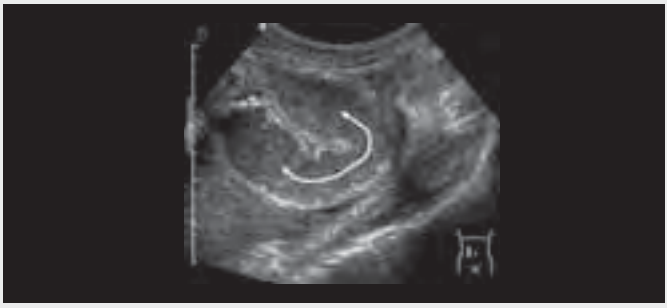

Fig. 11.50. Mechanical obstruction. (a) Jejunum with long Kerckring folds; (b) ileum with short folds

a

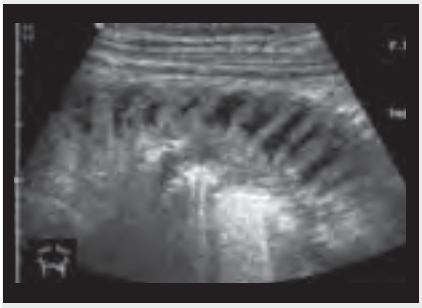

b

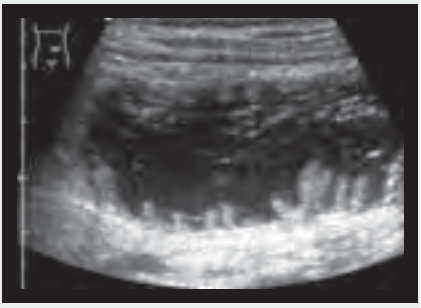

The content of the obstructed colon is not always echo poor (Fig. 11.51). In other cases the dilated colon contents mainly gas, as e.g. in a toxic megacolon or a congenital, aganglionic megacolon (Hirschsprung disease, Fig. 11.52).

Intussusception and volvulus are rare causes of bowel obstruction in adults. Both may form a palpable mass. Ultrasound shows an inhomogeneous process with smooth outlines. Precise analysis of two concentric rings ('ring-in-ring') enables diagnosis of the invagination (Fig. 11.53). The typical aspect is sometimes confused, as echo-rich parts of the mesentery or echo-poor fluid are also invaginated. Volvulus is diagnosed by analysing the course of the mesenteric vessels, which are twisted and congested. The possibility that a tumour is the cause of this disorder should be considered in adults.

Fig. 11.51. Obstruction of the colon (C): dilated colon (cross-section) with liquid content (right flexure) (Vc, vena cava)

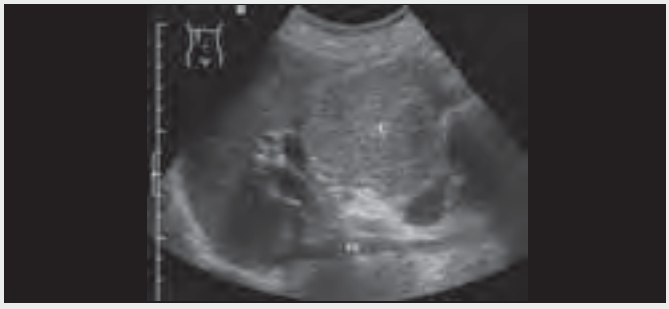

Fig. 11.52. Dilated descending, gas-filled colon (Hirschsprung disease; diameter, 7 cm)

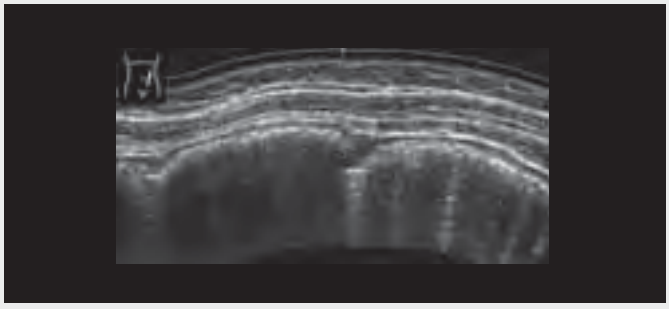

Fig. 11.53. Invagination: (a) transverse and (b) longitudinal scans. Ultrasound clearly demonstrates the 'ring-in-ring' sign

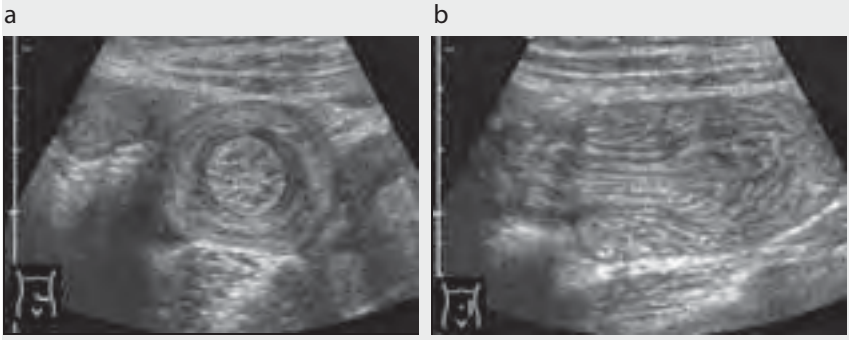

Appendicitis

Acute oedematous appendicitis causes thickening of the mucosal and submucosal layers. Ultrasound demonstrates a tubular structure with a blind end and a diameter greater than 8 mm (Fig. 11.54, Fig. 11.55). The different layers of the wall are still seen in the early stage. A cross-sectional scan shows a round shape, which is rigid under palpation. Coproliths cause strong echoes and an incomplete acoustic shadow.

Fig. 11.54. Normal appendix. Longitudinal (a) and transverse scans (b, 4 mm). The blind end and the oval cross-section are characteristic (C, caecum; I, ileum)

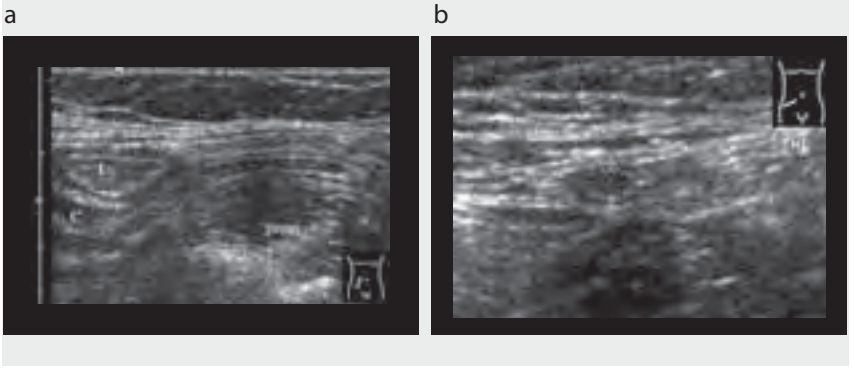

In the advanced stage of appendicitis, ultrasound demonstrates fluid in the lumen, an echo-poor wall with an irregular outline and oedema of the surrounding tissue. The wall of the caecum pole and of the ileum may also be thickened. Perforation causes abscess formation, visualized as echo-poor fluid around the appendix. The soft tissue reacts with adhesion of the neighbouring bowel segments. Ultrasound shows an inhomogeneous conglomerate in the region of the appendix (Fig. 11.56). Colour Doppler demonstrates the hyperaemia as a symptom of acute inflammation (Fig. 11.55 (b)).

Rare tumours of the appendix, such as a carcinoid tumour or a carcinoma, may be seen as echo-poor lesions. A mucocoele of the appendix shows dilatation of 20 mm or more, with a thin wall and an irregular, echo-poor pattern.

Fig. 11.55. Acute appendicitis (oedematous appendicitis). (a) Longitudinal scan shows a slightly thickened appendix (A) with an echo-poor wall (5.5 mm and 8.5 mm; ai, iliac artery). (b) Power Doppler shows striking hyperaemia of the wall. Note the round cross-section and compare with the normal appendix in Fig. 11.54

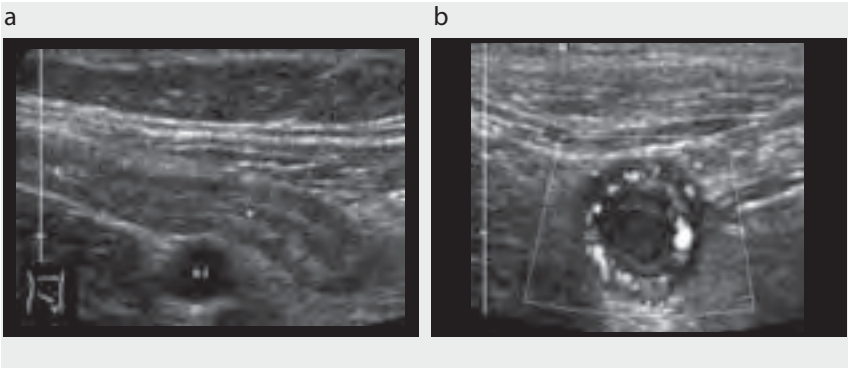

Fig. 11.56. a, Acute appendicitis (8 mm and 11.5 mm thick) with perforation, showing an irregular, interrupted contour and a small abscess (arrow); b, Abscess: 35 mm × 9 mm, heterogeneous, echo-poor mass, surrounded by the oedematous caecum (C)

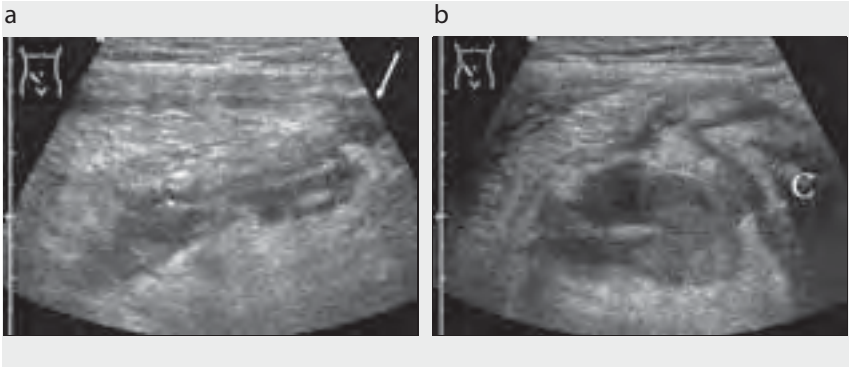

The normal appendix or even an inflamed appendix are difficult to visualize, but a careful ultrasound examination allows subdivision of patients with suspected appendicitis into the four groups listed in Table 11.3. Thus, the number of unnecessary appendectomies can be reduced. If the results of the ultrasound examination are not satisfactory because the appendix cannot be visualized, it is useful to wait and to repeat the examination after 4–6 h. Severe appendicitis can be demonstrated with ultrasound; a mild, initial appendicitis does not require an immediate intervention. A particular advantage of ultrasound examinations is the possibility of locating the pain point precisely with the transducer.

Table 11.3. Subdivision of patients with acute appendicitis on the basis of ultrasonography

Ultrasound finding	Consequence
Appendicitis	Appendectomy
Normal appendix	No appendectomy but examination for other disorders
Other disease, such as Crohn disease, adnexitis or lymphadenitis	No appendectomy but treatment of other diseases
Uncertain	Wait and control if clinical signs allow

AIDS

Opportunistic infections of the intestine and particularly of the small bowel are common in HIV-infected patients. The typical sonographic findings of acute enterocolitis are seen, such as fluid-filled small bowel loops and hyperperistalsis. The wall of the intestine is thickened, particularly the mucosal and submucosal layer. The transition between an inflammatory thickened wall and normal sections of the intestine is gradual.

In other cases, a sonographic feature, as in Crohn disease, may be found, with a segmental thickened wall and a narrowed lumen. Cytomegalovirus infections may cause appendicitis, with the characteristic sonographic findings of a thickened appendix. Other infections, such tuberculosis (Fig. 11.35), disseminated *Mycobacterium avium* complex and histoplasmosis cause pseudotumours. The affected bowel segments show considerably thickened, echo-poor walls with irregular but sometimes sharp margins. Enlarged lymph nodes, inflamed parts of the mesentery, abscesses and ascites form complex structured masses imitating large tumours (Fig. 11.47). None of these sonographic findings is specific, although neoplastic processes occur more frequently in HIV-infected patients than in the uninfected population. Differentiation between neoplastic lesions and inflammatory pseudotumours is difficult or impossible. Ultrasonic-guided fine-needle puncture is a suitable method in these situations to establish a final diagnosis (see Chapter 3, Interventional ultrasound).

Differential diagnosis

Advanced malignant tumours of the bowel show the typical target-like pattern. Thus, they can be differentiated from solid tumours of other abdominal or retroperitoneal structures, especially connective tissue tumours, which show a more homogeneous, echo-poor or echo-rich (liposarcoma) pattern.

The echo-poor structure of the wall and the relatively short longitudinal extension permit differentiation from benign disorders. A similar sonographic feature may be found in cases of colopathy associated with use of non-steroidal anti-inflammatory drugs. Chronic abuse of these drugs sometimes causes local damage of the colon wall with circumferential thickening of the wall and narrowing of the lumen.

As a complication of inflammatory diseases, infiltrated loops, inflamed soft tissue due to local peritonitis, abscesses between the loops, enlarged lymph nodes and fistulae may form 'conglomerate tumours', which are often palpable. The complex sonographic pattern of these benign masses usually allows their differentiation from malignant tumours. Such conglomerate tumours may be seen in cases of tuberculosis, in the complicated course of amoebic colitis, Crohn disease or diverticulitis, in perforated

appendicitis and in cases of inflamed and perforated Meckel diverticulum. It should also be noted that a tumour can cause an inflammatory pseudotumour if it produces (micro)-perforation and localized peritonitis.

Segmental thickening of the bowel wall is the common sonographic sign of bowel disorders but is, at the same time, ambiguous. It is also seen in acute infective and noninfective diseases, such as chronic inflammatory and other benign diseases, and even in secondary low-grade lymphomas. The clinical background, location and other symptoms may allow differentiation in many, but not all, situations, as shown in Table 11.2 and Table 11.4.

Table 11.4. Examples of differentiation of a segmental, thickened bowel wall

Location	Wall	Additional sonographic signs	Tentative diagnosis
Small bowel	Layers discernible	Hyperperistalsis	Acute inflammatory disease
Duodenum, small bowel	Layers discernible	Hyperperistalsis and flat mucosa	Tropical sprue, gluten enteropathy
Small bowel, stomach	Echo-poor swollen mucosa	Ascites	Angioneurotic oedema, parasites (*Anisakis marina*)
Terminal ileum	Layers discernible	Lymph nodes	*Yersinia* enteritis, Crohn disease
Small and large bowel	Layers discernible	Discontinuous involvement	Crohn disease
Large bowel	Layers discernible	Hyperperistalsis	Infective colitis, pseudomembranous colitis
Descending colon	Echo poor	Less or no flow	Ischaemic colitis
Distal colon	Echo poor	Augmented flow, fewer flow signals	Active ulcerative colitis, inactive colitis, radiation colitis
Sigmoid, descending colon	Echo poor	Echo-poor lesion outside wall	Diverticulitis
Distal colon	Echo poor or layers discernible	Echo-poor mesenteric lymph nodes	Low-grade lymphoma
Colon	Echo poor	Ascites	Graft-versus-host disease

Chapter 12

Adrenal glands

12

Adrenal glands

Introduction

The adrenal glands are difficult to study ultrasonically. CT scans are far easier, but if they are not available, ultrasound may be used, but with some limitations.

Examination technique

Equipment, transducer

A curved array or sector scanner should be used, with an ultrasound frequency as high as possible.

Preparation

No preparation is required.

Position of the patient

The patient should be in the supine or oblique position.

Scanning technique

The adrenals are scanned in a lateral oblique plane through the upper pole of the kidneys. The right adrenal gland may be seen by scanning obliquely through the vena cava and angling slightly medially. Normal adrenals and small tumours are often not seen, whereas larger lesions are seen more easily.

Normal findings

In neonates, the adrenal glands may be one third the size of the kidneys and are relatively easy to see. In adults, they are proportionately much smaller and are not often seen transabdominally. In thin patients, the right adrenal may be seen above and medial to the right kidney, posteromedial to the inferior vena cava. The left adrenal is above and medial to the left kidney and is not usually seen (Fig. 12.1).

Fig. 12.1. (a) Normal right adrenal gland (arrowhead); (b) normal left adrenal gland (arrowhead); (c) normal neonatal adrenal glands (arrowhead)

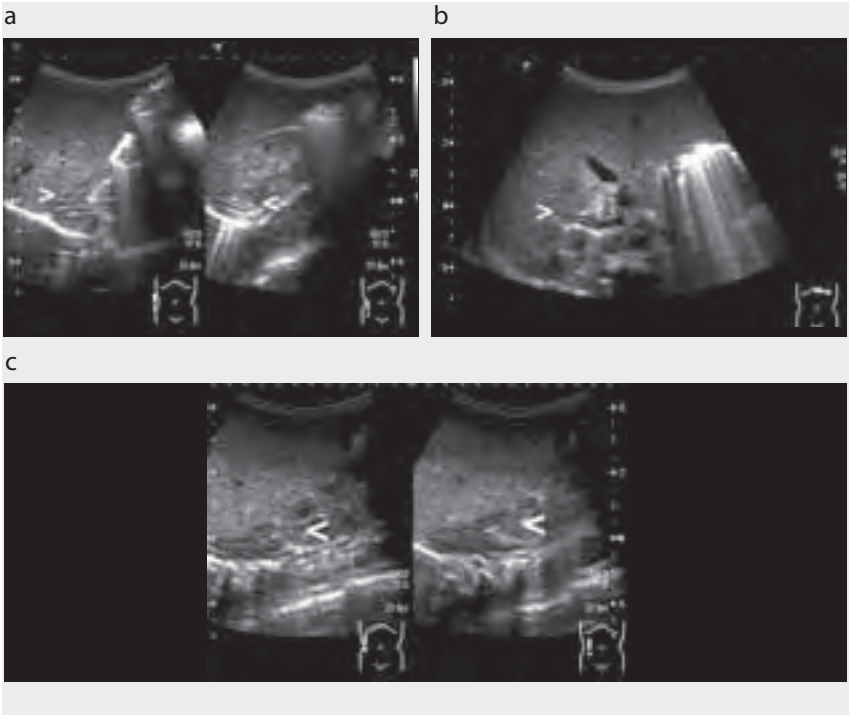

Pathological findings

Adrenal infections

Adrenal infections are commonly due to tuberculosis or histoplasmosis. Such infections cause enlargement with later calcification.

Ultrasound appearance

The dense calcification is echogenic, with posterior acoustic enhancement. Interpretation of ultrasound appearances may be difficult (Fig. 12.2).

As for any dense shadowing lesion seen on ultrasound, the nature of the shadowing should be confirmed by an abdominal X-ray.

Adrenal haemorrhage

Adrenal haemorrhage is not uncommon in neonates but rare in adults. It occurs secondary to trauma or severe physiological stress. The right side is most commonly affected. The ultrasound appearance is shown in Fig. 12.3.

The gland becomes enlarged and globular. Originally echogenic, the contents may liquefy and may become hypoechoic. The end-point is normally calcification.

Fig. 12.2. Old adrenal tuberculosis. (a) Dense shadowing above the kidney. (b) A plain X-ray film reveals calcified adrenals

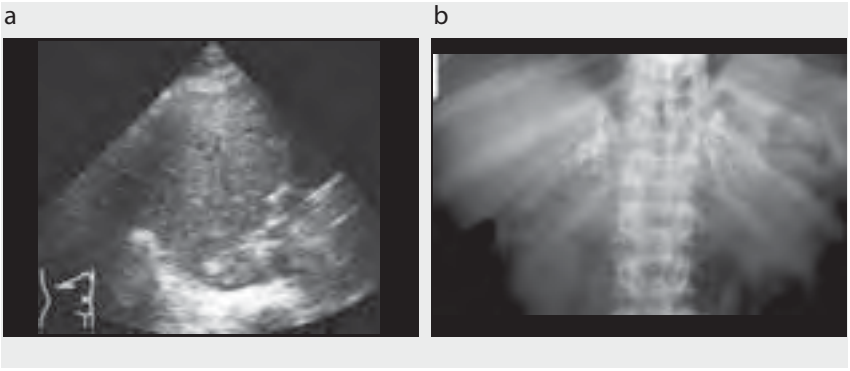

Fig. 12.3. Acute adrenal haemorrhage. The gland is enlarged, globular and hypoechoic

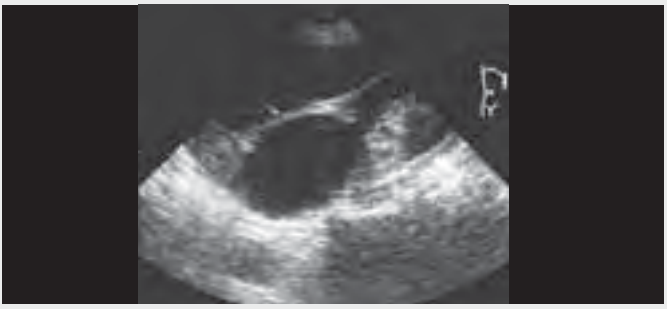

Adrenal tumours

Benign adenomas

While common, benign adenomas are often small and not seen by sonography. Only rarely are they functioning (hormone secreting). Other benign tumours are rare.

The ultrasound appearance is shown in Fig. 12.4.

As benign adenomas often contain fat, they may be echogenic.

Primary malignant tumours

Like benign tumours, primary malignant tumours may be functioning or non-functioning. All are rare. If the patient has hypertensive episodes, the tumour may be a phaeochromocytoma and biopsy is dangerous as it can precipitate a hypertensive crisis.

These tumours are often greater than 5 cm in diameter. They have a heterogeneous echo texture and may contain calcium, which causes shadowing (Fig. 12.5).

Fig. 12.4. (a, b) Adrenal adenomas

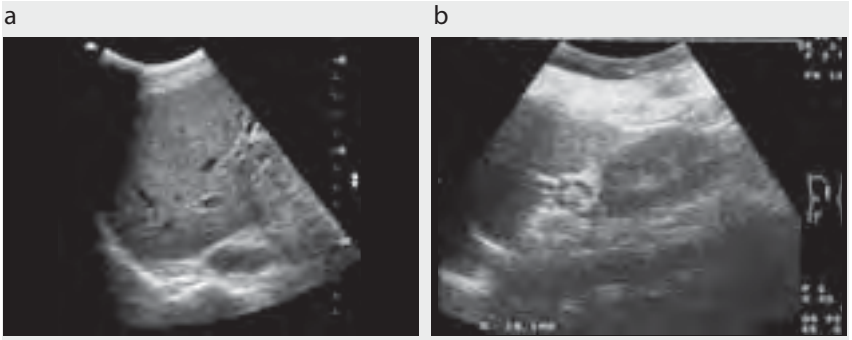

Fig. 12.5. (a, b) Malignant adrenal tumours shown by endoscopic ultrasound. The pattern is the same transabdominally. (c) Malignant adrenal tumour (phaeochromocytoma)

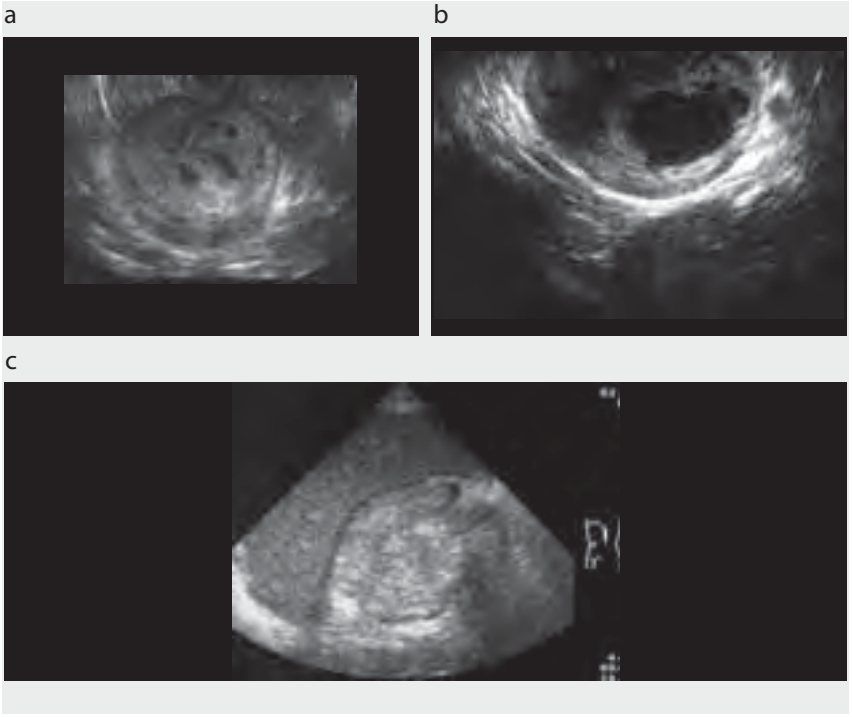

Secondary malignant tumours

Metastatic disease is common in advanced malignancy, especially from lung, breast, melanoma and renal primaries.

Metastatic adrenal tumours may be small and not visible ultrasonically. They are often heterogeneous due to necrosis (Fig. 12.6) and may be difficult to distinguish from upper-pole renal tumours.

Fig. 12.6. A secondary deposit from a bronchogenic carcinoma

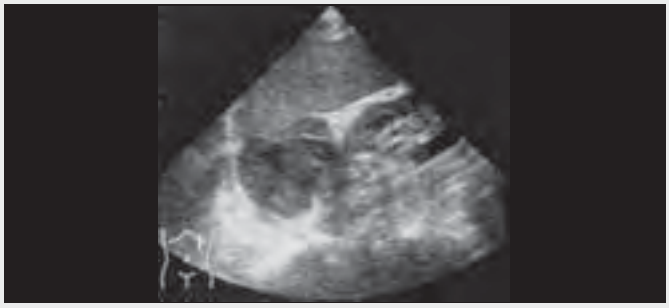

Adrenal cysts

Ultrasound appearance

Adrenal cysts are thin-walled, with anechoic contents, similar to all simple cysts (Fig. 12.7). Adrenal cysts are often misdiagnosed as renal cysts. As neither requires treatment, this is unimportant.

Fig. 12.7. Adrenal cyst

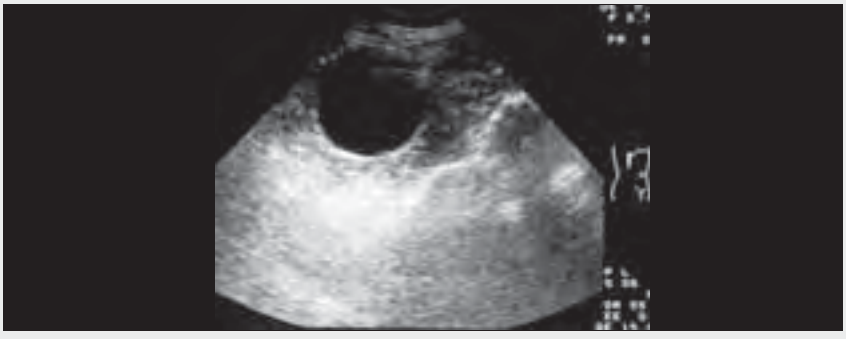

Chapter 13

Kidneys and ureters

13

Kidneys and ureters

Kidneys

Indications

The indications for ultrasonography of the kidneys are:

- renal or ureteric pain
- suspected renal mass (large kidney clinically)
- non-functioning kidney on urography
- haematuria
- recurrent urinary tract infections
- trauma
- suspected polycystic disease
- pyrexia of unknown origin
- renal failure of unknown origin
- schistosomiasis, genitourinary tuberculosis
- suspected congenital abnormality
- pelvic mass, exclude hydronephrosis.

Ultrasound cannot be used to assess renal function.

Examination technique

Equipment, transducer

For adults, use a 3.5-MHz (normal or obese patients) or 5-MHz (slim patients) transducer. If the transducer has variable frequency, deep structures can be adequately seen by lowering the frequency. A curvilinear transducer will usually be adequate, but a sector transducer may give better intercostal views.

Preparation

As the urinary bladder is commonly assessed at the same time as the kidneys or ureters, a full bladder is advised, although this is not necessary for isolated renal ultrasound.

Position of the patient

Start with the patient lying in the supine position.

Scanning technique

Place the transducer over the right upper abdomen. Set the focal depth for about the centre of the kidney, and adjust the gain to obtain the best image of the renal parenchyma. The focal depth that produces the best image varies somewhat among machines.

Like other organs, the kidneys should be scanned in longitudinal and transverse planes that include the whole organ. Care should be taken to ensure that the whole of the upper and lower poles are seen, to prevent missing an exophytic mass or a horseshoe kidney (lower poles united).

The cortical echogenicity should be compared with that of the liver, spleen and renal pyramids. The right kidney can be seen best when the patient is supine, with the liver as an acoustic window (anterolateral approach). Deep inspiration can help to visualize the upper pole, but remember to let the patient breathe! A left-lateral decubitus position may help show the lower pole.

The upper pole of the left kidney can usually be seen by using the spleen as an acoustic window, but in this position the lower pole is often obscured by bowel gas. The whole of the left kidney is often seen more easily when the patient's left side is raised, allowing a more posterior approach.

Ultrasound artefacts are useful for characterizing any pathological condition; for example, simple renal cysts contain fluid and have posterior acoustic enhancement. Calcification is echogenic or bright and causes 'clean' posterior acoustic shadowing, as in renal calculi. Gas or air will be echogenic but will cast a 'dirty' shadow.

Colour flow Doppler can be used to assess perfusion throughout the kidney. Spectral Doppler is used to assess possible renal artery stenosis and changes in renal diseases, such as acute tubular necrosis, in the waveform shape and with specific measurements, such as peak velocity and resistance index.

Ultrasound contrast agents can be used to demonstrate enhancement patterns of suspected pathological conditions and are safe. Specific software is, however, necessary.

Whatever technique is used, scan the kidneys in both the longitudinal and the transverse planes. When examining any part of the renal area, compare the two kidneys in different projections. Variations in size, contour and echogenicity may indicate an abnormality.

Doppler study

The intra-renal vessels are relatively easy to see and study. It is, however, important to scan in the correct plane. These vessels run from the hila to the periphery. As the kidney is usually tilted, with the hilum more anterior than the lateral edge, an oblique lateral plane is necessary to show the vessels well. At the poles of the kidney, the vessels run at a disadvantageous angle and may look underperfused. Changing the scan angle to the craniocaudal plane will show the polar vessels better.

If only perfusion is being assessed, colour Doppler alone is sufficient. If changes in renovascular resistance are being studied, pulse-wave Doppler is necessary, with analysis of the wave-form spectra.

The renal arteries are difficult to scan. The best initial approach is to scan through the kidney from a posterolateral approach and to follow the artery from the hilum to the aorta. In some patients, the renal artery origins and, sometimes, the arteries themselves are best seen on an anterior transverse scan. This is often the best plane for thin patients or children. For larger patients, the arteries are often too deep and are

obscured by the bowel. In all patients with an anterior approach the vessels lie almost parallel to the transducer. This is disadvantageous for a Doppler study.

The whole of the renal arteries may be difficult to see, with a technical failure rate of up to 40%. Accessory arteries are rarely visible.

Normal findings

The kidneys have a smooth outline (but see Normal variants, below). The cortex is of even, medium echodensity, similar to or slightly less than that of the liver or spleen. Significantly, they are less echo rich than a fatty liver.

The medullary pyramids are rounded triangular structures of lower echodensity than the cortex and are evenly arranged around the kidney. They are seen clearly, however, only when they lie 'end on' to the ultrasound beam. This allows them to be visualized, on a longitudinal scan, at the mid-kidney but not at the poles.

The central renal complex, comprising the calyceal system and the surrounding paracalyceal fat, appears as an echo-rich, white, irregular shape lying centrally.

The renal capsule is seen as a white line only when it is almost parallel to the transducer, i.e. at the mid-kidney on a longitudinal scan.

The normal calyces and infundibula may be seen to have a fine anechoic central area, due to urine; however, they are often collapsed and contain no visible urine.

The renal pelvis is a thin-walled anechoic structure that is variable in size. The renal artery, vein and ureter are seen as tubular structures at the hilum.

With low-resolution equipment or poor gain settings, the renal pyramids may look like dilated calyces or cysts.

Measurements

Normal adult kidneys measure 9–12 cm in length. The left kidney is commonly longer than the right, but there should be no more than 2 cm difference in length between the two kidneys. The renal cortex, measured from the outer border of a pyramid to the renal surface, is normally 10 mm in length. Normal measurements are available for all dimensions of the kidney, but only the length and cortical width are commonly used. Renal length is surprisingly difficult to measure accurately and consistently. If an oblique view is used, the renal length may be considerably underestimated.

Normal renal Doppler studies

The renal arteries run retroperitoneally from the aorta to the renal hila. An accessory renal artery usually supplies the lower pole in about 15% of kidneys. The intrarenal arteries branch from the hilum to supply the whole kidney. The intrarenal vessels are easily seen with a good colour Doppler machine. The renal arteries lie deep from an anterior approach; they are often partially obscured by the bowel and are therefore not usually well seen. The spectral waveform is low resistance with forward flow throughout the cardiac cycle (Fig. 13.1).

Paediatric kidneys

Paediatric kidneys appear broadly similar to adult kidneys, but there are some differences (see also Volume 2 of this manual). Corticomedullary differentiation is more pronounced in neonates and children up to 2 years of age (i.e. the renal pyramids

are more prominent). The collecting system is also seen more clearly than in normal adults. As there is little paracalyceal fat, the central renal complex is seen as a 'cleaner' image of the calyces.

The normal size of paediatric kidneys at different ages can be checked against various published tables (see Volume 2 of this manual) or ultrasonographs (Fig. 13.2).

Fig. 13.1. (a) Normal kidney, longitudinal plane. (b) Normal kidney, transverse plane. (c) Doppler study of intra-renal vessels. (d) Normal renal artery seen through the kidney. There is a normal low-resistance waveform. (e) Normal right renal artery and vein seen from an anterior approach (in a very thin patient)

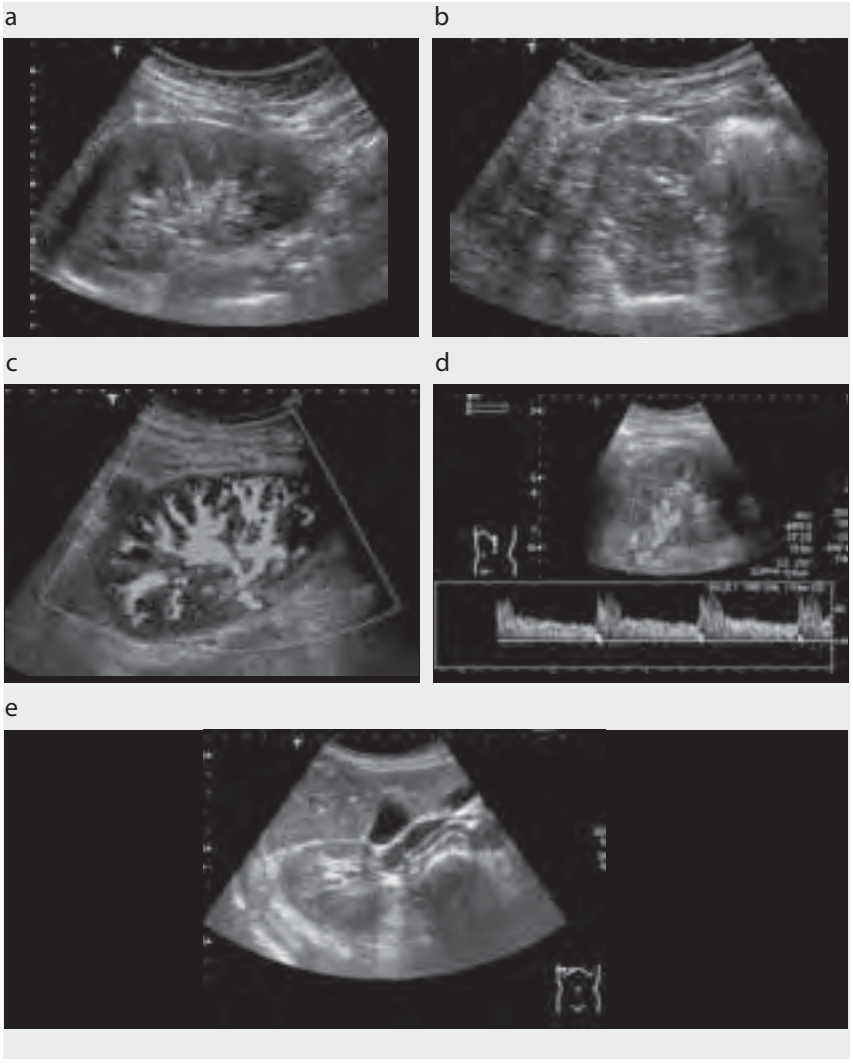

Fig. 13.2. (a) Normal infant kidney. (b) Normal neonatal kidney

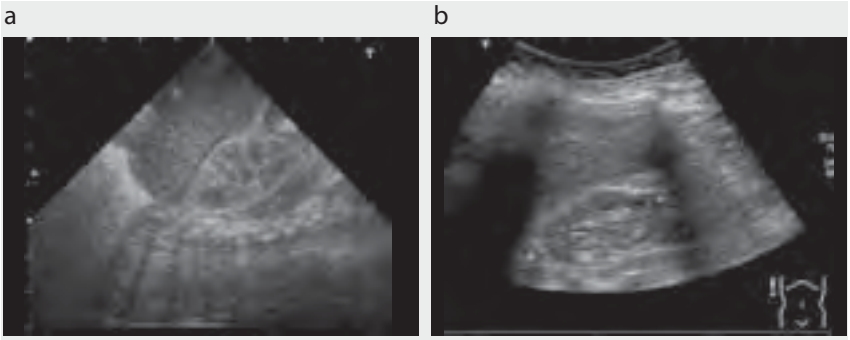

Normal variants

Normal variations in shape include the splenic hump, also known as the 'dromedary hump'. Splenic compression may produce a bulge on the lateral border of the mid-pole of the left kidney, which can be confused with a renal mass.

On ultrasound, the calyces should continue normally into the hump, and the cortex should have normal echogenicity (Fig. 13.3). If concern persists on CT, an isotope or follow-up ultrasound study may help.

Fig. 13.3. Dromedary hump

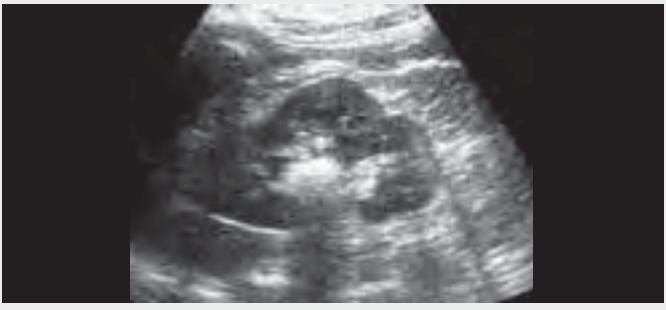

Congenital anomalies

These include a prominent septum or column of Bertin. Septa of Bertin usually separate the renal pyramids and are a continuation of the renal cortex. They can be hypertrophied, commonly in the mid-pole, and mistaken for a renal mass.

On ultrasound, as with a splenic hump, the normal cortical echogenicity is maintained (Fig. 13.4). In most cases, the ultrasound study is diagnostic. If there is doubt, CT or an isotope study is indicated.

Fig. 13.4. Hypertrophied column of Bertin

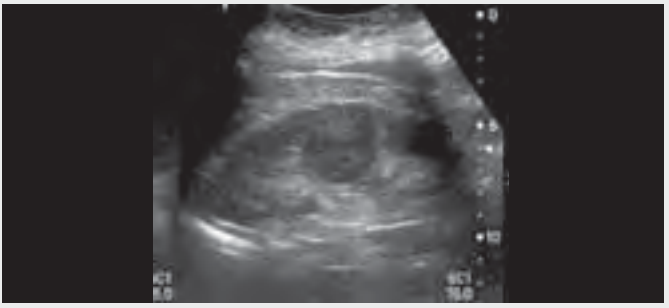

Fetal lobulation

Instead of being smooth, the renal outline may indent between the renal pyramids or calyces; this is differentiated from cortical scars, which lie over the calyces. Fetal lobulation is due to failure of fusion of grooves overlying the septa of Bertin in the fetus.

On ultrasound, the indentations in the renal surface lie between the renal pyramids, whereas scars are usually over the pyramids, and the indentations are more evenly spaced than scars (Fig. 13.5).

Fig. 13.5. Fetal lobulation (arrows)

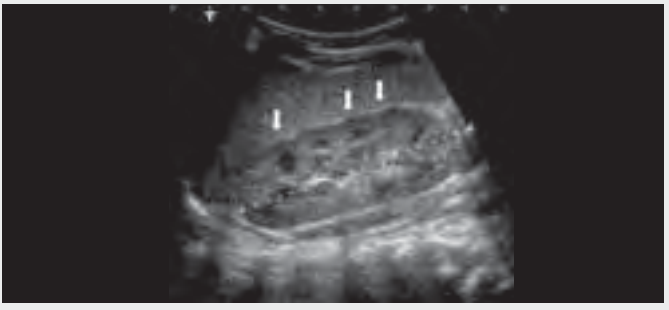

Duplex kidney

The renal pelvis and, to a certain extent, the ureters are duplicated. The ureters can continue and insert separately into the bladder or unite proximally to a single vesicoureteric junction.

On ultrasound (Fig. 13.6), the kidney is longer than normal but with the same number of calyces. The central renal sinus may be separated into two parts, and two renal hila may be seen. The upper pole moiety may be hydronephrotic and, if very hydronephrotic, may be mistaken for a renal or adrenal cyst.

Ultrasound is inadequate for detecting duplex kidneys, with high false-positive and false-negative rates. Confirmation is often not clinically important, but the condition should be confirmed by excretion urography or CT, if necessary.

Fig. 13.6. Duplex kidney. The kidney is long with a slight waist

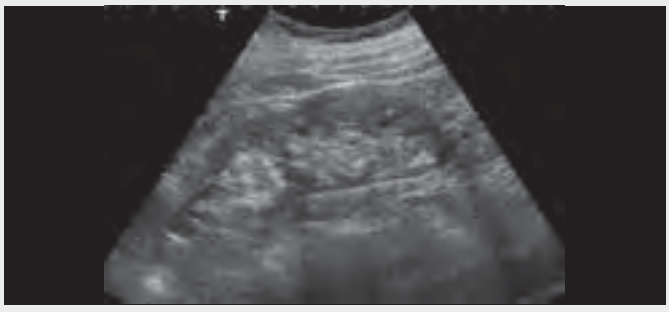

Hypoplastic kidney

A hypoplastic kidney is a small but functioning kidney.

On ultrasound (Fig. 13.7), the kidney is small but with a normal shape and echo pattern, like a small version of a normal kidney.

Fig. 13.7. Hypoplastic kidney. Right longitudinal view. The kidney is small but has a normal echo pattern

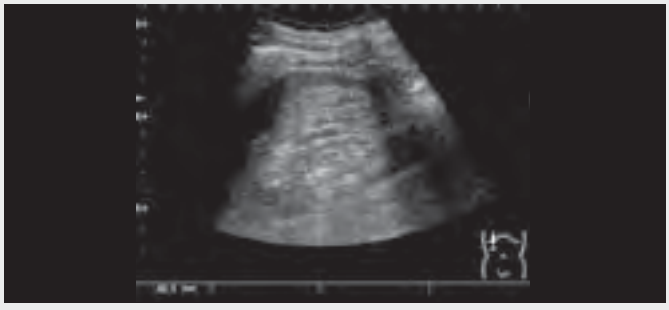

A hypoplastic kidney cannot be distinguished from a small ischaemic kidney. Due to chronic renal disease, small 'end-stage' kidneys usually, but not always, have an abnormal echo texture. Hypoplastic kidneys function normally. This cannot be assessed by ultrasound but can be determined by intravenous urography or an isotope study.

Dysplastic kidney

This is a small, non-functioning kidney.

On ultrasound (Fig. 13.8), the kidney is small and contains multiple cysts. The non-function of dysplastic kidneys cannot be assessed by ultrasound but can be determined by intravenous urography or an isotope study.

Fig. 13.8. Dysplastic kidneys, which are small with multiple cysts. (a) Transverse view and (b) longitudinal view of left kidney

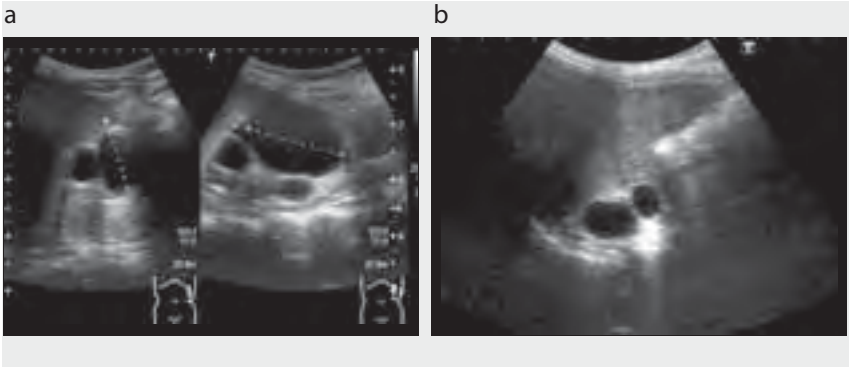

Renal ectopia

In renal ectopia, a kidney lies in an abnormal position. Ultrasound is often diagnostic, but confirmation by excretion urography may be necessary.

Ptotic kidney

In this condition, the kidney lies lower than normal in the abdomen and may be malrotated. The condition is not usually clinically important. On ultrasound, the low position is obvious. If it is malrotated, the kidney appears obviously abnormal, although at first it may not be clear why (Fig. 13.9). Colour Doppler may confirm the anterior hilum.

Fig. 13.9. Ptotic kidney. The kidney lies low on the psoas muscle and is malrotated

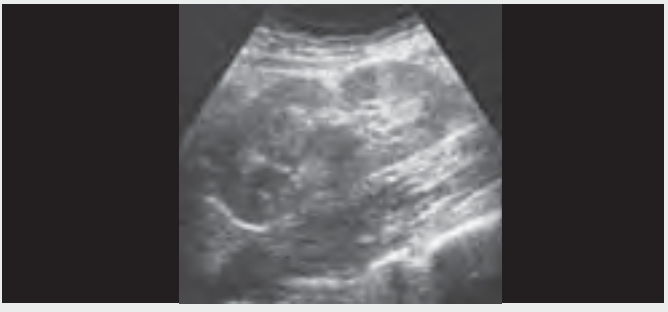

Horseshoe kidney

This condition involves fusion of the lower poles of the two kidneys (rarely the upper poles). The union or isthmus may be fibrous or thick and contain functioning renal tissue.

On ultrasound (Fig. 13.10), the kidneys are ectopic in that they lie lower than is normal. Their ascent appears to be confined by the inferior mesenteric artery crossing the isthmus. The lower poles are more medial than usual. The renal pelves are rotated more anteriorly than normal and may be dilated. The ureters pass anteriorly over the isthmus. A fibrous isthmus may be difficult or impossible to see on ultrasound. A thick isthmus is seen as a midline mass and may be mistaken for a retroperitoneal tumour.

Horseshoe kidneys are more prone to trauma, pelviureteric junction obstruction, renal calculi and Wilms tumours in children. The renal isthmus may be mistaken for a retroperitoneal tumour.

Fig. 13.10. Horseshoe kidney. (a) The kidney lies obliquely and low with a medial lower pole. Note the transverse processes posterior to the kidney. (b) The lower pole is bent medially, and there are calculi in the kidney. (c) The isthmus is seen crossing anterior to the aorta (A) and vena cava (VC)

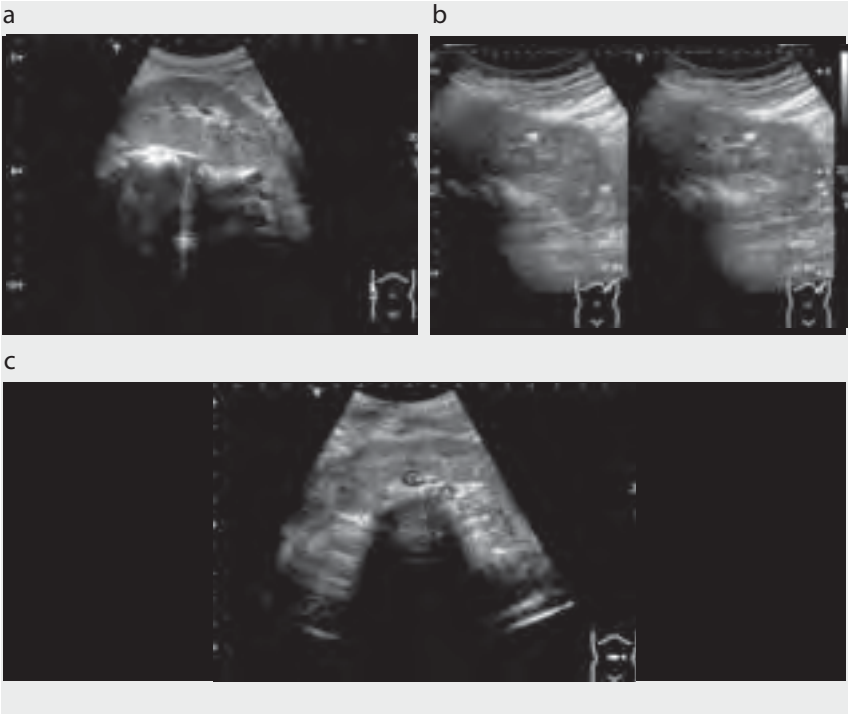

Pelvic kidney

Failure of ascent can result in a pelvic kidney. Rarely, both kidneys fail to ascend and fuse into a pelvic disc kidney.

On ultrasound, a pelvic kidney usually appears normal except for its position. The kidney is malrotated, with the hilum lying anterior. A pelvic kidney should be examined carefully if one kidney appears to be absent.

Crossed-fused ectopia

In this condition, one kidney crosses the midline and fuses with the other. The two ureters drain to their normal side.

On ultrasound, the kidney appears long, and there may be a waist between the two fused kidneys. There is no kidney on the other side (Fig. 13.11).

Fig. 13.11. Crossed renal ectopia. (a) The two kidneys lie on the right and are not joined. (b) There is no kidney on the left side

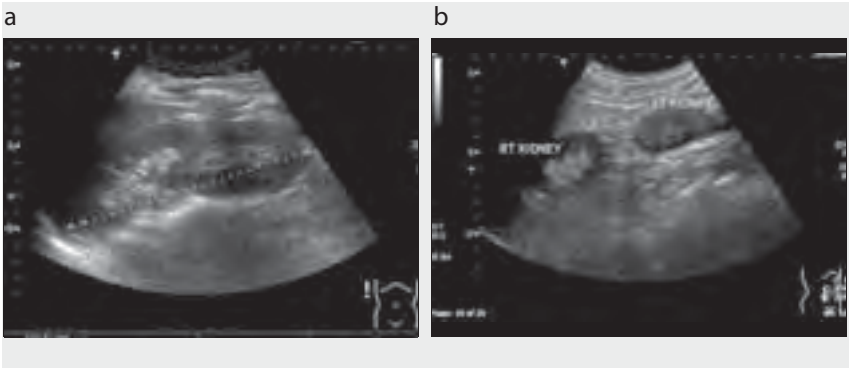

Thoracic kidney

The kidney lies more cranially than is normal and may be seen as a retrocardiac mass on a chest X-ray. On ultrasound, there is no kidney in the normal position, and the thoracic kidney itself is not visible.

Other conditions

Compensatory hypertrophy

A single functioning kidney will hypertrophy to compensate. This effect is most marked in children and young adults. On ultrasound, the kidney is large but otherwise usually appears normal (Fig. 13.12). In scarred kidneys, the normal parenchyma can hypertrophy, producing pseudotumours.

Renal sinus lipomatosis

The fat in the renal sinus can proliferate, producing a larger central echo complex, and may be associated with cortical loss. On ultrasound (Fig.13.13), the white central complex is enlarged, and there may be associated cortical loss.

Pathological findings

Renal cysts

Simple renal cyst

More than 70% of renal cysts are due to benign cystic disease. These cysts occur in up to one half of people over 50 years of age and may be bilateral. They seldom cause problems.

Fig. 13.12. Compensatory hypertrophy. The kidney measures 13.6 cm

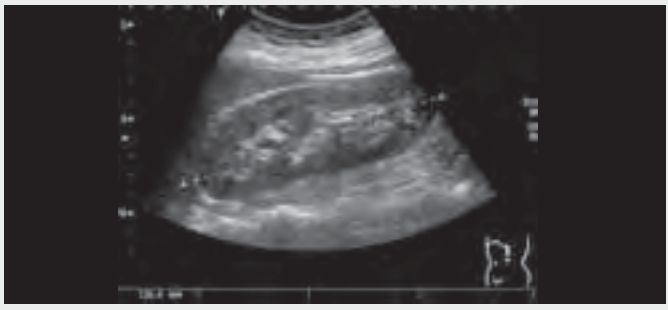

Fig. 13.13. Renal sinus lipomatosis. Longitudinal view of left kidney (arrows point to increase in renal sinus fat)

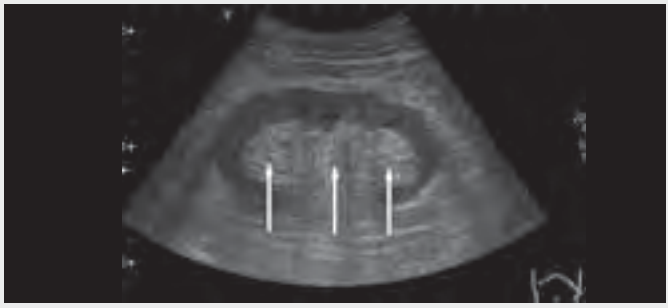

They are usually cortical but may be medullary or in the renal sinus. Renal sinus cysts can be confused with hydronephrosis; however, in the latter condition, dilated calyces should be demonstrated to be communicating with a dilated renal pelvis.

On ultrasound (Fig. 13.14), simple renal cysts are echo free or hypoechoic, with posterior acoustic enhancement. They may have a clearly defined smooth wall, with no internal echoes.

Complex cyst classification

Bosniak classification (Fig. 13.14, Fig. 13.15, Fig. 13.16, Fig. 13.17): This is the most commonly used set of criteria to assess the benign or malignant potential of a renal cyst. Although originally described for CT findings, it has been widely extrapolated to other imaging modalities such as ultrasound. Category 2F (F for follow-up) has been added to the revised classification.

- Category 1: benign simple cysts, thin-walled, no septa, calcification, solid components or internal echoes. They need no follow-up.
- Category 2: benign cysts, may have a few hairline septa, fine calcification or short area of minimally thickened calcification. They need no follow-up.

- Category 2F: cysts that are not clearly in either category 2 or 3. These require follow-up.
- Category 3: cystic masses with thickened walls, septa or calcification. Up to one half of these are malignant; the rest are haemorrhagic cysts, infected cysts or multilocular cystic nephromas. Nephrectomy should be strongly considered.
- Category 4: malignant cystic masses, which on CT have enhancing components, separate from the wall or septa. These require nephrectomy.

If the cyst contains thin septa (less than 1 mm) or fine calcification, it may be considered benign.

Irregular thickened septa, calcification, mural nodules, thick walls or a multiloculated appearance are indicative of a cystic or necrotic neoplasm. These changes and cyst debris can, however, occur in haemorrhagic or infected cysts. Aspiration is advised if infection is likely.

Fig. 13.14. Simple renal cyst. (a) A large simple renal cyst arising from the lower pole of the right kidney. (b) A small simple renal cyst. Note the posterior acoustic enhancement

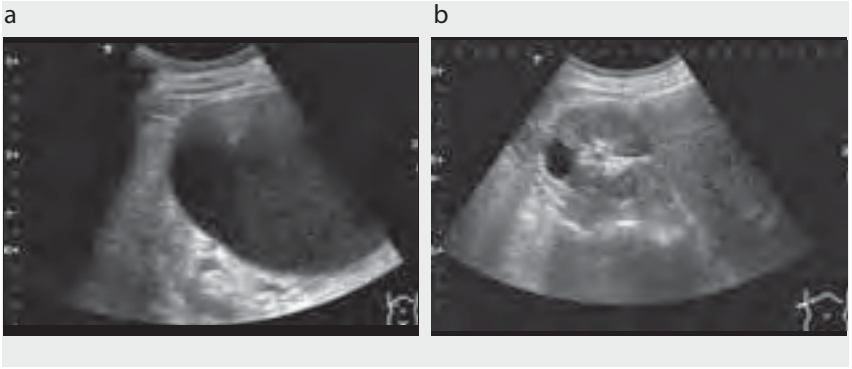

Fig. 13.15. (a) Bosniak category 2 renal cyst with a short area of thickened calcification (arrow). (b) Bosniak category 2 renal cyst with thin septa

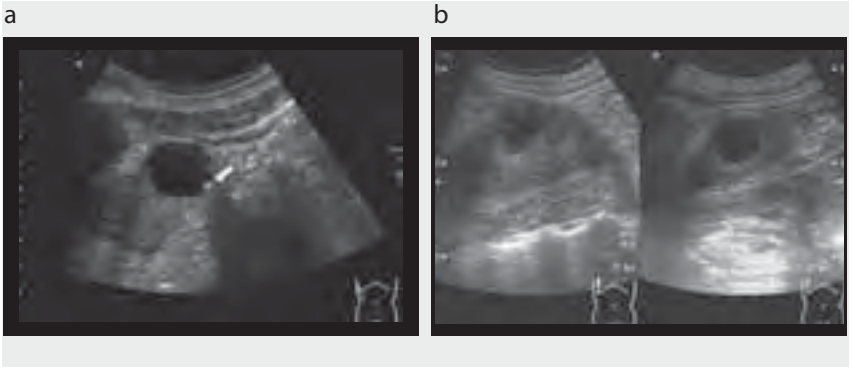

Fig. 13.16. Bosniak category 3 renal cyst with thickened calcified septa (arrow)

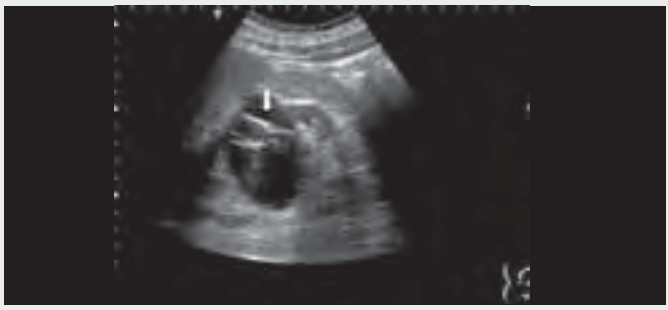

Fig. 13.17. Bosniak category 4 renal cyst with a thickened wall

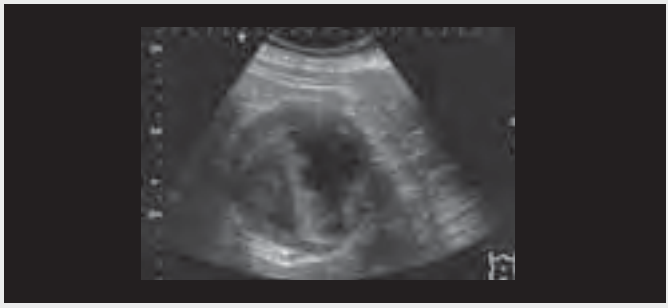

Autosomal dominant polycystic kidney disease

This inherited disorder is bilateral, although early in the course of the disease only one kidney may appear to be affected sonographically. There are bilateral renal cysts in the cortex and medulla. Hepatic cysts are commonly associated, but pancreatic cysts are rarely present.

On ultrasound (Fig. 13.18), the kidneys may appear massive due to the large number of cysts. Most of the cysts are simple; however, calcification and haemorrhage into cysts occur, as does infection. Haemorrhagic cysts have echogenic contents. There is also an increased risk for renal calculi.

In at-risk individuals, the following criteria are consistent with autosomal dominant polycystic kidney disease:

- < 30 years of age: two or more renal cysts
- 30–59 years of age: two or more cysts on each kidney
- ≥ 60 years of age: four or more cysts on each kidney.

Since multiple simple cysts occur with increasing age, the diagnosis can be difficult.

Fig. 13.18. (a) Polycystic kidney (arrows). (b) A polycystic kidney with echogenic haemorrhagic cysts (arrow). (c) A polycystic kidney with a solid lesion (arrows): a tumour confirmed by magnetic resonance imaging

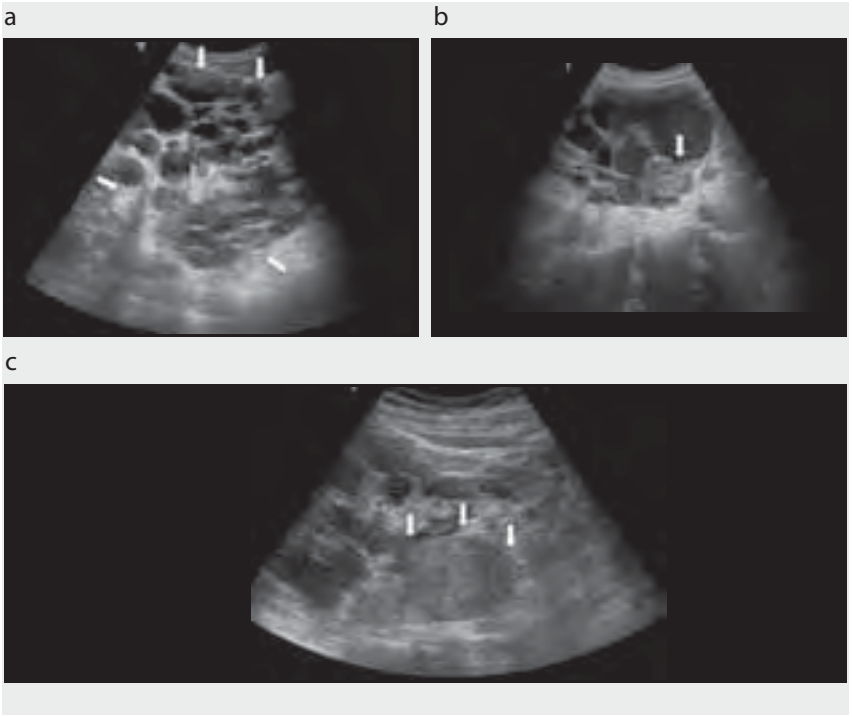

Acquired cystic kidney disease

Multiple cysts form in end-stage kidneys of renal dialysis patients. There is a risk for malignant change in these cysts, although the risk is not as great as early research suggested.

On ultrasound (Fig. 13.19), small echogenic kidneys are seen, with multiple simple cysts. Calcification or hydronephrosis, depending on the etiology of the renal failure, may also be present.

Fig. 13.19. Small echogenic kidney with a cystic renal tumour in end-stage dialysis

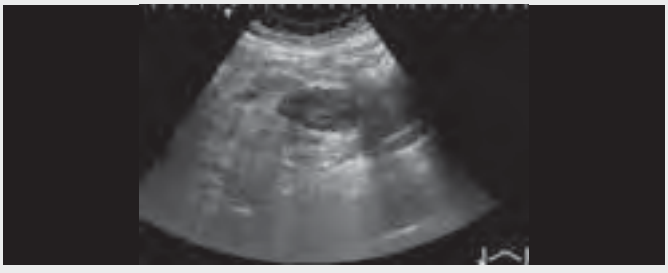

Infections

Renal complications of HIV and AIDS are discussed separately, below; however, the infections outlined may all occur in HIV-infected patients. If calcification is a feature of a particular infection, excretion urography may be helpful. If gas or air is thought to be a feature, a plain film will suffice.

Pyelonephritis

Pyelonephritis is an infection involving the renal parenchyma. Sonography is most often normal in acute pyelonephritis (Fig. 13.20). Renal enlargement and focal hypoechoic or hyperechoic areas may occur, which is termed 'focal pyelonephritis' or 'focal nephronia'. Loss of the normal central renal sinus renal parenchyma interface may occur, as may loss of corticomedullary differentiation.

Focal pyelonephritis may be mistaken for a tumour. It resolves after treatment, often leaving a scar.

Fig. 13.20. (a) Acute pyelonephritis, with swelling and reduced echodensity of the lower pole (arrow). (b) Focal pyelonephritis, with an area of altered echo pattern, mostly increased echodensity, in the mid-pole (arrow). (c) Focal pyelonephritis, with an area of focal pyelonephritis in the mid-pole. In this case, it has reduced echodensity (arrow)

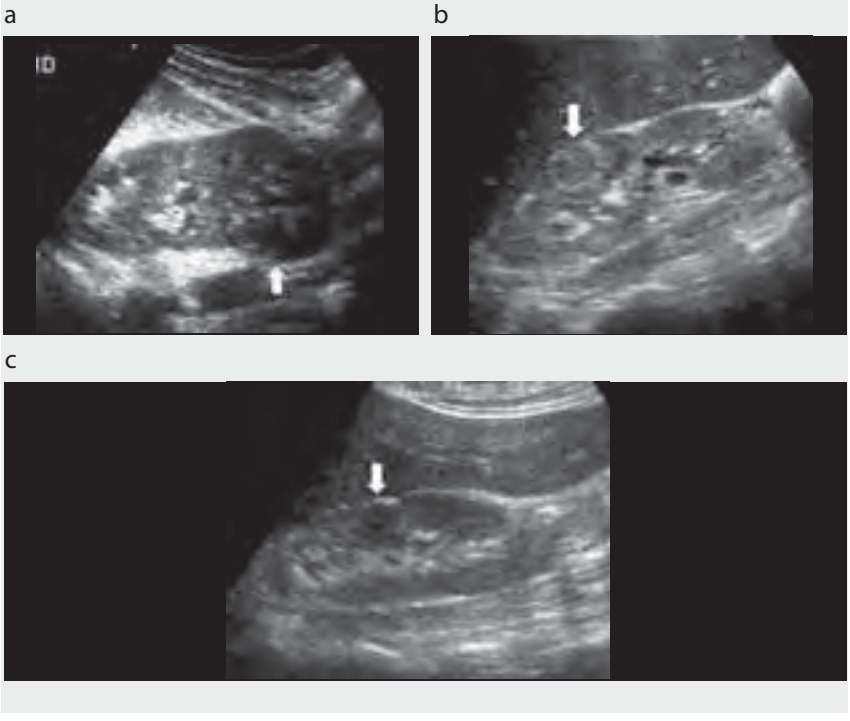

Emphysematous pyelonephritis

Emphysematous pyelonephritis is an uncommon, life-threatening condition, which is more frequent in patients with diabetes. It is an infection with gas-forming organisms, resulting in gas in the collecting systems (emphysematous pyelitis), renal parenchyma and sometimes the perinephric space.

On ultrasound, the gas produces 'dirty' acoustic shadowing, as opposed to 'clean' shadowing from renal calculi (Fig. 13.21).

Fig. 13.21. Emphysematous pyelonephritis. The shadowing lesions were shown on CT to be due to gas in the collecting system

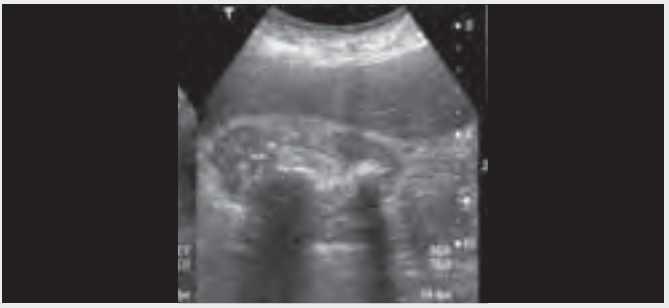

Pyonephrosis

Pyonephrosis consists of pus in an obstructed collecting system. On ultrasound, there is usually a dilated collecting system containing echogenic material or debris (Fig. 13.22). There may be associated perinephric collection.

Fig. 13.22. Pyonephrosis of the upper moiety in duplex kidney. The dilated moiety contains echogenic pus

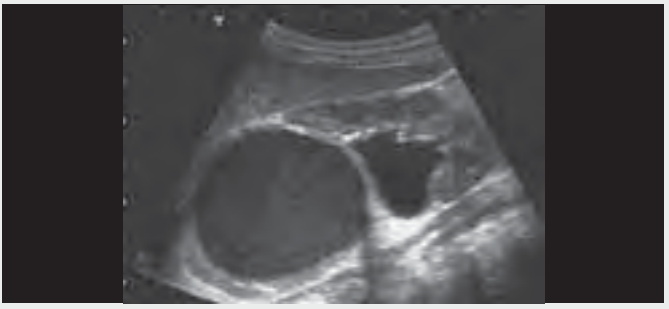

Renal and perinephric abscesses

A renal abscess consists of a collection of pus lying in the renal parenchyma. A perinephric abscess lies in the retroperitoneum adjacent to the kidney.

On ultrasound (Fig. 13.23), a renal abscess is commonly a rounded complex mass but is rarely hypoechoic. 'Dirty' posterior acoustic shadowing secondary to gas within it is an uncommon but helpful sign. Perinephric abscesses have a similar appearance to renal abscesses but lie adjacent to the kidney. There is often associated obstruction or pyonephrosis.

A renal abscess may be confused with a tumour. The centre of an abscess is avascular on Doppler. The pus may be seen to move or swirl.

Fig. 13.23. (a) Renal abscess (arrow), with a round abscess of mixed echodensity and some irregular layering of the pus in the upper pole. (b) Perinephric abscess (arrow)

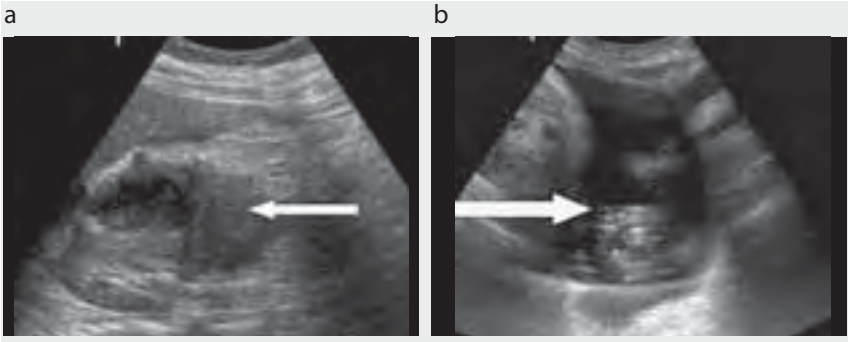

Xanthogranulomatous pyelonephritis

This is a rare chronic inflammatory process usually associated with obstruction secondary to a calculus. It is commoner in women than men and is rarely focal. Ultrasound (Fig. 13.24) shows a large kidney, with echogenic calcification and hypoechoic areas without posterior acoustic enhancement. There may be extension into the perinephric tissues, and the condition is frequently mistaken for a tumour.

Fig. 13.24. (a) Xanthogranulomatous pyelonephritis in a child. (b) A CT scan of the same patient, which shows the pattern better than the ultrasound

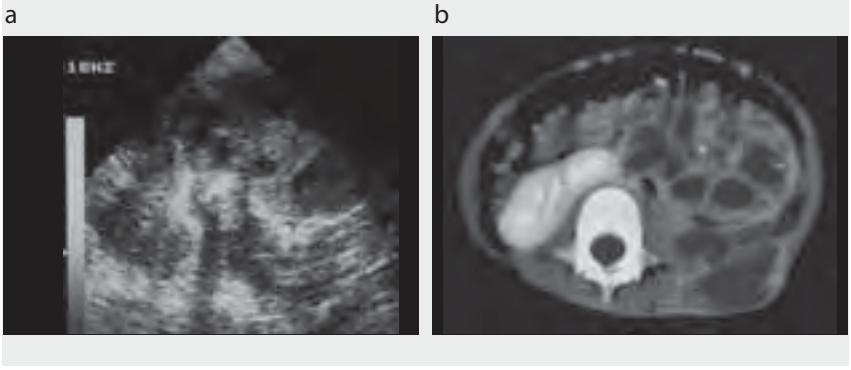

Hydatid disease (Hydatid cysts)

Hydatid disease (echinococcus infestation) in the kidney results in cyst formation. On ultrasound (Fig. 13.25), there is classically a mother cyst with smaller daughter cysts. The cyst walls may be fully or partially calcified and contain debris (hydatid sand). The disease has a predilection for the upper or lower poles. See WHO classification (see Chapter 7).

Fig. 13.25. Right kidney lower pole longitudinal scan of a hydatid cyst. The cyst has a calcified wall and echoic contents

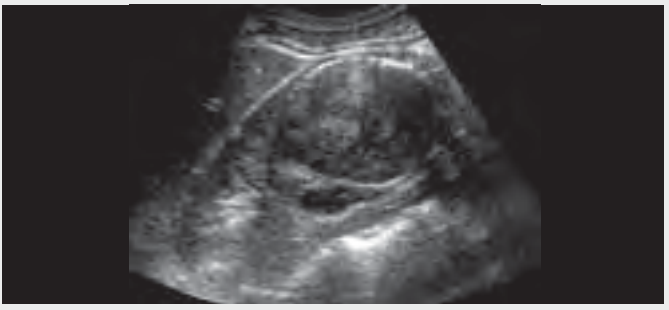

Fungal infections

Candida spp. are the commonest organisms involved; the resulting fungal infections occur in immunocompromised or debilitated patients. Fungal balls can occur in the collecting system.

On ultrasound (Fig. 13.26), echogenic masses are seen without posterior acoustic shadowing, which may be mobile. Disseminated infections can produce multiple abscesses in both kidneys and other organs. Any opportunistic infection, but particularly fungal infections, can cause thickening of the epithelial layer.

Tuberculosis

As **tuberculosis and brucellosis** have similar imaging features, the latter is not discussed separately. These conditions affect the kidney first and may later spread to the bladder.

Instillation of bacillus Calmette-Guérin (BCG) vaccine into the bladder for the treatment of bladder cancer can occasionally cause a renal infection identical to that caused by tuberculosis.

On ultrasound (Fig. 13.27), hypoechoic lesions are seen in the cortex early in the disease, which may later form calcified granulomata that are echogenic with posterior acoustic shadowing. Infundibular and pelvic stenoses cause calyceal dilatation proximally. Later in the disease, progression to autonephrectomy, or a 'putty' kidney, may occur, when the kidney becomes densely calcified. This echogenic appearance can be mistaken for bowel gas. An abdominal X-ray will prevent confusion.

Fig. 13.26. Fungal infections. (a) Right kidney longitudinal scan showing echogenic fungal balls in a paediatric kidney with a dilated collecting system. (b) A fungal ball in the upper pole calyx (crosses and dots on right image are measurements). (c) Fungal infection causing epithelial thickening

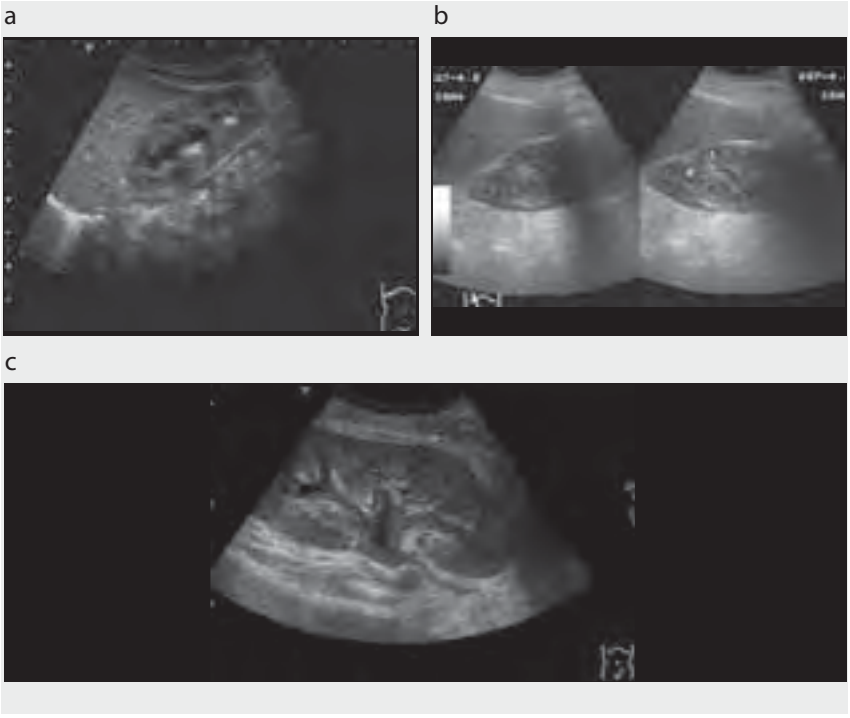

Renal manifestations of HIV/AIDS

HIV-associated nephropathy is a term used to describe the progressive renal failure that occurs in HIV infection and AIDS. Most patients with AIDS nephropathy have normal kidneys sonographically (Fig. 13.28). They can, however, have enlarged, echogenic kidneys (more echogenic than adjacent liver or spleen) with bilateral pelvicalyceal thickening. There can be loss of corticomedullary differentiation and a decrease in renal sinus fat.

HIV-related neoplasms

The incidences of all lymphomas are increased; Burkitt and large-cell lymphomas are considered AIDS-defining illnesses.

On ultrasound, the kidney may contain hypoechoic masses or less commonly be diffusely infiltrated and enlarged (Fig. 13.29). Retroperitoneal lymphadenopathy can displace the kidney or ureter, rarely causing hydronephrosis.

Fig. 13.27. Renal tuberculosis. (a) Right kidney longitudinal scan. Isolated infundibular stenosis causing calycectasis. (b, c) Left kidney: Hypoechoic granulomas (arrow) throughout the parenchyma. (d) Late stage: granulomas are calcified

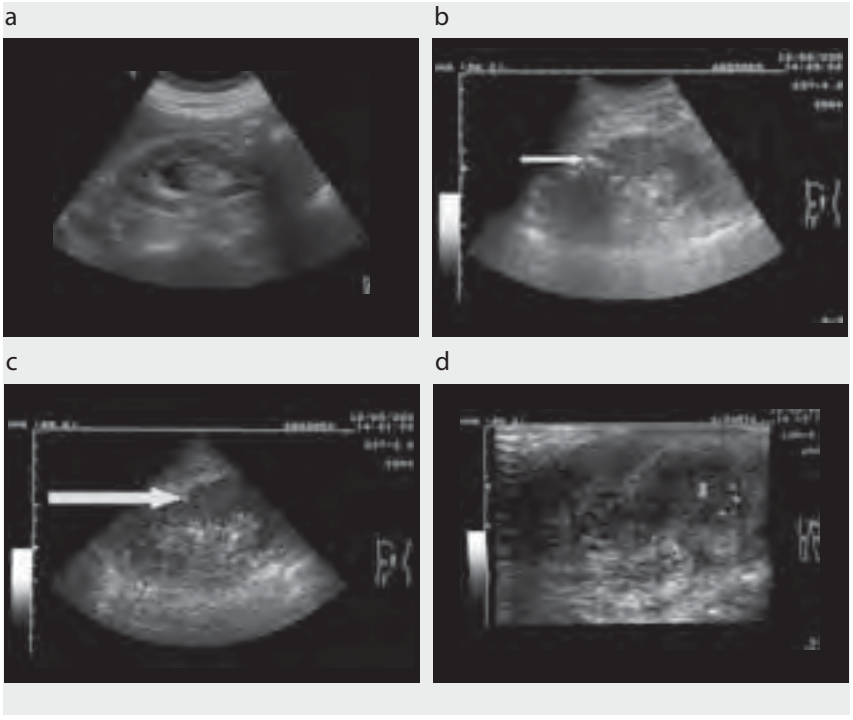

Fig. 13.28. HIV-associated nephropathy (two cases). Echogenic kidneys. (a) Right kidney longitudinal scan of enlarged echogenic kidney. (b) Right kidney longitudinal scan of echogenic kidney, less marked changes than in (a)

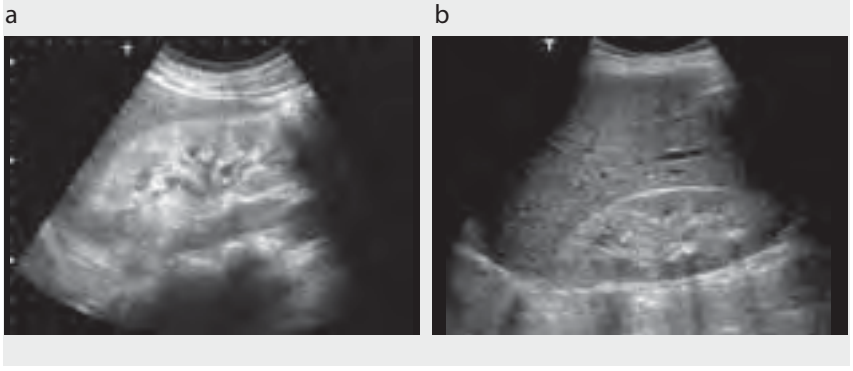

Fig. 13.29. HIV-related lymphoma, with a hypoechoic focus of lymphoma (broken line is renal length measurement) (see also Fig. 13.39)

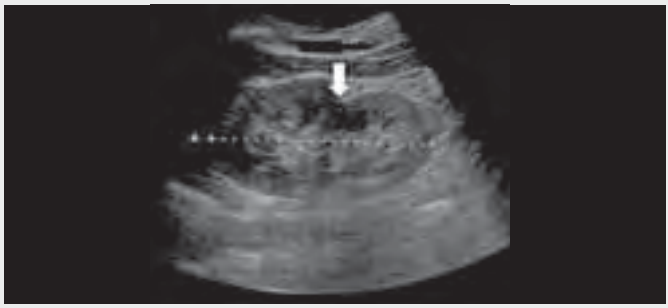

Opportunistic infections

Infection with *Pneumocystis jiroveci* or *Mycobacterium avium-intracellulare* may occur, and these are also considered AIDS-defining illnesses. The incidences of pyelonephritis and of genitourinary tuberculosis are also increased.

P. jiroveci and *M. avium-intracellulare* can both cause tiny focal echogenic densities, without posterior acoustic shadowing, in the renal cortex. (The appearances of pyelonephritis and tuberculosis have already been discussed above.)

Fungal balls can occur in the collecting system of immunocompromised patients.

Renal scarring

Renal scars can be due to previous reflux, infection, surgery or trauma. On ultrasound (Fig. 13.30), scars appear as indentations on the renal surface. Characteristically, they lie above the renal pyramids, whereas fetal lobulation causes indentations between the pyramids. There may be a triangular or irregular white defect. Broad scars appear as areas of focal cortical loss. 'Global scarring' is scarring that is so extensive that the kidney appears to be small with cortical thinning and no focal scars.

Fig. 13.30. (a) Renal scar. (b) Global scarring in a 16-year-old girl with recurrent renal tract infections since childhood

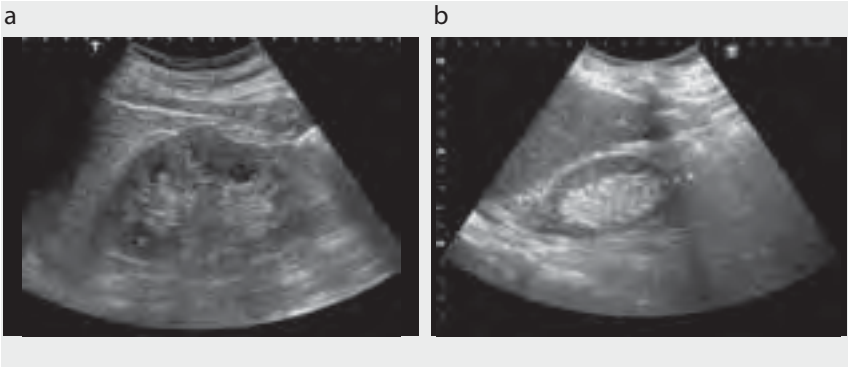

The presence of several scars can give the false appearance of a mass due to compensatory hypertrophy, which can be mistaken for a tumour.

Renal tumours

Ultrasound is highly sensitive for the detection of renal tumours. Although it may suggest that a tumour is benign or malignant, unfortunately, it is usually not possible to differentiate them reliably.

Benign tumours

Oncocytomas: These are usually benign but may metastasize. As they cannot be distinguished reliably from renal cell carcinoma by imaging, they should be excised, if appropriate. On ultrasound, oncocytomas are well defined, homogeneous tumours. A low-echodensity, central, stellate scar is a characteristic feature (Fig. 13.31). They are slightly more echogenic than renal parenchyma.

Fig. 13.31. Oncocytoma. The tumour is round, and an anechoic central scar is just visible (arrow)

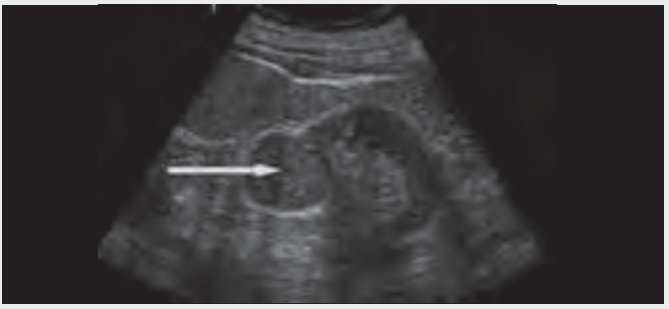

Angiomyolipomas: These tumours contain fat, blood vessels and smooth muscle elements in variable proportions. Small angiomyolipomas are invariably found incidentally; larger ones may present with flank pain secondary to haemorrhage. This is more likely when they are more than 4 cm in diameter. If they are bilateral, tuberose sclerosis should be considered as a diagnosis.

As angiomyolipomas have a high fat content, they have an echodensity similar to that of renal sinus fat (Fig. 13.32). Unfortunately, small renal cell tumours can have a similar appearance. If fat can be demonstrated within the tumour by other imaging modalities, it is likely to be an angiomyolipoma.

Large angiomyolipomas may contain anechoic and hyperechoic foci. Small angiomyolipomas of less than 1 cm in diameter are common. They appear as small, round, evenly echo-dense lesions and are usually assumed to be angiomyolipomas (although, rarely, one may be a hyperechoic renal cell carcinoma; see below).

Multilocular cystic tumours (cystic nephromas): These tumours have an unusual age and sex distribution: they occur in boys under the age of 4 years, 90% of whom are under 2 years of age. They also occur in girls under 5 years of age and women aged 40–60 years.

Fig. 13.32. Angiomyolipoma. (a) Large echogenic angiomyolipoma; presence of fat confirmed by CT. (b) Small angiomyolipoma of the upper pole of the left kidney

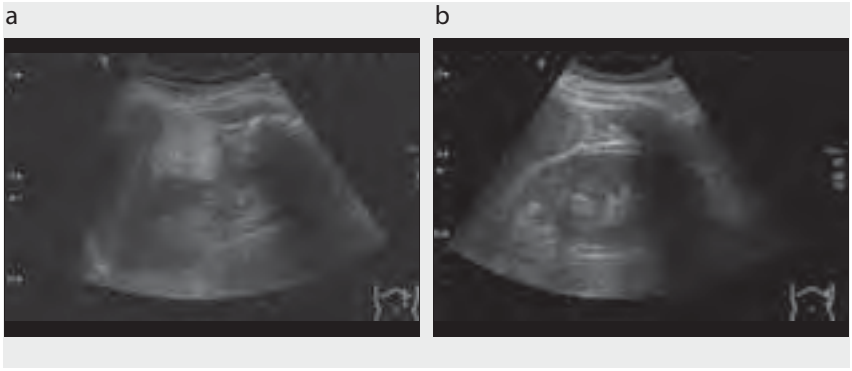

On ultrasound (Fig. 13.33), these tumours are well defined, multiloculated, partly solid and partly cystic masses. Although the septa are regular rather than nodular, it is not possible to distinguish them reliably from renal cell carcinoma.

Small hyperechoic cortical lesions: Small (< 6 mm) hyperechoic nonshadowing lesions are not infrequently seen in the renal cortex. They are often reported as granulomas or possible angiomyolipomas, but, as they are never excised, their nature is uncertain. We do know, however, that they are benign lesions that do not progress and require no treatment or follow-up (Fig. 13.34).

Fig. 13.33. (a) Small multilocular cystic nephroma (arrow). (b) Large multilocular cystic nephroma (arrow)

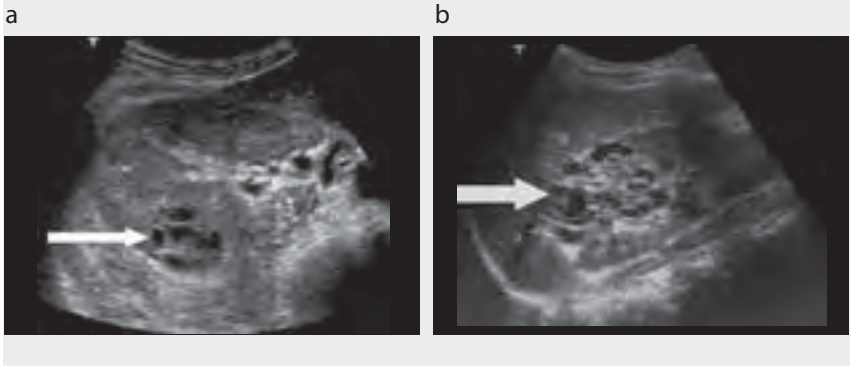

Fig. 13.34. Small hyperechoic cortical lesion

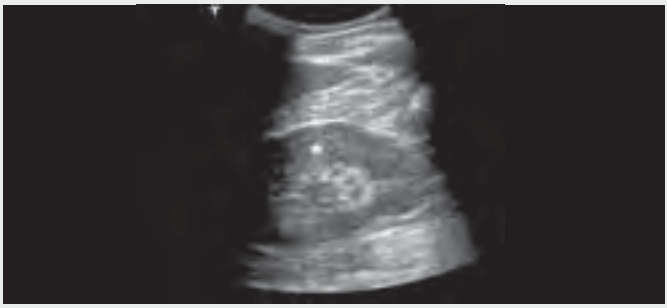

Malignant tumours

Renal cell carcinoma is the commonest malignant adult renal tumour. Transitional cell carcinomas arising from the collecting system are less common. Lymphoma and metastases comprise the majority of other malignant renal tumours.

Renal cell carcinoma: On ultrasound (Fig. 13.35), these tumours have a range of imaging characteristics. They are usually solid, partly cystic or with irregular hypoechoic areas of necrosis; or they may be predominantly cystic. Almost half are hyperechoic to the renal cortex. If they are small, they may be echogenic, resembling an angiomyolipoma. Almost one half are isoechoic; however, they are often heterogeneous and usually distort the cortex. A small number are hypoechoic without posterior enhancement and may look like solitary deposits of lymphoma.

Calcification, both punctuate and curvilinear, can occur, appearing as echogenic lines or foci with posterior shadowing.

Renal cell cancers are unusual tumours in that they may extend with tumour thrombus or a mixture of tumour and bland thrombus into the renal vein. From there, they may extend into the inferior vena cava and the right atrium. The extent of venous involvement will affect their prognosis and also determine the surgical approach. Therefore, it is important to categorize venous involvement as being of the renal vein only, of the subhepatic inferior vena cava, of the intrahepatic inferior vena cava, or of the right atrium and beyond. If available, CT or magnetic resonance imaging (MRI) will help, but ultrasound, although more difficult, is usually sufficient.

Pathological local lymphadenopathy results in a poor prognosis and should be considered when the nodes are larger than 2 cm. Ultrasound is not as good as CT for detecting lymphadenopathy, but may be used if it is the only means available.

As metastases to the lungs, liver and bone are common, staging with a thorax, abdomen and pelvis CT is advised for surgical candidates. If CT is not available, a chest X-ray and hepatic ultrasound should be performed.

As renal cell cancers, particularly papillary cancers, may be bilateral, both synchronously and metachronously, it is important to obtain good views of the contralateral kidney.

A venous tumour thrombus (Fig. 13.36) is echogenic and expands the vein. A tumour thrombus may contain blood vessels, which can be demonstrated by colour Doppler.

Lymphadenopathy (Fig. 13.37) consists of a hypoechoic mass or masses near the renal hilum or aorta.

Transitional cell carcinoma: These are infiltrative tumours arising from the epithelium of the collecting system. When they are advanced, they can also invade the renal veins and the inferior vena cava. They are often assessed by excretion urography and staged by CT. Transitional cell cancers can sometimes be seen ultrasonically (Fig. 13.38) but are often not visible. They are less echogenic than renal sinus fat and commonly cause separation or cut-off of the central echo complex. They may expand and fill the collecting system with an echogenic soft tissue mass. Renal invasion is usually hypoechoic to renal parenchyma.

Fig. 13.35. (a, b) Heterogeneous renal tumours (in (a) the arrow indicates calcification and in (b), the tumour). (c, d) Hyperechoic renal tumours (arrow). (e, f) Isoechoic renal tumours (arrows). The tumour (arrow) is seen only because in (e) it indents the central renal complex and in (f) it bulges out from the kidney. (g) A hypoechoic upper-pole renal cell cancer (arrow). (h) A cystic renal tumour

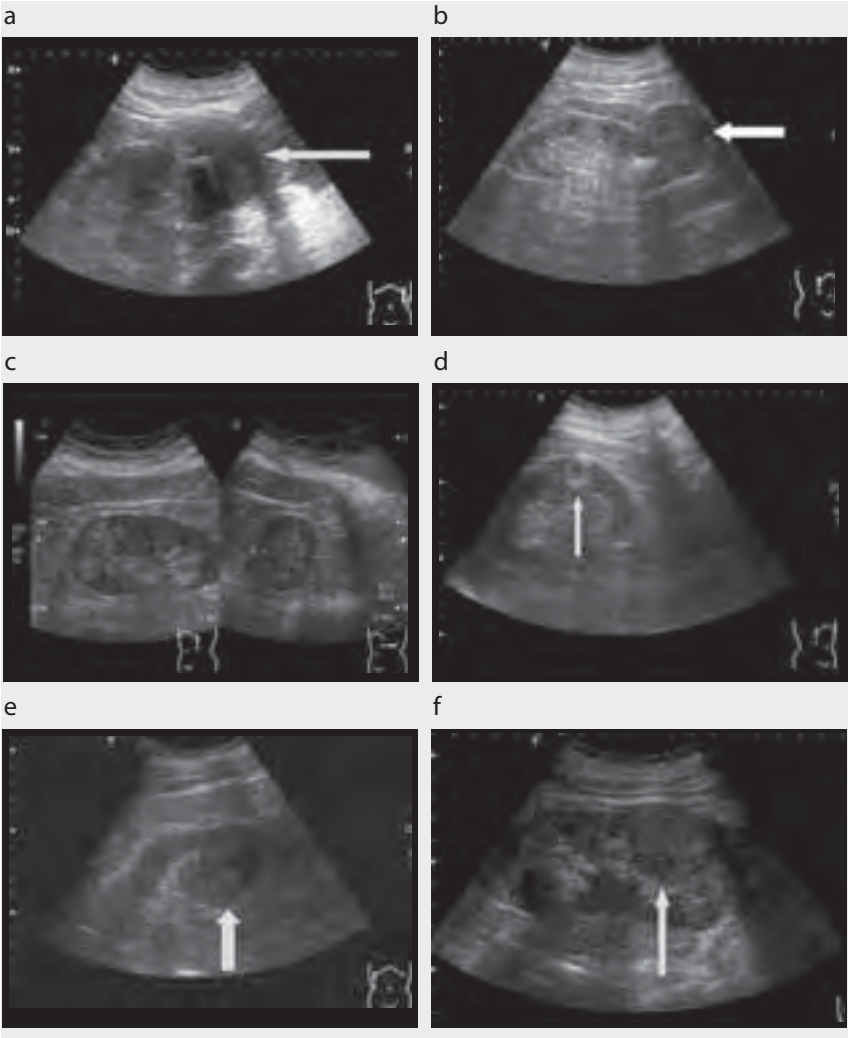

Fig. 13.35. *continued*

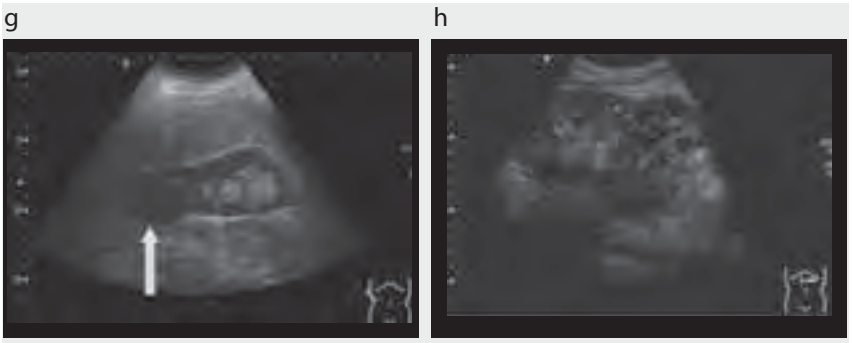

Fig. 13.36. (a) Tumour thrombus (arrow) in the renal vein. (b) Tumour thrombus (arrow) in the inferior vena cava extending to mid-hepatic level

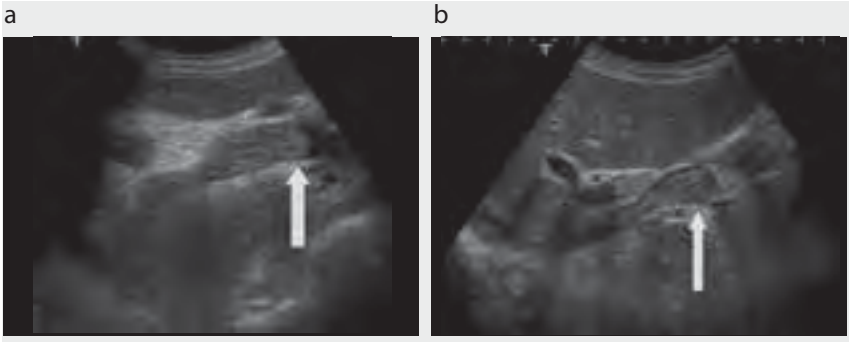

Fig. 13.37. (a) Lymphadenopathy associated with cystic renal tumour. (b) Para-aortic nodes secondary to a renal cell cancer

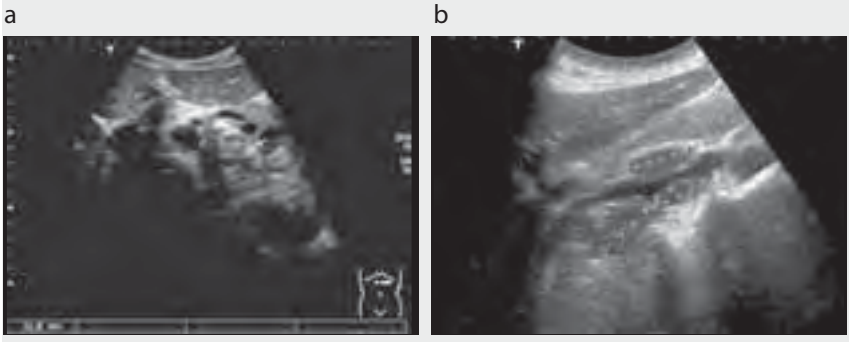

Fig. 13.38. A transitional cell carcinoma (arrow) filling and expanding the renal pelvis and calyces (see also Fig. 13.55)

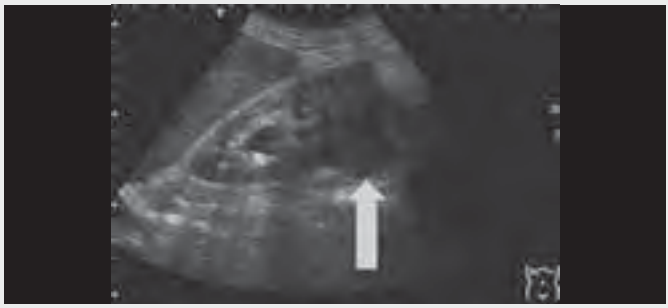

Renal lymphoma: Renal lymphoma usually occurs in widespread disease, with considerable lymphadenopathy. Occasionally there is only renal involvement. The ultrasonic appearance (Fig. 13.39) is similar to that of HIV-associated lymphoma (see section on Renal manifestations of HIV/AIDS in this chapter). The kidney may contain hypoechoic masses or, less commonly, be diffusely infiltrated and enlarged. Rarely, retroperitoneal lymphadenopathy can displace the kidney or ureter, causing hydronephrosis.

Metastases: These are common in advanced disease and are therefore frequently seen at autopsy. They are less commonly seen in clinical practice. On ultrasound, multiple small solid renal masses or, occasionally, solitary renal masses are seen in the presence of a known primary tumour elsewhere. They may be hyper- or hypoechoic with respect to the renal parenchyma.

Calculi and calcifications

Renal calculi

Urinary stasis predisposes to calculus formation. Ultrasound can be used to detect anatomical and congenital factors such as pelvicalyceal diverticula, pelviureteric junction obstruction, polycystic kidneys and ectopic kidneys. Most, however, occur in otherwise normal systems.

Excretion urography and CT urography are used in the detection of urinary tract calculi. Sonography is accurate for detecting renal calculi, especially if they are larger than 5 mm. It is poor for detecting ureteric calculi, because of overlying bowel gas, unless the calculi lie in the distal ureter, where the full bladder acts as an acoustic window (see section on Ureters below).

On ultrasound (Fig. 13.40), calculi are echogenic, with a clean shadow. If they measure less than 5 mm, posterior acoustic shadowing may not be present. Careful attention must be paid to setting the focus at, or just below, the level of the calculus. Harmonic imaging, if available, increases the acoustic shadow.

An echogenic cortex can prevent visualization of calculi. Pure matrix stones do not contain calcium and appear as a soft tissue mass; however, most matrix stones contain some calcium. Indinavir stones secondary to retroviral therapy are radiolucent and may not be seen even sonographically. If suspected clinically, secondary signs of obstruction should be assessed. Calyceal or pelvis ureter junction calculi may be hard to distinguish from surrounding echogenic fat.

Fig. 13.39. Renal lymphoma. (a, b) Hypoechoic tumour (arrow) in the upper pole of the right kidney. (c) A larger tumour in the left kidney

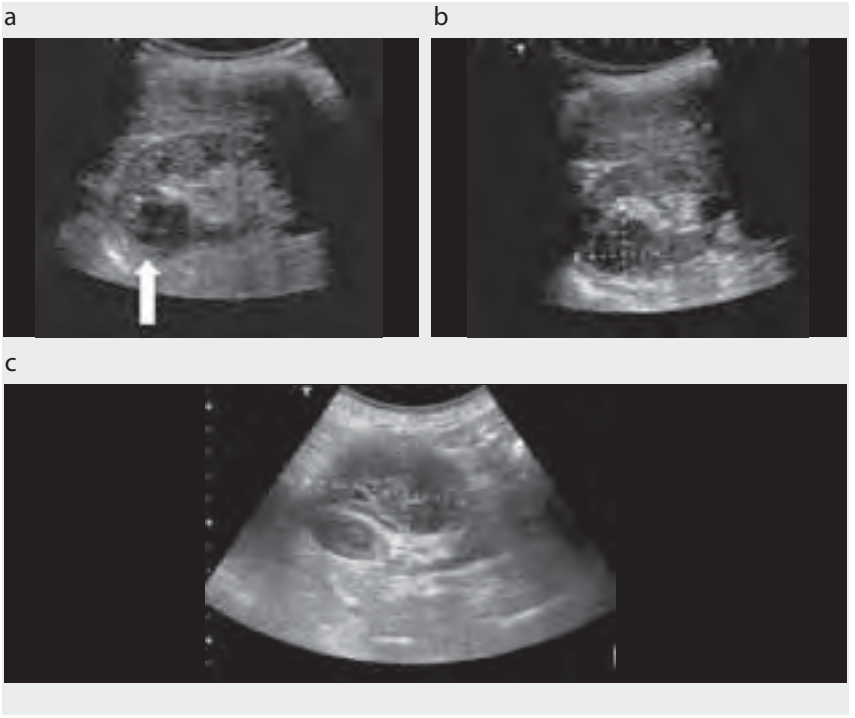

Nephrocalcinosis

Nephrocalcinosis is calcification in the cortex or medulla; the two may occur together. The condition can be idiopathic or secondary to urinary stasis, hyperparathyroidism, renal tubular acidosis, medullary sponge kidney, hypercalcaemia, AIDS-associated infections, tuberculosis and other causes.

On ultrasound (Fig. 13.41), calcification often starts as tiny clusters of echogenic foci in the pyramids. Later, the calcification may fill the pyramids.

Milk of calcium

Milk of calcium is a suspension of calcium that occurs secondary to urinary stasis; it layers in a dependent fashion in the collecting system, i.e. the heavier calcium forms a layer with urine above it. It may also be seen in renal cysts.

On ultrasound (Fig. 13.42), highly echogenic dependent layering is seen, with a sharp anterior line. Posterior acoustic shadowing may be present if there is a large amount of milk of calcium. The suspension moves when the patient turns.

Trauma

While it is clearly important to assess renal damage in cases of trauma, it is also important to identify a contralateral functioning kidney, if present. Excretion urography and ultrasound should be used when CT is not available. Trauma is more likely to affect an ectopic kidney than a normally placed one.

Fig. 13.40. (a) Staghorn calculus. An echogenic shadowing calculus (arrow) fills the collecting system. (b) Pelvis ureter junction calculus (arrow) with associated calyceal dilatation. (c) Kidney with bifid renal pelvis and two small lower pole renal calculi (arrow), the larger showing posterior acoustic shadowing

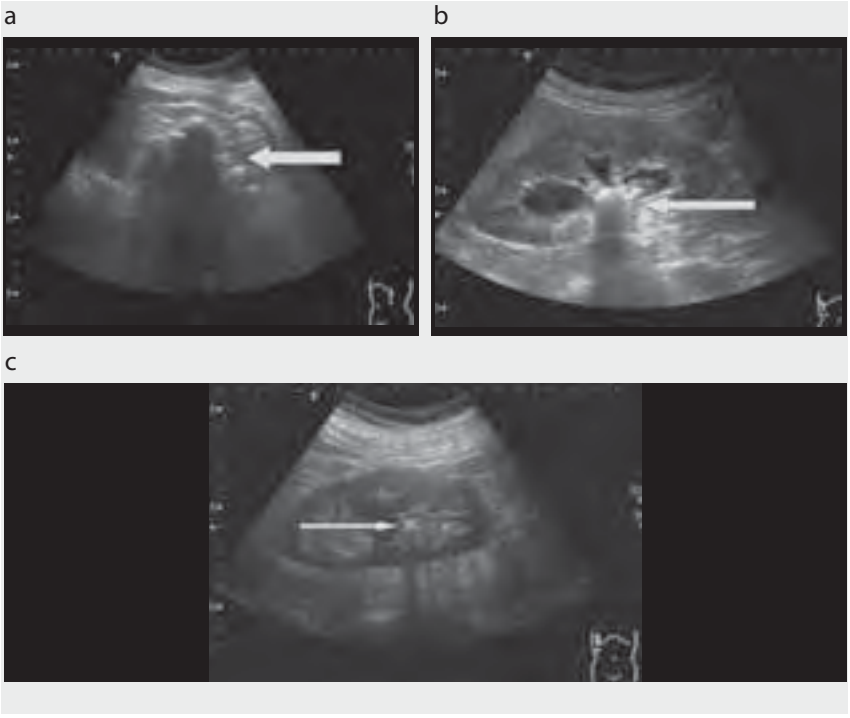

The most severe injuries, i.e. avulsion of the renal pedicle and a shattered kidney, usually require surgery. As patients with suspected renal trauma have usually had a severe injury, it is important to look also for injuries in adjacent organs, such as the spleen and liver. The abdomen should also be examined for the presence of free blood.

In severe trauma (Fig. 13.43), avulsion of the renal pedicle can appear normal on grey-scale sonography, and Doppler or excretion urography is required to visualize absent perfusion or an absent nephrogram. A shattered kidney involves multiple lacerations, which show as echo-poor areas if they contain urine or blood. There is also likely to be perirenal fluid. As the blood clots, it becomes echogenic.

Less severe trauma, including lacerations, contusions, segmental infarcts and subcapsular haematoma, is less likely to require surgery. On ultrasound (Fig. 13.44), infarcts have variable echogenicity, depending on their age, but they are often segmental. Subcapsular haematomas have low echogenicity in the acute phase but can be hard to detect if their echogenicity is similar to that of the cortex.

Collecting system injuries often result in a urinoma. If this contains urine only, it will be hypoechoic, but if it also contains blood, it will have variable echogenicity. Excretion urography should be used if these injuries are suspected.

Fig. 13.41. Nephrocalcinosis. (a) Medullary calcification (arrow) in a small-end stage kidney. (b) The calcifications (arrow) almost fill the pyramids. (c) Cortical nephrocalcinosis (arrow), in this case secondary to cortical necrosis

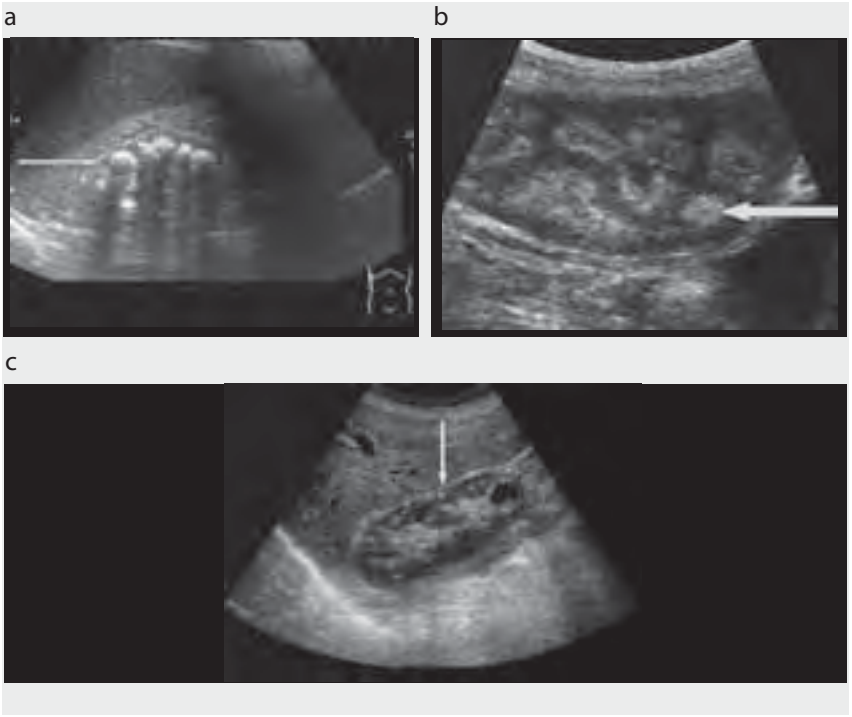

Fig. 13.42. Milk of calcium in a renal cyst

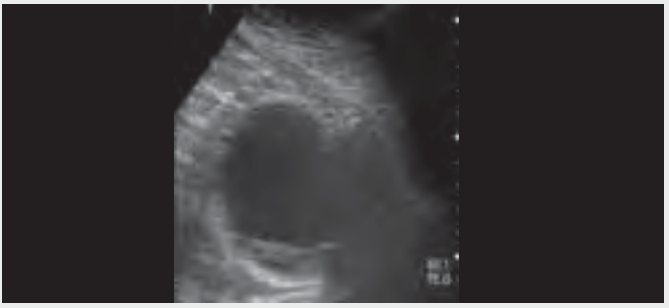

Fig. 13.43. (a) Longitudinal scan, ruptured left kidney with hypoechoic blood in the centre (arrow). (b) Perinephric haematoma (arrow), with a blood clot and anechoic blood around the upper pole. (c) Intraperitoneal blood: large volume of fluid (arrow) and clotted blood (arrowhead) in the peritoneal cavity

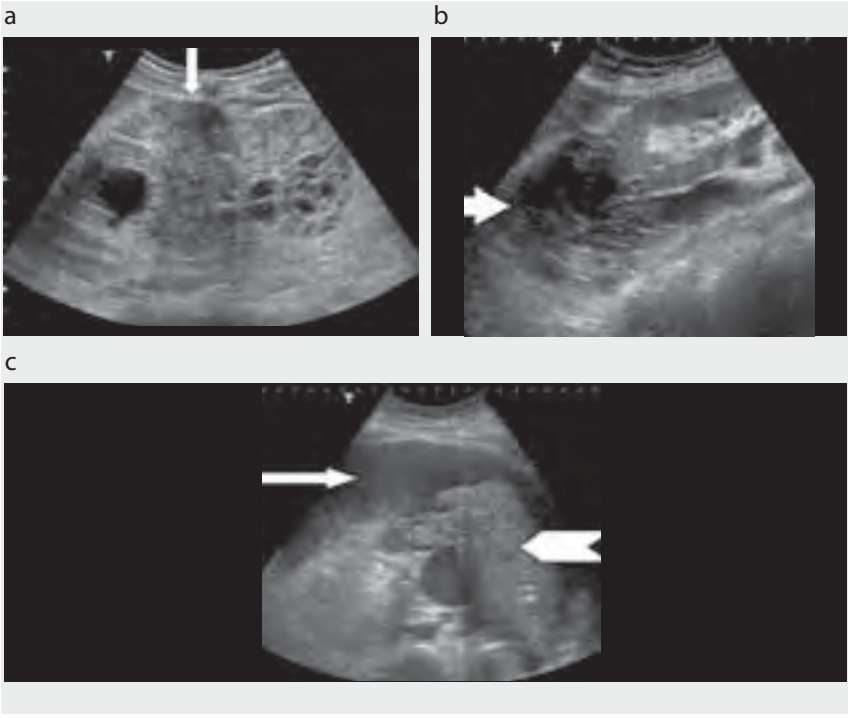

Fig. 13.44. (a) Urinoma, showing fluid around the upper pole (arrow). Aspiration revealed urine. (b) Subcapsular and small perinephric haematoma (arrow)

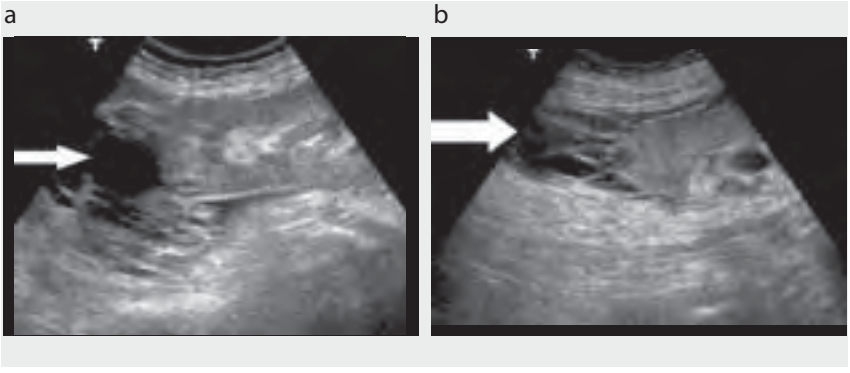

Renal failure

Renal failure can have pre-renal, renal or post-renal causes, each of which can be acute, chronic or acute on chronic. Renal failure is most accurately assessed by a fall in the glomerular filtration rate; however, in clinical practice, raised serum creatinine is used as a guide. Ultrasound is used predominantly to exclude obstruction, as changes in parenchymal disease are non-specific.

In patients who are dehydrated, pre-renal failure should be considered. In patients who have had an episode of hypotension, acute tubular necrosis should be considered.

Hydronephrosis must be presumed to indicate obstruction, which should be relieved by an appropriate method. Small end-stage kidneys, less than 7 cm in length, will not recover any significant function, and the patient should be put on a dialysis or a transplantation programme. No further investigation is necessary. Normal-size kidneys with no hydronephrosis may have a normal or altered echo pattern. Increased cortical or cortical and medullary echodensity indicates parenchymal disease, but the patterns are not specific. Diagnosis requires biopsy. Occasionally, polycystic kidneys will be found.

Vascular causes, such as bilateral renal artery emboli or renal vein thromboses, are extremely rare.

Renal failure associated with hypertension suggests renal artery stenosis. A rise in creatinine after administration of angiotensin-converting enzyme inhibitors also suggests renal artery stenosis.

Acute renal failure

All pre-renal causes of renal failure result in decreased renal perfusion, whatever the underlying cause, but dehydration is the commonest. Renal artery stenosis is the main structural cause that can be identified; this requires investigation with both colour and spectral Doppler. Unfortunately, it is technically demanding, even in expert hands, and often may not be successful. Renal causes of renal failure are common and include acute tubular necrosis, vascular disease, glomerulonephritis and papillary necrosis.

Post-renal causes of renal failure are obstruction or, rarely, renal vein thrombosis.

Chronic renal failure

Chronic renal failure is commonly due to intrarenal causes, such as diabetic nephropathy, hypertension, adult polycystic disease and glomerulonephritis. Less commonly, renal artery stenosis or chronic obstruction is responsible.

Parenchymal diseases

Glomerulonephritis: Many diseases can cause glomerular damage resulting in impairment of renal function. Glomerulonephritis can be acute or chronic.

On ultrasound, acute glomerulonephritis often causes smoothly enlarged, echogenic kidneys with associated loss of corticomedullary differentiation (Fig. 13.45 (a)). Chronic glomerulonephritis often results in shrunken echogenic kidneys, sometimes with proliferation of renal sinus fat (Fig. 13.45 (b)). The ultrasound appearance may, however, be normal in both acute and chronic glomerulonephritis. Diagnosis requires biopsy.

Tubulointerstitial disease

Acute tubular necrosis is the commonest reason for acute renal failure, resulting in oliguria or anuria. Ischaemia is the commonest cause, whether pre-renal, renal or

Fig. 13.45. (a) An echogenic right kidney (arrow) in acute glomerulonephritis, with a small volume of ascites (arrowhead). (b) Chronic glomerulonephritis. The right kidney is small (6.5 cm) and hyperechoic (longitudinal scan)

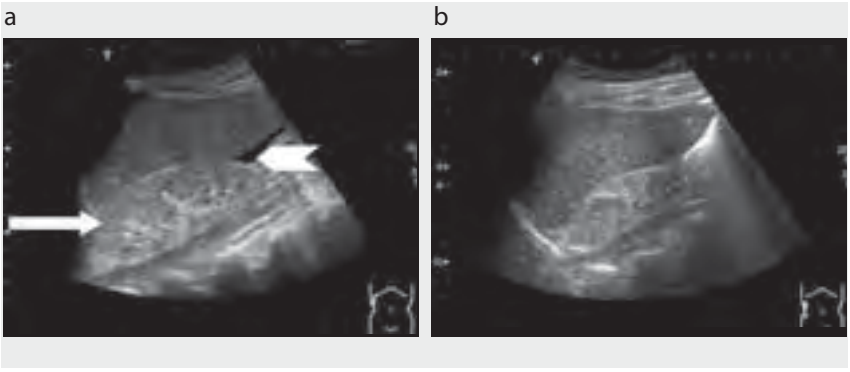

post-renal. It most often occurs after trauma or surgery for an acute illness that has caused an episode of severe hypotension, but certain toxins may be responsible.

On ultrasound (Fig. 13.46), the kidneys appear smoothly enlarged and are rounded in the anteroposterior direction rather than flattened as normally. Other findings are more variable, including parenchymal echogenicity and corticomedullary differentiation, although the medullary pyramids are often enlarged and hypoechoic, particularly in cases due to toxins. In Doppler studies, there is reduced diastolic velocity, measured as an increased resistance index. Mild or moderate cases recover; however, in severe cases, there is zero or reversed diastolic flow, and this has a poor prognosis. Many cases of reversed flow progress to cortical necrosis.

Renal artery stenosis

Renal artery stenosis may be suspected in patients with:

- severe hypertension that does not respond to treatment, particularly in young patients;
- a bruit heard over the renal arteries;
- combined hypertension and renal impairment; or
- renal impairment after administration of angiotensin-converting enzyme inhibitors.

Ultrasound on the grey scale shows a small kidney with a normal echo pattern in severe cases. There may be a discrepancy in the length of the two kidneys. Doppler studies for renal artery stenosis are technically difficult and time-consuming and require high-quality equipment. They may be accurate for children, very slim patients and renal transplants, but in other patients there is a relatively high technical failure rate.

Doppler ultrasound (Fig. 13.47) shows that, at the stenosis, the arterial blood velocity is high (> 2 m/s). Up to about 1 cm distal to the stenosis, there is turbulence, with a spiky, ragged waveform. In the intrarenal arteries, there is a damped waveform (parvus tardus) with a rounded, low systolic peak. As there is less reduction in diastolic flow, the resistance index is low.

The damped flow in the renal arteries is easiest to detect, but for diagnostic purposes it lacks sensitivity and specificity. It is found in cases of severe stenoses but also occurs in cases of severe renal impairment without stenosis.

Fig. 13.46. Acute tubular necrosis. (a) Enlarged echo-poor pyramids. (b) Reduced diastolic velocity, resistance index (RI) 86. (c) Severe acute tubular necrosis, with no diastolic flow

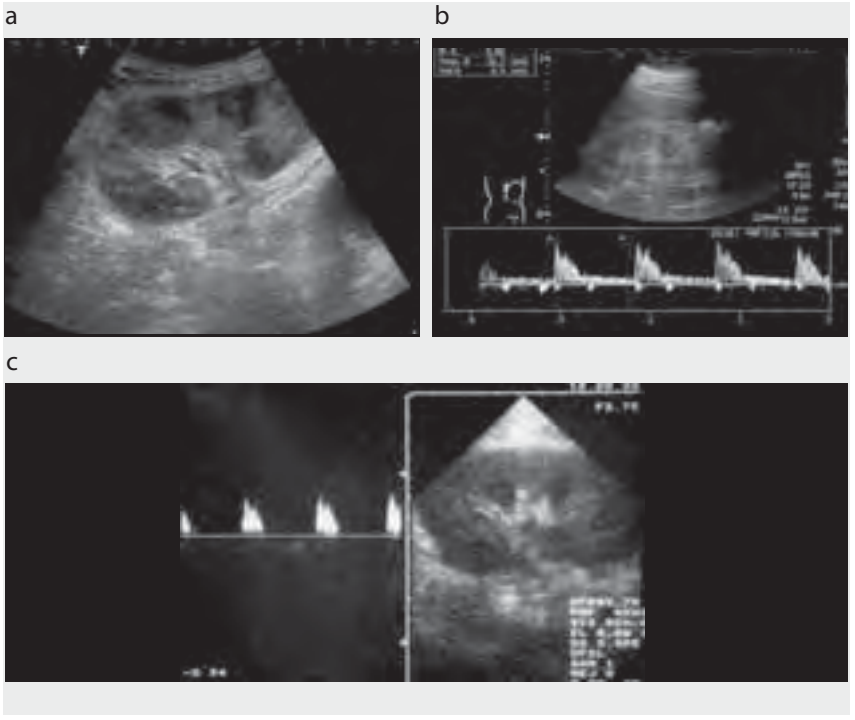

As Doppler changes at the stenosis occur only over a 1-cm length of the artery, it is important to study the Doppler signals from at least three points along the renal artery: origin, mid- and distal. This is, however, often not technically possible. A Doppler angle (between the beam and the artery) of less than about 60° may produce a waveform that looks damped.

Aortic valve disease, particularly incompetence, modifies the renal artery waveform, making interpretation difficult.

Obstruction and hydronephrosis

Obstruction implies resistance in the urinary tract and can be difficult to assess by sonography. It may result in cortical loss and renal failure. **Hydronephrosis**, or pelvocaliectasis, consists of dilatation of the collecting system of the kidney and is easier to assess.

A dilated system is not necessarily an obstructed one, and, conversely, acute obstruction does not immediately cause dilatation. Isotope renography can be used to distinguish between the two.

Hydronephrosis can be categorized into three grades on the basis of sonographic appearance (see also Fig. 13.48):

- Mild: blunt fornices, enlarged calyces, flattened visible papillae and separation of the central sinus echo. This appearance can be seen with a full bladder, in which case it resolves when the bladder is emptied.

Fig. 13.47. Renal artery stenosis. (a) At the stenosis, there is high velocity and turbulence. (b) Immediately distal to the stenosis, the flow is turbulent. (c) Damped flow in the intrarenal arteries

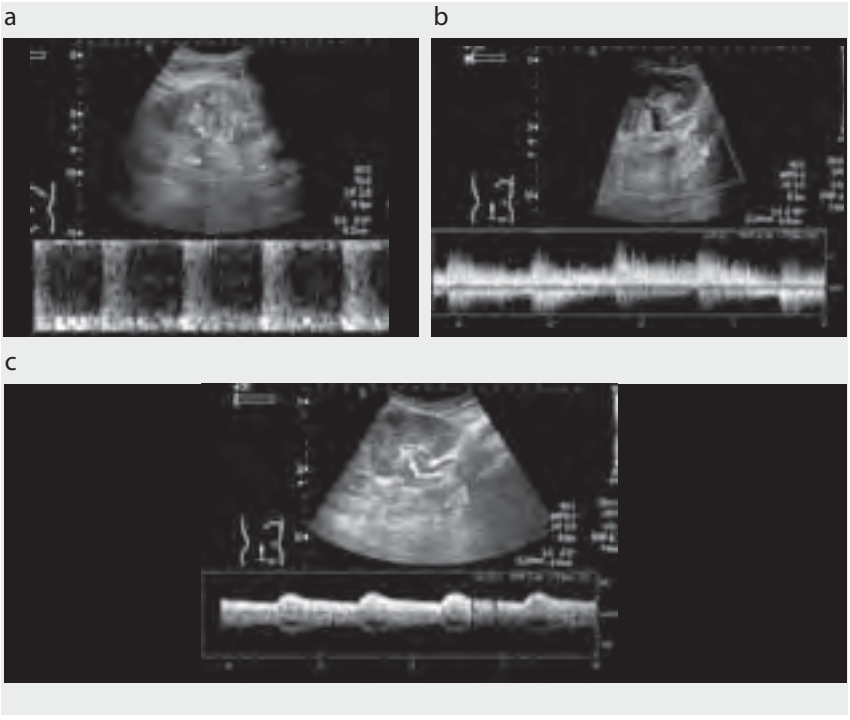

- Moderate: calyces rounded, papillae obliterated.
- Severe: grossly dilated calyces, often thin cortex. Fig 13.48 illustrates longstanding gross hydronephrosis, secondary to advanced prostate cancer, with almost no residual cortex.

It is important to look for separation of the central sinus echo in early hydronephrosis, although a certain degree of separation may be normal.

The resistance index is elevated in cases of acute obstruction, relative to that of the other kidney. The increase is, however, small and is useful only in identifying unilateral obstruction, when the two sides can be compared. The difference can be accentuated by administering intravenous furosemide.

Ureteric jets are absent from the bladder on the obstructed side, and colour Doppler can help to show their presence or absence.

The level and, if possible, the cause of obstruction should be sought (see section on Ureters in this chapter).

The difficulties in making a diagnosis are illustrated by the images in Fig. 13.49. Renal sinus cysts can look like a dilated renal pelvis, although it is not possible to show them communicating with the calyces. An extrarenal pelvis can look like hydronephrosis, but the calyces will be normal. If in doubt, excretion urography will help. Obstructed systems are not dilated for three main reasons:

- Acute obstruction may not cause dilatation during the first few hours.
- The system has been decompressed, i.e. there is a forniceal tear.

- The renal pelvis is scarred, e.g. secondary to tuberculosis, and will not dilate as it normally does.

Fig. 13.48. Hydronephrosis. (a) Mild; (b, c) moderate; (d) severe with marked cortical loss; and (e) total loss of cortex

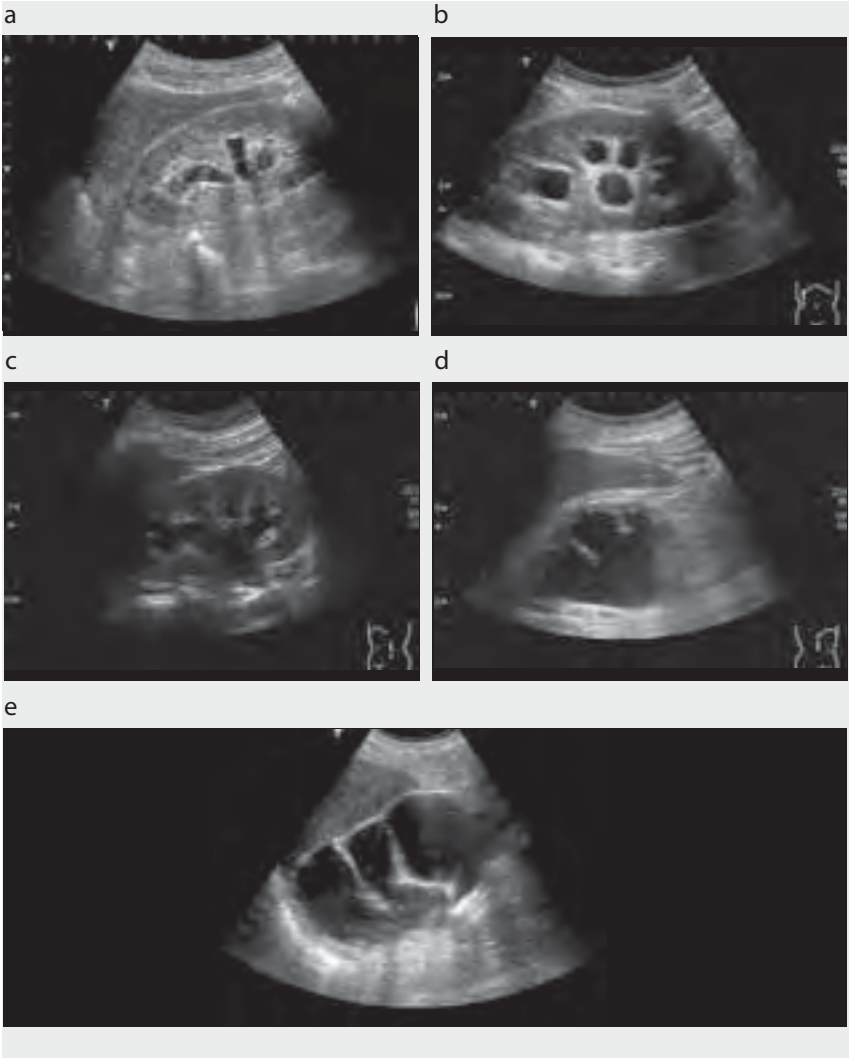

Urinary debris or gas may suggest infection in an obstructed system. This may, however, occur for other reasons. Conversely, the absence of debris or gas does not entirely exclude infection.

Infundibular obstruction or stenosis will cause a hydrocalyx, which is indistinguishable from a calyceal diverticulum. This can be due to tuberculosis, a calculus, a tumour or a blood clot. In Fig. 13.27 (a), a dilated calyx is seen, often with thinning of the overlying cortex. An associated calculus will be echogenic with

Fig. 13.49. (a) Right renal sinus cyst (arrow) demonstrated to be separate from the pelvicalyceal collecting system. (b) Extrarenal pelvis (arrow), confirmed by an intravenous pyelogram

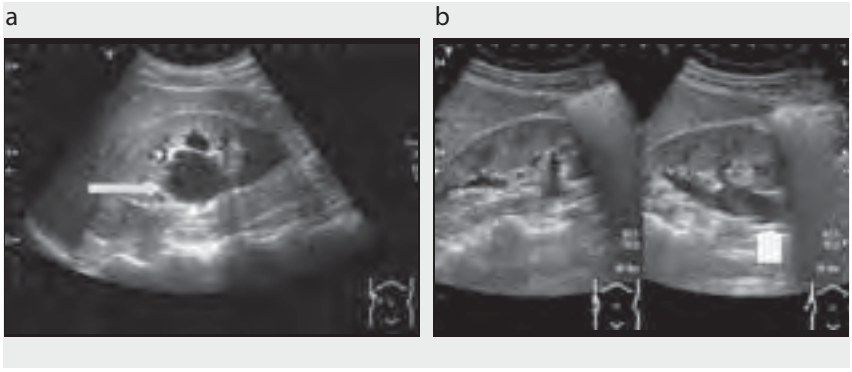

posterior acoustic shadowing. An isolated dilated calyx, particularly in the upper pole, may be due to previous reflux nephropathy.

Pelviureteric junction obstruction is commonly congenital and is due to a functional obstruction at this level or an aberrant blood vessel, although it may present at any age. All the causes of infundibular obstruction can be responsible for both this and ureteric obstruction.

Fig. 13.50 shows a dilated renal pelvis, with variable calyceal dilatation. The upper ureter is not dilated. The diagnosis may be strongly suspected from the ultrasound appearance but requires an intravenous urography or CT for confirmation. Surgery depends on whether there is high pressure (partial obstruction) or normal pressure. This is normally assessed by an isotope renogram.

Fig. 13.50. (a) Pelviureteric junction obstruction, with normal left junction and marked right junction obstruction. (b) Pelviureteric junction obstruction (arrow) in a horseshoe kidney

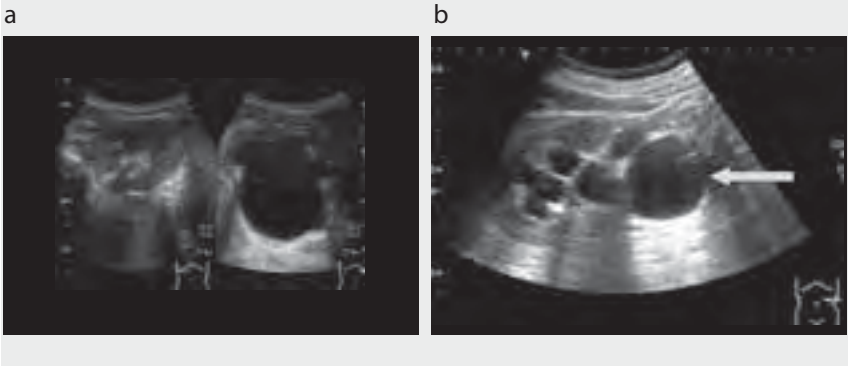

Doppler ultrasound may be used. The diastolic flow (higher resistance index) in a kidney with high pressure at the pelviureteric junction is lower than that in the other kidney. The difference is accentuated after intravenous furosemide.

Ureteric obstruction: See the section on Ureters.

Ureters

The ureters are narrow muscular tubes 4–6 mm in diameter, with a lumen of 2–8 mm, depending on peristalsis. They start at the pelviureteric junction and run a retroperitoneal course, typically just lateral to the tips of the spinal transverse processes, although often more medial or lateral. Subsequently, they cross the iliac artery and veins anteriorly; then, at mid-pelvic level, they turn medially to enter the bladder. The ureters are divided into retroperitoneal, pelvic and intramural portions.

Indications

To determine the level of obstruction of the ureters and, if possible, to determine its cause, ultrasound is a poor method of imaging, as much of their length is usually obscured by overlying bowel and other structures. It is far inferior to CT or intravenous urography. Nevertheless, examination of the ureters is frequently an important part of a renal ultrasound study, which often provides enough sufficient information about them, so that there is no need to proceed to CT or intravenous urography.

Examination technique

Equipment, transducer

For adults, use a 3.5-MHz (normal or obese) or 5-MHz (slim patients) transducer.

Preparation

The ureters are usually scanned as part of a general scan of the urinary tract. It is usual to give 1 litre of fluid 1 h before the scan to fill the bladder.

Position of the patient

Start with the patient lying in the supine position.

Scanning technique

The proximal ureter, just distal to the pelviureteric junction, can usually be seen if it is dilated; it is seen inconsistently if it is not dilated.

A longitudinal plane, scanning obliquely from the flank, with the patient in a lateral oblique position, may show the upper ureter, with the kidney as a sonic window. Sometimes, a transverse plane makes it possible to follow the ureter from the renal pelvis. Much in the same way, it can be followed on a CT scan (Fig. 13.51).

The distal ureter, as it passes behind the bladder, is similarly visible if dilated, but if not dilated is seen inconsistently. A moderately full, but not overfull, bladder is best.

The ureter can be identified in real time by its peristalsis. It is possible to mistake the iliac vessels for the ureter, but the use of colour Doppler eliminates this problem (Fig. 13.52).

The ureter is often seen in relatively slim patients as it crosses anterior to the iliac artery and vein. This may be important in distinguishing pathological dilatation from the physiological dilatation of pregnancy. An angled longitudinal, transverse or oblique scan plane is used. The pregnant patient is scanned in a 45° oblique position so that the scan plane passes behind the uterus. Non-pregnant patients can be scanned supine. The iliac vessels are easily identified, although colour Doppler may be helpful.

The ureter is seen passing obliquely anterior to them (Fig. 13.53). The rest of the ureter is not seen in most patients, unless it is highly dilated.

Fig. 13.51. Upper ureter seen through the kidney. (a) Normal ureter. (b) Dilated ureter for comparison. (c) Measurement of the upper ureter

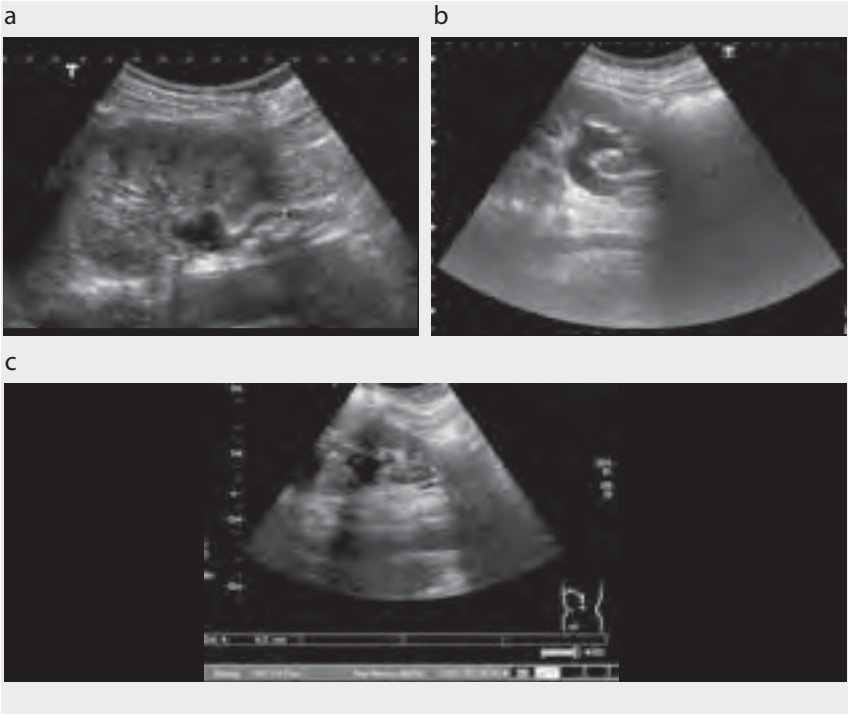

Fig. 13.52. The normal lower ureters are just visible posterior to the bladder (arrows)

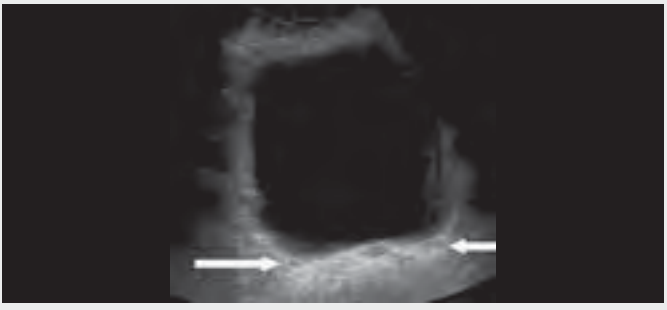

Fig. 13.53. Normal mid-ureter crossing the iliac vessels. The ureter is seen crossing anterior to the vessels (arrow). Colour flow (here in black and white) distinguishes the vessels

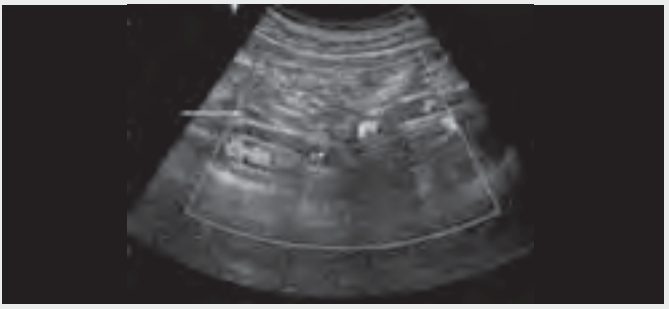

Ureteric obstruction

The commonest reason for imaging the ureter is hydronephrosis. In such cases, the level and, if possible, the cause of the obstruction must be established. Although the entire ureter may not be visualized, those portions that are visible often allow a diagnosis to be made.

Dilated calyces, a dilated renal pelvis and a non-dilated proximal ureter suggest pelviureteric junction obstruction (Fig. 13.54). Dilatation of the proximal but not the distal ureter suggests mid-ureteric obstruction but does not establish the cause. Dilatation of the distal ureter can be due to a calculus at the vesicoureteric junction or a bladder tumour, both of which are usually visible on ultrasound. The absence of any demonstrable cause in cases of poor bladder emptying suggests bladder outflow obstruction.

Pregnancy can cause physiological dilatation down to a smooth taper as the ureter crosses the iliac vessels, but not beyond (Fig. 13.54 (c)).

While a definitive cause of an obstruction may be established on an ultrasound scan, often only a probable cause can be established, which may have to be confirmed by intravenous urography or CT.

Tumours

Transitional cell cancer is the commonest ureteric tumour. Although such tumours are occasionally demonstrated by ultrasound, the diagnosis usually requires CT or retrograde pyelography. When tumours are seen on ultrasound (Fig. 13.55), they appear as soft tissue masses within a dilated ureter. Transitional cell cancers are often multiple, and other tumours may be seen in the pelvicalyceal system or bladder. Bladder tumours are often the cause of obstruction and should be explored.

Calculi

Ureteric calculi may often be seen when they lie at the pelviureteric junction or at the vesicoureteric junction and may occasionally be seen with proximal dilatation in the mid-ureter. In general, however, ultrasound is unreliable for the detection of ureteric calculi, especially in the mid-ureter. When calculi are seen on ultrasound (Fig. 13.56),

they appear on an echo-dense, curved line representing the surface of the calculus nearest to the transducer, with distal acoustic shadowing. The ureter proximal to them is usually, although not always, dilated.

Fig. 13.54. Pelviureteric junction obstruction. (a) The calyces and renal pelvis are dilated, but there is no upper ureteric dilatation. (b) The upper ureter is dilated (arrow), indicating that the obstruction is below this level. (c) The dilated mid-ureter is seen crossing the iliac vessels (arrow), indicating that the obstruction is below this level. (d) The lower left (LT) ureter is dilated, indicating that the obstruction is below this level. In this case, there is a bladder tumour. (e) The ureter of this pregnant woman is dilated (between calipers) down to an even taper at the level of the iliac vessels, the typical pattern of dilatation in pregnancy

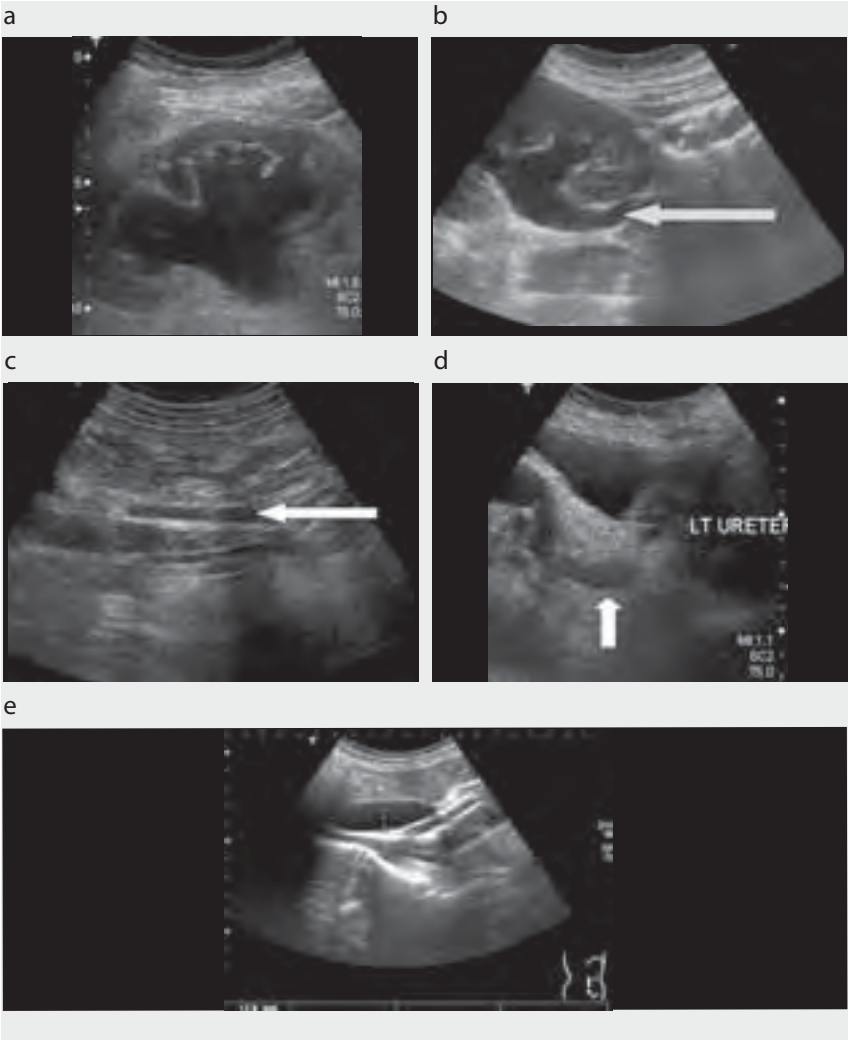

Fig. 13.55. Ureteric tumour. (a) The lower right ureter is dilated down to a small irregular tumour (arrow), a transitional cell carcinoma, within the lumen. (b) The same case, showing a second tumour within the right renal pelvis. (c) A bladder tumour (arrow) causing ureteric obstruction

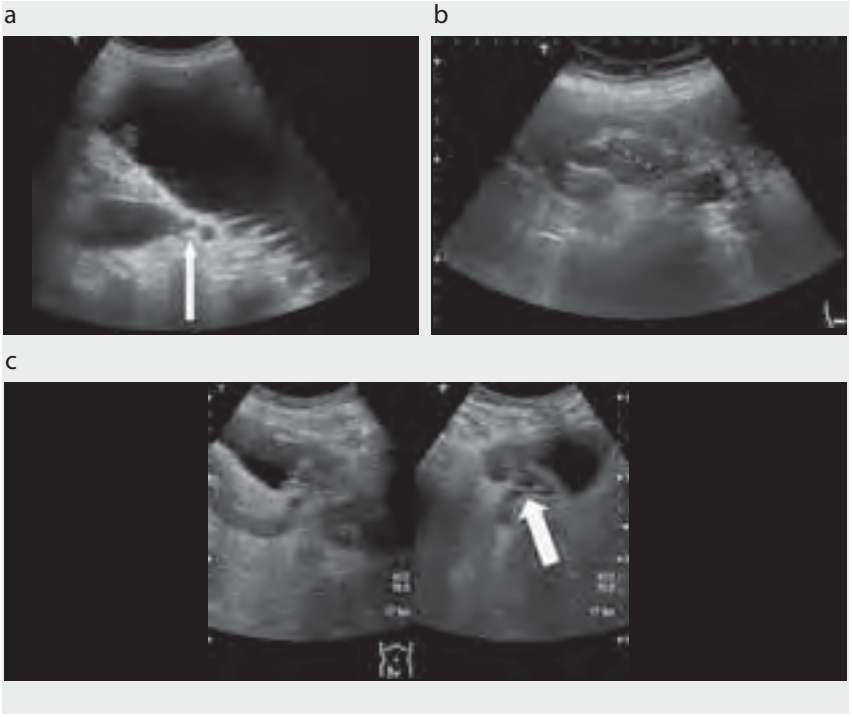

Fig. 13.56. Ureteric calculus. (a) Mid-ureteric calculus. It is echo dense with posterior shadowing, and there is dilatation of the ureter proximal to it. (b) Small calculus at the vesicoureteric junction casting a shadow

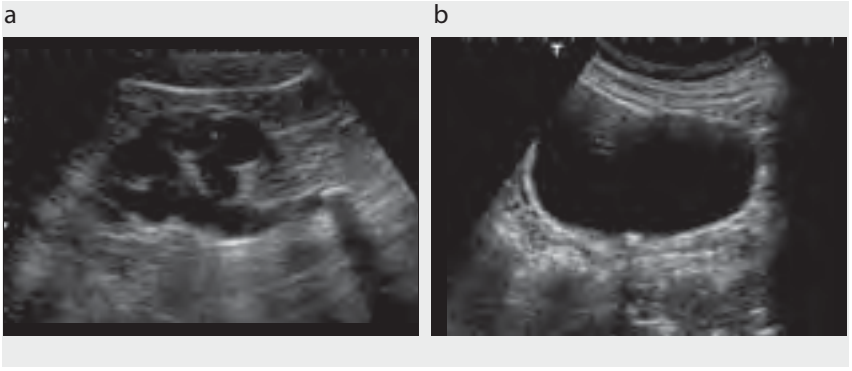

Ureterocoele

A ureterocoele is a thin-walled protrusion of the intramural portion of the ureter into the bladder lumen. In children, ureterocoeles present with symptoms of urinary tract infection or back pain due to obstruction and, in girls, less often, with incontinence. Those found in adults are usually asymptomatic and are found incidentally.

In 90% of girls and 50% of boys, a ureterocoele occurs as a duplex ureter draining the upper pole moiety of the kidney. This is often hydronephrotic, may cause back pain and may predispose to urinary tract infection.

Occasionally, a large ureterocoele fills the bladder and obstructs the outflow, and the ureter containing the ureterocoele opens into the vagina, causing urine incontinence.

Ureterocoeles appear ultrasonically as thin-walled, balloon-like structures that protrude into the bladder lumen and increase and decrease in size with ureteric peristalsis (Fig. 13.57). The ureteric jet can be visualized as it arises from the tip of the ureterocoele, from its base or ectopically.

Large ureterocoeles may fill the bladder. These are difficult or impossible to see by ultrasound. Ureteroceles can invert and lie partly or completely outside the bladder and may be misdiagnosed as diverticula (Fig. 13.58).

If a ureterocoele is found, it is important to scan the upper tracts carefully for a duplex system.

Fig. 13.57. Ureterocoele. (a) Typical thin-walled ureterocele projecting into the bladder lumen. (b) Small ureterocele on the left. The ureteric jet projects from its base, at a lower velocity than the normal jet on the right (colour flow, illustrated here in white)

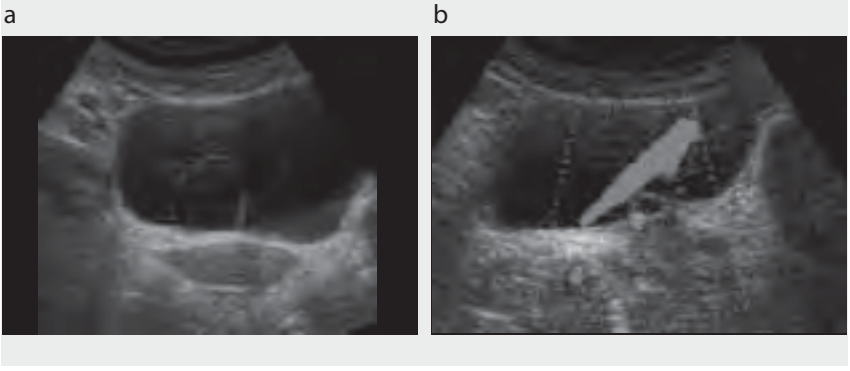

Fig. 13.58. Partly inverted ureterocoele (arrow), partly bulging out of the bladder

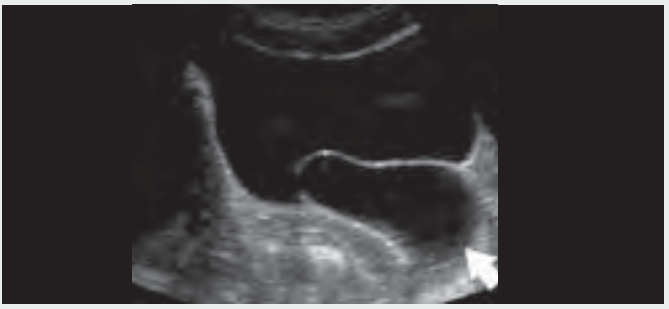

Reproduced with permission from: Cochlin DLL, Dubbins PA, Goldberg BB, Halpern EJ. *Urogenital ultrasound*, 2nd edition. London, Taylor & Francis Group, 2006. Fig. 2.25, p. 121.

Hydroureter, megaureter

Hydroureter consists of abnormal enlargement of the ureters, usually due to obstruction of flow or vesicoureteric reflux of urine into the bladder. Strictly speaking, the term 'megaureter' should be reserved for dilatation of the ureter, usually severe, due to replacement of the normal muscle tissue in the lower ureter with inactive fibrous tissue, resulting in partial obstruction due to lack of peristalsis. Some authors, however, use the term 'megaureter' for any marked dilatation of the ureter, whatever the cause. Care is therefore needed to avoid confusion. The distinction is, however, unimportant and, except for the degree of dilatation, a distinction cannot be made on the basis of imaging alone.

On ultrasound (Fig. 13.59), the upper level of a hydroureter can be seen by scanning through the lower pole of the kidney and the lower level by scanning through the bladder. The lumen is dilated, often considerably. Between these levels, a hydroureter is usually seen only when it is marked and in slim patients, although the dilated ureter is sometimes seen as it crosses the iliac vessels. Hydroureter due to vesicoureteric reflux looks similar to that due to obstruction.

Congenital megaureter, due to lack of peristalsis at the lower end of the ureter, tends to involve more dilatation than others (typically to > 7 mm in diameter, often much more) (Fig. 13.59 (c)). The ureter often becomes tortuous, so that it appears as multiple cystic structures on any single ultrasound plane, rather than as a tubular structure.

Ureteric jets and vesicoureteric reflux

Jets of urine passing from the ureters into the bladder can be seen on grey-scale ultrasound and appear to be slightly more echogenic than the rest of the urine in the bladder. The reason for this difference in echodensity is not fully understood, but it makes the jets visible. They are, however, far easier to study with colour Doppler. Much has been written about the significance of different jet patterns in obstruction and vesicoureteric reflux, but none of the techniques involved is in general clinical use.

On colour Doppler (Fig. 13.60), the ureteric jets are seen as jets of colour shooting well into the bladder. They point obliquely to the opposite side of the bladder and occur intermittently, often several minutes apart. They occur more frequently in well hydrated patients. Although easier to see on colour Doppler, they are usually easily seen

Fig. 13.59. Hydroureter. (a) Fairly marked dilatation of the upper right ureter. This degree of dilatation would normally be termed 'hydroureter'. (b) Hydroureter or (as some would term it) megaureter. (c) Definite megaureter. There is such marked dilatation of the left (LT) ureter in this case that it strongly suggests congenital megaureter

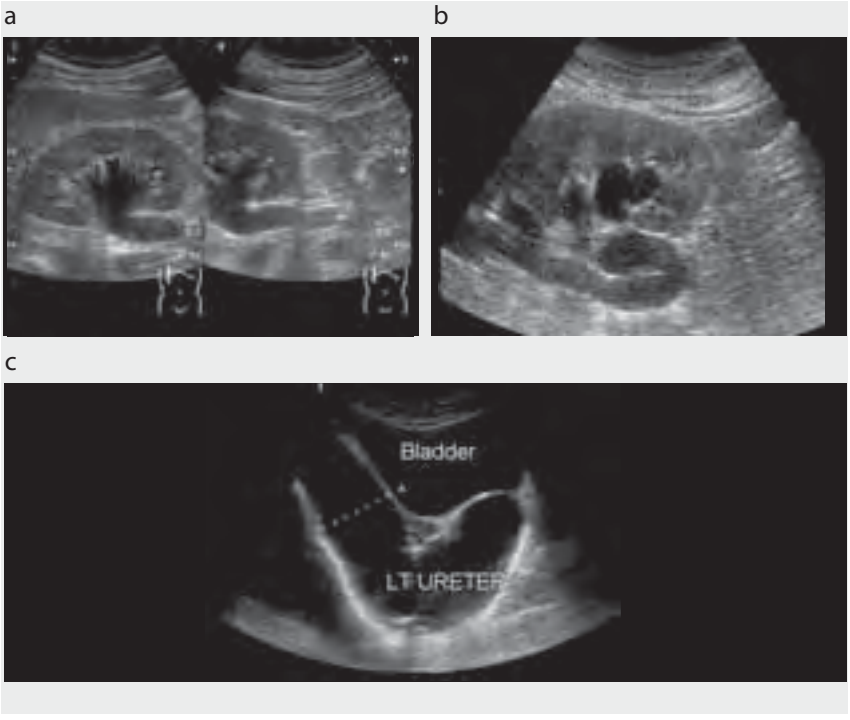

Reproduced with permission from: Cochlin DLL, Dubbins PA, Goldberg BB, Halpern EJ. *Urogenital ultrasound*, 2nd edition. London, Taylor & Francis Group, 2006. Fig. 2.27, p. 122.

Fig. 13.60. Normal ureteric jet (arrow) seen projecting into the bladder lumen at about 45° (compare with **Fig. 13.57 (b)**)

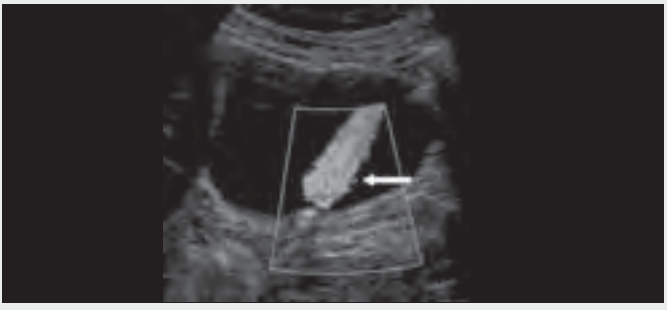

on grey-scale ultrasound. The presence of a jet excludes complete, but not incomplete, obstruction. The absence of a jet suggests, but does not prove, obstruction.

Ureteric diversions

The ureters may be diverted into various types of stoma or conduits fashioned from loops of bowel that empty through the abdominal wall. Ultrasound can be used to investigate the resultant dysfunction or complications by assessing the upper urinary tract for dilatation. In the region of the stoma or conduit, interpretation is difficult. A fluid-filled conduit may sometimes be seen, as may an abscess adjacent to the conduit. In general, however, use of ultrasound is disappointing for investigating ureteric diversions.

Retroperitoneal pathological conditions affecting the ureters

As the ureters run a retroperitoneal course throughout most of their length, any retroperitoneal pathological condition may affect them, usually causing obstruction. The principal causes are retroperitoneal fibrosis, retroperitoneal tumours and inflammatory conditions such as a psoas abscess.

Fibrosis

Retroperitoneal fibrosis is a tumour-like proliferation of fibrous tissue into the retroperitoneal space. About 68% of cases are idiopathic, probably caused by an autoimmune response to lipid leaking from damaged atheromatous vessel walls. This conclusion is supported by the frequent association with an atheromatous or aneurysmal aorta and other autoimmune conditions. Retroperitoneal fibrosis can occur secondary to local inflammation caused by urine, blood, inflammatory abdominal aortic aneurysm or surgery. Malignancy, such as lymphoma or metastatic lymphadenopathy, can also be responsible, as may certain drugs, radiotherapy and chemotherapy.

Retroperitoneal fibrosis is often not seen sonographically, but the effects commonly include ureteric obstruction, which can be visualized. In good-quality images of the retroperitoneum, retroperitoneal fibrosis can be seen as a smooth medium echo-density mass surrounding the aorta and vena cava (Fig. 13.61). There are often hydronephroses. On ultrasound, much or all of the retroperitoneum is often obscured by the bowel, and CT is a far more reliable method for imaging the peritoneum. Excretion urography may show medial deviation of the ureters and hydronephrosis.

Fig. 13.61. Retroperitoneal fibrosis. (a) Transverse scan, (b) longitudinal scan. A medium echo-density band of tissue can be seen around the atheromatous aneurysmal aorta (arrow)

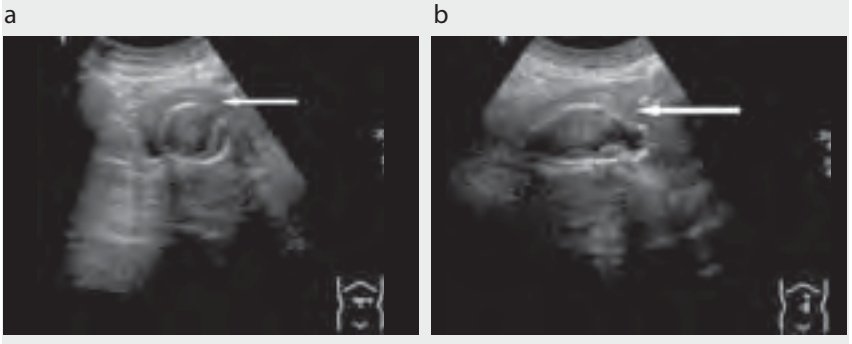

Tumours

Metastatic lymphadenopathy and lymphoma are the commonest tumours after those of the solid organs. Retroperitoneal tumours, including lymph nodes involved in metastatic tumours, can cause ureteric obstruction by direct involvement or an associated desmoplastic reaction. (Lymphoma nodes do not cause obstruction.)

On ultrasound (Fig. 13.62), the retroperitoneum is often obscured by the bowel, but retroperitoneal tumours can be seen in slim patients with little bowel gas. As for retroperitoneal fibrosis, CT is more reliable than ultrasound for imaging retroperitoneal tumours.

Most retroperitoneal tumours are nonspecific, medium echo-density masses. Lobulation suggests nodal masses. Lymphoma nodes are characteristically echo poor and do not cause ureteric obstruction. Sarcomas are uncommon and are normally large at presentation. They have a variable appearance, depending on their subtype and how well differentiated they are (see section on Retroperitoneal space in Chapter 6).

Fig. 13.62. Retroperitoneal tumour (a mass of lymph nodes involved with secondary deposits) has caused a lobulated mass obstructing both ureters

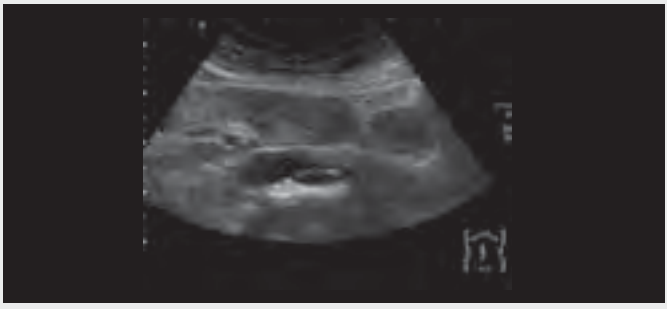

Haemorrhage

Retroperitoneal haemorrhage is commonly iatrogenic in developed countries, secondary to angiography due to femoral artery puncture, renal biopsy or use of anticoagulants. Other causes are trauma, ruptured abdominal aortic aneurysm and haemorrhage from a renal angiomyolipoma.

Retroperitoneal haemorrhage is usually difficult to detect by sonography (Fig. 13.63; see also Fig. 6.27), but the underlying cause may be identified. CT is the best modality, as the psoas muscle outline is lost on an abdominal X-ray.

Infection

Apart from infections in retroperitoneal organs, psoas abscesses are the most commonly found retroperitoneal infections. They may be secondary to spinal or urinary infection, classically tuberculosis, or to a gastrointestinal cause, such as diverticulitis.

On ultrasound (Fig. 13.64), psoas abscesses are often obscured by bowel gas when an anterior approach is used. Pressing hard with the transducer may displace the gas, although this may be painful if an abscess is present. Psoas abscesses can be seen when the scan is made from a posterior approach or because they extend into the groin. They

Fig. 13.63. Retroperitoneal haemorrhage

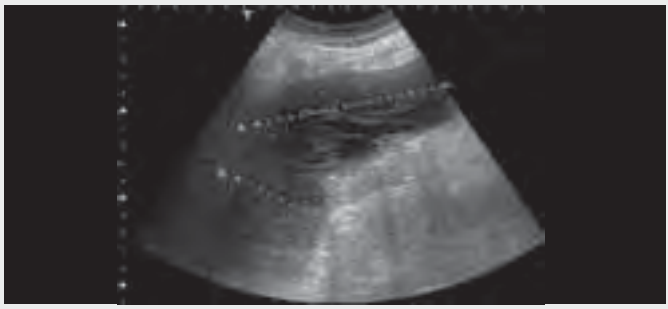

Fig. 13.64. Psoas abscess. (a) Longitudinal (arrow) and (b) transverse views

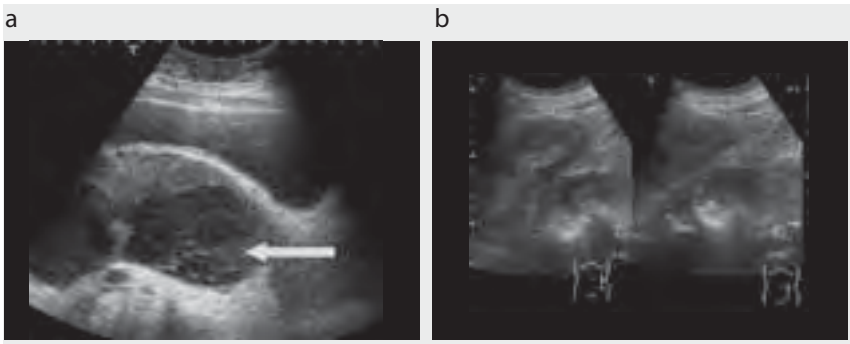

Fig. 13.65. Pelvic tumour. This large ovarian tumour (arrow) obstructed both ureters

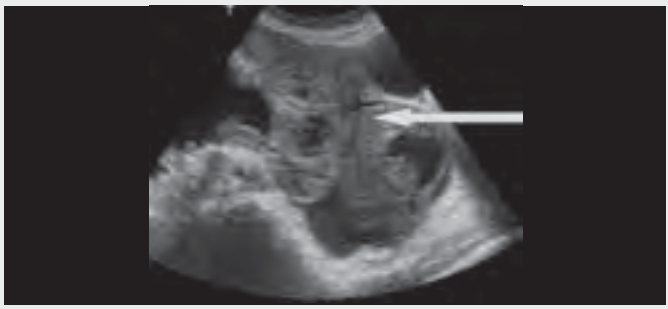

commonly contain fluid and gas, making them difficult to detect sonographically. The gas may be seen as areas of shadowing but is often mistaken for overlying bowel gas. The psoas muscle is swollen and the lines representing the muscle structure disrupted. An abscess cavity containing variably echodense fluid (pus) may be visible.

Pelvic tumours

Pelvic tumours cause ureteric obstruction (Fig. 13.65; see also Fig. 6.29). They are discussed in Chapter 6.

Differential diagnoses

Differential diagnoses of pathological conditions of the kidneys and ureters are listed in Table 13.1.

Pitfalls and pearls

Obstruction

Watch out for:

- renal sinus cysts;
- extra-renal pelvis;
- chronically dilated non-obstructed system;
- Acute obstruction: non-dilated system but absent ureteric jet, increased resistance index.

Calcification

Watch out for:

- Small calculi or small angiomyolipoma with no acoustic shadow
- Collecting system gas: need abdominal plain radiography or CT for confirmation.

Trauma

Ultrasound is less sensitive and less specific than CT. If CT is not available, intravenous pyelography confirms functioning kidneys.

Retroperitoneum

Ultrasound is less sensitive than CT.

Table 13.1. Differential diagnoses of pathological conditions of the kidneys and ureters

Diagnosis	Comments
Apparently absent kidney	
Ectopic kidney	
End-stage kidney atrophy	Small kidney with echogenicity similar to that of surrounding faty
Developmental abnormality	
Large kidney	
Unilateral	
Compensatory hypertrophy	
Obstructed	
Congenital fusion abnormality	
Tumour	
Cystic disease	
Inflammatory	Nephropathy, pyelonephritis, acute tubular necrosis
Vascular	Renal vein thrombosis
Bilateral	
Any unilateral cause	
Cysts (autosomal dominant polycystic kidney disease)	
Infiltrative tumours	Lymphoma
Protein deposition	Amyloid and myeloma
Small kidneys	
Unilateral	
Congenital	Dysplastic or hypoplastic
Atrophy	Post-obstructive, ischaemic end-stage kidney in chronic renal failure
Bilateral	
End-stage kidneys in renal failure	
Renal mass	
Cystic	
Benign cysts	
Complex cysts	
Cystic tumours	
Hydronephrosis	
Infective	Abscess, hydatid
Vascular	Aneurysm, flow on colour Doppler
Solid	
Congenital	Fusion anomaly
Pseudotumours	Splenic hump, hypertrophied septa of Bertin, focal compensatory hypertrophy
Tumours	Benign, malignant
Infection	Abscess, lobar nephronia, xanthogranulomatous pyelonephritis
Vascular	Haematoma

Table 13.1. *continued*

Diagnosis	Comments
Hyperechoic renal mass	
Calcification	
Tumour	Renal cell carcinoma, acute myelogenous leukaemia
Inflammatory	Nephritis
Vascular	Infarct
Infection	Fungal ball
Diffusely echogenic kidney	
Inflammatory	Glomerulonephritis, glomerulosclerosis, HIV nephropathy, acute tubular necrosis
End-stage kidney	
Calcification	
Hypoechoic renal mass	
Renal cyst	
Tumour	Renal cell carcinoma, metastasis, lymphoma
Infection	Lobar nephronia, abscess
Vascular	Haematoma, infarct
Trauma	Urinoma
Diffusely hypoechoic kidney	Right kidney may appear hypoechoic in the presence of an echogenic liver
Renal calcification	
Nephrolithiasis	
Nephrocalcinosis	
Tumour	Renal cell carcinoma
Infective	Tuberculosis, hydatid disease or cyst
Vascular	Aneurysm, calcified haematoma
Renal sinus mass or filling defect	
Calculus	
Renal sinus cyst	
Tumour	Transitional cell carcinoma, renal cell carcinoma, squamous cell carcinoma, benign polyp
Vascular	Clot
Infection	Fungal ball
Inflammatory	Sloughed papilla

Chapter 14

Urinary bladder, urethra, prostate and seminal vesicles and penis

14

Urinary bladder, urethra, prostate and seminal vesicles and penis

Urinary bladder

Indications

The indications for ultrasonography of the urinary bladder are:

- to assess bladder emptying in cases of suspected bladder outlet obstruction;
- to look for tumours in cases of macroscopic haematuria;
- to look for a predisposing cause of urinary tract infection, such as calculus, diverticulum or poor emptying.

Examination technique

Equipment, transducer

A standard transducer used for abdominal scanning, such as a 3- to 5-MHz curved linear, is appropriate.

Preparation

The bladder can be properly assessed only when it is full. Patients should drink 1 litre of fluid per hour before the examination and not empty their bladders. For some patients, however, this is not practical. For example, patients with incontinence might not be able to retain a full bladder, and those with renal failure might fill their bladder very slowly. In such cases, compromise is necessary, and patients should be instructed to attend with as full a bladder as possible.

For patients with urinary catheters, the catheter should be clamped 1 h before the examination, and the patient should drink 1 litre of fluid. If, for whatever reason, the bladder of a catheterized patient is not full, it can be filled by instilling sterile water through the catheter. Great care must be taken not to introduce any air, which will cause shadowing artefacts on the scan; however, even when care is exercised, some air is often introduced.

Position of the patient

The patient should be in the supine position.

Scanning technique

The bladder is scanned from an anterior approach, with the transducer just above the pubic symphysis. The bladder is scanned in both axial and sagittal planes, sweeping through the bladder in an arc. In the axial plane, the transducer is swept from cephalad to caudad to include the whole bladder. To examine the bladder base and the prostate, the transducer should be moved cephalad to the dome of the bladder, receive some pressure and then be angled so that the scan plane passes behind the pubic symphysis. In the sagittal plane, the transducer is initially placed in the midline and then swept in an arc to both sides to ensure that the whole bladder is examined.

The lateral walls of the bladder may be difficult to visualize, as the transducer beam is often tangential to them. To overcome this, the transducer is moved to the opposite side and then angled steeply towards the wall being examined. Visualization of the anterior wall is difficult for various reasons. It is close to the transducer and, unless the settings are changed, is often not in the maximal focal zone. Also, as it is parallel to the skin surface, marked reverberation artefacts usually degrade the image. The focus and gain settings must be optimized to minimize these effects.

The technique explained above may appear complicated. In practice, ultrasound of the bladder is straightforward, provided the operator takes basic steps to ensure that every part is shown as well as possible. Careful technique is particularly important when looking for tumours.

Normal findings

The normal bladder is a fluid-filled structure with a volume when full of about 500 ml. The contents are largely anechoic, although there is usually a band of increased echodensity due to reverberation artefact across the anterior part. With high-resolution systems, very small speckles may be seen within the urine. If they are excessive, they suggest poor bladder emptying, infection or haematuria.

The bladder may be thought of as a roughly ovoid structure, although the shape varies with distension and with pressure from adjacent organs, becoming more of a rectangle in the transverse plane, particularly in women, and pyramidal in the sagittal plane.

The adjacent organs depend on the sex of the patient. In males, the prostate and seminal vesicles may be at the bladder apex and the rectum at the posterior. In females, the uterus and ovaries lie posterior to the bladder. These are the only important anatomical relations.

The thickness of the normal bladder wall is about 3 mm for a full bladder and 5 mm for a non-distended bladder. The wall has four anatomical layers: the mucosa, submucosa, muscularis and serosal layers. There is also a layer of perivesical fat, which may appear as part of the wall on the ultrasound image.

Ultrasound appearance

Ultrasonically, the wall is often seen as a single, medium echodense band with no distinction between the layers. With high-definition systems, three layers can often be

identified. The mucosa appears as a highly echo-rich line, the muscularis layer as an echo-poor line and the serosal layer, often together with the perivesical fat, as a highly echo-rich line (Fig. 14.1).

The definition depends on the system being used, the build of the patient and what part of the bladder wall is being examined. The separate layers of the bladder wall are not seen with sufficient reliability to stage bladder tumours accurately, although in the absence of access to magnetic resonance imaging (MRI) or CT, a good guess can be made at local staging (see also Fig. 14.19). Nodal staging is not possible by ultrasound.

Fig. 14.1. Normal bladder. (a) Longitudinal and (b) transverse views showing a thin wall with the separate layers barely visible and almost anechoic contents. (c) In this case, the wall is seen as three separate layers anteriorly

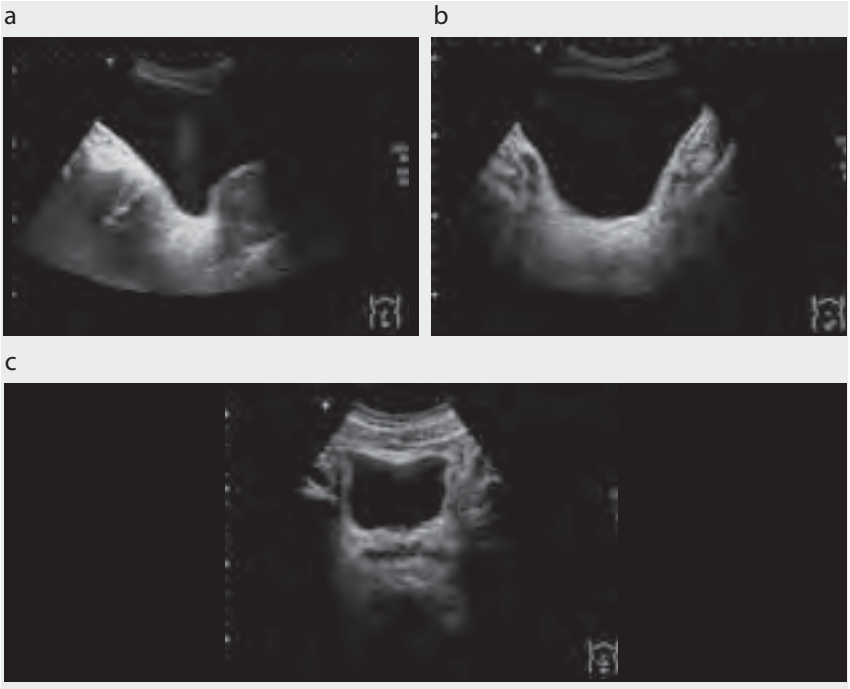

Pathological findings

Functional disorders

Micturition disorders (poor bladder emptying)

Assessment of bladder emptying is the commonest reason for an ultrasound study of the bladder. Poor emptying may be due to various causes.

- Primary bladder dysfunction is often associated with prostatic hypertrophy in older men. It is debatable whether prostatic hypertrophy alone causes outlet obstruction, but it may be the cause of dysfunction. Primary bladder dysfunction may occur in either sex.
- Neurogenic bladder may be caused by injury or multiple sclerosis, spina bifida and several less common causes.

- In young boys, urethral valves may cause outlet obstruction.

Whatever the cause of outlet obstruction, assessment of bladder emptying is often necessary for management decisions.

In an ultrasound study, the upper tracts (kidneys and ureters) are always examined at the same time as the bladder, primarily to assess hydronephrosis or scarring. The bladder is examined full. It is important to fill the bladder well, as a falsely high post-micturition residue may result with a half-full bladder. The reason for imaging the full bladder is primarily to check that it is sufficiently full for the post-micturition study, but other pathological signs may be seen. In outlet obstruction, a thick muscularis layer may be found, often showing the irregular pattern of trabeculation, with projection of the muscle bundles into the lumen (Fig. 14.2). This should not be confused with a polypoidal tumour. Generalized trabeculation is not usually a diagnostic problem, but trabeculation is sometimes focal and may look like a tumour. Conversely, in the presence of trabeculation, it is difficult to exclude small tumours. The presence of trabeculation indicates that the outlet obstruction is longstanding.

The appearance of a neurogenic bladder varies with the level of the neurological lesion. In general, spinal lesions result in hypertrophy with trabeculation, which occurs at various times after the onset of the condition. Cerebral lesions usually result in a thin-walled, distended bladder.

Fig. 14.2. Trabeculated bladder, with bundles of mucosa-covered hypertrophied muscle on the posterior wall. Trabeculation is often more marked and better visualized on the posterior wall

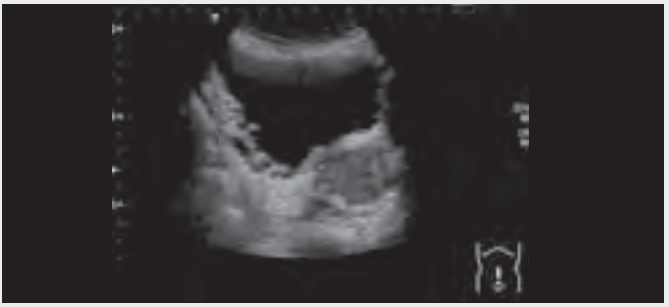

The second step is to assess the bladder after micturition. Patients should be instructed to empty their bladder as usual. For instance, if double micturition is their normal practice, they should do this. In patients who self-catheterize, a post-catheter residue is sometimes requested. Patients should be scanned with minimal delay after micturition as the bladder immediately starts to refill.

The post-micturition residue is assessed by measuring the bladder diameter from front-to-back, side-to-side and head-to-feet, keeping the measurements at approximately right angles to each other. The three diameters are multiplied together and then multiplied by $\pi/6$ ($\pi/6 = 0.52$) (Fig. 14.3). This estimate is based on the assumption that the bladder has an even, ovoid shape. This is not true in all patients. In practice, clinical assessment requires not a highly accurate measurement but rather an approximate

figure on which management can be based. The method outlined will achieve this even for a very irregular bladder, such as one that has been surgically augmented.

Theoretically, the normal bladder should empty completely after micturition. In practice, a residue of less than 20 ml in an adult and 10 ml in a child is accepted as normal or at least as clinically insignificant.

Fig. 14.3. Estimation of post-micturition residue. The bladder has been measured in three orthogonal planes and the volume calculated.

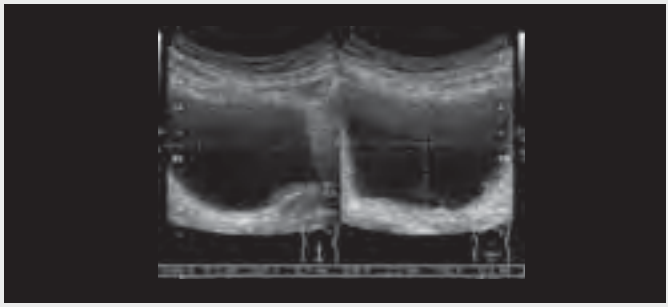

Cystitis

Cystitis is inflammation of the bladder, which can be caused by infection, mechanical or other irritation, toxic bladder contents, allergy or radiotherapy:

- bacterial infections: *Escherichia coli*, *Streptococcus aureus*, *Streptococcus faecalis*, tuberculosis; less commonly: *Proteus* spp., *Pseudomonas aeruginosa*, malakoplakia;
- iatrogenic infections: instillation of bacillus Calmette-Guérin vaccine (BCG) for treatment of bladder cancer.
- protozoal infection: schistosomiasis;
- fungal infections: *Candida*, actinomycoses;
- viral infections: *herpes, adenovirus*;
- non-infectious causes: foreign body, such as catheter, stent, self-inserted object, calculus;
- adjacent causes: pelvic inflammatory disease, inflammatory bowel disease;
- toxic drugs: cyclophosphamide, other chemotherapeutic drugs;
- allergy: interstitial, eosinophilic;
- radiotherapy.

Cystitis is diagnosed from the patient's history and from bacteriological examination of the urine. Nevertheless, the ultrasound appearance (Fig. 14.4) should be recognized, as some views may mimic other pathological conditions, principally bladder cancer. In many cases of cystitis, the bladder appears ultrasonically normal. There may be diffuse thickening of the bladder wall or focal thickening, in which some parts of the wall are thicker than others and the rest of the bladder appears normal. These cases may be misinterpreted as tumours. The safe option is cystoscopy, but an alternative is a follow-up scan after appropriate treatment. Any residual thickening requires cystoscopy, as, even in proven cystitis, there may be a coexisting cancer. These

appearances may occur in association with any of the causes of cystitis listed above. In some types of cystitis, however, there may be additional or different appearances, as discussed below.

Fig. 14.4. Cystitis. (a) Generalized echogenic thickening of the mucosa and hypoechoic submucosal oedema. (b) Generalized mucosal thickening, more marked on the posterior wall. (c) Focal cystitis. (d) Focal cystitis causing a mass simulating a tumour. Diagnosis was made by cystoscopy and biopsy

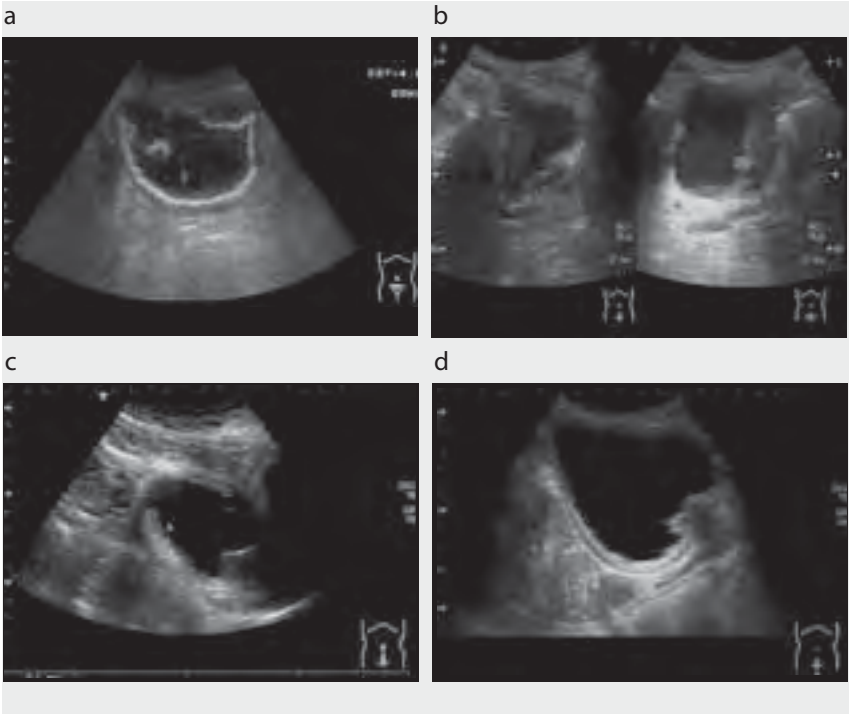

Fungal cystitis

Fungal cystitis occurs in immunocompromised patients. The diagnosis is made by finding mycelia in the urine. On ultrasound, there may be fungal balls within the bladder or in the dilated upper tracts. These appear as medium echodensity, rounded or lobulated masses with no shadowing. Those in the bladder are mobile (Fig. 14.5).

Schistosomiasis

Schistosomiasis (bilharzia) is caused by a parasitic worm. In the urinary tract, it mainly affects the lower ureters, leading to obstruction and renal failure, and the bladder, causing cystitis. The ultrasound appearance of acute cases is similar to that of bacterial cystitis. Chronic schistosomiasis causes a thick-walled bladder. In early cases the wall is non-calcified. In chronic cases there is usually linear or punctuate calcification, appearing as highly echogenic foci casting shadows. By the time the bladder wall is thickened, the lower ureters are almost invariably strictured by hydronephroses. There are often calculi in the bladder (Fig. 14.6).

Squamous cell cancers are a common complication of chronic schistosomiasis. Ultrasound is a cheaper and less invasive alternative to cystoscopy in surveillance for tumours. It must be accepted, however, that an ultrasound study is significantly less sensitive than cystoscopy, particularly in the detection of small tumours.

Fig. 14.5. Fungal cystitis. (a) Two balls in the bladder, which were mobile when the patient was turned. (b) In the same patient, a fungal ball is present in the dilated calyceal system.

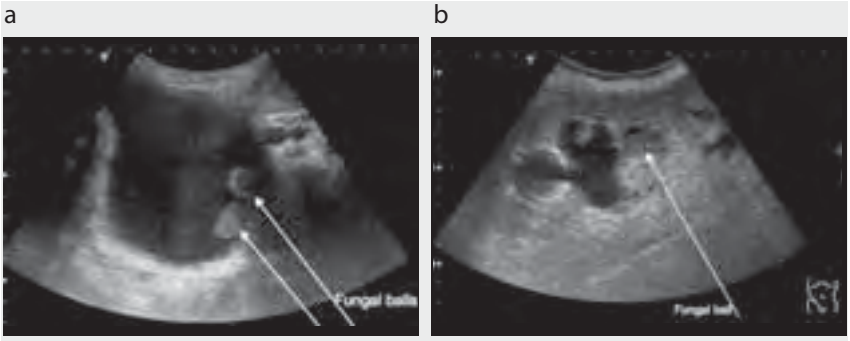

Fig. 14.6. Schistosomiasis. Transverse scan of the bladder of a 12-year-old child, with thickening and irregularity of the wall (arrows)

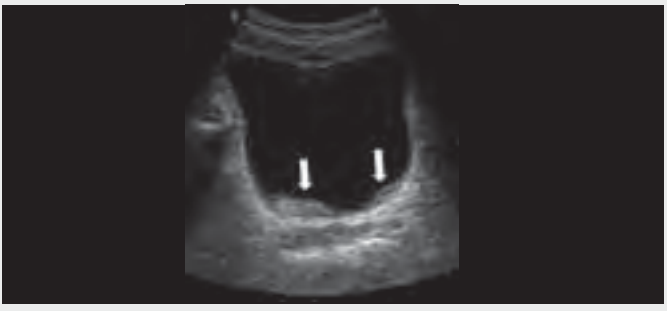

Tuberculosis

Urinary tract tuberculosis affects primarily the kidneys but may spread to the lower ureters and bladder. It is a common complication of AIDS. Instillation of BCG into the bladder for the treatment of bladder tumours may also result in cystitis, similar to that caused by tuberculosis. Bladder tuberculosis spreads from the kidney and is therefore accompanied by the renal changes described in Chapter 13. Early cases have an ultrasound appearance similar to those in pyogenic infections and other causes of cystitis. There may be focal or generalized wall thickening.

In late cases, the wall becomes markedly thickened and fibrotic, resulting in a thick-walled, nondistensible bladder. There are often areas of linear calcification within the wall, causing shadowing (Fig. 14.7). Fibrosis of the ureteric orifices holds them open, resulting in the vesicoureteric reflux and ureteric dilatation.

Fig. 14.7. Chronic tuberculous cystitis. The patient could not fill the bladder any further. The bladder is small and thick-walled, with echogenic areas of calcification

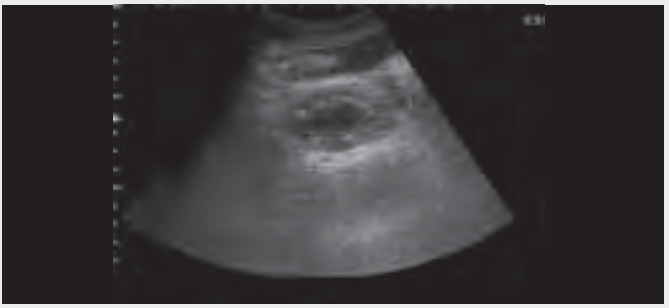

Emphysematous cystitis

This is a form of cystitis found particularly in patients with diabetes, in whom any pyogenic bacteria, but usually *Escherichia coli*, cause fermentation in the bladder wall, with release of gas (carbon dioxide and hydrogen), which tracts between the layers of the bladder wall. It is often associated with retention of urine. The gas causes shadowing on the ultrasound. In some cases, the shadowing is intermittent, and it is clear that there is gas within the bladder wall. The differential diagnosis in such cases is calcification due to tuberculosis. In cases where the shadowing is more intense, the ultrasound appearance may be more difficult to interpret; it is easy to misinterpret the image as an empty bladder with shadowing from bowel gas. In all cases, a plain X-ray provides a clear diagnosis (Fig. 14.8).

Fig. 14.8. Emphysematous cystitis. (a) The ultrasound scan shows shadowing, which was interpreted as bowel gas with an empty bladder. (b) A plain X-ray clearly demonstrates that the shadowing is due to gas in the bladder wall.

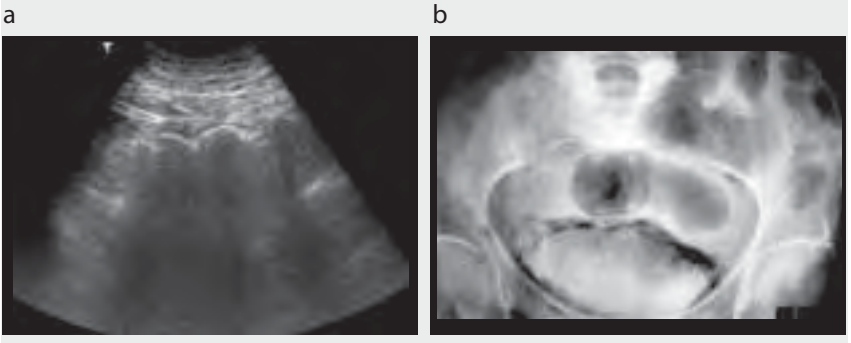

Malakoplakia

Malakoplakia is a rare form of cystitis occurring in immunocompromised patients. Incomplete phagocytosis or bacteria cause yellow plaques on the bladder wall. Malakoplakia plaques are ultrasonically identical to flat bladder tumours (Fig. 14.9). A diagnosis can be made only by cystoscopy and biopsy.

Fig. 14.9. Malakoplakia. A shallow mass in the bladder mucosa. The appearance could not be distinguished from a tumour; diagnosis was made by cystoscopy and biopsy.

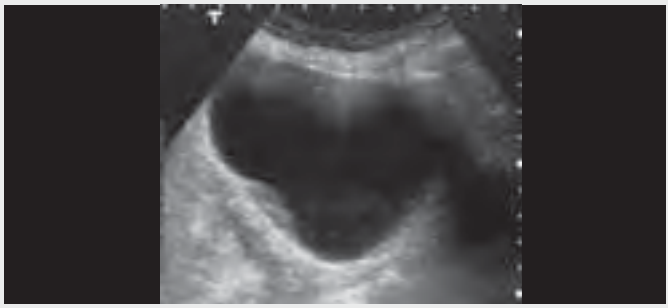

Catheter or foreign body cystitis

An indwelling bladder catheter, stent or other foreign body can cause mechanical cystitis. Infective cystitis is also commoner in catheterized patients. Mechanical cystitis typically causes focal wall thickening at the point at which a catheter or other object touches or irritates the opposite bladder wall. Generalized thickening may also occur. The catheter, stent or other foreign body may also be seen on ultrasound (Fig. 14.10).

Fig. 14.10. Catheter cystitis. Mucosal thickening in the posterior wall where the catheter balloon touches the wall

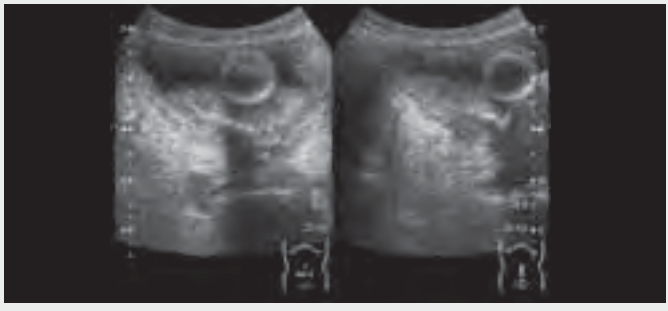

Cyclophosphamide cystitis

The breakdown products of several chemotherapeutic agents, but particularly cyclophosphamide, are excreted in the urine and may cause haemorrhagic cystitis. Other agents are usually given to minimize this, but cystitis may still occur. On ultrasound, the bladder wall is thickened and usually contains medium echodense blood clots. Sometimes, calcifications in the bladder wall caused shadowing (Fig. 14.11).

Fig. 14.11. Cyclophosphamide cystitis. Generalized, irregular mucosal thickening due to haemorrhagic cystitis. The cause can be found only from a history of cyclophosphamide treatment.

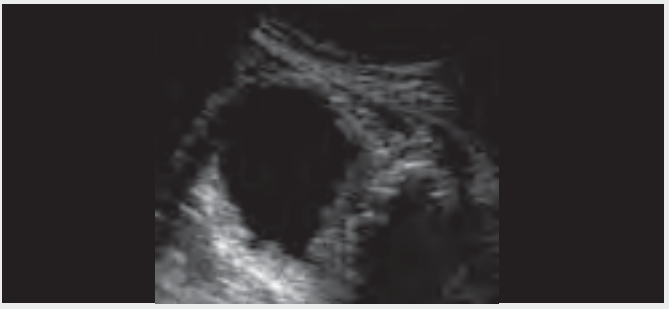

Tumours

Most bladder tumours are malignant transitional cell cancers or benign papillomas, which are usually small. The common malignant tumours are transitional cell cancer and squamous cell cancer, while less common malignant tumours include adenocarcinoma, small cell cancer (carcinosarcoma), sarcoma and lymphoma (the last two in the paediatric age group). The common benign tumours of the bladder are leiomyoma and fibroepithelial polyp; less common types are haemangioma, adenoma and phaeochromocytoma (endometrioma).

With a few exceptions, tumours cannot be distinguished from each other. Benign tumours are usually small, although small tumours may also be malignant; large tumours are likely to be malignant. Endometriomas are often associated with pelvic endometriomas and may give the characteristic symptom of haematuria, occurring only at the menses. Tumours in adjacent organs, particularly the uterus, prostate or bowel, may invade the bladder.

Ultrasound is less sensitive than cystoscopy for the detection of bladder tumours, and its sensitivity is lower for small and flat tumours. Nevertheless, recent studies have shown a sensitivity of 80–95% with high-resolution equipment. It has been suggested that real-time three-dimensional (four-dimensional) ultrasound improves the sensitivity, but this has not been proven. Meticulous technique, as outlined earlier in the chapter, is vitally important for high sensitivity.

On ultrasound, most small tumours are similar whatever their pathology. They appear as medium echodense masses protruding into the bladder (Fig. 14.12).

Larger tumours have various appearances and can be classified by their shape (Table 14.1).

Fig. 14.12. Small superficial bladder tumour, which could not be categorized ultrasonically. At cystoscopy and histology, it was found to be a papilloma

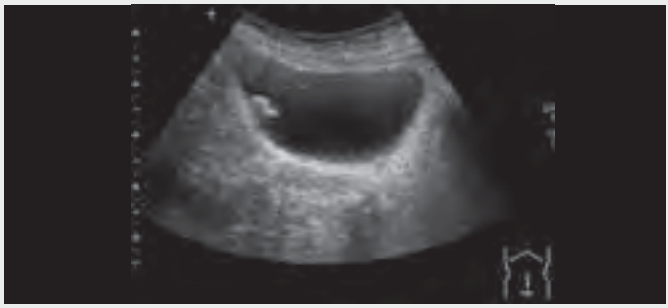

Table 14.1. Classification of bladder tumours by shape

Small flat	Often not visible on ultrasound
Polypoidal	Broad-based, narrow stalk or frond-like
Ellipsoid	Smooth or irregular surface
Massive	Usually lobular outline
Obliterans	Obscures the normal bladder anatomy
Infiltrating	Spreads into or through the bladder wall, but this pattern may be found with most of the other patterns

This classification adds little to the histological characterization of tumours and merely emphasizes the wide variation in appearance that may be found (Fig. 14.13).

Differential diagnosis

Ultrasound cannot differentiate the histological nature of bladder tumours. In a trabeculated bladder, the mucosa-covered hypertrophied muscle protrudes into the lumen. If these protrusions are focal, these may be mistaken for a tumour (see Fig. 14.2). Conversely, small tumours may not be detected ultrasonically in the presence of trabeculation.

The surface of tumours can become encrusted with minerals. These tumours are very echodense and cast a shadow (Fig. 14.14); they may be misdiagnosed as bladder calculi. The diagnosis is made by moving the patient into different positions, which usually causes a calculus to change its position. Calculi may, however, be reluctant to move, and quite extreme, prolonged changes in the patient's position may be necessary.

An enlarged prostate, particularly in benign prostatic hypertrophy, may indent the bladder, simulating a tumour (Fig. 14.15). The nature of the lesion is usually clear from its continuity with the prostate, and, if good resolution is possible, the intact bladder mucosa may be seen to cover its surface. Sometimes, however, particularly in irregular prostate enlargement, it may be difficult to distinguish prostatic indentation from a bladder tumour. It should be remembered that prostatic hypertrophy and bladder tumours are both common and may coexist in the same patient (Fig. 14.16).

Fig. 14.13. Bladder tumours. (a) Flat tumour. (b) Polypoidal tumour. (c) Ovoid tumour. (d) Massive tumour. (e) Tumour obliterans; the lumen is virtually obliterated leaving room only for the catheter balloon.

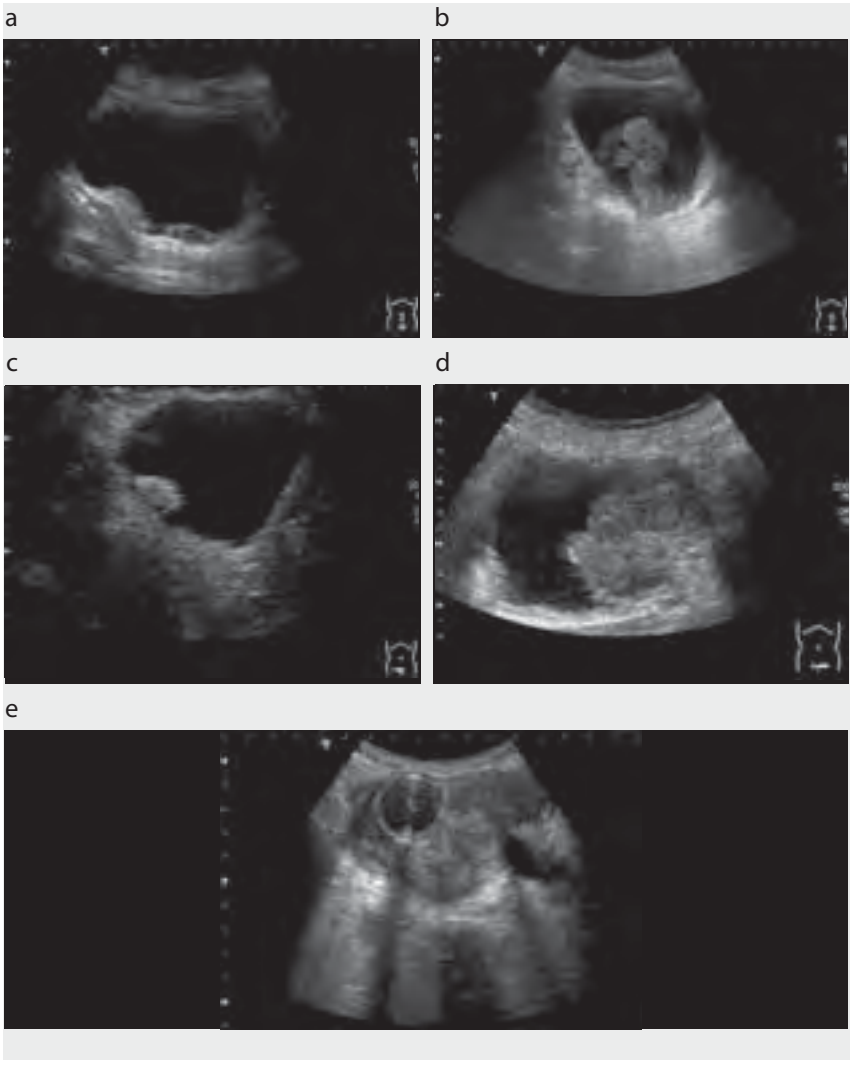

Fig. 14.14. Encrusted bladder tumour. The encrusted salts on the surface of the tumour cause shadowing, simulating a bladder calculus. The mass was not, however, mobile when the patient was turned

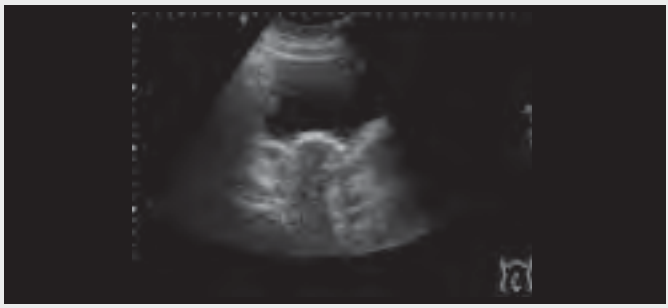

Fig. 14.15. Prostate enlargement. Benign enlargement of the so-called median lobe, which is indenting the bladder base, simulating a tumour

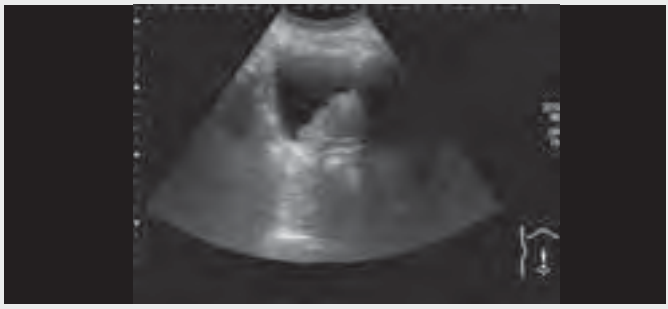

Fig. 14.16. Prostate enlargement with coexisting tumour. The indentation at the bladder base is due to prostatic hypertrophy. The mass in the posterior wall is the coexisting tumour

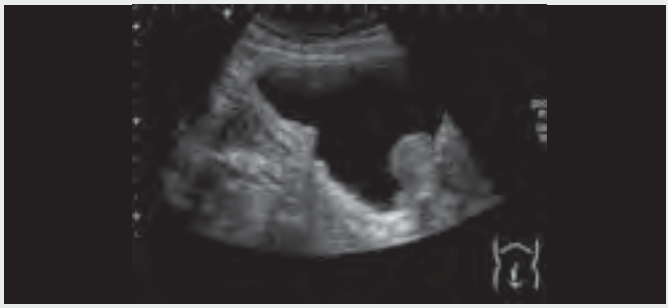

A blood clot within the bladder can simulate a tumour (Fig. 14.17). This is a particularly difficult problem, as a blood clot may overlie a causative bladder tumour. It is sometimes useful to use colour Doppler: if blood vessels are seen in part of the mass, it must represent tumour. Conversely, failure to find blood vessels does not exclude a tumour. Short-term follow-up scans may help, as blood clots usually change, while tumours do not. In practice, however, in the presence of unexplained haematuria, cystoscopy is usually used to make a diagnosis.

Tumours may arise within a diverticulum and appear as filling defects adjacent to the bladder (Fig. 14.18).

There is often a fold across the posterior wall of the bladder, which may look like a tumour in some views (Fig. 14.19). Different planes will show that it is a fold rather than a tumour.

Tumours in adjacent organs, particularly the uterus, prostate or bowel, may invade the bladder. A diagnosis can be made if their continuity with the organ of origin is demonstrated (Fig. 14.20). This is not always possible.

Fig. 14.17. Blood clot causing a mass effect which simulated a tumour. It had cleared on a follow-up scan

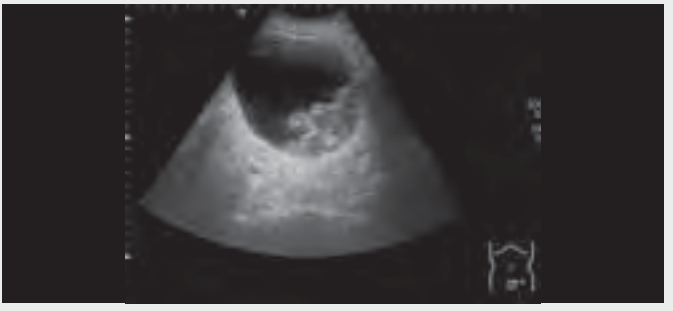

Fig. 14.18. A tumour in a bladder diverticulum and a mass in the diverticulum extending through the neck into the bladder. The diverticular mass was a transitional cell carcinoma, while the mass extending through the neck was a blood clot

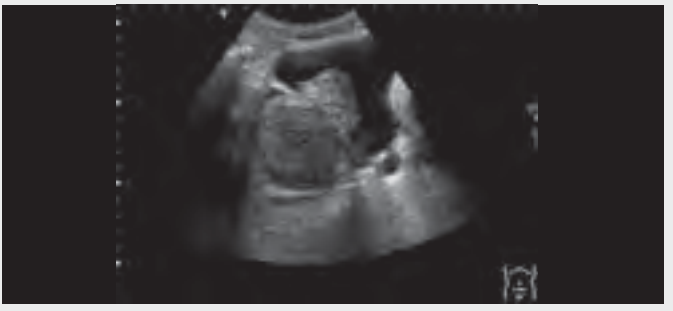

Fig. 14.19. Bladder fold. The indentation into the bladder could, at first glance, be interpreted as a tumour. On closer inspection, it is clear that all layers of the wall are present in the indentation, making it a fold

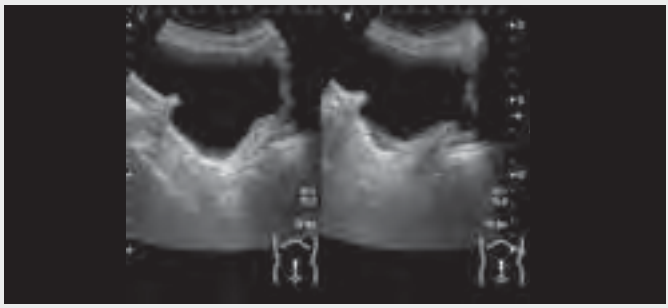

Fig. 14.20. Uterine tumour invading the bladder. Continuity of the tumour with the uterus provides the diagnosis

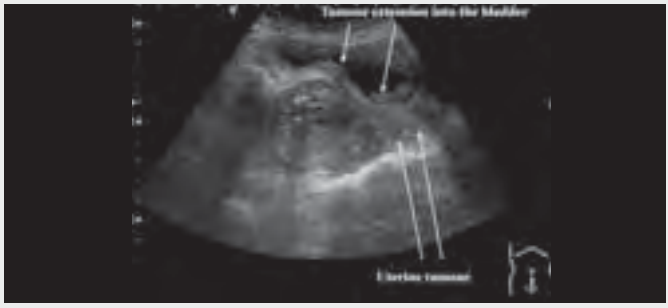

Fig. 14.21. Endometrioma. (a) Longitudinal scan, (b) transverse scan. The tumour lies in the muscularis layer with intact mucosa over it. Co-existing pelvis endometriomas are often found, although none were visible in this case

a

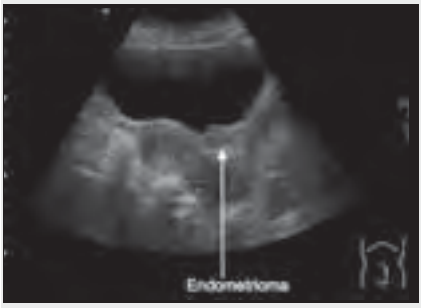

b

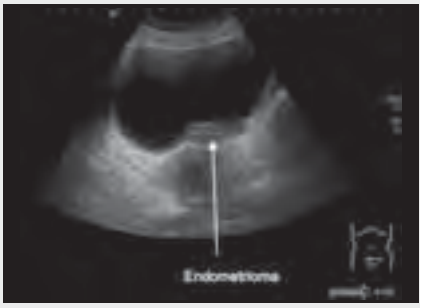

Endometrioma can occur in the bladder wall, often associated with pelvic endometriomas. Ultrasonically, they can be seen to lie in the muscularis layer rather than arising from the epithelium (Fig. 14.21).

Staging of bladder tumours

Bladder tumours must be staged to allow planning of treatment. For small tumours, histological examination of a cytoscopically excised tumour gives both the tumour type and the stage, provided that some of the underlying muscularis layer is included in the biopsy. For larger tumours, MRI or CT may be used to assess nodal status. As this is not possible with ultrasound, it is usual to use one of these modalities for both nodal and local staging. MRI is superior for local staging.

Usually, therefore, ultrasound is not used in staging. If, however, for any reason, such as lack of access to CT or MRI, staging must be assessed by ultrasound, it may be assessed significantly less accurately. Stage I or II is likely if an intact muscularis layer is seen beneath the base of the tumour. Stage III or IV is likely if the muscularis layer is obliterated, and stage IV if the tumour is seen to extend through the bladder wall (Fig. 14.22).

Fig. 14.22. Staging of bladder tumour. (a) Superficial T1–T2 tumour. The muscularis layer appears to be intact. (b) T3 tumour. The tumour has spread through the bladder wall

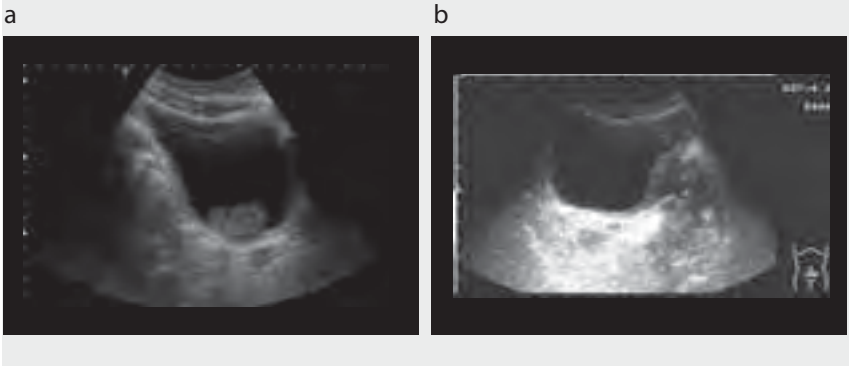

Calculi

On ultrasound, bladder calculi appear, like all calculi, as highly echogenic structures with a crescentic, dense line on the side nearest to the transducer and shadowing posteriorly (Fig. 14.23). Encrustation of the surface of a bladder tumour may give a similar appearance (see Fig. 14.14). Turning the patient will cause a calculus to move, although severe angulation of the patient, often into the semi-prone position, may be necessary.

Bladder diverticulum

A bladder diverticulum is an outpouching of the bladder mucosa through a defect in the muscular layer of the bladder wall. Diverticula may be congenital, in which case they usually occur near the urethral orifices, and are usually bilateral (Hutch diverticula) (Fig. 14.24). More often, they occur secondary to chronic bladder outlet obstruction. Most are uncomplicated and cause no symptoms. They may contain calculi.

Fig. 14.23. Bladder calculus, which is echo rich, with shadowing. It moved when patient was turned

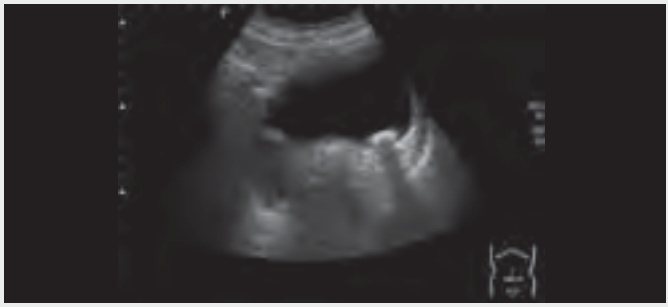

Fig. 14.24. Congenital Hutch diverticula. Diverticula are typically bilateral and near the ureteric orifices

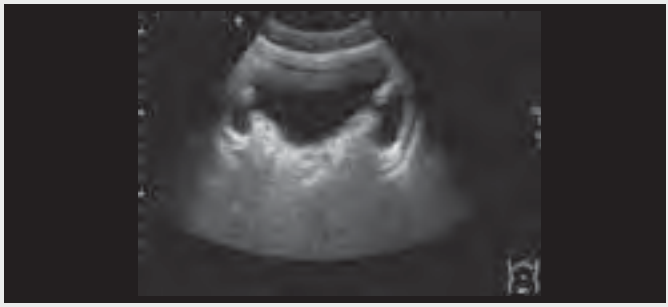

Tumours may develop within a diverticulum. They are histologically similar to other bladder tumours, but the malignant ones have a poor prognosis, probably because they spread through the thin wall of the diverticulum more rapidly than they would through the thicker normal bladder wall.

On ultrasound, uncomplicated diverticula are thin-walled, round or ovoid structures with anechoic contents bulging out from the outer bladder wall. The neck of the diverticulum is often, but not always, seen (Fig. 14.25). Colour Doppler can be used to show the neck in difficult cases. When intermittent pressure is applied over the bladder, the jet of urine through the neck of the diverticulum may be seen (Fig. 14.25 (b)). The technique does not always work, particularly for small or deeply placed diverticula.

Fig. 14.25. Acquired diverticulum. (a) The narrow neck of the diverticulum is clearly seen. (b) In a different case, the Doppler jet is seen passing from the bladder lumen into the diverticulum after sharp pressure on the bladder.

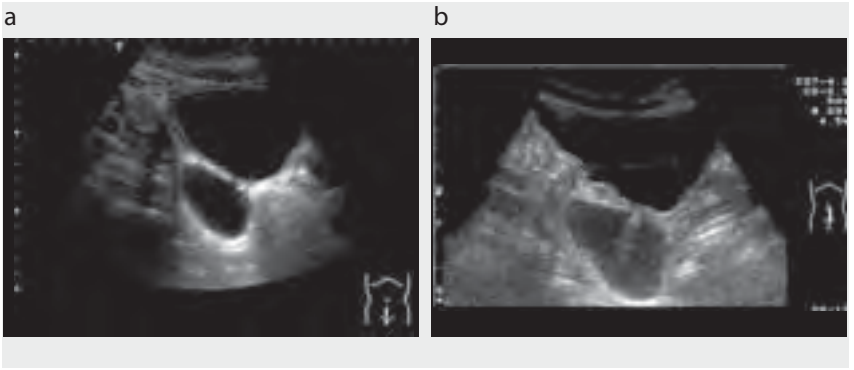

Differential diagnosis

The main differential diagnosis is an ovarian cyst. True differentiation can be made by demonstrating a definite separation from the bladder, which indicates that it is an ovarian cyst, or demonstration of the neck, which indicates that it is a diverticulum. Emptying the bladder and transvaginal scanning may help. Diverticula often do not empty when the bladder empties.

Patent urachus or urachal cyst

The urachus is a primitive connection between the bladder and the allantois, which usually closes and obliterates at birth. In some cases, the urachus remains patent, causing a channel between the bladder and the umbilicus. Sometimes, the whole urachus remains patent, communicating with the bladder and the umbilicus. Alternatively, only part of the mid-urachus may remain patent, causing a urachal cyst. Urachal cysts may be found incidentally or, if large, may present as a lower abdominal mass.

Complications include infection and malignant change. They sometimes present with a chronic umbilical discharge.

On ultrasound, an uncomplicated urachal cyst appears as a cystic structure lying anterior in the abdomen in or near the midline between the bladder and the umbilicus (Fig. 14.26). Complicated cysts, either infected or neoplastic, appear as complex structures with solid and cystic elements and echogenic contents (Fig. 14.27). A diagnosis is made from the position of the cyst and by demonstrating a connection with the umbilicus or the bladder. This is easily demonstrated on a sagittal MRI image but can usually be established by a careful ultrasound study.

Fig. 14.26. Urachal cyst. The diagnosis is made from the position of the cyst, which is antero-cranial to the bladder

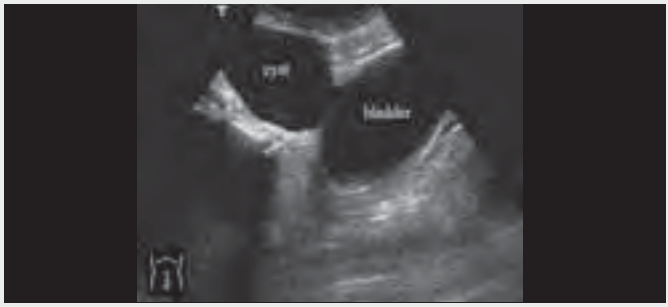

Fig. 14.27. Malignant urachal cyst. (a) The cyst has solid contents, indicating a tumour. (b) Continuity with the bladder

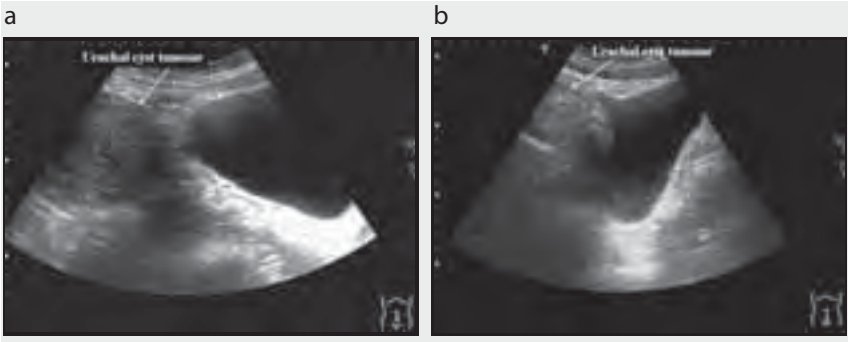

Urethra

Ultrasound has little place in imaging the urethra, contrast urethrography being the preferred mode of investigation. A sonourethrography technique has, however, been described in which the urethra is filled with fluid, either through a catheter, by clamping the urethral tip or by micturition against a pinched glans penis. The urethra is then scanned with a high-frequency transducer. Sonourethrography produces detailed images of the urethra, similar to those of a contrast urethrogram (Fig. 14.28). It shows the tissues around the urethra, which may give more information about the nature of a structure. Contrast urethrography cannot achieve this. Sonourethrography does not demonstrate fissures or fistulae as well as contrast urethrography. Despite its advantages, sonourethrography has not gained widespread acceptance.

Fig. 14.28. (a) Sonourethrogram with (b) a contrast urethrogram of the same case. There is a complex urethral stricture with mucosal tags (arrowheads)

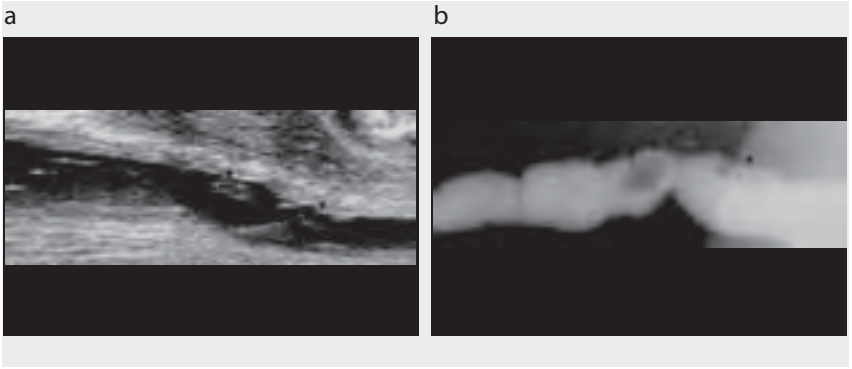

Reproduced with permission from: Cochlin DLL, Dubbins PA, Goldberg BB, Halpern EJ. *Urogenital ultrasound*, 2nd edition. London, Taylor & Francis Group, 2006. Fig. 6.16.

Prostate and seminal vesicles

Transabdominal scanning shows the prostate sufficiently well to allow approximate measurement of its size (for accurate measurement, a transrectal study is necessary). Transabdominal scanning is not good enough for any other purpose. The seminal vesicles may be seen sufficiently to determine whether they are present or absent (Fig. 14.29).

Fig. 14.29. (a) Transabdominal measurement of the prostate. (b) Seminal vesicles imaged transabdominally

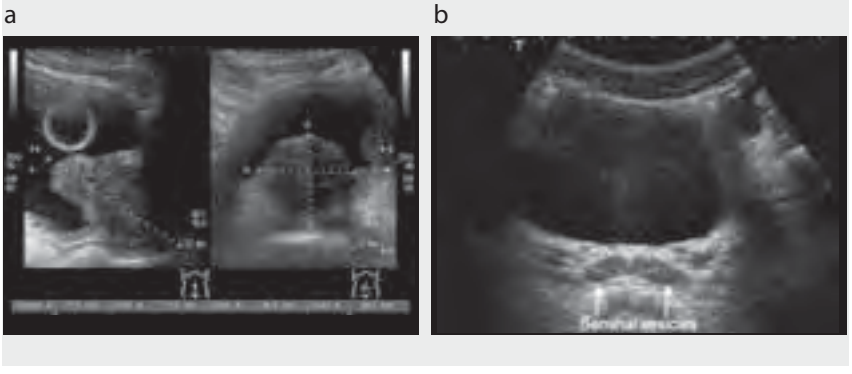

Transrectal ultrasound is necessary for the diagnosis of prostate cancer. The main use of imaging is to position systematic biopsies of the prostate accurately (Fig. 14.30 (a)). The diagnosis is then made by histological examination. Advanced local invasion of cancer may be seen (Fig. 14.30 (b)), but transrectal ultrasound is otherwise poor for local staging and of no use for nodal staging.

Imaging of the prostate, seminal vesicles and vasa deferentia has a small role in investigations of infertility, to assess the presence or absence of these structures or signs of obstruction. This can be done only by transrectal imaging (Fig. 14.31).

Prostate abscesses or other low-lying pelvic abscesses can be imaged and drained by transrectal ultrasound (Fig. 14.32).

Fig. 14.30. (a) Transrectal biopsy of the prostate. The needle is seen in the left lobe of the prostate following the dotted line of the biopsy guide. (b) Invasive prostate cancer. An irregular hyperechoic tumour is seen to invade the bladder. This could also be a bladder tumour invading the prostate

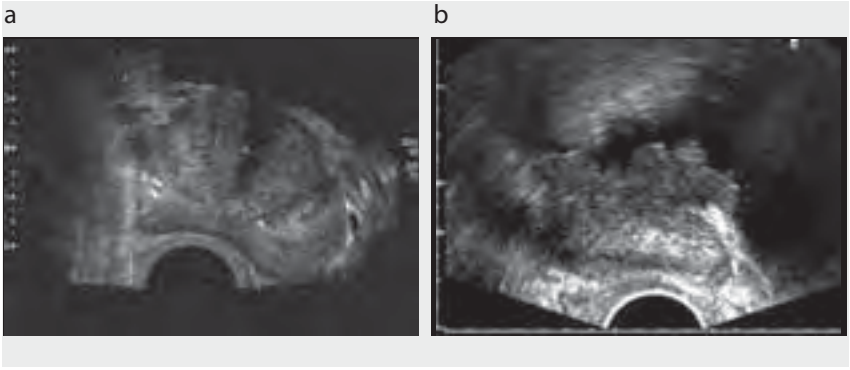

Fig. 14.31. Obstructed seminal vesicles. The lumina of both vesicles are dilated

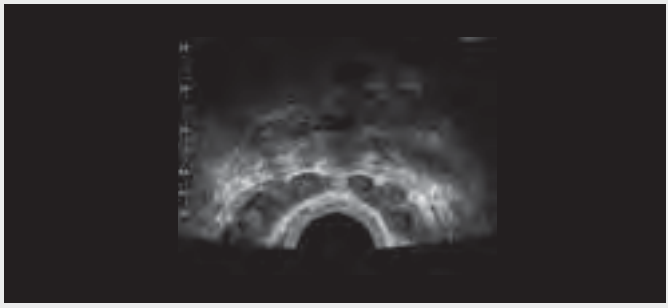

Fig. 14.32. Prostate abscess. Hypoechoic abscess (arrows) with post-lesion enhancement in the left lobe of the prostate

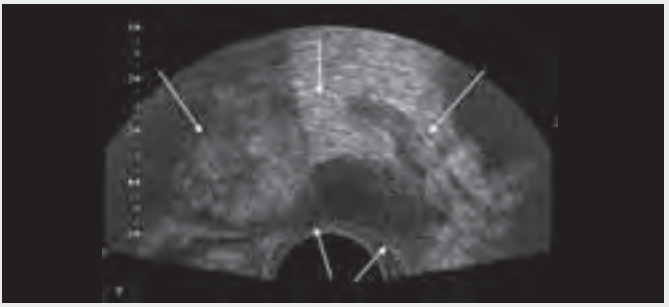

Penis

Requests for ultrasound scanning of the penis are few, but there are some applications.

Poor erection

In cases of failed or poor erection, the penile arterial waveforms may be studied and their response to intracavernosal papaverine or oral sildenafil citrate may be assessed. This can, with some accuracy, distinguish insufficient arterial input from loss of venous occlusion. This technique is now far less often used than previously. The detail of the procedure is beyond the scope of this text.

Peyronie disease

Peyronie disease is a condition in which fibrous plaques, which sometimes calcify, form on the tunical layers of the corpora. These cause painful bending of the penis during erection. The plaques are often difficult to see on ultrasound. They may be demonstrated as medium echodense, thickened areas within the tunica (Fig. 14.33 (a)). Calcified plaques can be distinguished by their increased echodensity and shadowing (Fig. 14.33 (b)). The presence of calcification affects management options.

Trauma

Rupture of the corporal tunica (fractured penis) requires surgical repair, while a simple haematoma can be treated conservatively. The diagnosis is often made clinically, but ultrasound is sometimes helpful. The pathognomonic sign of a fractured penis is disruption of the line representing the tunica (Fig. 14.34). There is always an associated haematoma.

Fig. 14.33. Peyronie disease. (a) Fibrous plaque causing a subtle hypoechoic, ovoid lesion disrupting the echogenic line of the tunica. (b) Calcified plaque in the ventral tunica. The dotted lines indicate measurement of the lesion

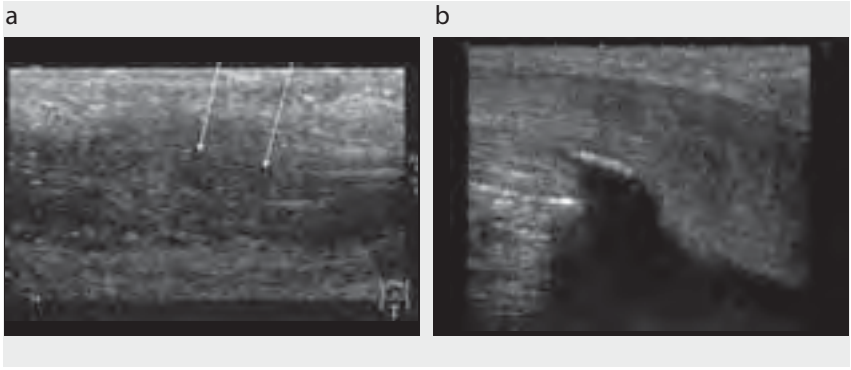

Fig. 14.34. Penile trauma. The posterior tunica is discontinuous, indicating rupture, with an associated hyperechoic haematoma.

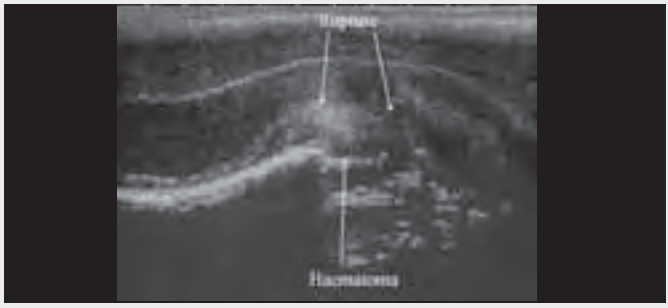

Tumours

Penile tumours are usually primary and occasionally secondary. Primary tumours start in the glans and are nearly always assessed clinically. Ultrasound is occasionally requested to assess the extent of the tumour along the penile shaft. Some cases present with a mass in the shaft, which are usually secondary deposits from the prostate or bowel. Penile tumours appear ultrasonically as hypoechoic masses (Fig. 14.35). They may be lobulated. Tumours in the shaft may cause priapism. The appearances are similar whatever the tumour type.

Fig. 14.35. Penile tumour. Transverse (a) and longitudinal (b) scans show the irregular hyperechoic tumour in the shaft. There is a catheter in situ

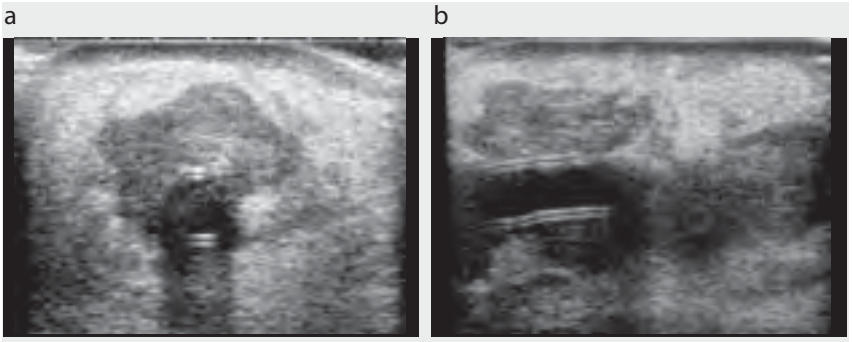

Priapism

Priapism is a condition of prolonged, painful penile erection. It can be due to several causes, but it is perhaps most important to distinguish between high-flow and low-flow priapism. Low-flow priapism is the commonest form, caused by impaired venous drainage. It may be idiopathic or secondary to hypercoagulability states, particularly sickle-cell disease, spinal cord stenosis or a variety of drugs, including sildenafil citrate (Viagra). High-flow priapism is due to high arterial flow caused by an arteriovenous fistula, usually traumatic or post-surgical.

In cases of low-flow priapism, a hyperechoic blood clot may be seen by ultrasound in the corpora. Penile tumours may be the cause. In cases of high-flow priapism, the arteriovenous fistula may be seen on colour Doppler (Fig. 14.36).

Fig. 14.36. Priapism. (a) Obstructive priapism. There is an echogenic clot in the dilated corpora. (b) In this case of high-flow priapism, the vertical line indicates the colour image of a post-traumatic arteriovenous (AV) fistula crossing the tunica

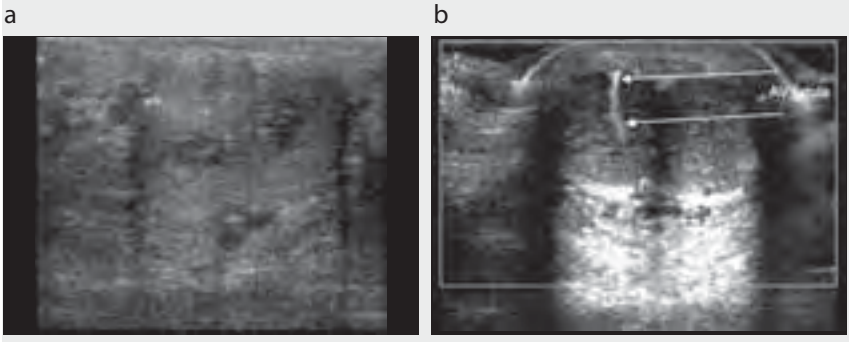

Chapter 15

Scrotum

15

Scrotum

Indications

The indications for scrotal ultrasound are complex; whether an ultrasound examination is warranted or not will depend on available resources and local attitudes. This chapter, therefore, does not provide a prescriptive list of indications, but rather discusses the potential benefits of ultrasound in the different conditions.

There are several possible indications for ultrasound study of the scrotum, ranging in strength from absolute to very weak. Until relatively recently, all scrotal pathology was managed on the basis of symptoms and signs alone. However, the introduction of high-frequency small-parts transducers allowed the scrotum to be imaged in greater detail. At first, ultrasound was used to study scrotal masses, allowing them to be categorized as intratesticular (and thus requiring orchidectomy) or extratesticular (not requiring orchidectomy). The applications of ultrasound have increased rapidly, so that now in many centres almost all patients with suspected scrotal pathology are scanned. If resources were unlimited, this would be a reasonable policy. Health care resources, however, are limited everywhere, particularly in developing countries, and it is essential not to waste them. The indications for scrotal scanning, therefore, need to be rationalized and classified according to importance.

Testicular masses

Scrotal masses that are clinically suspected to be intratesticular or that are of indeterminate position are an absolute indication for an ultrasound scan. More than 90% of palpable intratesticular masses are malignant tumours requiring orchidectomy; the remaining 10% are benign and can be treated conservatively. A small but significant minority of masses that clinically appear to be intratesticular are found on ultrasound to be extratesticular. These are usually inflammatory masses that are inherent to the testis. It is clear, therefore, that ultrasound imaging can determine the clinical management of a significant number of patients.

Extratesticular masses

Most masses suspected clinically to be extratesticular will be epididymal cysts, spermatoceles, or inflammatory or post-inflammatory masses. A few will be benign tumours. Malignant extratesticular tumours do occur, but are extremely rare. Primary malignant epididymal or paratesticular tumours generally present as large, irregular, craggy masses – which raises clinical suspicions of malignancy – and have a rapid rate of growth. They are, therefore, not really in the category discussed here. Secondary

deposits (usually from prostatic or rectal primaries), or lymphoma or leukaemia deposits may occur in the extratesticular scrotum. These are seen only in patients with established disease, so that the nature of the mass will be clinically suspected.

It is arguable, therefore, that – with the rare exceptions of large craggy masses, masses that are rapidly growing, and patients with known disease – ultrasound scanning of clinically suspected extratesticular masses is not necessary. The risk of such a policy would be very small. Many centres, nevertheless, choose to scan all such patients to provide reassurance.

Pain

Scrotal pain may be divided into severe pain of acute onset and chronic dull pain.

Severe pain

Severe pain of acute onset is usually due to epididymo-orchitis, far less often to testicular torsion or, in boys, torsion of the testicular or epididymal appendices. Less common causes include testicular infarcts, haemorrhage into a tumour and, in boys, Henoch–Schönlein purpura and appendicitis.

It is important to distinguish torsion from other causes. An ultrasound study with Doppler may achieve this and, with an experienced operator, is more accurate than clinical assessment. In cases of torsion, however, surgical detorsion of the testis with minimal delay is of paramount importance. In most centres, organizing an ultrasound scan with high-quality equipment and an experienced operator is likely to delay surgery, and it is common practice, therefore, to operate without performing an ultrasound examination. This policy results in several unnecessary operations (which is considered acceptable since the operation is minor).

The majority of cases of epididymo-orchitis can be managed clinically with antibiotics. An ultrasound scan is necessary only for severe cases, where an abscess may be suspected, and for patients who do not fully respond to a course of antibiotics. It is, in fact, common for patients not to respond to the first course of antibiotics, but there is always the possibility that the case may have been misdiagnosed and that the pain may be due to a tumour.

Adherence to this policy will result in relatively few scrotal ultrasound examinations. In practice, however, the boundaries are blurred, and what constitutes severe pain is subjective. Usually, therefore, far more patients in this group are scanned than is strictly necessary.

Dull pain or ache

A chronic pain, a dull pain, or a dull testicular ache is a more difficult problem. Most of these patients will have no obvious pathological process. The condition is sometimes termed idiopathic orchalgia. A small number will be suffering from mild epididymo-orchitis, while a very small but important group will have a testicular tumour. It is the possibility of the existence of a tumour that has led to a policy in many centres of scanning all these patients. The number of tumours found that are not clinically palpable, however, is extremely small – so small that, in most centres, patients with a dull ache are given low priority and often have to wait a long time for a scan. If the rationale of scanning this group is to detect impalpable cancers, then this policy is illogical. A careful clinical examination should be performed, and those thought to

have epididymo-orchitis should be given appropriate antibiotics. If resources permit, the addition of an ultrasound scan is undoubtedly the ultimate safe option. If, however, resources are limited, the patient should be reassured and advised to self-examine. He should return to the clinic if symptoms get worse or fail to respond to antibiotic treatment after 10 days or so. This policy will entail only a very small clinical risk.

Hydrocele

A tense hydrocele makes the testis impalpable. It is possible that clinical tumours may present with a hydrocele and, for that reason, an ultrasound scan is usually requested. In practice, hydroceles secondary to a tumour are small and lax, leaving the tumour palpable. The rationale for scanning this group of patients is therefore doubtful. In the absence of published evidence to the contrary, however, ultrasound should be performed.

While scrotal ultrasound is widely used in the management of a large spectrum of pathological conditions, a pragmatic analysis of its benefits shows that it necessary or strongly indicated only in a small proportion of cases. The policy adopted should be decided by the individual centre or clinician.

Examination technique

Equipment, transducer

Use a medium-high frequency (approximately 8 MHz) small-parts linear transducer. In cases of marked scrotal enlargement, such as a large hydrocele, a general-purpose curved linear transducer is needed to achieve sufficient depth of field.

Preparation

No preparation is required.

Position of the patient

The patient lies with his legs together. Place a paper or linen towel behind the scrotum to bring it forward.

Scanning technique

Both testes and epididymides should be scanned in the longitudinal and transverse planes, sweeping from side to side and top to bottom. Oblique planes may be used when necessary.

It is quite common that small palpable masses are not detected at first. In such cases, palpate the lesion. Leave one finger in contact with the lesion while scanning from the opposite side of the testis with the other hand. Moving the lesion slightly with the finger will aid detection, even if the lesion is almost isoechoic with the surrounding tissues.

Normal findings

The testes are a pair of smooth ovoid organs lying within the left and right compartments of the scrotal sac. The epididymides curve around the testes, usually posteromedially, though anatomical variants are common (Fig. 15.1). The testes are covered by a fibrous membrane, the tunica albuginea, which also covers the inner wall of the scrotum. The space so formed contains a small but variable volume of fluid which is visible on ultrasound scans as an anechoic band or crescent.

The hilum of the testis may be seen as a variably sized and shaped hyperechoic structure, which is often a long triangular structure in the longitudinal plane, shorter in the transversal plane (Fig. 15.2).

Fig. 15.1. Diagram of the normal scrotal anatomy

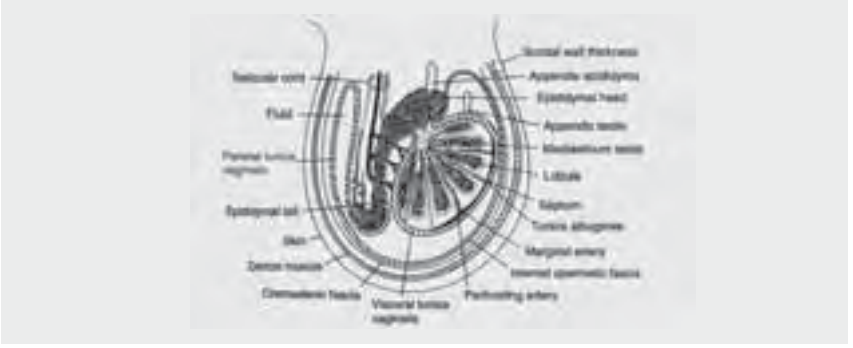

Reproduced with permission from: Cochlin DLL, Dubbins PA, Goldberg BB, Halpern EJ. *Urogenital ultrasound*, 2nd edition. London, Taylor & Francis Group, 2006. Fig. 5.1.

Fig. 15.2. Normal testis. (a) Longitudinal scan. (b) Transverse scan showing the hilum. The parenchyma is of even echodensity, except for the echogenic hilum and the rete testis, which is seen as a group of tubules just beneath the hilum. The tunica albuginea is partly seen as an echogenic line covering the testis

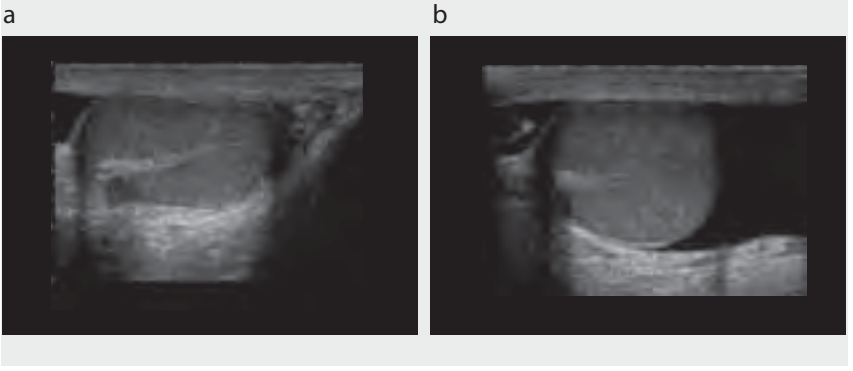

The testicular parenchyma may have a homogeneous appearance on ultrasound. With high-resolution systems, slightly curved hypoechoic lines may be seen radiating from the hilum, like the segments of an orange. These represent the fibrous septae of the testis. The individual tubules of the hilum, the rete testis, may also be seen (Fig. 15.3).

Fig. 15.3. The rete testis is seen at the right-hand side of the image. The tubules are just visible with anechoic lumens and echogenic walls

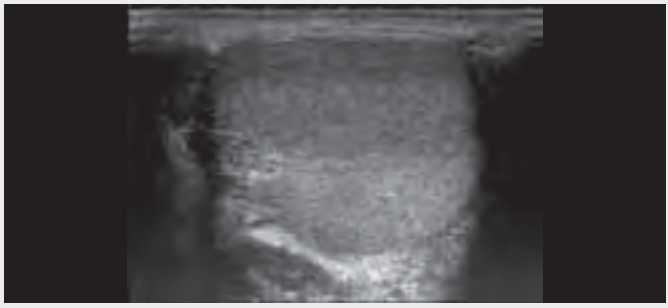

The tunica albuginea is seen as a hyperechoic line around the testis, and is more visible in the parts parallel to the transducer.

The epididymis is divided into three parts. The head lies cephalad to the testis, the body lies alongside the testis – usually but not always posteromedially – and the tail lies caudad to the testis. The position is highly variable. Both cranial–caudal and anteroposterior inversion occur.

The epididymal head is a discrete, smooth, pyramidal structure, which appears triangular on a longitudinal scan, with echodensity equal to or slightly greater than the testis (Fig. 15.4). The epididymal body is a looser structure and is rarely seen as a discrete entity, since it merges with the cord and pampiniform plexus (Fig. 15.5). The epididymal tail is a loose irregular structure (Fig. 15.6).

Fig. 15.4. The normal epididymal head is seen as a triangular structure to the right of the testis. The echo pattern is even and the texture similar to that of the testis

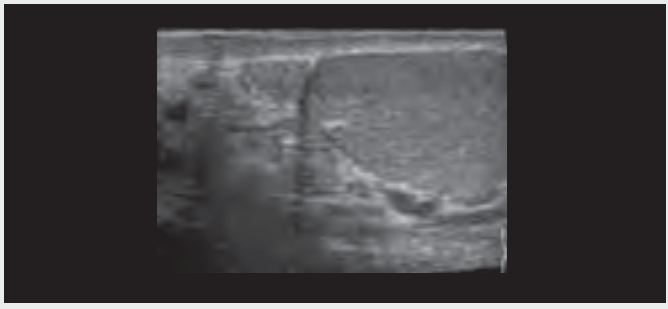

Fig. 15.5. The body of the epididymis, seen as a less compact structure alongside the testis (arrows)

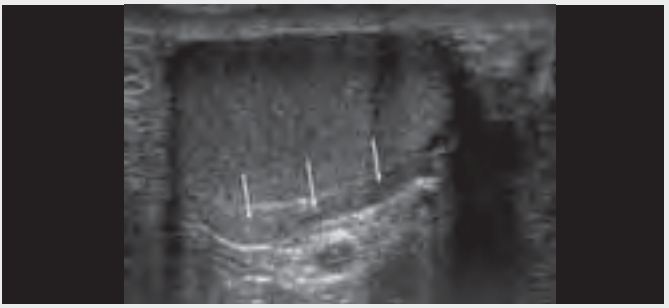

Fig. 15.6. The tail of the epididymis (arrows). This is a loosely bound, irregular structure

The spermatic cord is also a loosely bound structure, which is often difficult to see or follow on ultrasound scans.

Doppler ultrasound can identify short sections of blood vessels within the testis or epididymis and cord. The number and length of the vessels seen vary widely. The vessels are usually tortuous and small in diameter, so that only short lengths are seen (Fig. 15.7). In about 10% of men, a large straight artery and vein run between the periphery of the testis and the hilum; these are termed the transmediastinal artery and vein (Fig. 15.8).

With any reasonable Doppler system, vascularity can always be seen in men and post-pubertal boys. This is important in excluding torsion. In young boys, however, intratesticular vessels may not be visible on Doppler scans; results will depend on the age and size of the boy and the system used (see section on Testicular torsion in this chapter).

The normal testes vary in size from 3 cm to 5 cm in length and 2 cm to 3 cm in diameter.

Fig. 15.7. Normal scrotal Doppler ultrasound scan. Sections of the marginal arteries are seen on the surface of the testis and sections of the penetrating arteries are seen passing into the parenchyma. The size of the vessels is highly variable and in many men far fewer vessels are seen (see also Fig. 15.8)

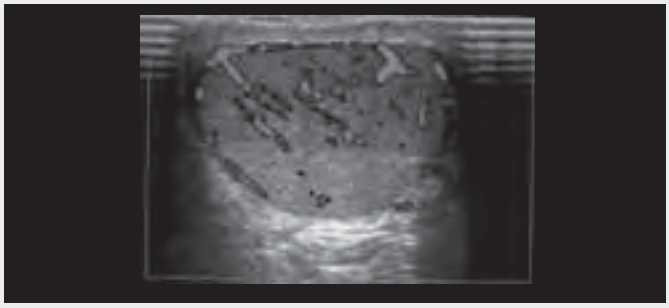

Fig. 15.8. The transmediastinal artery and vein are seen crossing the testis from the periphery to the hilum. They are present in 10% of men. Note that apart from these vessels, only a few perforating vessels are seen (compare with Fig. 15.7)

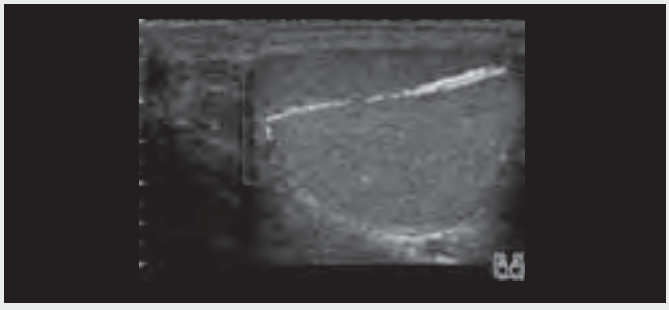

Pathological findings

Epididymo-orchitis

Epididymo-orchitis is inflammation of the epididymis and, less often, the testis. In young men, the majority of infections are sexually transmitted; in older men (aged > 60 years), they are usually due to spread from urinary tract infections and often follow bladder catheterization. Viral infections also occur, most commonly caused by the mumps virus, and these cause primary orchitis rather than epididymitis.

Tuberculosis and schistosomiasis also cause epididymo-orchitis, but they present differently, both clinically and on ultrasound imaging. They are therefore discussed separately.

As noted earlier, probably the majority of patients with epididymo-orchitis can be diagnosed clinically and treated with appropriate antibiotics. Ultrasound may be

performed in severe cases to look for complications – usually abscess – or to assess cases that do not respond to antibiotic therapy.

Bacterial epididymo-orchitis

In many cases of bacterial epididymo-orchitis, particularly mild or partially treated cases, the ultrasound appearance is normal.

In many cases, there is mild equivocal enlargement and inhomogeneity of the epididymis. The tail is usually affected first, followed by the body and then the head, though in some cases the head may be most severely affected.

On Doppler scans, the epididymis may appear hyperaemic. This has to be assessed subjectively, on the basis of the number and diameter of vessels seen compared with those seen with the same equipment and settings in normal subjects (Fig. 15.9). The asymptomatic side may be used for comparison. The size, echo pattern and vascularity of the epididymal tail is, however, variable in normal subjects, and the ultrasound signs of mild epididymitis are often equivocal. In mild cases the testis usually appears normal. It follows that a normal ultrasound scan does not exclude a diagnosis of epididymo-orchitis.

Fig. 15.9. Moderately severe epididymitis. (a) The epididymal tail is swollen and contains hypoechoic areas. (b) A Doppler scan showing moderate hyperaemia

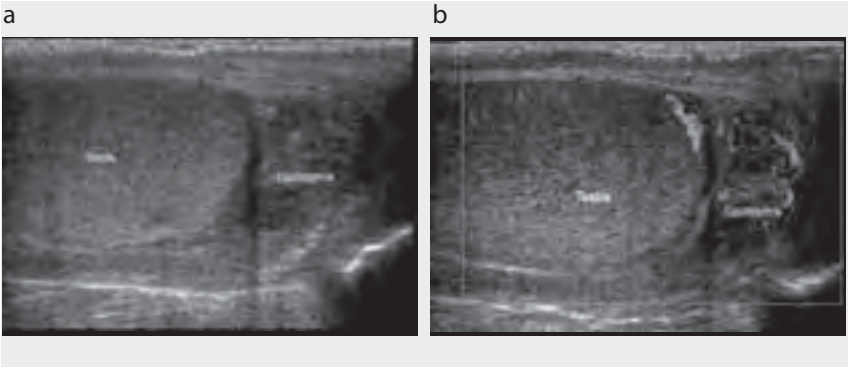

In more severe cases there is definite swelling and inhomogeneity of the epididymis. There are hypoechoic and sometimes also hyperechoic foci, and there is often a small reactive echogenic hydrocele (Fig. 15.10).

If the testis is involved, it is usually larger than the one on other side, often with hypoechoic bands radiating from the hilum, representing oedema around the septae and the enlarged blood vessels than run alongside them (Fig. 15.11). Doppler scans will show hyperaemia. This is assessed partly subjectively but there are some objective findings. The normal intratesticular arteries spiral, so that only small lengths are seen in a single ultrasound plane. They are also of small diameter, typically less than 1 mm. In hyperaemia, the vessels become straighter and larger (Fig. 15.12).

The spermatic cord may be involved in the inflammatory process, with thickening and hyperaemia. In a minority of cases this feature is predominant (Fig. 15.13).

In a very few severe cases, swelling of the cord within the inguinal canal (funiculitis) causes ischaemia of the testis, with reduced or absent blood flow on Doppler study.

Fig. 15.10. Severe epididymitis. (a) The tail of the epididymis is very swollen. In addition to hypoechoic areas, there are hyperechoic foci, probably due to haemorrhage. (b) Marked hyperaemia

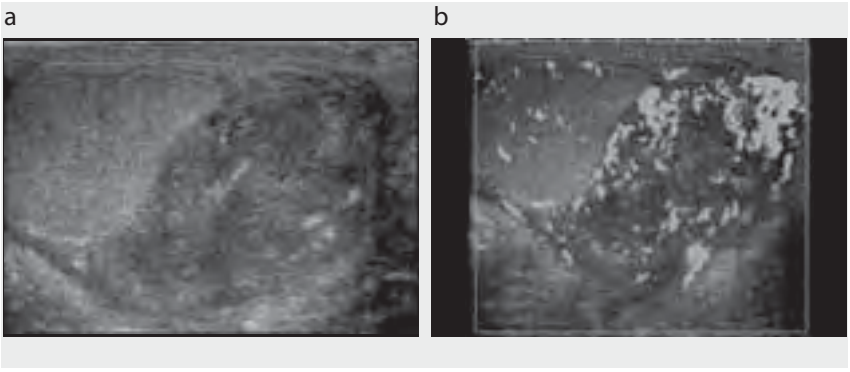

Fig. 15.11. Orchitis – grey-scale appearance. The testis is generally hypoechoic but with hyperechoic foci

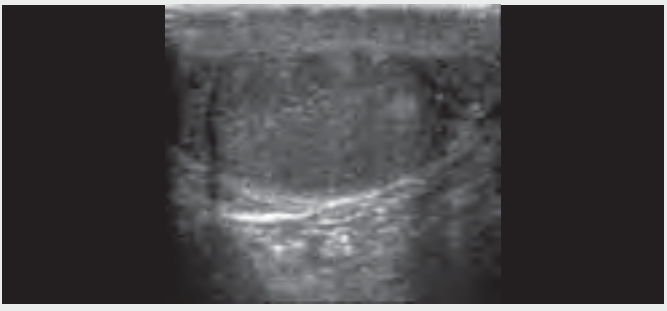

Fig. 15.12. Doppler scan of orchitis. Intense hyperaemia with a high number of vessels visible. The vessels are straight and have a wide diameter

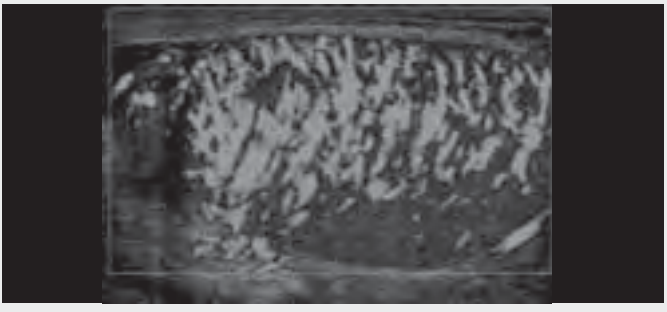

Fig. 15.13. Funiculitis. The spermatic cord is swollen and contains prominent vessels

Such cases are so uncommon that they may be discounted in the interpretation of the scan. Most such cases are misdiagnosed as torsion.

There may be cellulitis of the scrotal wall, with thickening and hyperechoic areas, but this is more easily assessed clinically.

The main complications of epididymo-orchitis are abscess formation and focal orchitis:

- Abscesses usually occur in the epididymis and may discharge through the scrotal wall. On ultrasound they are seen to have a thick wall and fluid contents of variable echogenicity (Fig. 15.14). Intratesticular abscesses are far less common but have a similar appearance.
- In focal orchitis, areas of the testis are severely inflamed. There are hypoechoic and sometimes also hyperechoic foci. In some cases, there are mass-like lesions within the testis, which may be indistinguishable from tumour (Fig. 15.15). The diagnosis may be suggested by the presence of orchitis, but it should be remembered that orchitis and testicular tumours can coexist. Indeed, there is some evidence that testicular tumours may predispose to orchitis by obstructing the tubules. Any mass lesion in the testis, therefore, must be closely followed. Areas of focal orchitis become less prominent with treatment and either resolve completely or leave a scar. Tumours do not resolve, but become larger, usually rapidly. In this situation, serum tumour markers should also be measured: elevated levels indicate a tumour, though normal levels do not exclude tumour.

Focal orchitis may sometimes progress to testicular abscess

Tuberculous epididymo-orchitis

Tuberculous epididymo-orchitis is a chronic condition, often presenting as a mass with little pain. Because of this, it is not common to scan early cases.

Ultrasound appearance

- Scans of early cases show epididymal swelling similar to that in bacterial epididymitis, sometimes also with areas of calcification (Fig. 15.16).

Fig. 15.14. Epididymal abscess. (a) A small abscess with anechoic contents (arrow). (b) A larger abscess (arrows) with contents of medium echodensity

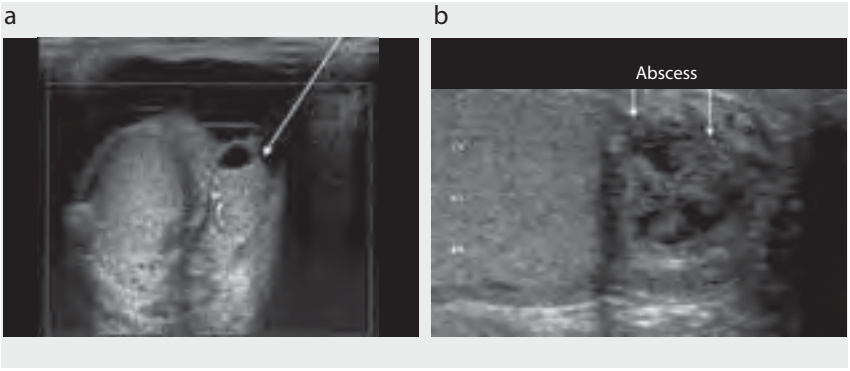

Fig. 15.15. Focal orchitis. (a, b) Hypoechoic areas within the testis

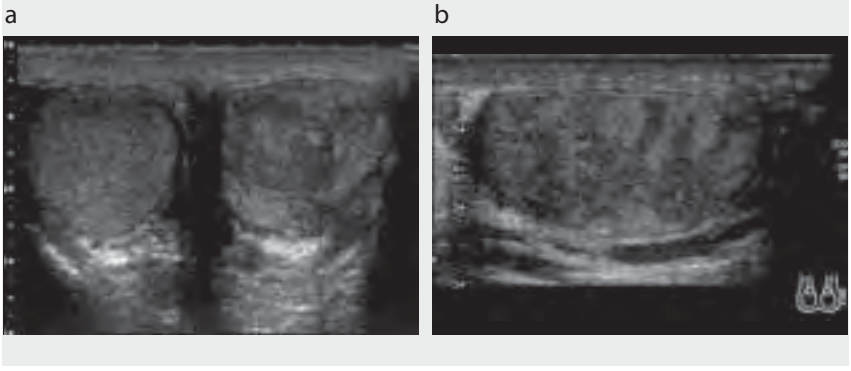

Fig. 15.16. Early tuberculous epididymo-orchitis. The epididymis is swollen and adherent to the testis. There are echodense foci of calcification

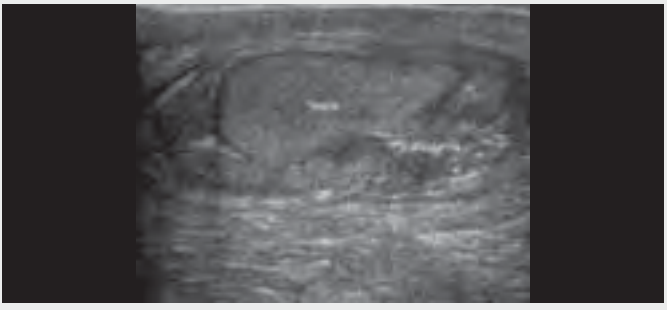

- Often, because there is no pain, patients present late, by which time there is severe enlargement of the epididymis with hyperechoic and hypoechoic areas. There are often calcifications, which cause shadow. The epididymis is usually widely adherent to the testis. The testis may also be inhomogeneous. The ultrasound appearance, therefore, is often of a single inhomogeneous mass in which it is difficult to distinguish the testis from the epididymis (Fig. 15.17). There is usually no discernible hyperaemia. It is sometimes impossible to distinguish tuberculous epididymo-orchitis from a tumour.

Fig. 15.17. Advanced tuberculous epididymo-orchitis. (a) Marked swelling of the epididymis with calcified foci. The epididymis is adherent to the testis. (b) An advanced case. The epididymis and testis are fused into a single inflammatory mass

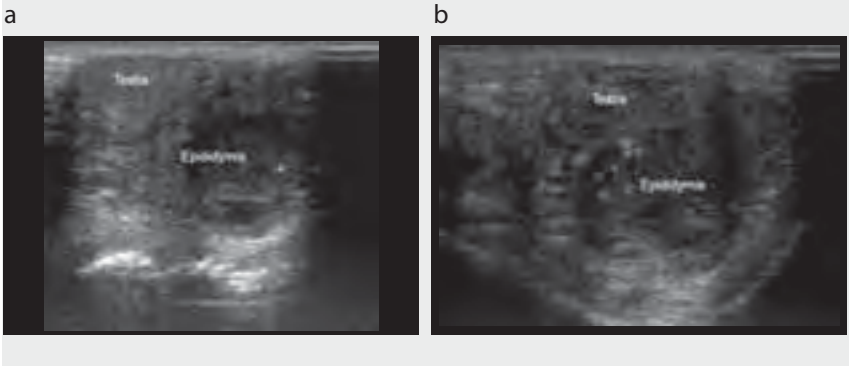

Schistosomiasis (bilharzia)

Schistosoma haematobium often affects the urinary tract and the epididymis, causing mild epididymitis. It less often causes orchitis.

Ultrasound appearance

The characteristic feature on ultrasound scans is multiple, hyperechoic rounded foci, about 1–1.5 mm in diameter throughout the epididymis or testis. These are calcified ova. There are also fewer small hypoechoic areas, representing granulomas. These are more easily visible when they occur in the testis. If the testis if affected, it will be enlarged.

Often, both epididymides or testes are involved (Fig. 15.18).

Late changes of epididymo-orchitis

The majority of cases of epididymo-orchitis return to normal after antibiotic treatment. Sometimes hard areas remain within the epididymis. These are easier to palpate than to see on an ultrasound scan.

Ultrasound appearance

The echo texture of the hard areas is usually very similar to the surrounding epididymis, which makes them difficult to see ultrasonically (Fig. 15.19). It is often necessary to palpate the lesion while scanning with the other hand. With this technique the

hard area, usually in the epididymal tail, may be seen to move differently from the surrounding epididymis.

Focal orchitis may leave hyperechoic or hypoechoic scars or hypoechoic infarcts (Fig. 15.19). Mumps orchitis usually causes atrophy.

Fig. 15.18. Schistosomiasis. (a) Epididymitis with rounded hyperechoic foci representing ova. (b) Orchitis. There are hyperechoic ova throughout the testis, as well as small hypoechoic foci representing granulomas

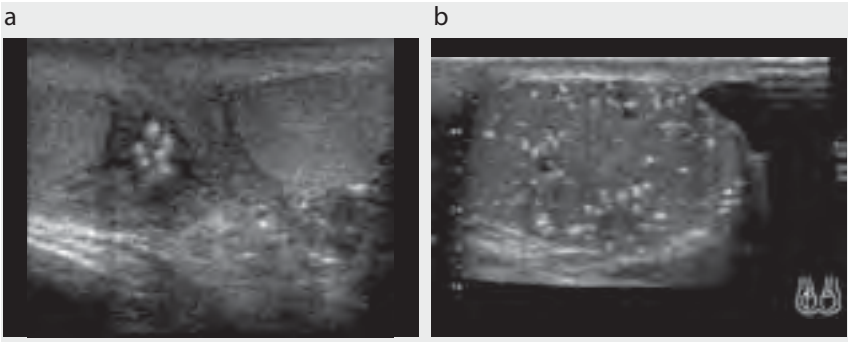

Fig. 15.19. Post-inflammatory mass. Three months after an episode of severe epididymitis, there is residual enlargement of the testicular tail. This was hard on palpation. It is indenting the lower pole of the testis (see also Fig. 15.46)

Testicular torsion

Testicular torsion is a condition in which the testis twists, resulting in obstruction of the spermatic artery and vein. The spermatic artery is essentially the only artery that supplies blood to the testis, which quickly becomes ischaemic and after 6–24 h becomes infarcted. The epididymis has a triple blood supply. It initially becomes ischaemic, but collateral vessels quickly enlarge so that the tissues survive. Torsion is most common in adolescents but it may occur at any age. Neonatal torsion differs in its mechanism. The testis and cord twist between the two tunical layers (intravaginal torsion). This is discussed in Volume 2 of this manual.

In childhood, adolescent or adult torsion, the testis and cord twist together with both tunical layers (extravaginal torsion). This can only occur when the attachment of the testis and epididymis to the scrotal wall, the pedicle, is abnormally narrow. This allows the testis and its covering tunica layers to twist.

The end result of both types of torsion is the same. Neonatal torsion, however, has a different presentation from childhood and adolescent torsion. Childhood torsion also has a different differential diagnosis from adult torsion. Neonatal torsion is discussed in Volume 2 of this manual.

Adolescent and adult torsion

As noted earlier, if adequate equipment and expertise are not immediately available, it is better to rely on clinical findings and perform a surgical exploration if torsion is suspected.

Torsion produces changes in the grey-scale appearance of the testis and epididymis, but it is the Doppler study that confirms or excludes the diagnosis. Good-quality equipment is essential. The Doppler settings need to be optimized, particularly in younger boys.

Ultrasound appearance

- On the grey-scale image, the testis is swollen and initially mildly heterogeneous with hypoechoic areas. Later these changes become more marked. If the torsion has been present for more than 24 h, there is often a hypoechoic band around the periphery of the testis.
- The epididymis is swollen and heterogeneous, with characteristic hyperechoic areas due to haemorrhage.
- There is usually a reactive haematohydrocele, with echogenic fluid and strands crossing it (Fig. 15.20).

These features all overlap with those of epididymo-orchitis.

- The cardinal feature of torsion on a Doppler scan is severely reduced blood flow within the testis.
- It was previously thought that blood flow stops completely, but with high-resolution equipment flow may be seen to persist in a few vessels. This is because the testis does have some collateral blood supply, although it is insufficient to prevent infarction (Fig. 15.21).
- Initially, blood flow to the epididymis is also reduced, but quickly increases as collateral vessels open up. The epididymis and tunica layers and scrotal wall rapidly become hyperaemic (Fig. 15.22).
- Careful Doppler study of the cord may show the position of the twist, or so-called torsion knot. This appears as a star-shaped pattern of vessels (Fig. 15.23). It is worth searching for this feature as it is totally diagnostic; however, it is not visible in all cases.
- Ultrasound contrast agents (intravascular injected microbubbles) are highly sensitive and specific for the diagnosis of torsion. Used with contrast-specific software they give a perfusion image in which the testis is shown to be non-perfused. The image is similar to that from a nuclear medicine study (Fig. 15.24). However, the appropriate software is expensive and the technique is not in general use.

Fig. 15.20. Testicular torsion, grey-scale appearance. (a) Testis and epididymis are swollen and inhomogeneous. (b) An echogenic haematohydrocele. The hyperechoic foci in the epididymis are due to haemorrhage

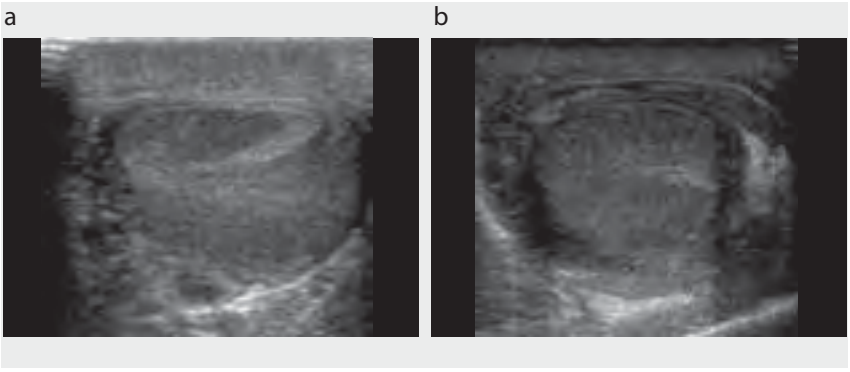

Fig. 15.21. Early testicular torsion, Doppler scan. Vessels are clearly seen around the testis but there is a marked reduction in the intratesticular vessels

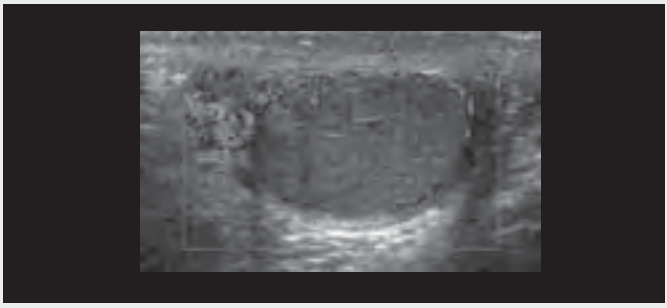

Fig. 15.22. Late testicular torsion. (a) The testis is very swollen and inhomogeneous, and there is a hyperechogenic haematohydrocele. (b) Hyperaemia of the paratesticular tissues. No intratesticular vessels are visible

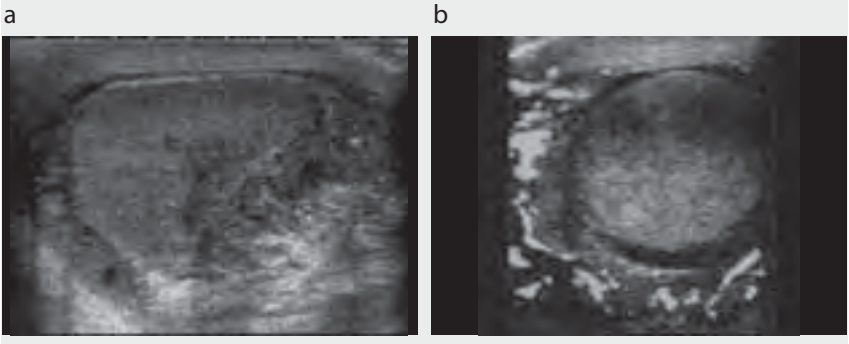

Fig. 15.23. Torsion knot. (a) The twist in the cord is seen as a star-shaped pattern of vessels. (b) A less definite star-shaped pattern that is, nevertheless, diagnostic

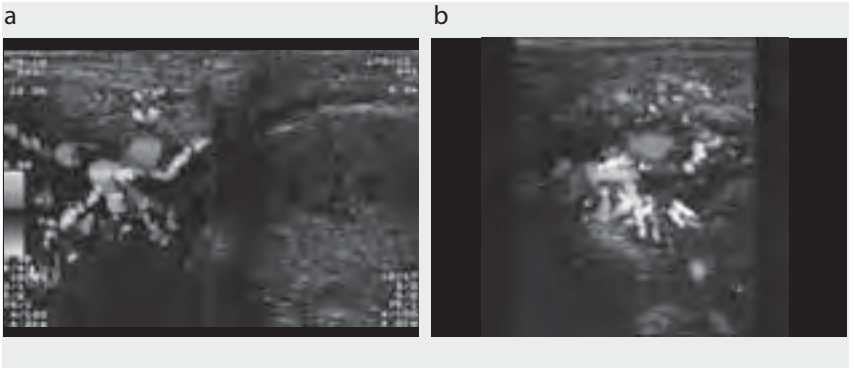

Image (a) reproduced with permission from: Cochlin DLL, Dubbins PA, Goldberg BB, Halpern EJ. *Urogenital ultrasound*, 2nd edition. London, Taylor & Francis Group, 2006. Fig. 5.84.

Fig. 15.24. Testicular torsion, contrast-enhanced ultrasound scan. (a) Transverse view. (b) Longitudinal view. These are pure perfusion images (there is virtually no grey-scale image). The white dots represent perfusion. The testis is seen to be non-perfused, except for a small area at the hilum (arrows)

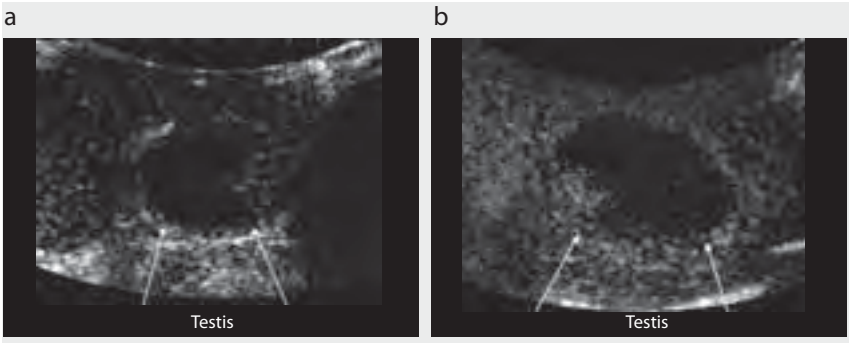

Incomplete torsion

The term 'incomplete torsion' describes a twist of the cord of 360° or less. The result is that the arterial supply is compromised but not totally occluded. The venous return is, however, occluded so that testicular infarction still occurs.

Ultrasound appearance

The difference from complete torsion is that a significant number of vessels may be seen, particularly at the testicular hilum. As stated previously, some vessels may also be seen in complete torsion so that the distinction on Doppler study may not be clear. Distinction, however, is not important as both conditions require surgery.

Spontaneous detorsion

In some cases, the testis may twist, causing ischaemia, but then spontaneously untwist before infarction occurs. This makes diagnosis very difficult both clinically and ultrasonically. In a significant number of cases, the testis will subsequently re-twist and eventually complete torsion will occur.

Ultrasound appearance

- The grey-scale findings seen in early torsion may be present but are not diagnostic.
- On a Doppler scan there is rebound hyperaemia simulating epididymo-orchitis. Indeed many cases are misdiagnosed in this way.
- The diagnosis of spontaneous detorsion is usually made clinically from a history of several episodes of severe acute pain. Clinical examination of the testis may reveal a narrow testicular hilum (bell-clapper deformity). Anteroposterior inversion of the testis often accompanies a narrow hilum and may be detected clinically.
- These features may be seen on an ultrasound scan, but only if there is a hydrocele surrounding the testis (Fig. 15.25).

Fig. 15.25. Narrow testicular hilum (bell-clapper deformity) (arrows). Torsion can occur as a result of this anomaly

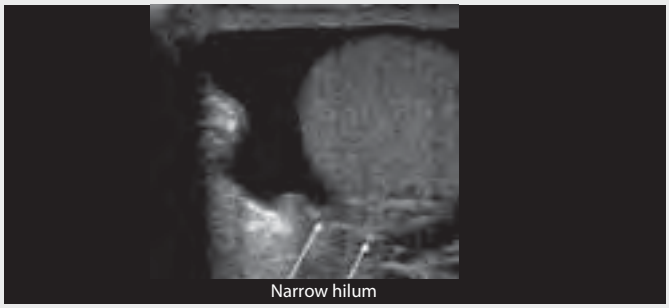

Neonatal torsion

This is discussed in Volume 2 of this manual.

Henoch–Schönlein purpura

Henoch–Schönlein purpura may cause testicular vasculitis, producing acute scrotal pain identical to that of torsion.

Ultrasound appearance

- The characteristic appearance is of a very stranded hydrocele. This gives the appearance of branching echogenic lines crossing the hydrocele fluid. As the strands attach to the tunica albuginea, they cause the testicular surface to appear ragged.

- There is normal flow on a Doppler scan.
- The knowledge that the child is suffering from Henoch–Schönlein purpura provides the diagnosis (Fig. 15.26).

Fig. 15.26. Henoch–Schönlein purpura. There is a characteristic very stranded hydrocele causing a ragged-looking testicular surface

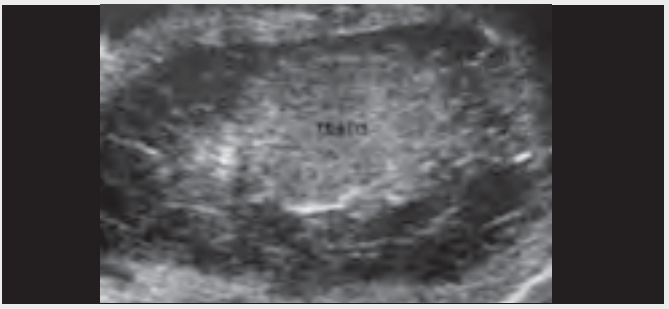

Focal testicular infarcts

Testicular infarcts occur in hypercoagulability states, including sickle-cell disease, but may also be idiopathic. They cause acute pain similar to that of torsion.

Ultrasound appearance

- A wedge-shaped or angular hypoechoic area is typical of an infarct (Fig. 15.27).
- In many cases, however, the hypoechoic areas are more rounded, simulating tumours. A Doppler scan will show the infarct to be avascular. However, some tumours, particularly small ones, are also hypovascular and no blood vessels may be seen within them on a Doppler scan. Such cases should have follow-up scans.
- Contrast ultrasound studies may be useful in showing the avascular infarct. Their accuracy, however, is not proven (Fig. 15.28, Fig. 15.29).

Fig. 15.27. Testicular infarct. The wedge-shaped hypoechoic lesions are typical of infarcts

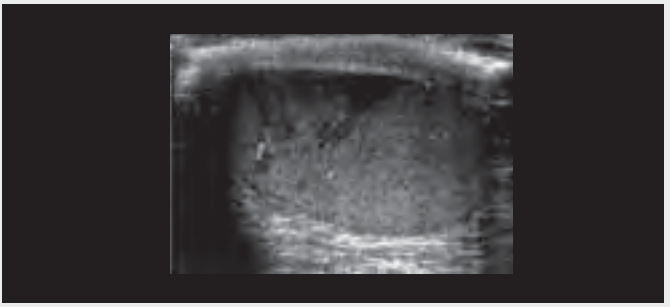

Fig. 15.28. A large hypoechoic testicular infarct. (a) Longitudinal scan. (b) Transverse scan. The straight border is typical

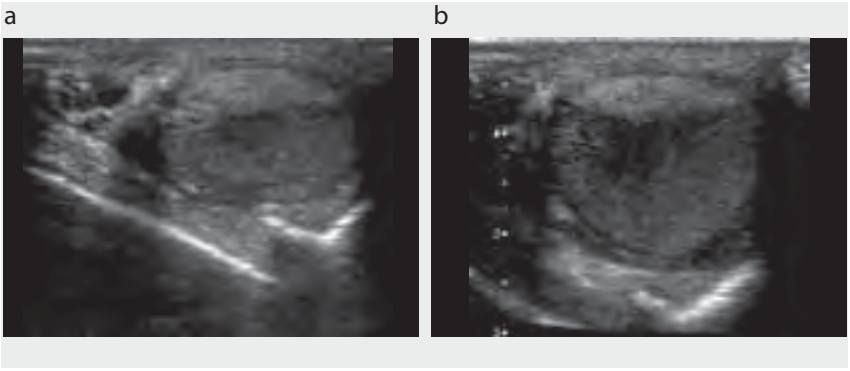

Fig. 15.29. Testicular infarct. (a) This small round infarct looks like a tumour. (b) This contrast-enhanced study shows the infarct to be non-perfused. Although small tumours are hypovascular, they show perfusion on contrast studies

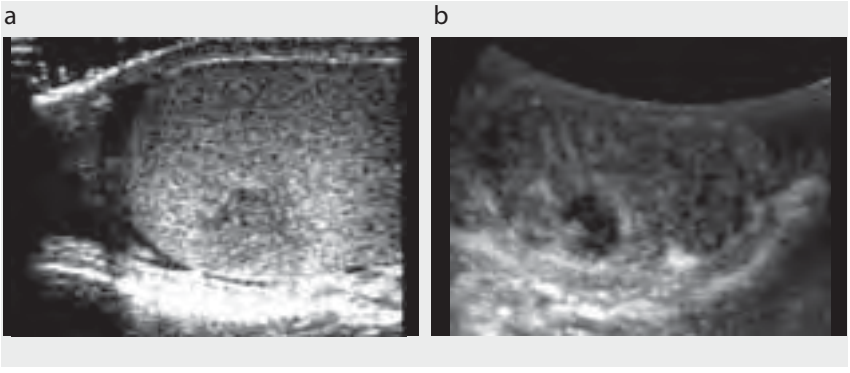

Idiopathic orchalgia

This term is used for a dull scrotal ache with no apparent cause. The pain is self-limiting, though it may last for several months. Although there are no ultrasound findings, the condition is included here as it represents a large proportion of cases seen in most ultrasound practices.

Ultrasound appearance

- As the name implies there is no specific ultrasound appearance. The scan may be normal or may show incidental findings, such as epididymal cysts.

Malignant intratesticular tumours and masses, lymphoma and leukaemia

Over 90% of intratesticular masses are malignant tumours, mostly germ cell tumours. It used to be standard practice to perform orchidectomy on all clinically diagnosed intratesticular masses. The first role of ultrasound was to distinguish more clearly intratesticular from extratesticular masses in cases of uncertainty.

The classification of malignant tumours is complex, but this has little impact on their detection by ultrasound. They may be divided very broadly into seminomas and non-seminomas (usually termed teratomas). Seminomas are seen most often in 30- to 40-year-olds, while teratomas are most common in 20- to 30-year-olds. However, both types may occur at any age from puberty onwards, although they are rare above the age of 60 years.

The characteristic appearances of seminomas and non-seminomas are described. Histological distinction is not necessary at the time of the scan, since the initial treatment of all malignant intratesticular tumours is radical orchidectomy. Subsequent treatment is then based on histological analysis of the excised specimen.

It is now possible to characterize some, though not all, benign tumours and masses, thus avoiding orchidectomy in some cases. The appearances that may distinguish benign tumours or masses are described. It is still, however, recommended to perform orchidectomy if there is any doubt about malignancy.

Boys have a different spectrum of testicular tumours and these are discussed in Volume 2 of this manual.

Seminoma

Ultrasound appearance

- Seminomas are typically rounded or lobulated hypoechoic masses.
- They are occasionally multiple.
- They may vary in size from a few millimetres in diameter to large tumours filling the testis.
- Tumours of less than about 1 cm are hypovascular. Above this size they become progressively hypervascular. Doppler study, however, usually adds little to the diagnosis (Fig. 15.30).

Fig. 15.30. Seminoma. This rounded hypoechoic tumour is typical of a seminoma (arrows)

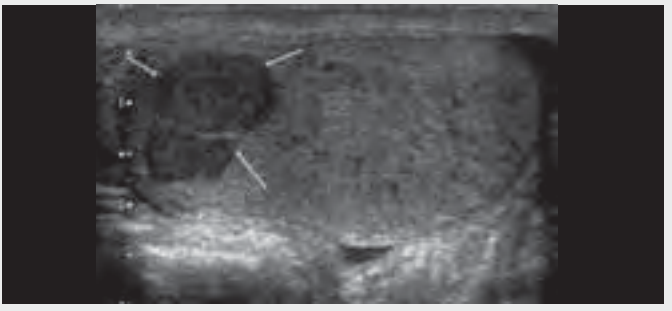

Teratoma

Ultrasound appearance

- Teratomas have a varied appearance. They usually have a mixed echo pattern with hypoechoic, hyperechoic and anechoic cystic elements.
- They may be smooth or irregular in outline.
- Small teratomas tend to be fairly uniformly hypoechoic, resembling seminomas.
- Small tumours are hypovascular. Large tumours are hypervascular. The vessels tend to be more irregular than those seen in seminomas.
- A teratoma is never multiple, but may be lobulated, giving the appearance of more than one tumour if several lobules cut across the scan plane (Fig. 15.31 and see also Fig. 15.37).

Fig. 15.31. Teratoma. The tumour has a mixed echo pattern but is predominantly hypoechoic

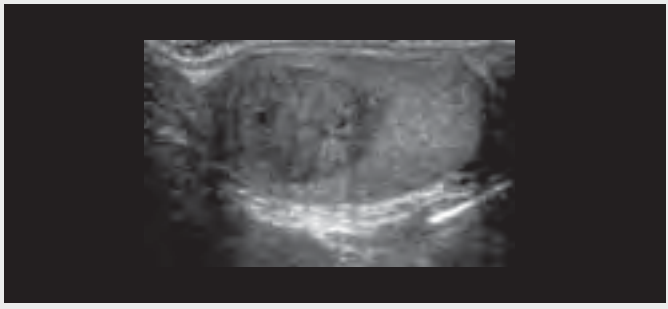

Testicular microcalcification

This is a condition in which tiny foci of calcification are scattered throughout the testis. It may be associated with several syndromes, notably Klinefelter syndrome, and is more common in infertile men. The majority of cases, however, are found incidentally. It used to be thought that such calcifications were associated with a high risk of developing germ cell tumours.

More recent research suggests that the risk, if any, is small. Follow-up is no longer advised.

Ultrasound appearance

- There are multiple small, intensely hyperechoic foci.
- The number may vary from a few to very many.
- They are less than 2 mm in diameter and, because of their small size, do not cast a shadow (Fig. 15.32).

Fig. 15.32. Typical testicular microcalcification

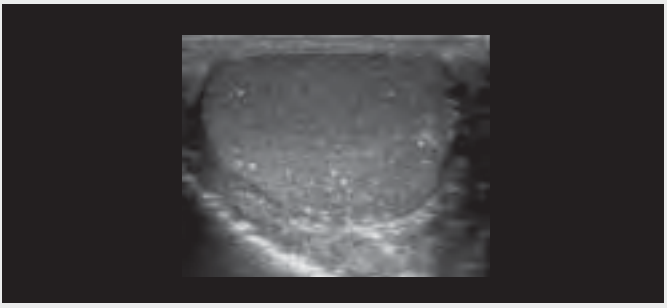

Lymphoma

Lymphoma is the most common testicular tumour in older men, though it may occur at any age. It may occur as part of already established disease or may be the first sign of disease.

Ultrasound appearance

- The tumours are hypoechoic. They may be solitary or multiple, rounded or lobulated.
- They may be unilateral or bilateral.
- They may also have a hypoechoic infiltrative pattern (Fig. 15.33).

Leukaemia

The testes are a sanctuary site in leukaemia, i.e. the disease may remain active in the testes when the patient is in clinical remission. Deposits often occur in the acute phase of the disease and often may also be found when the disease is apparently in remission.

Ultrasound appearance

- Leukaemia deposits are always hypoechoic.
- They tend to follow the septae of the testis, producing hypoechoic bands.
- They may cause more rounded deposits, although these also have a tendency to spread along the septae.
- There is a mass infiltrative pattern, involving part or all of the testis.
- The tumours are hypervascular. On Doppler study large infiltrative lesions may simulate acute orchitis (Fig. 15.34).

Benign intratesticular tumours and masses

These include testicular cysts, ectasia of the rete testis, epidermoid cysts, sarcoidosis, stromal tumours, haematomas, focal orchitis and infarcts. Some have a characteristic appearance on ultrasound scans, others are difficult to distinguish from malignant tumours.

Fig. 15.33. Lymphoma. (a) Longitudinal plane. (b) Transverse plane. Different cases with multiple rounded, hypoechoic tumours. These are typical of lymphoma, although in a young man the differential diagnosis could be multifocal seminoma. (c) Longitudinal plane. A large infiltrative hypoechoic lymphoma

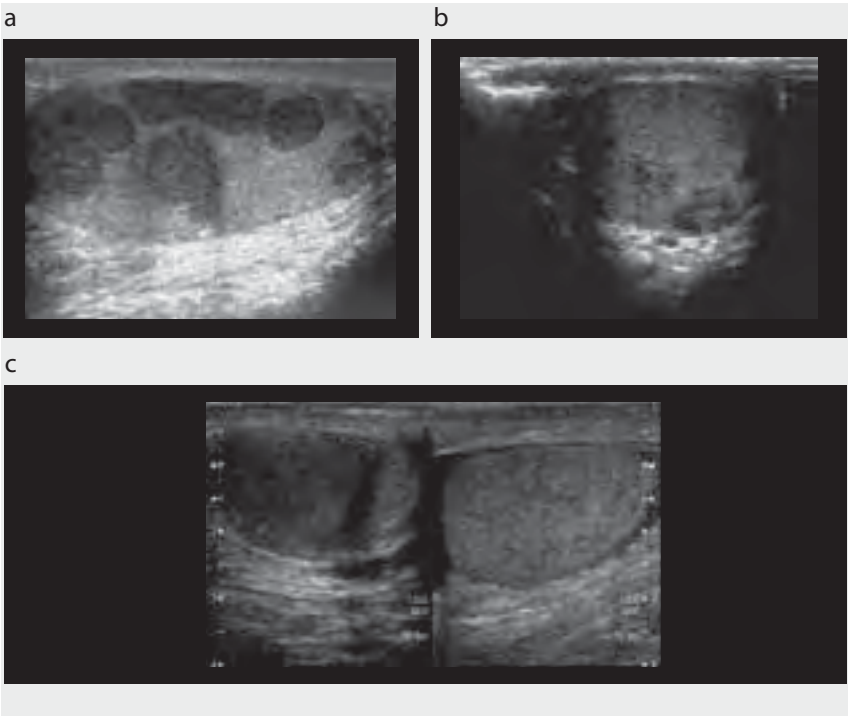

Images (a) and (b) reproduced with permission from: Cochlin DLL, Dubbins PA, Goldberg BB, Halpern EJ. *Urogenital ultrasound*, 2nd edition. London, Taylor & Francis Group, 2006. Fig. 5.26.

Fig. 15.34. Leukaemia. (a) Hypoechoic bands of tumour follow the septae. (b) More rounded tumour foci, also tending to follow the septae

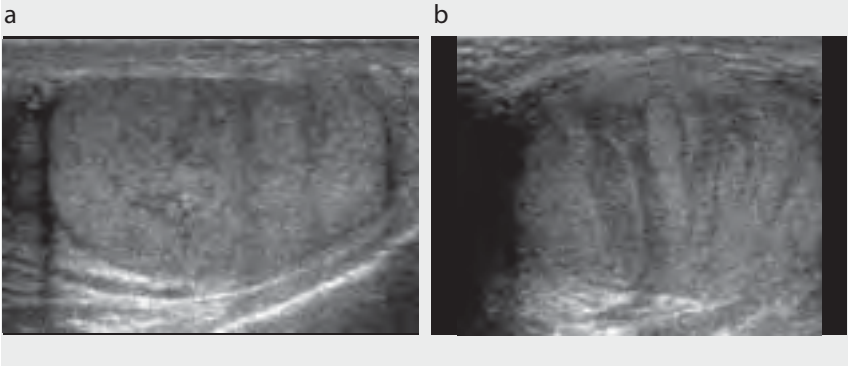

Testicular cysts

Some testicular cysts arise from the tunica albuginea and may bulge into or out of the testis. Others arise from the tubules and tend to occur near the hilum.

Ultrasound appearance

- The cysts are thin-walled with anechoic contents, acoustic enhancement posteriorly and no solid elements.
- They are usually small, but may occasionally grow large (≥ 5 cm).

In contrast, cystic teratomas always have solid elements and thick walls or thick septae (Fig. 15.35, Fig. 15.36, Fig. 15.37).

Fig. 15.35. Tunica albuginea cyst. A typical tunical cyst, situated at the periphery of the testis and bulging into the testis. It is thin-walled with anechoic contents

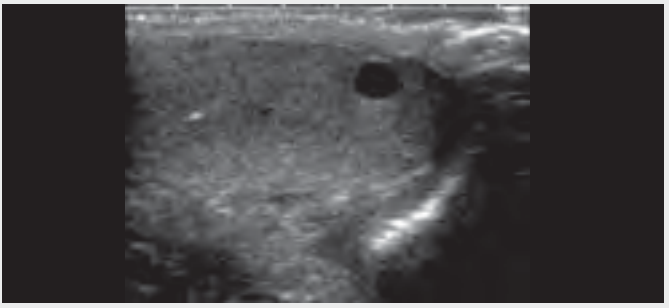

Fig. 15.36. Cyst of the rete testis. It is thin-walled with anechoic contents

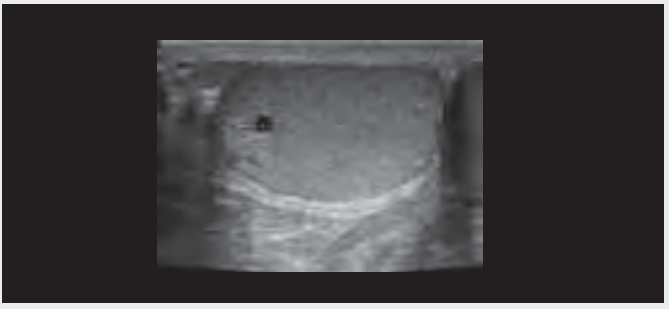

Fig. 15.37. Cystic teratoma. Although the lesion is predominantly cystic, there are marked solid elements which confirm the diagnosis

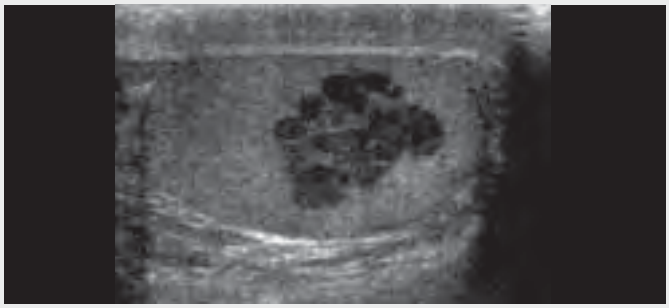

Cystic ectasia of the rete testis

The rete testis is the area at the hilum of the testis where the tubules leave to enter the epididymis. The tubules are of variable size and are often just visible on the ultrasound image as multiple thin-walled tubes converging at the hilum. Varying degrees of dilatation or ectasia can occur, assumed to be due to obstruction of the sperm transport mechanism (epididymis or vas deferens). The most common cause is vasectomy, though other causes are possible. Ectasia of the rete testis is relatively common in older men. It is not known whether all cases are due to obstruction. The condition is sometimes associated with multiple epididymal cysts.

In older men the condition is not important but, in younger men, bilateral ectasia suggests infertility. Dilatation of the rete has sometimes been misdiagnosed as cystic teratoma, particularly if scanned with low-resolution equipment. With good imaging, the misdiagnosis should not be made.

Carcinoma of the rete testis also produces tubular dilatation in its early stages, but there are coexisting solid elements. These tumours are extremely rare and frequently present with haematospermia. A history of haematospermia should raise the suspicion of the diagnosis and in the absence of the symptom it can be discounted. The tumour usually presents at a later stage as a large solid mass, indistinguishable on ultrasound from a germ cell tumour.

Ultrasound appearance

- Mild-to-moderate ectasia appears as multiple tubular structures at the testicular hilum.
- In more severe cases, the tubules are rounded. This may be termed cystic ectasia.
- There are often associated multiple epididymal cysts (Fig. 15.38).

Epidermoid cyst

Testicular epidermoid cysts are benign cystic lesions that, unlike simple cysts, are full of keratin rather than fluid. They are uncommon, comprising about 1% of testicular tumours. It is important to recognize them because, if a firm ultrasound diagnosis can be made, they can be excised, and the testis conserved.

Fig. 15.38. Ectasia of the rete testis. (a) The tubules of the rete testis are moderately enlarged. (b) A more marked case. (c) Gross enlargement (cystic ectasia)

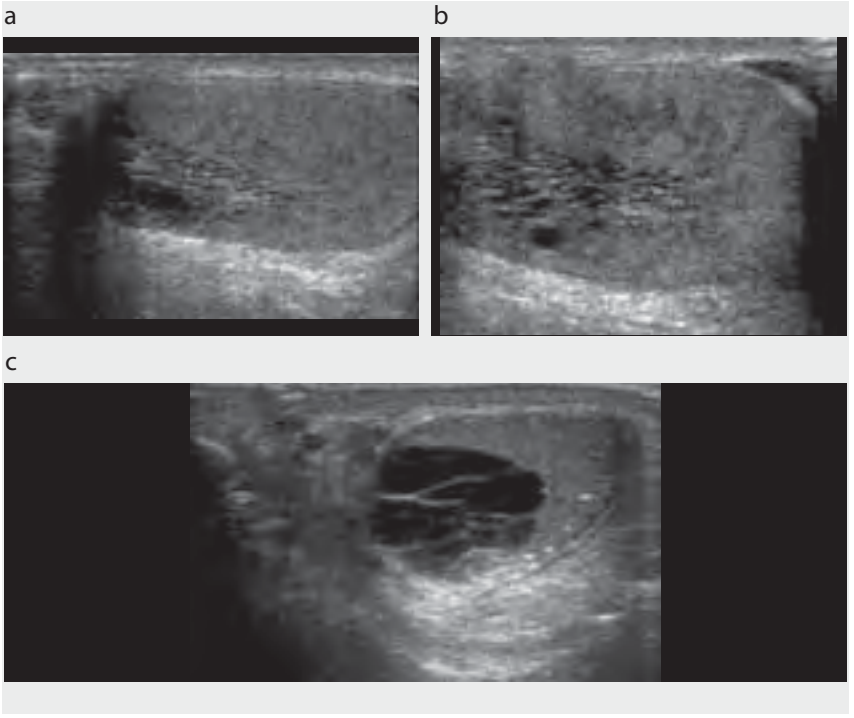

Ultrasound appearance

- The most typical appearance is of concentric rings, representing layers of keratin within the cyst. They may also have a more speckled appearance.
- The centre of the lesion is avascular. If any vessels are seen within the lesion then it is not an epidermoid cyst (Fig. 15.39).

Granuloma of the tunica albuginea

This benign granuloma may be caused by infection or trauma, but is more often idiopathic. Multiple granulomas may occur, for instance in granulomatous periorchitis. Although not truly intratesticular lesions, they may cause clinical concern. Small granulomas characteristically feel like a small hard grain of rice on the surface of the testis. Larger ones feel like testicular tumours.

Ultrasound appearance

- Granulomas may be hypoechoic or hyperechoic.
- They clearly lie within the tunica albuginea.
- They may calcify (Fig. 15.40).

Fig. 15.39. Testicular epidermoid cysts. (a) A typically hyperechoic round wall with concentric hyperechoic and hypoechoic rings within it. (b) A more speckled appearance. (c) Multiple epidermoid cysts. In this case the contents are more linear

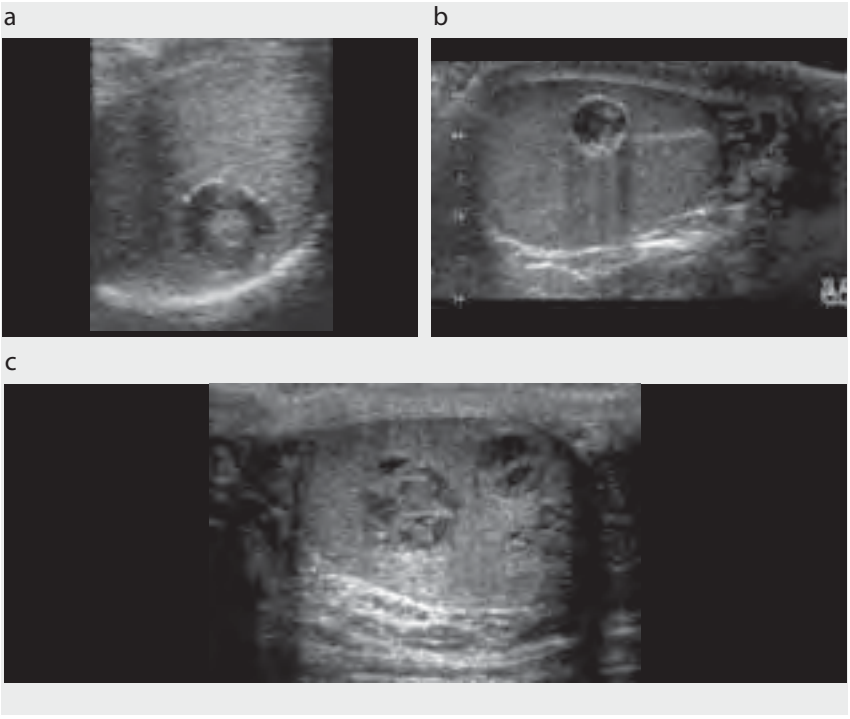

Image (b) reproduced with permission from: Cochlin DLL, Dubbins PA, Goldberg BB, Halpern EJ. *Urogenital ultrasound*, 2nd edition. London, Taylor & Francis Group, 2006. Fig. 5:3.

Small intratesticular tumours

With high-resolution ultrasound systems, very small tumours down to a few millimetres in size can be detected. Hyperechoic lesions are invariably benign, and are rarely, if ever, excised. They are often labelled granulomas, though their true nature is uncertain. Small hypoechoic lesions are more of a problem, and may cause a diagnostic dilemma (Fig. 15.41). A small germ cell tumour must be considered. However, most lesions of less than 5-mm diameter prove to be benign stromal tumours or cell rests. If orchidectomy is not performed, these lesions must be closely followed up.

Intratesticular haematomas

Intratesticular haematomas can be caused by severe trauma. They are included here as they may appear to be tumours. While a history of trauma would seem to point to the diagnosis, it is common for patients to present with a testicular tumour after trauma. This may be because the trauma causes a bleed into the tumour, or because the trauma prompts the patient to examine his scrotum. As with any intratesticular mass, estimation of serum tumour markers and follow-up are mandatory.

Fig. 15.40. Tunica granuloma. (a) A calcified granuloma casting a shadow. (b) A predominantly fibrous hypoechoic granuloma with a small fleck of calcification. It is lying posteromedially. (c) Granulomatous periorchitis. Two hypoechoic fibrous granulomas are seen in this plane on the anterior tunica. More were seen in other planes

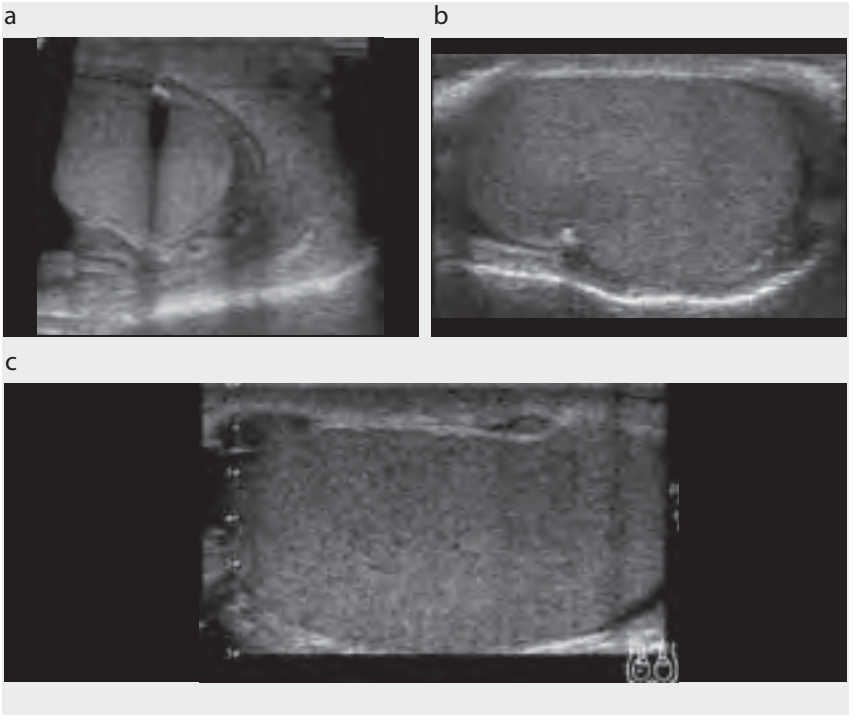

Fig. 15.41. Small intratesticular tumour. (a) Longitudinal plane. (b) Transverse plane. This tumour was found incidentally. The patient opted for orchidectomy. The tumour was a benign Leydig cell rest

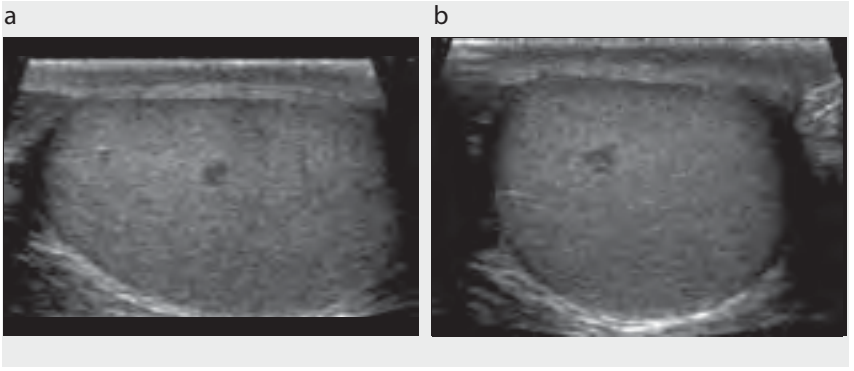

Ultrasound appearance

- See section on Trauma in this chapter.

Focal orchitis and infarcts

Focal orchitis and infarcts may both appear to be tumours.

Ultrasound appearances

- See sections on Epididymo-orchitis and Focal testicular infarcts in this chapter.

Testicular atrophy

The atrophic testis, whatever the cause, becomes small and heterogeneous with hypoechoic and hyperechoic areas, some due to scarring, others due to Leydig cell rests. Some of these areas may resemble germ cell tumours (Fig. 15.42). In older men with ischaemic atrophy and in younger men with a history of atrophy following mumps infection, these changes may be assumed to be due to atrophy alone. Conversely in men with atrophy due to previously undescended testes, congenital atrophy or hypotrophy, the testes are also likely to be dysplastic. This increases the risk of developing germ cell tumours. Abnormal areas within these testes must therefore be treated cautiously, with careful follow-up.

Fig. 15.42. Testicular atrophy. The testis is typically less than 3 cm in length and inhomogeneous with a prominent hypoechoic area. This appearance mimics a tumour

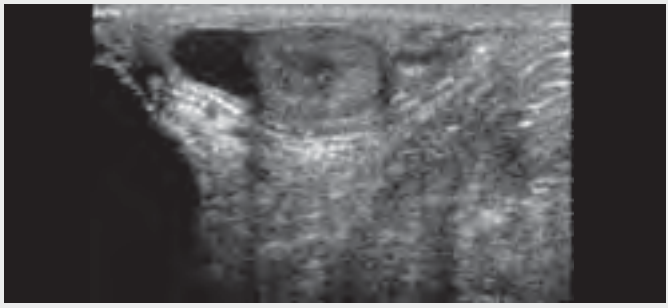

Ultrasound appearance

- The testis is small.
- There is an inhomogeneous parenchymal texture with irregular hyperechoic and hypoechoic areas (Fig. 15.42).

Extratesticular scrotal masses

An extratesticular scrotal mass may be:

- an epididymal cyst or spermatocele
- a benign epididymal tumour (sperm granuloma, adenomatoid tumour)
- an inflammatory or post-inflammatory epididymal mass
- tubular ectasia of the epididymis
- a malignant tumour, such as sarcoma or mesothelioma (but these are extremely rare).

Epididymal cysts and spermatoceles

It is often not possible to distinguish between these two benign cystic lesions. This is, however, not important as both are usually treated conservatively. Large symptomatic lesions may be excised.

Ultrasound appearance

- Both cysts and spermatoceles are thin-walled, spherical or ovoid structures. Larger ones may be indented by surrounding structures.
- They are often multiple.
- Their size varies from a few millimetres to several centimetres.
- Spermatoceles tend to be larger than cysts and have speckly echogenic contents (Fig. 15.43).
- Occasionally they may have an irregular shape, or apparently solid contents, possibly because of haemorrhage.

Whatever their appearance, epididymal cysts are always benign.

Fig. 15.43. Epididymal cysts. (a) A small cyst. (b) A large cyst or spermatocele. These are thin-walled with anechoic contents

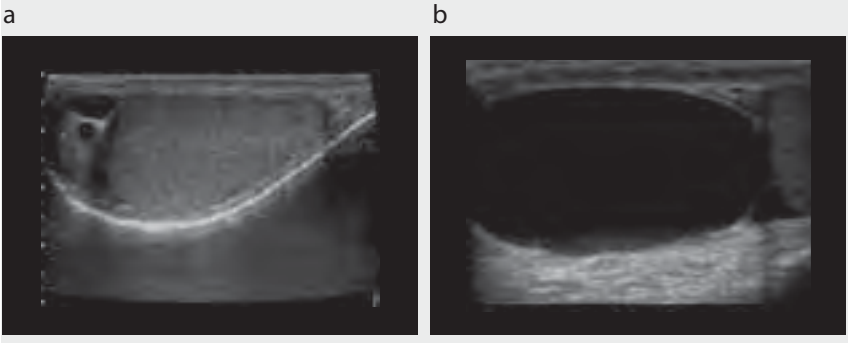

Differential diagnosis

- Large cysts that are indented by the testis may look like hydroceles. They do not, however, surround the testis.
- Tunica albuginea cysts that bulge out from the testis may look like epididymal cysts. Their attachment to the tunica distinguishes them.

Sperm granulomas

A granuloma, or scar tissue, may develop in response to sperm that has exuded from the tubules. They are more common following vasectomy, but often occur in patients who have not had a vasectomy. They typically cause a dull ache for a few months and thereafter are asymptomatic apart from a palpable mass.

Ultrasound appearance (Fig. 15.44)

- Granulomas are rounded masses, less than 1 cm in diameter.
- They have even or slightly mixed echodensity and are often almost isoechoic with the epididymis.
- If they are almost isoechoic, they are often easier to palpate than to demonstrate on an ultrasound scan.

Placing a finger of one hand against the palpable lesion while scanning with the other hand will often make the lesion easier to demonstrate.

Fig. 15.44. Sperm granuloma. There is a round lesion within the epididymis. This granuloma is significantly hypoechoic and is thus easy to see (transverse view of the epididymis; the testis is out of plane)

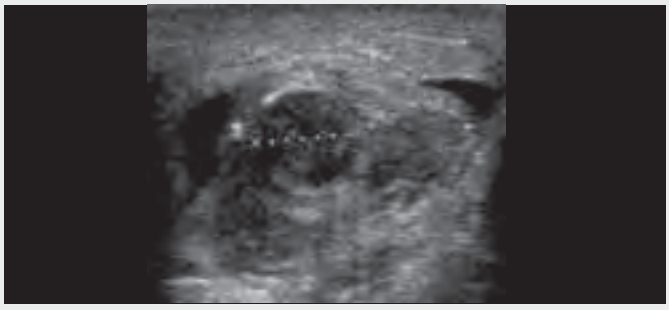

Adenomatoid tumours

These are benign tumours of the epididymis that typically occur in middle-aged men. They are asymptomatic and usually present as a mass less than 1.5 cm in diameter.

Ultrasound appearance (Fig. 15.45)

- Apart from their size and different history, they are indistinguishable from sperm granulomas.
- Distinction from sperm granulomas is unimportant as both lesions are treated conservatively.

As with sperm granulomas, palpating the lesion while scanning may be necessary to visualize it.

Inflammatory and post-inflammatory epididymal masses

Epididymitis causes swelling of the epididymis, which is sometimes focal. In the acute phase the nature of the mass is obvious. Focal swellings may persist for a considerable

time after the clinical symptoms have cleared and may be permanent. Tuberculous epididymo-orchitis usually results in a permanent irregular craggy mass.

Fig. 15.45. Adenomatoid tumour. There is a well circumscribed, significantly hypoechoic tumour within the epididymis. Many are only slightly hypoechoic

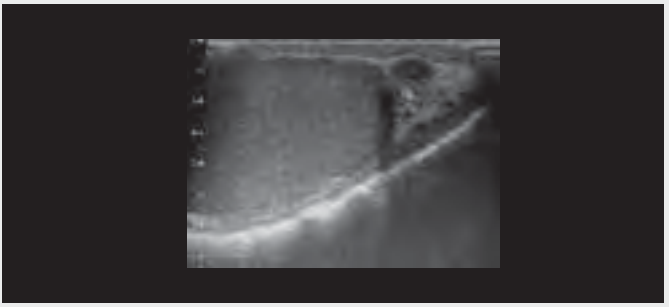

*Ultrasound appearance (**Fig. 15.46**)*

- The masses are typically of similar echodensity to the rest of the epididymis, making them difficult to see.
- If the mass is palpated while scanning, it can be seen to move differently from the normal epididymis.
- Tuberculous masses are irregular with a mixed echo pattern involving the testis and epididymis (see also Fig. 15.16).

Fig. 15.46. Post-inflammatory mass. There is a round, almost isoechoic area in the epididymal tail. This persisted after an episode of epididymitis

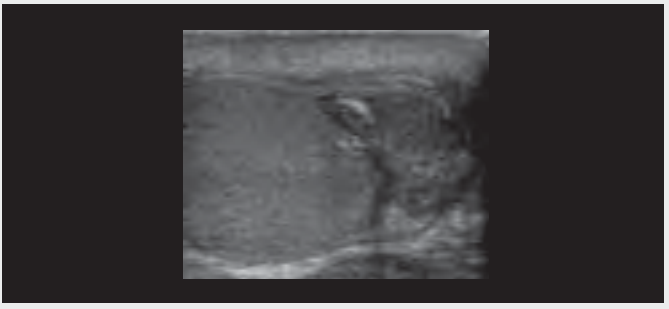

Tubular ectasia of the epididymis

Tubular ectasia of the epididymis is a condition that occurs in older men, often, though not exclusively, in men who have had a vasectomy. Commonly the whole epididymis is enlarged. Occasionally one part of the epididymis is more affected and presents as a palpable mass.

Ultrasound appearance (**Fig. 15.47**)

- High-resolution ultrasound systems can demonstrate that the epididymal enlargement or mass is a result of dilated tubules.
- Low-resolution systems will show non-specific enlargement of all or part of the epididymis, but may not demonstrate the individual tubules.
- The condition is often associated with tubular ectasia of the rete testis.

Fig. 15.47. Tubular ectasia of the epididymis. (a) The whole of the epididymis is enlarged. The individual dilated tubules can be seen. (b) Focal enlargement of the epididymal head. (c) A focal mass-like lesion in the tail of the epididymis. The dilated tubules making up the lesion are easily seen

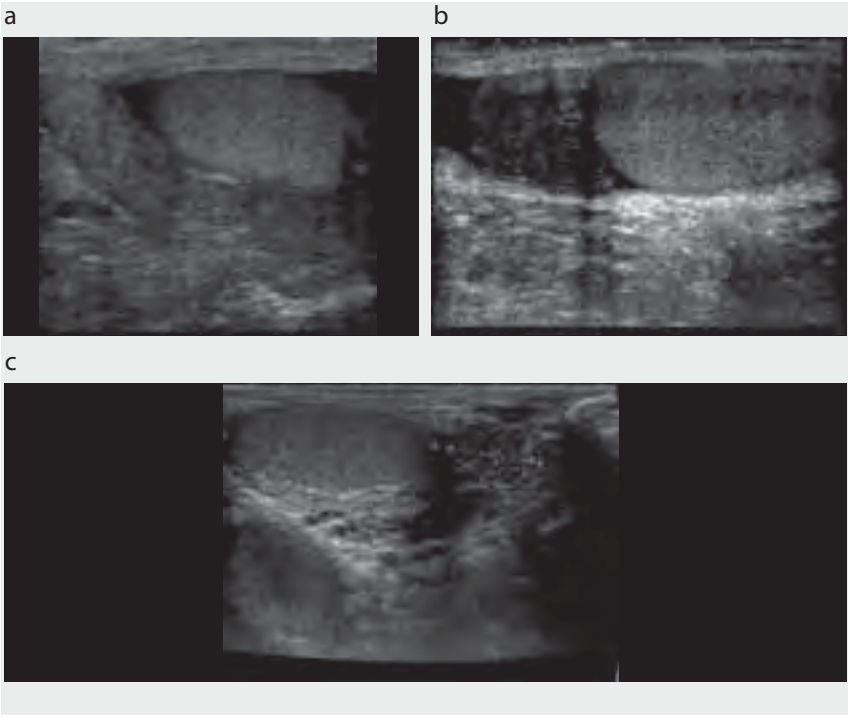

Varicocele

A varicocele is a pathological dilatation of the intrascrotal veins (the pampiniform plexus). Most are due to incompetent venous valves and reflux. A small minority may be due to obstruction by a pelvic tumour or, on the left side only, a renal tumour invading the renal vein. Rarely, they can be caused by an arteriovenous communication (high-flow varicocele). They are common: 10% of men have a left varicocele.

Ultrasound appearance

- The veins are enlarged to more than 2 mm supine, 2.5 mm standing.
- On a colour Doppler scan, there is little spontaneous flow. However, on coughing or with the Valsalva manoeuvre, reflux flow occurs, causing the veins to fill with colour (Fig. 15.48).
- Obstructed varicoceles do not have reflux flow. High-flow varicoceles have high spontaneous flow (without cough or Valsalva manoeuvre).
- Some specialists advocate scanning the left kidney in cases of left varicocele, to look for a tumour. The positivity rate, however, is very small.

Fig. 15.48. Varicocele. (a) A grey-scale image showing the enlarged veins. (b) A Doppler scan performed after a Valsalva manoeuvre. The reflux blood flow into the dilated veins is shown

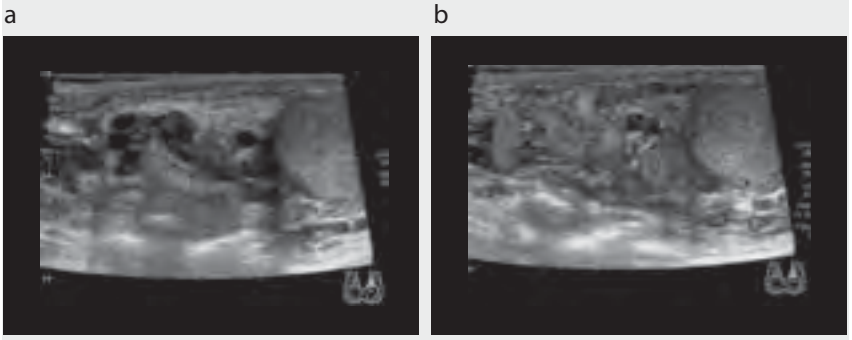

Inguinal hernia

An inguinal hernia may present as a scrotal mass. In most cases the diagnosis is made clinically. If there is clinical doubt, an ultrasound study may be requested.

Ultrasound appearance

- The echo pattern of a hernia is highly variable, depending on whether it contains omentum or bowel.
- The diagnostic feature is that a hernia can be shown to extend through the inguinal canal into the abdomen (Fig. 15.49).

Scrotal lymphangioma

Scrotal lymphangioma is caused by lymphatic obstruction. It presents as a large soft scrotal mass. It is most common in infants, though it may occur at any age.

Ultrasound appearance

- A large, loculated, cystic structure fills the extratesticular space.
- The lesion often extends through the inguinal canal into the pelvis (Fig. 15.50).

Fig. 15.49. Inguinal hernia. (a) A complex mass is seen above the testis. (b) The mass can be seen to pass through the inguinal canal into the abdomen

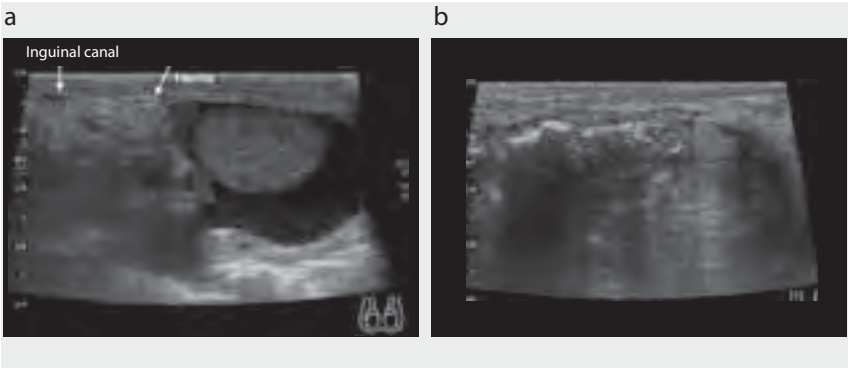

Fig. 15.50. Scrotal lymphangioma. This infant presented with a scrotal mass. The testis (which is not shown in this plane) was normal. There is a multiloculated, fluid-filled lesion within the scrotum, extending up to the inguinal canal (seen on the right side of the image)

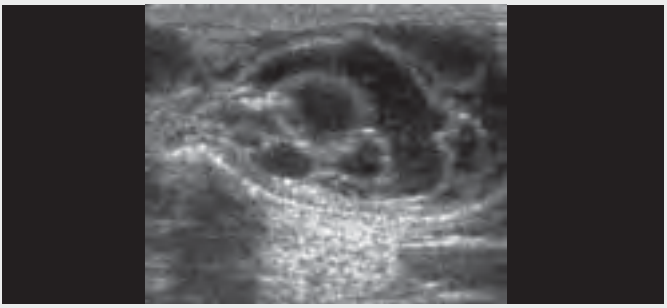

It is important to determine the total extent of the lesion, as incomplete surgical excision leads to recurrence. The pelvic component is better assessed by magnetic resonance imaging or computerized tomography.

Hydrocele

A hydrocele is a pathological increase in the volume of the fluid that normally surrounds the testis. In developed countries, the majority of hydroceles are idiopathic. In areas endemic for filariasis, the majority are due to this disease. Hydroceles may occur as a reaction to other scrotal pathology, particularly epididymo-orchitis, torsion or tumour.

***Ultrasound appearance* (*Fig. 15.51*)**

- There is fluid surrounding the testis, which is usually anechoic.
- Chronic hydroceles, inflammatory hydroceles and those due to filariasis have echogenic material floating in the fluid and may have fine lines, representing synechia, crossing them. In acute infection there is also epididymo-orchitis.

Fig. 15.51. Hydrocele. Anechoic fluid surrounds the testis

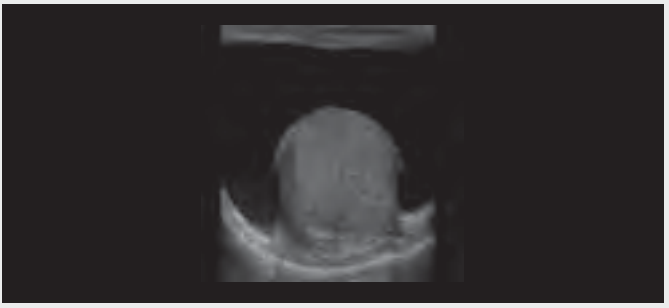

- High-resolution systems will show very fine speckles due to crystals in the hydrocele.

Trauma

Blunt trauma to the scrotum may cause swelling, usually as a result of a haematohydrocele. In severe trauma there may also be intratesticular haematoma. The ultrasound study has two main aims:

- to exclude the uncommon condition of a ruptured or fractured testis in which the tunica is torn; these cases should be surgically repaired;
- if there is a palpable testicular mass, to distinguish between haematoma and tumour.

Patients often present with a testicular tumour following an episode of trauma. The distinction may be difficult and follow-up is often required.

***Ultrasound appearance* (*Fig. 15.52*)**

- A haematohydrocele appears as echogenic fluid surrounding the testis, sometimes with a fluid–fluid level. This gives the appearance of a layer of moderately hyperechoic fluid separated from a less echoic layer of fluid by a straight horizontal line.
- An extratesticular haematoma is initially anechoic, then of mixed echodensity, then anechoic but with multiple echoic lines of septae crossing it.
- An intratesticular haematoma appears similar to a tumour. It is avascular on a Doppler scan (but small tumours may also have no blood flow on a Doppler scan). A haematoma is non-perfused on ultrasound contrast study.

- If there is any doubt as to the diagnosis, follow-up is essential. Haematomas slowly resolve, while tumours grow larger.
- A ruptured tunica albuginea appears as a defect in the line of the tunica, with an irregular appearance – like the bristles on an old toothbrush – representing the testicular tubules spilling out.
- The coexistence of an intratesticular and extratesticular haematoma strongly suggests a ruptured testis, even if a tunical defect is not seen.
- Intratesticular haematomas appear as hypoechoic areas. They may be indistinguishable from tumours except by follow-up.

Fig. 15.52. Scrotal trauma. (a) A ruptured testis. There are hypoechoic haemorrhages within the testis, and an echogenic haematocele. The tunica between the testis and the epididymis is discontinuous, indicating rupture (arrows). (b) Haematohydrocele. There is a fluid–fluid level, and haemorrhage into the epididymis, causing dilatation of the tubules

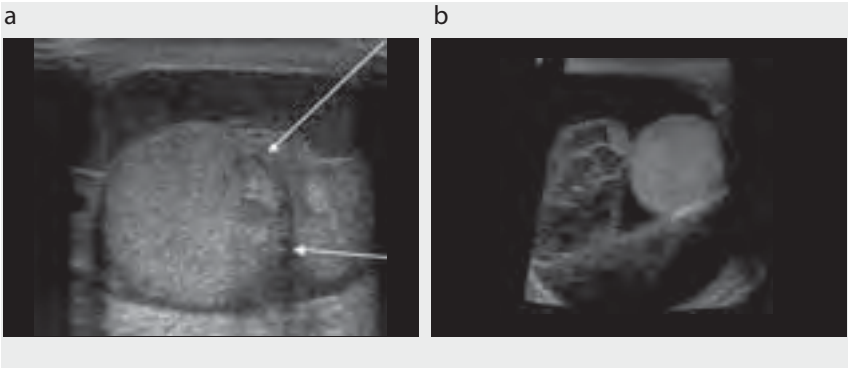

Swelling of the scrotal wall

Enlargement of the scrotum may be due to swelling of the wall. This may occur in any condition that causes oedema. Of particular note is idiopathic scrotal oedema, in which the oedema affects only the scrotum. It occurs in young boys and less often in older men. The cause is unknown and the condition is self-limiting.

Swelling of the scrotal wall may also be due to soft tissue infection. This may be secondary to severe epididymo-orchitis or may be a primary infection of the scrotal wall. A particularly virulent form is **Fournier gangrene**, a necrotizing infection of the perineum characterized by the formation of gas in the tissues.

Ultrasound appearance

- Oedema of the scrotal wall causes a thick wall with separation of the normal tissue planes by hypoechoic tissue (Fig. 15.53).
- If the cause is infection, abscesses may be present. Fournier gangrene will show shadowing from gas in the tissues (Fig. 15.54).

Fig. 15.53. Idiopathic scrotal oedema. The scrotal wall is thickened and hypoechoic with separation of the tissue layers

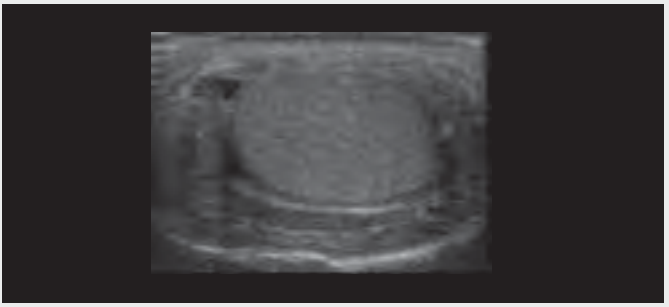

Fig. 15.54. Fournier gangrene. (a) There is marked oedema of the scrotal wall. The echogenic area medial to the right testis suggests gas in the soft tissues. (b) There are obvious pockets of gas in the adjacent perineum, casting shadows

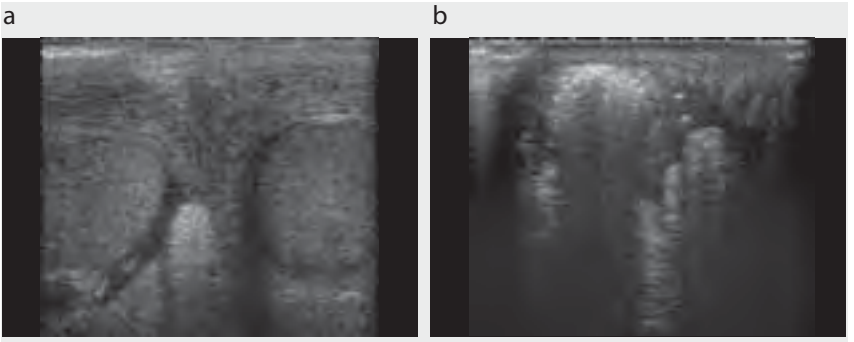

Chapter 16

Special aspects of abdominal ultrasound

16

Special aspects of abdominal ultrasound

Acute abdomen

Acute abdomen is defined as a sudden onset of severe abdominal pain connected with tenderness, visceral dysfunction and – possibly delayed – circulatory decompensation. Many different pathological processes may cause this syndrome, including inflammatory diseases, perforations, bowel obstruction, and circulatory disturbance of the feeding vessels. Even extra-abdominal disorders may cause these symptoms. In many of the causative diseases, surgery is needed.

After a detailed history and thorough physical examination, imaging can be useful, provided it can be carried out without loss of time at the bedside, without further stress for the patient, and without special preparation – conditions that are met nearly completely by ultrasound.

The ultrasound examination should be done systematically, independent of the expected disorder or the statistical likelihood of the various possible diseases. It is useful to start by examining the liver, even though diseases of the liver are rarely the reason for an acute abdomen. This is because the examination of the liver allows the settings of the equipment to be adjusted to the particular situation and gives a first topographical orientation before the more difficult parts of the abdomen are scanned.

A complete examination should always be performed, even if a pathological process (e.g. gallstones) is found at the beginning. Otherwise, the main diagnosis may be missed. Table 16.1 shows the recommended course of the examination, together with a checklist of features to be looked for in the various organs and regions. Details and images are given in the relevant chapters.

Table 16.1. Acute abdomen: ultrasound examination of the abdomen

Organ/region	Features to be looked for
Liver	Abscess; tumour with (spontaneous) haemorrhage; complicated parasitic cyst
Gallbladder	Cholecystitis (thickened wall, fluid); perforation. (*Note: gallstones alone do not cause acute symptoms.*)
Pancreas	Acute pancreatitis (oedema, necrosis)
Stomach, duodenum	Perforation (ulcer, tumour); obstruction
Spleen	Abscess; infarction; rupture
Bowel	Obstruction; perforation (diverticulitis, abscess, fistulas); ischemic disorder (thickened wall, paralytic ileus, gas in the portal vein)
Appendix	Swelling; abscess
Abdomen	Fluid (ascites, blood, abscess); free gas
Abdominal wall	Abscess; hernia; spontaneous haemorrhage (rectus sheath)
Retroperitoneum	Aortic aneurysm (bleeding); urinary congestion; stones; fluid (pelvic rupture, abscess, spontaneous bleeding or bleeding from tumour)
Small pelvis	Adnexitis; ruptured endometrial cyst; torsion; ectopic pregnancy
Chest	Pleural effusion; pulmonary embolism; basal pneumonia; pericardial effusion

Blunt abdominal trauma

Blunt abdominal trauma can cause diagnostic problems for various reasons. First, it may occur together with other more obvious injuries in patients with multiple traumas (for instance, in traffic accidents). Second, the patient may have few symptoms at first. Finally, the examination may have to be carried out in an emergency service under difficult conditions, e.g. in a brightly lit room, while other health staff are dealing with other injuries. The examination has to be carried out systematically and the abdominal organs should be checked following a clear schema, as recommended in Table 16.2.

Table 16.2. Ultrasound diagnosis in blunt abdominal trauma

Region/organ	Ultrasound features	Interpretation
Abdominal cavity, particularly Morison's pouch, splenic bed, retrovesical space	– Echo-free or echo-poor fluid	– Haemoperitoneum (the location does not always correspond to the location of the bleeding)
Retroperitoneal space	– Echo-free or echo-poor fluid	– Urinoma (echo free), haemorrhage (within renal fascia)
Liver, spleen, pancreas, kidneys (parenchymal organs)	– Fluid around the organ – Irregular or double contour, – Enlargement, irregular vascularity, or lack of Doppler signals	– Contusion or rupture (for details, see Table 16.3)
Urinary bladder	– Echoes in the fluid	– Blood, injury to the bladder or kidney
Gallbladder	– Echoes in the fluid	– Blood, injury to the gallbladder or liver
Arteries, aorta	– Lack of pulsation on B-scan – No signal on colour Doppler	– Avulsion

If the findings of the first examination are normal or inconclusive, the examination should be repeated after 4–6 h, especially if the time between the trauma and the first examination was short. Not infrequently, a small amount of blood in the abdomen may be missed at the first examination, especially if the conditions for the systematic examination are poor. Furthermore, the initial ultrasound indications of bleeding due to a contusion or even a rupture of a parenchymatous organ may be inconclusive (Fig. 16.1, Fig. 16.2 and Fig. 16.3).

Fig. 16.1. Contusion of the liver. (a) The diffuse echo-rich zone with an irregular border in the right lobe indicates a diffuse bleeding. This scan was made 2 h after an accident. (b) Blood in Morison's pouch (arrow) and an echo-rich area in the liver, 6 h after an accident (K, kidney)

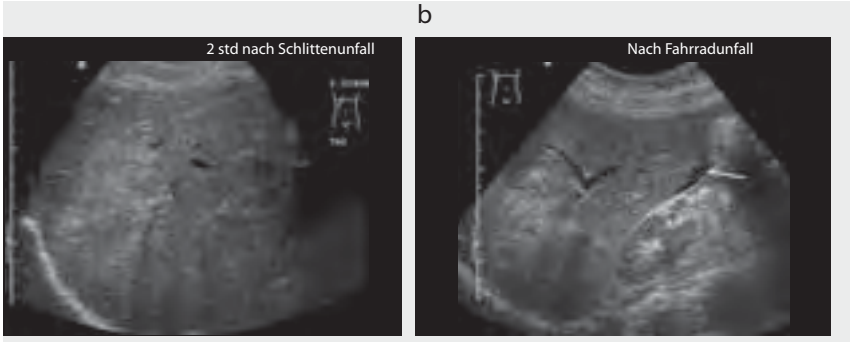

Fig. 16.2. Haematoma in the liver. Several days after a blunt trauma, a partially echo-free and partially echo-poor lesion with sharp margins can be seen in the liver

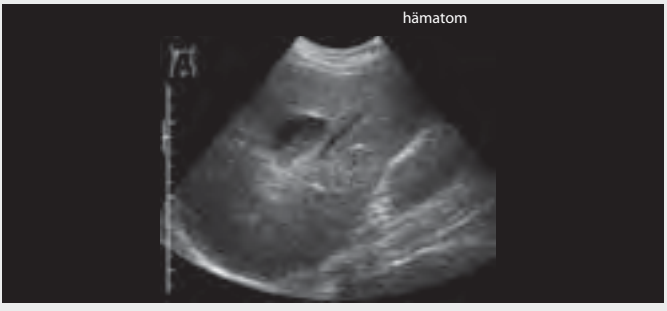

Fig. 16.3. Trauma to the spleen. (a) The inconspicuous (on initial view) spleen (S) is surrounded by echo-poor blood, shortly after a traffic accident. (b) Careful examination of all parts of the spleen shows a tear (arrow)

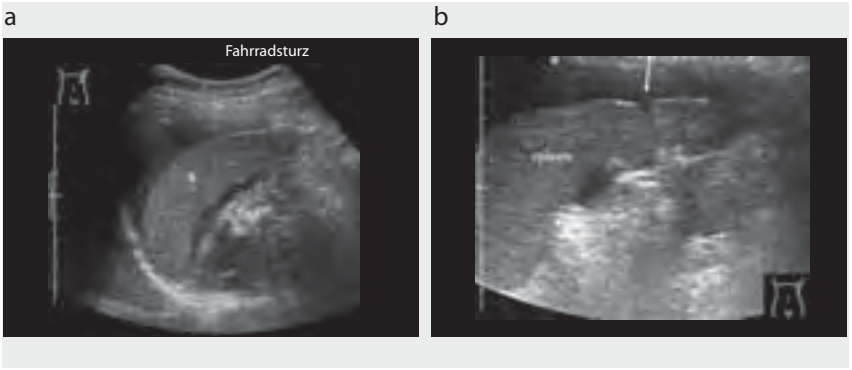

It is necessary, therefore, to look carefully for indirect symptoms of an injury to a parenchymal organ, such as blood in the abdominal cavity (Fig. 16.4) or the retroperitoneal space, changes in the contour of organs, a blurred echo pattern or a lack of (respiratory) movement (see also Fig. 6.17, Fig. 7.34, Fig. 10.15, Fig. 13.43 and Table 16.3). Echoes, i.e. blood, in the gallbladder or the urinary bladder may indicate an injury to the liver or the kidneys, respectively.

Table 16.3. Ultrasound features of parenchymal injuries

Ultrasound feature	Interpretation/diagnosis
Fluid around an organ	Tear(s) of the organ
Double contour	Subcapsular haematoma
Contour break (irregular outline)	Rupture
Organ enlargement	Parenchymal bleeding
Blurred echo pattern, 'clouds' of fine echoes	Parenchymal bleeding
Loss of 'movability'	Inconclusive, but may indicate a severe injury (needs follow-up and examination with contrast agents)
Irregular vascularity or lack of Doppler signals	Contusion (check), rupture or avulsion of a feeding vessel (contrast agents)

An additional Doppler examination, particularly with power Doppler, can demonstrate normal or abnormal vascularity. Abnormal vascularity may indicate avulsion of a vessel, a severe rupture of a parenchymal organ, or a contusion. This can be clarified by using contrast agents and by follow-up examinations within hours.

If blood is demonstrated with B-scan ultrasound, colour Doppler may allow the source of a still-active bleeding to be found.

Fig. 16.4. Blunt abdominal trauma. The fluid (blood) behind the bladder indicates bleeding in the abdominal cavity. Note the difference between the echo-free fluid in the bladder and the echo-poor blood behind the bladder

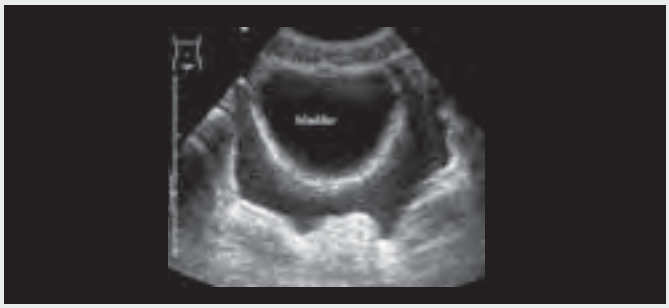

Examination of HIV-infected patients

Ultrasound is useful as a first-level imaging modality for patients with HIV infection, particularly for examination of the abdomen. It is likely to find particular application in developing countries, where HIV infection rates may range from 5% to 25%, and where computerized tomography and magnetic resonance imaging may be unavailable or unaffordable. Practitioners in general, and not only those in developing countries, should become familiar with the wide variety of ultrasound findings in HIV patients.

Precautions are required to avoid the transmission of infectious material from HIV patients to others. It is advisable to cover the transducer with a glove, to use disinfectants and to protect health-care personnel, especially if invasive procedures (guided puncture) are carried out.

It is important to be aware that patients with HIV infection may present with atypical features of common diseases, or with rare diseases not usually seen in immunocompetent subjects, e.g. extrapulmonary tuberculosis or *Mycobacterium avium* complex (MAC) infections.

Depending on the stage of the HIV infection, several organs may be affected and a wide variety of infectious diseases may be seen. Atypical neoplastic diseases also occur. In many situations, the ultrasound findings will be aspecific and the particular disease will not be evident. It is often difficult to differentiate between infectious and neoplastic diseases; for example, if atypical enlarged lymph nodes (Fig. 16.5, Fig. 16.6, Fig. 16.7) or bulky tumours of the bowel are seen (lymphoma or tuberculous infection?) or focal lesions in the liver or the spleen are found (lymphoma or abscess?). Ultrasound-guided puncture is particularly useful in such situations. Table 16.4 lists common findings on abdominal scans of HIV patients. The details are given in the specific chapters (see also Fig. 7.14, Fig. 8.22, Fig. 10.8, Fig. 11.35, Fig. 11.47, Fig. 13.28 and Fig. 13.39).

Fig. 16.5. Enlarged lymph nodes in HIV-infected patients. (a) Enlarged echo-poor tuberculous lymph nodes around the coeliac trunk (arrows). (b) Echo-rich lymph node (arrows) in the hepatic hilum (HIV patient with lymphadenopathy)

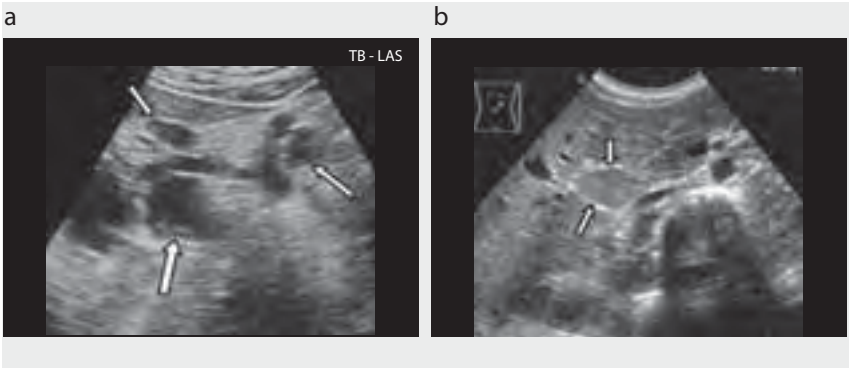

Fig. 16.6. Enlarged lymph nodes in HIV-infected patients (arrows). (a) Coinfection of HIV and hepatitis C (P, portal vein; V, vena cava; A, aorta). (b) Malignant lymphoma

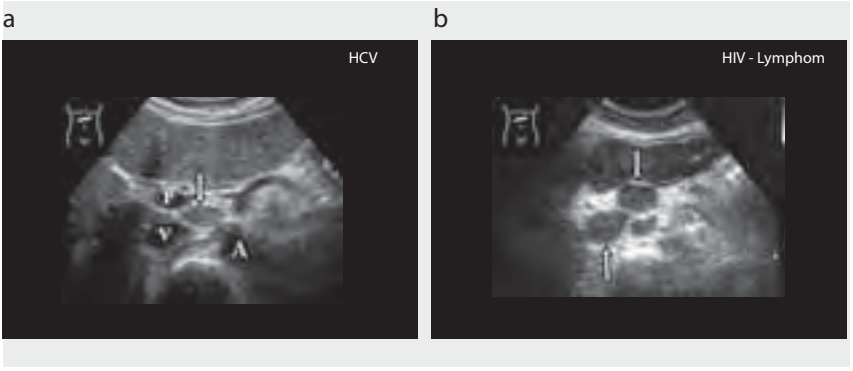

Fig. 16.7. Lymph nodes in HIV-infected patients. (a) Echo-poor, irregular, enlarged lymph nodes in a patient with non-Hodgkin lymphoma. (b) Mycotic abscess (A) in the left liver lobe and mycotic lymph nodes (arrows) around the coeliac trunk

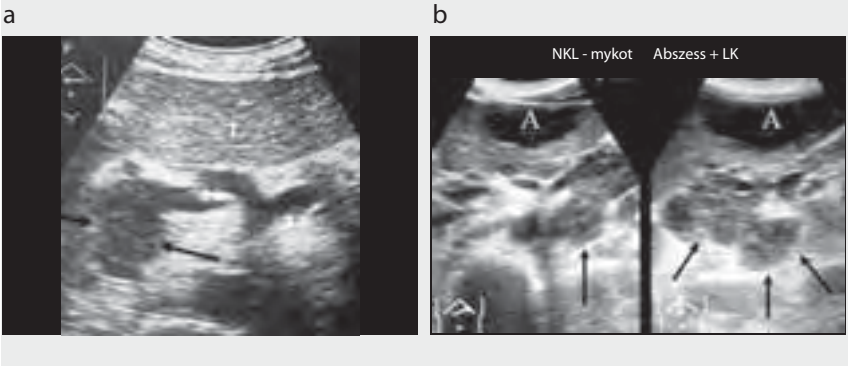

Table 16.4. Ultrasound examination of the abdomen in HIV-infected patients

Organ/ structure	Ultrasound features	Interpretation
Liver	– Enlargement	– Non-specific
	– Echo-rich pattern	– Fatty liver (alcohol), tuberculosis, concomitant hepatitis B virus infection, drugs, cirrhosis
	– Echo-rich spots (snow storm)	– Bartonella infection, *Pneumocystis jiroveci*
	– Echo-rich lesions > 10 mm	– Kaposi sarcoma
	– Echo-poor lesions > 1 cm	– Abscesses (tuberculosis) (Fig. 16.8), malignant lymphomas
	– Target-like lesions	– Mycotic abscesses, metastases)
Gallbladder	– Thickened wall	– Acalculous infectious cholecystitis (cytomegalovirus infection)
Bile ducts	– Thickened wall, irregular dilatation	– Sclerosing cholangitis
Pancreas	– Oedematous enlargement, dilated duct (abscesses)	– Pancreatitis (opportunistic infection)
Spleen	– Enlargement	– Nonspecific
	– Small echo-poor lesions	– Mycotic abscesses
	– Large echo-poor lesions	– Bacterial abscesses (tuberculosis)
	– Echo-poor masses of various sizes	– Malignant lymphoma
	– Echo-rich lesions of various sizes	– Kaposi sarcoma
	– Complex lesions	– *Candida* abscess, carcinoma
Gastrointestinal tract	– Dilated antrum	– Dysfunction
	– Thickened wall of various sections, hypermotility and stenoses	– Opportunistic infections
	– Complex masses with considerably thickened wall, enlarged lymph nodes	– Inflammatory pseudotumours (tuberculosis, MAC) (differential diagnosis malignant lymphomas)
Kidneys	– Enlargement, echo-rich structure	– Non-specific
	– Echo-poor lesions	– Malignant lymphoma (differential diagnosis abscesses)
Abdominal cavity	– Ascites	– Non-specific (infection, portal hypertension)
Lymph nodes	– Enlarged, oval-shaped lymph nodes (hilus sign)	– Lymphadenopathy
	– Enlarged, roundish, echo-poor lymph nodes (no hilus sign)	– Tuberculosis, granulomatous lymph nodes, malignant lymphomas
	– Echo-rich lymph nodes	– Kaposi sarcoma

Fig. 16.8. Tuberculosis of the liver in HIV-infected patients. (a) Granuloma in the right liver lobe (arrow). (b) Calcified regressive lesion under therapy

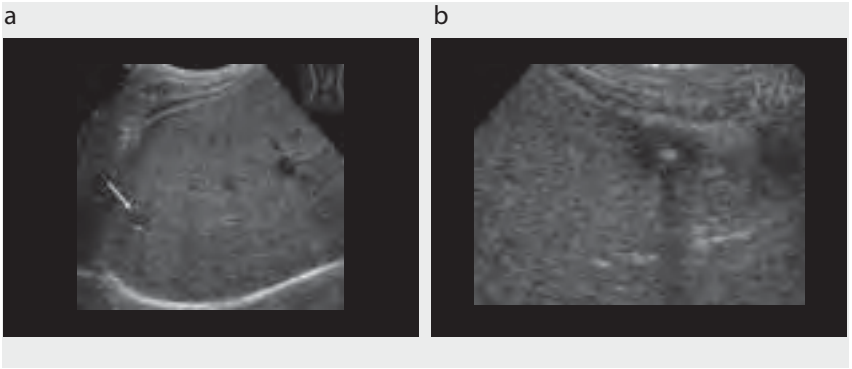

Recommended reading

- Bartolozzi C, Lencioni R, editors. *Liver malignancies: diagnostic and interventional radiology.* Berlin, Springer, 1999.
- Buscarini L, Campani R, editors. *Atlas of abdominal ultrasound.* Naples, Idelson Gnocchi, 2001.
- Buscarini E, Di Stasi M, editors. *Complications of interventional abdominal ultrasound.* Milan, Poletto, 1996.
- Cochlin DLL et al., editors. *Urogenital ultrasound,* 2nd edition. London, Taylor & Francis Group, 2006.
- Livraghi T, Makuuchi M, Buscarini L, editors. *Diagnosis and treatment of hepatocellular carcinoma.* London, Greenwich Medical Media, 1997.
- Lopez PM, Villanueva A, Llovet JM. Systematic review: evidence-based management of hepatocellular carcinoma–an updated analysis of randomized controlled trials. *Alimentary Pharmacology & Therapeutics,* 2006, 23:1535–1547. doi:10.1111/j.1365-2036.2006.02932.x PMID:16696801
- Lutz H, Gharbi HA, editors. *Manual of diagnostic ultrasound in infectious tropical diseases*. Springer, 2006.
- Mathis G, Lessnau KD, editors. *Atlas of chest sonography,* 2nd edition. Berlin, Springer, 2007.
- Pollack HM, editor. *Clinical urography,* 2nd edition. Philadelphia, WB Saunders, 2000.
- Rifkin MD, Cochlin DLL, editors. *Imaging of the scrotum and penis,* 2nd edition. London, Martin Dunnitz, 2002.
- Verslype C et al. The management of hepatocellular carcinoma. Current expert opinion and recommendations derived from the 10th World Congress on Gastrointestinal Cancer, Barcelona, 2008. *Annals of Oncology,* 2009, 20 Suppl 7;vii1–vii6. doi:10.1093/annonc/mdp281 PMID:19497945
- WHO Informal Working Group on Echinococcosis. *Puncture aspiration injection re-aspiration: an option for the treatment of cystic echinococcosis.* Geneva, World Health Organization, 2001 (WHO/GDS/CSR/APH/2001-6).

Glossary

Absorption:
Direct conversion of (ultra)sound energy into heat; leads to reduction of ultrasonic intensity in biological tissue and is a possible hazard (see Chapter 1).

Absorption coefficient:
Product of absorption constant (of a medium) and frequency (of ultrasound).

Acoustic enhancement:
Relative intensification of the echoes distal to areas causing attenuation below the average ('sonolucent' areas), especially fluid collections, due to a relative excess of time gain compensation.

Acoustic shadow:
Echo-free or relatively echo-poor (partial shadow) area on an ultrasonic image occurring distal to interfaces, resulting in total reflection of the ultrasound (gas, foreign bodies) or structures causing relatively high attenuation (bones, fibres).

Acoustic streaming:
Movement of fluid due to ultrasound (demonstrated as movement of the echoes arising within a non-homogeneous fluid).

Anechoic, anechogenic:
Denotes the absence of (internal) echoes, typically for fluid (synonym: Echo free).

Artefact:
Feature on an ultrasonic image that is not referable to real structures with regard to shape, intensity or location.

A-scan:
One-dimensional technique in which each echo causes a vertical deflection of the electron beam on a display proportional to its intensity; used for measurements.

Attenuation:
Loss of intensity of ultrasound in a tissue due to absorption, reflection and scattering, measured in decibels per centimetre.

Axial resolution:
The ability to distinguish objects in the direction of the ultrasound beam emitted by a transducer.

B-scan:
Mode of display in which echoes are presented as light spots on the screen.

Cavitation:
Formation of voids within a molecular structure during the negative-pressure phase of a (ultra) sound wave.

Colour Doppler technique:
Duplex technique in which the Doppler signals are displayed as coloured pixels, depending on their mean velocity.

Contrast agent:
Encapsulated microbubbles used intravenously to enhance the Doppler signal from streaming blood.

Contrast harmonic imaging:
Based on a technique to receive only echoes with a doubled frequency (second harmonic) rather than the fundamental (emitted) frequency. Enables better differentiation of the signals due to contrast agents, because microbubbles produce a much stronger second harmonic signal than tissue.

Coronal plane:
Plane corresponding to the long axis of the body but at a right angle to the longitudinal (sagittal) plane (e.g. a coronal scan may be obtained with the transducer placed on the side).

Coupling agent:
A gel or liquid used to obtain close contact of the surface of the transducer with the skin without air bubbles interfering with ultrasound transmission.

Crystal:
Polar crystals used as ultrasound transducers for converting electrical energy into ultrasound waves and vice versa.

Curved array:
Transducer with two or usually more crystals arranged on a convex surface.

Decibel (dB):
Logarithmic unit of measure of acoustic energy.

Depth gain compensation:
Synonym for time gain compensation.

Display:
Visual presentation of echoes.

Doppler effect:
Change in the original (emitted) frequency when it strikes an interface moving towards or away from the transducer.

Doppler frequency:
Difference between original (emitted) and received frequency.

Duplex technique:
Fixed combination of a Doppler system with the B-scan image.

Echo:
Reflected ultrasound signal that forms the basis for diagnostic ultrasonography.

Echo free:
Absence of (internal) echoes, typically for fluid (synonym: Anechoic).

Echogenicity:
Echo pattern.

Echo pattern:
Intensity and distribution of all echoes of a certain area (organ or tumour).

Echo poor:
Echo pattern consisting of a few weak echoes.

Echo rich:
Echo pattern consisting of many strong echoes.

Far field:
That part of the ultrasound field distal to the focus.

Focus:
Natural focus, the narrowest point of the ultrasound field between the near and the far field.

Focusing:
Adjustment of the ultrasound beam to a particular distance (depth), to obtain the best resolution of the region of interest.

Frequency:
Number of complete (ultra)waves per second.

Gain:
Relation between energy output and input in an amplification system, expressed in decibels.

Hertz:
Unit of frequency, equal to one cycle per second.

Hyperechoic (or hyperechogenic):
Synonym for echo rich.

Hypoechoic (or hypoechogenic):
Synonym for echo poor.

Impedance:
Resistance to an acoustic wave.

Impedance jump:
Sudden change in acoustic wave resistance at the interface between two materials (tissues) with different acoustic properties.

Intensity:
Acoustic energy per unit area.

Interface:
Technically, a part interposed between two structural components to compensate for their imperfect fit.

Lateral resolution:
(Poorer) resolution in a direction transversal to the ultrasound beam.

Linear array:
Linear arrangement of two or more crystals, which are activated electronically in groups.

Longitudinal scan:
Plan corresponding to the anterior–posterior long axis of the body.

Mechanical index:
Amount of negative acoustic pressure in the ultrasound field (measure of acoustic power).

Microbubble:
See Contrast agent.

Mirror effect:
Total reflection of ultrasound pulses by some structures, e.g. air-containing lung.

M-mode:
Continuous tracing of ultrasound echoes for moving structures (echocardiography). Synonyms: M-scan, TM-scan, time motion.

Near field:
Part of the ultrasound field between the transducer and the focus (synonym: Fresnel zone).

Parallel scan:
Two-dimensional B-scan with the single ultrasound beams running parallel (typical image of linear array transducer).

Phantom:
Device for testing or calibrating ultrasound equipment.

Piezoelectric effect:
Property of polar crystals to convert mechanical energy (pressure and tension) into electrical energy (ultrasound receiver) and vice versa (reverse piezoelectric effect: ultrasound transmitter).

Pulse-echo technique:
Ultrasound technique in which the ultrasound is emitted in very short pulses and the returned echoes are analysed.

Real time:
B-scan technique with rapid construction of images (about 15 per s), creating the impression of a continuous image.

Resolution:
See Axial resolution and Lateral resolution.

Reverberation:
Reflection of ultrasound between two nearly parallel surfaces backward and forward repeatedly. The repeated echoes arrive at the transducer with a delay and are positioned in the image at a doubled or multiple distance.

Sagittal scan:
Longitudinal scan.

Scanning plane:
Section of the body or organ passed by the ultrasound beams of the actual scan.

Scattering:
Reflection and refraction of an ultrasound beam non-directionally by a reflector smaller than the wavelength.

Sector scan:
Two-dimensional B-scan produced by diverging ultrasound beams (typical of mechanical real-time and curved array transducers).

Sonolucent:
Tissues and structures with a low (below average) attenuation of ultrasound.

Spectral Doppler:
Display of all frequencies of the Doppler signal over time.

Specular reflector:
Reflector (tissue surface or vessel wall) with a smooth surface and a diameter greater than the diameter of the wavelength.

Stimulated acoustic emission:
Short but strong signal created by destruction of microbubbles by ultrasound (high mechanical index) used e.g. for differentiation of liver tumours.

Thermal index:
Measure of heating of tissue by absorption; ratio of power used to that required to cause a maximum temperature increase of 1 °C.

Time gain compensation:
Electronic amplification of echoes, depending on their distance from the transducer (synonym: depth gain compensation).

Tissue harmonic imaging:
B-scan technique based on analysis and image construction only from echoes with doubled fundamental frequency (second harmonic).

TM scan:
Synonym for M-mode.

Transducer:
Device that converts one form of energy into another (in ultrasonography, electric energy into mechanical ultrasound waves) and vice versa.

Transverse scan:
Scanning plane at right angles to the long axis of the body.

Ultrasound:
Mechanical pressure waves beyond the upper limit of human hearing (> 20 000 Hz).

Wavelength:
Length of a single cycle of a (ultrasound) wave, inversely proportional to the frequency.

Index

Notes
Pages numbers ending in f refer to figures
Pages numbers ending in t refer to tables

[A]

[B]

[C]

[S]

[T]

[U]

Manual of diagnostic ultrasound

vol. 1

During the last decades , use of ultrasonography became increasingly common in medical practice and hospitals around the world, and a large number of scientific publications reported the benefit and even the superiority of ultrasonography over commonly used X-ray techniques, resulting in significant changes in diagnostic imaging procedures.

With increasing use of ultrasonography in medical settings, the need for education and training became essential. WHO took up this challenge and in 1995 published its first training manual in ultrasonography. Soon, however, rapid developments and improvements in equipment and indications for the extension of medical ultrasonography into therapy indicated the need for a totally new ultrasonography manual.

The manual (consisting of two volumes) has been written by an international group of experts of the World Federation for Ultrasound in Medicine and Biology (WFUMB), well-known for their publications regarding the clinical use of ultrasound and with substantial experience in the teaching of ultrasonography in both developed and developing countries. The contributors (more than 50 for the two volumes) belong to five different continents, to guarantee that manual content represents all clinical, cultural and epidemiological contexts.

This new publication, which covers modern diagnostic and therapeutic ultrasonography extensively, will certainly benefit and inspire medical professionals in improving 'health for all' in both developed and emerging countries.

ISBN 978 92 4 154745 1